

REPORT DOCUMENTATION PAGE

Form Approved
OMB NO. 0704-0188

Public Reporting burden for this collection of information is estimated to average 1 hour per response, including the time for reviewing instructions, searching existing data sources, gathering and maintaining the data needed, and completing and reviewing the collection of information. Send comment regarding this burden estimates or any other aspect of this collection of information, including suggestions for reducing this burden, to Washington Headquarters Services, Directorate for Information Operations and Reports, 1215 Jefferson Davis Highway, Suite 1204, Arlington, VA 22202-4302, and to the Office of Management and Budget, Paperwork Reduction Project (0704-0188), Washington, DC 20503.

1. AGENCY USE ONLY (Leave Blank)	2. REPORT DATE	3. REPORT TYPE AND DATES COVERED Final 01 May 98 - 30 Jun 01
4. TITLE AND SUBTITLE Constitutive Theories for Swelling Porous Media		5. FUNDING NUMBERS DAAG55-98-1-0228
6. AUTHOR(S) John H. Cushman		
7. PERFORMING ORGANIZATION NAME(S) AND ADDRESS(ES) Purdue Research Foundation Sponsored Program Service, 1063 Hovde Hall West Lafayette, IN 47907-1063		8. PERFORMING ORGANIZATION REPORT NUMBER
9. SPONSORING / MONITORING AGENCY NAME(S) AND ADDRESS(ES) U. S. Army Research Office P.O. Box 12211 Research Triangle Park, NC 27709-2211		10. SPONSORING / MONITORING AGENCY REPORT NUMBER 37641.2-EV

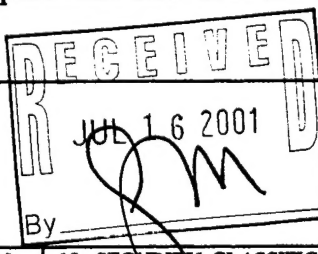
11. SUPPLEMENTARY NOTES
The views, opinions and/or findings contained in this report are those of the author(s) and should not be construed as an official Department of the Army position, policy or decision, unless so designated by other documentation.

12 a. DISTRIBUTION / AVAILABILITY STATEMENT Approved for public release; distribution unlimited.	12 b. DISTRIBUTION CODE
---	-------------------------

13. ABSTRACT (Maximum 200 words)

The macroscopic field equations (three-scale) and constitutive equations have been developed for various types of swelling porous media. One theory is general enough to account for electron quasi-static effects such as swelling induced ionic migration (change in electrolyte) upon drying or wetting. Another can handle generalized Kelvin-Voigt viscoelastic solid phases with arbitrary order time-rate-of-change in the macroscale solid phase strain tensor. Explicit relations have been developed between the macroscopic and microscopic variables. Tools employed in this analysis are derived from rational mechanics and mathematical homogenization theory.

Several fixed-grid and deforming-grid finite element solutions to the more elementary compaction and tearing problems have been developed. Of particular note here is the study of the deformation of a soil under both normal load and shear stress.

14. SUBJECT TERMS Swelling Porous Media Deformation Vehicle Simulation Constitutive Equations		 By _____	15. NUMBER OF PAGES 361
			16. PRICE CODE
17. SECURITY CLASSIFICATION OR REPORT UNCLASSIFIED	18. SECURITY CLASSIFICATION ON THIS PAGE UNCLASSIFIED	19. SECURITY CLASSIFICATION OF ABSTRACT UNCLASSIFIED	20. LIMITATION OF ABSTRACT UL

NSN 7540-01-280-5500

Standard Form 298 (Rev.2-89)
Prescribed by ANSI Std. Z39-18
298-102

Enclosure 1

20010725 031

MASTER COPY: PLEASE KEEP THIS "MEMORANDUM OF TRANSMITTAL" BLANK FOR REPRODUCTION PURPOSES. WHEN REPORTS ARE GENERATED UNDER THE ARO SPONSORSHIP, FORWARD A COMPLETED COPY OF THIS FORM WITH EACH REPORT SHIPMENT TO THE ARO. THIS WILL ASSURE PROPER IDENTIFICATION. NOT TO BE USED FOR INTERIM PROGRESS REPORTS; SEE PAGE 2 FOR INTERIM PROGRESS REPORT INSTRUCTIONS.

MEMORANDUM OF TRANSMITTAL

U.S. Army Research Office
ATTN: AMSRL-RO-BI (TR)
P.O. Box 12211
Research Triangle Park, NC 27709-2211

Reprint (Orig + 2 copies) Technical Report (Orig + 2 copies)
 Manuscript (1 copy) Final Progress Report (Orig + 2 copies)
 Related Materials, Abstracts, Theses (1 copy)

CONTRACT/GRANT NUMBER: DAAG55-98-1-0228

REPORT TITLE: Final Report on Constitutive Theories for Swelling Porous Media

is forwarded for your information.

SUBMITTED FOR PUBLICATION TO (applicable only if report is manuscript):

Sincerely,
John Cushman

Final Report, May 2001
on
Constitutive Theories for Swelling Porous Media

Executive Summary

Soils and soil moisture play a predominant role in off-road vehicular mobility, and as such they play an important role in the army's strategies, logistics, mobility and field operations. This is especially true in adverse terrain, such as muddy (expansive soils). Problems associated with simulating and predicting vehicle terrain interaction in adverse environments are immensely complicated, as soils are diverse and soil moisture dynamic. Yet it is the army's goal to develop an all-weather, all-terrain capability. This goal suggests the complicated, diverse and dynamic interaction of terrain with vehicles must be understood and simulated from a mechanistic perspective.

The army currently has an ability to model vehicular dynamics on smooth, hard terrain; yet the interaction of a vehicle with "real" terrain is beyond current simulation capability. It is this latter point that this report begins to address. Secondly, we have studied from first principles one of the most dynamic and restrictive conditions to army system performance; expansive-soil deformation.

As originally set out in the proposal, our goals were to develop constitutive models for expansive soils which incorporate the effects of electrolytes and heat transfer, and to begin development of numerical simulators for the resultant balances of mass, momentum and energy in the presence of dynamic loads. Over the three year funding period, significant advance toward achieving both goals was accomplished. In fact, in the area of constitutive model

development we have actually exceeded the goals of the original proposal. Below, in the form of bullets, we summarize what has been accomplished to date.

1. Capillary condensation and snap-off in nanoscale contacts (these results were highlighted on the Feb. 6, 2001 cover of the Amer. Chem. Soc. Journal of surfaces and colloids, Langmuir).

When a surface is placed in a vapor, several layers of molecules may adsorb depending on the intermolecular forces involved. As two such surfaces are brought together, a critical point is reached at which the gas condenses between the surfaces, forming a capillary across the gap. A cohesive force is associated with the condensed bridge. The reverse process wherein the capillary bridge degenerates as the surfaces are moved apart is called snap-off. These processes play a profound role on scales from the nano to the macro. We have studied this phenomenon via isostrain grand canonical Monte Carlo statistical mechanical simulations for Lennard-Jones fluids. Specifically, we have examined capillary condensation and snap-off between nanocontacts, infinite rectilinear nanowires, and finite rectilinear nanoplatelets, where macroscale concepts and theories are just about impossible to apply. These results are compared to condensation between infinite parallel plates. We discuss our results in terms of the Kelvin equation and van der Waals film-thickening model.

2. Coupled solvent and heat transport of a mixture of swelling porous particles and fluids: single time-scale problem.

A three-spatial scale, single time-scale model for both moisture and heat transport is developed for an unsaturated swelling porous media from first principles within a mixture theoretic framework. On the smallest (micro) scale, the system consists of macromolecules (clay particles, polymers, etc.) and a solvating liquid (vicinal fluid), each of which are viewed as individual phases or nonoverlapping continua occupying distinct regions of space and satisfying the classical field equations. These equations are homogenized forming overlaying continua on

the intermediate (meso) scale via hybrid mixture theory (HMT). On the mesoscale the homogenized swelling particles consisting of the homogenized vicinal fluid and colloid are then mixed with two bulk phase fluids: the bulk solvent and its vapor. At this scale, there exists three nonoverlapping continua occupying distinct regions of space. On the largest (macro) scale the saturated homogenized particles, bulk liquid and vapor solvent, are again homogenized forming four overlaying continua: doubly homogenized vicinal fluid, doubly homogenized macromolecules, and singly homogenized bulk liquid and vapor phases. Two constitutive theories are developed, one at the mesoscale and the other at the macroscale. Both are developed via the Coleman and Noll method of exploiting the entropy inequality coupled with linearization about equilibrium. The macroscale constitutive theory does not rely upon the mesoscale theory as is common in other upscaling methods. The energy equation on either the mesoscale or macroscale generalizes de Vries classical theory of heat and moisture transport. The momentum balance allows for flow of fluid via volume fraction gradients, pressure gradients, external force fields, and temperature gradients.

3. Thermomechanical dual porosity theories for swelling porous media with microstructure

Thermomechanical microstructural dual porosity models for swelling porous media incorporating coupled effects of hydration, heat transfer and mechanical deformation are proposed. These models are obtained by generalizing the three-scale system of Murad and Cushman [56,57] to accommodate heat transfer effects and their influence on swelling. The microscale consists of macromolecular structures (clay platelets, polymers, shales, biological tissues, gels) in a solvent (adsorbed water), both of which are considered as distinct nonoverlating continua. These continua are homogenized to the meso (intermediate scale) in the spirit of hybrid mixture theory (HMT), so that at the mesoscale they may be thought of as two

overlying continua. Application of HMT leads to a two-scale model which incorporates coupled thermal and physicochemical effects between the macromolecules and adsorbed solvent. Further, a three-scale model is obtained by homogenizing the particles (clusters consisting of macromolecules and adsorbed solvent) with the bulk solvent (solvent not within but next to the swelling particles). This yields a macroscopic microstructural model of dual porosity type. In the macroscopic swelling medium the mesoscale particles act as distributed sources/sinks of mass, momentum and energy to the macroscale bulk phase system. A modified Green's function method is used to reduce the dual porosity system to a single-porosity system with memory. The resultant theory provides a rigorous derivation of creep phenomena which are due to delayed intra-particle drainage (e.g. secondary consolidation of clay soils). In addition, the model reproduces a class of lumped-parameter models for fluid flow, heat conduction and momentum transfer where the distributed source/sink transfer function is a classical exchange term assumed proportional to the difference between the potentials in the bulk phase and swelling particles.

4. Macroscale thermodynamics and the chemical potential for swelling porous media

The thermodynamical relations for a two-phase, N -constituent, swelling porous medium are derived using a hybridization of averaging and the mixture-theoretic approach of Bowen. Examples of such media include 2-1 lattice clays and lyophilic polymers. A novel, scalar definition for the macroscale chemical potential for porous media is introduced, and it is shown how the properties of this chemical potential can be derived by slightly expanding the usual Coleman and Noll approach for exploiting the entropy inequality to obtain near-equilibrium results. The relationship between this novel scalar chemical potential and the tensorial chemical potential of Bowen is discussed. The tensorial chemical potential may be discontinuous between the solid and fluid phases at equilibrium; a result in clear contrast to Gibbsian theories. It is

shown that the macroscopic scalar chemical potential is completely analogous with the Gibbsian chemical potential. The relation between the two potentials is illustrated in three examples.

5. Thermomechanics of swelling viscoelastic two-scale porous media

A two-scale theory for swelling viscoelastic media is developed. At the microscale, the solid matrix interacts with the solvent through surface contact. The relaxation processes within the matrix were incorporated by modeling the solid phase as viscoelastic and the solvent phase as viscous at the mesoscale. We obtain novel equations for the total stress tensor, chemical potential of the solid phase, heat flux and the generalized Darcy's law all at the mesoscale. The constitutive relations are more general than those previously developed for the swelling colloids. The form of the generalized Fick's law is similar to that obtained in earlier works involving colloids. Using two-variable expansions, thermal gradients are coupled with the strain rate tensor for the solid phase and the deformation rate tensor for the liquid phase. This makes the experimental determination of the material coefficients easier and less ambiguous, and clearly illustrates the role of third-order tensors in anisotropic media.

6. Thermomechanics of swelling viscoelastic three-scale porous media with temporal nonlocality

A two-scale theory for swelling media with multiple species is developed. At the microscale, the interaction of the solid with the fluid phase is considered. The relaxation processes within the matrix are incorporated by modeling the solid phase as viscoelastic. Novel equations for the total stress tensor, chemical potential of the solid phase, heat flux and the generalized Darcy's law are obtained. The equations are more general than those developed for swelling colloids. The form of the generalized Fick's law remained similar to that obtained in the previous colloidal media studies. With two-variable Taylor series expansion, the thermal

gradient effects are coupled with the rate of strain tensor of the solid phase and the rate of deformation tensor of the liquid phase. This makes the experimental determination of the material coefficients easier and makes a clear distinction of the cross-effects exhibited by the anisotropic media.

7. Multicomponent, multiphase thermodynamics of swelling porous media with electroquasistatics: Macroscale field equations

A systematic development of the macroscopic field equations (conservation of mass, linear and angular momentum, energy, and Maxwell's equations) for a multiphase, multicomponent medium is presented. It is assumed that speeds involved are much slower than the speed of light and that the magnitude of the electric field significantly dominates over the magnetic field so that the electroquasistatic form of Maxwell's equations applies. A mixture formulation for each phase is averaged to obtain the macroscopic formulation. Species electric fields are considered, however it is assumed that it is the total electric field which contributes to the electrically induced forces and energy. The relationships between species and bulk phase variables and the macroscopic and microscopic variables are given explicitly. The resulting field equations are of relevance to many practical applications including, but not limited to, swelling clays (smectites), biopolymers, biological membranes, pulsed electrophoresis, and chromatography.

8. Multicomponent, multiphase thermodynamics of swelling porous media with electroquasistatics: Constitutive theory

We exploit the entropy inequality to obtain restrictions on constitutive relations at the macroscale for a 2-phase, multiple-constituent, polarizable mixture of fluids and solids. Specific emphasis is placed on charged porous media in the presence of electrolytes. The governing

equations for the stress tensors of each phase, flow of the fluid through a deforming medium, and diffusion of constituents through such a medium are derived. The results have applications in swelling clays (smectites), biopolymers, biological membranes, pulsed electrophoresis, chromatography, drug delivery, and other swelling systems.

9. Numerical methods and examples

Several finite element techniques are used to simulate consolidation coupled with pore-fluid transport. Several elastic and viscoelastic constitution theories are employed and capillarity is taken into account. Both moving and stationary grids are studied. Where possible model test cases are compared with analytical solutions. A novel problem, moving loads with shear and normal stress, was studied in detail.

Table of Contents

- I. Thermomechanics of swelling viscoelastic two-scale porous media
- II. Thermomechanics of swelling viscoelastic three-scale porous media with temporal nonlocality
- III. Multicomponent, multiphase thermodynamics of swelling porous media with electroquasistatics: Macroscale field equations
- IV. Multicomponent, multiphase thermomechanics of swelling porous media with electroquasistatics: Constitutive theory
- V. Numerical methods and examples
- VI. Students partially supported by this work
- VII. Publications and Presentations

Appendices

- 1. Capillary condensation and snap-off in nanoscale contacts (these results were highlighted on the Feb. 6, 2001 cover of the Amer. Chem. Soc. Journal of Surfaces and Colloids, Langmuir).
- 2. Coupled solvent and heat transport of a mixture of swelling porous particles and fluids: single time-scale problem
- 3. Thermomechanical theories for swelling porous media with microstructure
- 4. Macroscale thermodynamics and the chemical potential for swelling porous media

I. Thermomechanics of swelling viscoelastic two-scale porous media

1. Introduction

Swelling viscoelastic systems are ubiquitous; examples include soils, proteins, carbohydrates, foods, cartilages, membranes, plant seeds, drugs, contact lenses etc. In such systems a discrete hierarchy of scales is present due to their complex nested porous structures. Here we consider two scale systems.

Fig. 1 illustrates a three-scale (micro, meso, macro) system of interest. It is composed of a solid-matrix and solvating fluid. The solid matrix and the vicinal fluid (fluid solvating the matrix surface) exist as separate phases on the microscale (of the order of microns). The mixture of the solid matrix with the vicinal fluid on the mesoscale are represented by a particle in the diagram. The particle itself may exist in a bulk phase fluid, but we leave that problem to the future. At the mesoscale each constituent in each phase and in each interface and the phases themselves are considered as overlaying continua defined over all space. Most phenomenon exhibited at higher scales are a manifestation of interactions taking place at smaller scale. The mesoscale swelling/shrinkage exhibited by these systems results from the solvation of solid by the fluid on the microscale [24]. This necessitates the modeling of thermomechanical processes such as stress-cracking, extrusion, consolidation, and transport processes such as drying, conditioning, solvent-extraction, controlled drug and pesticide release, encapsulated germination over a hierarchy of scales.

Many methods are available for upscaling information from lower to higher scales [13,21]. We chose to use the hybrid mixture theory (HMT) approach. HMT involves volume averaging of equations of mass, momentum, energy and entropy at the microscale to obtain

equations at the mesoscale. In a two-scale approach, the constitutive equations are formulated at the mesoscale by exploiting the entropy inequality in the sense of Coleman and Noll [12].

HMT was developed by engineers to explain the thermomechanical behavior of natural geologic media. Many polymeric systems are porous and so amenable to a similar treatment. Experimental work by Etzler [15,16] has shown that the physics of interaction of water in silica and cellulosic surfaces is nearly identical. For these reasons, the HMT approach has been very successful in explaining the thermomechanical behavior of food gels [2]. HMT was introduced by Hassanizadeh and Gray [19,18] for non-interacting granular porous media. Achanta et al. [1], Bennethum and Cushman [3,4], Murad et al. [26], and Murad and Cushman [2729] extended these ideas to swelling and shrinking systems with multi-constituents where interactions between phases play an important role. However, in all previous works with HMT, the solid phase was assumed to be elastic solid and the liquid phase was assumed to be viscous. These studies were either aimed at swelling colloidal systems [26,3,4], or were adapted for polymeric systems from colloidal systems [1,3,4,2,9], for which the assumption of elastic solid phase holds. The systems exhibited viscoelastic behavior only at the macroscale, which resulted from microscale interaction of the elastic solid-phase with the viscous fluid-phase. These theories ignored the microscale relaxation processes of the polymeric matrix, which arise due to conformational changes in the flexible thread-like polymer chains [17]. The viscoelastic nature of the polymers is exhibited even at very small magnitudes of strains [17]. The focus of this study is on the viscoelastic swelling solid phase. We present a two-scale theory with the assumption that at the mesoscale the solid phase is a Kelvin-Voigt material and the liquid phase is a viscous fluid. This will make our work more general and applicable to a large class of polymeric and biopolymeric media subjected to a wide range of processes. Additionally, in previous HMT based theories

near-equilibrium equations were obtained by linearization around single variables, which made the coefficients a function of the thermal gradient. Here, we will use two-variable linearization to couple the thermal gradient with the rate of strain tensor of the solid phase and the rate of deformation tensor of the liquid phase. This will also make the linearization coefficients independent of the thermal gradient.

Notation

We consider a two-phase (e.g. solid-liquid) system with N components. The two phases are represented by α and β . For simplicity, we assume that the interface between the two phases is free from thermodynamic properties. Following the axiom of equipresence of constituents [1], we assume at the outset that each phase contains same set of N-constituents (some may be at zero concentration). The subscript α_j represents the property of the j^{th} constituent in the α phase. The hatted quantities, such as ${}^{\beta}\hat{e}^{\alpha_j}$, represent property transfer from one phase to the other. The hatted quantities like \hat{r}^{α_j} represent property gained by the j^{th} constituent within a phase due to chemical reactions. The complete nomenclature is presented in Appendix C. We lay out the equations in Eulerian coordinates with subscripts k and l representing the coordinate directions and repetition of these indices implying summation. The use of capital letters such as K and L with certain quantities represents Lagrangian coordinates. The indices k, l, K and L range from 1 to 3.

2. Constitutive Theory

The mesoscale field equations are applicable to all kinds of materials and are presented in the Appendix A. These equations are closed for specific materials by imposing restrictions on the

constitutive functions through the axioms of constitution [14] and entropy inequality in the sense of Coleman and Noll [12].

Here, we consider a two-phase solid (s)-liquid (w) system. At the mesoscale, the solid phase is considered viscoelastic and the liquid phase is considered viscous. The viscoelastic solid and the viscous liquid will interact to make the material behave as a viscoelastic solid at the mesoscale. For simplicity we assume that the viscoelastic solid is of Kelvin-Voigt type, whose constitutive variables depend upon the first order time derivative of the strain tensor. It is easy to further generalize the viscoelastic nature by including higher order time derivatives of the strain tensor but this adds little to our discussion here. Following is the list of unknown variables:

$$\varepsilon^\alpha, \varepsilon^\alpha \rho^{\alpha_j}, v_l^{\alpha_j}, T, {}^\beta \hat{e}^{\alpha_j}, \hat{r}^{\alpha_j}, t_{kl}^{\alpha_j}, {}^\beta \hat{T}_l^{\alpha_j}, \hat{i}_l^{\alpha_j}, A^{\alpha_j}, q_l^{\alpha_j}, {}^\beta \hat{Q}^{\alpha_j}, \hat{E}^{\alpha_j}, {}^\beta \hat{\phi}^{\alpha_j}, \eta^{\alpha_j}, \hat{\eta}^{\alpha_j}. \quad (2.1)$$

The mass conservation equation (A.1) corresponds to the unknown $\varepsilon^\alpha \rho^{\alpha_j}$. The momentum (A.10) and energy (A.18) balance equations, correspond to $v_l^{\alpha_j}$ and T , respectively. Additional equations are obtained by considering the following variables to be constitutive or dependent:

$$\dot{\varepsilon}^\alpha, {}^\beta \hat{e}^{\alpha_j}, \hat{r}^{\alpha_j}, t_{kl}^{\alpha_j}, {}^\beta \hat{T}_l^{\alpha_j}, \hat{i}_l^{\alpha_j}, A^{\alpha_j}, q_l^{\alpha_j}, {}^\beta \hat{Q}^{\alpha_j}, \hat{E}^{\alpha_j}, {}^\beta \hat{\phi}^{\alpha_j}, \eta^{\alpha_j}, \hat{\eta}^{\alpha_j}. \quad (2.2)$$

These constitutive variables are considered to be a function of the following set of independent variables:

$$\varepsilon^w, \varepsilon^\alpha \rho^{\alpha_j}, (\varepsilon^\alpha \rho^{\alpha_j})_j, v_l^{\alpha,s}, u_l^{\alpha_j}, T, T_j, E_{KL}^s, E_{KL,j}^s, \dot{E}_{KL}^s, d_{kl}^w, u_{k,l}^{w_j}. \quad (2.3)$$

In (2.3) only ε^w is listed because it is related to ε^s by (A.7). Therefore, we can chose either ε^w or ε^s as independent but not both. The variables ε^α and ρ^{α_j} always appear as a product $\varepsilon^\alpha \rho^{\alpha_j}$, which arose during the upscaling of the equations from micro to the mesoscale. All the variables have a corresponding equation, except for ε^α . This is the closure problem, and following

Bowen [11], we formulate the additional equation by postulating that $\dot{\varepsilon}^\alpha$ is a dependent variable. The variables ε^w and $(\varepsilon^w \rho^w)_j$ account for the liquid-solid interaction at moderate to high solvent content. The liquid-solid interaction occurs through solvation forces, which lower the chemical potential at the interfaces in comparison to the bulk liquid [25,22,23,11,24]. This causes liquid movement from the bulk phase to the interface, pushing apart the solid, which in turn produces swelling. The E_{KL}^s and $E_{KL,j}^s$ account for the elastic deformation of the solid matrix. At low moisture contents, $E_{KL,j}^s$ incorporates relative shear between two solid surfaces separated by only few molecular layers of water [27,7]. In a connected solid matrix a macroscopic deformation results in a gradient of the strain tensor at the mesoscale, which is also captured by the $E_{KL,j}^s$. At the mesoscale, the viscoelastic nature of the solid polymer is captured by \dot{E}_{KL}^s .

We assume that at least one of ${}^B\hat{e}^{\alpha_j}$ or \hat{r}^{α_j} is not equal to zero due to which $(\varepsilon^s \rho^{s_j})_j$ and \dot{E}_{KL}^s can be varied independently. Thus, both $(\varepsilon^s \rho^{s_j})_j$ and \dot{E}_{KL}^s are included in the list (2.3) of independent variables. Otherwise, $(\varepsilon^s \rho^{s_j})_j$ and \dot{E}_{KL}^s would be related by the mass balance equation (A.1) and the equation, $\dot{E}_{KL}^s = x_{k,K}^s x_{l,L}^s d_{kl}^s$, and only one would be required in the list (2.3).

Thermal energy production may arise in a material during deformation or due to an external source. The variables T and T_j account for the conduction of this thermal energy. At very high or low rates of heat transfer, T_j would not be required because in the former case the material responds so quickly that it can be considered to be at uniform temperature ($T_j \ll 1$), and in the latter case, the temperature change is so slow that its effects are negligible. At

intermediate rates of heat transfer, the thermal gradient becomes important. The viscous nature of the liquid phase is incorporated through the d_{kl}^w . The term $u_{k,l}^{w_j}$ leads to the viscous resistance of the fluid phase to the diffusion of species. For most practical purposes, the diffusion of species in the solid phase is negligible. Therefore, $u_{k,l}^{s_j}$ is not included in the list of independent variables.

The axiom of equipresence requires that initially all constitutive variables should be expressed in terms of the same list of independent variables until the contrary is proven[14]. It can be shown that the Helmholtz free energies are functions of the subsets of the list (2.3) [20]. Additionally, from physical knowledge of the system we know that the Helmholtz free energy of the solid phase depends upon $\varepsilon^s \rho^{s_j}$ and of the liquid phase depends upon $\varepsilon^w \rho^{w_j}$. Therefore, to save computations we postulate the dependence of the Helmholtz free energies on subsets of list (2.3) as:

$$A_l^w = A_l^w(\varepsilon^w, \varepsilon^w \rho^{w_j}, T, E_{KL}^s, \dot{E}_{KL}^s), \quad (2.4)$$

$$A_l^s = A_l^s(\varepsilon^s, \varepsilon^s \rho^{s_j}, T, E_{KL}^s, \dot{E}_{KL}^s). \quad (2.5)$$

All other dependent variables are considered to be a function of all independent variables in list (2.3). The free energies appear in the entropy inequality (A.41) as material derivatives. Using the chain rule, the following expressions for the material derivatives of the free energies can be obtained:

$$\begin{aligned} \frac{D^w A_l^w}{Dt} &= \frac{\partial A_l^w}{\partial \varepsilon^w} \frac{D^w \varepsilon^w}{Dt} + \sum_{j=1}^N \frac{\partial A_l^w}{\partial (\varepsilon^w \rho^{w_j})} \frac{D^w (\varepsilon^w \rho^{w_j})}{Dt} + \frac{\partial A_l^w}{\partial T} \frac{D^w T}{Dt} + \\ &\quad \frac{\partial A_l^w}{\partial E_{KL}^s} \frac{D^w E_{KL}^s}{Dt} + \frac{\partial A_l^w}{\partial \dot{E}_{KL}^s} \frac{D^w \dot{E}_{KL}^s}{Dt}, \end{aligned} \quad (2.6)$$

$$\begin{aligned} \frac{D^s A_l^s}{Dt} = & \frac{\partial A_l^s}{\partial \varepsilon^w} \frac{D^s \varepsilon^w}{Dt} + \sum_{j=1}^N \frac{\partial A_l^s}{\partial (\varepsilon^s \rho^{s_j})} \frac{D^s (\varepsilon^s \rho^{s_j})}{Dt} + \frac{\partial A_l^s}{\partial T} \frac{D^s T}{Dt} + \\ & \frac{\partial A_l^s}{\partial E_{KL}^s} \dot{E}_{KL}^s + \frac{\partial A_l^s}{\partial \dot{E}_{KL}^s} \ddot{E}_{KL}^s. \end{aligned} \quad (2.7)$$

The following identities will be needed to rewrite equations (2.6) and (2.7) in suitable forms before substitution into the entropy inequality (A.41):

$$\frac{D^w \phi}{Dt} = \frac{D^s \phi}{Dt} + v_k^{w,s} \phi_{,k} \quad (2.8)$$

$$\frac{D^{\alpha_j} \phi}{Dt} = \frac{D^{\alpha} \phi}{Dt} + u_k^{\alpha_j} \phi_{,k} \quad (2.9)$$

where, ϕ is a scalar function. The pressures and the chemical potential have been defined in more than one way in the literature [10,1,9]. For example, the chemical potential of Bowen [10] is a tensor, whereas in classical thermodynamics the chemical potential is a scalar. We will use the scalar valued definitions proposed by Bennethum et al. [9], which are equivalent to the definitions in classical thermodynamics. In classical thermodynamics, total Helmholtz energy, A^α is expressed as:

$$A^\alpha = A^\alpha(V^\alpha, M^{\alpha_j}, T) \quad (2.10)$$

Divide A^α by mass of the α phase and normalize V^α, M^{α_j} by the weighted averaging volume.

This gives:

$$A_l^\alpha = A_l^\alpha(\varepsilon^\alpha, \varepsilon^\alpha \rho^{\alpha_j}, T) \quad (2.11)$$

Here we used,

$$\frac{M^{\alpha_j}}{V} = \frac{M^{\alpha_j}}{V^\alpha} \frac{V^\alpha}{V} = \varepsilon^\alpha \rho^{\alpha_j} \quad (2.12)$$

The classical pressure, P^α is defined as:

$$\begin{aligned}
P^\alpha &= -\frac{\partial A^\alpha}{\partial V^\alpha} \Big|_{M^{\alpha_j}, T} = -\frac{\partial(M^\alpha A_I^\alpha)}{\partial V^\alpha} \Big|_{M^{\alpha_j}, T} = -\frac{\partial \left(\frac{V^\alpha M^\alpha}{V^\alpha V^\alpha} A_I^\alpha \right)}{\partial \left(\frac{V^\alpha}{V} \right)} \Big|_{M^{\alpha_j}, T} \\
&= -\frac{\partial(\varepsilon^\alpha \rho^\alpha A_I^\alpha)}{\partial \varepsilon^\alpha} \Big|_{\varepsilon^\alpha \rho^{\alpha_j}, T} = -\varepsilon^\alpha \rho^\alpha \frac{\partial A_I^\alpha}{\partial \varepsilon^\alpha} \Big|_{\varepsilon^\alpha \rho^{\alpha_j}, T}.
\end{aligned} \tag{2.13}$$

Thus we have the classical pressure defined in terms of the intensive variables needed to model open systems. Another quantity that needs to be defined is:

$$p^\alpha = \sum_{j=1}^N \rho^\alpha \rho^{\alpha_j} \frac{\partial A_I^\alpha}{\partial \rho^{\alpha_j}} \Big|_{\varepsilon^\alpha, T} \tag{2.14}$$

which we refer to as the thermodynamic pressure. For a single medium composed of single species only, p^α reduces to the classical thermodynamic pressure, P^α :

$$p^\alpha = \rho^{\alpha^2} \frac{\partial A_I^\alpha}{\partial \rho^\alpha} \Big|_{\varepsilon^\alpha, T} = P^\alpha \tag{2.15}$$

Further physical interpretation of p^α will be made clear after its relationship to the stress tensors are obtained from the exploitation of the entropy inequality.

The chemical potential, μ^{α_j} is defined as:

$$\begin{aligned}
\mu^{\alpha_j} &= \frac{\partial A^\alpha}{\partial M^{\alpha_j}} \Big|_{V^\alpha, T} = \frac{\partial(M^\alpha A_I^\alpha)}{\partial M^{\alpha_j}} \Big|_{V^\alpha, T} = \frac{\partial \left(\frac{V^\alpha M^\alpha}{V^\alpha V^\alpha} A_I^\alpha \right)}{\partial \left(\frac{V^\alpha M^{\alpha_j}}{V^\alpha V^\alpha} \right)} \Big|_{V^\alpha, T} \\
&= \frac{\partial(\varepsilon^\alpha \rho^\alpha A_I^\alpha)}{\partial(\varepsilon^\alpha \rho^{\alpha_j})} \Big|_{\varepsilon^\alpha, T} = A_I^\alpha + \rho^\alpha \frac{\partial A_I^\alpha}{\partial \rho^{\alpha_j}} \Big|_{\varepsilon^\alpha, T}.
\end{aligned} \tag{2.16}$$

In the entropy inequality, the terms involving $u_l^{\alpha_j}$ and $u_{k,l}^{\alpha_j}$ have N-1 independent variables and

one dependent variable because, $\sum_{j=1}^N \rho^{\alpha_j} u_l^{\alpha_j} = 0$. Thus, the following identities due to Bennethum et al. [9] will be needed to rewrite these terms as N-1 independent terms:

$$\sum_{j=1}^N F_k^{\alpha_j} u_k^{\alpha_j} = \sum_{j=1}^{N-1} u_k^{\alpha_j} \left(F_k^{\alpha_j} - \frac{\rho^{\alpha_j}}{\rho^{\alpha_N}} F_k^{\alpha_N} \right). \quad (2.17)$$

$$\sum_{j=1}^N G_{kl}^{\alpha_j} u_{k,l}^{\alpha_j} = \sum_{j=1}^{N-1} u_{k,l}^{\alpha_j} \left(G_{kl}^{\alpha_j} - \frac{\rho^{\alpha_j}}{\rho^{\alpha_N}} G_{kl}^{\alpha_N} \right) - G_{kl}^{\alpha_N} \sum_{j=1}^{N-1} \left(\frac{\rho^{\alpha_j}}{\rho^{\alpha_N}} \right)_{,l} u_k^{\alpha_j}. \quad (2.18)$$

where, $F_k^{\alpha_j}$ and $G_{kl}^{\alpha_j}$ are the vector and tensor valued coefficients of $u_k^{\alpha_j}$ and $u_{k,l}^{\alpha_j}$, respectively.

Substituting equations (2.6) and (2.7) in the entropy inequality (A.41) and simplifying using identities and definitions (2.8) – (2.18), we obtain:

$$\begin{aligned}
\Lambda = & -\sum_{\alpha} \frac{\varepsilon^{\alpha} \rho^{\alpha}}{T} \left(\frac{\partial A_I^{\alpha}}{\partial T} + \eta^{\alpha} \right) \frac{D^s T}{Dt} \\
& - \frac{1}{T} (\mathbf{P}^s - \mathbf{P}^w) \dot{\varepsilon}^w \\
& + \frac{1}{T} \left[\left(\varepsilon^s p^s \delta_{kl} - \varepsilon^s t_{kl}^{se} - \varepsilon^w t_{kl}^{sh} + \varepsilon^s \sum_{j=1}^N t_{kj}^{sj} \right) X_{K,k}^s X_{L,l}^s \right] \dot{E}_{KL}^s \\
& + \frac{\varepsilon^w}{T} \left(p^w \delta_{kl} + \sum_{j=1}^N t_{kj}^{wj} \right) d_{kl}^w \\
& + \sum_{\alpha} \frac{\varepsilon^{\alpha}}{T} \sum_{j=1}^{N-1} \left[(\mu^{\alpha_j} - \mu^{\alpha_N}) \rho^{\alpha_j} \delta_{kl} + \left(t_{kl}^{\alpha_j} - \frac{\rho^{\alpha_j}}{\rho^{\alpha_N}} t_{kl}^{\alpha_N} \right) - \rho^{\alpha_j} (A^{\alpha_j} - A^{\alpha_N}) \delta_{kl} \right] u_{k,l}^{\alpha_j} \\
& - \frac{1}{T} \left(\varepsilon^s \rho^s \frac{\partial A_I^s}{\partial \dot{E}_{KL}^s} + \varepsilon^w \rho^w \frac{\partial A_I^w}{\partial \dot{E}_{KL}^s} \right) \ddot{E}_{KL}^s \\
& + \frac{T_l}{T^2} \sum_{\alpha} \varepsilon^{\alpha} \left\{ q_l^{\alpha} + \sum_{j=1}^N \left[-t_{kl}^{\alpha_j} u_k^{\alpha_j} + \left(A^{\alpha_j} + \frac{1}{2} u_k^{\alpha_j} u_k^{\alpha_j} \right) \rho^{\alpha_j} u_l^{\alpha_j} \right] \right\} \\
& - \frac{1}{T} \sum_{j=1}^N \left(\mu^{s_j} - \mu^{w_j} + \frac{1}{2} u_l^{s_j} u_l^{s_j} - \frac{1}{2} u_l^{w_j} u_l^{w_j} - \frac{1}{2} v_l^{w,s} v_l^{w,s} \right)^w \hat{e}^{s_j} \\
& - \frac{1}{T} \sum_{\alpha} \sum_{j=1}^N \left(\mu^{\alpha_j} - A_l^{\alpha} + \frac{1}{2} u_l^{\alpha_j} u_l^{\alpha_j} \right) \hat{r}^{\alpha_j} \\
& - \frac{1}{T} \left[-\mathbf{P}^w \varepsilon^w_{,k} + \varepsilon^w \rho^w \left(\frac{\partial A_I^w}{\partial E_{KL}^s} E_{KL,k}^s + \frac{\partial A_I^w}{\partial \dot{E}_{KL}^s} \dot{E}_{KL,k}^s \right) + \right. \\
& \quad \left. \varepsilon^w \rho^w \left(\frac{\partial A_I^w}{\partial T} + \eta^w \right) T_{,k} + {}^s \hat{T}_k^w \right] v_k^{w,s} \\
& + \frac{1}{T} \sum_{\alpha} \sum_{j=1}^{N-1} \left\{ (\mu^{\alpha_j} - \mu^{\alpha_N}) \left(\varepsilon^{\alpha} \rho^{\alpha_j} \right)_{,k} - \left[\varepsilon^{\alpha} \rho^{\alpha_j} (A^{\alpha_j} - A^{\alpha_N}) \right]_{,k} - \right. \\
& \quad \left. \varepsilon^{\alpha} t_{kl}^{\alpha_N} \left(\frac{\rho^{\alpha_j}}{\rho^{\alpha_N}} \right)_{,l} - \left({}^{\beta} \hat{T}_k^{\alpha_j} + \hat{i}_k^{\alpha_j} \right) + \frac{\rho^{\alpha_j}}{\rho^{\alpha_N}} \left({}^{\beta} \hat{T}_k^{\alpha_N} + \hat{i}_k^{\alpha_N} \right) \right\} u_k^{\alpha_j} \geq 0. \tag{2.19}
\end{aligned}$$

where the terms t_{kl}^{se} and t_{kl}^{sh} are the Terzaghi and hydration stresses, respectively:

$$t_{kl}^{se} = \rho^s \frac{\partial A_I^s}{\partial E_{KL}^s} x_{k,K}^s x_{l,L}^s \tag{2.20}$$

$$t_{kl}^{sh} = \rho^w \frac{\partial A_l^w}{\partial E_{KL}^s} x_{k,K}^s x_{l,L}^s \quad (2.21)$$

The Terzaghi stress, t_{kl}^{se} is the elastic component of stress in the medium and t_{kl}^{sh} results from physico-chemical forces between the solid and solvent [8]. If the solid phase had been assumed to be elastic, the terms in the 3rd row of the entropy inequality (2.19), would have been grouped as a coefficient of d_{kl}^s . However, since we are modeling the solid phase as viscoelastic, d_{kl}^s was converted to the independent variable \dot{E}_{KL}^s using the equation:

$$d_{kl}^s = \dot{E}_{KL}^s X_{K,k}^s X_{L,l}^s \quad (2.22)$$

3. General Non-Equilibrium Relations

In the entropy inequality (2.19) the variables \dot{T} , $u_{k,l}^{s_j}$ and \ddot{E}_{KL}^s are neither dependent nor independent. These variables can vary arbitrarily. Therefore, to satisfy the entropy inequality for all processes, the coefficients of these variables must be zero. This leads to the following non-equilibrium equations:

$$\sum_{\alpha} \varepsilon^{\alpha} \rho^{\alpha} \left(\frac{\partial A_l^{\alpha}}{\partial T} + \eta^{\alpha} \right) = 0 \quad (3.1)$$

$$\varepsilon^s \rho^s \frac{\partial A_l^s}{\partial \dot{E}_{KL}^s} + \varepsilon^w \rho^w \frac{\partial A_l^w}{\partial \dot{E}_{KL}^s} = 0 \quad (3.2)$$

$$t_{kl}^{s_j} - \frac{\rho^{s_j}}{\rho^{s_N}} t_{kl}^{s_N} = \rho^{s_j} \left(A^{s_j} - A^{s_N} - \mu^{s_j} + \mu^{s_N} \right) \delta_{kl} \quad (3.3)$$

Equation (3.1) implies that the sum of terms over α is zero, but in accordance with the classical thermodynamics of one phase we are assuming the following:

$$\eta^\alpha = -\frac{\partial A_I^\alpha}{\partial T} \quad (3.4)$$

The free energy of one-phase Kelvin-Voigt solids is not a function of the rate of strain tensor because during exploitation of the entropy inequality, $\partial A_I^s / \partial \dot{E}_{KL}^s$ becomes zero [14]. However, such a conclusion cannot be made from (3.2), unless we assume that the entropy inequality holds for the solid and the liquid phase separately. But in the most general framework, this of course need not be true.

The variables for the j^{th} component in equation (3.3) depend upon the variables for the N^{th} component. Thus, (3.3) depends upon labeling of species. To remove this dependence, we sum (3.3) from $j = 1$ to N and simplify using (A.12), (A.39), (2.14) and (2.16). We obtain:

$$\frac{t_{kl}^{s_N}}{\rho^{s_N}} - A^{s_N} \delta_{kl} + \mu^{s_N} \delta_{kl} = \frac{t_{kl}^s}{\rho^s} + \frac{1}{\rho^s} \sum_{j=1}^N \rho^{s_j} u_k^{s_j} u_l^{s_j} + \frac{p^s}{\rho^s} \delta_{kl}. \quad (3.5)$$

To simplify (3.5) further we need an expression for t_{kl}^s , whose equilibrium and near-equilibrium forms will be obtained in the consecutive sections.

4. Equilibrium Restrictions

We define the thermodynamic equilibrium when the following variables become zero:

$$\dot{\varepsilon}^w, \dot{E}_{KL}^s, d_{kl}^w, u_{k,l}^{w_j}, T_j, {}^\beta \hat{e}^{\alpha_j}, v_k^{w,s}, u_k^{\alpha_j} \quad (4.1)$$

here, $j = 1$ to $N-1$ for $u_{k,l}^{w_j}$, $u_k^{\alpha_j}$ and $j = 1$ to N for ${}^\beta \hat{e}^{\alpha_j}$. The list (4.1) does not contain \hat{r}^{α_j} because it requires the equations of chemical reactions, which we have not incorporated. At equilibrium the entropy reaches its maximum value and the net generation of entropy, Λ , attains a minima. Thus, $\partial \Lambda / \partial x = 0$ and $\partial^2 \Lambda / \partial x \partial y \geq 0$. Where x and y are the variables in list (4.1). We obtain the following results:

$$\mathbf{P}^s = \mathbf{P}^w \quad (4.2)$$

$$t_{kl}^s = -p^s \delta_{kl} + t_{kl}^{se} + \frac{\varepsilon^w}{\varepsilon^s} t_{kl}^{sh} \quad (4.3)$$

$$t_{kl}^w = -p^w \delta_{kl} \quad (4.4)$$

$$\left(\mu^{w_j} - \mu^{w_N}\right) \rho^{w_j} \delta_{kl} + \left(t_{kl}^{w_j} - \frac{\rho^{w_j}}{\rho^{w_N}} t_{kl}^{w_N}\right) - \rho^{w_j} \left(A^{w_j} - A^{w_N}\right) \delta_{kl} = 0 \quad (4.5)$$

$$\sum_{\alpha} \varepsilon^{\alpha} q_l^{\alpha} = 0 \quad (4.6)$$

$$\mu^{s_j} = \mu^{w_j} \quad (4.7)$$

$${}^s \hat{T}_k^w = \mathbf{P}^w \varepsilon_{,k}^w - \varepsilon^w \rho^w \left(\frac{\partial A_I^w}{\partial E_{KL}^s} E_{KL,k}^s + \frac{\partial A_I^w}{\partial \dot{E}_{KL}^s} \dot{E}_{KL,k}^s \right) \quad (4.8)$$

$$\begin{aligned} {}^{\beta} \hat{T}_k^{\alpha_j} + \hat{i}_k^{\alpha_j} - \frac{\rho^{\alpha_j}}{\rho^{\alpha_N}} \left({}^{\beta} \hat{T}_k^{\alpha_N} + \hat{i}_k^{\alpha_N} \right) &= \left(\mu^{\alpha_j} - \mu^{\alpha_N} \right) \left(\varepsilon^{\alpha} \rho^{\alpha_j} \right)_{,k} - \\ &\left[\varepsilon^{\alpha} \rho^{\alpha_j} \left(A^{\alpha_j} - A^{\alpha_N} \right) \right]_{,k} - \varepsilon^{\alpha} t_{kl}^{\alpha_N} \left(\frac{\rho^{\alpha_j}}{\rho^{\alpha_N}} \right)_{,l} \end{aligned} \quad (4.9)$$

where $j = 1$ to $N-1$ in (4.5) and (4.9). To obtain an expression for μ^{s_j} at equilibrium, substitute t_{kl}^s from (4.3) in (3.5). This yields:

$$\frac{t_{kl}^{s_N}}{\rho^{s_N}} - A^{s_N} \delta_{kl} + \mu^{s_N} \delta_{kl} = \frac{t_{kl}^{se}}{\rho^s} + \frac{\varepsilon^w}{\varepsilon^s \rho^s} t_{kl}^{sh} \quad (4.10)$$

Substituting (4.10) into (3.3) to eliminate the N^{th} constituent variables and rearranging yields the following equation for μ^{s_j} at equilibrium:

$$\mu^{s_j} \delta_{kl} = A^{s_j} \delta_{kl} - \frac{t_{kl}^{s_j}}{\rho^{s_j}} + \frac{t_{kl}^{se}}{\rho^s} + \frac{\varepsilon^w}{\varepsilon^s \rho^s} t_{kl}^{sh} \quad (4.11)$$

To remove the N component dependence from (4.5), sum (4.5) from $j = 1$ to N and substitute the expression for t_{kl}^w from (4.4) into the result. We get:

$$\frac{t_{kl}^{w_N}}{\rho^{w_N}} - A^{w_N} \delta_{kl} + \mu^{w_N} \delta_{kl} = 0 \quad (4.12)$$

which, upon substitution in (4.5), results in the following expression for μ^{w_j} at equilibrium:

$$\mu^{w_j} \delta_{kl} = A^{w_j} \delta_{kl} - \frac{t_{kl}^{w_j}}{\rho^{w_j}}. \quad (4.13)$$

This equation states that at equilibrium the shear components of $t_{kl}^{w_j}$ are zero. This is expected because comparison of this equation to (4.4) shows that at equilibrium the stress in the liquid phase arises only due to the thermodynamic pressure.

To remove the N component dependence from (4.9), sum (4.9) from $j = 1$ to N . Using (2.16), we obtain:

$$\begin{aligned} {}^\beta \hat{T}_k^\alpha - \frac{\rho^\alpha}{\rho^{\alpha_N}} \left({}^\beta \hat{T}_k^{\alpha_N} + \hat{i}_k^{\alpha_N} \right) &= \sum_{j=1}^N \rho^\alpha \frac{\partial A_l^\alpha}{\partial \rho^{\alpha_j}} \left(\varepsilon^\alpha \rho^{\alpha_j} \right)_{,k} - \mu^{\alpha_N} \left(\varepsilon^\alpha \rho^\alpha \right)_{,k} - \\ &\quad A_{l,k}^\alpha \varepsilon^\alpha \rho^\alpha + \left(\varepsilon^\alpha \rho^\alpha A^{\alpha_N} \right)_{,k} - \varepsilon^\alpha t_{kl}^{\alpha_N} \left(\frac{\rho^\alpha}{\rho^{\alpha_N}} \right)_{,j} \end{aligned} \quad (4.14)$$

Here we used $\sum_{j=1}^N {}^\beta \hat{T}_k^{\alpha_j} = {}^\beta \hat{T}_k^\alpha$ and $\sum_{j=1}^N \hat{i}_k^{\alpha_j} = 0$, since at equilibrium $u_l^{\alpha_j} = 0$. Let us take

$\beta = s$ and $\alpha = w$. Based upon (2.4) the term $A_{l,k}^w$ can be computed as:

$$\begin{aligned} A_{l,k}^w &= \frac{\partial A_l^w}{\partial \varepsilon^w} \varepsilon^w_{,k} + \sum_{j=1}^N \frac{\partial A_l^w}{\partial (\varepsilon^w \rho^{w_j})} (\varepsilon^w \rho^{w_j})_{,k} + \frac{\partial A_l^w}{\partial T} T_{,k} + \\ &\quad \frac{\partial A_l^w}{\partial E_{KL}^s} E_{KL,k}^s + \frac{\partial A_l^w}{\partial \dot{E}_{KL}^s} \dot{E}_{KL,k}^s \end{aligned} \quad (4.15)$$

Substituting ${}^s \hat{T}_k^w$ from (4.8) and $A_{l,k}^w$ from (4.15) in (4.14) and simplifying we obtain:

$$\frac{\rho^w}{\rho^{w_N}} \left({}^s \hat{T}_k^{w_N} + \hat{i}_k^{w_N} \right) - \mu^{w_N} \left(\varepsilon^w \rho^w \right)_{,k} + \left(\varepsilon^w \rho^w A^{w_N} \right)_{,k} - \varepsilon^w t_{kl}^{w_N} \left(\frac{\rho^w}{\rho^{w_N}} \right)_{,l} = 0 \quad (4.16)$$

Finally, by substituting (4.16) in (4.9), we obtain the following expression for ${}^s \hat{T}_k^{w_j} + \hat{i}_k^{w_j}$ at equilibrium:

$${}^s \hat{T}_k^{w_j} + \hat{i}_k^{w_j} = \mu^{w_j} \left(\varepsilon^w \rho^{w_j} \right)_{,k} - \left(\varepsilon^w \rho^{w_j} A^{w_j} \right)_{,k} . \quad (4.17)$$

where (4.17) holds for $j = 1$ to N .

5. Near-Equilibrium Relations

In the entropy inequality (2.19), the coefficients of variables becoming zero at equilibrium [list 4.1)] are functions of these variables. For example, the coefficient of T_j is a function of all variables in the list (4.1). To satisfy the inequality, these coefficients are linearized to form positive quadratic terms. Linearization is performed by Taylor series expansion around the variables becoming zero at equilibrium and truncating the second and higher order terms. Because of truncation, the results hold only near-equilibrium. Taylor series expansion of each coefficient can be performed around one or more variables vanishing at equilibrium. For example, let z_1 and z_2 be two variables becoming zero at equilibrium. Let $f(z_1, z_2)$ be the coefficient of z_1 in entropy inequality. Linearization of f around z_1 yields the following expression:

$$f_{\text{neq}} = f_{\text{eq}} + C_1(z_2)z_1 \quad (5.1)$$

Where C_1 is a function of z_2 . Linearization of f around z_1 and z_2 leads to:

$$f_{\text{neq}} = f_{\text{eq}} + C_1 z_1 + C_2 z_2 \quad (5.2)$$

In this expression C_1 and C_2 are not functions of z_1 and z_2 . Equation (5.1) gives fewer terms in the linearized equations but the form of the coefficient must be evaluated as a function of z_2 . The choice of whether to linearize around one or more than one variable leads to different results which have advantages and disadvantages. Linearizing around two variables as in (5.2) yields linear forms for both variables, but introduces a linear truncation error related to the second variable. Experimentally, constant coefficients are preferred as they are easier to evaluate than functions.

Technically, each term in the entropy inequality involving variables given in (4.1) can be linearized about each of the variables in (4.1). However, this yields unwieldy expressions. Therefore, we perform one term Taylor series expansions of the coefficients of all variables in the list (4.1) except for the coefficients T_s, \dot{E}_{KL}^s and d_{kl}^w , where we perform a two-term expansion. To obtain thermoviscoelastic and thermoviscous effects we perform a two-term linearization around T_s and \dot{E}_{KL}^s for the solid phase; and T_s and d_{kl}^w for the liquid phase. The resulting linearization coefficients are a function of the remaining independent variables $(\dot{E}_{KL}^s, d_{kl}^w, u_{k,l}^{ws}, T_s, v_k^{ws}, u_k^{\alpha_s})$ listed in (4.1).

Let us elucidate another important issue related to linearization before presenting the results. Consider a variable V vanishing at equilibrium and appearing in the entropy inequality as follows:

$$(A+B+C)V \geq 0 \quad (5.3)$$

Here, the variables A , B and C are functions of V . Suppose, we are interested in the near-equilibrium form for the variable A . Linearization can be performed in the following two ways:
First,

$$A_{\text{neq}} = A_{\text{eq}} + A_D \quad (5.4)$$

$$A_{\text{eq}} = -(B+C) \quad (5.5)$$

$$A_D = \mu V \quad (5.6)$$

Here, A_D is called the dissipative part of the variable A . A_D is zero at equilibrium and non-zero near-equilibrium. The coefficient μ resulted during linearization. By substituting (5.5) and (5.6) in (5.4), we get:

$$A_{\text{neq}} = -(B+C)_{\text{eq}} + \mu V. \quad (5.7)$$

An alternative method of obtaining near-equilibrium relations for A is:

$$(A+B+C)_{\text{neq}} = (A+B+C)_{\text{eq}} + (A+B+C)_D, \quad (5.8)$$

$$(A+B+C)_{\text{eq}} = 0 \quad (5.9)$$

$$(A+B+C)_D = \mu V \quad (5.10)$$

By substituting (5.9) and (5.10) in (5.8) we obtain:

$$A_{\text{neq}} = -(B+C)_{\text{neq}} + \mu V. \quad (5.11)$$

The relation (5.11) is more general than the relation (5.7), unless $(B+C)_{\text{eq}}$ is equal to the $(B+C)_{\text{neq}}$. Often in the continuum mechanics literature the forms (5.7) and (5.11) are used without clarifying the underlying reasons. We suggest that whenever possible, form (5.11) be used initially and later the simplifications be made using physical arguments. In the following discussion we will obtain results based on (5.11) except when removing the N -component dependence from variables. In the latter case it is easy to perform manipulations by using form (5.7). By linearizing around $\dot{\varepsilon}^w$ we obtain the following equation:

$$P^w - P^s = M \dot{\varepsilon}^w \quad (5.12)$$

where M is a scalar coefficient. Equation (5.12) implies that the rate of swelling, $\dot{\varepsilon}^w$ of the polymeric system is directly proportional to the difference in classical pressure between the solid and the liquid phases. Equation (5.12) is similar to Thomas and Windle's [31] equation 8.

For t_{kl}^s forms (5.7) and (5.11) yield similar results. We will linearize t_{kl}^s and the heat flux about T_J and \dot{E}_{KL}^s . Let,

$$_{neq} \left(\sum_{j=1}^N t_{kl}^{sj} \right) = _{eq} \left(\sum_{j=1}^N t_{kl}^{sj} \right) + _D \left(\sum_{j=1}^N t_{kl}^{sj} \right) \quad (5.13)$$

where, the equilibrium part is given by (4.3). Thus,

$$_{neq} \left(\sum_{j=1}^N t_{kl}^{sj} \right) = -p^s \delta_{kl} + t_{kl}^{se} + \frac{\varepsilon^w}{\varepsilon^s} t_{kl}^{sh} + _D \left(\sum_{j=1}^N t_{kl}^{sj} \right) \quad (5.14)$$

Let us denote the solid phase coefficient of T_J by Q_l^s :

$$Q_l^s \equiv q_l^s + \sum_{j=1}^N \left[-t_{kl}^{sj} u_k^{sj} + \left(A^{sj} + \frac{1}{2} u_k^{sj} u_k^{sj} \right) \rho^{sj} u_l^{sj} \right] \quad (5.15)$$

Substituting (5.14) and (5.15) into the T_J and \dot{E}_{KL}^s terms of the entropy inequality, (2.19) we get:

$$\frac{\varepsilon^s}{T} _D \left(\sum_{j=1}^N t_{kl}^{sj} \right) X_{K,k}^s X_{L,l}^s \dot{E}_{KL}^s + \frac{\varepsilon^s}{T^2} Q_l^s T_J \geq 0 \quad (5.16)$$

By linearizing we obtain:

$$_D \left(\sum_{j=1}^N t_{kl}^{sj} \right) = G_{KLMN}^s \dot{E}_{MN}^s x_{k,K}^s x_{l,L}^s + H_{klm}^s T_m \quad (5.17)$$

$$Q_l^s = K_{kl}^s T_k + J_{klm}^s x_{l,K}^s \dot{E}_{LM}^s \quad (5.18)$$

here, the coefficients G_{KLMN}^s , H_{klm}^s , K_{kl}^s and J_{klm}^s are not functions of \dot{E}_{KL}^s and T_J . G_{KLMN}^s is a fourth order positive semi-definite tensor responsible for stress dissipation due to relaxation

processes within the solid polymers. H_{klm}^s and J_{KLM}^s are third order tensors. The H_{klm}^s term causes thermal gradients to affect the stress field inside an anisotropic solid phase. Because of the J_{KLM}^s term, the heat flux arises inside an anisotropic solid phase due to the strain rate. Given that the third order tensors are zero under full orthogonal group of transformations, H_{klm}^s and J_{KLM}^s would vanish for the isotropic solids [30]. Due to symmetry of the stress tensor and the strain rate, the third and fourth-order coefficients satisfy the following symmetry relationships:

$$\begin{aligned} G_{KLMN}^s &= G_{LKNM}^s = G_{KLNM}^s \\ H_{klm}^s &= H_{lkm}^s \\ J_{KLM}^s &= J_{KML}^s \end{aligned} \quad (5.19)$$

By substituting (5.17) in (5.14) and (5.18) in (5.15), we obtain the following near equilibrium equations:

$$t_{kl}^s = -p^s \delta_{kl} + t_{kl}^{se} + \frac{\varepsilon^w}{\varepsilon^s} t_{kl}^{sh} - \sum_{j=1}^N \rho^{sj} u_k^{sj} u_l^{sj} + G_{KLMN}^s \dot{E}_{MN}^s x_{k,K}^s x_{l,L}^s + H_{klm}^s T_{,m}. \quad (5.20)$$

$$q_l^s = \sum_{j=1}^N \left[t_{kl}^{sj} u_k^{sj} - \left(A^{sj} + \frac{1}{2} u_k^{sj} u_k^{sj} \right) \rho^{sj} u_l^{sj} \right] + K_{kl}^s T_{,k} + J_{KLM}^s x_{l,K}^s \dot{E}_{LM}^s. \quad (5.21)$$

Similarly, we can linearize about d_{kl}^w and $T_{,l}$ to obtain the following near-equilibrium equations

for t_{kl}^w and q_l^w :

$$t_{kl}^w = -p^w \delta_{kl} + v_{klmn}^w d_{mn}^w + H_{klm}^w T_{,m} - \sum_{j=1}^N \rho^{wj} u_k^{wj} u_l^{wj}. \quad (5.22)$$

$$q_l^w = \sum_{j=1}^N \left[t_{kl}^{wj} u_k^{wj} - \left(A^{wj} + \frac{1}{2} u_k^{wj} u_k^{wj} \right) \rho^{wj} u_l^{wj} \right] + K_{kl}^w T_{,k} + G_{lmn}^w d_{mn}^w. \quad (5.23)$$

Here, v_{klmn}^w is a fourth order, positive semi-definite viscous dissipation tensor. Similar to the solid phase, the third order tensors, H_{klm}^w and G_{lmn}^w introduce the cross-effects of the temperature

gradient on the stress tensor, and the rate of deformation on the heat flux. For an isotropic fluid phase H_{klm}^w and G_{lmn}^w disappear. Due to symmetry of the stress tensor and the rate of deformation tensor, the v_{klmn}^w , H_{klm}^w and G_{lmn}^w satisfy the following symmetry relationships:

$$\begin{aligned} v_{klmn}^w &= v_{lkmn}^w = v_{klnm}^w \\ H_{klm}^w &= H_{lkm}^w \\ G_{lmn}^w &= G_{lnm}^w \end{aligned} \quad (5.24)$$

Substituting t_{kl}^s from (5.20) in (3.5) and further substituting the resulting N-component terms in (3.3), we obtain the following equation for μ^{s_j} near equilibrium:

$$\mu^{s_j} \delta_{kl} = A^{s_j} \delta_{kl} - \frac{t_{kl}^{s_j}}{\rho^{s_j}} + \frac{1}{\rho^s} \left(t_{kl}^{se} + \frac{\varepsilon^w}{\varepsilon^s} t_{kl}^{sh} + G_{KLMN}^s \dot{E}_{MN}^s x_{k,K}^s x_{l,L}^s + H_{klm}^s T_{,m} \right). \quad (5.25)$$

In the solid-phase chemical potential equation (5.25), the term $G_{KLMN}^s \dot{E}_{MN}^s x_{k,K}^s x_{l,L}^s$ has not been reported in previous colloidal-media studies. This implies that the solid-phase chemical potential of the polymeric systems is a function of the strain rate.

Performing single-variable linearization about ${}^w \hat{e}^{s_j}$, $u_{k,l}^{w_j}$, $v_k^{w,s}$ and $u_k^{w_j}$, we obtain the following near-equilibrium equations:

$$\mu^{s_j} - \mu^{w_j} = \kappa^{j,s} \hat{e}^{w_j} - \frac{1}{2} u_l^{s_j} u_l^{s_j} + \frac{1}{2} u_l^{w_j} u_l^{w_j} + \frac{1}{2} v_l^{w,s} v_l^{w,s} \quad (5.26)$$

$$\mu^{w_j} \delta_{kl} = C_{klmn}^{w_j} u_{m,n}^{w_j} + A^{w_j} \delta_{kl} - \frac{t_{kl}^{w_j}}{\rho^{w_j}} \quad (5.27)$$

$${}^s \hat{T}_k^w = -R_{kl} v_l^{w,s} + P^w \varepsilon_{,k}^w - \varepsilon^w \rho^w \left[\frac{\partial A_I^w}{\partial E_{KL}^s} E_{KL,I}^s + \frac{\partial A_I^w}{\partial \dot{E}_{KL}^s} \dot{E}_{KL,I}^s + \left(\eta^w + \frac{\partial A_I^w}{\partial T} \right) T_{,k} \right] \quad (5.28)$$

$${}^s \hat{T}_k^{w_j} + \hat{i}_k^{w_j} = -R_{kl}^j u_l^{w_j} + \mu^{w_j} \left(\varepsilon^w \rho^{w_j} \right)_{,k} - \left(\varepsilon^w \rho^{w_j} A^{w_j} \right)_{,k}. \quad (5.29)$$

The coefficients κ^j , $C_{klmn}^{w_j}$, R_{kl} and R_{kl}^j are the linearization coefficients of these equations. In (5.28) the term in round brackets will vanish due to (3.4). We did not linearize about $u_k^{s_j}$ because in our system solid-phase diffusion was assumed negligible so that $u_k^{s_j}$ was not an independent variable. Hence, the coefficient of $u_k^{s_j}$ cannot be a function of $u_k^{s_j}$.

Total Stress and Heat Flux

The total particle stress tensor and the particle thermodynamic pressure are obtained by summing over the solid and the liquid phase. These are defined as [8]:

$$t_{kl} = \varepsilon^s t_{kl}^s + \varepsilon^w t_{kl}^w \quad (5.30)$$

$$p = \varepsilon^s p^s + \varepsilon^w p^w \quad (5.31)$$

Substituting (5.20) and (5.22) in (5.30) and using (5.31), we obtain:

$$\begin{aligned} t_{kl} = -p\delta_{kl} + \varepsilon^s & \left(t_{kl}^{se} + \frac{\varepsilon^w}{\varepsilon^s} t_{kl}^{sh} + G_{KLMN}^s \dot{E}_{MN}^s x_{k,K}^s x_{l,L}^s + H_{klm}^s T_{,m} \right) + \\ & \varepsilon^w \left(v_{klmn}^w d_{mn}^w + H_{klm}^w T_{,m} \right). \end{aligned} \quad (5.32)$$

Here, the second order term $\sum_{j=1}^N \rho^{\alpha_j} u_k^{\alpha_j} u_k^{\alpha_j}$ was neglected because the diffusion velocities are of small magnitude. In the total stress tensor equation (5.32), the $G_{KLMN}^s \dot{E}_{MN}^s x_{k,K}^s x_{l,L}^s$ term accounts for the relaxation processes within the solid polymeric matrix. In the previous porous media studies [19,18,1,26,3,4,28], this term could not be obtained due to the assumption of an elastic solid phase.

The total heat flux of a particle can be taken as [5]:

$$q_l = \varepsilon^s q_l^s + \varepsilon^w q_l^w \quad (5.33)$$

Substituting (5.21) and (5.23) in (5.33) to eliminate q_l^s and q_l^w we obtain:

$$\begin{aligned} q_l = \sum_{\alpha} \sum_{j=1}^N \varepsilon^{\alpha} \left[t_{kl}^{\alpha_j} u_k^{\alpha_j} - \left(A^{\alpha_j} + \frac{1}{2} u_k^{\alpha_j} u_k^{\alpha_j} \right) \rho^{\alpha_j} u_l^{\alpha_j} \right] + (\varepsilon^s K_{kl}^s + \varepsilon^w K_{kl}^w) T_{,k} + \\ \varepsilon^s J_{KLM}^s x_{l,K}^s \dot{E}_{LM}^s + \varepsilon^w G_{lmn}^w d_{mn}^w. \end{aligned} \quad (5.34)$$

Given that diffusion velocities are small, the third order term in $u_l^{\alpha_j}$ can be neglected.

Isotropic Stress and Heat Flux

If the solid and liquid phases have isotropic properties, the third order tensors disappear. The second and fourth-order coefficients follow these relations [30]:

$$\begin{aligned} K_{kl}^{\alpha} &= K^{\alpha} \delta_{kl}, \quad \alpha = s, w \\ G_{KLMN}^s &= \lambda^s \delta_{KL} \delta_{MN} + \mu^s (\delta_{KM} \delta_{LN} + \delta_{KN} \delta_{LM}) \\ v_{klmn}^w &= \lambda^w \delta_{kl} \delta_{mn} + \mu^w (\delta_{km} \delta_{ln} + \delta_{kn} \delta_{lm}) \end{aligned} \quad (5.35)$$

Substituting (5.35) in (5.32) and (5.34), and simplify to obtain the following equations for the total stress:

$$\begin{aligned} t_{kl} = -p \delta_{kl} + \varepsilon^s \left(t_{kl}^{se} + \frac{\varepsilon^w}{\varepsilon^s} t_{kl}^{sh} + \lambda^s \dot{E}_{MM}^s c_{kl}^{s^{-1}} + 2\mu^s \dot{E}_{KL}^s x_{k,K}^s x_{l,L}^s \right) + \\ \varepsilon^w (\lambda^w \delta_{kl} d_{mm}^w + 2\mu^w d_{kl}^w), \end{aligned} \quad (5.36)$$

$$c_{kl}^{s^{-1}} \equiv x_{k,K}^s x_{l,K}^s. \quad (5.37)$$

here, $c_{kl}^{s^{-1}}$ is the Finger deformation tensor for the solid phase, and the heat flux:

$$q_l = \sum_{\alpha} \sum_{j=1}^N \varepsilon^{\alpha} \left[t_{kl}^{\alpha_j} u_k^{\alpha_j} - \left(A^{\alpha_j} + \frac{1}{2} u_k^{\alpha_j} u_k^{\alpha_j} \right) \rho^{\alpha_j} u_l^{\alpha_j} \right] + (\varepsilon^s K^s + \varepsilon^w K^w) \delta_{kl} T_{,k}. \quad (5.38)$$

Note that the coefficients G_{KLMN}^s , H_{klm}^s , v_{klmn}^w , H_{klm}^w , λ^s , μ^s , λ^w and μ^w are not functions of the local thermal gradients because a two-variable Taylor series expansion was performed. The remaining terms in the stress tensor equations (5.32) and (5.36) depend upon A_I^α , which is a function of temperature but not of temperature gradient. Based upon these equations the stress field inside an anisotropic polymeric system is a function of the local thermal gradients. But inside an isotropic polymeric system it depends upon temperature only. This simplifies experiments because the anisotropic systems require measurement of material coefficients as a function of local temperature only. In isotropic solids both material coefficients and stress field require only temperature dependent measurements. In the previous porous media studies the material coefficients required determination as a function of the temperature as well as temperature gradient at different spatial locations because one variable Taylor-series expansions were performed. Similarly, in our heat flux equation, the material coefficients are not functions of the strain rate. The strain rate affects heat flux of the anisotropic system only (5.34), but not of the isotropic system (5.38). Similar deductions could be made using one-scale thermoviscoelasticity theory presented in reference [14].

Generalized Darcy's Law

Substituting \hat{T}_k^w from (5.28) and t_{kl}^w from (5.22) in the momentum balance equation (A.11) and neglecting the inertia and the second order terms in $u_l^{w,j}$, we get:

$$\begin{aligned} R_{kl}v_l^{w,s} = & -\left(\varepsilon^w p^w\right)_{,k} + \left(\varepsilon^w v_{klmn}^w d_{mn}^w\right)_{,l} + \left(\varepsilon^w H_{klm}^w T_{,m}\right)_{,l} + \varepsilon^w \rho^w g_k^w + \\ & P^w \varepsilon^w_{,k} - \varepsilon^w \rho^w \left(\frac{\partial A_I^w}{\partial E_{KL}^s} E_{KL,k}^s + \frac{\partial A_I^w}{\partial \dot{E}_{KL}^s} \dot{E}_{KL,k}^s \right). \end{aligned} \quad (5.39)$$

The thermal gradient term and the last term in (5.39) are new. We will explain this further in a subsequent discussion.

Generalized Fick's Law

Substitute $\hat{T}_k^{w_j} + \hat{i}_k^{w_j}$ from (5.29) and $i_{kl}^{w_j}$ from (5.27) in the momentum balance equation for species (A.10) and neglecting the inertia term to get:

$$R_{kl}^j u_l^{w_j} = -\varepsilon^w \rho^{w_j} \mu_{,k}^{w_j} + \varepsilon^w \rho^{w_j} g_k^{w_j} + \left(\varepsilon^w \rho^{w_j} C_{klmn}^{w_j} u_{m,n}^{w_j} \right)_{,l}. \quad (5.40)$$

This form of Fick's law is similar to that obtained for the colloidal systems in previous studies [8]. The last term in (5.40) is often neglected in literature as it is of second order.

Swelling Pressure

Bennethum [6] has derived a relation between classical pressure, thermodynamic pressure and swelling pressure. This relation can be obtained from a comparison of our choice of independent variables with the alternate choice [1], where A_I^w was considered to be a function of $\varepsilon^w, \rho^w, C^{w_j}$. For simplicity, let us write free energies only as a function of the variables required for this derivation:

$$A_I^w = A_I^w(\varepsilon^w, \varepsilon^w \rho^{w_j}), \quad \bar{A}_I^w = \bar{A}_I^w(\varepsilon^w, \rho^w, C^{w_j}) \quad (5.41)$$

where \bar{A}_I^w is the free energy in the alternative formulation. Now,

$$dA_I^w = \frac{\partial A_I^w}{\partial \varepsilon^w} \Bigg|_{\varepsilon^w, \rho^{w_j}} d\varepsilon^w + \sum_{j=1}^N \frac{\partial A_I^w}{\partial \rho^{w_j}} \Bigg|_{\varepsilon^w} d\rho^{w_j} + \sum_{j=1}^N \frac{\rho^{w_j}}{\varepsilon^w} \frac{\partial A_I^w}{\partial \rho^{w_j}} \Bigg|_{\varepsilon^w} d\varepsilon^w \quad (5.42)$$

$$d\bar{A}_I^w = \frac{\partial \bar{A}_I^w}{\partial \varepsilon^w} \Bigg|_{\rho^w, C^{w_j}} d\varepsilon^w + \frac{\partial \bar{A}_I^w}{\partial \rho^w} \Bigg|_{\varepsilon^w, C^{w_j}} d\rho^w + \sum_{j=1}^N \frac{\partial \bar{A}_I^w}{\partial C^{w_j}} \Bigg|_{\varepsilon^w, \rho^w} dC^{w_j} \quad (5.43)$$

Compare the coefficients of $d\varepsilon^w$:

$$\frac{\partial \bar{A}_I^w}{\partial \varepsilon^w} \Bigg|_{\rho^w, C^w} = \frac{\partial A_I^w}{\partial \varepsilon^w} \Bigg|_{\varepsilon^w, \rho^w} + \sum_{j=1}^N \frac{\rho^w_j}{\varepsilon^w} \frac{\partial A_I^w}{\partial \rho^w_j} \Bigg|_{\varepsilon^w} \quad (5.44)$$

Multiply throughout by $\varepsilon^w \rho^w$:

$$\varepsilon^w \rho^w \frac{\partial \bar{A}_I^w}{\partial \varepsilon^w} \Bigg|_{\rho^w, C^w} = \varepsilon^w \rho^w \frac{\partial A_I^w}{\partial \varepsilon^w} \Bigg|_{\varepsilon^w, \rho^w} + \sum_{j=1}^N \rho^w_j \rho^w \frac{\partial A_I^w}{\partial \rho^w_j} \Bigg|_{\varepsilon^w} \quad (5.45)$$

The terms on the right hand side can be identified as $-P^w$ and p^w using (2.13) and (2.15), respectively. The term on the left hand side is the swelling pressure obtained in the alternative formulation [1]. Thus, the expression for the swelling pressure is:

$$\bar{\pi}^w \equiv -\varepsilon^w \rho^w \frac{\partial \bar{A}_I^w}{\partial \varepsilon^w} \Bigg|_{\rho^w, C^w} \quad (5.46)$$

where, the over-bar is used to signify that the swelling pressure definition requires the use of free energy, \bar{A}_I^w , in the alternative formulation. The swelling pressure is measured by keeping the density and mass composition fixed and changing the volume fraction of the liquid by for example letting the liquid enter or exit the system. The (5.45) becomes:

$$-\bar{\pi}^w = -P^w + p^w \quad (5.47)$$

$$\text{or, } p^w(\varepsilon^w, \underline{\varepsilon^w} \rho^w_j) = P^w(\varepsilon^w, \underline{\varepsilon^w} \rho^w_j) - \bar{\pi}^w(\varepsilon^w, \underline{\rho^w}). \quad (5.48)$$

where the underlined terms are held constant when evaluating the pressures, but the pressures themselves may vary with these variables.

Recalling that the stress tensors represent the physical stress on the system through the momentum equations, and examining the relationship between the stress tensors and the thermodynamic pressures [equations (5.20) and (5.22)] we may conclude that the thermodynamic pressure is related to the physical pressures of the system when there are negligible shear deformations, temperature gradients and fluid flow. Thus, (5.48) states that the

thermodynamic pressure of each phase is composed of the classical pressure and the swelling pressure. See [6] for further discussion.

Low's Swelling Pressure Relation

Low [22,24] conducted extensive experiments on swelling clays and obtained the following relation for the swelling pressure, P_{ap} at equilibrium:

$$P_{ap} = A \exp(B/\delta^w) \quad (5.49)$$

where, A and B are the empirical constants. Achanta et al. [1] obtained the first non-heuristic derivation of this relation using the framework of HMT. Here we will derive this relation using equations obtained in previous sections after making simplifying assumptions. Consider the experiment depicted in Fig. 2, where pure water is in contact with the swelling colloids via a semi-permeable membrane under isothermal conditions. The semi-permeable membrane allows water to pass towards the colloids but prevents the passage of colloids towards water. Piston pressure, P_{ap} , is applied over the porous matrix to balance the swelling pressure. The colloids have a highly layered structure, with solid platlets parallel to each other. Multiplying the equilibrium equation (4.13) by ρ^w and summing the result from $j = 1$ to N , we obtain:

$$\sum_{j=1}^N \mu^{wj} \rho^{wj} \delta_{kj} = A_I^w \rho^w \delta_{kj} - t_k^w. \quad (5.50)$$

Substitute the expression for t_k^w from (4.4) to (5.50), and divide the both sides of (5.50) by ρ^w to obtain the equation for Gibbs free energy:

$$G^w \equiv \sum_{j=1}^N \mu^{wj} C^{wj} = A_I^w + \frac{p^w}{\rho^w} \quad (5.51)$$

Taking the differential of this equation in the alternative formulation, we get:

$$\begin{aligned}
D\bar{G}^w &= \frac{\partial \bar{A}_I^w}{\partial \varepsilon^w} \Big|_{\rho^w} d\varepsilon^w + \frac{\partial \bar{A}_I^w}{\partial \rho^w} \Big|_{\varepsilon^w} d\rho^w + \frac{1}{\rho^w} \left[\frac{\partial p^w}{\partial \varepsilon^w} \Big|_{\rho^w} d\varepsilon^w + \frac{\partial p^w}{\partial \rho^w} \Big|_{\varepsilon^w} d\rho^w \right] - \frac{p^w}{\rho^{w^2}} d\rho^w \\
&= \left[\frac{\partial \bar{A}_I^w}{\partial \varepsilon^w} \Big|_{\rho^w} + \frac{1}{\rho^w} \frac{\partial p^w}{\partial \varepsilon^w} \Big|_{\rho^w} \right] d\varepsilon^w + \left[\frac{\partial \bar{A}_I^w}{\partial \rho^w} \Big|_{\varepsilon^w} + \frac{1}{\rho^w} \frac{\partial p^w}{\partial \rho^w} \Big|_{\varepsilon^w} - \frac{p^w}{\rho^{w^2}} \right] d\rho^w
\end{aligned} \tag{5.52}$$

since, the definition of thermodynamic pressure, p^w , remains the same in both formulations, we did not use an over-bar with its representation in (5.52). The chemical potential of the water is maintained constant, because the lowered chemical potential due to hydration forces is compensated by the increase in applied pressure, P_{ap} . Thus, $D\bar{G}^w = 0$. This makes the bracketed terms in the second line of (5.52) equal to zero. Multiplying the first bracketed term in the second line of (5.52) with $\varepsilon^w \rho^w$ and using (5.46) we get:

$$\bar{\pi}^w = \varepsilon^w \frac{\partial p^w}{\partial \varepsilon^w} \Big|_{\rho^w} \tag{5.53}$$

As shown in Appendix B, at low and moderate moisture contents the pressure, P^w , is small in comparison to the swelling pressure, $\bar{\pi}^w$. Therefore, we neglect P^w in (5.48) to obtain:

$$p^w = -\bar{\pi}^w. \tag{5.54}$$

In layered clayey soils, due to balance of forces between the applied pressure and the thermodynamic pressure of solid and liquid phases we have:

$$P_{ap} = p^w = p^s. \tag{5.55}$$

Using (5.53), (5.54) and (5.55) we get:

$$P_{ap} = -\varepsilon^w \frac{\partial P_{ap}}{\partial \varepsilon^w} \Big|_{\rho^w} \tag{5.56}$$

For parallel layers of clay platlets the ε^w can be written as:

$$\varepsilon^w = \frac{\delta^w}{\delta^w + \delta^s} \quad (5.57)$$

and,

$$\frac{d\varepsilon^w}{\varepsilon^w} = \frac{d\delta^w}{\frac{\delta^{w^2}}{\delta^s} + \delta^w} \quad (5.58)$$

Here it should be noted that δ^s is an effective thickness since in general some packets of clay layers remain unexpanded. Assuming that $\delta^s \ll \delta^w$, (5.58) reduces to:

$$\frac{d\varepsilon^w}{\varepsilon^w} = \frac{\delta^s}{\delta^{w^2}} d\delta^w \quad (5.59)$$

Substituting (5.59) in (5.56) and integrating, we get:

$$P_{ap} = A \exp(\delta^s / \delta^w) \quad (5.60)$$

which is similar to the swelling pressure eqn.

Viscoelastic Effects in the Generalized Darcy's Law

Let us replace π^w in the generalized Darcy's law (5.39) by (5.48):

$$\begin{aligned} R_{kl} v_l^{w,s} &= - \left[\varepsilon^w (P^w - \bar{\pi}^w) \right]_k + P^w \varepsilon^w,_k + \text{Remaining Terms} \\ &= (\varepsilon^w \bar{\pi}^w)_{,k} - \varepsilon^w P^w,_k + \text{R.Ts} \end{aligned} \quad (5.61)$$

Substituting the expression for P^w from (5.12) in (5.61),

$$\begin{aligned} R_{kl} v_l^{w,s} &= (\varepsilon^w \bar{\pi}^w)_{,k} - \varepsilon^w P^s,_k - \varepsilon^w (M \dot{\varepsilon}^w)_{,k} + \text{R.Ts} \\ &= \varepsilon^w,_k \bar{\pi}^w + \varepsilon^w (\bar{\pi}^w - P^s)_{,k} - \varepsilon^w (M \dot{\varepsilon}^w)_{,k} + \text{R.Ts} \end{aligned} \quad (5.62)$$

The, P^s is small [see (2.13) and (5.46)] in comparison to the $\bar{\pi}^w$ (See Appendix B). Thus, we drop the P^s term in (5.62) to get:

$$R_{kl}v_l^{w,s} = (\varepsilon^w \bar{\pi}^w)_{,k} - \varepsilon^w (M \dot{\varepsilon}^w)_{,k} + (\varepsilon^w v_{klmn}^w d_{mn}^w)_{,l} + (\varepsilon^w H_{klm}^w T_{,m})_{,l} + \varepsilon^w \rho^w g_k^w - \varepsilon^w \rho^w \left(\frac{\partial A_l^w}{\partial E_{KL}^s} E_{KL,k}^s + \frac{\partial A_l^w}{\partial \dot{E}_{KL}^s} \dot{E}_{KL,k}^s \right). \quad (5.63)$$

On the right hand side of this equation the first two terms resemble the Darcy's law equation (7) obtained by Achanta et al. [2]. These account for the interaction of the solid polymer matrix with the fluid phase, which leads to time dependent swelling. The third term is called Brinkman's correction in the porous media literature. It accounts for the viscous resistance to the flow of liquid in the fluid boundary layer formed on the surface of the solid. In high velocity flows, this term will have significant magnitude, but it is often neglected at low moisture contents. The fourth term is novel. It results in flow due to thermal gradients for anisotropic fluids. For isotropic fluids this term will vanish. In the earlier porous media studies, the coefficient v_{klmn}^w was a function of T_l . Thus, the thermal gradient effect was neglected when the rate of deformation term was dropped. For anisotropic fluids of low thermal conductivity, the thermal gradient term could be significant in magnitude even when flow velocities are small. In the second line of (5.63) the first term in brackets has been reported by [27,7]. At low moisture contents when a few layers of fluid are present, the free energy of the fluid phase is a function of the shear strain in the solid phase. Then this term is of significant magnitude. At high moisture contents, the solid phase alters the liquid free energy only through normal components of the strain tensor and this term reduces to the swelling pressure [27]. The last term in (5.63) is nonlinear in \dot{E}_{KL}^s . It has not been reported before. In the previous studies, this term did not arise because an elastic solid phase does not depend upon the rate of strain. This term results from interaction of the viscoelastic solid phase with the liquid phase. More insight can be obtained by comparing this term to $\varepsilon^w (M \dot{\varepsilon}^w)_{,k}$ and $(\partial A_l^w / \partial E_{KL}^s) E_{KL,k}^s$. It appears that the rate of strain in the

polymeric matrix would affect the free energy of the liquid phase, which would add a component to the flow of liquid. This term is also related to $\partial A_l^s / \partial \dot{E}_{KL}^s$ by (3.2). It warrants additional investigation.

6. Conclusions

We developed a two-scale theory of swelling viscoelastic systems. At the mesoscale, the solid phase was modeled as a Kelvin-Voigt solid and the liquid phase was assumed viscous. Thus, we accounted for the relaxation processes within the solid matrix, which have been ignored in the previous porous media studies. At the mesoscale, the viscoelastic nature of our system resulted from two microscale effects – the relaxation of the solid and the interaction of the solid phase with the viscous fluid. We obtained novel equations for the total stress tensor (5.32), chemical potential of the solid phase (5.25), heat flux (5.34) and generalized Darcy's law (5.39), which are applicable to a large class of materials. The form of the generalized Fick's law (5.40) remained similar to that obtained in previous colloidal media studies. With two-variable Taylor series expansions, the thermal gradient effects were coupled with the rate of strain tensor of the solid phase and the rate of deformation tensor of the liquid phase. This made material parameters of the equations involving stress tensor and heat flux independent of the thermal gradient effects, and thus their experimental determination becomes easier in comparison to the parameters obtained in the previous porous media studies. Additionally, two-variable linearization helps make clear distinctions between the stress tensor, heat flux and Darcy's law equations for anisotropic and isotropic systems.

7. Appendix A. Mesoscale Field Equations

Here we consider mesoscale balance laws for a vicinal fluid solvating (or partially solvating) the solid. These equations were obtained by averaging the microscale laws. Details of the averaging procedure are laid out in references [18,3,13].

Mass Balance

The mesoscale mass balance equation for the j^{th} species in the phase α is:

$$\frac{D^{\alpha_j}(\varepsilon^\alpha \rho^{\alpha_j})}{Dt} + \varepsilon^\alpha \rho^{\alpha_j} v_{l,j}^{\alpha_j} = \sum_{\beta \neq \alpha} {}^\beta \hat{e}^{\alpha_j} + \hat{r}^{\alpha_j} \quad (\text{A.1})$$

Unlike classical mass balance equation of one scale, the quantities on the right hand side are not zero. In multi-scale equations such quantities appear at a higher scale during the averaging procedure. These act as a source or sink term. The ε^α multiplying with ρ^{α_j} also emerged during averaging. Similar quantities appear in the laws of conservation of momentum, energy and entropy.

Summing this equation over N components, gives the mass balance equation for phase α :

$$\frac{D^\alpha(\varepsilon^\alpha \rho^\alpha)}{Dt} + \varepsilon^\alpha \rho^\alpha v_{l,I}^\alpha = \sum_{\beta \neq \alpha} {}^\beta \hat{e}^\alpha, \quad (\text{A.2})$$

where, the phase variables are related to the species variables by:

$$\rho^\alpha = \sum_{j=1}^N \rho^{\alpha_j} \quad (\text{A.3})$$

$$v_l^\alpha = \sum_{j=1}^N C^{\alpha_j} v_l^{\alpha_j} \quad (\text{A.4})$$

$$C^{\alpha_j} = \frac{\rho^{\alpha_j}}{\rho^\alpha} \quad (\text{A.5})$$

$$\beta \hat{e}^\alpha = \sum_{j=1}^N \beta \hat{e}^{\alpha_j} \quad (\text{A.6})$$

The following restrictions apply:

$$\sum_\alpha \varepsilon^\alpha = 1 \quad (\text{A.7})$$

$$\sum_{j=1}^N \hat{r}^{\alpha_j} = 0, \quad \forall \alpha \quad (\text{A.8})$$

$$\beta \hat{e}^{\alpha_j} + \alpha \hat{e}^{\beta_j} = 0, \quad \alpha \neq \beta, \quad \forall j. \quad (\text{A.9})$$

The restriction (A.7) implies that the sum of volume fraction of phases in an REV is equal to one. The restriction (A.8) ensures that during chemical reactions, the mass lost by one component is gained by the other. The equation (A.9) ensures that the mass exchanged between the two phases remains conserved.

Momentum Balance

The mesoscale momentum balance equation for the j^{th} species in phase α :

$$\varepsilon^\alpha \rho^{\alpha_j} \frac{D^{\alpha_j} v_l^{\alpha_j}}{Dt} - (\varepsilon^\alpha t_{lk}^{\alpha_j})_{,k} - \varepsilon^\alpha \rho^{\alpha_j} g_l^{\alpha_j} = \sum_{\beta \neq \alpha} \beta \hat{T}_l^{\alpha_j} + \hat{i}_l^{\alpha_j} \quad (\text{A.10})$$

Summing this equation over the N components, we obtain the momentum balance equation for phase α :

$$\varepsilon^\alpha \rho^\alpha \frac{D^\alpha v_l^\alpha}{Dt} - (\varepsilon^\alpha t_{lk}^\alpha)_{,k} - \varepsilon^\alpha \rho^\alpha g_l^\alpha = \sum_{\beta \neq \alpha} \beta \hat{T}_l^\alpha, \quad (\text{A.11})$$

The relations between the phase and the species variables are:

$$t_{lk}^\alpha = \sum_{j=1}^N (t_{lk}^{\alpha_j} - \rho^{\alpha_j} u_l^{\alpha_j} u_k^{\alpha_j}) \quad (\text{A.12})$$

$$u_l^{\alpha_j} = v_l^{\alpha_j} - v_l^\alpha \quad (\text{A.13})$$

$$g_l^\alpha = \sum_{j=1}^N C^{\alpha_j} g_l^{\alpha_j} \quad (\text{A.14})$$

$${}^\beta \hat{T}_l^\alpha = \sum_{j=1}^N \left({}^\beta \hat{T}_l^{\alpha_j} + {}^\beta \hat{e}^{\alpha_j} u_l^{\alpha_j} \right) \quad (\text{A.15})$$

The following restrictions apply to the momentum balance equations:

$$\sum_{j=1}^N \left(\hat{i}_l^{\alpha_j} + \hat{r}^{\alpha_j} u_l^{\alpha_j} \right) = 0, \quad \forall \alpha \quad (\text{A.16})$$

$${}^\beta \hat{T}_l^{\alpha_j} + {}^\beta \hat{e}^{\alpha_j} v_l^{\alpha_j} + {}^\alpha \hat{T}_l^{\beta_j} + {}^\alpha \hat{e}^{\beta_j} v_l^{\beta_j} = 0, \quad \alpha \neq \beta, \quad \forall j. \quad (\text{A.17})$$

Energy Balance

The energy balance law for the j^{th} species in the phase α is:

$$\varepsilon^\alpha \rho^{\alpha_j} \frac{D^{\alpha_j} E^{\alpha_j}}{Dt} - \varepsilon^\alpha t_{kl}^{\alpha_j} v_{l,k}^{\alpha_j} - (\varepsilon^\alpha q_l^{\alpha_j})_l - \varepsilon^\alpha \rho^{\alpha_j} h^{\alpha_j} = \sum_{\beta \neq \alpha} {}^\beta \hat{Q}^{\alpha_j} + \hat{E}^{\alpha_j} \quad (\text{A.18})$$

Summing this equation over the N components:

$$\varepsilon^\alpha \rho^\alpha \frac{D^\alpha E^\alpha}{Dt} - \varepsilon^\alpha t_{kl}^\alpha v_{l,k}^\alpha - (\varepsilon^\alpha q_l^\alpha)_l - \varepsilon^\alpha \rho^\alpha h^\alpha = \sum_{\beta \neq \alpha} {}^\beta \hat{Q}^\alpha \quad (\text{A.19})$$

The relations between the phase and the species variables are:

$$E^\alpha = \sum_{j=1}^N C^{\alpha_j} (E^{\alpha_j} + \frac{1}{2} u_l^{\alpha_j} u_l^{\alpha_j}) \quad (\text{A.20})$$

$$q_l^\alpha = \sum_{j=1}^N \left[q_l^{\alpha_j} + t_{kl}^{\alpha_j} u_k^{\alpha_j} - \rho^{\alpha_j} (E^{\alpha_j} + \frac{1}{2} u_k^{\alpha_j} u_k^{\alpha_j}) u_l^{\alpha_j} \right] \quad (\text{A.21})$$

$$\rho^\alpha h^\alpha = \sum_{j=1}^N \rho^{\alpha_j} (h^{\alpha_j} + g_l^{\alpha_j} u_l^{\alpha_j}) \quad (\text{A.22})$$

$${}^\beta \hat{Q}^\alpha = \sum_{j=1}^N \left[{}^\beta \hat{Q}^{\alpha_j} + {}^\beta \hat{T}_l^{\alpha_j} u_l^{\alpha_j} + {}^\beta \hat{e}^{\alpha_j} (E^{\alpha_j, \alpha} + \frac{1}{2} u_l^{\alpha_j} u_l^{\alpha_j}) \right] \quad (\text{A.23})$$

The following restrictions apply to the energy balance equations:

$$\sum_{j=1}^N \left[\hat{E}^{\alpha_j} + \hat{i}_l^{\alpha_j} u_l^{\alpha_j} + \hat{r}^{\alpha_j} (E^{\alpha_j} + \frac{1}{2} u_l^{\alpha_j} u_l^{\alpha_j}) \right] = 0, \quad \forall \alpha \quad (\text{A.24})$$

$$\begin{aligned} {}^\beta \hat{Q}^{\alpha_j} + {}^\beta \hat{T}_l^{\alpha_j} v_l^{\alpha_j} + {}^\beta \hat{e}^{\alpha_j} (E^{\alpha_j} + \frac{1}{2} v_l^{\alpha_j} v_l^{\alpha_j}) + {}^\alpha \hat{Q}^{\beta_j} + {}^\alpha \hat{T}_l^{\beta_j} v_l^{\beta_j} \\ + {}^\alpha \hat{e}^{\beta_j} (E^{\beta_j} + \frac{1}{2} v_l^{\beta_j} v_l^{\beta_j}) = 0, \quad \alpha \neq \beta, \quad \forall j. \end{aligned} \quad (\text{A.25})$$

Entropy

The second law of thermodynamics requires that the evolution of processes must proceed in such away that the net internal entropy gained by the system increases. We begin by expressing an entropy balance law for each constituent of each phase:

$$\varepsilon^\alpha \rho^{\alpha_j} \frac{D^{\alpha_j} \eta^{\alpha_j}}{Dt} - (\varepsilon^\alpha \phi_l^{\alpha_j})_j - \varepsilon^\alpha \rho^{\alpha_j} b^{\alpha_j} = \sum_{\beta \neq \alpha} {}^\beta \hat{\phi}^{\alpha_j} + \hat{\eta}^{\alpha_j} + \Lambda^{\alpha_j} \quad (\text{A.26})$$

Summing the entropy balance equation over the N species:

$$\varepsilon^\alpha \rho^\alpha \frac{D^\alpha \eta^\alpha}{Dt} - (\varepsilon^\alpha \phi_l^\alpha)_j - \varepsilon^\alpha \rho^\alpha b^\alpha = \sum_{\beta \neq \alpha} {}^\beta \hat{\phi}^\alpha + \Lambda^\alpha, \quad (\text{A.27})$$

The relations between the phase and the species variables are:

$$\eta^\alpha = \sum_{j=1}^N \eta^{\alpha_j} \quad (\text{A.28})$$

$$\phi_l^\alpha = \sum_{j=1}^N (\phi_l^{\alpha_j} - \rho^{\alpha_j} u_l^{\alpha_j} \eta^{\alpha_j}) \quad (\text{A.29})$$

$$b^\alpha = \sum_{j=1}^N C^{\alpha_j} b^{\alpha_j} \quad (\text{A.30})$$

$${}^\beta \hat{\phi}^\alpha = \sum_{j=1}^N ({}^\beta \hat{\phi}^{\alpha_j} + {}^\beta \hat{e}^{\alpha_j} \eta^{\alpha_j, \alpha}) \quad (\text{A.31})$$

$$\Lambda^\alpha = \sum_{j=1}^N \Lambda^{\alpha_j} \quad (\text{A.32})$$

Restrictions on the entropy balance equations are:

$$\sum_{j=1}^N (\hat{r}^{\alpha_j} \eta^{\alpha_j} + \hat{\eta}^{\alpha_j}) = 0, \quad \forall \alpha \quad (\text{A.33})$$

$${}^\beta \hat{\phi}^{\alpha_j} + {}^\beta \hat{e}^{\alpha_j} \eta^{\alpha_j} + {}^\alpha \hat{\phi}^{\beta_j} + {}^\alpha \hat{e}^{\beta_j} \eta^{\beta_j} = 0, \quad \alpha \neq \beta, \quad \forall j. \quad (\text{A.34})$$

We assume that the system is at local thermal equilibrium, which causes different phases to have the same local temperature. The temperature is allowed vary spatially

$$T^{\alpha_j} = T^{\beta_j} = T. \quad (\text{A.35})$$

We also assume that the sources of entropy are solely due to heat flux and the body source of heat

$$\phi_i^{\alpha_j} = \frac{q_i^{\alpha_j}}{T} \quad (\text{A.36})$$

$$b^{\alpha_j} = \frac{h^{\alpha_j}}{T}. \quad (\text{A.37})$$

A thermodynamic process satisfying (A.36) and (A.37) is called a simple thermomechanical process. In the energy balance equation (A.18) the internal energy E^{α_j} is a function of the entropy, η^{α_j} . Since entropy can not be directly measured from experiments, a Legendre transformation is performed on E^{α_j} to convert it into the Helmholtz free energy, A^{α_j} , which is a function of temperature

$$A^{\alpha_j} = E^{\alpha_j} - T\eta^{\alpha_j} \quad (\text{A.38})$$

Summing A^{α_j} over the N components, we obtain the inner part of the total Helmoltz free energy:

$$A_I^\alpha = \sum_{j=1}^N C^{\alpha_j} A^{\alpha_j}. \quad (\text{A.39})$$

Entropy Inequality

All independent processes taking place inside a body must satisfy the axioms of mechanical and thermodynamic admissibility (see Eringen [14]). Equations of conservation of mass, momentum and energy ensure that the processes are mechanically admissible. To be thermodynamically admissible, the processes must satisfy the second law of thermodynamics. This is imposed using entropy inequality, which states that the net rate of entropy generation in the universe is always greater than or equal to zero.

$$\Lambda = \sum_{\alpha} \Lambda^{\alpha} = \sum_{\alpha} \sum_{j=1}^N \Lambda^{\alpha_j} \geq 0 \quad (\text{A.40})$$

Eliminating h^{α_j} between equations of energy and entropy balance and simplifying, we obtain:

$$\begin{aligned} \Lambda = \sum_{\alpha} \Lambda^{\alpha} = & - \sum_{\alpha} \frac{\varepsilon^{\alpha} \rho^{\alpha}}{T} \left(\frac{D^{\alpha} A_l^{\alpha}}{Dt} + \eta^{\alpha} \frac{D^{\alpha} T}{Dt} \right) \\ & + \sum_{\alpha} \frac{\varepsilon^{\alpha}}{T} \left(\sum_{j=1}^N t_{kl}^{\alpha_j} \right) d_{kl}^{\alpha} \\ & + \sum_{\alpha} \frac{\varepsilon^{\alpha}}{T} \sum_{j=1}^N \left(t_{kl}^{\alpha_j} - \rho^{\alpha_j} A^{\alpha_j} \delta_{kl} \right) u_{k,l}^{\alpha_j} \\ & + \sum_{\alpha} \frac{\varepsilon^{\alpha} T_l}{T^2} \left\{ q_l^{\alpha} + \sum_{j=1}^N \left[-t_{kl}^{\alpha_j} u_k^{\alpha_j} + \left(A^{\alpha_j} + \frac{1}{2} u_k^{\alpha_j} u_k^{\alpha_j} \right) \rho^{\alpha_j} u_l^{\alpha_j} \right] \right\} \\ & - \frac{1}{T} \sum_{\alpha} \sum_{j=1}^N \left[(\varepsilon^{\alpha} \rho^{\alpha_j} A^{\alpha_j})_l + \sum_{\beta \neq \alpha} \beta \hat{T}_l^{\alpha_j} + \hat{i}_l^{\alpha_j} \right] u_l^{\alpha_j} \\ & - \frac{1}{2T} \sum_{\alpha} \sum_{j=1}^N u_l^{\alpha_j} u_l^{\alpha_j} \left[\sum_{\beta \neq \alpha} \beta \hat{e}^{\alpha_j} + \hat{r}^{\alpha_j} \right] \\ & - \frac{1}{T} \sum_{\alpha} \sum_{\beta \neq \alpha} \beta \hat{T}_l^{\alpha} v_l^{\alpha,s} \\ & - \frac{1}{T} \sum_{\alpha} \sum_{\beta \neq \alpha} \beta \hat{e}^{\alpha} \left[A_l^{\alpha} + \frac{1}{2} v_l^{\alpha,s} v_l^{\alpha,s} \right] \geq 0. \end{aligned} \quad (\text{A.41})$$

8. Appendix B

In this section we prove that the magnitude of $\bar{\pi}^w$ is significantly greater than the magnitudes of P^w and P^s except at high moisture contents ($\varepsilon^w \sim 1$). First we convert $\bar{\pi}^w$ [eq. (5.46)] and P^w [eq. (2.13)] to extensive variables.

$$P^w = -\frac{\partial(\varepsilon^w \rho^w A_I^w)}{\partial \varepsilon^w} \Bigg|_{\varepsilon^w, \rho^w, T} = -\frac{\partial \left(\frac{V^w M^w}{V} \frac{A^w}{V^w} A_I^w \right)}{\partial \left(\frac{V^w}{V} \right)} \Bigg|_{\varepsilon^w, \rho^w, T} = -\frac{\partial \left(\frac{A^w}{V} \right)}{\partial \left(\frac{V^w}{V} \right)} \Bigg|_{\frac{M^w}{V}, T}. \quad (\text{B.1})$$

$$\bar{\pi}^w = -\varepsilon^w \rho^w \frac{\partial \bar{A}_I^w}{\partial \varepsilon^w} \Bigg|_{\rho^w, T} = -\varepsilon^w \frac{\partial(\rho^w \bar{A}_I^w)}{\partial \varepsilon^w} \Bigg|_{\rho^w, T} = -\varepsilon^w \frac{\partial \left(\frac{\bar{A}^w}{V^w} \right)}{\partial \left(\frac{V^w}{V} \right)} \Bigg|_{\rho^w, T}. \quad (\text{B.2})$$

Here, V is not the REV. REV is the averaging volume, which is held constant over time and space. Once the intensive variables like density have been upscaled from micro to mesoscale using REV, the total mass and free energy can be computed inside volume, V , of size different than REV. We take V , which increases proportionately with the whole body.

In (B.1), the ratio M^w/V is maintained constant and in (B.2) ρ^w is maintained constant during swelling or shrinkage. Let us expand the differentials in the numerator and denominator of (B.1) and (B.2):

$$P^w = -\frac{\frac{\partial A^w}{V} - \frac{A^w}{V^2} \partial V}{\frac{\partial V^w}{V} - \frac{V^w}{V^2} \partial V} \Bigg|_{\frac{M^w}{V}, T} = -\frac{V \partial A^w - A^w \partial V}{V \partial V^w - V^w \partial V} \Bigg|_{\frac{M^w}{V}, T}. \quad (\text{B.3})$$

$$\bar{\pi}^w = - \frac{\frac{\partial \bar{A}^w}{V} - \frac{\bar{A}^w}{VV^w} \partial V^w}{\frac{\partial V^w}{V} - \frac{V^w}{V^2} \partial V} \Bigg|_{\rho^w, T} = - \frac{V \partial \bar{A}^w - \frac{\bar{A}^w}{\varepsilon^w} \partial V^w}{V \partial V^w - V^w \partial V} \Bigg|_{\rho^w, T}. \quad (\text{B.4})$$

With assumption that the solid phase is incompressible at the mesoscale, the total volume increase will only be due change in the volume of fluid phase:

$$\partial V = \partial V^w \quad (\text{B.5})$$

Substitute (B.5) in (B.3) and (B.4), to get:

$$P^w = - \frac{V \partial A^w - A^w \partial V}{(V - V^w) \partial V} \Bigg|_{\frac{M^w}{V}, T} = - \frac{V \partial A^w - A^w \partial V}{V^s \partial V} \Bigg|_{\frac{M^w}{V}, T}. \quad (\text{B.6})$$

$$\bar{\pi}^w = - \frac{V \partial \bar{A}^w - \frac{\bar{A}^w}{\varepsilon^w} \partial V}{(V - V^w) \partial V} \Bigg|_{\rho^w, T} = - \frac{V \partial \bar{A}^w - \frac{\bar{A}^w}{\varepsilon^w} \partial V}{V^s \partial V} \Bigg|_{\rho^w, T}. \quad (\text{B.7})$$

Comparison of (B.6) and (B.7) shows that at low moisture contents ($\varepsilon^w < 1$) $\bar{\pi}^w$ will be greater than P^w . With increase in moisture content as ε^w approaches 1, $\bar{\pi}^w$ will asymptotically approach P^w . As $P^s = P^w$ at equilibrium [eq. (4.2)], $\bar{\pi}^w$ will also be greater than P^s when $\varepsilon^w < 1$.

9. Appendix C. Nomenclature

Latin Symbols

A^{α_j}	Helmholtz free energy of the j^{th} component in the α phase
A^α	Total Helmholtz free energy of the α phase computed in volume V ($= A_I^\alpha M^\alpha$)
A_I^α	Inner part of the Helmholtz free energy of the α phase
b^{α_j}	External entropy source for the j^{th} component in the α phase
b^α	External entropy source for the α phase
$c_{kl}^{s^{-1}}$	Finger deformation tensor of the solid phase
C^{α_j}	Mass concentration of the j^{th} component in the α phase ($= \rho^{\alpha_j} / \rho^\alpha$)
$C_{klmn}^{w_j}$	Material coefficient in equation (5.27)
d_{kl}^α	Rate of deformation tensor of the α phase
${}^\beta\hat{e}^{\alpha_j}$	Net mass transfer from the phase β to the j^{th} component in the α phase
${}^\beta\hat{e}^\alpha$	Net mass transfer from the phase β to the phase α
E^{α_j}	Internal energy of the j^{th} component in the α phase
E^α	Internal energy of the α phase
\hat{E}^{α_j}	Energy gained by the j^{th} component from other components in the same phase
E_{KL}^s	Lagrangian strain tensor of the solid phase
\dot{E}_{KL}^s	Material derivative of the E_{KL}^s with respect to the solid phase velocity
\ddot{E}_{KL}^s	Material derivative of the \dot{E}_{KL}^s with respect to the solid phase velocity
$g_l^{\alpha_j}$	Gravitational force on the j^{th} component in the α phase

g_i^α Gravitational force on the α phase

G^w Gibbs free energy

G_{lmn}^w Material coefficient in equation (5.23)

G_{KLMN}^s Material coefficient in equation (5.17)

h^{a_j} Net external energy source for the j^{th} component in the α phase

h^α Net external energy source for the α phase

h_{klm}^s Material coefficient in equation (5.20)

h_{klm}^w Material coefficient in equation (5.22)

$\hat{i}_l^{\alpha_j}$ Momentum transfer to the j^{th} component due to interaction with other components in the same phase

J_{KLM}^s Material coefficient in equation (5.21)

K_{kl}^s Thermal conductivity tensor of the solid phase

K_{kl}^w Thermal conductivity tensor of the liquid phase

K^α Isotropic thermal conductivity of the phase α

M^{a_j} Total mass of j^{th} component in the α phase contained in V ($= \rho^{a_j} V^\alpha$)

M^α Total mass of the α phase contained in V ($= \rho^\alpha V^\alpha$)

p^α Thermodynamic pressure in the α phase

p Total thermodynamic pressure for the particle (solid+liquid)

P^α Classical pressure of the α phase

P_{ap} Piston pressure applied in swelling experiment. See Fig. 2.

P_∞	Atmospheric or reference pressure
$q_l^{\alpha_j}$	Heat flux vector for the j^{th} component in the α phase
q_l^α	Heat flux vector for the α phase
q_l	Total heat flux vector for the particle (solid+liquid)
${}^\beta \hat{Q}^{\alpha_j}$	Net heat gained by the j^{th} component in the phase α from the phase β
${}^\beta \hat{Q}^\alpha$	Net heat gained by the phase α from the phase β
\hat{r}^{α_j}	Mass transfer to the j^{th} component due to interaction with other components in the same phase
R_{kl}^j	Material coefficient in equation (5.29)
R_{kl}	Material coefficient in equation (5.28)
REV	Representative elementary volume
t	Time
$t_{kl}^{\alpha_j}$	Stress tensor of the j^{th} component in the phase α
t_{kl}^α	Stress tensor of the phase α
t_{kl}	Total stress tensor of the particle (solid+liquid)
t_{kl}^{se}	Terzaghi stress
t_{kl}^{sh}	Hydration stress
T^{α_j}	Temperature of the j^{th} component in the phase α
T	Temperature
${}^\beta \hat{T}_l^{\alpha_j}$	Momentum transfer to the j^{th} component in the phase α due to mechanical interactions with the phase β

\hat{T}_l^α	Momentum transfer to the phase α due to mechanical interactions with the phase β
$u_k^{\alpha_j}$	Diffusion velocity of the j^{th} component in the phase α
$v_l^{\alpha_j}$	Velocity of the j^{th} component in the phase α
v_l^α	Velocity of the α phase
V^α	Volume of the α phase contained in V
V	Sample volume used to compute total free energy and total mass
x_k^α	Eulerian coordinate in the phase α
X_k^α	Lagrangian coordinate in the phase α

Greek Symbols

δ_{kl}	Kronecker delta function in Eulerian coordinates
δ_{KL}	Kronecker delta function in Lagrangian coordinates
ε^α	Volume fraction of the phase α
η^{α_j}	Entropy of the j^{th} component in the α phase
η^α	Entropy of the α phase
$\hat{\eta}^{\alpha_j}$	Entropy gained by the j^{th} component in a phase by interaction with other components in the same phase
δ^w	Thickness of the water layer between solid platlets. See Fig. 2.
δ^s	Thickness of solid platlets. See Fig. 2.
κ^j	Material coefficient in equation (5.26)
λ^s, λ^w	Isotropic material coefficients. See equation (5.35)
Λ^{α_j}	Net entropy production for the j^{th} component in the α phase

Λ^α	Net entropy production in the α phase
Λ	Net entropy production in the system at mesoscale
μ_j^α	Chemical potential of the j^{th} component in the α phase
ρ_j^α	Density of the j^{th} component in the α phase
ρ^α	Density of the α phase
$\bar{\pi}^\alpha$	Swelling pressure of the α phase
ϕ_l^α	Entropy flux vector for the j^{th} component in the α phase
ϕ_l^α	Entropy flux vector for the α phase
$\beta \hat{\phi}^\alpha$	Entropy transfer to the j^{th} component in the α phase from the β phase
$\beta \hat{\phi}^\alpha$	Entropy transfer to the α phase from the β phase
v_{klmn}^w	Material coefficient in equation (5.22)

Subscripts

D	Dissipative
eq	Equilibrium
neq	Near equilibrium
k, l	Coordinate indices

Superscripts

s	solid phase
w	water (or liquid) phase
α, β	General representation of phases
j	A given component of species

Special Symbols

$\frac{D^{\alpha_j}}{Dt}$ Material derivative of a function with respect to velocity of j^{th} component in the α phase

$\frac{D^\alpha}{Dt}$ Material derivative of a function with respect to velocity of the α phase

$v_i^{\alpha,s}$ Velocity of the α phase relative to the solid phase ($= v_i^\alpha - v_i^s$)

$$E^{\alpha_j, \alpha} = E^{\alpha_j} - E^\alpha$$

References

1. Achanta, S., Cushman, J. H. and Okos, M. R.: 1994, On multicomponent, multiphase thermomechanics with interfaces, *Int. J. Engng Sci.* **32**(11), 1717-1738.
2. Achanta, S., Okos, M. R., Cushman, J. H. and Kessler, D. P.: 1997, Moisture transport in shrinking gels during saturated drying, *A.I.Ch.E.J.* **43**(8), 2112-2122.
3. Bennethum, L. S. and Cushman, J. H.: 1996, Multiscale, hybrid mixture theory for swelling systems .1. Balance laws, *Int. J. Engng Sci.* **34**(2), 125-145.
4. Bennethum, L. S. and Cushman, J. H.: 1996, Multiscale, hybrid mixture theory for swelling systems .2. Constitutive theory, *Int. J. Engng Sci.* **34**(2), 147-169.
5. Bennethum, L. S. and Cushman, J. H.: 1999, Coupled solvent and heat transport of a mixture of swelling porous particles and fluids: Single time-scale problem, *Transp. Porous Media* **36**(2), 211-244.
6. Bennethum, L. S. and Cushman, J. H.: 2001, Three pressures in swelling porous media, *Submitted to: Transp. Porous Media*.
7. Bennethum, L. S. and Giorgi, T.: 1997, Generalized Forchheimer equation for two-phase flow based on hybrid mixture theory, *Transp. Porous Media* **26**(3), 261-275.
8. Bennethum, L. S., Murad, M. A. and Cushman, J. H.: 1997, Modified Darcy's law, Terzaghi's effective stress principle and Fick's law for swelling clay soils, *Comput. Geotech.* **20**(3-4), 245-266.
9. Bennethum, L. S., Murad, M. A. and Cushman, J. H.: 2000, Macroscale thermodynamics and the chemical potential for swelling porous media, *Transp. Porous Media* **39**(2), 187-225.
10. Bowen, R. M., Ed. 1971, *Theory of mixtures*, In: Continuum physics Vol. 3., New

York,, Academic Press, 2-127.

11. Bowen, R. M.: 1982, Compressible Porous-Media Models by Use of the Theory of Mixtures, *Int. J. Engng Sci.* **20**(6), 697-735.

12. Coleman, B. D. and Noll, W.: 1963, The thermodynamics of elastic materials with heat conduction and viscosity., *Arch. Rat. Mech. Anal.* **13**, 167-178.

13. Cushman, J. H.: 1997, *The physics of fluids in hierarchical porous media : angstroms to miles*, Dordrecht ; Boston, Kluwer Academic Publishers.

14. Eringen, A. C.: 1980, *Mechanics of continua*, Huntington, N.Y., R. E. Krieger Pub. Co.

15. Etzler, F. M. and Conners, J. J.: 1991, Structural Transitions in Vicinal Water - Pore-Size and Temperature-Dependence of Heat-Capacity of Water in Small Pores, *Langmuir* **7**(10), 2293-2297.

16. Etzler, F. M. and Conners, J. J.: 1991, The Structure and Properties of Vicinal Water - Recent Advances, *Abstr. Pap. Am. Chem. Soc.* **201**, 246-COLL.

17. Ferry, J. D.: 1980, *Viscoelastic properties of polymers*, New York, Wiley, pp:1-3.

18. Hassanizadeh, S. M. and Gray, W. G.: 1979, General conservation equations for multiphase systems: 1. Averaging procedure, *Adv. Wat. Resour.* **2**, 131-144.

19. Hassanizadeh, S. M. and Gray, W. G.: 1979, General conservation equations for multiphase systems: 2. Mass, Momenta, energy, and entropy equations, *Adv. Wat. Resour.* **2**, 191-208.

20. Hassanizadeh, S. M. and Gray, W. G.: 1980, General conservation equations for multiphase systems: 3. Constitutive theory for porous media flow, *Adv. Wat. Resour.* **3**, 25-40.

21. Hornung, U.: 1997, *Homogenization and porous media*, New York, Springer.
22. Low, P. F.: 1980, The Swelling of Clay .2. Montmorillonites, *Soil Sci. Soc. Am. J.* **44**(4), 667-676.
23. Low, P. F.: 1981, The Swelling of Clay .3. Dissociation of Exchangeable Cations, *Soil Sci. Soc. Am. J.* **45**(6), 1074-1078.
24. Low, P. F.: 1987, Structural Component of the Swelling Pressure of Clays, *Langmuir* **3**(1), 18-25.
25. Low, P. F. and Margheim, J. F.: 1979, Swelling of Clay .1. Basic Concepts and Empirical Equations, *Soil Sci. Soc. Am. J.* **43**(3), 473-481.
26. Murad, M. A., Bennethum, L. S. and Cushman, J. H.: 1995, A Multiscale Theory of Swelling Porous-Media .1. Application to One-Dimensional Consolidation, *Transp. Porous Media* **19**(2), 93-122.
27. Murad, M. A. and Cushman, J. H.: 1996, Multiscale flow and deformation in hydrophilic swelling porous media, *Int. J. Engng Sci.* **34**(3), 313-338.
28. Murad, M. A. and Cushman, J. H.: 1997, Multiscale theory of swelling porous media: II. Dual porosity models for consolidation of clays incorporating physicochemical effects, *Transp. Porous Media* **28**(1), 69-108.
29. Murad, M. A. and Cushman, J. H.: 2000, Thermomechanical theories for swelling porous media with microstructure, *Int. J. Engng Sci.* **38**(5), 517-564.
30. Segel, L. A. and Handelman, G. H.: 1977, *Mathematics applied to continuum mechanics*, New York, Macmillan.
31. Thomas, N. L. and Windle, A. H.: 1982, A Theory of Case-II Diffusion, *Polymer* **23**(4), 529-542.

II. Thermomechanics of swelling viscoelastic three-scale porous media with temporal nonlocality

Introduction

The swelling colloids exhibit a hierarchy of scales and often there is a distinct scale separation. Fig. 1 illustrates a three-scale (micro, meso, macro) system of interest composed of a solid-matrix and solvating fluid. The solid matrix and the vicinal fluid (fluid solvating the matrix surface) exist as separate phases on the microscale (of the order of microns). The homogeneous mixture of solid matrix and the vicinal fluid at mesoscale is represented as a particle, A, in the diagram. The particles themselves are immersed in two bulk phase fluids B and C (eg. liquid water and water vapor). At the macroscale each constituent in each phase and the phases themselves are considered as overlaying continua defined over all space. Most phenomenon exhibited at higher scales are a manifestation of interactions taking place at smaller scales. The macroscale swelling/shrinkage exhibited by these systems results from the solvation of solid by the fluid on the microscale [1].

Many methods are available for upscaling information from lower to higher scales [2, 3]. We chose to use the hybrid mixture theory (HMT) approach. HMT involves volume averaging of equations of mass, momentum, energy and entropy at the microscale to obtain equations at the mesoscale. In a three-scale approach, the mesoscale balance laws are further averaged to obtain balance laws at macroscale. At macroscale constitutive equations are formulated by exploiting the entropy inequality in the sense of Coleman and Noll [4].

HMT was introduced by Hassanizadeh and Gray [5, 6] for non-interacting granular porous media. Achanta et al. [7], Bennethum and Cushman [8, 9], Murad et al. [10], and Murad and Cushman [11-13] extended these ideas to swelling and shrinking systems with multi-

constituents where interactions between phases play an important role. However, in all previous works with HMT, the solid phase was assumed to be elastic and the liquid phase was assumed to be viscous. These studies were either aimed at swelling soil systems [8-10], or were adapted for polymeric systems from soil systems [7-9, 14, 15], for which the assumption of elastic solid phase does not really hold. The systems exhibited viscoelastic behavior only at the macroscale, which resulted from microscale interaction of the elastic solid-phase with the viscous fluid-phase. These theories ignored the microscale relaxation processes of the natural clays, which arise due to conformational changes in the flexible clay platelets [16]. These relaxation processes provide a force term, which affects liquid movement through porous matrix [17-20]. This force term plays a fundamental role when the time-scale of relaxation is the same as the time scale of the liquid transport. Incorporation of relaxation processes in the definition of the chemical potential, stress tensor and balance laws would make them sufficiently general to explain both Fickian and non-Fickian types of liquid transport, and general viscoelastic deformation.

In a previous section, we developed a two-scale theory of swelling colloidal media, which considered solid phase as a Kelvin-Voigt solid at mesoscale [21]. In this section we extend our work by incorporating the third (macro) scale, and by further generalizing the solid matrix to a generalized Kelvin-Voigt solid. This will make our work applicable to a large class of polymeric and biopolymeric media subjected to a wide range of processes.

System Description and Notation

Meso and macroscale variables are represented by Greek and capital superscripts, respectively. At microscale the variable volume fraction does not exist, because a spatial point is either in the solid or in the liquid phase. In the homogeneous mixture formed at the mesoscale,

the volume fraction of a phase is represented as ε^α . The solid and liquid components of the particle are denoted as sA and wA , respectively. At the mesoscale, the sA and wA interact with the bulk fluids B and C and the macroscale volume fraction does not exist, because a spatial point is either inside a particle, or inside one of the bulk fluids. At the macroscale the particles and the bulk fluids B and C form a homogeneous mixture. The macroscale volume fraction of a component is represented by ε^K . The fluids B and wA are of the same type and the fluid C is of different type. For example, the fluid B and wA could be considered as water and the fluid C could be considered as oil or air. For simplicity, we assume that the interface between the two phases is free from thermodynamic properties. Following the axiom of equipresence of constituents [22], we assume at the outset that each phase contains the same set of N-constituents (some may be at zero concentration). Superscript K_j represents the property of the j^{th} constituent in the K phase at macroscale. Hatted quantities, such as ${}^L\hat{e}^{K_j}$ represent property transfer from the phase L to the phase K . The hatted quantities like \hat{r}^{K_j} represent property gained by the j^{th} constituent within a phase due to chemical reactions. The complete nomenclature is presented in Appendix B. We lay out the equations in indicial notation using Eulerian coordinates. The indices k and l represent the coordinate directions and repetition of these indices implies summation. The use of capital indices such as K and L with certain quantities represents Lagrangian coordinates. The indices k , l , K and L range from 1 to 3.

Constitution

The macroscale field equations are applicable to all kinds of materials and are presented in the Appendix A. These equations are closed for specific materials by imposing restrictions on the constitutive functions through the axioms of constitution [2] and entropy inequality in the sense of Coleman and Noll [3].

At macroscale the solid phase is considered viscoelastic and the liquid phases, B and C are considered viscous. We assume that the viscoelastic solid is of generalized Kelvin-Voigt type. Thus, the constitutive variables for the solid phase depend upon the material time derivatives of the strain tensor from order zero to p . Due to its vicinity to the solid phase, the fluid wA has different thermodynamic properties than its bulk counterpart B . Following is the list of unknown variables:

$$\begin{aligned} \varepsilon^A, \dot{\varepsilon}^B, \rho^K, C^{K_J}, v_l^{K_J}, T, {}^L\hat{e}^{K_J}, \hat{r}^{K_J}, t_{kl}^{K_J}, {}^L\hat{T}_l^{K_J}, \hat{i}_l^{K_J}, A^{K_J}, q_l^{K_J}, {}^L\hat{Q}^{K_J}, \hat{E}^{K_J}, \eta^{K_J}, \hat{\eta}^{K_J} \\ j = 1..N, \quad K, L = sA, wA, B, C \text{ and } K \neq L. \end{aligned} \quad (2.1)$$

we consider only two volume fractions as unknowns because the third can be determined using (A.7). The mass conservation equation (A.1) corresponds to the unknown C^{K_J} . The momentum (A.10) and energy (A.19) balances correspond to $v_l^{K_J}$ and T , respectively. Additional equations are obtained by considering the following variables to be constitutive or dependent:

$$\begin{aligned} \dot{\varepsilon}^A, \dot{\varepsilon}^B, A^{K_J}, q_l^{K_J}, \eta^{K_J}, t_{kl}^{K_J}, {}^L\hat{e}^{K_J}, \hat{r}^{K_J}, {}^L\hat{T}_l^{K_J}, \hat{i}_l^{K_J}, {}^L\hat{Q}^{K_J}, \hat{E}^{K_J}, \hat{\eta}^{K_J} \\ K, L = sA, wA, B, C \text{ and } K \neq L. \end{aligned} \quad (2.2)$$

The constitutive variables are considered to be functions of the following set of independent variables:

$$\begin{aligned} \varepsilon^A, \dot{\varepsilon}^B, \varepsilon_J^A, \dot{\varepsilon}_J^B, T, T_J, \\ \rho^{sA}, C^{sA_J}, E_{KL}^{sA}, \overset{(m)}{E}_{KL}^{sA}, E_{KL,J}^{sA}, \overset{(m)}{E}_{KL,J}^{sA}, \\ \rho^{wA}, C^{wA_J}, v_l^{wA,SA}, u_l^{wA_J}, d_{kl}^{wA}, u_{k,l}^{wA_J}, \\ \rho^B, C^{B_J}, v_l^{B,SA}, u_l^{B_J}, d_{kl}^B, u_{k,l}^{B_J}, \\ \rho^C, C^{C_J}, v_l^{C,SA}, u_l^{C_J}, d_{kl}^C, u_{k,l}^{C_J}. \end{aligned} \quad (2.3)$$

where $m = 1$ to p . In (2.2) and (2.3) the time derivatives are computed by following the velocity of the solid phase at the macroscale:

$$\dot{g} \equiv \frac{D^{sA} g}{Dt} = \frac{\partial g}{\partial t} + v_l^{sA} g_J \quad (2.4)$$

$$\overset{(m)}{g} \equiv \frac{D^{sA^m} g}{Dt^m} \quad (2.5)$$

where m represents the order of the derivative. Before upscaling, all independent variables had a corresponding equation at the microscale except ε^K ($K = A, B$). As ε^K did not exist at microscale, it remains unaccounted after upscaling the microscale equations. This is the closure problem, and following Bowen [23], we close the system by postulating that $\dot{\varepsilon}^K$ is a dependent variable. The variables ε^K and $\dot{\varepsilon}_J^K$ account for the liquid-solid interaction at moderate to high solvent contents. The liquid-solid interaction occurs through solvation forces, which lower the chemical potential at the interfaces in comparison to the bulk liquid [1, 23-26]. This causes liquid movement from the bulk phase to the interface, pushing apart the solid, which in turn produces swelling.

The system under consideration is assumed to be governed by single time scale dependence on the volume fraction. Therefore, in our list of independent variables we include both volume fractions ($\varepsilon^A, \varepsilon^B$) at macroscale. In such a system the macropores are not in direct contact with the surrounding medium and they drain (or absorb) liquid only through micropores. The systems of dual porosity type, where both micro and macropores could directly exchange fluids with the surrounding medium, are governed by both meso and macroscale volume fractions. Such systems were beyond the scope of our current study.

The E_{KL}^{sA} and $E_{KL,I}^{sA}$ account for the elastic deformation of the solid matrix. At low fluid contents, $E_{KL,I}^{sA}$ incorporates relative shear between two solid surfaces separated by only few molecular layers of fluid [11, 27]. In a connected solid matrix a macroscopic deformation results in a gradient of the strain tensor, which is also captured by the $E_{KL,I}^s$. At the macroscale, the

viscoelastic nature of the solid polymers is captured by E_{KL}^{sA} , $m = 1$ to p ; where (m) indicates the order of the time material derivative. The variables T and T_l account for the conduction of thermal energy at intermediate rates of heat transfer and we are assuming local thermal equilibrium so only one energy equation is required. The viscous nature of the fluid phase is incorporated through the d_{kl}^K ($K = wA, B, C$). The term $u_{k,l}^{K_j}$ ($K = wA, B, C$) leads to the viscous resistance of the fluid phase to the diffusion of species. For most practical purposes, the diffusion of species in the solid phase is negligible. Therefore, $u_{k,l}^{sA_j}$ is not included in the list of independent variables.

If both ${}^L\hat{e}^{sA_j}$ and \hat{r}^{sA_j} are zero, the ε^{sA} , ρ^{sA} and E_{KL}^{sA} cannot be varied independently as they are related by the mass balance equation (A.3) and the equation, $\dot{E}_{KL}^{sA} = x_{k,K}^{sA} x_{l,L}^{sA} d_{kl}^{sA}$. Similarly, ε^K , ρ^K and d_{kl}^K ($K = wA, B$ and C) are related by the mass balance equations. To allow greater flexibility in variation of these variables we weakly impose the mass conservation equations in the entropy inequality (A.38) using the Lagrange multiplier technique [28]. Furthermore, this will allow making equations applicable to incompressible phases without re-exploiting the entropy inequality. We modify the entropy inequality as follows:

$$\begin{aligned}
 T\rho\Lambda_{new} &= T\rho\Lambda_{old} + \\
 &+ \sum_{K=sA,wA,B,C} \lambda^K \left[\frac{D^K(\varepsilon^K \rho^K)}{Dt} + \varepsilon^K \rho^K v_{l,l}^K - \sum_{\substack{L=sA,wA,B,C \\ L \neq K}} \varepsilon^K \rho^K {}^L\hat{e}^K \right] \\
 &+ \sum_{K=sA,wA,B,C} \sum_{j=1}^N \lambda^{K_j} \left[\varepsilon^K \rho^K \frac{D^K C^{K_j}}{Dt} + (\varepsilon^K \rho^{K_j} u_l^{K_j})_j - \left(\sum_{\substack{L=sA,wA,B,C \\ L \neq K}} \varepsilon^K \rho^{K_j} {}^L\hat{e}^{K_j} \right. \right. \\
 &\quad \left. \left. + \varepsilon^K \rho^{K_j} \hat{r}^{K_j} - C^{K_j} \sum_{\substack{L=sA,wA,B,C \\ L \neq K}} \varepsilon^K \rho^K {}^L\hat{e}^K \right) \right] \geq 0. \tag{2.6}
 \end{aligned}$$

where $T\rho\Lambda_{old}$ is equation (A.38). The form of the mass balance equations for species [(A.1) and (A.4)] was converted from density into concentration representation before substituting it in (2.6). Since the last two rows of (2.6) are independent for only N-1 values of j , we select $\lambda^{K_N} = 0$.

The axiom of equipresence requires that initially all constitutive variables should be expressed in terms of the same list of independent variables until the contrary is proven [22]. It can be shown that the Helmholtz free energies are functions of the subsets of the list [29]. Additionally, from physical knowledge of the system we know that the Helmholtz free energy of the solid phase depends upon ρ^{sA_j} and of the liquid phase depends upon ρ^{wA_j} . Therefore, to save computations we postulate the dependence of the Helmholtz free energies on subsets of the list (2.3) as:

$$A_I^{sA} = A_I^{sA}(\varepsilon^A, \varepsilon^B, T, \rho^{sA}, C^{sA_j}, E_{KL}^{sA}, \dot{E}_{KL}^{sA}, \dots \overset{(p)}{E}_{KL}^{sA}), \quad (2.7)$$

$$A_I^{wA} = A_I^{wA}(\varepsilon^A, \varepsilon^B, T, \rho^{wA}, C^{wA_j}, E_{KL}^{wA}, \dot{E}_{KL}^{wA}, \dots \overset{(p)}{E}_{KL}^{wA}), \quad (2.8)$$

$$A_I^B = A_I^B(\varepsilon^A, \varepsilon^B, T, \rho^B, C^B_j), \quad (2.9)$$

$$A_I^C = A_I^C(\varepsilon^A, \varepsilon^B, T, \rho^C, C^C_j). \quad (2.10)$$

All other dependent variables are considered to be functions of all independent variables in list (2.3). The free energies appear in the entropy inequality (A.38) as material derivatives. Using the chain rule, the following expressions for the material derivatives of the free energies can be obtained:

$$\begin{aligned} \frac{D^{sA} A_I^{sA}}{Dt} &= \frac{\partial A_I^{sA}}{\partial \varepsilon^A} \dot{\varepsilon}^A + \frac{\partial A_I^{sA}}{\partial \varepsilon^B} \dot{\varepsilon}^B + \frac{\partial A_I^{sA}}{\partial T} \dot{T} + \frac{\partial A_I^{sA}}{\partial \rho^{sA}} \dot{\rho}^{sA} + \sum_{j=1}^{N-1} \tilde{\mu}^{sA_j} \dot{C}^{sA_j} \\ &\quad + \frac{\partial A_I^{sA}}{\partial E_{KL}^{sA}} \dot{E}_{KL}^{sA} + \sum_{m=1}^p \frac{\partial A_I^{sA}}{\partial E_{KL}^{(m)}} \overset{(m+1)}{E}_{KL}^{sA}, \end{aligned} \quad (2.11)$$

$$\begin{aligned}
\frac{D^{wA} A_I^{wA}}{Dt} = & \frac{\partial A_I^{wA}}{\partial \varepsilon^A} \dot{\varepsilon}^A + \frac{\partial A_I^{wA}}{\partial \varepsilon^B} \dot{\varepsilon}^B + \frac{\partial A_I^{wA}}{\partial T} \dot{T} + \frac{\partial A_I^{wA}}{\partial \rho^{wA}} \dot{\rho}^{wA} + \sum_{j=1}^{N-1} \tilde{\mu}^{wA_j} \dot{C}^{wA_j} \\
& + \frac{\partial A_I^{wA}}{\partial E_{KL}^{sA}} \dot{E}_{KL}^{sA} + \sum_{m=1}^p \frac{\partial A_I^{wA}}{\partial E_{KL}^{(m)}} \dot{E}_{KL}^{(m)} + \frac{\partial A_I^{wA}}{\partial \varepsilon^A} v_l^{wA,sA} \varepsilon_{,l}^A + \frac{\partial A_I^{wA}}{\partial \varepsilon^B} v_l^{wA,sA} \varepsilon_{,l}^B \\
& + \frac{\partial A_I^{wA}}{\partial T} v_l^{wA,sA} T_{,l} + \frac{\partial A_I^{wA}}{\partial \rho^{wA}} v_l^{wA,sA} \rho_{,l}^{wA} + \sum_{j=1}^{N-1} \tilde{\mu}^{wA_j} v_l^{wA,sA} C^{wA_j,l} \\
& + \frac{\partial A_I^{wA}}{\partial E_{KL}^{sA}} v_l^{wA,sA} E_{KL,l}^{sA} + \sum_{m=1}^p \frac{\partial A_I^{wA}}{\partial E_{KL}^{(m)}} v_l^{wA,sA} E_{KL,l}^{(m)}
\end{aligned} \tag{2.12}$$

$$\begin{aligned}
\frac{D^K A_I^K}{Dt} = & \frac{\partial A_I^K}{\partial \varepsilon^A} \dot{\varepsilon}^A + \frac{\partial A_I^K}{\partial \varepsilon^B} \dot{\varepsilon}^B + \frac{\partial A_I^K}{\partial T} \dot{T} + \frac{\partial A_I^K}{\partial \rho^K} \dot{\rho}^K + \sum_{j=1}^{N-1} \tilde{\mu}^{K_j} \dot{C}^{K_j} + \frac{\partial A_I^K}{\partial \varepsilon^A} v_l^{K,sA} \varepsilon_{,l}^A \\
& + \frac{\partial A_I^K}{\partial \varepsilon^B} v_l^{K,sA} \varepsilon_{,l}^B + \frac{\partial A_I^K}{\partial T} v_l^{K,sA} T_{,l} + \frac{\partial A_I^K}{\partial \rho^K} v_l^{K,sA} \rho_{,l}^K + \sum_{j=1}^{N-1} \tilde{\mu}^{K_j} v_l^{K,sA} C^{K_j,l}, \quad K = B, C.
\end{aligned} \tag{2.13}$$

To obtain (2.12) and (2.13), we wrote total derivatives with respect to the solid phase using the following identity:

$$\frac{D^K \varphi}{Dt} = \frac{D^{sA} \varphi}{Dt} + v_l^{K,sA} \varphi_{,l} \quad K = wA, B, C. \tag{2.14}$$

where, φ is a scalar function. C^{K_j} is a dependent variable due to restriction (A.8). This gives

rise to the relative chemical potential $\tilde{\mu}^{K_j}$ in (2.12) and (2.13), which is defined as follows:

$$\begin{aligned}
\tilde{\mu}^{K_j} &\equiv \mu^{K_j} - \mu^{K_N}, \\
\mu^{K_j} &\equiv \frac{\partial A_I^K}{\partial C^{K_j}}, \quad K = sA, wA, B, C, \quad j = 1..N.
\end{aligned} \tag{2.15}$$

Additional macroscale quantities of interest are:

$$\text{Thermodynamic pressure} \quad p^K \equiv \rho^{K^2} \frac{\partial A_I^K}{\partial \rho^K}, \quad K = sA, wA, B, C, \tag{2.16}$$

$$\text{Terzaghi stress} \quad t_{kl}^{seA} \equiv \rho^{sA} \frac{\partial A_I^{sA}}{\partial E_{KL}^{sA}} x_{k,K}^{sA} x_{l,L}^{sA} \tag{2.17}$$

$$\text{Hydration stress} \quad t_{kl}^{shA} \equiv \rho^{wA} \frac{\partial A_I^{wA}}{\partial E_{KL}^{wA}} x_{k,K}^{wA} x_{l,L}^{wA}. \tag{2.18}$$

The Terzaghi stress, t_{kl}^{seA} is the elastic component of stress in the solid medium and t_{kl}^{shA} results from physico-chemical forces between the solid and solvent [30]. In the entropy inequality, the terms involving $u_i^{K_j}$ and $u_{k,l}^{K_j}$ have N-1 independent variables and one dependent variable because, $\sum_{j=1}^N \rho^{K_j} u_i^{K_j} = 0$. Thus, the following identities due to Bennethum et al. [15] will be needed to rewrite these terms as N-1 independent terms:

$$\sum_{j=1}^N F_k^{K_j} u_k^{K_j} = \sum_{j=1}^{N-1} u_k^{K_j} \left(F_k^{K_j} - \frac{\rho^{K_j}}{\rho^{K_N}} F_k^{K_N} \right). \quad (2.19)$$

$$\sum_{j=1}^N G_{kl}^{K_j} u_{k,l}^{K_j} = \sum_{j=1}^{N-1} u_{k,l}^{K_j} \left(G_{kl}^{K_j} - \frac{\rho^{K_j}}{\rho^{K_N}} G_{l,N}^{K_N} \right) - G_{k,N}^{K_N} \sum_{j=1}^{N-1} \left(\frac{\rho^{K_j}}{\rho^{K_N}} \right) u_k^{K_j}. \quad (2.20)$$

where, $F_k^{K_j}$ and $G_{kl}^{K_j}$ are the vector and tensor valued coefficients of $u_k^{K_j}$ and $u_{k,l}^{K_j}$, respectively.

Substituting equations (2.11)-(2.13) in the entropy inequality (A.38), using (2.6) and simplifying we obtain:

$$\begin{aligned} T\rho\Lambda = & - \sum_{K=sA,wA,B,C} \varepsilon^K \rho^K \left(\frac{\partial A_I^K}{\partial T} + \eta^K \right) \dot{T} \\ & - \left(\varepsilon^A \rho^{sA} \frac{\partial A_I^{sA}}{\partial \varepsilon^A} + \varepsilon^A \rho^{wA} \frac{\partial A_I^{wA}}{\partial \varepsilon^A} + \varepsilon^B \rho^B \frac{\partial A_I^B}{\partial \varepsilon^A} \right. \\ & \quad \left. + \varepsilon^C \rho^C \frac{\partial A_I^C}{\partial \varepsilon^A} - \lambda^{sA} \rho^{sA} - \lambda^{wA} \rho^{wA} + \lambda^C \rho^C \right) \dot{\varepsilon}^A \\ & - \left(\varepsilon^A \rho^{sA} \frac{\partial A_I^{sA}}{\partial \varepsilon^B} + \varepsilon^A \rho^{wA} \frac{\partial A_I^{wA}}{\partial \varepsilon^B} + \varepsilon^C \rho^C \frac{\partial A_I^C}{\partial \varepsilon^B} - \lambda^B \rho^B + \lambda^C \rho^C \right) \dot{\varepsilon}^B \\ & + \sum_{K=sA,wA,B,C} \varepsilon^K \left(-\frac{p^K}{\rho^K} + \lambda^K \right) \dot{\rho}^K \\ & + \sum_{K=sA,wA,B,C} \varepsilon^K \rho^K \left(-\tilde{\mu}^{K_j} + \lambda^{K_j} \right) \dot{C}^{K_j} \end{aligned}$$

$$\begin{aligned}
& + \varepsilon^A \left[\left(t_{kl}^{sA} - t_{kl}^{seA} - t_{kl}^{shA} + \sum_{j=1}^N \rho^{sA_j} u_k^{sA_j} u_l^{sA_j} + \lambda^{sA} \rho^{sA} \delta_{kl} \right) X_{K,k}^{sA} X_{L,l}^{sA} \right] \dot{E}_{KL}^{sA} \\
& - \varepsilon^A \sum_{m=1}^p \left(\rho^{sA} \frac{\partial A_I^{sA}}{\partial E_{KL}^{sA}} + \rho^{wA} \frac{\partial A_I^{wA}}{\partial E_{KL}^{sA}} \right) E_{KL}^{sA} \\
& + \sum_{K=wA,B,C} \varepsilon^K \left(t_{kl}^K + \sum_{j=1}^N \rho^{K_j} u_k^{K_j} u_l^{K_j} + \lambda^K \rho^K \delta_{kl} \right) d_{kl}^K \\
& + \sum_{K=sA,wA,B,C} \sum_{j=1}^{N-1} \varepsilon^K \left(t_{kl}^{K_j} - \frac{\rho^{K_j}}{\rho^{K_N}} t_{kl}^{K_N} - \rho^{K_j} A^{K_j} \delta_{kl} + \rho^{K_j} A^{K_N} \delta_{kl} + \lambda^{K_j} \rho^{K_j} \delta_{kl} \right) u_{k,l}^{K_j} \\
& + \sum_{K=sA,wA,B,C} \frac{\varepsilon^K T_J}{T} \left\{ q_I^K + \sum_{j=1}^N \left[\rho^{K_j} u_l^{K_j} \left(A^{K_j} + \frac{1}{2} u_k^{K_j} u_k^{K_j} \right) - t_{kl}^{K_j} u_k^{K_j} \right] \right\} \\
& - \varepsilon^A \rho^{wA} \left[\frac{\partial A_I^{wA}}{\partial \varepsilon^A} \varepsilon^A_{,I} + \frac{\partial A_I^{wA}}{\partial \varepsilon^B} \varepsilon^B_{,I} + \left(\eta^{wA} + \frac{\partial A_I^{wA}}{\partial T} \right) T_{,I} + \sum_{L=sA,B,C} {}^L \hat{T}_I^{wA} \right. \\
& + \frac{p^{wA}}{\rho^{wA^2}} \rho^{wA}_{,I} + \sum_{j=1}^{N-1} \tilde{\mu}^{wA_j} C_{,I}^{wA_j} + \frac{\partial A_I^{wA}}{\partial E_{KL}^{sA}} E_{KL,I}^{sA} \\
& \left. + \sum_{m=1}^p \frac{\partial A_I^{wA}}{\partial E_{KL}^{sA}} E_{KL,I}^{(m)} - \frac{\lambda^{wA}}{\varepsilon^A \rho^{wA}} (\varepsilon^A \rho^{wA})_{,I} - \sum_{j=1}^{N-1} \lambda^{wA_j} C_{,I}^{wA_j} \right] v_I^{wA,sA} \\
& - \sum_{K=B,C} \varepsilon^K \rho^K \left[\frac{\partial A_I^K}{\partial \varepsilon^A} \varepsilon^A_{,I} + \frac{\partial A_I^K}{\partial \varepsilon^B} \varepsilon^B_{,I} + \left(\eta^K + \frac{\partial A_I^K}{\partial T} \right) T_{,I} + \sum_{\substack{L=sA,wA,B,C \\ L \neq K}} {}^L \hat{T}_I^K \right. \\
& + \frac{p^K}{\rho^{K^2}} \rho^K_{,I} + \sum_{j=1}^{N-1} \tilde{\mu}^{K_j} C_{,I}^{K_j} - \frac{\lambda^K}{\varepsilon^K \rho^K} (\varepsilon^K \rho^K)_{,I} - \sum_{j=1}^{N-1} \lambda^{K_j} C_{,I}^{K_j} \left. \right] v_I^{K,sA} \\
& + \sum_{K=sA,wA,B,C} \sum_{j=1}^{N-1} u_l^{K_j} \left\{ -\varepsilon^K \rho^{K_j} \left(\sum_{\substack{L=sA,wA,B,C \\ L \neq K}} {}^L \hat{T}_I^{K_j} + \hat{i}_l^{K_j} \right) + \varepsilon^K \rho^{K_j} \left(\sum_{\substack{L=sA,wA,B,C \\ L \neq K}} {}^L \hat{T}_I^{K_N} + \hat{i}_l^{K_N} \right) \right. \\
& \left. - \left[\varepsilon^A \rho^{K_j} (A^{K_j} - A^{K_N}) \right]_{,I} - \varepsilon^K t_{kl}^{K_N} \left(\frac{\rho^{K_j}}{\rho^{K_N}} \right)_{,k} + (\varepsilon^A \rho^{K_j})_{,I} \lambda^{K_j} \right\}
\end{aligned}$$

$$\begin{aligned}
& - \sum_{K=sA, wA, B, C} \sum_{j=1}^N \varepsilon^K \rho^K \left(\frac{1}{2} u_l^{K_j} u_l^{K_j} + \lambda^{K_j} \right) \dot{r}^{K_j} \\
& - \sum_{K=sA, wA, B, C} \sum_{\substack{L=sA, wA, B, C \\ L \neq K}} \varepsilon^K \rho^K \hat{e}^K \left(A_l^K + \frac{1}{2} v_l^{K, sA} v_l^{K, sA} + \lambda^K - \sum_{j=1}^{N-1} \lambda^{K_j} C^{K_j} \right) \\
& - \sum_{K=sA, wA, B, C} \sum_{\substack{L=sA, wA, B, C \\ L \neq K}} \sum_{j=1}^{N-1} \varepsilon^K \rho^{K_j L} \hat{e}^{K_j} \left(\frac{1}{2} u_l^{K_j} u_l^{K_j} + \lambda^{K_j} \right) \geq 0,
\end{aligned} \tag{2.21}$$

where, $\varepsilon^{\alpha A}$, ($\alpha = s, w$) implies ε^A . We used $\lambda^{K_N} \equiv 0$, while writing the last two rows of (2.21).

If the solid phase had been assumed to be elastic, the terms in the 7th row of (2.21), would have been grouped as a coefficient of d_{kl}^{sA} . However, since we are modeling the solid phase as viscoelastic, d_{kl}^{sA} was converted to the independent variable \dot{E}_{KL}^{sA} using the equation:

$$d_{kl}^{sA} = \dot{E}_{KL}^{sA} X_{K,k}^{sA} X_{L,l}^{sA}. \tag{2.22}$$

Non-Equilibrium Relations

In the entropy inequality (2.21) the variables \dot{T} , $\dot{\rho}^K$, \dot{C}^{K_j} , \dot{E}_{KL}^{sA} ^(p+1) and $u_{k,j}^{sA}$ are neither dependent nor independent. They can vary arbitrarily. To satisfy the entropy inequality for all processes, the coefficients of these variables must be zero. This leads to the following non-equilibrium equations:

$$\sum_{K=sA, wA, B, C} \varepsilon^K \rho^K \left(\frac{\partial A_l^K}{\partial T} + \eta^K \right) = 0 \tag{3.1}$$

$$\lambda^K = \frac{p^K}{\rho^K}, \quad K = sA, wA, B, C, \tag{3.2}$$

$$\lambda^{K_j} = \tilde{\mu}^{K_j}, \quad K = sA, wA, B, C, \tag{3.3}$$

$$\rho^{sA} \frac{\partial A_l^{sA}}{\partial E_{KL}^{sA}} + \rho^{wA} \frac{\partial A_l^{wA}}{\partial E_{KL}^{sA}} = 0 \tag{3.4}$$

$$t_{kl}^{sA_j} - \frac{\rho^{sA_j}}{\rho^{sA_N}} t_{kl}^{sA_N} = \rho^{sA_j} \left(A^{sA_j} - A^{sA_N} - \tilde{\mu}^{sA_j} \right) \delta_{kl} \tag{3.5}$$

Equation (3.1) implies that the sum of terms over K phases is zero, however in accordance with the classical thermodynamics of one phase we make the following assumption:

$$\eta^K = -\frac{\partial A_I^K}{\partial T}, \quad K = sA, wA, B, C. \quad (3.6)$$

For single-phase viscoelastic solids $\rho^s(\partial A_I^s / \partial E_{kl}^s) = 0$ [22]. Such a conclusion cannot be drawn for multiphase systems, where viscoelastic solids interact with vicinal liquid, because in (3.4) $\partial A_I^{wA} / \partial E_{KL}^{sA}$ is also involved.

In (3.5) we used (3.3) to replace λ^{sA_j} with $\tilde{\mu}^{sA_j}$. In the subsequent manuscript, we will use (3.2) and (3.3) to replace λ^{K_j} and λ^K , with $\tilde{\mu}^{K_j}$ and p^K / ρ^K , respectively.

Equilibrium Restrictions

At thermodynamic equilibrium the following variables are zero:

$$\dot{\varepsilon}^A, \dot{\varepsilon}^B, \overset{(m)}{E}_{KL}^{sA}, d_{kl}^K, u_{k,l}^{K_j}, T_j, v_l^{K,sA}, u_l^{K_j}, {}^L\hat{e}^{K_j} \quad (4.1)$$

here, m = 1 to p+1; j = 1 to N-1 for $u_{k,l}^{K_j}, u_k^{K_j}$, and j = 1 to N for ${}^L\hat{e}^{K_j}$. K = wA, B, C for d_{kl}^K , and K = sA, wA, B and C for other variables. The list (4.1) does not contain \hat{r}^{K_j} because it requires the equations of chemical reactions, which we have not incorporated. At equilibrium the entropy reaches its maximum value and the net generation of entropy, Λ , attains a minima. Thus, $\partial\Lambda/\partial x = 0$ and $\partial^2\Lambda/\partial x\partial y \geq 0$. Where x and y are the variables in list (4.1). We obtain the following results:

$$\varepsilon^A \rho^{sA} \frac{\partial A_I^{sA}}{\partial \varepsilon^A} + \varepsilon^A \rho^{wA} \frac{\partial A_I^{wA}}{\partial \varepsilon^A} + \varepsilon^B \rho^B \frac{\partial A_I^B}{\partial \varepsilon^A} + \varepsilon^C \rho^C \frac{\partial A_I^C}{\partial \varepsilon^A} - p^{sA} - p^{wA} + p^C = 0, \quad (4.2)$$

$$\varepsilon^A \rho^{sA} \frac{\partial A_I^{sA}}{\partial \varepsilon^B} + \varepsilon^A \rho^{wA} \frac{\partial A_I^{wA}}{\partial \varepsilon^B} + \varepsilon^B \rho^B \frac{\partial A_I^B}{\partial \varepsilon^B} + \varepsilon^C \rho^C \frac{\partial A_I^C}{\partial \varepsilon^B} - p^B + p^C = 0, \quad (4.3)$$

$$t_{kl}^{sA} = -p^{sA} \delta_{kl} + t_{kl}^{seA} + t_{kl}^{shA}, \quad (4.4)$$

$$\rho^{sA} \frac{\partial A_I^{sA}}{\partial E_{KL}^{sA}} + \rho^{wA} \frac{\partial A_I^{wA}}{\partial E_{KL}^{sA}} = 0, \quad m = 1..p, \quad (4.5)$$

$$t_{kl}^K = -p^K \delta_{kl}, \quad K = wA, B, C, \quad (4.6)$$

$$t_{kl}^{K_j} - \frac{\rho^{K_j}}{\rho^{K_N}} t_{kl}^{K_N} = \rho^{K_j} \left(A^{K_j} - A^{K_N} - \tilde{\mu}^{K_j} \right) \delta_{kl}, \quad K = wA, B, C, \quad (4.7)$$

$$\sum_{K=sA, wA, B, C} \varepsilon^K q_l^K = 0, \quad (4.8)$$

$$\sum_{\substack{L=sA, wA, B, C \\ L \neq K}} \varepsilon^K \rho^K L \hat{T}_l^K = -\varepsilon^K \rho^K \frac{\partial A_l^K}{\partial \varepsilon^A} \varepsilon^A{}_l - \varepsilon^K \rho^K \frac{\partial A_l^K}{\partial \varepsilon^B} \varepsilon^B{}_l + p^K \varepsilon^K{}_l, \quad (4.9)$$

$$K = B, C,$$

$$\begin{aligned} \sum_{L=sA, B, C} \varepsilon^A \rho^{wA} L \hat{T}_l^{wA} &= -\varepsilon^A \rho^{wA} \frac{\partial A_l^{wA}}{\partial \varepsilon^A} \varepsilon^A{}_l - \varepsilon^A \rho^{wA} \frac{\partial A_l^{wA}}{\partial \varepsilon^B} \varepsilon^B{}_l + p^{wA} \varepsilon^A{}_l \\ &\quad - \varepsilon^A \rho^{wA} \frac{\partial A_l^{wA}}{\partial E_{KL}^{sA}} E_{KL,l}^{sA} - \varepsilon^A \rho^{wA} \sum_{m=1}^p \frac{\partial A_l^{wA}}{\partial E_{KL}^{(m)}} E_{KL,l}^{(m)}, \quad K = B, C, \end{aligned} \quad (4.10)$$

$$\begin{aligned} \varepsilon^K \rho^{K_j} \left(\sum_{\substack{L=sA, wA, B, C \\ L \neq K}} L \hat{T}_l^{K_j} + \hat{t}_l^{K_j} \right) - \varepsilon^K \rho^{K_j} \left(\sum_{\substack{L=sA, wA, B, C \\ L \neq K}} L \hat{T}_l^{K_N} + \hat{t}_l^{K_N} \right) &= \\ \tilde{\mu}^{K_j} \left(\varepsilon^K \rho^{K_j} \right)_l - \left[\varepsilon^K \rho^{K_j} \left(A^{K_j} - A^{K_N} \right) \right]_l - \varepsilon^K t_{kl}^{K_N} \left(\frac{\rho^{K_j}}{\rho^{K_N}} \right)_{,k} &, \end{aligned} \quad (4.11)$$

$$K = sA, wA, B, C,$$

$$A_l^K + \frac{p^K}{\rho^K} - \sum_{j=1}^{N-1} \tilde{\mu}^{K_j} C^{K_j} = A_l^L + \frac{p^L}{\rho^L} - \sum_{j=1}^{N-1} \tilde{\mu}^{L_j} C^{L_j}, \quad K, L = sA, wA, B, C, \quad K \neq L, \quad (4.12)$$

$$\tilde{\mu}^{sA_j} = \tilde{\mu}^{wA_j} = \tilde{\mu}^{B_j} = \tilde{\mu}^{C_j} \quad (4.13)$$

Removing the Nth component Dependence

In classical Gibbsian thermodynamics, when extensive variables such as number of molecules are used as independent variables, the species equations do not depend upon the Nth component. However, in mixture theories when concentrations of species are used as independent variables, the resulting equations become a function of the Nth component. To reproduce classical Gibbsian results we follow [31] and choose the equilibrium chemical potential of the Nth component appropriately. We take

$$\mu^{K_N} \delta_{kl} = A^{K_N} \delta_{kl} - \frac{t_{kl}^{K_N}}{\rho^{K_N}}, \quad K = wA, B, C, \quad (4.14)$$

$$\mu^{sA_N} \delta_{kl} = A^{sA_N} \delta_{kl} - \frac{t_{kl}^{sA_N}}{\rho^{sA_N}} + \frac{t_{kl}^{seA}}{\rho^{seA}} + \frac{t_{kl}^{shA}}{\rho^{shA}}. \quad (4.15)$$

Substituting (4.14) in (4.7) we get:

$$\mu^{K_j} \delta_{kl} = A^{K_j} \delta_{kl} - \frac{t_{kl}^{K_j}}{\rho^{K_j}}, \quad K = sA, wA, B, C, \quad (4.16)$$

Similarly, by substituting (4.15) in (3.5) we obtain:

$$\mu^{sA_j} \delta_{kl} = A^{sA_j} \delta_{kl} - \frac{t_{kl}^{sA_j}}{\rho^{sA_j}} + \frac{1}{\rho^{sA}} (t_{kl}^{seA} + t_{kl}^{shA}). \quad (4.17)$$

Multiplying (4.16) and (4.17) by C^{K_j} , summing over N species and using expressions for t_{kl}^K

[(4.4) and (4.6)], we retrieve the equation for Gibbs energy for the phase K:

$$G^K = \sum_{j=1}^N C^{K_j} \mu^{K_j} = A_I^K + \frac{p^K}{\rho^K}, \quad K = sA, wA, B, C. \quad (4.18)$$

Equation (4.13) says that the relative chemical potential of species coexisting in different phases is equal at equilibrium. However in classical thermodynamics, the absolute chemical potential of species present in various phases is equal at equilibrium. To obtain this later result, we rewrite (4.12) as

$$A_I^K + \frac{p^K}{\rho^K} - \sum_{j=1}^N C^{K_j} \mu^{K_j} + \mu^{K_N} = A_I^L + \frac{p^L}{\rho^L} - \sum_{j=1}^N C^{L_j} \mu^{L_j} + \mu^{L_N}, \quad K, L = sA, wA, B, C, \quad K \neq L, \quad (4.19)$$

and substitute (4.18) in (4.19), to obtain

$$\mu^{K_N} = \mu^{L_N}, \quad K, L = sA, wA, B, C, \quad K \neq L, \quad (4.20)$$

Finally, substituting (4.20) into (4.13), we obtain the classical result:

$$\mu^{sA_j} = \mu^{wA_j} = \mu^{B_j} = \mu^{C_j}. \quad (4.21)$$

To remove N component dependence from (4.11), sum this equation from j = 1 to N

$$\begin{aligned} \varepsilon^K \rho^K \sum_{\substack{L=sA, wA, B, C \\ L \neq K}} {}^L \hat{T}_I^K - \varepsilon^K \rho^K \left(\sum_{\substack{L=sA, wA, B, C \\ L \neq K}} {}^L \hat{T}_I^{K_N} + \hat{t}_I^{K_N} \right) = \\ \sum_{j=1}^N \tilde{\mu}^{K_j} \left(\varepsilon^K \rho^{K_j} \right)_J - \left(\varepsilon^K \rho^K A_I^K \right)_J - \varepsilon^K t_{kl}^{K_N} \left(\frac{\rho^K}{\rho^{K_N}} \right)_k + \left(\varepsilon^K \rho^K A^{K_N} \right)_J, \quad (4.22) \\ K = sA, wA, B, C, \end{aligned}$$

Here we used $\sum_{j=1}^N {}^L\hat{T}_l^{K_j} = {}^L\hat{T}_l^K$ and $\sum_{j=1}^N \hat{i}_l^{K_j} = 0$, since at equilibrium $u_l^{K_j} = 0$. Using (2.8)-(2.10)

compute $A_{I,J}^K$ as follows:

$$\begin{aligned} A_{I,J}^{wA} &= \frac{\partial A_I^{wA}}{\partial \varepsilon^A} \varepsilon^A_{,J} + \frac{\partial A_I^{wA}}{\partial \varepsilon^B} \varepsilon^B_{,J} + \frac{\partial A_I^{wA}}{\partial T} T_{,J} + \frac{\partial A_I^{wA}}{\partial \rho^{wA}} \rho^{wA}_{,J} + \sum_{j=1}^{N-1} \tilde{\mu}^{wA_j} C^{wA_j}_{,J} + \\ &\quad \frac{\partial A_I^{wA}}{\partial E_{KL}^{sA}} E_{KL,I}^{sA} + \sum_{m=1}^p \frac{\partial A_I^{wA}}{\partial E_{KL}^{sA}} \overset{(m)}{E}_{KL,I}^{sA} \end{aligned} \quad (4.23)$$

$$A_{I,J}^K = \frac{\partial A_I^K}{\partial \varepsilon^A} \varepsilon^A_{,J} + \frac{\partial A_I^K}{\partial \varepsilon^B} \varepsilon^B_{,J} + \frac{\partial A_I^K}{\partial T} T_{,J} + \frac{\partial A_I^K}{\partial \rho^K} \rho^K_{,J} + \sum_{j=1}^{N-1} \tilde{\mu}^{K_j} C^{K_j}_{,J}, \quad K = B, C. \quad (4.24)$$

Substitute $A_{I,J}^K$, ($K = wA, B, C$) and ${}^L\hat{T}_l^K$ [eqs. (4.9), (4.10)] in (4.22) and simplify to get:

$$\begin{aligned} \varepsilon^K \rho^K \left(\sum_{\substack{L=wA, wB, wC \\ L \neq K}} {}^L\hat{T}_l^{K_N} + \hat{i}_l^{K_N} \right) - (\varepsilon^K \rho^K)_{,J} \mu^{K_N} + (\varepsilon^K \rho^K A^{K_N})_{,J} \\ - \varepsilon^K t_{kl}^{K_N} \left(\frac{\rho^K}{\rho^{K_N}} \right)_{,k} = 0, \quad K = wA, B, C, \end{aligned} \quad (4.25)$$

Finally, substituting (4.25) in (4.22) and reversing one step in derivation, we obtain:

$$\varepsilon^K \rho^{K_J} \left(\sum_{\substack{L=wA, wB, wC \\ L \neq K}} {}^L\hat{T}_l^{K_J} + \hat{i}_l^{K_J} \right) = (\varepsilon^K \rho^{K_J})_{,J} \mu^{K_J} - (\varepsilon^K \rho^{K_J} A^{K_J})_{,J}, \quad K = wA, B, C. \quad (4.26)$$

Near-Equilibrium Relations

In the entropy inequality, the coefficients of variables becoming zero at equilibrium [list (4.1)] are functions of these variables. For example, the coefficient of T_l is a function of remaining variables in the list (4.1). To satisfy the inequality, these coefficients are linearized using Taylor series expansion to form positive quadratic terms. Because of truncation, the results hold only near-equilibrium. In the previous section we have clarified the linearization procedure within the context of hybrid mixture theory.

Here, we perform one term Taylor series expansions of the coefficients of all variables in the list (4.1) except for the coefficients of T_J , E_{KL}^{sA} and d_{kl}^K , where we perform a two-term expansion. To obtain thermoviscoelastic and thermoviscous effects we perform a two-term linearization around T_J and E_{KL}^{sA} for the solid phase; and T_J and d_{kl}^K for the liquid phase. The resulting linearization coefficients are a function of the remaining independent variables listed in (4.1).

Thermoviscoelasticity

We linearize t_{kl}^{sA} and q_l^{sA} about T_J and E_{KL}^{sA} . Let,

$${}_{neq} \left(\sum_{j=1}^N t_{kl}^{sA_j} \right) = {}_{eq} t_{kl}^{sA} + {}_D t_{kl}^{sA} \quad (5.1)$$

where, the equilibrium part is given by (4.4). Let us denote the solid phase coefficient of T_J by Q_l^{sA} :

$$Q_l^{sA} \equiv q_l^{sA} + \sum_{j=1}^N \left[\left(A^{sA_j} + \frac{1}{2} u_k^{sA_j} u_k^{sA_j} \right) \rho^{sA_j} u_l^{sA_j} - t_{kl}^{sA_j} u_k^{sA_j} \right] \quad (5.2)$$

Substituting (5.1) and (5.2) into the T_J and E_{KL}^{sA} terms of the entropy inequality (2.21), we get:

$$\varepsilon^A {}_D t_{kl}^{sA} X_{K,k}^{sA} X_{L,l}^{sA} \dot{E}_{KL}^{sA} - \varepsilon^A \sum_{m=1}^p \left(\rho^{sA} \frac{\partial A_l^{sA}}{\partial E_{KL}^{sA}} + \rho^{wA} \frac{\partial A_l^{wA}}{\partial E_{KL}^{sA}} \right) E_{KL}^{sA} + \frac{\varepsilon^A}{T} Q_l^{sA} T_J \geq 0 \quad (5.3)$$

Notice that in (5.3) upon linearizing ${}_D t_{kl}^{sA}$ appears as a linear function of E_{KL}^{sA} whereas A_l^{sA}

appears as a nonlinear function because linearization is performed on $\partial A_l^{sA} / E_{KL}^{sA}$. If $E_{KL}^{sA} = 0$ and

$T_J = 0$, then $\partial A_l^{sA} / E_{KL}^{sA} = 0$ and $Q_l^{sA} = 0$. By linearizing we obtain:

$${}_D t_{kl}^{sA} = \sum_{m=1}^p \left(G_{KLMN}^{sA} E_{MN}^{(m)} x_{k,K}^{sA} x_{l,L}^{sA} \right) + H_{klm}^{sA} T_{,m} \quad (5.4)$$

$$Q_l^{sA} = K_{kl}^{sA} T_{,k} + \sum_{m=1}^p J_{KLM}^{sA} x_{l,K}^{sA} E_{LM}^{(m)} \quad (5.5)$$

where G_{KLMN}^{sA} is the coefficients of m^{th} time derivative of strain rate ($E_{MN}^{(m)}$). The coefficients

G_{KLMN}^{sA} , H_{klm}^{sA} , K_{kl}^{sA} and J_{KLM}^{sA} are not functions of $E_{KL}^{(m)}$ and $T_{,l}$. G_{KLMN}^{sA} is a fourth order positive semi-definite tensor responsible for stress dissipation due to relaxation processes within the solid phase. H_{klm}^{sA} and J_{KLM}^{sA} are third order tensors. K_{kl}^{sA} is the second order positive semi-definite tensor representing the thermal conductivity of the solid phase at macroscale. The H_{klm}^{sA} term causes thermal gradients to affect the stress field inside an anisotropic solid phase. Because of the J_{KLM}^{sA} term, heat flux arises inside an anisotropic solid phase due to the strain rate. Given that the third order tensors are zero under the full orthogonal group of transformations, H_{klm}^{sA} and J_{KLM}^{sA} would vanish for the isotropic solids [32]. Due to symmetry of the stress tensor and the strain rate, the third and fourth-order coefficients satisfy the following symmetry relationships:

$$\begin{aligned} G_{KLMN}^{sA} &= G_{LKNM}^{sA} = G_{KLN M}^{sA}, \quad m=1..p, \\ H_{klm}^{sA} &= H_{lkm}^{sA}, \\ J_{KLM}^{sA} &= J_{KML}^{sA}, \quad m=1..p. \end{aligned} \quad (5.6)$$

By substituting (5.4) and (4.4) in (5.1); and (5.5) in (5.2), we obtain the following near equilibrium equations:

$$t_{kl}^{sA} = -p^{sA} \delta_{kl} + t_{kl}^{seA} + t_{kl}^{shA} - \sum_{j=1}^N \rho^{sA_j} u_k^{sA_j} u_l^{sA_j} + \sum_{m=1}^p \left(G_{KLMN}^{sA} E_{MN}^{(m)} x_{k,K}^{sA} x_{l,L}^{sA} \right) + H_{klm}^{sA} T_{,m}, \quad (5.7)$$

$$q_l^{sA} = \sum_{j=1}^N \left[t_{kl}^{sA_j} u_k^{sA_j} - \left(A^{sA_j} + \frac{1}{2} u_k^{sA_j} u_k^{sA_j} \right) \rho^{sA_j} u_l^{sA_j} \right] + K_{kl}^{sA} T_{,k} + \sum_{m=1}^p J_{KLM}^{sA} x_{l,K}^{sA} E_{LM}^{(m)}. \quad (5.8)$$

Thermoviscous Effects

We can similarly, linearize about d_{kl}^K and $T_{,l}$ to obtain the following near-equilibrium equations for t_{kl}^K and q_l^K :

$$t_{kl}^K = -p^K \delta_{kl} + v_{klmn}^K d_{mn}^K + H_{klm}^K T_{,m} - \sum_{j=1}^N \rho^{K_j} u_k^{K_j} u_l^{K_j}, \quad K = wA, B, C, \quad (5.9)$$

$$q_l^K = \sum_{j=1}^N \left[t_{kl}^{K_j} u_k^{K_j} - \left(A^{K_j} + \frac{1}{2} u_k^{K_j} u_k^{K_j} \right) \rho^{K_j} u_l^{K_j} \right] + K_{kl}^K T_{,k} + G_{lmn}^K d_{mn}^K \quad K = wA, B, C. \quad (5.10)$$

Here, v_{klmn}^K is a fourth order, positive semi-definite viscous dissipation tensor. Similar to the solid phase, the third order tensors, H_{klm}^K and G_{lmn}^K introduce the cross-effects of the temperature gradient on the stress tensor, and the rate of deformation on the heat flux. For isotropic fluid phases H_{klm}^K and G_{lmn}^K disappear. Due to symmetry of the stress tensor and the rate of deformation tensor, the v_{klmn}^K , H_{klm}^K and G_{lmn}^K satisfy the following symmetry relationships:

$$\begin{aligned} v_{klmn}^K &= v_{lkmn}^K = v_{klnm}^K \\ H_{klm}^K &= H_{lkm}^K \\ G_{lmn}^K &= G_{lnm}^K, \quad K = wA, B, C. \end{aligned} \quad (5.11)$$

Remaining Near Equilibrium Equations

To obtain a more general equation for the chemical potential of a species in the solid phase, we may choose the near-equilibrium chemical potential of the N^{th} component in a very special way. We take

$$\mu^{sA_N} \delta_{kl} = A^{sA_N} \delta_{kl} - \frac{t_{kl}^{sA_N}}{\rho^{sA_N}} + \frac{1}{\rho^{sA}} \left(t_{kl}^{seA} + t_{kl}^{shA} + \sum_{m=1}^p G_{KLMN}^{sA} E_{MN}^{(m)} x_{k,K}^{sA} x_{l,L}^{sA} + H_{klm}^{sA} T_{,m} \right), \quad (5.12)$$

Substituting (5.12) in (3.5) we obtain:

$$\mu^{sA_j} \delta_{kl} = A^{sA_j} \delta_{kl} - \frac{t_{kl}^{sA_j}}{\rho^{sA_j}} + \frac{1}{\rho^{sA}} \left(t_{kl}^{seA} + t_{kl}^{shA} + \sum_{m=1}^p G_{KLMN}^{sA} E_{MN}^{sA} x_{k,K}^{sA} x_{l,L}^{sA} + H_{klm}^{sA} T_{,m}^{(m)} \right). \quad (5.13)$$

In the solid-phase chemical potential (5.13), the term $\sum_{m=1}^p G_{KLMN}^{sA} E_{MN}^{sA} x_{k,K}^{sA} x_{l,L}^{sA}$ has not been reported in previous colloidal-media studies. This term implies that the solid-phase chemical potential of the swelling systems is a function of various orders of strain rate.

Performing single-variable linearization about $\dot{\varepsilon}^A, \dot{\varepsilon}^B, u_{k,l}^{K_j}, {}^L\hat{e}^{K_j}, v_k^{K,sA}$ and $u_k^{K_j}$, we obtain the following near-equilibrium equations:

$$\varepsilon^A \rho^{sA} \frac{\partial A_l^{sA}}{\partial \varepsilon^A} + \varepsilon^A \rho^{wA} \frac{\partial A_l^{wA}}{\partial \varepsilon^A} + \varepsilon^B \rho^B \frac{\partial A_l^B}{\partial \varepsilon^A} + \varepsilon^C \rho^C \frac{\partial A_l^C}{\partial \varepsilon^A} - p^{sA} - p^{wA} + p^C = -M^A \dot{\varepsilon}^A, \quad (5.14)$$

$$\varepsilon^A \rho^{sA} \frac{\partial A_l^{sA}}{\partial \varepsilon^B} + \varepsilon^A \rho^{wA} \frac{\partial A_l^{wA}}{\partial \varepsilon^B} + \varepsilon^B \rho^B \frac{\partial A_l^B}{\partial \varepsilon^B} + \varepsilon^C \rho^C \frac{\partial A_l^C}{\partial \varepsilon^B} - p^B + p^C = -M^B \dot{\varepsilon}^B, \quad (5.15)$$

$$\mu^{K_j} \delta_{kl} = C_{klmn}^{K_j} u_{m,n}^{K_j} + A^{K_j} \delta_{kl} - \frac{t_{kl}^{K_j}}{\rho^{K_j}}, \quad K = wA, B, C, \quad (5.16)$$

$$\mu^{L_j} - \mu^{K_j} = \kappa^{LK_j} {}^L\hat{e}^{K_j} - \frac{1}{2} u_l^{L_j} u_l^{L_j} + \frac{1}{2} u_l^{K_j} u_l^{K_j}, \quad K, L = sA, wA, B, C, \quad K \neq L, \quad (5.17)$$

$$\sum_{L=sA,B,C} \varepsilon^K \rho^K {}^L\hat{T}_k^{wA} = -R_{kl}^{wA} v_l^{wA,sA} + p^{wA} \varepsilon^A,_k - \varepsilon^A \rho^{wA} \left(\frac{\partial A_l^{wA}}{\partial \varepsilon^A} \varepsilon^A,_k + \frac{\partial A_l^{wA}}{\partial \varepsilon^B} \varepsilon^B,_k + \frac{\partial A_l^{wA}}{\partial E_{KL}^{sA}} E_{KL}^{sA} + \sum_{m=1}^p \frac{\partial A_l^{wA}}{\partial E_{KL}^{(m)}} E_{KL}^{(m)} \right) \quad (5.18)$$

$$\sum_{\substack{L=sA,wA,B,C \\ L \neq K}} \varepsilon^K \rho^K {}^L\hat{T}_k^K = -R_{kl}^K v_l^{K,sA} + p^K \varepsilon^K,_k - \varepsilon^K \rho^K \left(\frac{\partial A_l^K}{\partial \varepsilon^A} \varepsilon^A,_k + \frac{\partial A_l^K}{\partial \varepsilon^B} \varepsilon^B,_k \right), \quad (5.19)$$

$$K = B, C,$$

$$\sum_{\substack{L=sA,wA,B,C \\ L \neq K}} \varepsilon^K \rho^K \left({}^L\hat{T}_k^{K_j} + \hat{i}_k^{K_j} \right) = -R_{kl}^{K_j} u_l^{K_j} + \mu^{K_j} \left(\varepsilon^K \rho^K \right)_{,k} - \left(\varepsilon^K \rho^K A^{K_j} \right)_{,k}. \quad (5.20)$$

$$K = wA, B, C.$$

The coefficients $M^A, M^B, C_{klmn}^{K_j}, \kappa^{LK_j}, R_{kl}^K$ and $R_{kl}^{K_j}$ are the linearization coefficients of these equations. We did not linearize about $u_k^{sA_j}$ because in our system solid-phase diffusion was

assumed negligible so that $u_k^{sA_j}$ was not an independent variable. Hence, the coefficient of $u_k^{sA_j}$ cannot be a function of $u_k^{sA_j}$.

Total Stress and Heat Flux

The total stress tensor and total thermodynamic pressure at macroscale are obtained by summing over the solid and the liquid phases [30]. These are defined as:

$$t_{kl} = \sum_{K=sA,wA,B,C} \varepsilon^K t_{kl}^K \quad (5.21)$$

$$p = \sum_{K=sA,wA,B,C} \varepsilon^K p^K \quad (5.22)$$

Substituting (5.20) and (5.22) in (5.30) and using (5.31), we obtain:

$$\begin{aligned} t_{kl} = & -p\delta_{kl} + \varepsilon^A \left[t_{kl}^{seA} + t_{kl}^{shA} + \sum_{m=1}^p \left(G_{KLMN}^{sA} E_{KL}^{(m)} x_{k,K}^{sA} x_{l,L}^{sA} \right) + H_{klm}^{sA} T_{,m} \right] \\ & + \sum_{K=wA,B,C} \varepsilon^K \left(v_{klmn}^K d_{mn}^K + H_{klm}^K T_{,m} \right). \end{aligned} \quad (5.23)$$

Here, the second order term $\sum_{j=1}^N \rho^{K_j} u_k^{K_j} u_k^{K_j}$ was neglected because the diffusion velocities are of small magnitude. In the total stress tensor equation (5.32), the $G_{KLMN}^{sA} E_{KL}^{(m)} x_{k,K}^{sA} x_{l,L}^{sA}$ term accounts for the relaxation processes within the solid polymeric matrix. In the previous porous media studies [5-10, 12], this term could not be obtained due to the assumption of an elastic solid phase.

The total heat flux of a particle can be taken as [33]:

$$q_l = \sum_{K=sA,wA,B,C} \varepsilon^K q_l^K \quad (5.24)$$

Substituting (5.21) and (5.23) in (5.33) to eliminate q_l^{sA} and q_l^K we obtain:

$$\begin{aligned} q_l = & \sum_{K=sA,wA,B,C} \sum_{j=1}^N \varepsilon^K \left[t_{kl}^{K_j} u_k^{K_j} - \left(A^{K_j} + \frac{1}{2} u_k^{K_j} u_k^{K_j} \right) \rho^{K_j} u_l^{K_j} \right] + \sum_{K=sA,wA,B,C} \varepsilon^K K_{kl}^K T_{,k} + \\ & \sum_{m=1}^p J_{KLIM}^{sA} x_{l,K}^{sA} E_{LM}^{(m)} + \sum_{K=wA,B,C} \varepsilon^K G_{lmn}^K d_{mn}^K. \end{aligned} \quad (5.25)$$

Given that diffusion velocities are small, the third order term in $u_l^{K_j}$ can be neglected.

Isotropic Stress and Heat Flux

If the solid and liquid phases have isotropic properties, the third order tensors disappear.

The second and fourth-order coefficients follow these relations [32]:

$$\begin{aligned} K_{kl}^K &= K^K \delta_{kl}, \quad \alpha = sA, wA, B, C \\ G_{KLMN}^{sA} &= \lambda^{sA} \delta_{KL} \delta_{MN} + \mu^{sA} (\delta_{KM} \delta_{LN} + \delta_{KN} \delta_{LM}) \\ v_{klmn}^K &= \lambda^K \delta_{kl} \delta_{mn} + \mu^K (\delta_{km} \delta_{ln} + \delta_{kn} \delta_{lm}), \quad K = wA, B, C. \end{aligned} \quad (5.26)$$

Substitute (5.35) in (5.32) and (5.34), and simplify to obtain the following equations for the total stress

$$\begin{aligned} t_{kl} &= -p \delta_{kl} + \varepsilon^A \left[t_{kl}^{seA} + t_{kl}^{shA} + \sum_{m=1}^P \left(\lambda^{sA} E_{MM}^{sA} c_{kl}^{sA^{-1}} + 2\mu^{sA} E_{KL}^{sA} x_{k,K}^{sA} x_{l,L}^{sA} \right) \right] + \\ &\quad \sum_{K=wA, B, C} \varepsilon^K (\lambda^K \delta_{kl} d_{mm}^K + 2\mu^K d_{kl}^K), \end{aligned} \quad (5.27)$$

$$c_{kl}^{sA^{-1}} \equiv x_{k,K}^{sA} x_{l,K}^{sA}, \quad (5.28)$$

(here $c_{kl}^{sA^{-1}}$ is the Finger deformation tensor for the solid phase) and the heat flux

$$q_l = \sum_{K=sA, wA, B, C} \sum_{j=1}^N \varepsilon^K \left[t_{kl}^{Kj} u_k^{Kj} - \left(A^{Kj} + \frac{1}{2} u_k^{Kj} u_k^{Kj} \right) \rho^{Kj} u_l^{Kj} \right] + \sum_{K=sA, wA, B, C} \varepsilon^K K^K T_j. \quad (5.29)$$

Note that the coefficients G_{KLMN}^{sA} , H_{klm}^{sA} , v_{klmn}^K , H_{klm}^K , λ^{sA} , μ^{sA} , λ^K and μ^K are not functions of the local thermal gradients because a two-variable Taylor series expansion was performed. The remaining terms in the stress tensor equations (5.32) and (5.36) depend upon A_l^K , which is a function of temperature but not of temperature gradient. Based upon these equations the stress field inside an anisotropic system is a function of the local thermal gradients. But inside an isotropic system it depends upon temperature only. This simplifies experiments because the anisotropic systems require measurement of material coefficients as a function of local temperature only. In isotropic solids both material coefficients and stress fields require only temperature dependent measurements. In earlier works the material coefficients were a function of the temperature as well as the temperature gradient at different spatial locations, because one

variable Taylor-series expansions were performed. Similarly, in our heat flux equation, the material coefficients are not functions of the strain rate. The strain rate affects heat flux of the anisotropic system only (5.34), but not of the isotropic system (5.38). Similar deductions could be made using one-scale thermoviscoelasticity theory presented in reference [22].

Generalized Darcy's Law

Note that Darcy's law used in porous media literature is often called Fick's law in polymer science literature. Here we let Darcy's law apply to flow of fluid phase and Fick's Law to transport of species. By substituting $\sum_{\substack{L=sA, wA, B, C \\ L \neq K}} {}^L \hat{T}_k^K$ [eqs. (5.28), (5.19)] and t_{kl}^K from (5.22) in the momentum balance equations [(A.12), (A.14)], and neglecting the inertia and the second order terms in $u_l^{K_j}$, we obtain

$$R_{kl}^{wA} v_l^{wA, sA} = -\varepsilon^A p^{wA, k} - \varepsilon^A \rho^{wA} \left(\frac{\partial A_I^{wA}}{\partial \varepsilon^A} \varepsilon^A, k + \frac{\partial A_I^{wA}}{\partial \varepsilon^B} \varepsilon^B, k + \frac{\partial A_I^{wA}}{\partial E_{KL}^{sA}} E_{KL, k}^{sA} \right. \\ \left. + \sum_{m=1}^p \frac{\partial A_I^{wA}}{\partial E_{KL}^{sA}} \overset{(m)}{E}_{KL, k}^{sA} \right) + (\varepsilon^A v_{klmn}^{wA} d_{mn}^{wA})_j + (\varepsilon^A H_{klm}^{wA} T_{,m})_j + \varepsilon^A \rho^{wA} g_k^{wA}, \quad (5.30)$$

$$R_{kl}^K v_l^{K, sA} = -\varepsilon^K p^K, k - \varepsilon^K \rho^K \left(\frac{\partial A_I^K}{\partial \varepsilon^A} \varepsilon^A, k + \frac{\partial A_I^K}{\partial \varepsilon^B} \varepsilon^B, k \right) + (\varepsilon^K v_{klmn}^K d_{mn}^K)_j \\ + (\varepsilon^K H_{klm}^K T_{,m})_j + \varepsilon^K \rho^K g_k^K, \quad K = B, C. \quad (5.31)$$

The thermal gradient term and the last term in (5.30) and (5.31) are new. We will discuss this further subsequently.

Generalized Fick's Law

Substitute $\sum_{\substack{L=sA, wA, B, C \\ L \neq K}} {}^L \hat{T}_k^{K_j} + \hat{i}_k^{K_j}$ from (5.29) and $t_{kl}^{K_j}$ from (5.16) in the momentum balance equations for species [(A.10), (A.13)] and neglect the inertia terms to get

$$R_{kl}^{K_j} u_l^{K_j} = -\varepsilon^K \rho^{K_j} \mu^{K_j, k} + \varepsilon^K \rho^{K_j} g_k^{K_j} + (\varepsilon^K \rho^{K_j} C_{klmn}^{K_j} u_{m,n}^{K_j})_j. \quad (5.32)$$

This form of Fick's law is similar to that obtained for the colloidal systems in previous studies [30]. The last term in (5.40) is often neglected in literature as it is of second order.

Swelling Pressure

Swelling occurs due to liquid transport from the bulk phase, B, to the particles, A. Derjaguin and Churaev [34] defined swelling pressure at mechanical equilibrium to be the difference in pressure between the particle interlayers and the bulk fluid exchanging fluid with the interlayers. Following this definition we take swelling pressure as:

$$\pi^w = \left(\varepsilon^A \rho^{wA} \frac{\partial A_I^{wA}}{\partial \varepsilon^A} - p^B \right) - p^B \quad (5.33)$$

Achanta et al. [7] showed that (5.33) leads to the empirical swelling pressure relationship of Low [1]. This relationship is:

$$\pi^w = A \exp(\delta^s / \delta^w), \quad (5.34)$$

This equation indicates that swelling pressure decays at an exponential rate with increase in spacing between parallel solid platlets (or liquid content of particles).

Eliminating $\varepsilon^A \rho^{wA} \partial A_I^{wA} / \partial \varepsilon^A$ between (5.33) and (5.14) we obtain:

$$\pi^w = p^{wA} - p^B - p^C - M^A \dot{\varepsilon}^A. \quad (5.35)$$

Here we assumed that

$$\frac{\partial A_I^{sA}}{\partial \varepsilon^A} = 0, \quad (5.36)$$

$$\frac{\partial A_I^B}{\partial \varepsilon^A} = \frac{\partial A_I^C}{\partial \varepsilon^A} = 0. \quad (5.37)$$

Assumption (5.36) holds except at the lowest vicinal liquid contents. At very low vicinal liquid content, the layers of liquid molecules will exert stress on the molecules of the solid phase, which would make the free energy of solid phase a function of the liquid content. The assumption (5.37) is true for unconfined bulk fluid phases. This assumption could also be made

for a bulk fluid phase, which is free to move inside a connected porous matrix. Notice that the first three terms on right hand side of (5.35) relate swelling pressure to thermodynamic pressures at thermodynamic equilibrium. $M^A \dot{\varepsilon}^A$ is the near-equilibrium term relating time dependent swelling of the matrix to the swelling pressure. This term is similar to Thomas and Windle's [35] equation (9), used for relating swelling pressure to the Case-II sorption of solvent in the polymeric matrix.

Darcy's Law - Swelling Pressure Relationship

Eliminating $\varepsilon^A \rho^{wA} \partial A_I^{wA} / \partial \varepsilon^A$ and p^{wA} from (5.30) using (5.33) and (5.35), we obtain the following equation for the flow of vicinal fluid:

$$R_{kl}^{wA} v_l^{wA,sA} = -\left(\varepsilon^A \pi^w\right)_{,k} - \varepsilon^A \left(M^A \dot{\varepsilon}^A\right)_{,k} \left(\varepsilon^A v_{klmn}^{wA} d_{mn}^{wA}\right)_{,l} + \left(\varepsilon^A H_{klm}^{wA} T_{,m}\right)_{,l} + \varepsilon^A \rho^{wA} g_k^{wA} - \varepsilon^A \rho^{wA} \left(\frac{\partial A_I^{wA}}{\partial \varepsilon^B} \varepsilon^B_{,k} + \frac{\partial A_I^{wA}}{\partial E_{KL}^{sA}} E_{KL,k}^{sA} + \sum_{m=1}^p \frac{\partial A_I^{wA}}{\partial E_{KL}^{(m)}} E_{KL,k}^{(m)} \right). \quad (5.38)$$

On the right hand side of this equation the first two terms resemble the Darcy's law equation (7) obtained by Achanta et al. [14]. These account for the interaction of the solid matrix with the fluid phase, which leads to time dependent swelling. The third term is called Brinkman's correction in the porous media literature. It accounts for the viscous resistance to the flow of liquid in the fluid boundary layer formed on the surface of the solid. In high velocity flows, this term will have significant magnitude, but it is often neglected at low fluid contents. The fourth term is novel. It gives rise to flow via thermal gradients for anisotropic fluids. For isotropic fluids this term will vanish. In the earlier porous media studies, the coefficient v_{klmn}^w was a function of T_J . Thus, the thermal gradient effect was neglected when the rate of deformation

term was dropped. For anisotropic fluids of low thermal conductivity, the thermal gradient term could be significant in magnitude even when flow velocities are small.

In the second line of (5.38), the first term in brackets appears only when three phases (A, B, C) are present at macroscale. It causes flow of vicinal fluid due to gradient in bulk phase liquid content. The second term in brackets has been reported by [11, 27]. At low moisture contents when a few layers of fluid are present, the free energy of the fluid phase is a function of the shear strain in the solid phase. At high moisture contents, the solid phase alters the liquid free energy only through normal components of the strain tensor and this term reduces to the swelling pressure [11]. The last term is nonlinear in various order time derivatives of strain rate. It couples the effect of near-equilibrium relaxation processes with fluid transport when the time scale of relaxation is similar to the time scale of transport. Such coupling has been suggested for predicting the non-Fickian transport of fluids in polymeric materials [17-19]. Thus, our equations are sufficiently general to describe both Fickian and non-Fickian transport of fluids in porous polymeric media. Using single scale theory of continuum thermodynamics Lustig et al. [20] obtained a similar effect of polymer relaxation on diffusion velocity of low molecular weight fluids. To our knowledge, this is the first attempt to obtain this coupling at the macroscale in a three-scale theory of swelling porous media.

Conclusions

We developed a three-scale theory of swelling viscoelastic systems. At the microscale, we considered interaction of the vicinal fluid with solid matrix. At mesoscale, the homogenized vicinal fluid and solid phase interact with two bulk fluids. The mesoscale particle and bulk fluids form a homogeneous mixture at macroscale. The solid phase was modeled as a

generalized Kelvin-Voigt solid and the liquid phases were assumed viscous. Thus, we accounted for the relaxation processes within the solid matrix, which have been ignored in the previous polymeric porous media studies. The macroscale viscoelastic nature of our system resulted from two micro and mesoscale effects – the relaxation of the solid on the microscale, and the interaction of the solid phase with the viscous fluid at mesoscale and bulk fluids at macroscale. We obtained novel equations for the total stress tensor (5.23), chemical potential of the solid phase (5.13), heat flux (5.29) and generalized Darcy's law for vicinal fluid (5.38), which are applicable to a large class of porous materials. The generalized Darcy's law for vicinal fluid incorporated the effect of stress relaxation on transport of fluid. Literature suggests that such coupling between stress relaxation and fluid transport can describe both Darcian and non-Darcian phenomenon [17-20, 35]. The form of the generalized Fick's law (5.32) remained similar to that obtained in previous colloidal media studies. With two-variable Taylor series expansions, the thermal gradient effects were coupled with the rate of strain tensor of the solid phase and the rate of deformation tensor of the liquid phase. This made material parameters of the equations involving stress tensor and heat flux independent of the thermal gradient effects, and thus their experimental determination becomes easier in comparison to the parameters obtained in the previous porous media studies. Additionally, two-variable linearization helps make clear distinctions between the stress tensor, heat flux and Darcy's law equations for anisotropic and isotropic systems.

Appendix-A

Here we present the macroscale balance laws of Bennethum and Cushman [8], which were obtained by averaging the mesoscale balance laws. The equations for bulk fluid phases have similar form at meso and macroscale.

Mass Balance

The macroscale mass balance equation for the j^{th} species in the particle is:

$$\frac{D^{\alpha A_j} (\varepsilon^A \rho^{\alpha A_j})}{Dt} + \varepsilon^A \rho^{\alpha A_j} v_{l,j}^{\alpha A_j} = \sum_{\substack{L=sA, wA, B, C \\ L \neq \alpha}} \varepsilon^A \rho^{\alpha A_j} {}_L \hat{e}^{\alpha A_j} + \varepsilon^A \rho^{\alpha A_j} \hat{r}^{\alpha A_j}, \quad \alpha = w, s, j = 1..N \quad (\text{A.1})$$

Here, the macroscale variables were obtained by volume, $\langle \rangle^A$, or mass averaging, $\overline{(\)}^A$, the mesoscale variables in the phase A as shown in the following set:

$$\begin{aligned} \rho^{\alpha A_j} &\equiv \left\langle \varepsilon^\alpha \rho^{\alpha_j} \right\rangle^A, \quad v_l^{\alpha A_j} \equiv \overline{v_l^{\alpha_j}}^A, \\ {}_L \hat{e}^{\alpha A_j} &\equiv \frac{1}{\varepsilon^A \rho^{\alpha A_j} |\Delta v|} \int \varepsilon^\alpha \rho^{\alpha_j} \left(v_k|_{AL_j} - v_k^{\alpha_j} \right) n_k^A da, \quad L = B, C, \alpha = s, w \\ {}^{\beta A} \hat{e}^{\alpha A_j} &\equiv \overline{{}^{\beta A} \hat{e}^{\alpha_j}}^A, \quad \hat{r}^{\alpha A_j} \equiv \overline{\hat{r}^{\alpha_j}}^A, \quad \alpha, \beta = sA, wA, \alpha \neq \beta. \end{aligned} \quad (\text{A.2})$$

Here, $|\Delta v|$ is the volume of the macroscale REV, ΔA_{AL} is the surface area of interface between the particle and the bulk fluid, $v_k|_{AL_j}$ is the velocity of the j^{th} component at the particle-bulk fluid interface and n_k^A is the vector normal to the particle.

Summing (A.1) for N species yields:

$$\frac{D^{\alpha A} (\varepsilon^A \rho^{\alpha A})}{Dt} + \varepsilon^A \rho^{\alpha A} v_{l,j}^{\alpha A} = \sum_{\substack{K=sA, wA, B, C \\ K \neq \alpha}} \varepsilon^K \rho^{\alpha A} {}_K \hat{e}^{\alpha A}, \quad \alpha = w, s. \quad (\text{A.3})$$

For the bulk fluid phase the mass balance equations for the species are:

$$\begin{aligned} \frac{D^{K_j} (\varepsilon^K \rho^{K_j})}{Dt} + \varepsilon^K \rho^{K_j} v_{l,j}^{K_j} &= \sum_{\substack{L=sA, wA, B, C \\ L \neq K}} \varepsilon^K \rho^{K_j} {}_L \hat{e}^{K_j} + \varepsilon^K \rho^{K_j} \hat{r}^{K_j}, \\ K &= B, C, j = 1..N \end{aligned} \quad (\text{A.4})$$

Summing (A.4) for N species, we get:

$$\frac{D^K(\varepsilon^K \rho^K)}{Dt} + \varepsilon^K \rho^K v_{l,l}^K = \sum_{\substack{L=sA,wA,B,C \\ L \neq K}} \varepsilon^K \rho^K {}^L \hat{e}^K, \quad K = B, C. \quad (\text{A.5})$$

Relationships between the macroscopic species variables and their bulk counterparts are:

$$\begin{aligned} \rho^K &= \sum_{j=1}^N \rho^{K_j}, \quad C^{K_j} = \frac{\rho^{K_j}}{\rho^K}, \quad v_l^K = \sum_{j=1}^N C^{K_j} v_l^{K_j}, \\ {}^L \hat{e}^K &= \sum_{j=1}^N C^{K_j} {}^L \hat{e}^{K_j}, \quad L \neq K, \quad L, K = sA, wA, B, C. \end{aligned} \quad (\text{A.6})$$

The following restrictions apply:

$$\varepsilon^A + \varepsilon^B + \varepsilon^C = 1 \quad (\text{A.7})$$

$$\sum_{j=1}^N C^{K_j} = 1, \quad \sum_{j=1}^N \rho^{K_j} \hat{r}^{K_j} = 0, \quad (\text{A.8})$$

$$\varepsilon^L \rho^{L_j} {}^K \hat{e}^{L_j} + \varepsilon^K \rho^{K_j} {}^L \hat{e}^{K_j} = 0, \quad K \neq L, \quad K, L = sA, wA, B, C, \quad J = 1..N. \quad (\text{A.9})$$

The $\varepsilon^{\alpha A}$ arising in (A.9) implies ε^A .

Momentum Balance

The macroscale momentum balance equation for the j^{th} species in the particle is:

$$\varepsilon^A \rho^{\alpha A_j} \frac{D^{\alpha A_j} v_l^{\alpha A_j}}{Dt} - (\varepsilon^A t_{kl}^{\alpha A_j})_{,k} - \varepsilon^A \rho^{\alpha A_j} g_l^{\alpha A_j} = \sum_{\substack{L=sA,wA,B,C \\ L \neq \alpha A_j}} \varepsilon^A \rho^{\alpha A_j} {}^L \hat{T}_l^{\alpha A_j} + \varepsilon^A \rho^{\alpha A_j} \hat{t}_l^{\alpha A_j}, \quad (\text{A.10})$$

$$\alpha = w, s, \quad j = 1..N$$

The macroscale variables in (A.10) are related to the mesoscale variables by the following set of equations:

$$\begin{aligned} t_{kl}^{\alpha A_j} &\equiv \left(t_{kl}^{\alpha_j} \right)^A - \rho^{\alpha_j} \overline{v_l^{\alpha_j} v_l^{\alpha_j}}^A, \quad \overline{v_k^{\alpha_j}}^A \equiv v_k^{\alpha A_j} - \overline{v_k^{\alpha_j}}^A, \quad g_l^{\alpha A_j} \equiv \overline{g_l^{\alpha_j}}^A \\ {}^L \hat{T}_l^{\alpha A_j} &\equiv \frac{1}{\varepsilon^A \rho^{\alpha A_j} |\Delta v|_{\Delta A_{AL}}} \int \varepsilon^\alpha \left[t_{kl}^{\alpha_j} + \rho^{\alpha_j} \overline{v_l^{\alpha_j}}^A \left(v_k|_{\Delta L_j} - \overline{v_k^{\alpha_j}}^A \right) \right] n_k^A da, \quad L = B, C \quad (\text{A.11}) \\ \beta A \hat{T}_l^{\alpha A_j} &\equiv \overline{\beta \hat{T}_l^{\alpha_j}}^A + \overline{\beta \hat{e}^{\alpha_j} v_l^{\alpha_j}}^A, \quad \hat{t}_l^{\alpha A_j} \equiv \overline{\hat{t}_l^{\alpha_j}}^A + \overline{\hat{r}^{\alpha_j} v_l^{\alpha_j}}^A, \quad \alpha, \beta = sA, wA, \quad \alpha \neq \beta. \end{aligned}$$

Summing (A.10) from $j = 1$ to N , we get momentum balance equations for the solid and liquid phases present in the particle:

$$\varepsilon^A \rho^{\alpha A} \frac{D^{\alpha A} v_l^{\alpha A}}{Dt} - (\varepsilon^A t_{kl}^{\alpha A})_{,k} - \varepsilon^A \rho^{\alpha A} g_l^{\alpha A} = \sum_{\substack{L=sA, wA, B, C \\ L \neq \alpha A}} \varepsilon^A \rho^{\alpha A} {}^L \hat{T}_l^{\alpha A}, \quad \alpha = w, s. \quad (\text{A.12})$$

For the species present in the bulk fluid phases:

$$\varepsilon^K \rho^{K_j} \frac{D^{K_j} v_l^{K_j}}{Dt} - (\varepsilon^K t_{kl}^{K_j})_{,k} - \varepsilon^K \rho^{K_j} g_l^{K_j} = \sum_{\substack{L=sA, wA, B, C \\ L \neq K}} \varepsilon^K \rho^{K_j} {}^L \hat{T}_l^{K_j} + \varepsilon^K \rho^{K_j} \hat{i}_l^{K_j}, \quad (\text{A.13})$$

$K = B, C, \quad j = 1..N$

Summing (A.13) from $j = 1$ to N , we get:

$$\varepsilon^K \rho^K \frac{D^K v_l^K}{Dt} - (\varepsilon^K t_{kl}^K)_{,k} - \varepsilon^K \rho^K g_l^K = \sum_{\substack{L=sA, wA, B, C \\ L \neq K}} \varepsilon^K \rho^K {}^L \hat{T}_l^K, \quad K = B, C. \quad (\text{A.14})$$

Relation between the macroscopic constituent and the bulk variables are:

$$t_{kl}^K = \sum_{j=1}^N (t_{kl}^{K_j} - \rho^{K_j} u_k^{K_j} u_l^{K_j}), \quad (\text{A.15})$$

$$u_k^{K_j} = v_k^{K_j} - v_k^K \quad (\text{A.16})$$

$$g_l^K = \sum_{j=1}^N C^{K_j} g_l^{K_j}, \quad {}^L \hat{T}_l^K = \sum_{j=1}^N {}^L \hat{T}_l^{K_j}, \quad L, K = sA, wA, B, C, \quad L \neq K. \quad (\text{A.17})$$

Restriction upon the source and sink variables are:

$$\sum_{j=1}^N \rho^{K_j} (\hat{i}_l^{K_j} + \hat{r}^{K_j} v_l^{K_j}) = 0, \quad \varepsilon^K \rho^{K_j} ({}^L \hat{T}_l^{K_j} + {}^L \hat{e}^{K_j} v_l^{K_j}) + \varepsilon^L \rho^{L_j} ({}^K \hat{T}_l^L) = 0, \quad K, L = sA, wA, B, C, \quad K \neq L. \quad (\text{A.18})$$

The $\varepsilon^{\alpha A}$ arising in (A.18) implies ε^A .

Energy Balance

The equation of conservation of energy for the j^{th} species in the particle is:

$$\varepsilon^A \rho^{\alpha A_j} \frac{D^{\alpha A_j} E^{\alpha A_j}}{Dt} - \varepsilon^A t_{kl}^{\alpha A_j} v_{l,k}^{\alpha A_j} - (\varepsilon^A q_l^{\alpha A_j})_{,j} - \varepsilon^A \rho^{\alpha A_j} h^{\alpha A_j} = \sum_{\substack{L=sA, wA, B, C \\ L \neq \alpha A}} \varepsilon^A \rho^{\alpha A_j} {}^L \hat{Q}^{\alpha A_j} + \varepsilon^A \rho^{\alpha A_j} \hat{E}^{\alpha A_j}, \quad \alpha = w, s, \quad j = 1..N \quad (\text{A.19})$$

The macroscale variables in (A.19) are related to the mesoscale variables by the following set of equations:

$$\begin{aligned}
E^{\alpha A_j} &\equiv \overline{E^{\alpha_j} + \frac{1}{2} \widetilde{v}_l^{\alpha_j} \widetilde{v}_l^{\alpha_j}}^A, \\
q_l^{\alpha A_j} &\equiv \left\langle q_l^{\alpha_j} \right\rangle^A + \overline{t_{kl}^{\alpha_j} \widetilde{v}_k^{\alpha_j}}^A - \rho^{\alpha A_j} v_l^{\alpha A_j} \left(\overline{\widetilde{E}^{\alpha_j}}^A + \frac{1}{2} \overline{\widetilde{v}_l^{\alpha_j} \widetilde{v}_l^{\alpha_j}}^A \right)^A, \\
h^{\alpha A_j} &\equiv \overline{h^{\alpha_j} + \widetilde{v}_l^{\alpha_j} g_l^{\alpha_j}}^A, \\
{}^L \hat{Q}^{\alpha A_j} &\equiv \frac{1}{\varepsilon^A \rho^{\alpha A_j} |\Delta V|_{\Delta A_{AL}}} \int \varepsilon^A \left[\rho^{\alpha_j} \left(v_k |_{AL_j} - v_k^{\alpha_j} \right) \left(\overline{\widetilde{E}^{\alpha_j}}^A + \frac{1}{2} \overline{\widetilde{v}_l^{\alpha_j} \widetilde{v}_l^{\alpha_j}}^A \right) \right. \\
&\quad \left. + t_{kl}^{\alpha_j} \widetilde{v}_l^{\alpha_j} + q_k^{\alpha_j} \right] n_k^A da, \quad L = B, C, \\
{}^\beta A \hat{Q}^{\alpha A_j} &\equiv \overline{{}^\beta \hat{Q}^{\alpha_j}}^A + \overline{{}^\beta \hat{T}_l^{\alpha_j} \widetilde{v}_l^{\alpha_j}}^A + \overline{{}^\beta \hat{e}^{\alpha_j}}^A \left(\overline{\widetilde{E}^{\alpha_j}}^A + \frac{1}{2} \overline{\widetilde{v}_l^{\alpha_j} \widetilde{v}_l^{\alpha_j}}^A \right)^A, \\
\hat{E}^{\alpha A_j} &\equiv \overline{\hat{E}^{\alpha_j}}^A + \overline{\hat{t}_l^{\alpha_j} \widetilde{v}_l^{\alpha_j}}^A + \overline{\hat{r}^{\alpha_j}}^A \left(\overline{\widetilde{E}^{\alpha_j}}^A + \frac{1}{2} \overline{\widetilde{v}_l^{\alpha_j} \widetilde{v}_l^{\alpha_j}}^A \right)^A, \\
\alpha, \beta &= sA, wA, \quad \alpha \neq \beta.
\end{aligned} \tag{A.20}$$

Summing (A.19) over N species, we obtain the following equations for the solid and liquid phases forming the particles:

$$\begin{aligned}
\varepsilon^A \rho^{\alpha A} \frac{D^{\alpha A} E^{\alpha A}}{Dt} - \varepsilon^A t_{kl}^{\alpha A} v_{l,k}^{\alpha A} - (\varepsilon^A q_l^{\alpha A})_j - \varepsilon^A \rho^{\alpha A} h^{\alpha A} = \\
\sum_{\substack{L=sA, wA, B, C \\ L \neq \alpha}} \varepsilon^A \rho^{\alpha A} {}^L \hat{Q}^{\alpha A}, \quad \alpha = w, s.
\end{aligned} \tag{A.21}$$

For the species present in the bulk phases:

$$\begin{aligned}
\varepsilon^K \rho^{K_j} \frac{D^K E^K}{Dt} - \varepsilon^K t_{kl}^{K_j} v_{l,k}^{K_j} - (\varepsilon^K q_l^{K_j})_j - \varepsilon^K \rho^{K_j} h^{K_j} = \\
\sum_{\substack{L=sA, wA, B, C \\ L \neq K}} \varepsilon^K \rho^{K_j} {}^L \hat{Q}^{K_j} + \varepsilon^K \rho^{K_j} \hat{E}^{K_j}, \quad K = B, C, \quad j = 1..N,
\end{aligned} \tag{A.22}$$

Summing (A.22) from j = 1 to N, we get:

$$\begin{aligned}
\varepsilon^K \rho^K \frac{D^K E^K}{Dt} - \varepsilon^K t_{kl}^K v_{l,k}^K - (\varepsilon^K q_l^K)_j - \varepsilon^K \rho^K h^K = \\
\sum_{\substack{L=sA, wA, B, C \\ L \neq K}} \varepsilon^K \rho^K {}^L \hat{Q}^K, \quad K = B, C.
\end{aligned} \tag{A.23}$$

The macroscopic constituent variables are related to their bulk counterparts by the following set of equations:

$$\begin{aligned}
 E^K &= \sum_{j=1}^N C^{K_j} (E^{K_j} + \frac{1}{2} u_k^{K_j} u_k^{K_j}), \\
 q_l^K &= \sum_{j=1}^N \left[q_l^{K_j} + t_{kl}^{K_j} u_k^{K_j} - \rho^{K_j} u_l^{K_j} \left(E^{K_j} + \frac{1}{2} u_k^{K_j} u_k^{K_j} \right) \right], \\
 h^K &= \sum_{j=1}^N C^{K_j} \left(h^{K_j} + g_l^{K_j} u_l^{K_j} \right), \\
 {}^L \hat{Q}^K &= \sum_{j=1}^N C^{K_j} \left[{}^L \hat{Q}^{K_j} + {}^L \hat{T}_l^{K_j} u_l^{K_j} + {}^L \hat{e}^{K_j} \left(E^{K_j, K} + \frac{1}{2} u_l^{K_j} u_l^{K_j} \right) \right], \\
 L, K &= sA, wA, B, C, \quad L \neq K.
 \end{aligned} \tag{A.24}$$

The following restrictions apply:

$$\begin{aligned}
 \sum_{j=1}^N \rho^{K_j} \left[\hat{E}^{K_j} + \hat{i}_l^{K_j} v_l^{K_j} + \hat{r}^{K_j} \left(E^{K_j} + \frac{1}{2} v_l^{K_j} v_l^{K_j} \right) \right] &= 0, \\
 \varepsilon^K \rho^{K_j} \left[{}^L \hat{Q}^{K_j} + {}^L \hat{T}_l^{K_j} v_l^{K_j} + {}^L \hat{e}^{K_j} \left(E^{K_j} + \frac{1}{2} v_l^{K_j} v_l^{K_j} \right) \right] + \\
 \varepsilon^L \rho^{L_j} \left[{}^K \hat{Q}^{L_j} + {}^K \hat{T}_l^{L_j} v_l^{L_j} + {}^K \hat{e}^{L_j} \left(E^{L_j} + \frac{1}{2} v_l^{L_j} v_l^{L_j} \right) \right] &= 0, \\
 K, L &= sA, wA, B, C, \quad K \neq L.
 \end{aligned} \tag{A.25}$$

The ε^{wA} arising in (A.25) implies ε^A .

Entropy Production

The equation of entropy balance for the j^{th} species in the particle is:

$$\begin{aligned}
 \varepsilon^A \rho^{\alpha A_j} \frac{D^{\alpha A_j} \eta^{\alpha A_j}}{Dt} - (\varepsilon^A \phi_l^{\alpha A_j})_j - \varepsilon^A \rho^{\alpha A_j} b^{\alpha A_j} = \\
 \sum_{\substack{L=sA, wA, B, C \\ L \neq \alpha}} \varepsilon^A \rho^{\alpha A_j} {}^L \hat{\phi}^{\alpha A_j} + \varepsilon^A \rho^{\alpha A_j} \hat{\eta}^{\alpha A_j} + \varepsilon^A \rho^{\alpha A_j} \Lambda^{\alpha A_j}, \quad \alpha = w, s, \quad j = 1..N
 \end{aligned} \tag{A.26}$$

The macroscopic variables in (A.26) are related to the mesoscale variables by the following set of equations:

$$\begin{aligned}
\eta^{\alpha A_j} &\equiv \overline{\eta^{\alpha_j}}^A, b^{\alpha A_j} \equiv \overline{b^{\alpha_j}}^A, \phi_l^{\alpha A_j} \equiv \left(\phi_l^{\alpha_j} \right)^A - \rho^{\alpha A_j} \overline{\eta^{\alpha_j}}^A, \\
{}^L \hat{\phi}^{\alpha A_j} &\equiv \frac{1}{\varepsilon^A \rho^{\alpha A_j} |\Delta v|_{\Delta A_{AL}}} \int \varepsilon^A \left[\phi_k^{\alpha_j} + \rho^{\alpha_j} \overline{\eta^{\alpha_j}}^A \left(v_k|_{AL_j} - v_k^{\alpha_j} \right) \right] n_k^A da, \quad L = B, C, \\
{}^B \hat{\phi}^{\alpha A_j} &\equiv \overline{{}^B \hat{\phi}^{\alpha_j}}^A + \overline{{}^B \hat{e}^{\alpha_j}}^A \overline{\eta^{\alpha_j}}^A, \hat{\eta}^{\alpha A_j} \equiv \overline{\hat{\eta}^{\alpha_j}}^A + \overline{{}^B \hat{e}^{\alpha_j}}^A \overline{\eta^{\alpha_j}}^A, \\
\Lambda^{\alpha A_j} &= \overline{\Lambda^{\alpha_j}}^A \quad \alpha, \beta = sA, wA, \quad \alpha \neq \beta.
\end{aligned} \tag{A.27}$$

Summing (A.26) from $j = 1$ to N , we obtain:

$$\begin{aligned}
\varepsilon^A \rho^{\alpha A} \frac{D^{\alpha A} \eta^{\alpha A}}{Dt} - (\varepsilon^A \phi_l^{\alpha A})_j - \varepsilon^A \rho^{\alpha A} b^{\alpha A} &= \sum_{\substack{L=sA, wA, B, C \\ L \neq \alpha A}} \varepsilon^A \rho^{\alpha A L} \hat{\phi}^{\alpha A} + \varepsilon^A \rho^{\alpha A} \Lambda^{\alpha A}, \\
&\quad \alpha = w, s.
\end{aligned} \tag{A.28}$$

The entropy balance equation for the species present in the bulk fluids is:

$$\begin{aligned}
\varepsilon^K \rho^K \frac{D^K \eta^K}{Dt} - (\varepsilon^K \phi_l^K)_j - \varepsilon^K \rho^K b^K &= \\
\sum_{\substack{L=sA, wA, B, C \\ L \neq K}} \varepsilon^K \rho^K L \hat{\phi}^K + \varepsilon^K \rho^K \hat{\eta}^K + \varepsilon^K \rho^K \Lambda^K, \quad K = B, C, \quad j = 1..N
\end{aligned} \tag{A.29}$$

Summing (A.29) over N species, we get:

$$\begin{aligned}
\varepsilon^K \rho^K \frac{D^K \eta^K}{Dt} - (\varepsilon^K \phi_l^K)_j - \varepsilon^K \rho^K b^K &= \\
\sum_{\substack{L=sA, wA, B, C \\ L \neq K}} \varepsilon^K \rho^K L \hat{\phi}^K + \varepsilon^K \rho^K \Lambda^K, \quad K = B, C.
\end{aligned} \tag{A.30}$$

The relations between the macroscale constituent and bulk variables is:

$$\begin{aligned}
\eta^K &= \sum_{j=1}^N C^{K_j} \eta^{K_j}, \phi_l^K = \sum_{j=1}^N \left(\phi_l^{K_j} - \rho^{K_j} \eta^{K_j} u_l^{K_j} \right), \\
b^K &= \sum_{j=1}^N C^{K_j} b^{K_j}, {}^L \hat{\phi}^K = \sum_{j=1}^N C^{K_j} \left({}^L \hat{\phi}^{K_j} + {}^L \hat{e}^{K_j} \eta^{K_j, K} \right), \\
\Lambda^K &= \sum_{j=1}^N C^{K_j} \Lambda^{K_j} \quad L, K = sA, wA, B, C, \quad L \neq K.
\end{aligned} \tag{A.31}$$

The following restrictions apply to the entropy balance equations:

$$\begin{aligned} \sum_{j=1}^N \rho^{K_j} \left[\hat{\eta}^{K_j} + \hat{r}^{K_j} \eta^{K_j} \right] &= 0, \\ \varepsilon^K \rho^{K_j} \left({}^L \hat{\phi}^{K_j} + {}^L \hat{e}^{K_j} \eta^{K_j} \right) + \varepsilon^L \rho^{L_j} \left({}^K \hat{\phi}^{L_j} + {}^K \hat{e}^{L_j} \eta^{L_j} \right) &= 0, \\ K, L = sA, wA, B, C, \quad K \neq L. \end{aligned} \quad (\text{A.32})$$

Total Entropy Inequality

The entropy inequality states that the net rate of generation of entropy inside the universe is always greater than or equal to zero. Thus, at macroscale all independent processes taking place inside the body must satisfy the following inequality:

$$\rho \Lambda = \sum_{j=1}^N \left(\varepsilon^A \rho^{wA_j} \Lambda^{wA_j} + \varepsilon^A \rho^{sA_j} \Lambda^{sA_j} + \varepsilon^B \rho^B \Lambda^B + \varepsilon^C \rho^C \Lambda^C \right) \geq 0 \quad (\text{A.33})$$

We assume that at each spatial location inside the body, different phases are at local thermal equilibrium. The temperature is allowed to vary from one spatial location to the other

$$T^{sA_j} = T^{wA_j} = T^B = T^C = T. \quad (\text{A.34})$$

We also assume the sources of entropy are solely due to heat flux and the body source of heat. Thus, our system is thermomechanically a simple system

$$\phi_i^{K_j} = \frac{q_i^{K_j}}{T}, \quad b^{K_j} = \frac{h^{K_j}}{T}, \quad K = sA, wA, B, C. \quad (\text{A.35})$$

Since entropy cannot be directly measured from experiments, a Legendre transformation is performed on E^{K_j} to convert it into the Helmholtz free energy, A^{K_j} , which is a function of temperature

$$A^{K_j} = E^{K_j} - T\eta^{K_j} \quad (\text{A.36})$$

Summing A^{K_j} over the N components, we obtain the inner part of the total Helmholtz free energy

$$A_I^K = \sum_{j=1}^N C^{K_j} A^{K_j}. \quad (\text{A.37})$$

Eliminating h^{K_j} between the equations of energy and entropy balance and simplifying, we get the following entropy inequality. The $\varepsilon^{\alpha A}$ in this equation implies ε^A .

$$\begin{aligned}
T\rho\Lambda = & - \sum_{K=sA,wA,B,C} \varepsilon^K \rho^K \left(\frac{D^K A_I^K}{Dt} + \eta^K \frac{D^K T}{Dt} \right) \\
& + \sum_{K=sA,wA,B,C} \varepsilon^K d_{kl}^K \left(t_{kl}^K + \sum_{j=1}^N \rho^{K_j} u_k^{K_j} u_l^{K_j} \right) \\
& + \sum_{K=sA,wA,B,C} \sum_{j=1}^N \varepsilon^K u_{k,l}^{K_j} \left(t_{kl}^{K_j} - \rho^{K_j} A^{K_j} \delta_{kl} \right) \\
& + \sum_{K=sA,wA,B,C} \frac{\varepsilon^K T_{,l}}{T} \left\{ q_l^K + \sum_{j=1}^N \left[\rho^{K_j} u_l^{K_j} \left(A^{K_j} + \frac{1}{2} u_k^{K_j} u_k^{K_j} \right) - t_{kl}^{K_j} u_k^{K_j} \right] \right\} \\
& - \sum_{K=sA,wA,B,C} \sum_{j=1}^N u_l^{K_j} \left[\varepsilon^K \rho^{K_j} \hat{i}_l^{K_j} + \sum_{\substack{L=sA,wA,B,C \\ L \neq K}} \varepsilon^K \rho^{K_j} {}^L \hat{T}_l^{K_j} + (\varepsilon^K \rho^{K_j} A^{K_j})_{,l} \right] \\
& - \sum_{K=sA,wA,B,C} \sum_{\substack{L=sA,wA,B,C \\ K \neq L}} \varepsilon^K \rho^K {}^L \hat{T}_l^K v_l^{K,sA} \\
& - \frac{1}{2} \sum_{K=sA,wA,B,C} \sum_{j=1}^N \varepsilon^K \rho^{K_j} u_l^{K_j} u_l^{K_j} \left(\sum_{\substack{L=sA,wA,B,C \\ L \neq K}} {}^L \hat{e}^{K_j} + \hat{r}^{K_j} \right) \\
& - \sum_{K=sA,wA,B,C} \sum_{\substack{L=sA,wA,B,C \\ L \neq K}} \varepsilon^K \rho^K {}^L \hat{e}^K \left(A_l^K + \frac{1}{2} v_l^{K,sA} v_l^{K,sA} \right) \geq 0. \tag{A.38}
\end{aligned}$$

here,

$$d_{kl}^K = \frac{1}{2} (v_{k,l}^K + v_{l,k}^K), \quad K = sA, wA, B, C. \tag{A.39}$$

Appendix-B

Latin Symbols

A^{K_j} Helmholtz free energy of the j^{th} component in the K phase
 A_I^K Inner part of the Helmholtz free energy of the K phase
 b^{K_j} External entropy source for the j^{th} component in the K phase
 b^K External entropy source for the K phase
 $c_{kl}^{SA^{-1}}$ Finger deformation tensor of the solid phase at macroscale
 C^{K_j} Mass concentration of the j^{th} component in the K phase ($= \rho^{K_j} / \rho^K$)
 $C_{klmn}^{K_j}$ Material coefficient in equation (5.16)
 d_{kl}^K Rate of deformation tensor of the K phase
 ${}^L\hat{e}^{K_j}$ Net mass transfer from the phase L to the j^{th} component in the K phase
 ${}^L\hat{e}^K$ Net mass transfer from the phase L to the K phase
 E^{K_j} Internal energy of the j^{th} component in the K phase
 E^K Internal energy of the K phase
 \hat{E}^{K_j} Energy gained by the j^{th} component from other components in the same phase
 E_{KL}^{SA} Lagrangian strain tensor of the solid phase at macroscale
 $E_{KL}^{(m)SA}$ m^{th} order material derivative of the E_{KL}^{SA} with respect to the macroscale solid phase velocity
 $g_l^{K_j}$ Gravitational force on the j^{th} component in the K phase
 g_l^K Gravitational force on the K phase
 G^K Gibbs free energy for the phase K

G_{lmn}^K Material coefficient in equation (5.23)

G_{klmN}^{sA} Material coefficient in equation (5.17)

h^{K_j} Net external energy source for the j^{th} component in the K phase

h^K Net external energy source for the α phase

H_{klm}^{sA} Material coefficient in equation (5.17)

H_{klm}^K Material coefficient in equation (5.22)

$\hat{i}_l^{K_j}$ Momentum transfer to the j^{th} component due to interaction with other components in the same phase

J_{klm}^{sA} Material coefficient in equation (5.5)

K_{kl}^K Thermal conductivity tensor of the K phase

K^K Isotropic thermal conductivity of the phase K

p^α Thermodynamic pressure in the α phase

p Total thermodynamic pressure for the homogenized mixture at macroscale

$q_l^{K_j}$ Heat flux vector for the j^{th} component in the K phase

q_l^K Heat flux vector for the K phase

q_l Total heat flux vector for the homogenized mixture of particles and bulk fluids at macroscale

${}^L\hat{Q}^{K_j}$ Net heat gained by the j^{th} component in the phase K from the phase L

${}^L\hat{Q}^K$ Net heat gained by the phase K from the phase L

\hat{r}^{K_j}	Mass transfer to the j^{th} component due to interaction with other components in the same phase
$R_{kl}^{K_j}$	Material coefficient in equation (5.29)
R_{kl}^{wA}	Material coefficient in equations (5.28)
R_{kl}^K	Material coefficient in equations (5.19)
REV	Representative elementary volume
t	Time
$t_{kl}^{K_j}$	Stress tensor of the j^{th} component in the phase K
t_{kl}^K	Stress tensor of the phase K
t_{kl}	Total stress tensor for the homogeneous mixture of particles and bulk fluids at macroscale
t_{kl}^{seA}	Terzaghi stress
t_{kl}^{shA}	Hydration stress
T^{K_j}	Temperature of the j^{th} component in the phase K
T	Temperature
${}^L\hat{T}_l^{K_j}$	Momentum transfer to the j^{th} component in the phase K due to mechanical interactions with the phase L
${}^L\hat{T}_l^K$	Momentum transfer to the phase K due to mechanical interactions with the phase L
$u_k^{K_j}$	Diffusion velocity of the j^{th} component in the phase K
$v_l^{K_j}$	Velocity of the j^{th} component in the phase K
v_l^K	Velocity of the K phase

x_k^K Eulerian coordinate in the phase K

X_K^K Lagrangian coordinate in the phase K

Greek Symbols

δ_{kl} Kronecker delta function in Eulerian coordinates

δ_{KL} Kronecker delta function in Lagrangian coordinates

ε^α Mesoscale volume fraction of the phase α

ε^K Macroscale volume fraction of the phase K

η^{K_j} Entropy of the j^{th} component in the K phase

η^K Entropy of the K phase

$\hat{\eta}^{K_j}$ Entropy gained by the j^{th} component in a phase by interaction with other components in the same phase

δ^w Thickness of the water layer between solid platlets. See Fig. 2.

δ^s Thickness of solid platlets. See Fig. 2.

κ^{LK_j} Material coefficient in equation (5.26)

λ^s, λ^K Isotropic material coefficients. See equation (5.35)

μ^s, μ^K Isotropic material coefficients. See equation (5.35)

Λ^{K_j} Net entropy production for the j^{th} component in the K phase

Λ^K Net entropy production in the K phase

Λ Net entropy production in the system at macroscale

μ^{K_j} Chemical potential of the j^{th} component in the K phase

ρ^{K_j} Density of the j^{th} component in the K phase

ρ^K Density of the K phase

π^w Swelling pressure due to interaction of particle A with the bulk fluid B

$\phi_l^{K_j}$ Entropy flux vector for the j^{th} component in the K phase

ϕ_l^K Entropy flux vector for the K phase

${}^L\hat{\phi}^{K_j}$ Entropy transfer to the j^{th} component in the K phase from the L phase

${}^L\hat{\phi}^K$ Entropy transfer to the K phase from the L phase

v_{klmn}^{wA} Material coefficient in equation (5.22)

Subscripts

D Dissipative

eq Equilibrium

neq Near equilibrium

k, l Eulerian coordinate indices

K, L Lagrangian coordinate indices

Superscripts

sA solid component of particle at macroscale

wA water (or liquid) component of particle at macroscale

B, C bulk fluid phases

α, β General representation of phases at mesoscale

K, L General representation of phases at macroscale

j A given component of species

Special Symbols

$\frac{D^{K_j}}{Dt}$ Material derivative of a function with respect to velocity of j^{th} component in the K phase

$\frac{D^K}{Dt}$ Material derivative of a function with respect to velocity of the K phase

$v_i^{K,sA}$ Velocity of the K phase relative to the solid phase at macroscale ($= v_i^K - v_i^{sA}$)

$$E^{K_j,K} = E^{K_j} - E^K$$

References

- [1] P.F. Low, *Langmuir*. **3**, 18 (1987).
- [2] U. Hornung, *Homogenization and porous media*. Interdisciplinary applied mathematics ; v. 6. 1997, New York: Springer.
- [3] J.H. Cushman, *The physics of fluids in hierarchical porous media : angstroms to miles. Theory and applications of transport in porous media* ; v. 10. 1997, Dordrecht ; Boston: Kluwer Academic Publishers.
- [4] B.D. Coleman and W. Noll, *Arch.* **13**, 167 (1963).
- [5] S.M. Hassanzadeh and W.G. Gray, *Adv. Wat. Resour.* **2**, 131 (1979).
- [6] S.M. Hassanzadeh and W.G. Gray, *Adv. Wat. Resour.* **2**, 191 (1979).
- [7] S. Achanta, J.H. Cushman, and M.R. Okos, *Int. J. Engng Sci.* **32**, 1717 (1994).
- [8] L.S. Bennethum and J.H. Cushman, *Int. J. Engng Sci.* **34**, 125 (1996).
- [9] L.S. Bennethum and J.H. Cushman, *Int. J. Engng Sci.* **34**, 147 (1996).
- [10] M.A. Murad, L.S. Bennethum, and J.H. Cushman, *Transp. Porous Media*. **19**, 93 (1995).
- [11] M.A. Murad and J.H. Cushman, *Int. J. Engng Sci.* **34**, 313 (1996).
- [12] M.A. Murad and J.H. Cushman, *Transp. Porous Media*. **28**, 69 (1997).
- [13] M.A. Murad and J.H. Cushman, *Int. J. Engng Sci.* **38**, 517 (2000).
- [14] S. Achanta, M.R. Okos, J.H. Cushman, and D.P. Kessler, *A.I.Ch.E.J.* **43**, 2112 (1997).
- [15] L.S. Bennethum, M.A. Murad, and J.H. Cushman, *Transp. Porous Media*. **39**, 187 (2000).
- [16] J.D. Ferry, *Viscoelastic properties of polymers*. 3d ed. 1980, New York: Wiley. pp:1.
- [17] G.S. Hartley, *Transactions of the Faraday Society*. **45**, 820 (1949).
- [18] G.S. Park, *Transactions of the Faraday Society*. **46**, 684 (1950).
- [19] L. Mandelkern and F.A. Long, *J. Polym. Sci.* **6**, 457 (1951).

- [20] S.R. Lustig, J.M. Caruthers, and N.A. Peppas, *Chemical Engineering Science.* **47**, 3037 (1992).
- [21] P.P. Singh, J.H. Cushman, and D.E. Maier, *Submitted to: Transp. Porous Media.* (2001).
- [22] A.C. Eringen, *Mechanics of continua.* 2d ed. 1980, Huntington, N.Y.: R. E. Krieger Pub. Co.
- [23] R.M. Bowen, *Int. J. Engng Sci..* **20**, 697 (1982).
- [24] P.F. Low and J.F. Margheim, *Soil Sci. Soc. Am. J..* **43**, 473 (1979).
- [25] P.F. Low, *Soil Sci. Soc. Am. J..* **44**, 667 (1980).
- [26] P.F. Low, *Soil Sci. Soc. Am. J..* **45**, 1074 (1981).
- [27] L.S. Bennethum and T. Giorgi, *Transp. Porous Media.* **26**, 261 (1997).
- [28] I.S. Liu, *Arch. Rat. Mech. Anal..* **46**, 131 (1972).
- [29] S.M. Hassanzadeh and W.G. Gray, *Adv. Wat. Resour..* **3**, 25 (1980).
- [30] L.S. Bennethum, M.A. Murad, and J.H. Cushman, *Comput. Geotech..* **20**, 245 (1997).
- [31] L.S. Bennethum, J.H. Cushman, and M.A. Murad, *Int. J. Engng Sci..* **34**, 1611 (1996).
- [32] L.A. Segel and G.H. Handelman, *Mathematics applied to continuum mechanics.* 1977, New York: Macmillan.
- [33] L.S. Bennethum and J.H. Cushman, *Transp. Porous Media.* **36**, 211 (1999).
- [34] B.V. Derjaguin and N.V. Churaev, *J. Colloid Interf. Sci..* **66**, 389 (1978).
- [35] N.L. Thomas and A.H. Windle, *Polymer.* **23**, 529 (1982).

III. Multicomponent, multiphase thermodynamics of swelling porous media with electroquasistatics: Macroscale field equations

Multicomponent, Multiphase Thermodynamics of Swelling Porous Media with Electroquasistatics:

I. Macroscale Field Equations

Lynn Schreyer Bennethum * John H. Cushman †

March 5, 2001

Abstract

A systematic development of the macroscopic field equations (conservation of mass, linear and angular momentum, energy, and Maxwell's equations) for a multiphase, multicomponent medium is presented. It is assumed that speeds involved are much slower than the speed of light and that the magnitude of the electric field significantly dominates over the magnetic field so that the electroquasistatic form of Maxwell's equations applies. A mixture formulation is presented for each phase and then averaged to obtain the macroscopic formulation. Species electric fields are considered, however it is assumed that it is the total electric field which contributes to the electrically induced forces and energy. The relationships between species and bulk phase variables and the macroscopic and microscopic variables are given explicitly. The resulting field equations are of relevance to many practical applications including, but not limited to, swelling clays (smectites), biopolymers, biological membranes, pulsed electrophoresis, and chromatography.

Key words: porous media, mixture theory, electrodynamics, averaging, swelling

1 Introduction

We attempt to address the following issue: in a composite or porous medium, how do the electro-thermodynamic variables of each individual constituent contribute to the electro-thermodynamic variables of the mixture as a whole? In other words, given information about individual materials, determine the relationship between the electro-thermodynamic properties of individual components and the electro-thermodynamic properties of the averaged multi-phase

*University of Colorado at Denver, Center for Computational Mathematics, Campus Box 170, P.O. Box 173364, Denver, CO 80217-3364. bennethum@math.cudenver.edu. To whom correspondence should be addressed.

†Center for Applied Math, Math Sciences Building, Purdue University, W. Lafayette, IN 47907.

multi-component material. We combine mixture theory and averaging to obtain macroscopic field equations for a deformable porous medium in which species may induce different electric fields but forces on the species are determined by the net electric field of the mixture.

The constituent forms of Maxwell's equations were first developed by Kellogg [24], although he did not consider deformable media. A binary mixture of electro-magnetic fluids has been used to model plasma with single electric and magnetic fields, see e.g. Kulsrud [25]. Benach and Müller [2] applied single electric and magnetic fields to model a mixture of dielectric fluids. The idea of using multiple electric fields has been used historically in modeling a binary mixture of superconducting fluids [9]. Eringen [14] developed a mixture theoretic approach for a multiple constituent electro-magnetic deformable medium with multiple electro-magnetic fields and applied the model to combinations of conducting/superconducting fluids and elastic solids. This article differs from [14] in that multiple phases are considered, a different philosophy is taken in the electric fields of constituents accounting for energy and momentum balance, and the mixture may swell. Mixture theory alone does not allow for this development. An upscaling approach is required to map microscopic information into well-defined macroscopic variables.

On the microscale one can distinguish between phases or materials, while the macroscale is defined to be the scale at which the material appears to be homogeneous. There are several upscaling techniques to choose between: homogenization (matched asymptotics) [5, 12, 35], volume averaging in the sense of Whitaker [31, 33, 34, 41, 42], spectral integral methods [17], generalized Taylor-Aris methods [7], and hybrid mixture theory [1, 3, 21, 22]. All but the latter of these methods upscale field equations and constitutive equations from the microscale to the macroscale. The hybrid mixture theoretic approach that we adapt does not upscale constitutive relations.

We present constituent, or species, electro-quasistatic equations for a mixture, give the relationship between the species and single-phase properties, and then volume average these governing equations for a multicomponent, multi-phase medium to obtain the governing equations for the medium at the macroscale. At this scale, the medium is viewed as a continuum where thermodynamic properties for each constituent of each phase exist spatially everywhere. The relationships between the microscale variables and the macroscale variables are explicitly given. For ease of exposition we assume that interfacial properties such as excess mass density, free charge on interfaces, and interface currents, are negligible; although the present theory can be extended to incorporate these effects [19]. The medium is referred to as multi-phase, but it is understood that this includes composites (e.g. a medium composed of two solid materials), or a porous medium, where the multiphases may be gas, immiscible liquids, and/or solid.

Maxwell's equations involve species electric fields, but the macroscale momentum and energy equations for species are based on the philosophy that the force or work induced by the electric field acting on a species is generated by the *total* electric field. This differs from what has been done in the past [14, 24].

The species electric fields are defined through Gauss' Law since the charge and polarization density are well defined for a species. The species electric fields then manifest themselves in the macroscale equations through terms involving gradients or time-rate-of-change of the volume fraction.

The resulting field equations may be used to obtain restrictions on admissible constitutive relations by applying the methods of either extended thermodynamics [30], or rational thermodynamics [13, 10]. The need for these equations, and the explicit relationships between the macroscopic and microscopic variables is demonstrated by the increasingly complex porous media being studied. Recent examples include Huyghe and Janssen [23] and Gu *et al.* [20] who both use a simplified version of the equations developed herein to model an incompressible porous medium composed of an electrically charged solid phase saturated with an ionic fluid.

2 Microscale Equations

In this section we present the governing field equations at the microscale. The equations include mass balance, conservation of linear and angular momentum, conservation of energy, entropy balance, and Maxwell's equations. The complete form of these equations for a bulk phase (single phase with no species) are given by Eringen [15] and Tiersten [38], and here we follow their formulation and notation. The derivation of these equations follows from the particle level in the spirit of Lorentz [27].

It is assumed that the dominant field source is the electric field and that velocities are small compared to the speed of light (non-relativistic). Following Melcher [28], the electroquasistatic system of equations are obtained by non-dimensionalizing Maxwell's equations, expanding each variable in a Taylor series about the variable representing the ratio of the electromagnetic wave transit time to the characteristic time of the problem, and taking the zero-order equations as the quasi-static formulation. The difference between the electroquasistatic formulation and the magneto-quasistatic formulation arises in the choice of the normalizing parameters: in the former a reference electric field is used, and in the latter a reference magnetic field is used.

It is necessary to postulate governing field equations which hold for each species. Following Truesdell [40], we adhere to the following principles: (1) all properties of the mixture must be mathematical consequences of properties of the constituents; (2) to describe the motion of a constituent, we may perceive it as being isolated from the rest of the mixture, provided we allow properly for the actions of the other constituents; (3) the motion of the mixture is governed by the same equations as is a single body. Further, due to the incorporation of electric fields, some assumptions must be made regarding the form of the momentum and energy balance laws. It is assumed that (4) the "primitive" form of the balance laws is the one incorporating the work and force, and not, e.g. the electro-stress tensors. This is in contrast to [8, 26] in which the electro-magnetic stresses are considered the primitive quantity. The forms are equivalent up to the

classical Maxwell's equations, but are not equivalent in the mixture formulation. Hence, until experiments prove otherwise, the choice is purely philosophical. The last principle is that (5) within the electrical work and force terms in the energy and momentum balance equations respectively, it is the *total* electric field which acts on the species, and not just the electric field associated with the species. This last assumption guarantees that principles (1), (2), and (3) are not violated.

Although the form of the equations for the constituents is natural for some balance laws (conservation of mass, conservation of charge density), it leads to un-intuitive variables in other equations, e.g. the partial stress tensor. However, we do not want to mix bulk phase equations with constitutive equations, and hence formulate constitutive equations for all field equations. To account for the effects of the other constituents, exchange terms, denoted by variables with a carrot $\hat{\cdot}$, are introduced.

The species' equations can then be summed to obtain the governing equation for the phase, and the relationship between the species properties and their bulk phase counterparts are then obtained. The details regarding this procedure for the field equations with no electric or magnetic effects can be found in Truesdell and Toupin [39] or Bowen [6]. For the parallel development of Maxwell's equations, see Kelly [24].

We now present the governing equations for a mixture in a single phase at the microscale assuming electroquasistatics. The relationships between the species' variables and the bulk phase variables are obtained by summing the field equation over all constituents and relating the variables so as to obtain the field equation at the bulk scale. These relationships are given in Appendix B.

Conservation of Mass

$$\frac{D^j(\rho^j)}{Dt} + \rho^j(\nabla \cdot \mathbf{v}^j) = \rho^j\hat{r}^j \quad (1)$$

where $\frac{D^j}{Dt}$ is the material time derivative given by

$$\frac{D^j}{Dt} = \frac{\partial}{\partial t} + \mathbf{v}^j \cdot \nabla \quad (2)$$

and where \hat{r}^j is the rate of mass transfer to species j from other species due to chemical reactions. Summing over constituents we obtain the bulk phase equation

$$\frac{D\rho}{Dt} + \rho(\nabla \cdot \mathbf{v}) = 0 \quad (3)$$

with the restriction

$$\sum_{j=1}^N \rho^j\hat{r}^j = 0. \quad (4)$$

This restriction merely states that within an isolated system consisting of a single phase there is no net loss of mass.

Gauss' Law

For this equation we introduce the electric field for species j , \mathbf{E}^j . Gauss' law for constituent j can then be expressed as

$$\nabla \cdot \mathbf{D}^j - q_e^j = \hat{d}^j \quad (5)$$

where \mathbf{D}^j is the displacement vector for the j th component only, q_e^j is the charge density of constituent j , and \hat{d}^j is the excess charge density due to the presence of other species. The displacement vector for constituent j is defined in terms of the electric field and polarization density as:

$$\mathbf{D}^j = \epsilon_0 \mathbf{E}^j + \mathbf{P}^j, \quad (6)$$

where ϵ_0 is the permittivity in a vacuum. In MKS units, the permittivity has the value of 8.854×10^{-12} Farads per meter [28].

The species' electric field, \mathbf{E}^j , must satisfy the restriction that the total electric field, \mathbf{E} , is the sum of the species' electric field, i.e. $\sum_{j=1}^N \mathbf{E}^j = \mathbf{E}$. If there is no external electric field then \mathbf{E} is just the electric field generated by all the species. There is no unique way of incorporating the externally applied electric field into these equations. One could treat the external electric field as the presence of another species, say species N , in which this "external" species has no other electro-thermodynamic properties. Then species N would have no charge density, no associated polarization, etc. and these terms would be set to zero in the governing equations. Alternately, a portion of the external field could be assigned to each \mathbf{E}^j so that \mathbf{E}^j is the sum of the electric field generated by species j and a weight, w^j , times the external electric field. The weights must sum to one, and may, for example, be proportional to the amount of charge, or maybe the mass fraction of species j . A third choice might be that the species electric field is defined such that the exchange term \hat{d}^j is zero. This would simplify computations down the road although its physical interpretation is not clear. These choices have no affect on the following derivation, as long as \mathbf{E}^j sum to the total electric field. However, in formulating a mathematical model it is necessary to choose a particular definition and remain consistent.

Summing over constituents gives the bulk phase Gauss law:

$$\nabla \cdot \mathbf{D} - q_e = 0 \quad (7)$$

where $\mathbf{D} = \sum_{j=1}^N \mathbf{D}^j$ and with the restriction

$$\sum_{j=1}^N \hat{d}^j = 0. \quad (8)$$

which states that the net effect of excess charge densities produced by the species acting on each other must sum to zero.

Faraday's Law

Faraday's law for the quasi-static case for species j is given by

$$\nabla \times \mathbf{E}^j = \hat{\sigma}^j \quad \text{or} \quad E_{k,l}^j - E_{l,k}^j = \varepsilon_{lkm} \hat{\sigma}_m^j, \quad (9)$$

where the second form of the equation is in indicial notation with repeated indices denoting summation, a comma denotes differentiation, and ε_{lkm} is the permutation tensor. Here $\hat{\sigma}^j$ incorporates the effect of the electric fields, \mathbf{E}^i , $i \neq j$.

Summing over species gives the bulk phase Faraday's law,

$$\nabla \times \mathbf{E} = \mathbf{0}, \quad (10)$$

where $\mathbf{E} = \sum_{j=1}^N \mathbf{E}^j$ is the total electric field. This relationship is assumed throughout. The required restriction obtained from this summation is that

$$\sum_{j=1}^N \hat{\sigma}^j = \mathbf{0}. \quad (11)$$

Ampère's Law

Ampère's law for the quasi-static case for species j is given by

$$\mathbf{J}^j = -\frac{\partial \mathbf{D}^j}{\partial t} + \nabla \times \mathbf{H}^j - \nabla \times (\mathbf{P}^j \times \mathbf{v}^j) + \hat{\mathbf{h}}^j \quad (12)$$

where \mathbf{H}^j is the magnetic field intensity and $\hat{\mathbf{h}}^j$ accounts for the effects of other constituents.

Summing over species gives the bulk phase version of this law,

$$\mathbf{J} = -\frac{\partial \mathbf{D}}{\partial t} + \nabla \times c\mathbf{H} - \nabla \times (\mathbf{P} \times \mathbf{v}) \quad (13)$$

where

$$\sum_{j=1}^N \hat{\mathbf{h}}^j = \mathbf{0}. \quad (14)$$

Conservation of Electric Charge

This equation can be derived by taking the divergence of Ampère's law and the time derivative of Gauss' Law and summing the results. Of all Maxwell's equations, this equation is the most accepted in mixture form since each component has a well defined physical interpretation. The conservation of electric charge for species j is

$$\nabla \cdot (\mathcal{J}^j + q_e^j \mathbf{v}^j) + \frac{\partial q_e^j}{\partial t} = \tilde{q}^j + \rho^j z^j \hat{r}^j, \quad (15)$$

where \mathbf{v}^j is the velocity of species j relative to a fixed frame of reference, \mathcal{J}^j is the free current density of constituent j measured relative to species j , z^j is the charge per unit mass and \tilde{q}^j is the rate of gain of charge density due to the presence of other constituents but not due to chemical reactions. The free current density, denoted by \mathcal{J}^j , is related to the free current density relative to a fixed (Eulerian) frame of reference, \mathbf{J}^j , by

$$\mathcal{J}^j = \mathbf{J}^j - q_e^j \mathbf{v}^j. \quad (16)$$

Another form of this equation is obtained by subtracting out the conservation of mass to reduce redundancy, and this yields

$$\rho^j \frac{D^j z^j}{Dt} + \nabla \cdot \mathcal{J}^j = \tilde{q}^j. \quad (17)$$

Summing over constituents yields

$$\nabla \cdot (\mathcal{J} + q_e \mathbf{v}) + \frac{\partial q_e}{\partial t} = 0, \quad (18)$$

where

$$\sum_{j=1}^N [\tilde{q}^j + \rho^j z^j \tilde{r}^j] = 0. \quad (19)$$

This equation states that the net gain or loss of total charge of constituent j due to ion transfer or chemical reactions is zero in an isolated system.

In addition, because of the coupling between Gauss' law, Ampère's law, and the conservation of charge, there is a coupling between the exchange terms:

$$\nabla \cdot \tilde{\mathbf{h}}^j - \frac{\partial \tilde{d}^j}{\partial t} = \tilde{q}^j + q_e^j \tilde{r}^j.$$

Linear Momentum Balance

This equation is given by

$$\rho^j \frac{D^j \mathbf{v}^j}{Dt} - \nabla \cdot \mathbf{t}^j - \rho^j \mathbf{g}^j - q_e^j \mathbf{E} - \mathbf{P}^j \cdot \nabla \mathbf{E} = \rho^j \tilde{\mathbf{i}}^j \quad (20)$$

where \mathbf{t}^j is the partial Cauchy stress tensor and \mathbf{g}^j is the external body force acting on constituent j . The exchange term, $\tilde{\mathbf{i}}^j$, takes into account all gain of momenta due to the presence of other species but not due to chemical reactions. The last term on the left-hand-side is usually referred to as the Kelvin force, and the adjacent term (on the LHS) is referred to as the Lorentz force [15]. Note that unlike [14, 24] we assume it is the *total* electric field which contributes to these forces.

Summing over constituents gives the conservation of linear momentum for the entire phase,

$$\rho \frac{D \mathbf{v}}{Dt} - \nabla \cdot \mathbf{t} - \rho \mathbf{g} - q_e \mathbf{E} - \mathbf{P} \cdot \nabla \mathbf{E} = \mathbf{0}. \quad (21)$$

In this form \mathbf{t} is the Cauchy stress tensor and is related to the partial Cauchy stress tensors, \mathbf{t}^j , in the same way as the purely thermo-mechanical mixture theory (no electric field). This is what naturally appears in the energy conservation equation given below, i.e. if other terms are incorporated into the definition of the bulk phase stress tensor, then these additional terms must be subtracted out where the stress tensor appears in the conservation of energy and the restriction must be modified. The specific relationship between the constitutive variables and the bulk phase variables are given in Appendix B. The restriction for the conservation of linear momentum is:

$$\sum_{j=1}^N [\rho^j \hat{\mathbf{i}}^j + \rho^j \mathbf{v}^j \hat{\mathbf{r}}^j] = \mathbf{0} \quad (22)$$

The restriction states that the net momentum gained between species due to mass transfer or mechanical momentum must be zero.

Angular Momentum Balance

In indicial notation, the angular momentum equation is

$$\epsilon_{klm} t_{kl}^j + \epsilon_{klm} P_k^j E_l = -\rho^j \hat{m}_m^j, \quad (23)$$

where \hat{m}_m^j is the m th component of the net rate of gain of angular momentum due to the presence of other species. The negative sign on the right hand side is in keeping with the convention that exchange terms (in this case \hat{m}^j) represents a rate of *gain* of a property.

Summing over constituents yields

$$\epsilon_{klm} t_{kl} + \epsilon_{klm} P_k E_l = 0_m \quad (24)$$

with the restriction that

$$\sum_{j=1}^N \rho^j \hat{m}^j = \mathbf{0}. \quad (25)$$

This equation states that the net internal angular momentum for this single-phase medium, consisting of the sum of angular momenta generated by species acting on each other, must be zero.

Conservation of Energy

The species energy balance is

$$\begin{aligned} \rho^j \frac{D^j e^j}{Dt} - \mathbf{t}^j : \nabla \mathbf{v}^j - \nabla \cdot \mathbf{q}^j - \rho^j h^j - \mathcal{J}^j \cdot \mathbf{E} - \frac{\partial \mathbf{P}^j}{\partial t} \cdot \mathbf{E} \\ - [\nabla \cdot (\mathbf{v}^j \mathbf{P}^j)] \cdot \mathbf{E} = \rho^j \hat{Q}^j \end{aligned} \quad (26)$$

where the colon indicates a tensor dot product (e.g. $\underline{\underline{a}} : \underline{\underline{b}} = \sum_{i,j} a_{ij} b_{ij}$) and \hat{Q}^j is the rate of energy gain due to the presence of other constituents but not due to chemical reactions (mass transfer) or momentum transfer. The sum of the last

three terms on the left-hand-side is the electrical energy source. As in the linear momentum balance we assume that electric energy is due to the *total* electric field, not just part of it. These three terms take on a variety of forms [15, 28] which are related through the Maxwell equations (Gauss' law, Faraday's law, Ampère's Law, and Conservation of Electric Charge). The form presented here is the one derived directly from microscale electrical forces using a statistical averaging approach (see Eringen [15]) making no use of Maxwell's equations, since otherwise exchange terms (\hat{d}^j , $\hat{\sigma}^j$, \hat{q}^j) appear.

Summing over constituents yields

$$\rho \frac{De}{Dt} - t : \nabla v - \nabla \cdot q - \rho h - \mathcal{J} \cdot E - \frac{\partial P}{\partial t} \cdot E - [\nabla \cdot (vP)] \cdot E = 0 \quad (27)$$

with the restriction

$$\sum_{j=1}^N \left[\rho^j \hat{Q}^j + \rho^j v^j \cdot \hat{i}^j + (e^j + \frac{1}{2} v^j \cdot v^j) \rho^j \hat{r}^j \right] = 0. \quad (28)$$

Entropy Balance

The entropy balance equation is one way of representing the second law of thermodynamics:

$$\rho^j \frac{D^j \eta^j}{Dt} - \nabla \cdot \phi^j - \rho^j b^j = \rho^j \hat{\eta}^j + \rho^j \hat{\Lambda}^j \quad (29)$$

where $\hat{\eta}^j$ is the rate of transfer of entropy from other constituents. Here $\hat{\Lambda}^j$ is the rate at which entropy is generated.

Summing over constituents yields

$$\rho \frac{D\eta}{Dt} - \nabla \cdot \phi - \rho b = \rho^j \hat{\Lambda} \quad (30)$$

with the restriction

$$\sum_{j=1}^N \left[\rho^j \hat{\eta}^j + \rho^j v^j \hat{r}^j \right] = 0. \quad (31)$$

It is postulated that the total rate of entropy generation, obtained by summing over all species, is non-negative. All relations for this equation remain unaltered from the purely thermo-mechanical mixture theory.

3 Macroscale Equations

In this section we average the microscale equations and obtain equations at the macroscale. At the macroscale, each thermodynamic variable is defined spatially everywhere, so that if there are 3 phases, with each phase containing N constituents, the medium is viewed as $3N$ overlaying continua. The first subsection discusses the notation and assumptions required to upscale, and the following

subsections present the macroscale field equations and how each variable relates to the microscale. To the authors' knowledge, the electroquasistatic equations have not been presented before.

3.1 Averaging Procedure

Consider a multi-constituent multi-phase medium where the phase is denoted by Greek letters (α, β, γ), and the constituent or species is denoted by $j, j = 1, \dots, N$. For ease of exposition we assume that interfaces contain no thermodynamic properties. Consequently it is assumed no amount of mass, momentum, energy, charge, current, etc. is lost when being transferred between phases. Interfacial effects can be included by pursuing any of the approaches of [18, 19, 29], however, we shall omit these terms to keep the level of algebra at a minimum.

The governing microscopic equations for each phase were given in Section 2, but to distinguish between phases we introduce the additional Greek superscript.

Assuming no surface discontinuities, the constituent, microscopic field equations of mass, charge, linear momentum, angular momentum, energy, and entropy can be expressed for a given phase, α , as (following the notation of Eringen, [13]):

$$\frac{\partial}{\partial t}(\rho^j \psi^j) + \nabla \cdot (\rho^j \mathbf{v}^j \psi^j) - \nabla \cdot \mathbf{i}^j - \rho^j f^j - F^j = \rho^j G^j + \rho^j \hat{\psi}^j \quad (32)$$

where ψ^j is the mass-average (over the phase) thermodynamic property of constituent j , \mathbf{v}^j is the mass-average velocity vector, ρ^j is the mass density, \mathbf{i}^j is the flux vector, f^j is the body source, F^j is the supply due to electrical effects, G^j is the net production, and $\hat{\psi}^j$ represents the influx of ψ from all other constituents (e.g. due to chemical reactions). If there is only one constituent, $\hat{\psi}^j$ is zero. For each of the respective equations, the quantities given in Table 1 are used.

Table 1: Quantities for Equation (32)

Quantity	ψ	\mathbf{i}	f	F	$\hat{\psi}$	G
Mass	1	0	0	0	\hat{r}	0
Charge	z	\mathcal{J}	0	0	$\hat{q} + \rho z \hat{r}$	0
Linear Momentum	\mathbf{v}	t	$\mathbf{g} + \mathbf{g}_I$	\mathbf{F}_e	$\hat{\mathbf{i}} + \hat{r}\mathbf{v}$	0
Angular Momentum	$\mathbf{r} \times \mathbf{v}$	$\mathbf{r} \times t$	$\mathbf{r} \times \mathbf{g}$	$\mathbf{r} \times \mathbf{F}_e + \mathbf{C}_e$	$\mathbf{r} \times (\hat{\mathbf{i}} + \hat{r}\mathbf{v})$	0
Energy	$e + \frac{1}{2}v^2$	$\mathbf{t}\mathbf{v} + \mathbf{q}$	$\mathbf{g} \cdot \mathbf{v} + h$	W_e	$\hat{Q} + \hat{\mathbf{i}} \cdot \mathbf{v} + \hat{r}(e + \frac{1}{2}v^2)$	0
Entropy	η	ϕ	b	0	$\hat{\eta} + \hat{r}\mathbf{v}$	Λ

For conciseness we also introduce the force, couple, and work due to the electric field, respectively:

$$\mathbf{F}_e^j = q_e^j \mathbf{E} + \mathbf{P}^j \cdot \nabla \mathbf{E} \quad (33)$$

$$\begin{aligned}
 &= -\nabla \cdot \left(\mathbf{D}^j \mathbf{E} - \frac{1}{2} \varepsilon_0 \mathbf{E}^j \cdot \mathbf{E} \mathbf{I} \right) + \hat{\mathbf{d}}^j \mathbf{E} + \frac{1}{2} \varepsilon_0 (\nabla \mathbf{E} \cdot \mathbf{E}^j - \nabla \mathbf{E}^j \cdot \mathbf{E}) \quad (34) \\
 \mathbf{C}_e^j &= \mathbf{P}^j \times \mathbf{E} \quad (35)
 \end{aligned}$$

$$W_e^j = \mathbf{J}^j \cdot \mathbf{E} + \frac{\partial \mathbf{P}^j}{\partial t} \cdot \mathbf{E} + \nabla \cdot (\mathbf{v}^j \mathbf{E} \cdot \mathbf{P}^j) \quad (36)$$

$$\begin{aligned}
 &= \frac{\partial}{\partial t} \left(-\frac{1}{2} \varepsilon_0 \mathbf{E}^j \cdot \mathbf{E} \right) - \nabla \cdot (\mathbf{E} \times \mathbf{H}^j) + \nabla \cdot (\mathbf{P}^j \mathbf{v}^j \cdot \mathbf{E}) \\
 &\quad + \hat{\mathbf{h}}^j \cdot \mathbf{E} - \frac{1}{2} \varepsilon_0 \left(\frac{\partial \mathbf{E}^j}{\partial t} \cdot \mathbf{E} - \frac{\partial \mathbf{E}}{\partial t} \cdot \mathbf{E}^j \right) \quad (37)
 \end{aligned}$$

(see also equations (20,23,26)). Definitions of all terms are given in Appendix A. The forms of \mathbf{F}_e^j and W_e^j are a consequence of which form one assumes to be the most primitive. If one assumes that the second forms of \mathbf{F}_e^j and W_e^j , (34, 37), are the most primitive then miscellaneous terms would appear in the first forms. The two forms are needed in order to obtain conditions which correspond directly with jump boundary conditions across an interface. The averaging procedure is based on ideas laid down in [16, 41, 42, 37]. Several methods are available, but we choose the computationally simplest. Equations are averaged by weighted integration using the indicator function of the α -phase. To avoid the mathematical difficulties of, for example, defining a derivative of the averaged quantities resulting from using such a weighting function, one must treat the averaged quantity as a distribution [36, 32].

It should be noted that using this simple weight function may mean that the averaged value may not represent the actual values being measured. To account for the measuring technique, one needs to choose a weight function which represents the instrument used to measure the physical properties [11]. Extensions of the presented theory to such cases are straight forward.

Let δV be a volume, δV_α the portion of δV in the α -phase, and $\delta A_{\alpha\beta}$ the portion of the interface within δV . It is assumed that δV_α and $\delta A_{\alpha\beta}$ are isolated simply connected regions. If the magnitude of δV is denoted by $|\delta V|$ then the volume fraction can be expressed as

$$\varepsilon^\alpha(\mathbf{x}, t) = \frac{|\delta V_\alpha|}{|\delta V|} \quad (38)$$

so that

$$\sum_\alpha \varepsilon^\alpha = 1. \quad (39)$$

The indicator function is

$$\gamma_\alpha(\mathbf{r}, t) = \begin{cases} 1 & \text{if } \mathbf{r} \in \delta V_\alpha \\ 0 & \text{if } \mathbf{r} \in \delta V_\beta, \quad \beta \neq \alpha. \end{cases}$$

We may write $\mathbf{r} = \mathbf{x} + \boldsymbol{\xi}$ where \mathbf{x} is the macroscale spatial variable, and $\boldsymbol{\xi}$ varies over δV . To obtain the macroscale equations formally, one multiplies

equation (2) by $\gamma_\alpha(\mathbf{r})$, integrates over δV with respect to ξ (x is held fixed) and divides by $|\delta V|$. Then in order to obtain equations of the forms which mirror the microscale equations, the following theorem is applied to interchange the order of differentiation and integration.

Theorem 1 *If $w_{\alpha\beta}$ is the microscopic velocity of interface $\alpha\beta$ and \mathbf{n}_α is the outward unit normal vector of δV_α indicating the integrand should be evaluated in the limit as the $\alpha\beta$ -interface is approached from the α -side then*

$$\frac{1}{|\delta V|} \int_{\delta V} \frac{\partial f}{\partial t} \gamma_\alpha dv(\xi) = \frac{\partial}{\partial t} \left[\frac{1}{|\delta V|} \int_{\delta V} f \gamma_\alpha dv(\xi) \right] - \sum_{\beta \neq \alpha} \frac{1}{|\delta V|} \int_{\delta A_{\alpha\beta}} f w_{\alpha\beta} \cdot \mathbf{n}_\alpha da(\xi) \quad (40)$$

$$\frac{1}{|\delta V|} \int_{\delta V} \nabla_r f \gamma_\alpha dv(\xi) = \nabla_x \left[\frac{1}{|\delta V|} \int_{\delta V} f \gamma_\alpha dv(\xi) \right] + \sum_{\beta \neq \alpha} \frac{1}{|\delta V|} \int_{\delta A_{\alpha\beta}} f \mathbf{n}_\alpha da(\xi). \quad (41)$$

After averaging equation (32), the system is considered to be a mixture so that each component in each phase and each bulk phase now have thermodynamic properties existing at each point within the macroscopic body. The macroscopic definition of each field variable in terms of its microscopic counterpart, making *no small perturbation assumptions*, is given in Appendix C.

For more details regarding this procedure for the field equations with no electric or magnetic effects see for example Whitaker [41], Slattery [37] and Plumb and Whitaker [31]. For the parallel development of Maxwell's equations with constitutive assumptions, see Rio and Whitaker [33, 34].

3.2 Macroscopic Conservation Equations

Conservation of Mass

The macroscopic mass balance for constituent j in phase α is

$$\frac{D^{\alpha_j} (\varepsilon^\alpha \rho^{\alpha_j})}{Dt} + \varepsilon^\alpha \rho^{\alpha_j} (\nabla \cdot \mathbf{v}^{\alpha_j}) = \sum_{\beta \neq \alpha} \varepsilon^\alpha \rho^{\alpha_j} \hat{e}_\beta^{\alpha_j} + \varepsilon^\alpha \rho^{\alpha_j} \hat{r}^{\alpha_j} \quad (42)$$

where $\frac{D^{\alpha_j}}{Dt}$ is the material time derivative given by

$$\frac{D^{\alpha_j}}{Dt} = \frac{\partial}{\partial t} + \mathbf{v}^{\alpha_j} \cdot \nabla, \quad (43)$$

and $\hat{e}_\beta^{\alpha_j}$ represents the net rate of mass gained by constituent j in phase α from phase β :

$$\hat{e}_\beta^{\alpha_j} = \frac{1}{\rho^{\alpha_j} |\delta V_\alpha|} \int_{\delta A_{\alpha\beta}} \rho^j (w_{\alpha\beta}^j - \mathbf{v}^j) \cdot \mathbf{n}^\alpha da, \quad (44)$$

where $w_{\alpha\beta}^j$ is the velocity of species j at interface $\alpha\beta$.

The bulk phase counterpart is given by

$$\frac{D^\alpha(\varepsilon^\alpha \rho^\alpha)}{Dt} + \varepsilon^\alpha \rho^\alpha (\nabla \cdot \mathbf{v}^\alpha) = \sum_{\beta \neq \alpha} \varepsilon^\alpha \rho^\alpha \hat{e}_\beta^\alpha. \quad (45)$$

The net gain of mass of the bulk phase must be zero, implying that:

$$\sum_{j=1}^N \rho^{\alpha_j} \hat{r}^{\alpha_j} = 0 \quad \forall \alpha. \quad (46)$$

Further, since the interface is assumed to be massless, we have the restriction:

$$\varepsilon^\alpha \rho^{\alpha_j} \hat{e}_\beta^{\alpha_j} + \varepsilon^\beta \rho^{\beta_j} \hat{e}_\alpha^{\beta_j} = 0, \quad j = 1, \dots, N. \quad (47)$$

Using (45) we can re-write (42) as

$$\varepsilon^\alpha \rho^\alpha \frac{D^\alpha C^{\alpha_j}}{Dt} + \nabla \cdot (\varepsilon^\alpha \rho^{\alpha_j} \mathbf{v}^{\alpha_j, \alpha}) = \sum_{\beta \neq \alpha} \varepsilon^\alpha \rho^{\alpha_j} (\hat{e}_\beta^{\alpha_j} - \hat{e}_\beta^\alpha) + \varepsilon^\alpha \rho^{\alpha_j} \hat{r}^{\alpha_j}. \quad (48)$$

Gauss' Law

The macroscopic form of Gauss' law for constituent j in phase α is

$$\nabla \cdot (\varepsilon^\alpha \mathbf{D}^{\alpha_j}) - \varepsilon^\alpha q_e^{\alpha_j} = \varepsilon^\alpha \hat{d}_\beta^{\alpha_j} + \sum_{\beta \neq \alpha} \varepsilon^\alpha \hat{d}_\beta^{\alpha_j} \quad (49)$$

where \mathbf{D}^{α_j} is the volume average of \mathbf{D}^j . Here $\hat{d}_\beta^{\alpha_j}$ represents the effect constituent j in phase β has on the charge of the same constituent in phase α :

$$\hat{d}_\beta^{\alpha_j} = -\frac{1}{|\delta V_\alpha|} \int_{\delta A_{\alpha\beta}} \mathbf{D}^j \cdot \mathbf{n}^\alpha \, da. \quad (50)$$

Other relations are given in Appendix C.

Summing over j yields the bulk phase form:

$$\nabla \cdot (\varepsilon^\alpha \mathbf{D}^\alpha) - \varepsilon^\alpha q_e^\alpha = \sum_{\beta \neq \alpha} \varepsilon^\alpha \hat{d}_\beta^\alpha. \quad (51)$$

The restrictions include

$$\sum_{j=1}^N \hat{d}^{\alpha_j} = 0 \quad \forall \alpha \quad (52)$$

$$\varepsilon^\alpha \hat{d}_\beta^{\alpha_j} + \varepsilon^\beta \hat{d}_\alpha^{\beta_j} = 0, \quad j = 1, \dots, N. \quad (53)$$

The first restriction states that the net effect constituents have on each other within phase α must be zero, and the second states that the interfacial displacement is zero, which is a consequence of assuming that the interface contains no

electric/thermodynamical properties. Recall that if there is no surface charge or polarization the jump condition between two materials states that the jump in the normal component of the displacement vector must be zero [15]:

$$\mathbf{n} \cdot [[\mathbf{D}]] = 0. \quad (54)$$

Integrating this equation over $\delta A_{\alpha\beta}$ shows that this theory is consistent with the classical formulation for the jump condition, equation (53).

Faraday's Law

The macroscopic form of Faraday's law for constituent j in phase α is

$$\nabla \times (\varepsilon^\alpha \mathbf{E}^{\alpha j}) = \varepsilon^\alpha \hat{\sigma}^{\alpha j} + \sum_{\beta \neq \alpha} \varepsilon^\alpha \hat{\sigma}_\beta^{\alpha j} \quad (55)$$

or in indicial notation

$$(\varepsilon^\alpha E_k^{\alpha j})_{,l} - (\varepsilon^\alpha E_l^{\alpha j})_{,k} = \varepsilon_{lkm} \varepsilon^\alpha \hat{\sigma}_m^{\alpha j} + \sum_{\beta \neq \alpha} \varepsilon_{lkm} \varepsilon^\alpha (\hat{\sigma}_\beta^{\alpha j})_m \quad (56)$$

where

$$\hat{\sigma}_\beta^{\alpha j} = -\frac{1}{|\delta V_\alpha|} \int_{\delta A_{\alpha\beta}} \mathbf{n}^\alpha \times \mathbf{E}^j da, \quad (57)$$

which represents the effect phase β has on the electric field of phase α . Upon summing, the bulk phase form of Faraday's law becomes:

$$\nabla \times (\varepsilon^\alpha \mathbf{E}^\alpha) = \sum_{\beta \neq \alpha} \varepsilon^\alpha \hat{\sigma}_\beta^\alpha \quad (58)$$

with restrictions

$$\sum_{j=1}^N \hat{\sigma}^{\alpha j} = 0 \quad \forall \alpha \quad (59)$$

$$\varepsilon^\alpha \hat{\sigma}_\beta^{\alpha j} + \varepsilon^\beta \hat{\sigma}_\alpha^{\beta j} = 0 \quad j = 1, \dots, N. \quad (60)$$

Equation (60) corresponds precisely with the classical jump condition across interfaces [15]

$$\mathbf{n} \times [[\mathbf{E}]] = \mathbf{0}, \quad (61)$$

where the double square brackets indicate the difference of the quantity evaluated on either side of the interval, if (61) is integrated over the surface $\delta A_{\alpha\beta}$.

Ampère's Law The macroscopic form of Ampère's law for the quasi-static case for species j of phase α is given by

$$\varepsilon^\alpha \mathbf{J}^{\alpha j} = -\frac{\partial(\varepsilon^\alpha \mathbf{D}^{\alpha j})}{\partial t} + \nabla \times (\varepsilon^\alpha \mathbf{H}^{\alpha j}) - \nabla \times (\varepsilon^\alpha \mathbf{P}^{\alpha j} \times \mathbf{v}^{\alpha j}) + \sum_{\beta \neq \alpha} \varepsilon^\alpha \hat{\mathbf{h}}_\beta^{\alpha j} + \varepsilon^\alpha \hat{\mathbf{h}}^{\alpha j} \quad (62)$$

where

$$\hat{\mathbf{h}}_\beta^{\alpha j} = \frac{1}{|\delta V_\alpha|} \int_{\delta A_{\alpha\beta}} \left[\mathbf{D}^j \mathbf{w}_{\alpha\beta}^j \cdot \mathbf{n}^\alpha - (\mathbf{H}^j - \mathbf{P}^j \times \mathbf{v}^j) \times \mathbf{n}^\alpha \right] da \quad (63)$$

represents the effect of phase β on phase α . Summing over species gives the bulk phase version of this law,

$$\varepsilon^\alpha \mathbf{J}^\alpha = -\frac{\partial(\varepsilon^\alpha \mathbf{D}^\alpha)}{\partial t} + \nabla \times \varepsilon^\alpha \mathbf{H}^\alpha - \nabla \times (\varepsilon^\alpha \mathbf{P}^\alpha \times \mathbf{v}^\alpha) + \sum_{\beta \neq \alpha} \varepsilon^\alpha \hat{\mathbf{h}}_\beta^\alpha \quad (64)$$

where the restrictions are

$$\sum_{j=1}^N \hat{\mathbf{h}}^{\alpha j} = \mathbf{0} \quad \forall \alpha \quad (65)$$

$$\varepsilon^\alpha \hat{\mathbf{h}}_\beta^{\alpha j} + \varepsilon^\beta \hat{\mathbf{h}}_\alpha^{\beta j} = \mathbf{0} \quad j = 1, \dots, N. \quad (66)$$

The jump condition associated with Ampère's law is given by [15]:

$$\mathbf{n} \times [[\mathbf{H} - \mathbf{w} \times \mathbf{D}]] = \mathbf{0} \quad (67)$$

where the polarization at the surface has been neglected. Equation (63) does not correspond directly with the jump condition given in [15] since (67) is derived directly from the global surface area form of Ampère's law, and (63) is derived from the bulk-phase form of the law. This causes a loss of information; specifically, (63) does not include a term corresponding to $\mathbf{w}^j(\mathbf{n} \cdot \mathbf{D}^j)$.

Conservation of Electric Charge

The conservation of charge equation at the macroscale becomes

$$\begin{aligned} \nabla \cdot (\varepsilon^\alpha \mathcal{J}^{\alpha j} + \varepsilon^\alpha q_e^{\alpha j} \mathbf{v}^{\alpha j}) + \frac{\partial}{\partial t} (\varepsilon^\alpha q_e^{\alpha j}) &= \varepsilon^\alpha \hat{q}^{\alpha j} + \varepsilon^\alpha \rho^{\alpha j} z^{\alpha j} \hat{r}^{\alpha j} \\ &+ \sum_{\beta \neq \alpha} \varepsilon^\alpha \rho^{\alpha j} (\hat{Z}_\beta^{\alpha j} + z^{\alpha j} \hat{e}_\beta^{\alpha j}) \end{aligned} \quad (68)$$

where

$$\begin{aligned} \hat{Z}_\beta^{\alpha j} &= \frac{1}{\rho^{\alpha j} |\delta V_\alpha|} \int_{\delta A_{\alpha\beta}} \left[q_e^j (\mathbf{w}_{\alpha\beta}^j - \mathbf{v}^j) - \mathcal{J}^j \right] \cdot \mathbf{n}^\alpha da \\ &- \frac{z^{\alpha j}}{\rho^{\alpha j} |\delta V_\alpha|} \int_{\delta A_{\alpha\beta}} \left[\rho^j (\mathbf{w}_{\alpha\beta}^j - \mathbf{v}^j) \right] \cdot \mathbf{n}^\alpha da \end{aligned} \quad (69)$$

which represents the rate of exchange of charge of constituent j from phase β to phase α not due to mass exchange. Using the continuity equation, (42), equation (68) may be re-written as:

$$\varepsilon^\alpha \rho^{\alpha_j} \frac{Dz^{\alpha_j}}{Dt} + \nabla \cdot (\varepsilon^\alpha \mathcal{J}^{\alpha_j}) = \varepsilon^\alpha \hat{q}^{\alpha_j} + \sum_{\beta \neq \alpha} \varepsilon^\alpha \rho^{\alpha_j} \hat{Z}_\beta^{\alpha_j} \quad (70)$$

Summing over constituents yields

$$\nabla \cdot (\varepsilon^\alpha \mathcal{J}^\alpha + \varepsilon^\alpha q_e^\alpha \mathbf{v}^\alpha) + \frac{\partial}{\partial t} (\varepsilon^\alpha q_e^\alpha) = \sum_{\beta \neq \alpha} \varepsilon^\alpha \rho^\alpha (\hat{Z}_\beta^\alpha + z^\alpha \hat{e}_\beta^\alpha), \quad (71)$$

where the following restrictions apply

$$\sum_{j=1}^N [\hat{q}^{\alpha_j} + \rho^{\alpha_j} z^{\alpha_j} \hat{r}^{\alpha_j}] = 0 \quad \forall \alpha \quad (72)$$

$$\varepsilon^\alpha \rho^{\alpha_j} (\hat{Z}_\beta^{\alpha_j} + z^{\alpha_j} \hat{e}_\beta^{\alpha_j}) + \varepsilon^\beta \rho^{\beta_j} (\hat{Z}_\alpha^{\beta_j} + z^{\beta_j} \hat{e}_\alpha^{\beta_j}) = 0 \quad j = 1, \dots, N. \quad (73)$$

Equation (73) corresponds precisely with the classical jump condition across a discontinuous interface [15]:

$$\mathbf{n} \cdot [[\mathcal{J} + q_e(\mathbf{v} - \mathbf{w})]] = 0. \quad (74)$$

Linear Momentum Balance

The macroscale linear momentum equation is given by

$$\begin{aligned} & \varepsilon^\alpha \rho^{\alpha_j} \frac{D^{\alpha_j} \mathbf{v}^{\alpha_j}}{Dt} - \nabla \cdot (\varepsilon^\alpha \mathbf{t}^{\alpha_j}) - \varepsilon^\alpha \rho^{\alpha_j} (\mathbf{g}^{\alpha_j} + \mathbf{g}_I^{\alpha_j}) - \varepsilon^\alpha q_e^{\alpha_j} \mathbf{E}_T \\ & + \frac{1}{2} \varepsilon_0 \mathbf{E}_T \cdot \mathbf{E}^{\alpha_j} \nabla \varepsilon^\alpha - \varepsilon^\alpha \mathbf{P}^{\alpha_j} \cdot \nabla \mathbf{E}_T = \varepsilon^\alpha \rho^{\alpha_j} \hat{\mathbf{i}}^{\alpha_j} + \sum_{\beta \neq \alpha} \varepsilon^\alpha \rho^{\alpha_j} \hat{\mathbf{T}}_\beta^{\alpha_j} \end{aligned} \quad (75)$$

where \mathbf{E}_T is the upscaled (total) electric field and is related to the species

electric field by $\mathbf{E}_T = \sum_{j=1}^N \sum_\alpha \varepsilon^\alpha \mathbf{E}^{\alpha_j}$, and

$$\begin{aligned} \hat{\mathbf{T}}_\beta^{\alpha_j} = & \frac{1}{\rho^{\alpha_j} |\delta V_\alpha|} \int_{\delta A_{\alpha\beta}} \left[(\mathbf{t}^j)^T + \mathbf{E} \mathbf{D}^j - \frac{1}{2} \varepsilon_0 \mathbf{E}^j \cdot \mathbf{E} I + \rho^j \mathbf{v}^j (\mathbf{w}_{\alpha\beta}^j - \mathbf{v}^j) \right] \cdot \mathbf{n}^\alpha da \\ & - \frac{\mathbf{v}^{\alpha_j}}{\rho^{\alpha_j} |\delta V_\alpha|} \int_{\delta A_{\alpha\beta}} \rho^j (\mathbf{w}_{\alpha\beta}^j - \mathbf{v}^j) \cdot \mathbf{n}^\alpha da + \frac{1}{\rho^{\alpha_j}} \hat{d}_\beta^{\alpha_j} \mathbf{E}_T \end{aligned} \quad (76)$$

represents the effect constituent j of phase β has on the rate of change of mechanical momentum of the same constituent in phase α . The relation between the other macroscale variables and their microscale counterparts are given in Appendix C.

There are a couple of additional forces in this form compared to the classical form due to the introduction of the species electric field, \mathbf{E}^{α_j} , and the volume fraction ε^α . The first we consider an additional (internal) body force, \mathbf{g}_I . It is due to the difference between \mathbf{E} and \mathbf{E}^j (see Appendix C), and so if the source of the electric field is dominated by one charged species, then this term is negligible. The other additional term involves the gradient of the volume fraction. If the medium is homogeneous in volume fraction (ε^α is constant), then this term is zero. The form of this equation is motivated by the form of $\hat{\mathbf{T}}_\beta^{\alpha_j}$, which we choose to be consistent with the jump condition associated with momentum balance.

Summing over j yields

$$\begin{aligned} \varepsilon^\alpha \rho^\alpha \frac{D^\alpha \mathbf{v}^\alpha}{Dt} - \nabla \cdot (\varepsilon^\alpha \mathbf{t}^\alpha) - \varepsilon^\alpha \rho^\alpha (\mathbf{g}^\alpha + \mathbf{g}_I^\alpha) - \varepsilon^\alpha q_e^\alpha \mathbf{E}_T - \varepsilon^\alpha \mathbf{P}^\alpha \cdot \nabla \mathbf{E}_T \\ = \sum_{\beta \neq \alpha} \varepsilon^\alpha \rho^\alpha \hat{\mathbf{T}}_\beta^\alpha, \end{aligned} \quad (77)$$

with restrictions

$$\sum_{j=1}^N \rho^{\alpha_j} (\hat{\mathbf{i}}^{\alpha_j} + \hat{\mathbf{r}}^{\alpha_j} \mathbf{v}^{\alpha_j}) = 0 \quad \forall \alpha \quad (78)$$

$$\varepsilon^\alpha \rho^{\alpha_j} (\hat{\mathbf{T}}_\beta^{\alpha_j} + \hat{\mathbf{e}}_\beta^{\alpha_j} \mathbf{v}^{\alpha_j}) + \varepsilon^\beta \rho^{\beta_j} (\hat{\mathbf{T}}_\alpha^{\beta_j} + \hat{\mathbf{e}}_\alpha^{\beta_j} \mathbf{v}^{\beta_j}) = 0 \quad j = 1, \dots, N. \quad (79)$$

The jump condition across a discontinuous interface is [15]:

$$\mathbf{n} \cdot [[\rho \mathbf{v}(\mathbf{v} - \mathbf{w}) - \mathbf{t} - \mathbf{t}_E]] = 0 \quad (80)$$

where \mathbf{w} is the speed of the discontinuity and for the electroquasistatic case considered here,

$$\mathbf{F}_e = \nabla \cdot \mathbf{t}_E = \nabla \cdot (\mathbf{D}\mathbf{E} - \frac{1}{2} \varepsilon_0 \mathbf{E} \cdot \mathbf{E}\mathbf{I}). \quad (81)$$

Equation (80) can be shown to correspond directly with (79) using (53).

Angular Momentum Balance

The macroscale form of the conservation of angular momentum equation in indicial notation is

$$\begin{aligned} -\varepsilon^\alpha \epsilon_{klm} t_{kl}^{\alpha_j} - \varepsilon^\alpha \epsilon_{klm} P_k^{\alpha_j} (\mathbf{E}_T)_l = \varepsilon^\alpha \rho^{\alpha_j} \hat{\mathbf{m}}_m^{\alpha_j} + \varepsilon^\alpha \rho^{\alpha_j} M_m^{\alpha_j} \\ + \sum_{\beta \neq \alpha} \varepsilon^\alpha \rho^{\alpha_j} (\hat{\mathbf{m}}_\beta^{\alpha_j})_m \end{aligned} \quad (82)$$

where the definitions of all variables are given in Appendix C. Thus the macroscale equation is composed of two parts. The equation consisting of all but the term involving $M_m^{\alpha_j}$ is the macroscale form of the microscale equation. The term $M_m^{\alpha_j}$ contains all terms arising from the the microscale conservation of linear

momentum crossed with ξ and volume averaged. These additional terms for the purely mechanical case have been derived before ([16, 22]). The term in M^{α_j} involving the time rate of change of velocity is known as inertial [16] or local [22] spin. The term in M^{α_j} involving t^j has been referred to as the first surface stress moment [16], or apparent couple stress tensor [22]. One observation which is painfully clear is that even in a medium which contains no electric field or charge, the mixture of two media which have symmetric stress tensors may result in a macroscopic medium which has a non-symmetric stress tensor.

Summing over j yields

$$-\varepsilon^\alpha \epsilon_{klm} t_{kl}^\alpha - \varepsilon^\alpha \epsilon_{klm} P_k^\alpha (E_T)_l = \varepsilon^\alpha \rho^{\alpha_j} M_m^\alpha + \sum_{\beta \neq \alpha} \varepsilon^\alpha \rho^\alpha (\hat{m}_\beta^\alpha)_m \quad (83)$$

where we note that symmetry of the stress tensor is lost due to possible polarization of the medium, the microscale angular momentum, and the interaction of the phase with other phases.

The restriction which must hold to preserve angular momentum within a phase is

$$\sum_{j=1}^N \rho^{\alpha_j} \hat{m}^{\alpha_j} = \mathbf{0} \quad \forall \alpha. \quad (84)$$

The restriction which arises from the assumption of no interfacial angular momentum is

$$\varepsilon^\alpha \rho^{\alpha_j} \hat{m}_\beta^{\alpha_j} + \varepsilon^\beta \rho^{\alpha\beta} \hat{m}_\alpha^{\beta_j} = 0 \quad j = 1, \dots, N. \quad (85)$$

Conservation of Energy

The conservation of energy equation is given by

$$\begin{aligned} & \varepsilon^\alpha \rho^{\alpha_j} \frac{D^{\alpha_j} e^{\alpha_j}}{Dt} - \varepsilon^\alpha t^{\alpha_j} : \nabla v^{\alpha_j} - \nabla \cdot (\varepsilon^\alpha q^{\alpha_j}) - \varepsilon^\alpha \rho^{\alpha_j} h^{\alpha_j} - \varepsilon^\alpha \mathcal{J}^{\alpha_j} \cdot E_T \\ & - \frac{\partial(\varepsilon^\alpha P^{\alpha_j})}{\partial t} \cdot E_T - \nabla \cdot (\varepsilon^\alpha v^{\alpha_j} P^{\alpha_j}) \cdot E_T - \frac{1}{2} \varepsilon_0 E_T \cdot E^{\alpha_j} \frac{D^{\alpha_j} \varepsilon^\alpha}{Dt} \\ & = \varepsilon^\alpha \rho^{\alpha_j} \hat{Q}^{\alpha_j} + \sum_{\beta \neq \alpha} \varepsilon^\alpha \rho^{\alpha_j} \hat{Q}_\beta^{\alpha_j} \end{aligned} \quad (86)$$

where

$$\begin{aligned} \hat{Q}_\beta^{\alpha_j} = & \frac{1}{\rho^{\alpha_j} |\delta V_\alpha|} \int_{\delta A_{\alpha\beta}} [q^j + (t^j + D^j E - \frac{1}{2} \varepsilon_0 (E^j \cdot E) I) \cdot v^j \\ & + \rho^j (e^j + \frac{1}{2} v^j \cdot v^j + \frac{1}{2} \varepsilon_0 E^j \cdot E) (w_{\alpha\beta}^j - v^j)] \cdot n^\alpha da \\ & - \frac{e^{\alpha_j} - \frac{1}{2} v^{\alpha_j} \cdot v^{\alpha_j}}{\rho^{\alpha_j} |\delta V_\alpha|} \int_{\delta A_{\alpha\beta}} \rho^j (w_{\alpha\beta}^j - v^j) \cdot n^\alpha da \\ & - \frac{v^{\alpha_j}}{\rho^{\alpha_j} |\delta V_\alpha|} \cdot \int_{\delta A_{\alpha\beta}} [(t^j)^T + E D^j - \frac{1}{2} \varepsilon_0 (E^j \cdot E) I + \rho^j v^j (w_{\alpha\beta}^j - v^j)] \cdot n^\alpha da \end{aligned}$$

$$+\frac{1}{\rho^{\alpha_j}|\delta V_\alpha|} \int_{\delta A_{\alpha\beta}} [(-\varepsilon_0 \mathbf{E}^j \cdot \mathbf{E} + \varepsilon_0 (\mathbf{E}^j \cdot \mathbf{E}) \mathbf{I}) \cdot \mathbf{v}^j + \mathbf{H}^j \times \mathbf{E}] \cdot \mathbf{n}^\alpha da \\ - \hat{d}_\beta^{\alpha_j} \mathbf{E}_T \cdot \mathbf{v}^{\alpha_j} - \hat{h}_\beta^{\alpha_j} \cdot \mathbf{E}_T \quad (87)$$

represents the effect constituent j of phase β has on the rate of change of energy of the same constituent in phase α due to non-mass transfer, non-mechanical means. The relation between the other macroscale variables and their microscale counterparts are given in Appendix C. As in the linear momentum equation, upscaling produces an additional term involving the material time rate of change of the volume fraction. This term would be negligible in a non-swelling porous medium. Additional effects of fluctuations in the species electric work terms manifest themselves in the flux term, q^{α_j} , and the external source term, h^{α_j} .

Summing over constituents yields

$$\varepsilon^\alpha \rho^\alpha \frac{D^\alpha e^\alpha}{Dt} - \varepsilon^\alpha t^\alpha : \nabla \mathbf{v}^\alpha - \nabla \cdot (\varepsilon^\alpha q^\alpha) - \varepsilon^\alpha \rho^\alpha h^\alpha - \varepsilon^\alpha \mathcal{J}^\alpha \cdot \mathbf{E}_T - \frac{\partial(\varepsilon^\alpha \mathbf{P}^\alpha)}{\partial t} \cdot \mathbf{E}_T \\ - \nabla \cdot (\varepsilon^\alpha \mathbf{v}^\alpha \mathbf{P}^\alpha) \cdot \mathbf{E}_T - \frac{1}{2} \varepsilon_0 \mathbf{E}^\alpha \cdot \mathbf{E}_T \frac{D^\alpha \varepsilon^\alpha}{Dt} = \sum_{\beta \neq \alpha} \varepsilon^\alpha \rho^\alpha \hat{Q}_\beta^\alpha \quad (88)$$

with the restrictions

$$\sum_{j=1}^N \left[\rho^{\alpha_j} \hat{Q}^{\alpha_j} + \rho^{\alpha_j} \hat{i}^{\alpha_j} \cdot \mathbf{v}^{\alpha_j} + \rho^{\alpha_j} \hat{r}^{\alpha_j} \left(e^{\alpha_j} + \frac{1}{2} (\mathbf{v}^{\alpha_j})^2 \right) \right] = 0. \quad \forall \alpha \quad (89)$$

$$\left[\varepsilon^\alpha \rho^{\alpha_j} \hat{Q}_\beta^{\alpha_j} + \varepsilon^\alpha \rho^{\alpha_j} \hat{T}_\beta^{\alpha_j} \cdot \mathbf{v}^{\alpha_j} + \varepsilon^\alpha \rho^{\alpha_j} \hat{e}_\beta^{\alpha_j} \left(e^{\alpha_j} + \frac{1}{2} (\mathbf{v}^{\alpha_j})^2 \right) \right] \\ + \left[\varepsilon^\beta \rho^{\beta_j} \hat{Q}_\alpha^{\beta_j} + \varepsilon^\beta \rho^{\beta_j} \hat{T}_\alpha^{\beta_j} \cdot \mathbf{v}^{\beta_j} + \varepsilon^\beta \rho^{\beta_j} \hat{e}_\alpha^{\beta_j} \left(e^{\beta_j} + \frac{1}{2} (\mathbf{v}^{\beta_j})^2 \right) \right] = 0 \quad j = 1, \dots, N. \quad (90)$$

The first restriction states that energy must be conserved within a phase, and the second states that the interface can hold no energy.

We wish to compare (90) with the jump discontinuity condition. Various forms exist depending on what is considered negligible and the use of Maxwell's equations. Here we consider

$$[[\mathbf{q} + \mathbf{t} \cdot \mathbf{v} + (\rho \mathbf{e} + \frac{1}{2} \rho \mathbf{v}^2)(\mathbf{w} - \mathbf{v}) + \frac{1}{2} \varepsilon_0 (\mathbf{E} \cdot \mathbf{E}) \mathbf{w} + \mathbf{H} \times \mathbf{E} + \mathbf{P} \mathbf{E} \cdot \mathbf{v}]] \cdot \mathbf{n} = 0. \quad (91)$$

Equation (90) can be re-written as:

$$\frac{1}{|\delta V|} \int_{\delta A_{\alpha\beta}} \left[\mathbf{q}^j + (\mathbf{t}^j + \mathbf{P}^j \mathbf{E}) \cdot \mathbf{v}^j + \rho^j (e^j + \frac{1}{2} (\mathbf{v}^j)^2) (\mathbf{w}_{\alpha\beta}^j - \mathbf{v}^j) \right. \\ \left. + \frac{1}{2} \varepsilon_0 (\mathbf{E}^j \cdot \mathbf{E}) \mathbf{w}_{\alpha\beta}^j + \mathbf{H}^j \times \mathbf{E} \right] \cdot \mathbf{n}^\alpha da \\ = \frac{1}{|\delta V|} \int_{\delta A_{\alpha\beta}} \left[\mathbf{q}^j + (\mathbf{t}^j + \mathbf{P}^j \mathbf{E}) \cdot \mathbf{v}^j + \rho^j (e^j + \frac{1}{2} (\mathbf{v}^j)^2) (\mathbf{w}_{\alpha\beta}^j - \mathbf{v}^j) \right]$$

$$+\frac{1}{2}\varepsilon_0(\mathbf{E}^j \cdot \mathbf{E})\mathbf{w}_{\alpha\beta}^j + \mathbf{H}^j \times \mathbf{E} \Big] \cdot \mathbf{n}^\beta da. \quad (92)$$

Comparing terms we see that the condition involving exchange of energy across the interface, (90), conforms exactly with the classical jump condition (91).

Entropy Balance

The entropy balance for constituent j in phase α is given by

$$\varepsilon^\alpha \rho^{\alpha_j} \frac{D^{\alpha_j} \eta^{\alpha_j}}{Dt} - \nabla \cdot \varepsilon^\alpha \phi^{\alpha_j} - \varepsilon^\alpha \rho^{\alpha_j} b^{\alpha_j} = \sum_{\beta \neq \alpha} \varepsilon^\alpha \rho^{\alpha_j} \hat{\Phi}_\beta^{\alpha_j} + \varepsilon^\alpha \rho^{\alpha_j} \hat{\eta}^{\alpha_j} + \varepsilon^\alpha \rho^{\alpha_j} \hat{\Lambda}^{\alpha_j}, \quad (93)$$

where $\hat{\Phi}_\beta^{\alpha_j}$ represents the rate at which entropy is gained from constituent j in phase β . Summing over constituents we get

$$\varepsilon^\alpha \rho^\alpha \frac{D^\alpha \eta^\alpha}{Dt} - \nabla \cdot (\varepsilon^\alpha \phi^\alpha) - \varepsilon^\alpha \rho^\alpha b^\alpha = \sum_{\beta \neq \alpha} \varepsilon^\alpha \rho^\alpha \hat{\Phi}_\beta^\alpha + \varepsilon^\alpha \rho^\alpha \hat{\Lambda}^\alpha, \quad (94)$$

with restrictions

$$\sum_{j=1}^N \rho^{\alpha_j} (\hat{\eta}^{\alpha_j} + \hat{r}^{\alpha_j} \eta^{\alpha_j}) = 0 \quad \forall \alpha. \quad (95)$$

$$\varepsilon^\alpha \rho^{\alpha_j} (\hat{\Phi}_\beta^{\alpha_j} + \hat{e}_\beta^{\alpha_j} \eta^{\alpha_j}) + \varepsilon^\beta \rho^{\beta_j} (\hat{\Phi}_\alpha^{\beta_j} + \hat{e}_\alpha^{\beta_j} \eta^{\beta_j}) = 0 \quad j = 1, \dots, N. \quad (96)$$

The second condition is exactly analogous to the classical jump boundary condition applied at an interface. This equation can be used to obtain restrictions on the forms of constitutive equations using, for example, the Coleman and Noll method (see e.g. [4, 13]). At this point we make no assumptions regarding the form of the entropy flux or source. It is now postulated that the rate of entropy production is non-negative after summing over both species and phases. Our statement at the end of Section 2 need not hold in this case, as it is the rate of entropy production of the universe which is non-negative.

4 Discussion

We have provided the microscale and macroscale balance laws for a multiphase, multi-species, swelling system which incorporates electroquasistatics. The microscale derivation follows the approach of Eringen and Maugin [15], while the upscaling to the macroscale is achieved via spatial averaging. The species electric field, \mathbf{E}^{α_j} , is carefully defined and the complete relations between the microscopic and macroscopic variables and the species and bulk phase variables are provided. Further comparisons were made between restrictions required to hold at interfaces and jump conditions classically used at interfaces.

In regards to the conservation of momentum and energy, there are several ways in which one can group together terms into the definitions of the macroscopic variables. In this paper, we choose the macroscopic definitions in a way which results in consistency between restriction conditions at interfaces and classical jump conditions used at interfaces. But as a consequence, additional body sources appear due not to external sources but due to species electric fields and microscopic fluctuations of the work terms. Further, there are additional terms which appear due to gradients in volume fractions and material time rate-of-change of the volume fractions in the conservation of momentum and energy equation, respectively. This is *not* due to the primitive choice of \mathbf{F}_e^j and W_e^j (see equations (33-35)). Rather it is a consequence of the choice of grouping terms so as to recover classical jump conditions. The consequence of these additional terms needs to be investigated. This is partially done in part II of these papers.

The field equations are required for many practical applications including, but not limited to, swelling clays (smectites), biopolymers, biological membranes, pulsed electrophoresis, and chromatography. In part II of these papers we exploit the entropy inequality with independent variables consistent with several natural systems and apply the resulting constitutive theory near equilibrium for two problems: electrolyte transport in swelling clays and pulsed electrophoresis.

Acknowledgments. JHC would like to acknowledge the ARO / Terrestrial Sciences and Mathematics divisions for support under grant DAAE55-98-1-0228.

References

- [1] S. Achanta, J. H. Cushman, and M. R. Okos. On multicomponent, multiphase thermomechanics with interfaces. *Int. J. Eng. Sci.*, 32(11):1717–1738, 1994.
- [2] R. Benach and I. Müller. Thermodynamics and the description of magnetizable dielectric mixtures of fluids. *Archive for Rational Mechanics and Analysis*, 53(4):312–346, 1973.
- [3] L. S. Bennethum and J. H. Cushman. Multiscale, hybrid mixture theory for swelling systems - I: Balance laws. *Int. J. Engrg. Sci.*, 34(2):125–145, 1996.
- [4] L. S. Bennethum and J. H. Cushman. Multiscale, hybrid mixture theory for swelling systems - II: Constitutive theory. *Int. J. Engrg. Sci.*, 34(2):147–169, 1996.
- [5] A. Bensoussan, J.L. Lions, and G. Papanicolau. *Asymptotic analysis of periodic structures*. North-Holland , Amsterdam, 1978.
- [6] R. M. Bowen. Theory of mixtures. In A. C. Eringen, editor, *Continuum Physics*. Academic Press, Inc., New York, 1976.

- [7] H. Brenner and D. A. Evans. *Macrotransport process*. Butterworth, Boston, 1993.
- [8] A. Castellanos. Basic concepts and equations in electrohydrodynamics. In A. Castellanos, editor, *Electrohydrodynamics*, pages 2–82. Springer-Verlag, New York, 1998.
- [9] M. W. Coffey. Coupled nonlinear electrodynamics of type-II superconductors in the mixed state. *Physical Review B*, 46(1):567–570, 1992.
- [10] B. D. Coleman and W. Noll. The thermodynamics of elastic materials with heat conduction and viscosity. *Arch. Rat. Mech. Anal.*, 13:167–178, 1963.
- [11] J. H. Cushman. On unifying the concepts of scale, instrumentation and stochastics in the development of multiple phase transport theory. *Water Res. Res.*, 20:1668–1676, 1984.
- [12] J. Douglas, Jr. and T. Arbogast. Dual porosity models for flow in naturally fractured reservoirs. In J. H. Cushman, editor, *Dynamics of Fluid in Hierarchical Porous Media*, pages 177–222. Academic Press, New York, 1990.
- [13] A. C. Eringen. *Mechanics of Continua*. John Wiley and Sons, New York, 1967.
- [14] A. C. Eringen. A mixture theory of electromagnetism and superconductivity. *International Journal of Engineering Science*, 36(5,6):525–543, 1998.
- [15] A. C. Eringen and G. A. Maugin. *Electrodynamics of Continua I*. Springer-Verlag, New York, 1990.
- [16] A. C. Eringen and E. S. Suhubi. Nonlinear theory of simple microelastic solids. *International Journal of Engineering Science*, 2:189–203, 1964.
- [17] L. W. Gelhar and C. L. Axness. Three-dimensional stochastic analysis of macrodispersion in aquifers. *Water Res. Res.*, 19:161–180, 1983.
- [18] W. G. Gray and S. M. Hassanizadeh. Averaging theorems and averaged equations for transport of interface properties in multiphase systems. *Intl. J. Multiphase Flow*, 15:81–95, 1989.
- [19] W. G. Gray and S. M. Hassanizadeh. Unsaturated flow theory including interfacial phenomena. *Water Resources Research*, 27:1855–1863, 1991.
- [20] W. Y. Gu, W. M. Lai, and V. C. Mow. Transport of multi-electrolytes in charged hydrated biological soft tissues. *Transport in Porous Media*, 34:143–157, 1999.
- [21] S. M. Hassanizadeh and W. G. Gray. General conservation equations for multiphase systems: 1. Averaging procedure. *Adv. Water Resour.*, 2:131–144, 1979.

- [22] S. M. Hassanzadeh and W. G. Gray. General conservation equations for multiphase systems: 2. Mass, momenta, energy, and entropy equations. *Advances in Water Resources*, 2:191–208, 1979.
- [23] J. M. Huyghe and J. D. Janssen. Thermo-chemo-electro-mechanical formulation of saturated charged porous solids. *Transport in Porous Media*, 34:129–141, 1999.
- [24] P. D. Kelly. A reacting continuum. *International Journal of Engineering Science*, 2:129–153, 1964.
- [25] R. M. Kulsrud. Mhd description of plasma. In M. N. Rosenbluth and R. Z. Sagdeev, editors, *Basic Plasma Physics I*, pages 115–123. North-Holland Publishing Company, New York, 1983.
- [26] L. M. Landau and E. M. Lifschitz. *Electrodynamique des Milieux Continus*. MIR, Moscow, 1990.
- [27] H. A. Lorentz. *The Theory of Electrons*. Dover, New York, 1952.
- [28] J. R. Melcher. *Continuum Electromechanics*. MIT Press, Cambridge, 1981.
- [29] G. P. Moeckel. Thermodynamics of an interface. *Arch. Rat. Mech. Anal.*, 57:255–280, 1975.
- [30] I. Müller and T. Ruggeri. *Extended Thermodynamics*. Springer-Verlag, New York, 1993.
- [31] O. A. Plumb and S. Whitaker. Diffusion, adsorption and dispersion in porous media: Small-scale averaging and local volume averaging. In J. H. Cushman, editor, *Dynamics of Fluid in Hierarchical Porous Media*, pages 97–176. Academic Press, New York, 1990.
- [32] J. I. Richards and H. K. Youn. *Theory of distributions: A non-technical introduction*. Cambridge Univ. Press, Cambridge, 1990.
- [33] J. A. del Rio and S. Whitaker. Maxwell's equations in two-phase systems I: Local electrodynamic equilibrium. *Transport in Porous Media*, 39:159–186, 2000.
- [34] J. A. del Rio and S. Whitaker. Maxwell's equations in two-phase systems II: Two-equation model. *Transport in Porous Media*, 39:259–287, 2000.
- [35] E. Sanchez-Palencia. Non-homogeneous media and vibration theory. In *Lecture Notes in Physics*. Springer-Verlag, New York, 1980.
- [36] L. Schwartz. *Théorie des distributions*. Hermann et Cie., Paris, 1950.
- [37] J. C. Slattery. Flow of viscoelastic fluids through porous media. *AIChEJ*, 13:1066–1071, 1967.

- [38] H. F. Tiersten. *A Development of the Equations of Electromagnetism in Material Continua*. Springer-Verlag, New York, 1990. In Series: Springer Tracts in Natural Philosophy, v. 36.
- [39] C. Truesdell and R. A. Toupin. The classical field theories. In S. Flügge, editor, *Handbuch der Physik*. Springer-Verlag, New York, 1960.
- [40] C. Truesdell and R. A. Toupin. *Rational Thermodynamics*. Springer-Verlag, New York, 1984.
- [41] S. Whitaker. Diffusion and dispersion in porous media. *AIChEJ*, 13:420–438, 1967.
- [42] S. Whitaker. Advances in theory of fluid motion in porous media. *Industrial and Engineering Chemistry*, 61(12):14–28, 1969.

Appendix A. Nomenclature

Superscripts, Subscripts, and Other Notations

- \cdot^{α_j} j^{th} component of α -phase on mesoscale
- \cdot^α α -phase on mesoscale
- $\cdot\tilde{}$ fluctuation from averaged quantity
- $\cdot\hat{}$ denotes exchange from other interface or phase
- $\cdot^{k,l}$ difference of the two quantities, i.e. $\cdot^k - \cdot^l$
- $\cdot|_{\alpha_j}$ microscopic property of constituent j in phase [subscript] (non-averaged)

Latin Symbols

- $\delta A_{\alpha\beta}$: Portion of $\alpha\beta$ -interface in representative elementary volume (REV)
- b^{α_j}, b^α : External entropy source [$J/(Kg\cdot s \cdot ^\circ K)$]
- C^{α_j} : Mass fraction of j^{th} component [-]
- D^{α_j}, D^α : Electric displacement [C/m^2]
- \widehat{d}^{α_j} : Net effect other constituents have on the charge of constituent j within phase α in Gauss' Law [C]
- $\widehat{d}_\beta^{\alpha_j}$: Net effect phase β has on the charge of constituent j in phase α in Gauss' Law [C]
- e^{α_j}, e^α : energy density [J/Kg]

$\hat{e}_\beta^{\alpha_j}$: Rate of mass transfer from phase [subscript] to phase [superscript] per unit mass density [1/s]

E^{α_j}, E^α : Electric Field intensity generated by (the j th constituent of) phase α [V/m]

g^{α_j}, g^α : External supply of momentum (gravity) [m/s²]

$g_I^{\alpha_j}, g_I^\alpha$: Internal supply of momentum due to fluctuations in Kelvin and Lorentz forces [m/s²]

h^{α_j}, h^α : External supply of energy [J/(Kg-s)]

$\hat{h}^{\alpha_j}, \hat{h}^\alpha$: Free current density induced by other species within the same phase within Ampère's law [A/m²]

$\hat{h}_\beta^{\alpha_j}, \hat{h}_\beta^\alpha$: Free current density induced by other phases on species j in Ampère's law [A/m²]

\hat{i}^{α_j} : Rate of momentum gain due to interaction with other species within the same phase per unit mass density [N/Kg]

H^{α_j}, H^α : Magnetic field intensity [A/m]

\hat{i}^{α_j} : Rate of momentum gain due to interaction with other species within the same phase per unit mass density [N/Kg]

J^{α_j}, J^α : Free current density in a fixed frame of reference [A/m²]

J^{α_j}, J^α : Free current density in the material frame of reference [A/m²] = [C/m²-s]; $J^{\alpha_j} = J^{\alpha_j} - q_e^{\alpha_j} v^{\alpha_j}$

\hat{m}^{α_j} : Rate of angular momentum gain due to interaction with other species within the same phase per unit mass density [N-m/Kg]

$\hat{m}_\beta^{\alpha_j}$: Rate of angular momentum gain by constituent j in phase α due to interaction with phase β [N-m/Kg]

M^{α_j} : Rate of angular momentum gain due to the microscale angular momentum terms - see Appendix C [N-m/Kg]

n^α : Unit normal vector pointing out of α -phase within mesoscopic REV [-]

P^{α_j}, P^α : Polarization density averaged over α -phase [C/m²]

$q_e^{\alpha_j}, q_e^\alpha$: Charge density averaged over α -phase [C/m³]

\hat{m}^{α_j} : Rate of gain of angular momentum of constituent j from other constituents in phase α [m²/s²]

\mathbf{q}^{α_j} : Partial heat flux vector for the j^{th} component of phase [$\text{J}/(\text{m}^2\cdot\text{s})$]

\mathbf{q}^α : Heat flux vector for phase α [$\text{J}/(\text{m}^2\cdot\text{s})$]

\hat{q}^{α_j} : Net rate of charge density gain by species j due to interaction with other species within phase α (does not include that gained to due mass transfer). [$\text{C}/\text{m}^3\cdot\text{s}$]

\hat{Q}^{α_j} : Rate of energy gain due to interaction with other species within the same phase per unit mass density not due to mass or momentum transfer [$\text{J}/(\text{Kg}\cdot\text{s})$]

$\hat{Q}_\beta^{\alpha_j}, \hat{Q}_\beta^\alpha$: Energy transfer rate from phase [subscript] to phase [superscript] per unit mass density not due to mass or momentum transfer [$\text{J}/(\text{Kg}\cdot\text{s})$]

\mathbf{r} : Microscale spatial variable [m]

\hat{r}^{α_j} : Rate of mass gain due to interaction with other species within the same phase per unit mass density [1/s]

t : Time [s]

T : Temperature [$^\circ\text{K}$]

\mathbf{t}^{α_j} : Partial stress tensor for the j^{th} component for phase [N/m^2]

\mathbf{t}^α : Total stress tensor for the phase [N/m^2]

$\hat{T}_\beta^{\alpha_j}, \hat{T}_\beta^\alpha$: Rate of momentum transfer through mechanical interactions from phase [subscript] to phase [superscript] per unit mass density [N/Kg]

$\mathbf{v}^{\alpha_j}, \mathbf{v}^\alpha$: Velocity [m/s]

δV : Representative elementary volume

δV_α : Portion of α -phase in REV

$w_{\alpha\beta}^j$: Velocity of constituent j at the interface between phases α and β [m/s]

\mathbf{x} : Macroscale spatial variable [m]

z^{α_j} : Charge per unit mass density of constituent j in phase α [C/Kg], $q_e^{\alpha_j} = \rho^{\alpha_j} z^{\alpha_j}$

$\hat{Z}_\beta^{\alpha_j}, \hat{Z}_\beta^\alpha$: Rate of exchange of charge of constituent j from phase β to phase α per unit mass [$\text{C}/\text{Kg}\cdot\text{s}$]

Greek Symbols

γ^α : Indicator function which is 1 if in mesoscopic region α and zero otherwise

ε^α : Volume fraction of α -phase in mesoscale REV [-]

ϵ_0 : Permittivity in a vacuum. In MKS units, the permittivity has the value of 8.854×10^{-12} Farads per meter.

ϵ_{klm} : Permutation tensor

$\hat{\Lambda}^{\alpha_j}, \hat{\Lambda}^\alpha$: Entropy production per unit mass density [J/(Kg-s-°K)]

ξ : Microscale spatial variable which varies over REV for fixed x : $r = x + \xi$ [m]

$\eta^{\alpha_j}, \eta^\alpha$: Entropy [J/(Kg-°K)]

$\hat{\eta}^{\alpha_j}$: Entropy gain due to interaction with other species within the same phase/interface per unit mass density [J/(Kg-s-°K)]

ϕ^{α_j} : Partial entropy flux vector for the j^{th} component for phase [J/(m²-s-°K)]

ϕ^α : Total entropy flux vector for the phase [J/(m²-s-°K)]

$\hat{\Phi}_\beta^{\alpha_j}, \hat{\Phi}_\beta^\alpha$: Entropy transfer through mechanical interactions from phase [subscript] to phase [superscript] per unit mass [J/(kg-s-°K)]

ρ^{α_j} : Partial mass density of j^{th} component of α -phase [Kg/m³] so that $\epsilon^\alpha \rho^\alpha$ is the total mass of j^{th} constituent in phase α divided by the volume of REV

ρ^α : Mass density of α -phase averaged over α -phase [Kg/m³]

$\hat{\sigma}^{\alpha_j}$: Induced curl of electric field of species j due to presence of other species within the same phase. See Faraday's law. [V/m]

$\hat{\sigma}_\beta^{\alpha_j}$: Effect constituent j of phase β has on the curl of the electric field of phase α [V/m]

Appendix B. Definition of Macroscopic Bulk Variables

The relationships between the macroscopic constituent variables and their bulk counterparts follow:

$$\rho^\alpha = \sum_{j=1}^N \rho^{\alpha_j}, \quad (B.1)$$

$$C^{\alpha_j} = \frac{\rho^{\alpha_j}}{\rho^\alpha}, \quad (B.2)$$

$$v^\alpha = \sum_{j=1}^N C^{\alpha_j} v^{\alpha_j}, \quad (B.3)$$

$$\hat{e}_\beta^\alpha = \sum_{j=1}^N C^{\alpha_j} \hat{e}_\beta^{\alpha_j}, \quad (\text{B.4})$$

$$\mathbf{J}^\alpha = \sum_{j=1}^N \mathbf{J}^{\alpha_j} \quad (\text{B.5})$$

$$\mathcal{J}^\alpha = \sum_{j=1}^N \mathcal{J}^{\alpha_j} + q_e^{\alpha_j} v^{\alpha_j, \alpha}, \quad (\text{B.6})$$

$$\mathbf{D}^\alpha = \sum_{j=1}^N \mathbf{D}^{\alpha_j} \quad (\text{B.7})$$

$$\mathbf{P}^\alpha = \sum_{j=1}^N \mathbf{P}^{\alpha_j} \quad (\text{B.8})$$

$$\mathbf{E}^\alpha = \sum_{j=1}^N \mathbf{E}^{\alpha_j} \quad (\text{B.9})$$

$$q_e^\alpha = \sum_{j=1}^N q_e^{\alpha_j}, \quad (\text{B.10})$$

$$\hat{d}_\beta^\alpha = \sum_{j=1}^N \hat{d}_\beta^{\alpha_j} \quad (\text{B.11})$$

$$\hat{\sigma}_\beta^\alpha = \sum_{j=1}^N \hat{\sigma}_\beta^{\alpha_j} \quad (\text{B.12})$$

$$\mathbf{H}^\alpha = \sum_{j=1}^N (\mathbf{H}^{\alpha_j} - \mathbf{P}^{\alpha_j} \times \mathbf{v}^{\alpha_j, \alpha}) \quad (\text{B.13})$$

$$\hat{h}_\beta^\alpha = \sum_{j=1}^N \hat{h}_\beta^{\alpha_j} \quad (\text{B.14})$$

$$z^\alpha = \sum_{j=1}^N C^{\alpha_j} z^{\alpha_j} \quad (\text{B.15})$$

$$\hat{Z}_\beta^\alpha = \sum_{j=1}^N C^{\alpha_j} (\hat{Z}_\beta^{\alpha_j} + \hat{e}_\beta^{\alpha_j} z^{\alpha_j, \alpha}) \quad (\text{B.16})$$

$$t^\alpha = \sum_{j=1}^N [t^{\alpha_j} - \rho^{\alpha_j} v^{\alpha_j, \alpha} v^{\alpha_j, \alpha}], \quad (\text{B.17})$$

$$g^\alpha = \sum_{j=1}^N C^{\alpha_j} g^{\alpha_j}, \quad (\text{B.18})$$

$$g_I^\alpha = \sum_{j=1}^N C^{\alpha_j} g_I^{\alpha_j} \quad (\text{B.19})$$

$$\hat{T}_\beta^\alpha = \sum_{j=1}^N C^{\alpha_j} \left(\hat{T}_\beta^{\alpha_j} + \hat{e}_\beta^{\alpha_j} v^{\alpha_j, \alpha} \right) + \frac{1}{\rho^\alpha} \hat{d}_\beta^\alpha E_T, \quad (\text{B.20})$$

$$\hat{m}_\beta^\alpha = \sum_{j=1}^N C^{\alpha_j} \hat{m}_\beta^{\alpha_j}, \quad (\text{B.21})$$

$$M^\alpha = \sum_{j=1}^N C^{\alpha_j} M^{\alpha_j}, \quad (\text{B.22})$$

$$e^\alpha = \sum_{j=1}^N C^{\alpha_j} \left(e^{\alpha_j} + \frac{1}{2} v^{\alpha_j, \alpha} \cdot v^{\alpha_j, \alpha} \right), \quad (\text{B.23})$$

$$q^\alpha = \sum_{j=1}^N \left[q^{\alpha_j} + t^{\alpha_j} \cdot v^{\alpha_j, \alpha} - \rho^{\alpha_j} v^{\alpha_j, \alpha} \left(e^{\alpha_j} + \frac{1}{2} (v^{\alpha_j, \alpha})^2 \right) + v^{\alpha_j, \alpha} P^{\alpha_j} \cdot E_T \right], \quad (\text{B.24})$$

$$h^\alpha = \sum_{j=1}^N C^{\alpha_j} (h^{\alpha_j} + (g^{\alpha_j} + g_I^{\alpha_j}) \cdot v^{\alpha_j, \alpha}), \quad (\text{B.25})$$

$$\begin{aligned} \hat{Q}_\beta^\alpha &= \sum_{j=1}^N C^{\alpha_j} \left[\hat{Q}_\beta^{\alpha_j} + \hat{T}_\beta^{\alpha_j} \cdot v^{\alpha_j, \alpha} + \hat{e}_\beta^{\alpha_j} \left(e^{\alpha_j, \alpha} + \frac{1}{2} (v^{\alpha_j, \alpha})^2 \right) \right. \\ &\quad \left. - \hat{d}_\beta^\alpha E_t \cdot v^\alpha - \hat{h}_\beta^\alpha \cdot E_T \right], \end{aligned} \quad (\text{B.26})$$

$$\eta^\alpha = \sum_{j=1}^N C^{\alpha_j} \eta^{\alpha_j}, \quad (\text{B.27})$$

$$\phi^\alpha = \sum_{j=1}^N (\phi^{\alpha_j} - \rho^{\alpha_j} \eta^{\alpha_j} v^{\alpha_j, \alpha}), \quad (\text{B.28})$$

$$b^\alpha = \sum_{j=1}^N C^{\alpha_j} b^{\alpha_j}, \quad (\text{B.29})$$

$$\hat{\Phi}_\beta^\alpha = \sum_{j=1}^N C^{\alpha_j} \left(\hat{\Phi}_\beta^{\alpha_j} + \hat{e}_\beta^{\alpha_j} \eta^{\alpha_j, \alpha} \right), \quad (\text{B.30})$$

$$\hat{\Lambda}^\alpha = \sum_{j=1}^N C^{\alpha_j} \hat{\Lambda}^{\alpha_j}, \quad (\text{B.31})$$

$$(\text{B.32})$$

Appendix C. Relationship between Macroscopic and Microscopic Variables

For notational brevity, define the volume average over phase α with angle brackets:

$$\langle \psi^j \rangle^\alpha(x, t) = \frac{1}{|\delta V_\alpha|} \int_{\delta V} \psi^j(\mathbf{r}, t) \gamma_\alpha(\mathbf{r}, t) dv(\xi) \quad (\text{C.1})$$

so that if for example, ρ^j is constant throughout phase α then $\langle \rho^j \rangle^\alpha$ would be that constant density.

Similarly we define the mass average to be

$$\overline{\psi^j}^\alpha(x, t) = \frac{1}{\langle \rho^j \rangle^\alpha |\delta V_\alpha|} \int_{\delta V} \rho^j(\mathbf{r}, t) \psi^j(\mathbf{r}, t) \gamma_\alpha(\mathbf{r}, t) dv(\xi). \quad (\text{C.2})$$

Thus for example, while the volume average of velocity makes no physical sense, the mass average (momentum) does.

The relationships between the macroscopic constituent variables and their microscopic counterparts follow. There are *no* assumptions made about small fluctuations about the average. What follows is exact.

$$\rho^{\alpha_j} = \langle \rho^j \rangle^\alpha \quad (\text{C.3})$$

$$\mathbf{v}^{\alpha_j} = \overline{\mathbf{v}^j}^\alpha \quad (\text{C.4})$$

$$\hat{\mathbf{r}}^{\alpha_j} = \overline{\hat{\mathbf{r}}^j}^\alpha \quad (\text{C.5})$$

$$\hat{\mathbf{e}}_\beta^{\alpha_j} = \frac{1}{\rho^{\alpha_j} |\delta V_\alpha|} \int_{\delta A_{\alpha\beta}} \rho^j (\mathbf{w}_{\alpha\beta}^j - \mathbf{v}^j) \cdot \mathbf{n}^\alpha da \quad (\text{C.6})$$

(C.7)

$$\mathbf{J}^{\alpha_j} = \langle \mathbf{J}^j \rangle^\alpha \quad (\text{C.8})$$

$$\mathcal{J}^{\alpha_j} = \langle \mathcal{J}^j \rangle^\alpha + \langle q_e^j \mathbf{v}^j \rangle^\alpha - q_e^{\alpha_j} \mathbf{v}^{\alpha_j} \quad (\text{C.9})$$

$$\mathbf{D}^{\alpha_j} = \langle \mathbf{D}^j \rangle^\alpha \quad (\text{C.10})$$

$$\mathbf{P}^{\alpha_j} = \langle \mathbf{P}^j \rangle^\alpha \quad (\text{C.11})$$

$$\mathbf{E}^{\alpha_j} = \langle \mathbf{E}^j \rangle^\alpha \quad (\text{C.12})$$

$$\mathbf{E}_T = \sum_\alpha \epsilon^\alpha \langle \mathbf{E} \rangle^\alpha = \frac{1}{|\delta V|} \int_{\delta V} \mathbf{E} dv \quad (\text{C.13})$$

$$q_e^{\alpha_j} = \langle q_e^j \rangle^\alpha \quad (\text{C.14})$$

$$\hat{\mathbf{d}}^{\alpha_j} = \langle \hat{\mathbf{d}}^j \rangle^\alpha \quad (\text{C.15})$$

$$\hat{\mathbf{d}}_\beta^{\alpha_j} = -\frac{1}{|\delta V_\alpha|} \int_{\delta A_{\alpha\beta}} \mathbf{D}^j \cdot \mathbf{n}^\alpha da \quad (\text{C.16})$$

$$\hat{\sigma}^{\alpha_j} = \langle \hat{\sigma}^j \rangle^\alpha \quad (\text{C.17})$$

$$\hat{\sigma}_{\beta}^{\alpha_j} = -\frac{1}{|\delta V_{\alpha}|} \int_{\delta A_{\alpha\beta}} \mathbf{n}^{\alpha} \times \mathbf{E}^j da \quad (\text{C.18})$$

$$\mathbf{H}^{\alpha_j} = <\mathbf{H}^j>^{\alpha} + [\mathbf{P}^{\alpha_j} \times \mathbf{v}^{\alpha_j} - <\mathbf{P}^j \times \mathbf{v}^j>^{\alpha}] \quad (\text{C.19})$$

$$\hat{h}_{\beta}^{\alpha_j} = \frac{1}{|\delta V_{\alpha}|} \int_{\delta A_{\alpha\beta}} [\mathbf{D}^j w_{\alpha\beta}^j \cdot \mathbf{n}^{\alpha} - (\mathbf{H}^j - \mathbf{P}^j \times \mathbf{v}^j) \times \mathbf{n}^{\alpha}] da \quad (\text{C.20})$$

$$\hat{h}^{\alpha_j} = <\hat{h}^j>^{\alpha} \quad (\text{C.21})$$

$$z^{\alpha_j} = \overline{z^j} \quad (\text{C.22})$$

$$\hat{q}_e^{\alpha_j} = <\hat{q}_e^j>^{\alpha} + \epsilon^{\alpha} \rho^{\alpha_j} \overline{z^j \hat{r}^j}^{\alpha} - \epsilon^{\alpha} \rho^{\alpha_j} \hat{r}^{\alpha_j} z^{\alpha_j} \quad (\text{C.23})$$

$$\begin{aligned} \hat{Z}_{\beta}^{\alpha_j} = & \frac{1}{\rho^{\alpha_j} |\delta V_{\alpha}|} \int_{\delta A_{\alpha\beta}} [q_e^j (w_{\alpha\beta}^j - \mathbf{v}^j) - \mathcal{J}^j] \cdot \mathbf{n}^{\alpha} da \\ & - \frac{z^{\alpha_j}}{\rho^{\alpha_j} |\delta V_{\alpha}|} \int_{\delta A_{\alpha\beta}} [\rho^j (w_{\alpha\beta}^j - \mathbf{v}^j)] \cdot \mathbf{n}^{\alpha} da \end{aligned} \quad (\text{C.24})$$

$$\begin{aligned} t^{\alpha_j} = & <\mathbf{t}^j>^{\alpha} + \rho^{\alpha_j} \mathbf{v}^{\alpha_j} \mathbf{v}^{\alpha_j} - \rho^{\alpha_j} \overline{\mathbf{v}^j \mathbf{v}^j}^{\alpha} + <\mathbf{D}^j \mathbf{E}>^{\alpha} - \mathbf{D}^{\alpha_j} \mathbf{E}_T \\ & + \frac{1}{2} \epsilon_0 [\mathbf{E}^{\alpha_j} \cdot \mathbf{E}_T - <\mathbf{E}^j \cdot \mathbf{E}>^{\alpha}] \mathbf{I} \end{aligned} \quad (\text{C.25})$$

$$\mathbf{g}^{\alpha_j} = \overline{\mathbf{g}^j}^{\alpha} \quad (\text{C.26})$$

$$\mathbf{g}_I^{\alpha_j} = \frac{\epsilon_0}{2\rho^{\alpha_j}} [\nabla \mathbf{E}_T \cdot \mathbf{E}^{\alpha_j} - <\nabla \mathbf{E} \cdot \mathbf{E}^j>^{\alpha} - \nabla \mathbf{E}^{\alpha_j} \cdot \mathbf{E}_T + <\nabla \mathbf{E}^j \cdot \mathbf{E}>^{\alpha}] \quad (\text{C.27})$$

$$\hat{\mathbf{i}}^{\alpha_j} = \overline{\hat{\mathbf{i}}^j}^{\alpha} + \overline{\hat{\mathbf{r}}^j \mathbf{v}^j}^{\alpha} - \hat{\mathbf{r}}^{\alpha_j} \mathbf{v}^{\alpha_j} + \frac{1}{\rho^{\alpha_j}} (\hat{\mathbf{d}}^{\alpha_j} \mathbf{E}_T - <\hat{\mathbf{d}}^j \mathbf{E}>^{\alpha}) \quad (\text{C.28})$$

$$\begin{aligned} \hat{T}_{\beta}^{\alpha_j} = & \frac{1}{\rho^{\alpha_j} |\delta V_{\alpha}|} \int_{\delta A_{\alpha\beta}} [(t^j)^T + \mathbf{E} \mathbf{D}^j - \frac{1}{2} \epsilon_0 \mathbf{E}^j \cdot \mathbf{E} \mathbf{I} + \rho^j \mathbf{v}^j (w_{\alpha\beta}^j - \mathbf{v}^j)] \cdot \mathbf{n}^{\alpha} da \\ & - \frac{\mathbf{v}^{\alpha_j}}{\rho^{\alpha_j} |\delta V_{\alpha}|} \int_{\delta A_{\alpha\beta}} \rho^j (w_{\alpha\beta}^j - \mathbf{v}^j) \cdot \mathbf{n}^{\alpha} da + \frac{1}{\rho^{\alpha_j}} \hat{d}_{\beta}^{\alpha_j} \mathbf{E}_T \end{aligned} \quad (\text{C.29})$$

$$\hat{m}^{\alpha_j} = <\hat{m}^j>^{\alpha} - \frac{1}{\rho^j} [<\mathbf{P}^j \times \mathbf{E}^j>^{\alpha} - \mathbf{P}^{\alpha_j} \times \mathbf{E}^{\alpha_j}] \quad (\text{C.30})$$

$$(\hat{m}_{\beta}^{\alpha_j})_m = \frac{1}{\rho^{\alpha_j} |\delta V_{\alpha}|} \int_{\delta A_{\alpha\beta}} [\epsilon_{klm} \xi_k (t_{nl} + v_l ((w_{\alpha\beta}^j)_n - v_n^j)) n_n da \quad (\text{C.31})$$

$$\begin{aligned} (M^{\alpha_j})_m = & -\frac{\partial}{\partial t} \left(\epsilon^{\alpha} \rho^{\alpha_j} \overline{\epsilon_{klm} \xi_k v_l^j}^{\alpha} \right) - \left[\epsilon^{\alpha} \rho^{\alpha_j} \overline{v_n^j (\epsilon_{klm} \xi_k v_l^j)}^{\alpha} \right]_{,n} \\ & + \left[\epsilon^{\alpha} <\epsilon_{klm} \xi_k t_{nl}^j>^{\alpha} \right]_{,n} + \epsilon^{\alpha} \rho^{\alpha_j} \overline{\epsilon_{klm} \xi_k g_l^j}^{\alpha} + \epsilon^{\alpha} <\epsilon_{klm} \xi_k (F_e^j)_l>^{\alpha} \\ & + \epsilon^{\alpha} <\epsilon_{klm} \xi_k (\rho^j \hat{i}_k^j + \rho^j \hat{r}^j v_k^j)>^{\alpha} \end{aligned} \quad (\text{C.32})$$

$$e^{\alpha_j} = \overline{e^j}^{\alpha} + \frac{1}{2} \overline{\mathbf{v}^j \cdot \mathbf{v}^j}^{\alpha} - \frac{1}{2} \mathbf{v}^{\alpha_j} \cdot \mathbf{v}^{\alpha_j} + \frac{\epsilon_0}{\rho^{\alpha_j}} [<\mathbf{E}^j \cdot \mathbf{E}>^{\alpha} - \mathbf{E}^{\alpha_j} \cdot \mathbf{E}_T] \quad (\text{C.33})$$

$$\begin{aligned} q^{\alpha_j} = & <\mathbf{q}^j>^{\alpha} + <\mathbf{t}^j \cdot \mathbf{v}^j>^{\alpha} - t^{\alpha_j} \cdot v^{\alpha_j} + \rho^{\alpha_j} \mathbf{v}^{\alpha_j} (e^{\alpha_j} + \frac{1}{2} \mathbf{v}^{\alpha_j} \cdot \mathbf{v}^{\alpha_j}) - \rho^{\alpha_j} \overline{\mathbf{v}^j (e^j + \frac{1}{2} \mathbf{v}^j \cdot \mathbf{v}^j)}^{\alpha} \\ & + <\mathbf{E} \times \mathbf{H}^j>^{\alpha} - \mathbf{E}_T \times \mathbf{H}^{\alpha_j} + <\mathbf{P}^j \mathbf{v}^j \cdot \mathbf{E}>^{\alpha} - \mathbf{P}^{\alpha_j} \mathbf{v}^{\alpha_j} \cdot \mathbf{E}_T \end{aligned} \quad (\text{C.34})$$

$$\begin{aligned} h^{\alpha_j} &= \overline{h^j}^\alpha + \overline{g^j \cdot v^j}^\alpha - \overline{g^j}^\alpha \cdot v^{\alpha_j} \\ &\quad + \frac{\varepsilon_0}{2\rho^{\alpha_j}} \left[\frac{\partial E^{\alpha_j}}{\partial t} \cdot E_T - \left\langle \frac{\partial E^j}{\partial t} \cdot E_T \right\rangle^\alpha + \left\langle \frac{\partial E}{\partial t} \cdot E^j \right\rangle^\alpha - \frac{\partial E_T}{\partial t} \cdot E^{\alpha_j} \right] \end{aligned} \quad (\text{C.35})$$

$$\begin{aligned} \widehat{Q}^{\alpha_j} &= \overline{\widehat{Q}^j}^\alpha + \overline{\widehat{i}^j \cdot v^j}^\alpha - \overline{\widehat{i}^{\alpha_j} \cdot v^{\alpha_j}} + \overline{(e^j + \frac{1}{2}v^j \cdot v^j)\widehat{r}^j}^\alpha - \overline{(e^j + \frac{1}{2}v^j \cdot v^j)}^\alpha \widehat{r}^{\alpha_j} \\ &\quad + \frac{1}{\rho^{\alpha_j}} \left[\langle \widehat{h}^j \cdot E \rangle^\alpha - \widehat{h}^{\alpha_j} \cdot E_T \right] \end{aligned} \quad (\text{C.36})$$

$$\begin{aligned} \widehat{Q}_\beta^{\alpha_j} &= \frac{1}{\rho^{\alpha_j} |\delta V_\alpha|} \int_{\delta A_{\alpha\beta}} [q^j + (t^j + D^j E - \frac{1}{2}e_0(E^j \cdot E)I) \cdot v^j \\ &\quad + \rho^j(e^j + \frac{1}{2}v^j \cdot v^j + \frac{1}{2}\varepsilon_0 E^j \cdot E)(w_{\alpha\beta}^j - v^j)] \cdot n^\alpha da \\ &\quad - \frac{e^{\alpha_j} - \frac{1}{2}v^{\alpha_j} \cdot v^{\alpha_j}}{\rho^{\alpha_j} |\delta V_\alpha|} \int_{\delta A_{\alpha\beta}} \rho^j(w_{\alpha\beta}^j - v^j) \cdot n^\alpha da \\ &\quad - \frac{v^{\alpha_j}}{\rho^{\alpha_j} |\delta V_\alpha|} \cdot \int_{\delta A_{\alpha\beta}} [(t^j)^T + ED^j - \frac{1}{2}\varepsilon_0(E^j \cdot E)I + \rho^j v^j(w_{\alpha\beta}^j - v^j)] \cdot n^\alpha da \\ &\quad + \frac{1}{\rho^{\alpha_j} |\delta V_\alpha|} \int_{\delta A_{\alpha\beta}} [(-\varepsilon_0 E^j E + \varepsilon_0(E^j \cdot E)I) \cdot v^j + H^j \times E] \cdot n^\alpha da \\ &\quad - \widehat{d}_\beta^{\alpha_j} E_T \cdot v^{\alpha_j} - \widehat{h}_\beta^{\alpha_j} \cdot E_T \end{aligned} \quad (\text{C.37})$$

$$\eta^{\alpha_j} = \overline{\eta^j}^\alpha \quad (\text{C.38})$$

$$\phi^{\alpha_j} = \langle \phi^j \rangle^\alpha + \rho^{\alpha_j} v^{\alpha_j} \eta^{\alpha_j} - \rho^{\alpha_j} \overline{v^j \eta^j}^\alpha \quad (\text{C.39})$$

$$b^{\alpha_j} = \overline{b^j}^\alpha \quad (\text{C.40})$$

$$\widehat{\Phi}^{\alpha_j} = \frac{1}{|\delta V|} \int_{\delta A_{\alpha\beta}} [\phi^j + \rho^j \eta^j (w_{\alpha\beta}^j - v^j)] \cdot n^\alpha da - \frac{\eta^{\alpha_j}}{|\delta V|} \int_{\delta A_{\alpha\beta}} \rho^j (w_{\alpha\beta}^j - v^j) \cdot n^\alpha da \quad (\text{C.41})$$

$$\widehat{\eta}^{\alpha_j} = \varepsilon^\alpha \rho^{\alpha_j} \left(\overline{\widehat{\eta}^j}^\alpha + \overline{\widehat{r}^j \eta^j}^\alpha - \widehat{r}^{\alpha_j} \eta^{\alpha_j} \right) \quad (\text{C.42})$$

$$\widehat{\Lambda}^{\alpha_j} = \overline{\Lambda^j}^\alpha \quad (\text{C.43})$$

**IV. Multicomponent, multiphase thermomechanics of swelling porous media
with electroquasistatics: Constitutive theory**

Multicomponent, Multiphase Thermodynamics of
Swelling Porous Media with Electroquasistatics:
II. Constitutive Theory

Lynn Schreyer Bennethum * John H. Cushman †

October 23, 2000

Abstract

In Part I macroscopic field equations of mass, linear and angular momentum, energy, and the quasistatic form of Maxwell's equations for a multiphase, multicomponent medium were derived. Here we exploit the entropy inequality to obtain restrictions on constitutive relations at the macroscale for a 2-phase, multiple-constituent, polarizable mixture of fluids and solids. Specific emphasis is placed on charged porous media in the presence of electrolytes. The governing equations for the stress tensors of each phase, flow of the fluid through a deforming medium, and diffusion of constituents through such a medium are derived. The results have applications in swelling clays (smectites), biopolymers, biological membranes, pulsed electrophoresis, chromatography, drug delivery, and other swelling systems.

Key words: porous media, mixture theory, electrodynamics, swelling, constitutive equations

1 Introduction

We continue our investigation into the form of the governing equations for a multiple-component, multiple-phase, polarizable, swelling porous medium with charged particles subject to an electric field. In Part I of this series we derived the macroscopic field equations under the assumption that it is the total electric field which affects the species' conservation of momentum and energy. For simplicity we consider only a liquid-solid system. The mixture is charge neutral, although neither the phases nor species face this requirement individually.

*University of Colorado at Denver, Center for Computational Mathematics, Campus Box 170, P.O. Box 173364, Denver, CO 80217-3364. bennethum@math.cudenver.edu. To whom correspondence should be addressed.

†Center for Applied Math, Math Sciences Building, Purdue University, W. Lafayette, IN 47907.

To derive restrictions on the form of the constitutive equations, we follow [15, 16] and view fluxes as constitutive. In earlier work, Eringen [16] considered constituent electric fields throughout for a non-swelling porous medium; Huyghe and Janssen [20] considered a single electric field in a deformable two-phase porous medium with no exchange terms from the conservation equations; and Gu et al. [17] considered a charged swelling medium with no electric field.

2 Constitutive Assumptions and the Entropy Inequality

The full entropy inequality which is exploited in subsequent sections is presented in Appendix B. The basic notation is found in Part I so only new terms are defined herein. We assume the medium consists of a liquid phase (denoted by $\alpha = l$), and a solid phase, (denoted by $\alpha = s$), and that the medium is macroscopically neutrally charged, however charges may move between constituents and phases.

We assume that entropy generation must be non-negative for the total body, i.e.

$$\rho \hat{\Lambda} = \sum_{\alpha} \sum_j \varepsilon^{\alpha} \rho^{\alpha_j} \hat{\Lambda}^{\alpha_j} \geq 0. \quad (1)$$

Further we assume a form of local equilibrium wherein there is one temperature for all constituents and all phases, i.e. $T^{\alpha_j}(\mathbf{x}, t) = T(\mathbf{x}, t)$ for all constituents j and all phases α . This effectively states that the rate of heat transfer between constituents is much faster than the time scales of interest to the problem.

To couple the entropy and energy equations, it is necessary to relate the fluxes and sources of entropy to the fluxes and sources of heat. We assume the processes are simple in the sense of [15]. In this sense several possible relations are admissible. Among these are:

$$\phi^{\alpha_j} = \frac{\mathbf{q}^{\alpha_j}}{T} \quad b^{\alpha_j} = \frac{h^{\alpha_j}}{T} \quad (2)$$

$$\phi^{\alpha} = \frac{\mathbf{q}^{\alpha}}{T} \quad b^{\alpha} = \frac{h^{\alpha}}{T} \quad (3)$$

$$\sum_{\alpha} \varepsilon^{\alpha} \phi^{\alpha} = \sum_{\alpha} \frac{\varepsilon^{\alpha} \mathbf{q}^{\alpha}}{T} \quad \sum_{\alpha} \varepsilon^{\alpha} b^{\alpha} = \sum_{\alpha} \frac{\varepsilon^{\alpha} h^{\alpha}}{T}. \quad (4)$$

The expressions in (4) have been used in [16], and the relations in (2) have been used in [1, 2, 3, 19]. More general expressions which simplify to the above are used in extended thermodynamics [21, 23]. The question is whether the processes governing the behavior of the constituents themselves, the individual phases, or the bulk material are simple. The assumption of any one of these does not imply any other due to microscale/macroscale relationships between

heat fluxes and heat sources [4]. This problem is complicated further because the macroscale definition of the heat flux depends on how one incorporates microscale fluctuations (see Part I, [4]). The differences manifest themselves explicitly in the constitutive relations obtained for diffusive fluxes and the chemical potential. For example, if the relations in (4) are used then it can be shown that that the chemical potentials of two “different” species at equilibrium must be equal, which is inconsistent with Gibbsian thermostatics [12]. To the authors’ knowledge, the relations in (2) do not result in any physical inconsistencies, and these are the relations used herein.

Define the Helmholtz free energy for the species and the internal Helmholtz free energy for the bulk phase as

$$A^{\alpha_j} = e^{\alpha_j} - T\eta^{\alpha_j} \quad A^\alpha = \sum_{j=1}^N C^{\alpha_j} A^{\alpha_j} \quad (5)$$

and introduce a modified Helmholtz free energy as

$$\tilde{A}^{\alpha_j} = e^{\alpha_j} - T\eta^{\alpha_j} - \frac{1}{\rho^{\alpha_j}} \mathbf{E}_T \cdot \mathbf{P}^{\alpha_j} \quad \tilde{A}^\alpha = \sum_{j=1}^N C^{\alpha_j} \tilde{A}^{\alpha_j}, \quad (6)$$

where C^{α_j} is the mass fraction of constituent j in phase α given by $C^{\alpha_j} = \rho^{\alpha_j}/\rho^\alpha$. The purpose of introducing the modified Helmholtz potential is to reduce the amount of manipulations required to obtain the entropy inequality, as either \mathbf{P}^{α_j} or \mathbf{E}_T must be constitutive (dependent) variables. With this notation, eliminating ϕ^{α_j} , b^{α_j} , $\hat{Q}_\beta^{\alpha_j}$, \hat{Q}^{α_j} , $\hat{\Phi}_\beta^{\alpha_j}$, and $\hat{\eta}^{\alpha_j}$ from the entropy balance and re-writing it in terms of bulk-phase variables one obtains

$$\begin{aligned} \sum_\alpha \varepsilon^\alpha \rho^\alpha T \hat{\Lambda}^\alpha &= - \sum_\alpha \varepsilon^\alpha \rho^\alpha \left(\frac{D^\alpha \tilde{A}^\alpha}{Dt} + \eta^\alpha \frac{D^\alpha T}{Dt} \right) + \sum_\alpha \varepsilon^\alpha \mathcal{J}^\alpha \cdot \mathbf{E}_T \\ &+ \sum_\alpha \left[\varepsilon^\alpha t^\alpha + \sum_{j=1}^N \varepsilon^\alpha \rho^{\alpha_j} \left(\tilde{A}^{\alpha_j} \mathbf{I} + \mathbf{v}^{\alpha_j, \alpha} \mathbf{v}^{\alpha_j, \alpha} \right) \right] : \nabla \mathbf{v}^\alpha \\ &+ \sum_\alpha \sum_{j=1}^N \left[\varepsilon^\alpha t^{\alpha_j} + \varepsilon^\alpha \mathbf{P}^{\alpha_j} \cdot \mathbf{E}_T \mathbf{I} \right] : \nabla \mathbf{v}^{\alpha_j, \alpha} + \sum_\alpha \dot{\varepsilon}^\alpha \left[\frac{1}{2} \varepsilon_o \mathbf{E}_T \cdot \mathbf{E}^\alpha \right] \\ &+ \sum_\alpha \frac{\varepsilon^\alpha}{T} \nabla T \cdot \left\{ \mathbf{q}^\alpha + \sum_{j=1}^N \left[\rho^{\alpha_j} \mathbf{v}^{\alpha_j, \alpha} (\tilde{A}^{\alpha_j} + \frac{1}{2} \mathbf{v}^{\alpha_j, \alpha} \cdot \mathbf{v}^{\alpha_j, \alpha}) - \mathbf{t}^{\alpha_j} \cdot \mathbf{v}^{\alpha_j, \alpha} \right] \right\} \\ &+ \sum_\alpha \sum_{j=1}^N \frac{D^s(\varepsilon^\alpha \rho^{\alpha_j})}{Dt} \left[\frac{1}{\rho^\alpha} \mathbf{E}_T \cdot \mathbf{P}^\alpha + A^{\alpha_j} \right] - \sum_\alpha \varepsilon^\alpha \dot{\mathbf{E}}_T \cdot \mathbf{P}^\alpha \\ &+ \mathbf{v}^{l,s} \cdot \left[-\varepsilon^l \rho^l \hat{\mathbf{T}}_s^l + \sum_{j=1}^N (A^{l,j} \nabla (\varepsilon^l \rho^{l,j}) + \frac{1}{\rho^{l,j}} \mathbf{E}_T \cdot \mathbf{P}^{l,j} \nabla (\varepsilon^l \rho^{l,j})) \right. \\ &\quad \left. - \varepsilon^l \nabla \mathbf{E}_T \cdot \mathbf{P}^{l,j} + \frac{1}{2} \varepsilon_o \mathbf{E}_T \cdot \mathbf{E}^{l,j} \nabla \varepsilon^l \right] \end{aligned}$$

$$\begin{aligned}
& + \sum_{\alpha} \sum_{j=1}^N \mathbf{v}^{\alpha_j, \alpha} \cdot [-\varepsilon^{\alpha} \rho^{\alpha} (\hat{\mathbf{i}}^{\alpha_j} + \sum_{\beta \neq \alpha} \hat{\mathbf{T}}_{\beta}^{\alpha_j}) - \varepsilon^{\alpha} \rho^{\alpha_j} \nabla \tilde{A}^{\alpha_j} - \varepsilon^{\alpha} q_e^{\alpha_j} \mathbf{E}_T \\
& \quad + \frac{1}{\rho^{\alpha_j}} \mathbf{E}_T \cdot \mathbf{P}^{\alpha_j} \nabla (\varepsilon^{\alpha} \rho^{\alpha_j}) - \varepsilon^{\alpha} \nabla \mathbf{E}_T \cdot \mathbf{P}^{\alpha_j} + \frac{1}{2} \varepsilon_o \mathbf{E}_T \cdot \mathbf{E}^{\alpha_j} \nabla \varepsilon^{\alpha} - \frac{\varepsilon^{\alpha}}{T} \mathbf{E}_T \cdot \mathbf{P}^{\alpha_j} \nabla T] \\
& \quad - \sum_{\alpha} \sum_{j=1}^N \sum_{\beta \neq \alpha} \varepsilon^{\alpha} \rho^{\alpha_j} \hat{e}_{\beta}^{\alpha_j} \left[\frac{1}{\rho^{\alpha_j}} \mathbf{E}_T \cdot \mathbf{P}^{\alpha_j} + \tilde{A}^{\alpha_j} + \tilde{A}^{\alpha} + \frac{1}{2} (\mathbf{v}^{\alpha, s})^2 + \frac{1}{2} (\mathbf{v}^{\alpha_j, \alpha})^2 \right] \\
& \quad + \sum_{\alpha} \sum_{j=1}^N \varepsilon^{\alpha} \rho^{\alpha_j} \hat{r}^{\alpha_j} \left[-\frac{1}{2} (\mathbf{v}^{\alpha_j, \alpha})^2 - \tilde{A}^{\alpha_j} - \frac{1}{\rho^{\alpha_j}} \mathbf{E}_T \cdot \mathbf{P}^{\alpha_j} \right] \geq 0,
\end{aligned} \tag{7}$$

where a comma in the superscript denotes difference (e.g. $\mathbf{v}^{\alpha, s} = \mathbf{v}^{\alpha} - \mathbf{v}^s$), a superimposed dot denotes the material time derivative with respect to the solid phase (e.g. $\dot{\varepsilon}^{\alpha} = \partial \varepsilon^{\alpha} / \partial t + \mathbf{v}^s \cdot \nabla \varepsilon^{\alpha}$), \mathbf{I} is the identity matrix, and the contraction operator $A : B$ is, in indicial notation, $A_{ij} B_{ij}$.

We enforce many of the balance laws weakly using the Lagrange Multiplier approach [22]. The equations and their associated Lagrange multipliers are listed below.

Lagrange Mult.	Equation from [4]	Lagrange Mult.	Equation from [4]
$\lambda_{\rho}^{\alpha_j}$ $\Lambda_E^{\alpha_j}$ Λ	Continuity Eqn α_j , (42) Faraday's Law (55) $\frac{D^s}{Dt} (\varepsilon^l q_e^l + \varepsilon^s q_e^s) = 0$	$\lambda_D^{\alpha_j}$ $\lambda_{q_e}^{\alpha_j}$	Gauss' Law (49) Conserv. of Charge (68)

Ampère's law is derivable from the conservation of charge and Gauss' law and so is not enforced directly. The expression corresponding to the Lagrange multiplier Λ enforces *charge neutrality* locally. This restriction alone would imply that the total charge could vary in space. However we have in mind that the mixture is charge neutral initially everywhere so that it is assumed the time scale at which imbalances may occur is small compared to the time scale involved with other processes.

The unknowns in this system include:

$$\varepsilon^l, \rho^{\alpha_j}, \mathbf{v}^{\alpha_j}, T, \mathbf{E}^{\alpha_j}, q_e^{\alpha_j}, \tag{8}$$

$$\hat{e}_{\beta}^{\alpha_j}, \hat{r}^{\alpha_j}, t^{\alpha_j}, t^{\alpha}, \hat{\mathbf{T}}_{\beta}^{\alpha_j}, \hat{\mathbf{T}}_{\beta}^{\alpha}, \hat{\mathbf{i}}^{\alpha_j}, \tag{9}$$

$$A^{\alpha_j}, q^{\alpha_j}, \eta^{\alpha_j}, \tag{10}$$

$$\mathbf{P}^{\alpha_j}, \hat{d}^{\alpha_j}, \hat{d}_{\beta}^{\alpha_j}, \hat{\sigma}^{\alpha_j}, \hat{\sigma}_{\beta}^{\alpha_j}, \mathcal{J}^{\alpha_j}, \hat{q}^{\alpha_j}, \hat{Z}_{\beta}^{\alpha_j}. \tag{11}$$

The variables in the first row, (8), are the primary unknowns. The remaining variables, (9–11), are considered constitutive and are a function of *constitutive independent variables*. In order to close the system, one additional equation is needed, which corresponds to the unknown ε^l . This is known as the closure problem, and it arises from the homogenization of the microscopic geometry.

To close the system we follow [1, 9, 11] and view the time rate of change of the volume fraction $D\varepsilon^l/Dt$ as a constitutive variable.

The choice of constitutive independent variables is made based on knowledge of the system being modeled. Here we assume the fluid may behave as a Newtonian fluid and the solid as an elastic solid, hence we include the rate of deformation tensor, \mathbf{d}^l , and the strain tensor, \mathcal{E}^s . Since the solid phase may be disconnected, the macroscale strain tensor is not the average of the microscale strain, but is defined in terms of the deformation gradient $\mathbf{F} = \nabla_o \mathbf{x}$, $\mathcal{E}^s = \frac{1}{2}(\mathbf{F}_s^T \mathbf{F}_s - \mathbf{I})$, where ∇_o denotes differentiation with respect to the macroscopic material particle. Thus the strain tensor is a measure of the geometry of the solid phase. Further, we are particularly interested in modeling materials in which the solid and fluid phases have electro-chemical interactions, so that the behavior of the liquid phase may strongly depend upon its proximity to the solid phase. Thus we incorporate the volume fraction, ε^l , as an independent variable. The independent variables which are used to define the constitutive variables include:

$$\begin{aligned} & \varepsilon^l, T, \varepsilon^\alpha \rho^{\alpha_j}, \mathbf{v}^{l,s}, \mathbf{v}^{\alpha_j,\alpha}, \mathcal{E}^s, \mathbf{E}_T, \varepsilon^\alpha q_e^{\alpha_j}, \\ & \nabla \varepsilon^l, \nabla T, \nabla(\varepsilon^\alpha \rho^{\alpha_j}), \mathbf{d}^l, \omega^\alpha, \nabla \mathbf{v}^{l,j,l}, \nabla \mathcal{E}^s, \nabla \mathbf{E}_T, \\ & j = 1, \dots, N, \quad \alpha = l, s \end{aligned} \quad (12)$$

where because the liquid phase may be polarizable and may depend strongly on the geometry of the solid phase [4], we have also included the vorticity tensor, $\omega^l = (\nabla \mathbf{v} - (\nabla \mathbf{v})^T)$. Note that we have incorporated the total electric field as an independent variable, as opposed to the electric fields of each constituent or each phase. This is because it is assumed that all constitutive variables are measured with respect to the total electric field.

The reason for incorporating the volume fraction into some of the independent variables is that this allows a direct comparison with more easily recognizable thermodynamic variables which are extensive. As an example, consider the extensive Helmholtz potential, A_T^α , which is the volume of the REV multiplied by $\varepsilon^\alpha \rho^\alpha A^\alpha$. One definition of the chemical potential is,

$$\mu^{\alpha_j} = \frac{\partial A_T^\alpha}{\partial M^{\alpha_j}} \quad (13)$$

where M^{α_j} is the total mass of constituent j in the α phase. Performing a change of variables to intensive variables [13] leads to

$$\mu^{\alpha_j} = \frac{\partial(\varepsilon^\alpha \rho^\alpha A^\alpha)}{\partial(\varepsilon^\alpha \rho^{\alpha_j})}. \quad (14)$$

Thus in order to compare the two approaches directly, the appropriate independent variable is $\varepsilon^\alpha \rho^{\alpha_j}$ and not ρ^{α_j} . A similar argument can be made with $q_e^{\alpha_j}$.

To simplify the results we relax the Principle of Equipresence [26] and assume that the modified Helmholtz potential energies \tilde{A}^α are a function of a subset of the above constitutive independent variables:

$$\begin{aligned}\tilde{A}^l &= \tilde{A}^l(\varepsilon^l, T, \varepsilon^l \rho^{l_j}, \mathbf{v}^{l,s}, \mathbf{v}^{l_j,l}, \mathcal{E}^s, \mathbf{E}_T, \varepsilon^l q_e^{l_j}, \\ &\quad \nabla T, \nabla(\varepsilon^l \rho^{l_j}), \mathbf{d}^l, \omega^l, \nabla \mathbf{v}^{l_j,l})\end{aligned}\quad (15)$$

$$\begin{aligned}\tilde{A}^s &= \tilde{A}^s(\varepsilon^l, T, \varepsilon^s \rho^{s_j}, \mathbf{v}^{s_j,s}, \mathcal{E}^s, \mathbf{E}_T, \varepsilon^s q_e^{s_j}, \\ &\quad \nabla T, \nabla(\varepsilon^s \rho^{s_j}), \omega^s).\end{aligned}\quad (16)$$

We note that including the additional independent variables does not change the results if one modifies the definitions of pressure, chemical potential, etc. see e.g. [3]. The entropy inequality is now expanded in the traditional manner [9, 15, 18] and is presented in Appendix B.

3 Non-Equilibrium Constitutive Restrictions

The following variables are neither constitutive nor independent,

$$\frac{D^s(\varepsilon^\alpha \rho^{\alpha_j})}{Dt}, \frac{D^s(\varepsilon^\alpha q_e^{\alpha_j})}{Dt}, \dot{T}, \dot{\mathbf{E}}_T, \mathbf{d}^s, \nabla \mathbf{v}^{s_j,s}, \nabla \dot{T}, \quad (17)$$

$$\dot{\mathbf{v}}^{\alpha_j,\alpha}, \nabla \left(\frac{D^s(\varepsilon^\alpha \rho^{\alpha_j})}{Dt} \right), \dot{\mathbf{v}}^{l,s}, \dot{\mathbf{d}}^l, \dot{\omega}^l, \nabla \dot{\mathbf{v}}^{l_j,l}, \quad (18)$$

$$\nabla \times \mathbf{E}^{\alpha_j}, \nabla \cdot \mathbf{E}^{\alpha_j}, \quad (19)$$

where $j = 1, \dots, N$ for all variables not containing $\mathbf{v}^{\alpha_j,\alpha}$, since $\sum_{j=1}^N \rho^{\alpha_j} \mathbf{v}^{\alpha_j,\alpha} = \mathbf{0}$. Thus for example, $\mathbf{v}^{s_j,s}$ is indexed from $j = 1, \dots, N - 1$ in order to keep the list of variables independent. Since these terms appear linearly in the entropy inequality, their coefficients must be zero. This results in the following restrictions (corresponding directly with the terms in (17)):

$$\lambda_\rho^{\alpha_j} = \rho^\alpha \frac{\partial \tilde{A}^\alpha}{\partial \rho^{\alpha_j}} - \tilde{A}^{\alpha_j} - \frac{1}{\rho^{\alpha_j}} \mathbf{E}_T \cdot \mathbf{P}^{\alpha_j}, \quad j = 1, \dots, N \quad (20)$$

$$\lambda_{q_e}^{\alpha_j} + \Lambda = \rho^\alpha \frac{\partial \tilde{A}^\alpha}{\partial q_e^{\alpha_j}} \quad (21)$$

$$\sum_{\alpha=l,s} \varepsilon^\alpha \rho^\alpha (\eta^\alpha + \frac{\partial \tilde{A}^\alpha}{\partial T}) = 0 \quad (22)$$

$$\sum_{\alpha} \varepsilon^\alpha \mathbf{P}^\alpha = - \sum_{\alpha} \varepsilon^\alpha \rho^\alpha \frac{\partial \tilde{A}^\alpha}{\partial \mathbf{E}_T} \quad (23)$$

$$\varepsilon^s \mathbf{t}_{\text{sym}}^s = - \sum_{j=1}^N \varepsilon^s \rho^{s_j} (\lambda_\rho^{s_j} + \tilde{A}^{s_j} + z^{s_j} \lambda_{q_e}^{s_j}) + \varepsilon^s \mathbf{t}_e^s + \frac{\varepsilon^l}{\varepsilon^s} \mathbf{t}_s^l - \sum_{j=1}^N \varepsilon^s \rho^{s_j} \mathbf{v}^{s_j,s} \mathbf{v}^{s_j,s} \quad (24)$$

$$\begin{aligned} \mathbf{t}^{s_j} - \frac{\rho^{s_j}}{\rho^{s_N}} \mathbf{t}^{s_N} &= -(\mathbf{P}^{\alpha_j} \cdot \mathbf{E}_T - \frac{\rho^{s_j}}{\rho^{s_N}} \mathbf{P}^{s_N} \cdot \mathbf{E}_T) \mathbf{I} - \rho^{s_j} (\lambda_{\rho}^{s_j} - \lambda_{\rho}^{s_N}) \mathbf{I} \\ &\quad - (q_e^{s_j} \lambda_{q_e}^{s_j} - \frac{\rho^{s_j}}{\rho^{s_N}} q_e^{s_N} \lambda_{q_e}^{s_N}) \mathbf{I} \end{aligned} \quad (25)$$

$$\varepsilon^l \rho^l \frac{\partial \tilde{A}^l}{\partial \nabla T} + \varepsilon^s \rho^s \frac{\partial \tilde{A}^s}{\partial \nabla T} = 0, \quad (26)$$

where we have defined the effective stress tensor and hydration stress tensor as

$$\mathbf{t}_e^s = \rho^s \nabla \mathbf{F}^s \cdot \frac{\partial \tilde{A}^s}{\partial \mathcal{E}^s} \cdot (\nabla \mathbf{F}^s)^T \quad \mathbf{t}_s^l = \rho^l \nabla \mathbf{F}^s \cdot \frac{\partial \tilde{A}^l}{\partial \mathcal{E}^s} \cdot (\nabla \mathbf{F}^s)^T, \quad (27)$$

respectively. The restrictions obtained from the coefficients of the variables listed in (18) indicate that the modified Helmholtz free energy is not a function of $\mathbf{v}^{\alpha_j, \alpha}$, $\nabla(\varepsilon^{\alpha} \rho^{\alpha_j})$, $\mathbf{v}^{l,s}$, d^l , ω^{α} , $\nabla \mathbf{v}^{l_j, l}$, and the restrictions corresponding to the variables listed in (19) require that the Lagrange multipliers, $\lambda_{q_e}^{\alpha_j}$, $\Lambda_E^{\alpha_j}$, and $\lambda_D^{\alpha_j}$ must all be identically zero.

Equations (20) and (21) define the Lagrange multipliers $\lambda_{\rho}^{\alpha_j}$ and $\lambda_{q_e}^{\alpha_j}$, respectively. Equation (22) states that η^{α} and T are dual variables with respect to the *modified* Helmholtz potential, and this is in agreement with [2, 16]. Equation (26) states that the modified Helmholtz potential of the entire system is independent of ∇T .

Equation (23) implies that it is the polarization of the entire medium which is dual to the electric field in this representation. This is in contrast with [16] in which it is shown that the polarization of each component is dual to the constituent's electric field. The disparity results from our choice of independent variables - we use \mathbf{E}_T and Eringen uses \mathbf{E}^{α_j} as independent variables.

We define the *thermodynamic pressure* by

$$\pi^{\alpha} = \sum_{j=1}^N \rho^{\alpha_j} (\lambda_{\rho}^{\alpha_j} + \tilde{A}^{\alpha_j}) \quad (28)$$

$$= \sum_{j=1}^N (\rho^{\alpha} \rho^{\alpha_j} \frac{\partial \tilde{A}^{\alpha}}{\partial \rho^{\alpha_j}}) - \mathbf{E}_T \cdot \mathbf{P}^{\alpha} \quad (29)$$

$$= \sum_{j=1}^N \left(\rho^{\alpha} \rho^{\alpha_j} \frac{\partial A^{\alpha}}{\partial \rho^{\alpha_j}} + \left(\frac{\rho^{\alpha_j}}{\rho^{\alpha}} \mathbf{P}^{\alpha} - \mathbf{P}^{\alpha_j} \right) \cdot \mathbf{E}_T - \rho^{\alpha_j} \mathbf{E}_T \cdot \frac{\partial \mathbf{P}^{\alpha}}{\partial \rho^{\alpha_j}} \right). \quad (30)$$

where equation (29) is written in terms of the modified Helmholtz potential and (30) is written in terms of the classical Helmholtz potential. From (30) we see that this definition agrees with the classical thermodynamic pressure ($(\rho^{\alpha})^2 \partial A^{\alpha} / (\partial \rho^{\alpha})$) only in the case where there is one constituent and polarization is negligible for both constituents and for the bulk phase. In this case, π^{α} is the same as the thermodynamic pressure in the absence of electric fields.

From (24), the solid-phase stress tensor is written as

$$\mathbf{t}_{\text{sym}}^s = -\pi^s \mathbf{I} + \mathbf{t}_e^s + \frac{\varepsilon^l}{\varepsilon^s} \mathbf{t}_s^l - \sum_{j=1}^N \rho^{s_j} \mathbf{v}^{s_j, s} \mathbf{v}^{s_j, s} + q_e^s \Lambda - \sum_{j=1}^N \rho^s q_e^{s_j} \frac{\partial \tilde{\mathbf{A}}^s}{\partial q_e^{s_j}}, \quad (31)$$

which is identical to that when $\mathbf{E}_T = \mathbf{0}$. Charges and the electric field enter into this expression through π^s and through the effective and hydration stress tensors through $\tilde{\mathbf{A}}^s$. The role played by the effective and hydration stress tensors are discussed in [8, 6, 24, 25]. We remark that if the solid phase is considered incompressible then the material time derivative of ρ^{s_j} is zero, ρ^{s_j} is not considered an independent variable, and $\lambda_\rho^{s_j}$ is the Lagrange multiplier which enforces the remaining part of the conservation of mass for constituent s_j . In that case we obtain the same results, except that π^s is a primary unknown which must be handled directly.

We define the electro-chemical potential as (see equation (14))

$$\mu^{\alpha_j} = \frac{\partial(\varepsilon^\alpha \rho^\alpha \tilde{\mathbf{A}}^\alpha)}{\partial(\varepsilon^\alpha \rho^{\alpha_j})} = \tilde{\mathbf{A}}^\alpha + \rho^\alpha \frac{\partial \tilde{\mathbf{A}}^\alpha}{\partial \rho^{\alpha_j}} \quad (32)$$

which does not incorporate the Lagrange Multiplier enforcing charge neutrality as is often done [17, 20]. With this definition and (25) we determine the relationship between the chemical potential and the partial stress tensors. By eliminating the Lagrange multipliers and using the definition of μ^{s_j} , (24) becomes

$$\mathbf{t}^{s_j} - \frac{\rho^{s_j}}{\rho^{s_N}} \mathbf{t}^{s_N} = \left\{ -\rho^{s_j} (\mu^{s_j} - \mu^{s_N}) + \rho^{s_j} (\tilde{\mathbf{A}}^{s_j} - \tilde{\mathbf{A}}^{s_N}) - \rho^s \left[q_e^{s_j} \frac{\partial \tilde{\mathbf{A}}^s}{\partial q_e^{s_j}} - \frac{\rho^{s_j}}{\rho^{s_N}} q_e^{s_N} \frac{\partial \tilde{\mathbf{A}}^s}{\partial q_e^{s_N}} \right] + (q_e^{s_j} - \frac{\rho^{s_j}}{\rho^{s_N}} q_e^{s_N}) \Lambda \right\} \mathbf{I}. \quad (33)$$

Summing these equation on j from 1 to N and using

$$\sum_{j=1}^N \rho^{s_j} \mu^{s_j} = \rho^s \tilde{\mathbf{A}}^s + \pi^s + \mathbf{E}_T \cdot \mathbf{P}^s \quad (34)$$

$$\sum_{j=1}^N \mathbf{t}^{s_j} = -\pi^s \mathbf{I} + \mathbf{t}_e^s + \frac{\varepsilon^l}{\varepsilon^s} \mathbf{t}_s^l + q_e^s \Lambda - \sum_{j=1}^N \rho^s q_e^{s_j} \frac{\partial \tilde{\mathbf{A}}^s}{\partial q_e^{s_j}}, \quad (35)$$

one obtains an expression for μ^{s_N} , which when substituted back into equation (33) yields

$$\mu^{s_j} \mathbf{I} = \tilde{\mathbf{A}}^{s_j} \mathbf{I} - \frac{1}{\rho^{s_j}} \mathbf{t}^{s_j} + \frac{1}{\rho^s} \left(\mathbf{t}_e^s + \frac{\varepsilon^l}{\varepsilon^s} \mathbf{t}_s^l \right) + z^{s_j} \left(\Lambda - \rho^s \frac{\partial \tilde{\mathbf{A}}^s}{\partial q_e^{s_j}} \right) \mathbf{I} + \frac{1}{\rho^s} \mathbf{E}_T \cdot \mathbf{P}^s \mathbf{I}. \quad (36)$$

The first two terms on the right-hand-side form the classical chemical potential (see Bowen, [10]), although these terms are not scalars. In [7, 9] it was shown that the first three terms yield an appropriate definition of chemical potential when no electric field or charges exist. Changing the effective stress or hydration stress in a porous medium will result in a change in the chemical potential, which in turn would produce a different balance of species within phases. The fourth term on the right-hand-side is the classical electrical contribution [13]. At the macroscale we get additional contributions which, like the stress tensors, can produce a shift in phase-equilibrium of the species. See [9] for further discussion.

In examining (36) we see that it does not make sense to both impose charge neutrality through the Lagrange multiplier Λ and to have q_e^{sj} as an independent variable. Either we have charge neutrality, in which case all terms involving $\partial \tilde{A}^s / (\partial q_e^{sj})$ are dropped, or one drops the charge neutrality condition and sets Λ to zero. We shall continue to carry both terms for generality.

Taking advantage of these relations and simplifying gives us the dissipative portion of the entropy inequality in Appendix A.

4 Near-Equilibrium Constitutive Restrictions

Equilibrium is defined to occur when the following variables, defined generically as x_a , are zero:

$$\mathbf{d}^l, \varepsilon^l, \mathbf{v}^{l,s}, \nabla \mathbf{v}^{l,j,l}, \mathbf{v}^{\alpha_j, \alpha}, \quad \alpha = l, s \quad j = 1, \dots, N - 1 \quad (37)$$

$$\nabla T, \varepsilon^l \rho^{l,j} \hat{e}_s^{l,j}, \omega^\alpha, \varepsilon^l \rho^{l,j} \hat{Z}_s^{l,j}, \quad \alpha = l, s \quad j = 1, \dots, N. \quad (38)$$

Using a dimensionality argument we can show that these variables are functionally independent. Hence we have

$$\left. \frac{\partial}{\partial x_a} \left(\sum_{\alpha=l,s} \varepsilon^\alpha \rho^\alpha T \hat{\Lambda}^\alpha \right)_D \right|_e = 0, \quad \left. \frac{\partial^2}{\partial (x_a x_b)} \left(\sum_{\alpha=l,s} \varepsilon^\alpha \rho^\alpha T \hat{\Lambda}^\alpha \right)_D \right|_e \geq 0, \quad (39)$$

where subscript e denotes equilibrium. Note that we have not incorporated \hat{r}^{α_j} and \hat{q}^{α_j} into the above set. This is because without incorporating specific chemical reactions, incorrect results are obtained.

So for example, considering $x_a = \mathbf{d}^l$, we have at equilibrium

$$\mathbf{t}_{\text{sym}}^l = -\pi^l \mathbf{I} + q_e^l \Lambda - \sum_{j=1}^N \rho^l q_e^{l,j} \frac{\partial \tilde{A}^l}{\partial q_e^{l,j}}. \quad (40)$$

To obtain results which hold near equilibrium, we expand linearly about equilibrium. For example

$$\left(\mathbf{t}_{\text{sym}}^l + \pi^l \mathbf{I} - q_e^l \Lambda + \sum_{j=1}^N \rho^l q_e^{l,j} \frac{\partial \tilde{A}^l}{\partial q_e^{l,j}} + \sum_{j=1}^N \rho^l q_e^{l,j} \mathbf{v}^{l,j,l} \mathbf{v}^{l,j,l} \right)$$

$$\approx \left(t_{\text{sym}}^l + \pi^l \mathbf{I} - q_e^l \Lambda + \sum_{j=1}^N \rho^l q_e^{lj} \frac{\partial \tilde{A}^l}{\partial q_e^{lj}} \right)_e + \mathbf{f}_1 : \mathbf{d}^l + f_2 \dot{\varepsilon}^l + \mathbf{f}_3 : \nabla T + \dots \quad (41)$$

where \mathbf{f}_1 and \mathbf{f}_3 are fourth order tensors and f_2 is a scalar. These linearization coefficients are functions of all independent variables which are not in the lists (37) or (38). In this manner one can obtain cross effects, e.g. [16], and nonlinear terms, e.g. [5]. We choose to linearize only about the one variable which produces a quadratic term in the entropy inequality, e.g. for the liquid phase stress tensor:

$$t_{\text{sym}}^l \approx -\pi^l \mathbf{I} + q_e^l \Lambda - \sum_{j=1}^N \rho^l q_e^{lj} \frac{\partial \tilde{A}^l}{\partial q_e^{lj}} + \nu : \mathbf{d}^l - \sum_{j=1}^N \rho^l q_e^{lj} v^{lj,l} v^{lj,l} \quad (42)$$

where ν is a fourth-order tensor.

We note that in order to obtain equilibrium results the x_a must be functionally independent. However near equilibrium, one can linearize about any independent variable which is zero at equilibrium.

Defining pressure in terms of extensive variables to be $p^l = -\partial \tilde{A}_T^l / (\partial V^l)$ where \tilde{A}_T^l is the total Helmholtz energy and V^l the total volume of phase l , we can convert to intensive variables and show that this is equivalent to

$$p^l = -\varepsilon^l \rho^l \left. \frac{\partial \tilde{A}^l}{\partial \varepsilon^l} \right|_{\varepsilon^l, \rho^l, T, \dots} \quad (43)$$

This pressure is equivalent to the thermodynamic pressure, π^l , only in the case of a single phase and single constituent.

Using this definition and linearizing about $\dot{\varepsilon}^l$, we obtain

$$\mu^l \dot{\varepsilon}^l = p^l - p^s + \frac{1}{2} \varepsilon_o \mathbf{E}_T \cdot (\mathbf{E}^l - \mathbf{E}^s), \quad (44)$$

where μ^l is the linearization coefficient and is not to be confused with the electrochemical potential. Thus if there are no effects of the electric field and $p^l > p^s$ the volume fraction will change so as to increase the amount of liquid phase. The last term involves the differences in the electro-stress tensor $t_E = \mathbf{D} \mathbf{E} - \frac{1}{2} \varepsilon_o \mathbf{E} \cdot \mathbf{E} \mathbf{I}$ (see the conservation of linear momentum equation in Part I). Thus if the contribution of the electric field of one phase is greater than the other, then the equilibrium volume fraction will be affected.

Linearizing about ∇T and ω^α yields the traditional results

$$\mathbf{K} \cdot \nabla T = \sum_{\alpha=l,s} \mathbf{q}^\alpha \quad (45)$$

$$\varepsilon^\alpha t_{as}^\alpha = \mathbf{Q}^\alpha : \omega^\alpha, \quad (46)$$

where \mathbf{K} and \mathbf{Q}^α are second order and fourth order tensors, respectively. The first is Fourier's law of heat conduction (where normally \mathbf{q}^α is defined with the

opposite sign) and (46) states that the stress tensors are not symmetric, which was known from the conservation of angular momentum (see Part I [4]). Cross effects can also be obtained [16].

Linearizing about the conservation of charge exchange term, $\widehat{Z}_s^{l_j}$, yields the following near-equilibrium result

$$\varepsilon^l \rho^{l_j} G^{l_j} \widehat{Z}_s^{l_j} = \rho^s \frac{\partial \tilde{A}^s}{\partial q_e^{s_j}} - \rho^l \frac{\partial \tilde{A}^l}{\partial q_e^{l_j}}, \quad (47)$$

where G^{l_j} is the linearization constant. Thus, only if there is an imbalance in the electric-potential terms will charges from constituent j move from one phase to the other. Note that the Lagrange multiplier enforcing charge neutrality does not appear in this expression, since if the medium is charge-neutral and \tilde{A}^α are independent of $q_e^{\alpha_j}$, and assuming no cross-effects, no net charge is transferred between phases.

Adsorption relations are obtained by linearizing about the rate at which mass is transferred from the solid phase to the liquid phase, $\varepsilon^l \rho^{l_j} \widehat{e}_s^{l_j}$. At equilibrium we obtain

$$\mu^{l_j} - \mu^{s_j} = 0. \quad (48)$$

so that phase-equilibrium is governed by the electro-chemical potential alone. Linearizing about equilibrium yields

$$\varepsilon^l \rho^{l_j} \mathbf{K}^{l_j} \widehat{e}_s^{l_j} + z^{l_j} \left(\rho^l \frac{\partial \tilde{A}^l}{\partial q_e^{l_j}} - \rho^s \frac{\partial \tilde{A}^s}{\partial q_e^{s_j}} \right) = \mu^{s_j} - \mu^{l_j} \quad (49)$$

where, by (47), the second term on the left-hand-side is zero at equilibrium.

The relationship between the chemical potential and the partial stress tensor of the liquid phase is obtained exactly as in the previous section for the solid phase, except that the liquid phase result holds only at equilibrium:

$$\mu^{l_j} \mathbf{I} = \tilde{A}^{l_j} \mathbf{I} - \frac{1}{\rho^{l_j}} \mathbf{t}^{l_j} + z^{l_j} \left(\Lambda - \rho^l \frac{\partial \tilde{A}^l}{\partial q_e^{l_j}} \right) \mathbf{I} + \frac{1}{\rho^l} \mathbf{E}_T \cdot \mathbf{P}^l \mathbf{I}. \quad (50)$$

5 Bulk-Phase Flow and Diffusion

The equations which govern momentum balance in porous media are known as generalized Darcy's equations, after Darcy, who in 1856 empirically derived the rather simple relationship that flux is proportional to the gradient in fluid pressure:

$$\varepsilon^l \mathbf{v}^{l,s} = -\mathbf{K} \nabla p^l + \varepsilon^l \rho^l \mathbf{g}, \quad (51)$$

where \mathbf{K} is the conductivity of the material. It is generally thought to be valid for slow-moving viscous fluids through a homogeneous granular media. We

would like to determine the generalization of this law for the swelling charged porous media considered here. To begin with, we linearize about $\mathbf{v}^{l,s}$ and obtain a near-equilibrium expression for the exchange of momentum term, $\hat{\mathbf{T}}_s^l$, which may then be substituted into the conservation of momentum equation. Neglecting inertial effects and using (40) to eliminate \mathbf{t}^l we obtain:

$$\begin{aligned} \mathbf{K} \cdot \mathbf{v}^{l,s} = & -\nabla(\varepsilon^l \pi^l) + \varepsilon^l \rho^l (\mathbf{g}^l + \mathbf{g}_I^l) + \left(p^l + \frac{1}{2} \varepsilon_o \mathbf{E}_T \cdot \mathbf{E}^l \right) \nabla \varepsilon^l + \varepsilon^l q_e^l \mathbf{E}_T \\ & - \varepsilon^l \rho^l \left(\eta^l + \frac{\partial \tilde{\mathbf{A}}^l}{\partial T} \right) \nabla T - \Lambda \nabla(\varepsilon^l q_e^l) - \varepsilon^l \rho^l \frac{\partial \tilde{\mathbf{A}}^l}{\partial \varepsilon^s} : (\nabla \mathcal{E}^s)^T \\ & - \varepsilon^l \rho^l \frac{\partial \tilde{\mathbf{A}}^l}{\partial \mathbf{E}_T} \cdot (\nabla \mathbf{E}_T)^T - \varepsilon^l \rho^l \frac{\partial \tilde{\mathbf{A}}^l}{\partial (\nabla T)} \cdot (\nabla^2 T). \end{aligned} \quad (52)$$

The linearization constant \mathbf{K} is positive definite by the minimization of entropy generation at equilibrium, and may be a function of all independent variables not equal to zero at equilibrium, including ε^l . For a homogeneous rigid medium ε^l is constant, and if there is an absence of electric fields, \mathbf{g}_I is zero so that we recover Darcy's equations. The terms not involving the electric field have been derived before [3] and these results are discussed in detail in [8]. They indicate that flow can be driven by a gradient in the volume fraction and gradients in shear strain, the latter of which may be appropriate for swelling media with low water content. These terms account for the chemical/hydration forces between the solid and liquid phase. The term involving ∇T suggests flow in porous media can be driven by a gradient in temperature. In addition to these terms, we have the Lorentz force ($\varepsilon^l q_e^l \mathbf{E}_T$), the Kelvin force (using equation (23)) $\varepsilon^l \mathbf{P}^l \cdot \nabla \mathbf{E}_T$, and a term enforcing charge neutrality, $\Lambda \nabla(\varepsilon^l q_e^l)$. Further, a portion of the electro-stress tensor, $1/2 \varepsilon_o \mathbf{E}_T \cdot \mathbf{E}^l$, magnifies the effects a gradient in the volume fraction has on the rate of flow.

Diffusion in a single-phase mixture is governed by *Fick's law*, which states diffusive velocity is proportional to the gradient of the chemical potential. Here we derive a novel form of Fick's law. Begin with the coefficient of $\mathbf{v}^{l,j,l}$ in the residual entropy inequality which, when set to zero, gives at equilibrium:

$$\begin{aligned} \varepsilon^\alpha \rho^{\alpha_j} (\hat{\mathbf{i}}^{\alpha_j} + \hat{\mathbf{T}}_\beta^{\alpha_j}) - \varepsilon^\alpha \rho^{\alpha_j} (\hat{\mathbf{i}}^{\alpha_N} + \hat{\mathbf{T}}_\beta^{\alpha_N}) = & -\nabla [\varepsilon^\alpha \rho^{\alpha_j} (\tilde{\mathbf{A}}^{\alpha_j} - \tilde{\mathbf{A}}^{\alpha_N})] \\ & - \varepsilon^\alpha \nabla \mathbf{E}_T \cdot (\mathbf{P}^{\alpha_j} - \frac{\rho^{\alpha_j}}{\rho^{\alpha_N}} \mathbf{P}^{\alpha_N}) + \frac{1}{2} \varepsilon_o \mathbf{E}_T \cdot (\mathbf{E}^{\alpha_j} - \frac{\rho^{\alpha_j}}{\rho^{\alpha_N}} \mathbf{E}^{\alpha_N}) \nabla \varepsilon^\alpha \\ & - \frac{\varepsilon^\alpha}{T} \mathbf{E}_T \cdot (\mathbf{P}^{\alpha_j} - \frac{\rho^{\alpha_j}}{\rho^{\alpha_N}} \mathbf{P}^{\alpha_N}) \nabla T + \rho^\alpha \left(\frac{\partial \tilde{\mathbf{A}}^\alpha}{\partial \rho^{\alpha_j}} - \frac{\partial \tilde{\mathbf{A}}^\alpha}{\partial \rho^{\alpha_N}} \right) \nabla (\varepsilon^\alpha \rho^{\alpha_j}) \\ & + \left(\rho^\alpha \frac{\partial \tilde{\mathbf{A}}^\alpha}{\partial q_e^{\alpha_j}} - \Lambda \right) \nabla (\varepsilon^\alpha q_e^{\alpha_j}) - \left(\rho^\alpha \frac{\partial \tilde{\mathbf{A}}^\alpha}{\partial q_e^{\alpha_N}} - \Lambda \right) \nabla \left(\varepsilon^\alpha \frac{\rho^{\alpha_j}}{\rho^{\alpha_N}} q_e^{\alpha_N} \right) \\ & - \varepsilon^\alpha (q_e^{\alpha_j} - \frac{\rho^{\alpha_j}}{\rho^{\alpha_N}} q_e^{\alpha_N}) \mathbf{E}_T - \varepsilon^\alpha \mathbf{t}^{\alpha_N} \cdot \nabla \left(\frac{\rho^{\alpha_j}}{\rho^{\alpha_N}} \right) \Big] \quad j = 1, \dots, N-1. \end{aligned} \quad (53)$$

In addition we have from (15)

$$\begin{aligned}
 -\nabla(\varepsilon^l \rho^l \tilde{A}^l) &= -\varepsilon^l \rho^l \frac{\partial \tilde{A}^l}{\partial \varepsilon^l} \nabla \varepsilon^l - \varepsilon^l \rho^l \frac{\partial \tilde{A}^l}{\partial T} \nabla T - \sum_{j=1}^N \rho^l \frac{\partial \tilde{A}^l}{\partial \rho^{lj}} \nabla(\varepsilon^l \rho^{lj}) \\
 &\quad - \sum_{j=1}^N \tilde{A}^l \nabla(\varepsilon^l \rho^{lj}) - \varepsilon^l \rho^l \frac{\partial \tilde{A}^l}{\partial \mathcal{E}^s} : (\nabla \mathcal{E}^s)^T - \varepsilon^l \rho^l \frac{\partial \tilde{A}^l}{\partial \mathbf{E}_T} \cdot \nabla \mathbf{E}_T \\
 &\quad - \sum_{j=1}^N \rho^l \frac{\partial \tilde{A}^l}{\partial q_e^{lj}} \nabla(\varepsilon^l q_e^{lj}) - \varepsilon^l \rho^l \frac{\partial \tilde{A}^l}{\partial (\nabla T)} \cdot \nabla^2 T
 \end{aligned} \tag{54}$$

so that from the coefficient of $v^{l,s}$ we have at equilibrium

$$\begin{aligned}
 \varepsilon^l \rho^l \tilde{T}_s^l &= -\varepsilon^l \rho^l \nabla \tilde{A}^l + \sum_{j=1}^N \rho^l \frac{\partial \tilde{A}^l}{\partial \rho^{lj}} \nabla(\varepsilon^l \rho^{lj}) + \sum_{j=1}^N \rho^l \frac{\partial \tilde{A}^l}{\partial q_e^{lj}} \nabla(\varepsilon^l q_e^{lj}) \\
 &\quad - \varepsilon^l \rho^l \eta^l \nabla T - \varepsilon^l \nabla \mathbf{E}_T \cdot \mathbf{P}^l + \frac{1}{2} \varepsilon_o \mathbf{E}_T \cdot \mathbf{E}^l \nabla \varepsilon^l \\
 &\quad - \Lambda \nabla(\varepsilon^l q_e^l).
 \end{aligned} \tag{55}$$

Summing (53) over j from 1 to N and making use of the two forms of the chemical potential, (32) and (50), we obtain (56) for the case $j = N$. Substituting this result back into (53) and again making use of (32) and (50) we obtain the equilibrium result:

$$\begin{aligned}
 \varepsilon^l \rho^{lj} (\tilde{i}^{lj} + \tilde{T}_s^{lj}) &= -\varepsilon^l \rho^{lj} \nabla \mu^{lj} - \nabla \cdot (\varepsilon^l \mathbf{t}^{lj}) \\
 &\quad + \varepsilon^l q_e^{lj} \nabla \left(\Lambda - \rho^l \frac{\partial \tilde{A}^l}{\partial q_e^{lj}} \right) - \varepsilon^l \nabla \mathbf{E}_T \cdot \mathbf{P}^{lj} + \frac{\rho^{lj}}{\rho^l} \nabla(\varepsilon^l \mathbf{E}_T \cdot \mathbf{P}^l) \\
 &\quad + \frac{\varepsilon^l}{T} \left(\frac{\rho^{lj}}{\rho^l} \mathbf{P}^l - \mathbf{P}^{lj} \right) \cdot \mathbf{E}_T \nabla T + \varepsilon^l \left(\frac{\rho^{lj}}{\rho^l} q_e^l - q_e^{lj} \right) \mathbf{E}_T + \frac{1}{2} \varepsilon_o \mathbf{E}_T \cdot \mathbf{E}^{lj} \nabla \varepsilon^l \\
 &\quad - \frac{\rho^{lj}}{\rho^l} \varepsilon^l \tilde{d}_s \mathbf{E}_T,
 \end{aligned} \tag{56}$$

where \tilde{d}_s represents the phase exchange term in Gauss' law. If the electric field for species is defined appropriately, \tilde{d}_s is zero [4]. Note that as in the chemical potential, the Lagrange multiplier enforcing charge neutrality, Λ , appears in combination with $\partial \tilde{A}^l / (\partial q_e^{lj})$ in the same manner throughout.

Next we linearize about equilibrium using the coefficient of $v^{lj,l}$ in the original entropy inequality given in Appendix B. This allows us to obtain non-relative results since $j = 1, \dots, N$. Here we make use of the fact that \tilde{A}^l and the primary independent variables, listed in (8), are the same at equilibrium and near-equilibrium. That this holds for \tilde{A}^l is justified by since \tilde{A}^l is not a function of any of the variables which define equilibrium. We also assume that the

constitutive equation for \mathbf{P}^{l_j} is the same at equilibrium and near-equilibrium. Using this result to eliminate $\varepsilon^l \rho^{l_j} (\hat{\mathbf{i}}^{l_j} + \hat{\mathbf{T}}_s^{l_j})$ in the conservation of momentum equation, neglecting the inertial term, and approximating μ^{l_j} using equation (50), we obtain

$$\begin{aligned} \mathbf{R}^{l_j} \mathbf{v}^{l_j, l} = & -\varepsilon^l \rho^{l_j} \nabla \mu^{l_j} + \varepsilon^l \rho^{l_j} (\mathbf{g}^{l_j} - \mathbf{g}_I^{l_j}) - \varepsilon^l q_e^{l_j} \nabla \left[\rho^l \frac{\partial \tilde{\mathbf{A}}^l}{\partial q_e^{l_j}} - \Lambda \right] \\ & + \varepsilon^l \frac{\rho^{l_j}}{\rho^l} q_e^l \mathbf{E}_T - \frac{\varepsilon^l}{T} \mathbf{P}^{l_j} \cdot \mathbf{E}_T \nabla T + \frac{\rho^{l_j}}{\rho^l} \nabla (\varepsilon^l \mathbf{E}_T \cdot \mathbf{P}^l) - \frac{\rho^{l_j}}{\rho^l} \varepsilon^l \hat{\mathbf{d}}_s^{l_j} \mathbf{E}_T, \end{aligned} \quad (57)$$

where \mathbf{R}^{l_j} is the linearization constant. Recall that $\hat{\mathbf{d}}_s^{l_j}$ is the exchange term from Gauss' equation, so that $\varepsilon^l \hat{\mathbf{d}}_s^{l_j} \mathbf{E}_T$ can be viewed as an additional body force, with the electric field producing the source.

To analyze this further, assume that \mathbf{E}^l is defined in such a way that $\hat{\mathbf{d}}_s^{l_j}$ is zero, body force, \mathbf{g}^{l_j} is gravity, \mathbf{g} , temperature gradients are negligible, and we enforce charge neutrality with the Lagrange multiplier, Λ , and that $\tilde{\mathbf{A}}^l$ is not a function of the charges, $q_e^{l_j}$. In this case (57) simplifies to

$$\begin{aligned} \mathbf{R}^{l_j} \mathbf{v}^{l_j, l} = & -\varepsilon^l \rho^{l_j} \nabla \mu^{l_j} + \varepsilon^l \rho^{l_j} (\mathbf{g} - \mathbf{g}_I^{l_j}) + \varepsilon^l q_e^{l_j} \nabla \Lambda \\ & + \frac{\rho^{l_j}}{\rho^l} \nabla (\varepsilon^l \mathbf{E}_T \cdot \mathbf{P}^l) + \varepsilon^l \frac{\rho^{l_j}}{\rho^l} q_e^l \mathbf{E}_T. \end{aligned} \quad (58)$$

The first two terms (on the right-hand-side) gives the standard Fick's law, where the body force has an additional term due to differences in \mathbf{E}_T and \mathbf{E}^{l_j} . The third term represents the electric potential due to charge of the specie, but unlike [17, 20], the charge density appears outside the gradient, and not within. If the charge of the species per unit mass density, z^{l_j} , is constant, as is assumed in [17, 20], then we get agreement with [17, 20]. The last two terms involve bulk-phase forces weighted by the mass fraction, just as the gravitational force is weighted by the mass density. These terms are new and should be evaluated carefully, although similar bulk terms have been derived before, [2]. The first of the last two terms originates from the last term in the relationship between the chemical potential and the partial stress tensor, (50), and is a term which affects the chemical potentials of all constituents in the liquid phase. That it is weighted by a mass concentration is a consequence of the fact that the bulk phase velocity is a sum of the mass concentrations weighted constituent velocities.

The last term in (58) comes from the energy work term $\varepsilon^l \mathcal{J}^{l_j} \cdot \mathbf{E}_T$. The presence of this term should be experimentally measured since it could easily be incorporated into the entropy source term in equation (2). If the work term were incorporated into the entropy source, the last term in (58) would not appear, no other relations would be affected, and there would be one less term in the dissipative entropy inequality which was not exploited here, $\sum_{\alpha=l,s} \varepsilon^\alpha \mathcal{J}^\alpha \cdot \mathbf{E}_T$

in Appendix A. Recall that (2) is an assumption, and although has been shown to give valid results for the case with no electric field, the exact form for the case considered herein is not known. This provides an excellent opportunity for determining the assumptions listed in (2) - any term in (58) which is determined to be not there physically could be absorbed (indirectly) into the entropy source or entropy flux. The remaining relations would then need to be modified in order to remain thermodynamically admissible.

6 Discussion

We exploited the entropy inequality to obtain constitutive relations for a swelling porous medium composed of a possibly polarizable solid and liquid phase, with charges and an electric field. We did so under the philosophy that it is the total electric field which contributes to the force and work terms in the conservation of momentum and energy terms, and that it is only the total electric field which is measurable. This produced an additional term involving the gradient of the volume fraction in the macroscale conservation of momentum equation, which manifests itself as an additional term in the generalized Darcy equation, (52). Further, the Lorentz force, Kelvin force, and charge neutrality (if enforced) also determine the overall flow rate.

The Lagrange multiplier which enforces charge neutrality is shown to appear almost unilaterally with the change in modified Helmholtz potential with respect to the charge density (see e.g. (36)). Since the volume fraction and density are held fixed while taking this partial derivative, we see that the Lagrange multiplier is related to the change in energy with respect to charge density, and that which constituent the charge is associated with is irrelevant.

The relation between the chemical potential and the partial stress tensors involves some novel bulk-scale quantities, see (36) and (50). These new terms affect phase equilibrium (see discussion in [9]), and affect diffusion, see (58). The exact form of the diffusion equation should be validated experimentally, and this would give a method for determining the exact form of the entropy source and entropy flux, which for this paper was assumed.

Other results include that the rate at which the medium swells is determined by the difference in the thermodynamic pressures $p^l - p^s$ and the difference of a portion of the electro-stress tensor, see equation (44). We also showed that it is the chemical potential which determines phase-equilibria (48), but that near equilibrium, the electric potential becomes a factor (49). Likewise we also note that the the stress tensor of each phase is not affected by the presence of the electric field other than through the dependence of the Helmholtz potential on the charged particles and electric field.

Acknowledgments. JHC would like to acknowledge the ARO / Terrestrial Sciences and Mathematics divisions for support under grant DAAG55-98-1-0228.

References

- [1] S. Achanta, J. H. Cushman, and M. R. Okos. On multicomponent, multiphase thermomechanics with interfaces. *Int. J. Eng. Sci.*, 32(11):1717–1738, 1994.
- [2] R. Benach and I. Müller. Thermodynamics and the description of magnetizable dielectric mixtures of fluids. *Archive for Rational Mechanics and Analysis*, 53(4):312–346, 1973.
- [3] L. S. Bennethum and J. H. Cushman. Multiscale, hybrid mixture theory for swelling systems - II: Constitutive theory. *Int. J. Engrg. Sci.*, 34(2):147–169, 1996.
- [4] L. S. Bennethum and J. H. Cushman. Multicomponent, multiphase thermodynamics of swelling porous media with electroquasistatics: I. macroscale field equations. *IJES*, submitted, 2000.
- [5] L. S. Bennethum and T. Giorgi. Generalized forchheimer law for two-phase flow based on hybrid mixture theory. *Transport in Porous Media*, 26(3):261–275, 1997.
- [6] L. S. Bennethum, M. A. Murad, and J. H. Cushman. Clarifying hybrid mixture theory and the macroscale chemical potential for porous media. *Int. J. Eng. Sci.*, , 1996.
- [7] L. S. Bennethum, M. A. Murad, and J. H. Cushman. Clarifying mixture theory and the macroscale chemical potential for porous media. *International Journal of Engineering Science*, 34(14):1611–1621, 1996.
- [8] L. S. Bennethum, M. A. Murad, and J. H. Cushman. Modified darcy's law, terzaghi's effective stress principle and fick's law for swelling clay soils. *Computers and Geotechnics*, 20(3/4):245–266, 1997.
- [9] L. S. Bennethum, M. A. Murad, and J. H. Cushman. Macroscale thermodynamics and the chemical potential for swelling porous media. *Transport in Porous Media*, to appear, 2000.
- [10] R. M. Bowen. Theory of mixtures. In A. C. Eringen, editor, *Continuum Physics*. Academic Press, Inc., New York, 1976.
- [11] R. M. Bowen. Compressible porous media models by use of the theory of mixtures. *International Journal of Engineering Science*, 20:697–735, 1982.
- [12] H. B. Callen. *Thermodynamics and an Introduction to Thermostatistics*. John Wiley and Sons, New York, 1985.
- [13] G. W. Castellan. *Physical Chemistry*. Benjamin/Cummings, Menlo Park, CA, 1983.

- [14] B. D. Coleman and W. Noll. The thermodynamics of elastic materials with heat conduction and viscosity. *Arch. Rat. Mech. Anal.*, 13:167–178, 1963.
- [15] A. C. Eringen. *Mechanics of Continua*. John Wiley and Sons, New York, 1967.
- [16] A. C. Eringen. A mixture theory of electromagnetism and superconductivity. *International Journal of Engineering Science*, 36(5,6):525–543, 1998.
- [17] W. Y. Gu, W. M. Lai, and V. C. Mow. Transport of multi-electrolytes in charged hydrated biological soft tissues. *Transport in Porous Media*, 34:143–157, 1999.
- [18] S. M. Hassanzadeh and W. G. Gray. General conservation equations for multiphase systems: 2. Mass, momenta, energy, and entropy equations. *Advances in Water Resources*, 2:191–208, 1979.
- [19] S. M. Hassanzadeh and W. G. Gray. General conservation equations for multiphase systems: 3. Constitutive theory for porous media. *Advances in Water Resources*, 3:25–40, 1980.
- [20] J. M. Huyghe and J. D. Janssen. Thermo-chemo-electro-mechanical formulation of saturated charged porous solids. *Transport in Porous Media*, 34:129–141, 1999.
- [21] D. Jou, J. Casas-Vázquez, and G. Lebon. *Extended Irreversible Thermodynamics*. Springer-Verlag, New York, 1996.
- [22] I-Shih Liu. Method of lagrange multipliers for exploitation of the entropy principle. *Archive for Rational Mechanics and Analysis*, 46:131–148, 1972.
- [23] I. Müller and T. Ruggeri. *Extended Thermodynamics*. Springer-Verlag, New York, 1993.
- [24] M. A. Murad, L. S. Bennethum, and J. H. Cushman. A multi-scale theory of swelling porous media: I. Application to one-dimensional consolidation. *Transport in Porous Media*, 19:93–122, 1995.
- [25] M. A. Murad and J. H. Cushman. Multiscale flow and deformation in hydrophilic swelling porous media. *International Journal of Engineering Science*, 34(3):313–336, 1996.
- [26] C. Truesdell and W. Noll. *The Non-Linear Field Theories of Mechanics. Handbuch der Physik III/3*. Springer-Verlag, 1965.

Appendix A. Dissipative Entropy Inequality

The dissipative portion of the entropy inequality is

$$\begin{aligned}
(\sum_{\alpha} \varepsilon^{\alpha} \rho^{\alpha} T \hat{\Lambda}^{\alpha})_D = & \\
d^l : [\varepsilon^l t_{\text{sym}}^l + \sum_{j=1}^N \varepsilon^l \rho^{l_j} v^{l_j, l} v^{l_j, l} + \varepsilon^l \pi^l - \varepsilon^l q_e^l \Lambda + \sum_{j=1}^N \varepsilon^l \rho^l q_e^{l_j} \frac{\partial \tilde{A}^l}{\partial q_e^{l_j}}] & \\
+ \varepsilon^l \left[-\varepsilon^l \rho^l \frac{\partial \tilde{A}^l}{\partial \varepsilon^l} - \varepsilon^s \rho^s \frac{\partial \tilde{A}^s}{\partial \varepsilon^l} + \frac{1}{2} \varepsilon_o \mathbf{E}_T \cdot (\mathbf{E}^l - \mathbf{E}^s) \right] & \\
+ \mathbf{v}^{l,s} \cdot \left[-\varepsilon^l \rho^l \left(\eta^l + \frac{\partial \tilde{A}^l}{\partial T} \right) \nabla T - \varepsilon^l \rho^l \tilde{T}_s^l - \varepsilon^l \rho^l \frac{\partial \tilde{A}^l}{\partial \varepsilon^l} \nabla \varepsilon^l \right. & \\
\left. - \varepsilon^l \rho^l \frac{\partial \tilde{A}^l}{\partial \varepsilon^s} : (\nabla \mathcal{E}^s)^T - \varepsilon^l \rho^l \frac{\partial \tilde{A}^l}{\partial \mathbf{E}_T} \cdot (\nabla \mathbf{E}_T)^T - \varepsilon^l \nabla \mathbf{E}_T \cdot \mathbf{P}^l \right. & \\
\left. + \frac{1}{2} \varepsilon_o \mathbf{E}_T \cdot \mathbf{E}^l \nabla \varepsilon^l - \Lambda \nabla (\varepsilon^l q_e^l) - \varepsilon^l \rho^l \frac{\partial \tilde{A}^l}{\partial \nabla T} \cdot \nabla^2 T \right] & \\
+ \sum_{j=1}^{N-1} \nabla v^{l_j, l} : \varepsilon^l \left[t^{l_j} - \frac{\rho^{l_j}}{\rho^{l_N}} t^{l_N} + \rho^l \rho^{l_j} \left(\frac{\partial \tilde{A}^l}{\partial \rho^{l_j}} - \frac{\partial \tilde{A}^l}{\partial \rho^{l_N}} \right) - \rho^{l_j} (\tilde{A}^{l_j} - \tilde{A}^{l_N}) \mathbf{I} \right. & \\
\left. + \rho^l \left(q_e^{l_j} \frac{\partial \tilde{A}^l}{\partial q_e^{l_j}} - \frac{\rho^{l_j}}{\rho^{l_N}} q_e^{l_N} \frac{\partial \tilde{A}^l}{\partial q_e^{l_N}} \right) \mathbf{I} - (q_e^{l_j} - \frac{\rho^{l_j}}{\rho^{l_N}} q_e^{l_N}) \Lambda \mathbf{I} \right] & \\
+ \sum_{\alpha=l,s} \sum_{j=1}^{N-1} \mathbf{v}^{\alpha_j, \alpha} \cdot \left[-\varepsilon^{\alpha} \rho^{\alpha_j} (\tilde{i}^{\alpha_j} + \tilde{T}_{\beta}^{\alpha_j}) + \varepsilon^{\alpha} \rho^{\alpha_j} (\tilde{i}^{\alpha_N} + \tilde{T}_{\beta}^{\alpha_N}) \right. & \\
\left. - \nabla (\varepsilon^{\alpha} \rho^{\alpha_j} (A^{\alpha_j} - A^{\alpha_N})) - \varepsilon^{\alpha} \nabla \mathbf{E}_T \cdot (\mathbf{P}^{\alpha_j} - \frac{\rho^{\alpha_j}}{\rho^{\alpha_N}} \mathbf{P}^{\alpha_N}) \right. & \\
\left. + \frac{1}{2} \varepsilon_o \mathbf{E}_T \cdot (\mathbf{E}^{\alpha_j} - \frac{\rho^{\alpha_j}}{\rho^{\alpha_N}} \mathbf{E}^{\alpha_N}) \nabla \varepsilon^{\alpha} - \frac{\varepsilon^{\alpha}}{T} \mathbf{E}_T \cdot (\mathbf{P}^{\alpha_j} - \frac{\rho^{\alpha_j}}{\rho^{\alpha_N}} \mathbf{P}^{\alpha_N}) \nabla T \right. & \\
\left. + \rho^{\alpha} \left(\frac{\partial \tilde{A}^{\alpha}}{\partial \rho^{\alpha_j}} - \frac{\partial \tilde{A}^{\alpha}}{\partial \rho^{\alpha_N}} \right) \nabla (\varepsilon^{\alpha} \rho^{\alpha_j}) + \left(\rho^{\alpha} \frac{\partial \tilde{A}^{\alpha}}{\partial q_e^{\alpha_j}} - \Lambda \right) \nabla (\varepsilon^{\alpha} q_e^{\alpha_j}) \right. & \\
\left. - \left(\rho^{\alpha} \frac{\partial \tilde{A}^{\alpha}}{\partial q_e^{\alpha_N}} - \Lambda \right) \nabla \left(\varepsilon^{\alpha} \frac{\rho^{\alpha_j}}{\rho^{\alpha_N}} q_e^{\alpha_N} \right) - \varepsilon^{\alpha} (q_e^{\alpha_j} - \frac{\rho^{\alpha_j}}{\rho^{\alpha_N}} q_e^{\alpha_N}) \mathbf{E}_T - \varepsilon^{\alpha} t^{\alpha_N} \cdot \nabla \left(\frac{\rho^{\alpha_j}}{\rho^{\alpha_N}} \right) \right] & \\
+ \sum_{\alpha=l,s} \frac{\varepsilon^{\alpha}}{T} \nabla T \cdot \left[q^{\alpha} + \sum_{j=1}^N \left(\rho^{\alpha_j} v^{\alpha_j, \alpha} (\tilde{A}^{\alpha_j} + \frac{1}{2} (v^{\alpha_j, \alpha})^2) - t^{\alpha_j} \cdot v^{\alpha_j, \alpha} \right) \right] & \\
+ \sum_{\alpha=l,s} \sum_{j=1}^N \varepsilon^l \rho^{l_j} \tilde{e}_s^{l_j} \left[-\tilde{A}^l + \tilde{A}^s - \rho^l \frac{\partial \tilde{A}^l}{\partial \rho^{l_j}} + \rho^s \frac{\partial \tilde{A}^s}{\partial \rho^{s_j}} - z^{l_j} (\rho^l \frac{\partial \tilde{A}^l}{\partial q_e^{l_j}} - \rho^s \frac{\partial \tilde{A}^s}{\partial q_e^{s_j}}) \right. & \\
\left. + \frac{1}{2} \mathbf{v}^{s_j, s} \cdot \mathbf{v}^{s_j, s} - \frac{1}{2} \mathbf{v}^{l_j, l} \cdot \mathbf{v}^{l_j, l} - \frac{1}{2} \mathbf{v}^{l,s} \cdot \mathbf{v}^{l,s} \right] &
\end{aligned}$$

$$\begin{aligned}
& + \sum_{\alpha=l,s} \sum_{j=1}^N \varepsilon^\alpha \rho^{\alpha_j} \hat{r}^{\alpha_j} \left[-\rho^\alpha \frac{\partial \tilde{A}^\alpha}{\partial \rho^{\alpha_j}} - (\rho^\alpha \frac{\partial \tilde{A}^\alpha}{\partial q_e^{\alpha_j}} - \Lambda) z^{\alpha_j} - \frac{1}{2} (\mathbf{v}^{\alpha_j,\alpha})^2 \right] \\
& + \sum_{\alpha=l,s} \omega^\alpha : [\varepsilon^\alpha t_{as}^\alpha] + \sum_{\alpha=l,s} \sum_{j=1}^N \mathbf{P}^{\alpha_j} \cdot [\mathbf{E}_T^{\alpha_j} \mathbf{v}^{\alpha_j} \cdot \nabla \varepsilon^\alpha] \\
& + \sum_{\alpha=l,s} \sum_{j=1}^N \nabla \cdot (\varepsilon^\alpha \mathcal{J}^{\alpha_j}) [\rho^\alpha \frac{\partial A_T}{\partial q_e^{\alpha_j}} - \Lambda] + \sum_{\alpha=l,s} \varepsilon^\alpha \mathcal{J}^\alpha \cdot \mathbf{E}_T \\
& - \sum_{\alpha=l,s} \sum_{j=1}^N \varepsilon^\alpha \hat{q}^{\alpha_j} [\rho^\alpha \frac{\partial \tilde{A}^\alpha}{\partial q_e^{\alpha_j}} - \Lambda] + \sum_{j=1}^N \varepsilon^l \rho^{l,j} \tilde{Z}_s^{l,j} [\rho^s \frac{\partial \tilde{A}^s}{\partial q_e^{s,j}} - \rho^l \frac{\partial \tilde{A}^l}{\partial q_e^{l,j}}] \geq 0,
\end{aligned} \tag{59}$$

where subscripted *sym* and *as* mean the symmetric and anti-symmetric part of the tensor, respectively.

Appendix B. Entropy Inequality

The entropy inequality in its entirety is:

$$\begin{aligned}
& \sum_{\alpha=l,s} \varepsilon^\alpha \rho^\alpha T \hat{\Lambda}^\alpha = \\
& \sum_{\alpha=l,s} \sum_{j=1}^N \frac{D^s(\varepsilon^\alpha \rho^{\alpha_j})}{Dt} \left[-\varepsilon^\alpha \rho^\alpha \frac{\partial \tilde{A}^\alpha}{\partial (\varepsilon^\alpha \rho^{\alpha_j})} + \lambda_\rho^{\alpha_j} + \tilde{A}^{\alpha_j} + \frac{1}{\rho^{\alpha_j}} \mathbf{E}_T \cdot \mathbf{P}^{\alpha_j} \right] \\
& + \dot{\mathbf{E}}_T \left[-\varepsilon^l \rho^l \frac{\partial \tilde{A}^l}{\partial \mathbf{E}_T} - \varepsilon^s \rho^s \frac{\partial \tilde{A}^s}{\partial \mathbf{E}_T} - \varepsilon^l \mathbf{P}^l - \varepsilon^s \mathbf{P}^s \right] \\
& + \dot{T} \left[-\varepsilon^l \rho^l \eta^l - \varepsilon^s \rho^s \frac{\partial \tilde{A}^l}{\partial T} - \varepsilon^s \rho^s \eta^s - \varepsilon^s \rho^s \frac{\partial \tilde{A}^s}{\partial T} \right] \\
& + \dot{\mathbf{d}}^l : \left[\varepsilon^l \mathbf{t}_{\text{sym}}^l + \sum_{j=1}^N \varepsilon^l \rho^{l_j} (\lambda_\rho^{l_j} \mathbf{I} + \tilde{A}^{l_j} \mathbf{I} + z^{l_j} \lambda_{q_e}^{l_j} \mathbf{I} + \mathbf{v}^{l_j,l} \mathbf{v}^{l_j,l}) \right] \\
& + \dot{\mathbf{d}}^s : \left[\varepsilon^s \mathbf{t}_{\text{sym}}^s + \sum_{j=1}^N \varepsilon^s \rho^{s_j} (\lambda_\rho^{s_j} \mathbf{I} + \tilde{A}^{s_j} \mathbf{I} + z^{s_j} \lambda_{q_e}^{s_j} \mathbf{I} + \mathbf{v}^{s_j,s} \mathbf{v}^{s_j,s}) \right. \\
& \quad \left. - \varepsilon^l \rho^l \nabla \mathbf{F}^s \cdot \frac{\partial \tilde{A}^l}{\partial \mathbf{E}^s} \cdot (\nabla \mathbf{F}^s)^T - \varepsilon^s \rho^s \nabla \mathbf{F}^s \cdot \frac{\partial \tilde{A}^s}{\partial \mathbf{E}^s} \cdot (\nabla \mathbf{F}^s)^T \right] \\
& + \sum_{\alpha=l,s} \omega^\alpha : \left[\varepsilon^\alpha t_{\text{as}}^\alpha \right] + \sum_{\alpha=l,s} \sum_{j=1}^{N-1} \frac{D^s \mathbf{v}^{\alpha_j, \alpha}}{Dt} \cdot \left[-\varepsilon^\alpha \rho^\alpha \frac{\partial \tilde{A}^\alpha}{\partial \mathbf{v}^{\alpha_j, \alpha}} \right] \\
& + \nabla \dot{T} \cdot \left[-\varepsilon^l \rho^l \frac{\partial \tilde{A}^l}{\partial \nabla T} - \varepsilon^s \rho^s \frac{\partial \tilde{A}^s}{\partial \nabla T} \right] \\
& + \sum_{\alpha=l,s} \sum_{j=1}^N \nabla \frac{D^s(\varepsilon^\alpha \rho^{\alpha_j})}{Dt} \left[-\varepsilon^\alpha \rho^\alpha \frac{\partial \tilde{A}^\alpha}{\partial \nabla (\varepsilon^\alpha \rho^{\alpha_j})} \right] \\
& + \dot{\varepsilon}^l \left[-\varepsilon^l \rho^l \frac{\partial \tilde{A}^l}{\partial \varepsilon^l} - \varepsilon^s \rho^s \frac{\partial \tilde{A}^s}{\partial \varepsilon^l} + \frac{1}{2} \varepsilon_o \mathbf{E}_T \cdot \mathbf{E}^l - \frac{1}{2} \varepsilon_o \mathbf{E}_T \cdot \mathbf{E}^s \right] \\
& + \dot{\mathbf{v}}^{l,s} \cdot \left[-\varepsilon^l \rho^l \frac{\partial \tilde{A}^l}{\partial \mathbf{v}^{l,s}} \right] + \dot{\mathbf{d}}^l : \left[-\varepsilon^l \rho^l \frac{\partial \tilde{A}^l}{\partial \mathbf{d}^l} \right] + \dot{\mathbf{w}}^l : \left[-\varepsilon^l \rho^l \frac{\partial \tilde{A}^l}{\partial \mathbf{w}^l} \right] \\
& + \nabla \dot{\mathbf{v}}^{l_j,l} : \left[-\varepsilon^l \rho^l \frac{\partial \tilde{A}^l}{\partial \nabla \mathbf{v}^{l_j,l}} \right] \\
& + \dot{\mathbf{v}}^{l,s} \cdot \left[-\varepsilon^l \rho^l \left(\eta^l + \frac{\partial \tilde{A}^l}{\partial T} \right) \nabla T - \varepsilon^l \rho^l \frac{\partial \tilde{A}^l}{\partial \varepsilon^l} \nabla \varepsilon^l - \sum_{j=1}^N \varepsilon^l \rho^l \frac{\partial \tilde{A}^l}{\partial (\varepsilon^l \rho^{l_j})} \nabla (\varepsilon^l \rho^{l_j}) \right. \\
& \quad \left. - \varepsilon^l \rho^l \frac{\partial \tilde{A}^l}{\partial \mathbf{E}^s} : (\nabla \mathbf{E}^s)^T - \varepsilon^l \rho^l \frac{\partial \tilde{A}^l}{\partial \mathbf{E}_T} \cdot (\nabla \mathbf{E}_T)^T - \sum_{j=1}^N \varepsilon^l \rho^l \frac{\partial \tilde{A}^l}{\partial (\varepsilon^l q_e^{l_j})} \nabla (\varepsilon^l q_e^{l_j}) - \varepsilon^l \nabla \mathbf{E}_T \cdot \mathbf{P}^l \right]
\end{aligned}$$

$$\begin{aligned}
& -\varepsilon^l \rho^l \tilde{\mathbf{T}}_s^l + \sum_{j=1}^N (\tilde{A}^{l_j} + \frac{1}{\rho^{l_j}} \mathbf{E}_T \cdot \mathbf{P}^{l_j}) \nabla(\varepsilon^l \rho^{l_j}) + \frac{1}{2} \mathbf{E}_T \cdot \mathbf{E}^l \nabla \varepsilon^l + \sum_{j=1}^N \lambda_{\rho}^{l_j} \nabla(\varepsilon^l \rho^{l_j}) \\
& + \sum_{j=1}^N \lambda_{q_e}^{l_j} \nabla(\varepsilon^l q_e^{l_j}) - \varepsilon^l \rho^l \frac{\partial \tilde{A}^l}{\partial \mathbf{v}^{l,s}} \cdot (\nabla \mathbf{v}^{l,s})^T \\
& - \sum_{j=1}^{N-1} \varepsilon^l \rho^l \frac{\partial \tilde{A}^l}{\partial \mathbf{v}^{l_j,l}} \cdot (\nabla \mathbf{v}^{l_j,l})^T - \varepsilon^l \rho^l \frac{\partial \tilde{A}^l}{\partial \nabla T} \cdot \nabla^2 T - \varepsilon^l \rho^l \frac{\partial \tilde{A}^l}{\partial \nabla \mathbf{v}^{l_j,l}} : \nabla^2 \mathbf{v}^{l_j,l} \\
& - \sum_{j=1}^N \varepsilon^l \rho^l \frac{\partial \tilde{A}^l}{\partial \nabla(\varepsilon^\alpha \rho^{l_j})} \cdot \nabla^2(\varepsilon^l \rho^{l_j}) - \varepsilon^l \rho^l \frac{\partial \tilde{A}^l}{\partial \mathbf{d}^l} : (\nabla \mathbf{d}^l)^T \\
& - \varepsilon^l \rho^l \frac{\partial \tilde{A}^l}{\partial \mathbf{w}^l} : (\nabla \mathbf{w}^l)^T \\
& + \sum_{\alpha=l,s} \sum_{j=1}^N (\nabla \mathbf{v}^{\alpha_j,\alpha})^T : \left[\varepsilon^\alpha \mathbf{t}^{\alpha_j} + \varepsilon^\alpha \mathbf{P}^{\alpha_j} \cdot \mathbf{E}_T \mathbf{I} + \varepsilon^\alpha \rho^{\alpha_j} \lambda_p^{\alpha_j} \mathbf{I} + \varepsilon^\alpha q_e^{\alpha_j} \lambda_{q_e}^{\alpha_j} \mathbf{I} \right] \\
& + \sum_{\alpha=l,s} \frac{\varepsilon^\alpha}{T} \nabla T \cdot \left[\mathbf{q}^\alpha + \sum_{j=1}^N \left(\rho^{\alpha_j} \mathbf{v}^{\alpha_j,\alpha} (\tilde{A}^{\alpha_j} + \frac{1}{2} (\mathbf{v}^{\alpha_j,\alpha})^2) - \mathbf{t}^{\alpha_j} \cdot \mathbf{v}^{\alpha_j,\alpha} \right) \right] \\
& + \sum_{\alpha=l,s} \sum_{j=1}^N \mathbf{v}^{\alpha_j,\alpha} \cdot \left[-\varepsilon^\alpha \rho^{\alpha_j} \tilde{\mathbf{i}}^{\alpha_j} - \sum_{\beta \neq \alpha} \varepsilon^\alpha \rho^{\alpha_j} \tilde{\mathbf{T}}_\beta^{\alpha_j} - \varepsilon^\alpha \rho^{\alpha_j} \nabla \tilde{A}^{\alpha_j} + \frac{1}{\rho^{\alpha_j}} \mathbf{E}_T \cdot \mathbf{P}^{\alpha_j} \nabla(\varepsilon^\alpha \rho^{\alpha_j}) \right. \\
& \quad \left. - \varepsilon^\alpha \nabla \mathbf{E}_T \cdot \mathbf{P}^{\alpha_j} + \frac{1}{2} \varepsilon_o \mathbf{E}_T \cdot \mathbf{E}^{\alpha_j} \nabla \varepsilon^\alpha - \frac{\varepsilon^\alpha}{T} \mathbf{E}_T \cdot \mathbf{P}^{\alpha_j} \nabla T + \lambda_\rho^{\alpha_j} \nabla(\varepsilon^\alpha \rho^{\alpha_j}) \right. \\
& \quad \left. + \lambda_{q_e}^{\alpha_j} \nabla(\varepsilon^\alpha q_e^{\alpha_j}) - \varepsilon^\alpha q_e^{\alpha_j} \mathbf{E}_T \right] \\
& + \sum_{\alpha=l,s} \varepsilon^\alpha \mathcal{J}^\alpha \cdot \mathbf{E}_T \\
& + \sum_{\alpha=l,s} \sum_{j=1}^N \sum_{\beta \neq \alpha} \varepsilon^\alpha \rho^{\alpha_j} \tilde{\mathbf{e}}_\beta^{\alpha_j} \left[-\tilde{A}^{\alpha_j} - \frac{1}{\rho^{\alpha_j}} \mathbf{E}_T \cdot \mathbf{P}^{\alpha_j} - \frac{1}{2} (\mathbf{v}^{\alpha_j,\alpha})^2 - \lambda_\rho^{\alpha_j} \right. \\
& \quad \left. - \tilde{A}^\alpha - \frac{1}{2} (\mathbf{v}^{\alpha,s})^2 - \lambda_{q_e}^{\alpha_j} z^{\alpha_j} \right] \\
& + \sum_{\alpha=l,s} \sum_{j=1}^N \varepsilon^\alpha \rho^{\alpha_j} \tilde{\mathbf{r}}^{\alpha_j} \left[-\tilde{A}^{\alpha_j} - \frac{1}{\rho^{\alpha_j}} \mathbf{E}_T \cdot \mathbf{P}^{\alpha_j} - \lambda_\rho^{\alpha_j} - z^{\alpha_j} \lambda_{q_e}^{\alpha_j} - \frac{1}{2} (\mathbf{v}^{\alpha_j,\alpha})^2 \right] \\
& + \sum_{\alpha=l,s} \nabla \cdot \mathbf{D}^{\alpha_j} \left[\varepsilon^\alpha \lambda_D^{\alpha_j} \right] \\
& + \sum_{\alpha=l,s} \sum_{j=1}^N \frac{D^s(\varepsilon^\alpha q_e^{\alpha_j})}{Dt} \left[-\varepsilon^\alpha \rho^\alpha \frac{\partial \tilde{A}^\alpha}{\partial (\varepsilon^\alpha q_e^{\alpha_j})} + \lambda_{q_e}^{\alpha_j} + \Lambda \right]
\end{aligned}$$

$$\begin{aligned}
& + \sum_{\alpha=l,s} \sum_{j=1}^N \nabla \times \mathbf{E}^{\alpha_j} \cdot \left[\Lambda_E^{\alpha_j} \varepsilon^\alpha \right] \\
& + \sum_{\alpha=l,s} \sum_{j=1}^N \lambda_D^{\alpha_j} \left[\mathbf{D}^{\alpha_j} \cdot \nabla \varepsilon^\alpha - \varepsilon^\alpha q_e^{\alpha_j} - \varepsilon^\alpha \hat{\mathbf{d}}^{\alpha_j} - \sum_{\beta \neq \alpha} \varepsilon^\alpha \hat{\mathbf{d}}_\beta^{\alpha_j} \right] \\
& + \sum_{\alpha=l,s} \sum_{j=1}^N \Lambda_E^{\alpha_j} \cdot \left[\nabla \varepsilon^\alpha \times \mathbf{E}^{\alpha_j} - \varepsilon^\alpha \hat{\boldsymbol{\sigma}}^{\alpha_j} - \sum_{\beta \neq \alpha} \varepsilon^\alpha \hat{\boldsymbol{\sigma}}_\beta^{\alpha_j} \right] \\
& + \sum_{\alpha=l,s} \sum_{j=1}^N \lambda_{q_e}^{\alpha_j} \left[\nabla \cdot (\varepsilon^\alpha \mathcal{J}^\alpha) - \varepsilon^\alpha \hat{q}^{\alpha_j} - \sum_{\beta \neq \alpha} \varepsilon^\alpha \rho^{\alpha_j} \hat{Z}_\beta^{\alpha_j} \right] \geq 0,
\end{aligned}$$

where subscripted *sym* and *as* mean the symmetric and anti-symmetric part of the tensor, respectively.

V. Numerical methods and examples

1. Introduction to the Numerical Approach

The study of coupling between stress and pore pressure in deformable, saturated porous media started with the work of Terzaghi [1], who proposed and developed a one dimensional consolidation model. Biot [2, 3, 4] extended this model to three-dimensional soil consolidation with physically consistent assumptions. Analytical solutions of consolidation problems based on Biot's theory have been developed by a number of researchers, e.g. Cryer [5]; McNamee and Gibson [6,7]; Gibson et al. [8]; Schiffman et al. [9] and Schiffman and Fungaroli [10]. In [5] and [6] the authors found that within the framework of the full Biot model, short time pore pressure in a poroelastic body loaded on the surface, could be higher than the surface load pressure. This was rationalized by noting that the tangential stress components take part in the pore pressure generation. This effect is specific to the full Biot model, and it differentiates Biot's model from Terzaghi's model.

Unfortunately, analytical solutions are available for only a very few restricted situations. For more realistic problems numerical methods must be employed. Early finite element formulations for consolidation problems have been espoused by Sandhu and Wilson [11]; Christian [12]; Christian and Boehmer [13]; Christian et al. [14]; Ghaboussi and Wilson [15]; and Matsumoto [16]. In these articles the authors obtained numerical solutions of many important engineering problems. Christian [17] summarized and presented in a systematical form the methodical issues of the finite element method as applied to consolidation problems. The development and investigation of various methods of implementing the finite element method has continued over the years by many investigators such as Sandhu, Liu and Singh [18] and Reed [19].

Booker [20] obtained the solution of settlement problem for a loaded layer by combining the Laplace transform and finite element method. A solution was obtained for different forms of load footing: strip, circle and square. Lewis and Schrefler [21], Safai and Pinder [22], and Kim and Parizek [23] applied the finite element method to consolidation for the problems related to settlement when pumping water or oil. Sandhu and Liu [24] and Budkowska and Fu [25] studied the application of the finite element method to consolidation of viscoelastic bodies. Khaled et al. [26] and Bai et al. [27] applied finite element method to simulate consolidation of porous media with dual porosity. Ng and Small [28] used the finite element method to study consolidation of unsaturated soil. The authors considered the high water content case (above 0.7-0.8) and reduced this model to the model of saturated soil with variable compressibility.

Haghghi [29], Irudayaraj and Haghghi [30], Irudayaraj et al. [31] developed finite element model for related problems involving stress in drying bodies. In these articles the authors used viscoelastic equations coupled with equations of conductive heat and moisture transfer. The temperature expansion of material was taken into account as well. Hasatami and Itaya [32], Itaya et al. [33], Itaya et al. [34], Hasatami and Itaya [35] considered similar processes as [29-30], and developed similar finite element models.

Nguyen and Selvadurai [36] and Selvadurai [37] developed the finite element technique to study rock consolidation in the presence of heat sources. In addition to the classical Biot consolidation equations, they included a convective heat transfer equation. Temperature was also taken into account. Zhou et al. [38] used to the finite element method to study mechanical hydro-thermo-moisture behavior in nonsaturated clay. In addition to the classical Biot's consolidation equations, their mathematical model included coupled convective heat transfer, moisture transfer, and vapor- and air- transfer. Guvanassen and Chang [39] developed three-

dimensional finite element models for thermohydromechanical elastic deformation of fractured rock with convective heat transfer.

Carter et al. [40, 42], Carter et al. [41] initiated finite element models for consolidation within finite deformation theory. Meijer [43] developed the Updated Lagrangian-Eulerian method for the same problem of consolidation with finite strain. The author used a moving finite element grid.

Chopra and Dargush [44] used the finite element method for consolidation with plasticity at finite strain. They derived and used Updated Lagrangian-Eulerian equations for moving grids with linearization of the governing equations for each time step, before applying the finite element method. This linearization was used for the stress-displacement equations, but not for pore pressure-volume change equation. The authors applied this model to the problem of extension of a cylindrical cavity in the subsurface.

Advani et al. [50] and Kim et al. [51] considered a coupled hydrothermomechanical finite element model of elastic-plastic media under thermal and mechanical loading at finite strain. They proposed updated Lagrangian-Eulerian equations via linearization, and then formulated the finite element model.

2. Finite Element Model of Consolidation Based on Biot's Classical Model

The classical Biot model accounts for the stress field, infinitesimal strain and pore pressure in a linear deforming porous body that is saturated with an incompressible fluid, within the framework of the small deformation theory.

The model includes:

- 1) equilibrium equations;
- 2) state equations for an elastic body;
- 3) boundary conditions.

The equilibrium equations in Cartesian coordinates are:

$$\frac{\partial \sigma_{ij}}{\partial x_j} + F_i - \frac{\partial p}{\partial x_i} = 0, \quad i = 1,2,3; j = 1,2,3; \quad (2.1)$$

$$\frac{\partial e_v}{\partial t} = \operatorname{div} \left(\frac{\kappa}{\mu} \cdot \nabla p \right), \quad (2.2)$$

Here x_j are Cartesian coordinates, σ_{ij} are components of Cauchi stress tensor (tension stresses are positive), p is pore pressure (positive for compression of the porous media), F_i are components of the vector of volume force, t is time, $e_v = \sum_{k=1}^3 \frac{\partial U_k}{\partial x_k}$ is the volume deformation (U_i , $i = 1,2,3$ are components of the displacement vector), κ is the permeability coefficient of the porous media, and μ is the fluid viscosity.

In geotechnical applications other forms of (2.2) are often used

$$\frac{\partial e_v}{\partial t} = \operatorname{div} (k \cdot \nabla h), \quad (2.2')$$

where h is the head, $h = \frac{p}{\rho g}$ (ρ is the fluid density and g is the gravitational constant), and k is

the hydraulic conductivity, $k = \frac{\kappa \cdot \rho g}{\mu}$. By introducing the head instead of the exceeded pore pressure, data may often be more easily understood.

We will use (2.2) for the analysis and the seepage coefficient and head for data presentation.

The infinitesimal strain is

$$\varepsilon_{ij} = \frac{1}{2} \left(\frac{\partial U_i}{\partial x_j} + \frac{\partial U_j}{\partial x_i} \right), \quad i,j = 1, 2, 3, \quad (2.3)$$

and we assume the Hookian stress field

$$\sigma_{ij} = \lambda \cdot \delta_{ij} \varepsilon_{kk} + 2\mu \cdot \varepsilon_{ij} = \lambda \cdot \delta_{ij} e_v + 2\mu \cdot \varepsilon_{ij} \quad (2.4)$$

Here λ and μ are Lame constants, which characterize the elasticity properties of the body; δ_{ij} is the Kronecker delta.

Another equivalent form of Hook's law is

$$\sigma_v = 3K e_v, \quad s_{ij} = 2G e_{ij}, \quad (2.5)$$

where

$$\sigma_v = \frac{1}{3} \sum_{k=1}^3 \sigma_{kk} \quad (2.6)$$

is mean (hydrostatic) stress (one third of the first invariant of stress tensor),

$$e_v = \sum_{k=1}^3 \varepsilon_{kk} \quad (2.7)$$

is the volume deformation (first invariant of the deformation tensor),

$$s_{ij} = \sigma_{ij} - \delta_{ij} \sigma_v, \quad i, j = 1, 2, 3 \quad (2.8)$$

are components of the stress deviator (shear stress tensor), and

$$e_{ij} = \varepsilon_{ij} - \frac{1}{3} \delta_{ij} e_v, \quad i, j = 1, 2, 3 \quad (2.9)$$

are components of deformations deviator (shear deformation tensor). Hook's law in form (2.5) establishes the proportionality between spherical parts of stress and strain tensors, and deviator tensors.

Coefficients K and G (the modulus of volume deformation and the shear modulus) are connected to Lame parameters by relations

$$K = \lambda + \frac{2}{3} \mu, \quad G = \mu.$$

Two types of boundary conditions are used on the boundary $\Gamma = \Gamma_1^{(e)} \cup \Gamma_2^{(e)}$. On $\Gamma_1^{(e)}$ the displacements are assigned:

$$U = U_0, \quad x \in \Gamma_1^{(e)},$$

while on $\Gamma_2^{(e)}$ the normal effective stress is specified:

$$\sigma_{ij} \cdot n_j - p \cdot n_i = t_i, \quad x \in \Gamma_2^{(e)}.$$

Here n is the unit outer normal to the body surface.

Similarly for the fluid flow, $\Gamma = \Gamma_1^{(p)} \cup \Gamma_2^{(p)}$, we specify

$$p = p_0, \quad x \in \Gamma_1^{(p)},$$

while on $\Gamma_2^{(p)}$ the normal flux of fluid flow is

$$\frac{\kappa}{\mu} \cdot \frac{\partial p}{\partial n_j} \cdot n_j = q, \quad x \in \Gamma_2^{(p)}.$$

It is also possible to represent sliding with traction. We do so by fixing the tangential component of stress and letting the normal displacement vanish.

Below we consider the plane stress elasticity problem. In this problem forces (both volume and surface loading) do not change in the x_3 -direction. Thus $U_3 = 0$, and displacements U_1 and U_2 are invariant with x_3 . Hence

$$\varepsilon_{33} = 0,$$

$$\varepsilon_{13} = \frac{1}{2} \left(\frac{\partial U_1}{\partial x_3} + \frac{\partial U_3}{\partial x_1} \right) = 0, \quad \varepsilon_{23} = \frac{1}{2} \left(\frac{\partial U_2}{\partial x_3} + \frac{\partial U_3}{\partial x_2} \right) = 0,$$

$$\sigma_{13} = 2G \cdot \varepsilon_{13} = 0, \quad \sigma_{23} = 2G \cdot \varepsilon_{23} = 0.$$

These relations have many consequences. For example, one can deduce

$$\sigma_{33} = G \cdot e_v + \frac{\sigma_{11} + \sigma_{22}}{2}, \quad e_v = \frac{3(\sigma_{11} + \sigma_{22})}{2(9K + G)},$$

$$\sigma_{33} = \frac{9K - 2G}{2(9K + G)} \cdot (\sigma_{11} + \sigma_{22}).$$

At this point the main importance of these results is that the stress component σ_{33} can be defined independently, after defining $\{\sigma_{ij}\}$, $i,j = 1,2$. In this fashion the problem is reduced to finding U_1 , U_2 and pore pressure p based on

$$\frac{\partial \sigma_{ij}}{\partial x_j} + F_i - \frac{\partial p}{\partial x_i} = 0, \quad i = 1,2; j = 1,2; \quad (2.10)$$

$$\frac{\partial}{\partial t} \left(\frac{\partial U_1}{\partial x_i} + \frac{\partial U_2}{\partial x_i} \right) = \frac{\partial}{\partial x_i} \left(\frac{k}{\rho g} \cdot \frac{\partial p}{\partial x_i} \right), \quad i = 1,2. \quad (2.11)$$

Here $\{\sigma_{ij}\}$, $i,j = 1,2$ is the Cauchy's plane stress tensor with $\sigma_{12} = \sigma_{21}$ by symmetry. We thus have by Hook's law relations (2.5)

$$\begin{pmatrix} \sigma_{11} \\ \sigma_{22} \\ \sigma_{12} \end{pmatrix} = \begin{pmatrix} K + \frac{4}{3}G & K - \frac{2}{3}G & 0 \\ K - \frac{2}{3}G & K + \frac{4}{3}G & 0 \\ 0 & 0 & G \end{pmatrix} \cdot \begin{pmatrix} \sigma_{11} \\ \sigma_{22} \\ \sigma_{12} \end{pmatrix}, \quad (2.12)$$

or

$$\bar{\sigma} = D \cdot \bar{\varepsilon}, \quad (2.13)$$

where

$$\bar{\sigma} = \begin{pmatrix} \sigma_{11} \\ \sigma_{22} \\ \sigma_{12} \end{pmatrix}, \quad D = \begin{pmatrix} K + \frac{4}{3}G & K - \frac{2}{3}G & 0 \\ K - \frac{2}{3}G & K + \frac{4}{3}G & 0 \\ 0 & 0 & G \end{pmatrix}, \quad \bar{\varepsilon} = \begin{pmatrix} \varepsilon_{11} \\ \varepsilon_{22} \\ \varepsilon_{12} \end{pmatrix}. \quad (2.14)$$

To implement the finite element method [48,49], we introduce the triangular grid (Figure 2.1). We use the linear elements for pore pressure (see Figure 2.2) and quadratic elements for displacements (Figure 2.3). In such a way we associate to each element six standard quadratic basis functions $\{\psi_\alpha\}$, $\alpha=1,\dots,6$ for determining displacement U_1 , six standard quadratic basis functions $\{\psi_\beta\}$, $\beta=1,\dots,6$ for determining displacement U_2 , and 3 standard linear basis functions $\{\varphi_\gamma\}$, $\gamma=1, 2, 3$ for determining pore pressure p [48,49].

As usual we find the solution $\begin{pmatrix} U_1 \\ U_2 \end{pmatrix}$, p in form of a linear combination of basis functions

$$\begin{pmatrix} U_1 \\ U_2 \end{pmatrix} = \sum_{\alpha} U_{\alpha}^{(1)} \cdot \bar{N}_{\alpha}^{(1)} + \sum_{\beta} U_{\beta}^{(2)} \cdot \bar{N}_{\beta}^{(2)}, \quad p = \sum_{\gamma} P_{\gamma} \cdot \varphi_{\gamma}, \quad (2.15)$$

Here

$$\bar{N}_\alpha^{(1)} = \begin{pmatrix} \psi_\alpha \\ 0 \end{pmatrix}, \quad \bar{N}_\beta^{(2)} = \begin{pmatrix} 0 \\ \psi_\beta \end{pmatrix}.$$

Using the Galerkin method the finite element equations are obtained by multiplying equation (2.10) at $i=1$ on the basis function $\psi_{\alpha'}$, equation (2.10) at $i=2$ on the basis function $\psi_{\beta'}$, equation (2.11) on the basis function $\varphi_{\gamma'}$ and integrating by parts and applying Green's formula, for all of the functions $\psi_{\alpha'}$, $\psi_{\beta'}$, and $\varphi_{\gamma'}$

The resultant is the system of linear algebraic equations for unknown coefficients $U_\alpha^{(1)}$, $U_\beta^{(2)}$, and P_r :

$$\begin{aligned} \sum_\alpha U_\alpha^{(1)} \cdot \int_V \frac{\partial \psi_{\alpha'}}{\partial x_1} \sigma_{11}(\bar{N}_\alpha^{(1)}) dv + \sum_\beta U_\beta^{(2)} \cdot \int_V \frac{\partial \psi_{\alpha'}}{\partial x_2} \sigma_{12}(\bar{N}_\beta^{(2)}) dv - \sum_r P_r \cdot \int_V \frac{\partial \psi_{\alpha'}}{\partial x_1} \varphi_r dv \\ = \int_V F_1 \cdot \psi_{\alpha'} dv + \int_{\Gamma_2^{(1)}} t_1 \cdot \psi_{\alpha'} ds, \end{aligned} \quad (2.16)$$

$$\begin{aligned} \sum_\alpha U_\alpha^{(1)} \cdot \int_V \frac{\partial \psi_{\beta'}}{\partial x_1} \sigma_{12}(\bar{N}_\alpha^{(1)}) dv + \sum_\beta U_\beta^{(2)} \cdot \int_V \frac{\partial \psi_{\beta'}}{\partial x_2} \sigma_{22}(\bar{N}_\beta^{(2)}) dv - \sum_r P_r \cdot \int_V \frac{\partial \psi_{\beta'}}{\partial x_2} \varphi_r dv \\ = \int_V F_2 \cdot \psi_{\beta'} dv + \int_{\Gamma_2^{(2)}} t_{21} \cdot \psi_{\beta'} ds, \end{aligned} \quad (2.17)$$

$$\begin{aligned} \sum_\alpha \frac{dU_\alpha^{(1)}}{dt} \cdot \int_V \frac{\partial \psi_\alpha}{\partial x_1} \varphi_r dv + \sum_\beta \frac{dU_\beta^{(2)}}{dt} \cdot \int_V \frac{\partial \psi_\beta}{\partial x_2} \varphi_r dv \\ + \sum_r P_r \cdot \int_V \frac{\kappa}{\mu} \left(\frac{\partial \varphi_r}{\partial x_1} \frac{\partial \varphi_r}{\partial x_1} + \frac{\partial \varphi_r}{\partial x_2} \frac{\partial \varphi_r}{\partial x_2} \right) dv = \int_{\Gamma_p^{(2)}} q \cdot \varphi_r ds. \end{aligned} \quad (2.18)$$

Using a finite difference scheme in time, one can write equations (2.16) - (2.18) in the compact matrix form:

$$K_{11} \cdot \bar{U} + K_{12} \cdot \bar{V} - C_1 \cdot P = F_1, \quad (2.19)$$

$$K_{21} \cdot \bar{U} + K_{22} \cdot \bar{V} - C_2 \cdot P = F_2, \quad (2.20)$$

$$C_1^T \cdot \frac{\bar{U} - U}{\Delta t} + C_2^T \cdot \frac{\bar{V} - V}{\Delta t} + H \cdot [\alpha \cdot \bar{P} + (1-\alpha) \cdot P] = Q, \quad (2.21)$$

where U is the vector of unknown coefficients $\{U_\alpha\}$, V is the vector of unknown coefficients $\{V_\beta\}$, and P is the vector of unknown coefficients $\{P_\gamma\}$. The overbar indicates $t = t_n + \Delta t$; otherwise $t = t_n$.

Matrixes are

$$\begin{pmatrix} K_{11} & K_{12} \\ K_{21} & K_{22} \end{pmatrix} = \begin{pmatrix} K_{11}^{\alpha',\alpha} & K_{12}^{\alpha',\alpha} \\ K_{21}^{\alpha',\alpha} & K_{22}^{\alpha',\alpha} \end{pmatrix} = \int_V \nabla \psi_{\alpha'}^T \cdot D \cdot \nabla \psi_\alpha dv;$$

$$C_1 = (C_1^{\alpha',\alpha}), \quad C_1^{\alpha',\alpha} = \int_V \frac{\partial \psi_{\alpha'}}{\partial x_1} \cdot \varphi_\alpha dv;$$

$$C_2 = (C_2^{\alpha',\alpha}), \quad C_2^{\beta',\beta} = \int_V \frac{\partial \psi_{\beta'}}{\partial x_2} \cdot \varphi_\beta dv;$$

$$H = (H^{\gamma',\gamma}), \quad H^{\gamma',\gamma} = \int_V \frac{K}{\mu} \cdot \left(\frac{\partial \varphi_{\gamma'}}{\partial x_1} \frac{\partial \varphi_\gamma}{\partial x_1} + \frac{\partial \varphi_{\gamma'}}{\partial x_2} \frac{\partial \varphi_\gamma}{\partial x_2} \right) dv,$$

where

$$\nabla \psi = \begin{pmatrix} \frac{\partial \psi}{\partial x_1} & 0 \\ 0 & \frac{\partial \psi}{\partial x_2} \\ \frac{\partial \psi}{\partial x_2} & \frac{\partial \psi}{\partial x_1} \end{pmatrix}$$

and D is the matrix (2.14).

Let us rewrite equations (2.19)-(2.21) again in the form

$$K \cdot \bar{U} - C \cdot \bar{P} = F, \quad (2.22)$$

$$C^T \cdot \frac{\bar{U} - U}{\Delta t} + H \cdot [\alpha \cdot \bar{P} + (1-\alpha) \cdot P] = Q, \quad (2.23)$$

or more compactly

$$\begin{bmatrix} K & -C \\ C^T & \alpha \cdot \Delta t \cdot H \end{bmatrix} \cdot \begin{pmatrix} \bar{U} \\ \bar{P} \end{pmatrix} = \begin{bmatrix} 0 & 0 \\ C^T & -(1-\alpha) \cdot \Delta t \cdot H \end{bmatrix} \cdot \begin{pmatrix} U \\ P \end{pmatrix} + \begin{pmatrix} F \\ \Delta t \cdot Q \end{pmatrix}, \quad (2.24)$$

which is adapted to the calculation of the solution at $t = t_n + \Delta t$ based on known data for $t = t_n$.

Equation (2.24) is solved by decomposing matrix A at each time step into the product

$$A = L \cdot U$$

of the lower triangular matrix L and upper triangular matrix U, using

$$A \cdot x = f$$

with

$$L \cdot y = f \quad \text{and} \quad U \cdot x = y.$$

We used subroutines dgbco and dgbsl from LINPACK [50,51], which employs Crout's decomposition with pivoting and back substitution [52].

For typical values of the elastic and permeability coefficients in poroelastic bodies, the matrix A in (2.24) is ill conditioned with condition number 10^{-8} . This ill conditioning is closely related to the fact that matrix A incorporates large values of the elastic characteristics but small values of the permeability (see typical data in the test description below). Neither the flow nor elastic problem when considered separately is ill conditioned.

The condition number may be increased [19] by rewriting the scheme (2.24) as

$$\begin{bmatrix} K & -s \cdot C \\ s \cdot C^T & s^2 \cdot \alpha \cdot \Delta t \cdot H \end{bmatrix} \cdot \begin{pmatrix} \bar{U} \\ \frac{1}{s} \cdot \bar{P} \end{pmatrix} = \begin{bmatrix} 0 & 0 \\ s \cdot C^T & -s^2 \cdot (1-\alpha) \cdot \Delta t \cdot H \end{bmatrix} \cdot \begin{pmatrix} U \\ \frac{1}{s} \cdot P \end{pmatrix} + \begin{pmatrix} F \\ s \cdot \Delta t \cdot Q \end{pmatrix} \quad (2.25)$$

where we have introduced the parameters. This parameter is chosen in such a way to maximize the condition number. We are able to increase the condition number in typical cases from 10^{-8} at $s=1$ to 10^{-6} for optimal values of s.

All our results were obtained by applying of this procedure. It should be noted that the search for the optimum value of s , and Crout's decomposition are performed only once during the solution procedure unless the time step is changed radically.

3. Test of the Elastic Model for Biot Consolidation

As a test we considered the one-dimensional consolidation problem for a column of elastic porous material, subjected to constant loading (see Figure 3.1). On the lower surface zero displacement is prescribed. On the vertical boundaries sliding without traction is imposed at zero horizontal displacement. On the upper boundary a uniformly distributed vertical load is prescribed. The upper boundary is drained with zero pore pressure, while the remaining boundaries are impermeable. The analytical solution to this problem is [54]

$$V^* = 1 - \frac{8}{\pi^2} \sum_{i=1,3,\dots}^{\infty} \frac{1}{i^2} \cdot \exp\left(-\frac{i^2 \pi^2 t^*}{4}\right). \quad (3.1)$$

Here $t^* = \frac{c_v \cdot t}{H^2}$ is dimensionless time, H is the column's height, $c_v = \frac{k}{\rho g \cdot a}$ is the consolidation

coefficient, $a = \frac{1}{K + \frac{4}{3} \cdot G}$ is the compressibility of soil, and $V^* = V/V_\infty$ is dimensionless

normalized settlement, where V is the settlement of the upper boundary of column at the current time, and $V_\infty = a \cdot H \cdot F$ is full final settlement of the upper boundary after pore pressure dissipation. Also, F is pressure outside the top surface, and V^* is sometimes called the degree of consolidation.

We have used the test data of [18] $h = 7$, $K = 10000$, $G = 2142$, $t_2 = 190$ (vertical stress component on the upper boundary) and the grid was the same as in [18]. In Fig. 3.2 a comparison of the numerical and analytical solutions is presented, $V^* = V^*(t^*)$. The numerical solution differs from analytical less than 2%.

We tested two versions of initial data

$$U(x, y, 0) = 0, \quad p(x, y, 0) = t_2 \quad (3.2)$$

(pore pressure at $t = 0$ is equal to the vertical stress); and the second initial data was obtained by solving (2.22), (2.23) adopted at $t = 0$, $\Delta t = 0$:

$$K \cdot U - C \cdot P = F, \quad (3.3)$$

$$C^T \cdot U = 0. \quad (3.4)$$

These two initial conditions give rise to essentially the same results for $t > 0$.

4. Finite Element Model of Consolidation for Viscoelastic Media

Following [54-58], we take the equations for consolidation of a viscoelastic porous medium in the form

$$\frac{\partial \sigma_{ij}}{\partial x_j} + F_i - \eta \cdot \frac{\partial}{\partial t} \left(\frac{\partial e_v}{\partial x_i} \right) - \frac{\partial p}{\partial x_i} = 0, \quad (4.1)$$

$$\frac{\partial e_v}{\partial t} = \operatorname{div} \left(\frac{\kappa}{\mu} \cdot \nabla p \right). \quad (4.2)$$

Here η is the viscoelasticity coefficient of the skeleton, and $\eta \cdot \frac{\partial}{\partial t} \left(\frac{\partial e_v}{\partial x_i} \right)$ describes the viscoelasticity effects. We consider the plane stress viscoelastic consolidation problem.

The boundary conditions for the part of boundary where loads are prescribed have the form

$$\sigma_{ij} \cdot \bar{n}_j - \eta \cdot \frac{\partial e_v}{\partial t} \cdot \bar{n}_i - p \cdot \bar{n}_i = t_i, \quad x \in \Gamma_2^{(e)}.$$

By applying the Galerkin procedure and using the same basis and trial functions as earlier, one can see that the additional term arises in the left side of (2.16)

$$\eta \cdot \sum_{\alpha} \frac{dU_{\alpha}^{(1)}}{dt} \cdot \frac{\partial \psi_{\alpha'}}{\partial x_1} \cdot \frac{\partial \psi_{\alpha}}{\partial x_1} + \eta \cdot \sum_{\beta} \frac{dU_{\beta}^{(2)}}{dt} \cdot \frac{\partial \psi_{\alpha'}}{\partial x_1} \cdot \frac{\partial \psi_{\beta}}{\partial x_2},$$

and an additional term arises in the left side of (2.17)

$$\eta \cdot \sum_{\alpha} \frac{dU_{\alpha}^{(1)}}{dt} \cdot \frac{\partial \psi_{\beta'}}{\partial x_2} \cdot \frac{\partial \psi_{\alpha}}{\partial x_1} + \eta \sum_{\beta} \frac{dU_{\beta}^{(2)}}{dt} \cdot \frac{\partial \psi_{\beta'}}{\partial x_2} \cdot \frac{\partial \psi_{\beta}}{\partial x_2}.$$

Thus one can write the resulting matrix equations as

$$K \cdot \bar{U} + \frac{\eta}{\Delta t} \cdot K_v \cdot \bar{U} - C \cdot \bar{P} = \frac{\eta}{\Delta t} \cdot K_v \cdot U + F, \quad (4.3)$$

$$C^T \cdot \frac{\bar{U} - U}{\Delta t} + H \cdot P = Q \quad (4.4)$$

(we take $\alpha = 1$). Here the additional matrix Kv , which is related to viscoelasticity terms, is

$$Kv = \begin{pmatrix} Kv_{11} & Kv_{12} \\ Kv_{21} & Kv_{22} \end{pmatrix} = \begin{pmatrix} Kv_{11}^{\alpha',\alpha} & Kv_{12}^{\alpha',\alpha} \\ Kv_{21}^{\alpha',\alpha} & Kv_{22}^{\alpha',\alpha} \end{pmatrix},$$

where

$$\begin{aligned} Kv_{11}^{\alpha',\alpha} &= \int_V \frac{\partial \psi_{\alpha'}}{\partial x_1} \cdot \frac{\partial \psi_\alpha}{\partial x_1} dv, & Kv_{12}^{\alpha',\alpha} &= \int_V \frac{\partial \psi_{\alpha'}}{\partial x_1} \cdot \frac{\partial \psi_\alpha}{\partial x_2} dv, \\ Kv_{21}^{\alpha',\alpha} &= \int_V \frac{\partial \psi_{\alpha'}}{\partial x_2} \cdot \frac{\partial \psi_\alpha}{\partial x_1} dv, & Kv_{22}^{\alpha',\alpha} &= \int_V \frac{\partial \psi_{\alpha'}}{\partial x_2} \cdot \frac{\partial \psi_\alpha}{\partial x_2} dv. \end{aligned}$$

We proceeded as in the previous section to compute the numerical solution, but we found considerable discrepancy with the analytical solution. So we changed the approach and instead of solving equations (4.3), (4.4) we solved the equivalent equation

$$\begin{pmatrix} K + \frac{\eta}{\Delta t} \cdot Kv & -C \\ C^T & \Delta t \cdot H \end{pmatrix} \cdot \begin{pmatrix} \delta U \\ \delta P \end{pmatrix} = \begin{pmatrix} K \cdot U - C \cdot P - F \\ \Delta t \cdot (H \cdot P - Q) \end{pmatrix} \quad (4.5)$$

for increments

$$\delta U = \bar{U} - U, \quad \delta P = \bar{P} - P, \quad (4.6)$$

by applying the same matrix conditioning technique for equation (4.5). With this approach the numerical and analytical solutions were nearly identical.

As a test we considered a one-dimensional problem of consolidation of viscoelastic porous material that had an analytical solution [54]

$$V^* = 1 - \frac{8}{\pi^2} \sum_{i=1,3,\dots}^{\infty} \frac{1}{i^2} \cdot \exp \left(-\frac{i^2 \pi^2 t^*}{4 \cdot \left(1 + \frac{i^2 \pi^2 S}{4} \right)} \right),$$

Here the parameters are as in (3.1) with $S = \frac{\kappa}{\mu} \cdot \frac{\eta}{H^2}$ the dimensionless viscoelasticity coefficient.

For the test we used the following data: $H = 10$, $K = 1000$, $G = 1600$, $\kappa / \mu = 0.001$, $t_2 = 10$ (vertical stress component on the upper boundary). A series of tests were performed for the sequence of viscoelasticity coefficient $\eta = 0, 10000, 20000, 50000$, and 100000 . This corresponds to values of the dimensionless parameter $S = 0, 0.1, 0.2, 0.5, 1$. In Fig. 4.1 we compare the numerical and analytical solution. As mentioned, results are in excellent agreement.

5. Finite Element Model for Consolidation of Viscoelastic porous media with additional flow
due to capillary forces

None of the previous models included the affects of colloidal swelling. Flow due to swelling is generally assumed proportional to the gradient of volume deformation [54-58]

$$\bar{u}_f = -\frac{\kappa}{\mu} \cdot \nabla p - \frac{\kappa}{\mu} \cdot \bar{p}_* \cdot \nabla e_v. \quad (5.1)$$

Here the first term in the right hand side is the usual Darcy flow, while the second term describes the additional flow due to volume fraction gradients. The material parameter \bar{p}_* has the dimension of pressure. The consolidation equations for viscoelastic porous media with the additional flow (5.1) have a form [54-58]

$$\frac{\partial \sigma_{ij}}{\partial x_j} + F_i - \eta \cdot \frac{\partial}{\partial t} \left(\frac{\partial e_v}{\partial x_i} \right) - \frac{\partial p}{\partial x_i} = 0, \quad (5.2)$$

$$\frac{\partial e_v}{\partial t} = \operatorname{div} \left(\frac{\kappa}{\mu} \cdot \nabla p \right) + \operatorname{div} \left(\frac{\kappa}{\mu} \bar{p}_* \cdot \nabla e_v \right). \quad (5.3)$$

Using the decomposition (2.15) and applying the Galerkin procedure, we see that in the left hand side of (2.18) the additional term

$$\begin{aligned} \frac{\kappa \bar{p}_*}{\mu} \cdot & \left\{ \int_V \frac{\partial \varphi_\gamma}{\partial x_1} \cdot \frac{\partial}{\partial x_1} \left[\sum_\alpha U_\alpha^{(1)} \frac{\partial \psi_\alpha}{\partial x_1} + \sum_\beta U_\beta^{(2)} \frac{\partial \psi_\beta}{\partial x_2} \right] dv + \right. \\ & \left. \int_V \frac{\partial \varphi_\gamma}{\partial x_2} \cdot \frac{\partial}{\partial x_2} \left[\sum_\alpha U_\alpha^{(1)} \frac{\partial \psi_\alpha}{\partial x_1} + \sum_\beta U_\beta^{(2)} \frac{\partial \psi_\beta}{\partial x_2} \right] dv \right\} \end{aligned}$$

arises. Thus the full finite element equations, as in development (2.22),(2.23) and (4.3),(4.4), have the form

$$K \cdot \bar{U} + \frac{\eta}{\Delta t} K v \cdot \bar{U} - C \cdot \bar{P} = \frac{\eta}{\Delta t} K v \cdot U + F, \quad (5.5)$$

$$C^T \cdot \frac{\bar{U} - U}{\Delta t} + \frac{\kappa \bar{p}_*}{\mu} K c \cdot \bar{U} + H \cdot \bar{P} = Q. \quad (5.6)$$

Here the “stiffness (sub)matrix” Kc for additional flow due to volume deformation is

$$Kc = (Kc_{\gamma\alpha}, Kc_{\gamma\beta}),$$

where

$$Kc_{\gamma\alpha} = \int_V \frac{\partial \varphi_\gamma}{\partial x_1} \cdot \frac{\partial^2 \psi_\alpha}{\partial x_1^2} dv + \int_V \frac{\partial \varphi_\gamma}{\partial x_2} \cdot \frac{\partial^2 \psi_\alpha}{\partial x_2 \partial x_1} dv,$$

$$Kc_{\gamma\beta} = \int_V \frac{\partial \varphi_\gamma}{\partial x_1} \cdot \frac{\partial^2 \psi_\beta}{\partial x_1 \partial x_2} dv + \int_V \frac{\partial \varphi_\gamma}{\partial x_2} \cdot \frac{\partial^2 \psi_\beta}{\partial x_2^2} dv.$$

We rewrite equations (5.5),(5.6) to solve it for increments dU and dP (4.6). The modified system, as (4.5), has the form

$$\begin{pmatrix} K + \frac{\eta}{\Delta t} \cdot Kv & -C \\ C^T + \Delta t \cdot Kc & \Delta t \cdot H \end{pmatrix} \cdot \begin{pmatrix} dU \\ dP \end{pmatrix} = -\begin{pmatrix} K \cdot U - C \cdot P - F \\ \Delta t \cdot (Kc \cdot U + H \cdot P - Q) \end{pmatrix}. \quad (5.7)$$

In a fashion similar to sec.3,4, we solve equation (5.7) by maximizing the condition number according to procedure (2.25), and then using Crout's decomposition. Maximization of condition number and Crout's decomposition is performed only once during the solution of (5.7).

As a test case we considered a one-dimensional problem of consolidation for a column of viscoelastic porous material, similar to those in sec.3,4. The analytical solution of this problem has a form (see [54], where a similar problem is considered)

$$V^* = 1 - \frac{8}{\pi^2} \sum_{i=1,3,\dots}^{\infty} \frac{1}{i^2} \cdot \exp \left(-\frac{i^2 \pi^2 t^*}{4 \cdot \left(1 + \frac{i^2 \pi^2 S}{4} \right)} \right),$$

The only difference between here and sec.3 is the form of dimensionless time

$$t^* = \frac{\kappa}{\mu} \cdot \left(K + \frac{4}{3}G + \bar{p}_* \right) \cdot \frac{t}{H^2} \quad \text{and} \quad \text{dimensionless viscoelasticity coefficient}$$

$$S = \frac{\kappa}{\mu} \cdot \frac{\eta}{H^2} \left(1 + \frac{\bar{p}_*}{K + \frac{4}{3}G} \right).$$

For the test we used the following data: $H = 10$, $K = 1000$, $G = 1600$, $\kappa/\mu = 0.001$, $t_2 = 10$ (vertical stress component on the upper boundary). Again a series of tests were performed for the sequence of viscoelasticity coefficients $\eta = 0, 10000, 20000, 50000$, and 100000 , which correspond to values of dimensionless parameter $S = 0, 0.1, 0.2, 0.5, 1$.

In Fig. 5.1 a comparison between the numerical and analytical solution is presented. Again results agree well.

6. Examples of Solutions for Two-Dimensional Problems

Here we consider 2-d examples of problems with a strip load on the upper boundary, which may be in motion with normal as well as tangential stress. We first consider elastic and viscoelastic models with fixed grids. In Fig. 6.1 the modeled areas and grids are shown. The domain has the length L and thickness H and represents one half of the symmetric body. The surface is loaded by a strip of half-length b . We consider both drained and undrained surfaces.

On the base zero displacements were prescribed:

$$U = 0, \quad V = 0 \quad \text{at} \quad 0 \leq x \leq L, \quad y = -H.$$

On the symmetry axis and the far boundary we had vanishing horizontal displacement and no shear stress:

$$\begin{aligned} U = 0, \quad \sigma_{12} = 0 \quad &\text{at} \quad x = 0, \quad -H \leq y \leq 0 \quad \text{and} \\ &x = L, \quad -H \leq y \leq 0. \end{aligned}$$

On the upper boundary away from the load, zero normal stress was prescribed:

$$\sigma_{22} = 0 \quad \text{at} \quad b < x \leq L, \quad y = 0.$$

For fluid flow the following boundary conditions were applied:

- impervious bottom

$$\frac{\partial p}{\partial n} = 0 \quad \text{at} \quad 0 \leq x \leq L, \quad y = -H;$$

- impervious symmetry axis

$$\frac{\partial p}{\partial n} = 0 \quad \text{at} \quad x = 0, \quad -H \leq y \leq 0;$$

- zero surplus pore pressure on the far vertical boundary and the upper boundary away from the load

$$p = 0 \quad \text{at} \quad x = L, \quad -H \leq y \leq 0 \quad \text{and} \quad b < x \leq L, \quad y = 0.$$

Two variants of boundary conditions were applied under the load $0 \leq x \leq b$, $y=0$:

a) for the drained case

$$\sigma_{22} = F, \quad p = 0,$$

and

b) for the undrained case

$$\sigma_{22} - p = F, \quad \frac{\partial p}{\partial n} = 0.$$

Two sets of initial data were considered. In the first the initial condition was calculated according to Biot's equations (2.22), (2.23), adopted for $t = 0$, $\Delta t = 0$ (3.3), (3.4), which in this case express the incompressibility of pore fluid at instantaneous loading:

$$\frac{\partial \sigma_{ij}}{\partial x_j} + F_i - \frac{\partial p}{\partial x_i} = 0, \quad (6.1)$$

$$\frac{\partial U_k}{\partial x_k} = 0. \quad (6.2)$$

In the second case we used zero initial conditions

$$U(x, y, 0) = 0, \quad p(x, y, 0) = 0 \quad (6.3)$$

It is readily seen for sufficiently small Δt , the solution of the Biot problem (2.22), (2.23) with initial condition (3.3), (3.4) coincides with (or be very close to) that with initial condition (6.3). Numerical tests did confirm this.

Soil data were $K = 1600 \text{ t/m}^2$, $G = 1000 \text{ t/m}^2$, $\kappa/\mu = 0.01 \text{ m/day}$, which correspond to compacted loam.

Figures 6.2-6.4 are for Biot's drained problem. Figure 6.2 displays isobars in the body at times $t = 0.1 \text{ day}$, 1 day and 3 days with $H = 20 \text{ m}$, $L = 20 \text{ m}$, $b = 10 \text{ m}$, and $F = 10 \text{ t/m}$. These data illustrate the generation of pore pressure shortly after loading and dissipation of pore

pressure later via boundary drainage. Figure 6.3 shows the settlement and position of the upper boundary for the same problem. Figure 6.4 illustrates the change in the displacement field with time. In order to make this field more visible, modeled displacements were increased 20 times.

Figures 6.5–6.7 are similar to Figures 6.2–6.4 except the loaded surface is undrained.

For ease in comparison, Figures 6.8 and 6.9 have been drafted to illustrate the difference in the two models. In Fig. 6.8 the surface settlement at the center of the load is displayed, while in Fig. 6.9 the integral volume deformation is displayed. These data also characterize the full volume of compressed pore fluid.

In Figure 6.10 the pore pressure is shown with strip tangential load on the surface. The footing of the load is drained. One can see that the pore pressure is symmetric, $p(-x, y, t) = -p(x, y, t)$, with regard to the axis $x = 0$. In Figure 6.11 the settlement of the upper boundary is shown for the same problem. It also has the same symmetry $V(-x, y = 0, t) = -V(x, y = 0, t)$. Figure 6.12 shows the displacement vector field with symmetry $U(-x, y, t) = U(x, y, t)$, $V(-x, y, t) = -V(x, y, t)$.

Next we consider the case where the normal load is moving with constant velocity v . Results are shown in Figures 6.13-6.21. It is obvious that if the load is moved quite fast, the layer has no time to dissipate pore pressure and to recharge fluid, so the settlement and compaction of the layer is small. On the other hand, if the load is moved quite slowly, the layer has enough time to dissipate pore pressure, so in this case the settlement is close to a stationary load. The question is what is fast and what is slow.

It is a well-known fact that for a stationary load the characteristic time of consolidation is $t_1 = H^2 / c_v$, where $c_v = \kappa / (\mu \cdot a)$ is the consolidation coefficient and $a = 1 / (K + \frac{4}{3}G)$ is the compressibility coefficient. On the other hand, the characteristic time for the moving load is

$t_2 = b/v$, where v is the velocity of the load. So it is natural to measure time on the t_1 scale and to compare it with t_2 . The ratio of t_1 to t_2 gives the dimensionless velocity $v_* = v \cdot H^2 / (c_v \cdot b)$. At $t_1 = t_2$, the characteristic velocity is $v = c_v \cdot b / H^2$. The data in Figs. 6.13 and 6.14 correspond to the dimensionless velocity $v_* = 1$; Figs. 6.15, 6.16 to $v_* = 2$; Figs. 6.17, 6.18 to $v_* = 0.5$; and Figs. 6.19, 6.20 to $v_* = 5$.

In Fig. 6.21 we collect all data related to the settlement of the layer for the various cases. One can see that the settlement under a moving load is not symmetric with regard to its middle point. At fixed velocity the settlement increases monotonically along the loading surface from its front to the back, and has maximum at the rear. Subsistence is decreased as velocity increases. At $v_* = 0.5$ the subsistence is very near that of the stationary load. The pore pressures in Figures 6.13, 6.15, 6.17 and 6.19 show the degree of consolidation. We depict in Figs. 6.22-6.25 dimensionless results for a moving load for four values of dimensionless velocity $v_* = 0.5, 1, 2, 5$ and two values of dimensionless length of loaded surface, $b/H = 10$ and $b/H = 5$. In Figures 6.22 and 6.24 the ratio p/F is shown in dimensionless coordinates $x/H, y/H$. In Figs. 6.23 and 6.25 the dimensionless settlement of the upper boundary

$$V_*(x; y=0) = \frac{V}{a \cdot H \cdot F}$$

is presented.

Fig. 6.26 illustrates the subsidence under the moving load when the move is just beginning. The solid line (at $t = t_0$) relates to the stationary condition: the normal load is stationary for a long time before t_0 . Starting at $t = t_0$ the load is then moved with a constant speed v . The subsequent three curves show the subsidence at 1, 2, and 3 minutes after movement starts.

Next we consider the 2-d numerical solution of the consolidation problem using deforming grids. In Figs. 6.28 and 6.30 deformed grids are shown for the classical Biot model and for consolidation of the viscoelastic soil. In the Lagrangian framework the grid is updated at each time step according to the calculated displacement vector field. To make the results more visible, we considered a very soft (weak) ground and very heavy load. For comparison, Figures 6.27 and 6.29 show deformed grids, which are calculated by using stationary grids. For the data used, a difference between the classical Biot's model and viscoelastic model is visible, but the two grids produce similar results.

To check the importance of the viscoelasticity factor, a series of cases was studied with a stationary grid. In Fig. 6.31 the settlement of the central point under the drained normal load is shown for viscoelastic coefficient values $\mu = 0, 1000, 3000$, and 5000 . These data show the viscoelasticity factor became important for quite high viscoelasticity coefficient values.

7. Summary

We have presented finite element solutions for a number of consolidation problems ranging from elastic to viscoelastic coupled with flow including capillarity's swelling systems. These models have been tested against analytical solutions whenever possible and good agreement was obtained.

Several novel test problems were considered for which there are no analytical solutions. The most interesting of these involves a moving load, consistent with vehicular traffic over a viscoelastic body, with both drained and undrained porous matrix.

References

1. K. Terzaghi. Theoretical soil mechanics. Wiley, New York, 1943.
2. M.A. Biot. General theory of three-dimensional consolidation. *J. Appl. Phys.*, v.12, 155-164 (1941).
3. M.A. Biot. Consolidation settlement under a rectangular load distribution. *J. Appl. Phys.*, v.12, 426-430 (1941).
4. M.A. Biot. Theory of elasticity and consolidation for a porous solid. *J. Appl. Phys.*, v.26, 182-185 (1955).
5. C.W. Cryer. A comparison of the three-dimensional consolidation theories of Biot and Terzaghi. *Quart. J. Mech. and Appl. Math.*, v.26, N 4, 401-412 (1963).
6. J. McNamee and R.E. Gibson. Plane strain and axially symmetric problems of the consolidation of a semi-infinite clay stratum. *Quart. J. Mech. and Appl. Math.*, v.13, 210-227 (1960).
7. R.E. Gibson and J. McNamee. The consolidation settlement of a load uniformly distributed over a rectangular area. *Proc. 4th Intern. Conf. Soil Mech.*, v.1, 297-299 (1957).
8. R.E. Gibson, R.L. Shiffman and S.L. Pu. Plane strain and axially symmetric consolidation of a clay layer on a smooth impervious base. *Quart. J. Mech. and Appl. Math.*, v.23, N 4, 505-519 (1970).
9. R.L. Shiffman, A.T-F. Chen and J.C. Jordan. An analysis of consolidation theories. *J. Soil Mech. and Found. Div., ASCE*, v.95 (SM1), 285-312 (1969).
10. R.L. Shiffman and A.A. Fungaroli. Pore pressure and effective stress generation due to slowly moving loads. *Geotechnique*, v.23, 271-278 (1973).
11. R.S. Sandhu and E.L. Wilson. Finite element analysis of flow in saturated porous media. *J. Eng. Mech. Div., ASCE*, v.95 (EM3), 641-652 (1969).
12. J.T. Christian. Undrained stress distribution by numerical methods. *J. Soil Mech. Div., ASCE*, v.94 (SM6), 1333-1345 (1968).

13. J.T. Christian and J.W. Boehmer. Plane strain consolidation by finite elements. *J. Soil Mech. and Found. Div., ASCE*, v.96 (SM4), 1435-1457 (1970).
14. J.T. Christian, J.W. Boehmer and P.P. Martin. Consolidation of a layer under a strip load. *J. Soil Mech. and Found. Div., ASCE*, v.98 (SM7), 693-707 (1972).
15. J. Ghaboussi and E.L. Wilson. Flow of compressible fluid in porous elastic media. *Intern. J. Numer. Meth. Engrg.*, v.5, 419-442 (1973).
16. T. Matsumoto. Finite element analysis of immediate and consolidation deformations based on effective stress principle. *Soils and Foundations (Japan. Soc. of Soil Mech. and Found. Engrg.)*, v.16, N 4, 23-34 (1976).
17. J.T. Christian. Two- and three- dimensional consolidation. In: *Numerical Methods in Geotechnical Engineering* (C.S. Desai and J.T. Christian, eds.), 399-426, McGraw Hill, 1977.
18. R.S. Sandhu, H. Liu and K.J. Singh. Numerical performance of some finite element schemes for analysis of seepage in porous elastic media. *Intern. J. Numer. Anal. Meth Geomech.*, v.1, 177-194 (1977).
19. M.B. Reed. An investigation of numerical errors in the analysis of consolidation by finite elements. *Intern. J. Numer. Anal. Meth Geomech.*, v.8, 243-257 (1984).
20. J.R. Booker. The consolidation of a finite layer subject to surface loading. *Intern. J. Solids and Structures*, v.10, 1053-1065 (1974).
21. R.W. Lewis and B.A. Schrefler. The finite element method in the deformation and consolidation of porous media. Wiley, New York, 1987.
22. N.M. Safai and G.F. Pinder. Vertical and horizontal land deformation in a desaturating porous media. *Advances in Water Resources*, v.2, 19-25, (1979).
23. J-M. Kim and R.P. Parizek. Three-dimensional finite element modelling for consolidation due to groundwater withdrawal in a desaturating anisotropic aquifer system. *Intern. J. Numer. Anal. Meth. Geomech.*, v.23, 549-571 (1999).

24. R.S. Sandhu and H. Liu. Analysis of consolidation of viscoelastic solids. In: Numerical Methods in Geomechanics / Proc. 3rd Intern. Conf. on Numerical Methods in Geomechanics, Aachen, 1979, (ed. by W. Wittke), v.4, 1255-1263, Balkema, Rotterdam, 1980.
25. B.B. Budkowska and Q. Fu. Some aspects of numerical analysis of creep in layered granular medium. Computers and Geomechanics, v.5, 285-306 (1988).
26. M.Y. Khaled, D.E. Beskos, and E.C. Ainfantis. On the theory of consolidation with double porosity - III. A finite element formulation. Intern. J. Numer. Anal. Meth. Geomech., v.8, 101-123 (1984).
27. M. Bai, Y. Abousleiman, L. Cui and J. Zhang. Dual-porosity poroelastic modeling of generalized plane strain. Intern. J. Rock Mech. and Mining Sci., v.36, 1087-1094 (1999).
28. A.K.L. Ng and J.C. Small. Use of coupled finite element analysis in unsaturated soil problems. Intern. J. Numer. Anal. Meth. Geomech., v.24, 73-94 (2000).
29. K. Haghghi. Finite element simulation of the thetrmo- hydro- stress in a viscoelastic sphere during drying. Drying Technology, v.8, N 3, 451-464 (1990).
30. J. Irudayaraj and K. Haghghi. Stress analysis of viscoelastic materials during drying: I- Theory and finite element formulation. Drying Technology, v.11, N 5, 901-927 (1993).
31. J. Irudayaraj, K. Hadgidgi and R. Strochine. Stress analysis of viscoelastic materials during drying: II-Application to grain kernels. Drying Technology, v.11, N 5, 929-959 (1993).
32. M. Hasatami and Y. Itaya. Fundamental study of shrinkage of formed clay during drying.- Viscoelastic strain-stress and heat/moisture transfer. Drying Technology, v.10, N 4, 1013-1036 (1992).
33. Y. Itaya, S. Mabuchi and M. Hasatami. Deformation behavior of ceramic slabs by nonuniform drying. Drying Technology, v.13, N 3, 801-819 (1995).
34. Y. Itaya S. Taniguchi and M. Hasatami. A numerical study of transient deformation and stress behavior of a slab clay during drying. Drying Technology, v.15, N 1, 1-21 (1997).
35. M. Hasatami and Y. Itaya. Drying induced strain and stress: a review. Drying technology, v.14, N 5, 1011-1040 (1996).

36. T.S. Nguen and A.P.S. Selvadurai. Coupled thermal-mechanical-hydrological behavior of sparsely fractured rock: implications for nuclear fuel waste disposal. *Intern. J. Rock. Mech. and Mining Sci.*, v.32, N 5, 465-479 (1995).
37. A.P.S. Selvadurai. Geomechanics of engineered and natural geological barriers in nuclear waste management endeavours. In: *Computer methods and Advances in Geomechanics* (Yuan, ed.), 2455-2468, Balkema, Rotterdam, 1998.
38. Y. Zhou, R.K.N.D. Rajapakse and J. Graham. Coupled heat-moisture-air transfer in deformable unsaturated media. *J. Engrg. Mech.*, v.124, N 10, 1090-1099 (1998).
39. V. Guvanasen and Tin Chan. A three-dimensional numerical model for thermohydromechanical deformation with hysteresis in a fractured rock mass. *Intern. J. Rock Mech. and Mining Sci.*, v.37, 89-106 (2000).
40. J.P. Carter, J.C. Small and J.R. Booker. A theory of finite elastic consolidation. *Intern. J. Solids and Structures*, v.13, 467-478 (1977).
41. J.P. Carter, J.R. Booker and E.H. Davis. Finite deformation of an elastoplastic soil. *Intern. J. Numer. Anal. Meth. Geomech.*, v.1, 25-43 (1997).
42. J.P. Carter, J.R. Booker and J.C. Small. The analysis of finite elasto- plastic consolidation. *Intern. J. Numer. Anal. Meth. Geomech.*, v.3, 107-129 (1979).
43. K.L. Meijer. Comparison of finite and infinitezimal strain consolidation by numerical experiments. *Intern. J. Numer. Anal. Meth. Geomech.*, v.8, 531-548 (1984).
44. M.B. Chopra and G.F. Dargush. Finite element analysis of time-dependent large-deformation problems. *Intern. J. Numer. Anal. Meth. Geomech.*, v.16, 101-130 (1992).
45. S.H. Advani, T.S. Lee, J.K. Lee and C.S. Kim. Hydrothermomechanical evaluation of porous media under finite deformation. Part I-Finite element formulation. *Intern. J. Numer. Meth. Eng.*, v.36, 147-160, (1993).
46. C.S. Kim, T.S. Lee, S.H. Advani and J.K. Lee. Hydrothermomechanical evaluation of porous media under finite deformation. Part II-Model validation and field simulation. *Intern. J. Numer. Meth. Eng.*, v.36, 161-179 (1993).

47. F. Armero. Formulation and finite element implementation of a multiplicative model of coupled poro-plasticity at finite strains under fully saturated conditions. *Comput. Meth. Appl. Mech. Engrg.*, v.171, 205-241.
48. O.C. Zienkiewicz. The finite element method in engineering science. McGraw-Hill, London, 1971.
49. T.G.R. Hughes. The finite element method: linear static and dynamic finite element analysis. Englewood Cliffs, N.J.: Prentice-Hall, 1987.
50. J.J. Dongarra, C.B. Moler, J.R. Bunch, G.W. Stewart. LINPACK Users' Guide. SIAM, Philadelphia, 1979.
51. LINPACK. <http://www.netlib.org/lapack>
52. W.H. Press, S.A. Teukolsky, W.T. Vetterling, B.P. Flannery. Numerical Recipies in Fortran 77. Cambridge University Press, 1992.
53. A. Verruijt. Computational Geomechanics. Kluwer Academic Publishers, Boston, 1995.
54. M.A. Murad, L.S. Bennethum, J.H. Cushman. A multi-scale theory of swelling porous media: I. Application to one-dimensional consolidation. *Transport in porous media*, v.19, p.93-122 (1995).
55. M.A. Murad, J.H. Cushman. New directions for modeling consolidation of swelling clay soils. *Trends in Soil Science*, v.2, p.1-35, (1997).
56. M.A. Murad, J.H. Cushman. A three-scale model for consolidation of swelling clay soils. *NUMOG-VI: Numerical Methods in Geomechanics* (ed. S. Petruszczak, G.N. Pande), Balkema, Rotterdam, p.117-122, 1997.
57. S. Achanta, M.R. Okos, J.H. Cushman, D.P. Kessler. Moisture transport in shrinking gels during saturated drying. *AIChE Journal*, v.43, N 8, 2112-2122 (1997).
58. M.A. Murad, J.H. Cushman. Thermomechanical theories for swelling porous media with microstructure. *Intern. J. of Engrg. Sci.*, v.38, p.517-564 (2000).

Fig. 2.1. An arbitrary finite element triangle grid.

Fig. 2.2. Linear basis functions in triangle, used for pore pressure approximation.

$$A = \text{area of entire triangle}; \quad A_i = \text{area of triangle opposite node } i; \quad \varphi_i = A_i / A.$$

Fig. 2.3. Quadratic basis functions in triangle, used for displacement approximation.

$$\psi_1 = \varphi_1(2\varphi_1 - 1), \quad \psi_2 = \varphi_2(2\varphi_2 - 1), \quad \psi_3 = \varphi_3(2\varphi_3 - 1),$$

$$\psi_4 = 4\varphi_2\varphi_3, \quad \psi_5 = 4\varphi_3\varphi_1 \quad \psi_6 = 4\varphi_1\varphi_2.$$

Fig. 3.1. Scheme for 1-d test problem.

Fig. 3.2. 1-d test problem for classical Biot model.

Displacement of the upper boundary, $V = V(t)$ (dimensionless V and t).

Fig. 4.1. 1-d test problem for consolidation model with viscoelasticity.

Displacement of the upper boundary, $V = V(t)$ (dimensionless V and t).

Fig. 5.1. 1-d test problem for consolidation model with viscoelasticity and additional capillary flow.

Displacement of the upper boundary, $V = V(t)$ (dimensionless V and t).

Fig. 6.1. The scheme and the grid for consolidation problem for layer loaded on the upper boundary.

$$H = 20 \text{ m}, L = 50 \text{ m}, b = 10 \text{ m}.$$

Fig. 6.2. Strip load. Drained loading surface. Pore pressure.

$$K = 1600 \text{ t/m}^2, G = 1000 \text{ t/m}^2, k = 0.01 \text{ m/day},$$

$$H = 20 \text{ m}, L = 50 \text{ m}, b = 10 \text{ m}, F = 10 \text{ t/m}.$$

Fig. 6.3. Settlement of the upper boundary $V = V(x | y = 0)$ of horizontal layer under drained strip

$$\text{load. } K = 1600 \text{ t/m}^2, G = 1000 \text{ t/m}^2, k = 0.01 \text{ m/day},$$

$$H = 20 \text{ m}, L = 50 \text{ m}, b = 10 \text{ m}, F = 10 \text{ t/m}.$$

Fig. 6.4. Strip load. Drained loading surface. Displacement vector field.

load. $K = 1600 \text{ t/m}^2$, $G = 1000 \text{ t/m}^2$, $k = 0.01 \text{ m/day}$,

$H = 20 \text{ m}$, $L = 50 \text{ m}$, $b = 10 \text{ m}$, $F = 10 \text{ t/m}$.

Fig. 6.5. Strip load. Undrained loading surface. Pore pressure.

$K = 1600 \text{ t/m}^2$, $G = 1000 \text{ t/m}^2$, $k = 0.01 \text{ m/day}$,

$H = 20 \text{ m}$, $L = 50 \text{ m}$, $b = 10 \text{ m}$, $F = 10 \text{ t/m}$.

Fig. 6.6. Settlement of the upper boundary $V = V(x | y = 0)$ of horizontal layer under undrained strip

load. $K = 1600 \text{ t/m}^2$, $G = 1000 \text{ t/m}^2$, $k = 0.01 \text{ m/day}$,

$H = 20 \text{ m}$, $L = 50 \text{ m}$, $b = 10 \text{ m}$, $F = 10 \text{ t/m}$.

Fig. 6.7. Strip load. Undrained loading surface. Displacement vector field.

load. $K = 1600 \text{ t/m}^2$, $G = 1000 \text{ t/m}^2$, $k = 0.01 \text{ m/day}$,

$H = 20 \text{ m}$, $L = 50 \text{ m}$, $b = 10 \text{ m}$, $F = 10 \text{ t/m}$.

Fig. 6.8. Settlement under the central point vs. time.

$K = 1600 \text{ t/m}^2$, $G = 1000 \text{ t/m}^2$, $k = 0.01 \text{ m/day}$,

$H = 20 \text{ m}$, $L = 50 \text{ m}$, $b = 10 \text{ m}$, $F = 10 \text{ t/m}$.

Fig. 6.9. Integral volume deformation vs. time.

$K = 1600 \text{ t/m}^2$, $G = 1000 \text{ t/m}^2$, $k = 0.01 \text{ m/day}$,

$H = 20 \text{ m}$, $L = 50 \text{ m}$, $b = 10 \text{ m}$, $F = 10 \text{ t/m}$.

Fig. 6.10. Strip tangential load. Drained loading surface. Pore pressure.

$K = 1600 \text{ t/m}^2$, $G = 1000 \text{ t/m}^2$, $k = 0.01 \text{ m/day}$,

$H = 20 \text{ m}$, $L = 100 \text{ m}$, $2b = 20 \text{ m}$, $F = 10 \text{ t/m}$.

Fig. 6.11. Settlement of the upper boundary $V = V(x | y = 0)$ of horizontal layer under drained strip

tangential load. $K = 1600 \text{ t/m}^2$, $G = 1000 \text{ t/m}^2$, $k = 0.01 \text{ m/day}$,

$H = 20 \text{ m}$, $L = 100 \text{ m}$, $2b = 20 \text{ m}$, $F = 10 \text{ t/m}$.

Fig. 6.12. Strip tangential load. Drained loading surface. Displacement vector field.

$$K = 1600 \text{ t/m}^2, G = 1000 \text{ t/m}^2, k = 0.01 \text{ m/day},$$

$$H = 20 \text{ m}, L = 100 \text{ m}, 2b = 20 \text{ m}, F = 10 \text{ t/m}.$$

Fig. 6.13. Moving load. Pore pressure.

$$K = 160 \text{ t/m}^2, G = 100 \text{ t/m}^2, k = 1 \text{ m/day},$$

$$H = 1 \text{ m}, b = 10 \text{ m}, F = 10 \text{ t/m}, v = 60 \text{ m/hour}.$$

Fig. 6.14. Moving load. Displacement of the upper boundary $V = V(x | y = 0)$.

$$K = 160 \text{ t/m}^2, G = 100 \text{ t/m}^2, k = 1 \text{ m/day},$$

$$H = 1 \text{ m}, b = 10 \text{ m}, F = 10 \text{ t/m}, v = 60 \text{ m/hour}.$$

Fig. 6.15. Moving load. Pore pressure.

$$K = 160 \text{ t/m}^2, G = 100 \text{ t/m}^2, k = 1 \text{ m/day},$$

$$H = 1 \text{ m}, b = 10 \text{ m}, F = 10 \text{ t/m}, v = 120 \text{ m/hour}.$$

Fig. 6.16. Moving load. Displacement of the upper boundary $V = V(x | y = 0)$.

$$K = 160 \text{ t/m}^2, G = 100 \text{ t/m}^2, k = 1 \text{ m/day},$$

$$H = 1 \text{ m}, b = 10 \text{ m}, F = 10 \text{ t/m}, v = 120 \text{ m/hour}.$$

Fig. 6.17. Moving load. Pore pressure.

$$K = 160 \text{ t/m}^2, G = 100 \text{ t/m}^2, k = 1 \text{ m/day},$$

$$H = 1 \text{ m}, b = 10 \text{ m}, F = 10 \text{ t/m}, v = 240 \text{ m/hour}.$$

Fig. 6.18. Moving load. Displacement of the upper boundary $V = V(x | y = 0)$.

$$K = 160 \text{ t/m}^2, G = 100 \text{ t/m}^2, k = 1 \text{ m/day},$$

$$H = 1 \text{ m}, b = 10 \text{ m}, F = 10 \text{ t/m}, v = 240 \text{ m/hour}.$$

Fig. 6.19. Moving load. Pore pressure.

$$K = 160 \text{ t/m}^2, G = 100 \text{ t/m}^2, k = 1 \text{ m/day},$$

$$H = 1 \text{ m}, b = 10 \text{ m}, F = 10 \text{ t/m}, v = 600 \text{ m/hour}.$$

Fig. 6.20. Moving load. Displacement of the upper boundary $V = V(x | y = 0)$.

$$K = 160 \text{ t/m}^2, G = 100 \text{ t/m}^2, k = 1 \text{ m/day},$$

$$H = 1 \text{ m}, b = 10 \text{ m}, F = 10 \text{ t/m}, v = 600 \text{ m/hour}.$$

Fig. 6.21. Moving load. Displacement of the upper boundary $V = V(x | y = 0)$.

$$K = 160 \text{ t/m}^2, G = 100 \text{ t/m}^2, k = 1 \text{ m/day},$$

$$H = 1 \text{ m}, b = 10 \text{ m}, F = 10 \text{ t/m}.$$

Fig. 6.22. Moving load. Dimensionless pore pressure. $b/H = 10$.

$$\text{Calculated at } K = 160 \text{ t/m}^2, G = 100 \text{ t/m}^2, k = 1 \text{ m/day},$$

$$H = 1 \text{ m}, b = 10 \text{ m}, F = 10 \text{ t/m}.$$

Fig. 6.23. Moving load. Dimensionless displacement of the upper boundary. $b/H = 10$.

$$\text{Calculated at } K = 160 \text{ t/m}^2, G = 100 \text{ t/m}^2, k = 1 \text{ m/day},$$

$$H = 1 \text{ m}, b = 10 \text{ m}, F = 10 \text{ t/m}.$$

Fig. 6.24. Moving load. Dimensionless pore pressure. $b/H = 5$.

$$\text{Calculated at } K = 160 \text{ t/m}^2, G = 100 \text{ t/m}^2, k = 1 \text{ m/day},$$

$$H = 1 \text{ m}, b = 10 \text{ m}, F = 10 \text{ t/m}.$$

Fig. 6.25. Moving load. Dimensionless displacement of the upper boundary. $b/H = 5$.

$$\text{Calculated at } K = 160 \text{ t/m}^2, G = 100 \text{ t/m}^2, k = 1 \text{ m/day},$$

$$H = 1 \text{ m}, b = 10 \text{ m}, F = 10 \text{ t/m}.$$

Fig. 6.26. Moving load. Dimensionless displacement of the upper boundary $V = V(x | y = 0)$ at time

moments near the starting point.

$$K = 160 \text{ t/m}^2, G = 100 \text{ t/m}^2, k = 1 \text{ m/day},$$

$$H = 1 \text{ m}, b = 10 \text{ m}, F = 10 \text{ t/m}, v = 120 \text{ m/hour}.$$

Fig. 6.27. Classical Biot consolidation. Strip load. Drained loading surface. Deformed grid.
(Small strain. The solution is calculated using stationary grid).

$$K = 160 \text{ t/m}^2, G = 100 \text{ t/m}^2, k = 0.01 \text{ m/day},$$

$$H = 10 \text{ m}, L = 50 \text{ m}, b = 10 \text{ m}, F = 100 \text{ t/m}.$$

Fig. 6.28. Classical Biot consolidation. Strip load. Drained loading surface. Deformed grid.

(Small strain. The solution is calculated using moving grid).

$$K = 160 \text{ t/m}^2, G = 100 \text{ t/m}^2, k = 0.01 \text{ m/day},$$

$$H = 10 \text{ m}, L = 50 \text{ m}, b = 10 \text{ m}, F = 100 \text{ t/m}.$$

Fig. 6.29. Consolidation of a viscoelastic body. Strip load. Drained loading surface. Deformed grid.

(Small strain. The solution is calculated using stationary grid).

$$K = 160 \text{ t/m}^2, G = 100 \text{ t/m}^2, \eta = 3000 \text{ t/m}\cdot\text{day}, k = 0.01 \text{ m/day},$$

$$H = 10 \text{ m}, L = 50 \text{ m}, b = 10 \text{ m}, F = 100 \text{ t/m}.$$

Fig. 6.30. Consolidation of a viscoelastic body. Strip load. Drained loading surface. Deformed grid.

(Small strain. The solution is calculated using moving grid).

$$K = 160 \text{ t/m}^2, G = 100 \text{ t/m}^2, \eta = 3000 \text{ t/m}\cdot\text{day}, k = 0.01 \text{ m/day},$$

$$H = 10 \text{ m}, L = 50 \text{ m}, b = 10 \text{ m}, F = 100 \text{ t/m}.$$

Fig. 6.31. Settlement of the central point vs. time for classical Biot and viscoelastic models.

$$K = 160 \text{ t/m}^2, G = 100 \text{ t/m}^2, k = 0.01 \text{ m/day},$$

$$H = 10 \text{ m}, L = 50 \text{ m}, b = 10 \text{ m}.$$

An arbitrary finite element triangle grid

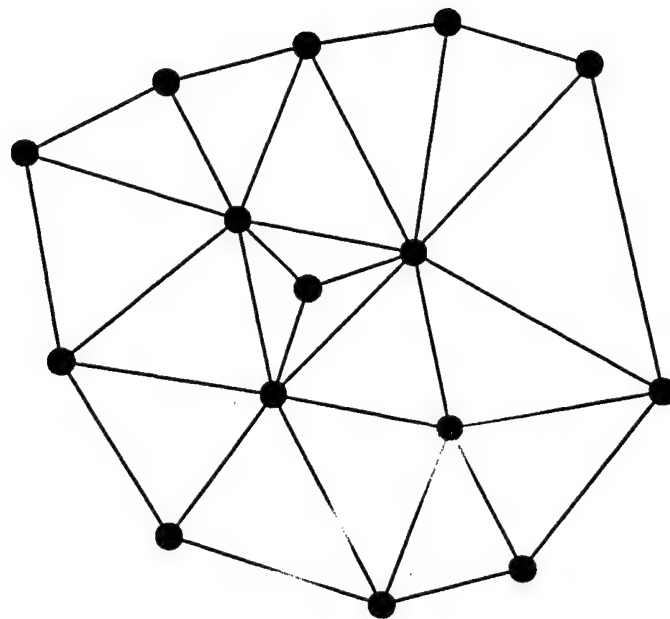


Figure 2.1

Linear basis functions in triangle,
used for pore pressure approximation

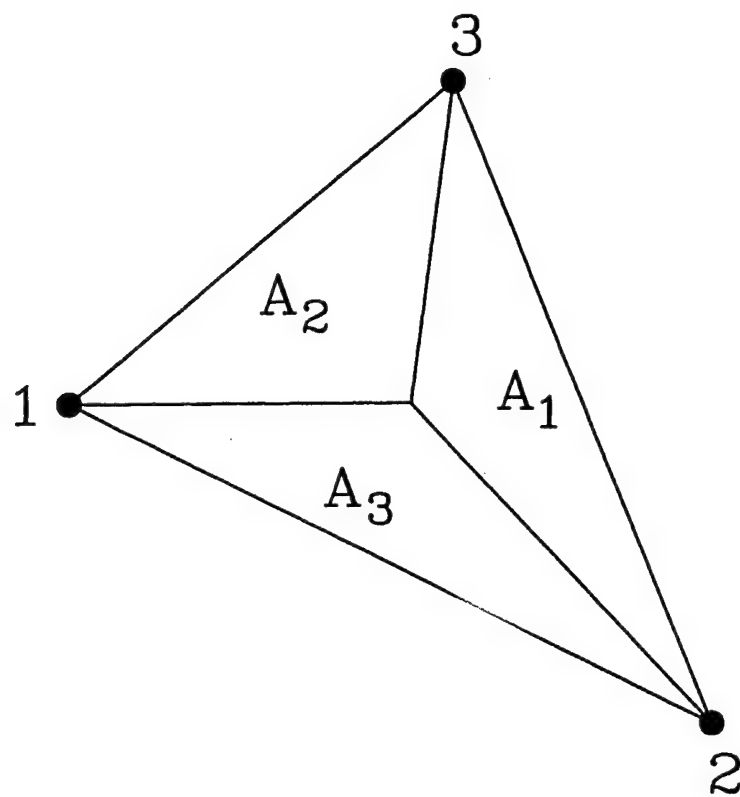


Figure 2.2

Quadratic basis functions in triangle,
used for displacements approximation

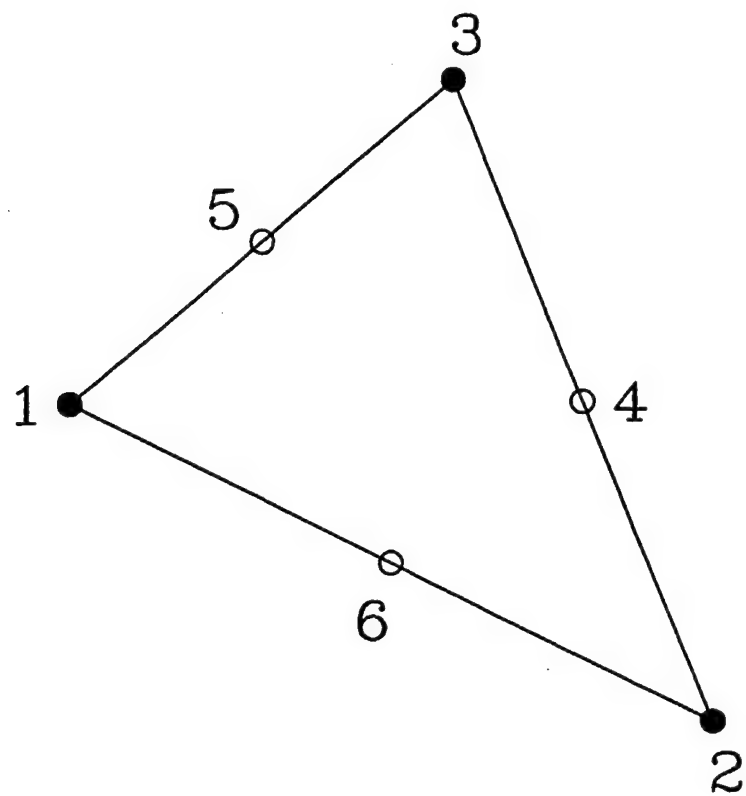


Figure 2.3

Scheme for 1-d test problem

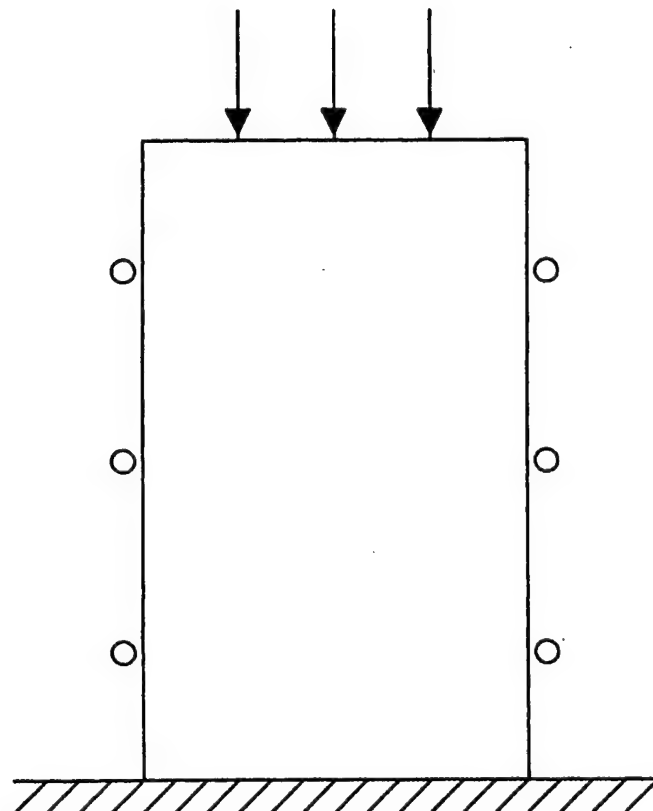


Figure 3.1

1-d test problem
for classical Biot model.

Displacement of the upper boundary, $V=V(t)$

(dimensionless V and t)

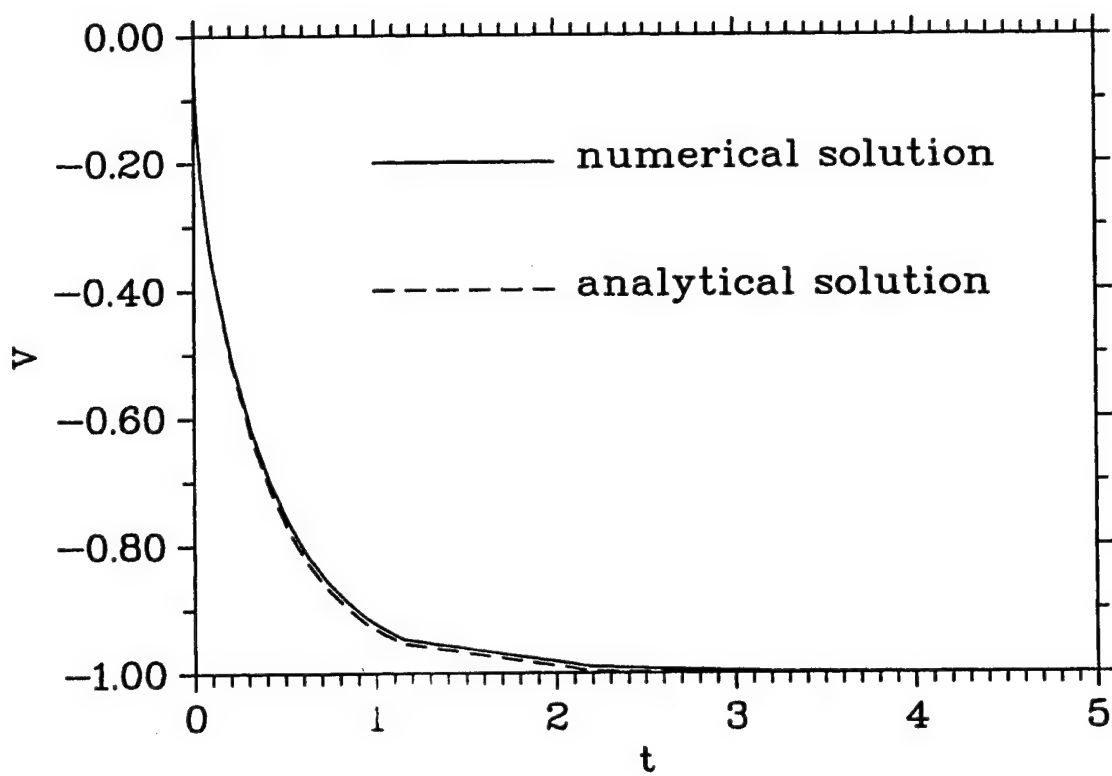


Figure 3.2

1-d test problem
for consolidation model with viscoelasticity

Displacement of the upper boundary, $V = V(t)$

(dimensionless V and t)

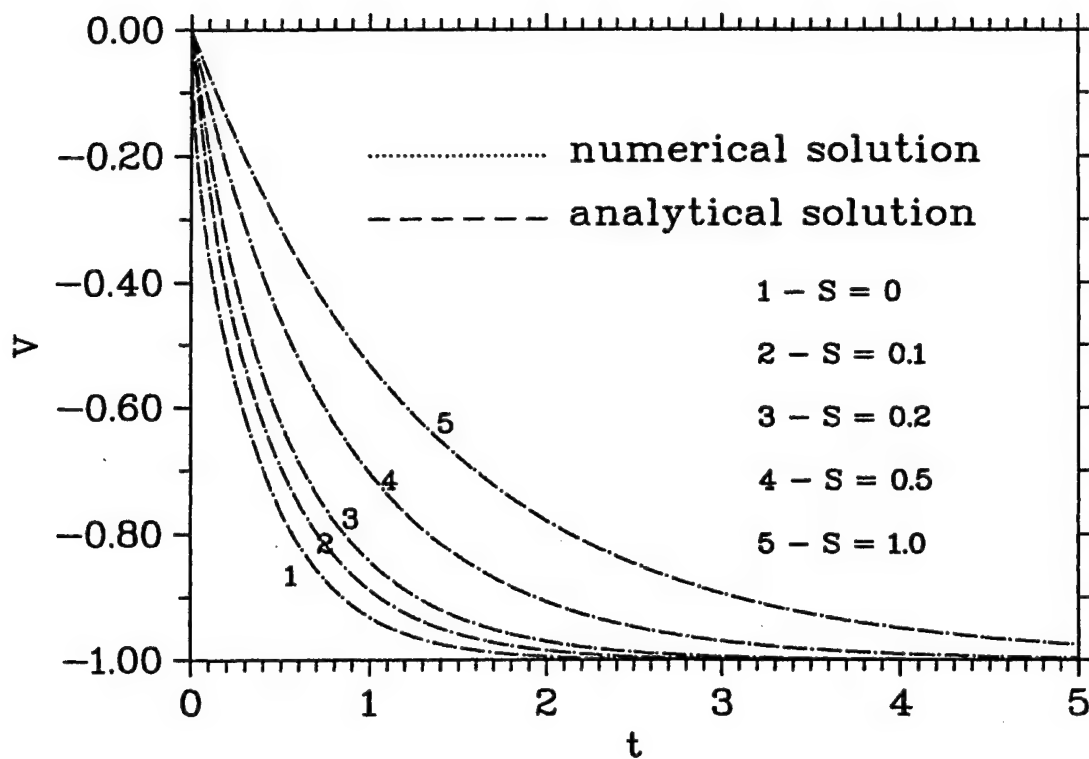


Figure 4.1

1-d test problem
for consolidation model with viscoelasticity
and additional capillary flow

Displacement of the upper boundary, $V=V(t)$

(dimensionless V and t)

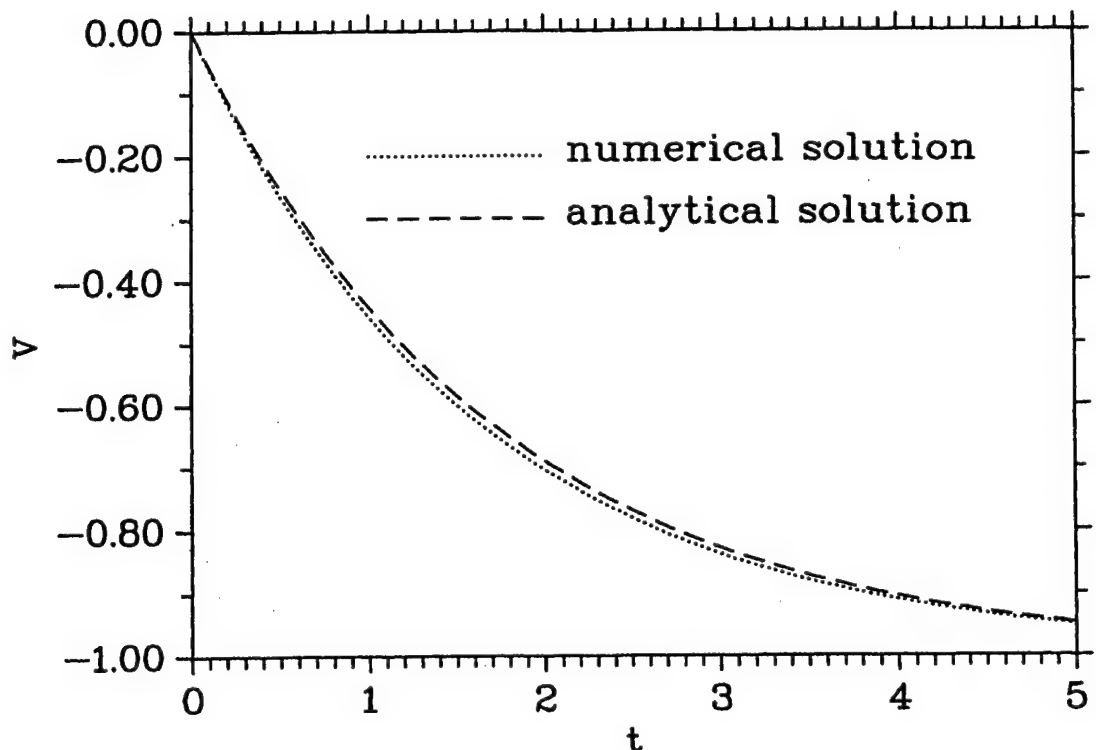


Figure 5.1

The Scheme and the Grid
for consolidation problem
for Layer Loaded on Upper Boundary

$$H=20 \text{ m}, \quad L=50\text{m}, \quad b=10\text{m}$$

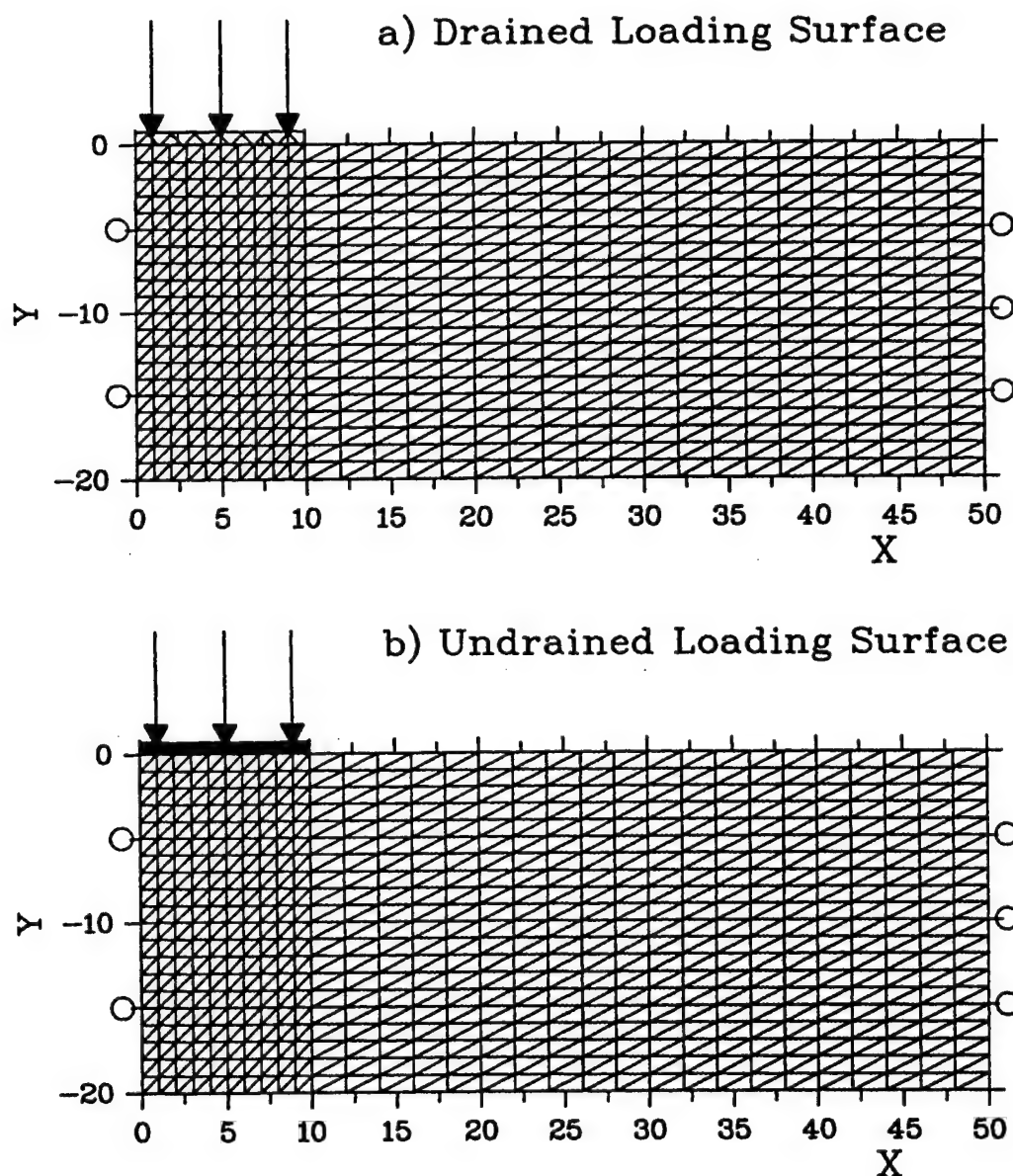


Figure 6.1

Strip Load. Drained Loading Surface.
Pore pressure

$K=1600 \text{ t/m}^2\text{ day}$, $G=1000 \text{ t/m}^2\text{ day}$, $k=0.01 \text{ m/day}$

$H=20 \text{ m}$, $L=50 \text{ m}$, $b=10 \text{ m}$, $F=10 \text{ t/m}$

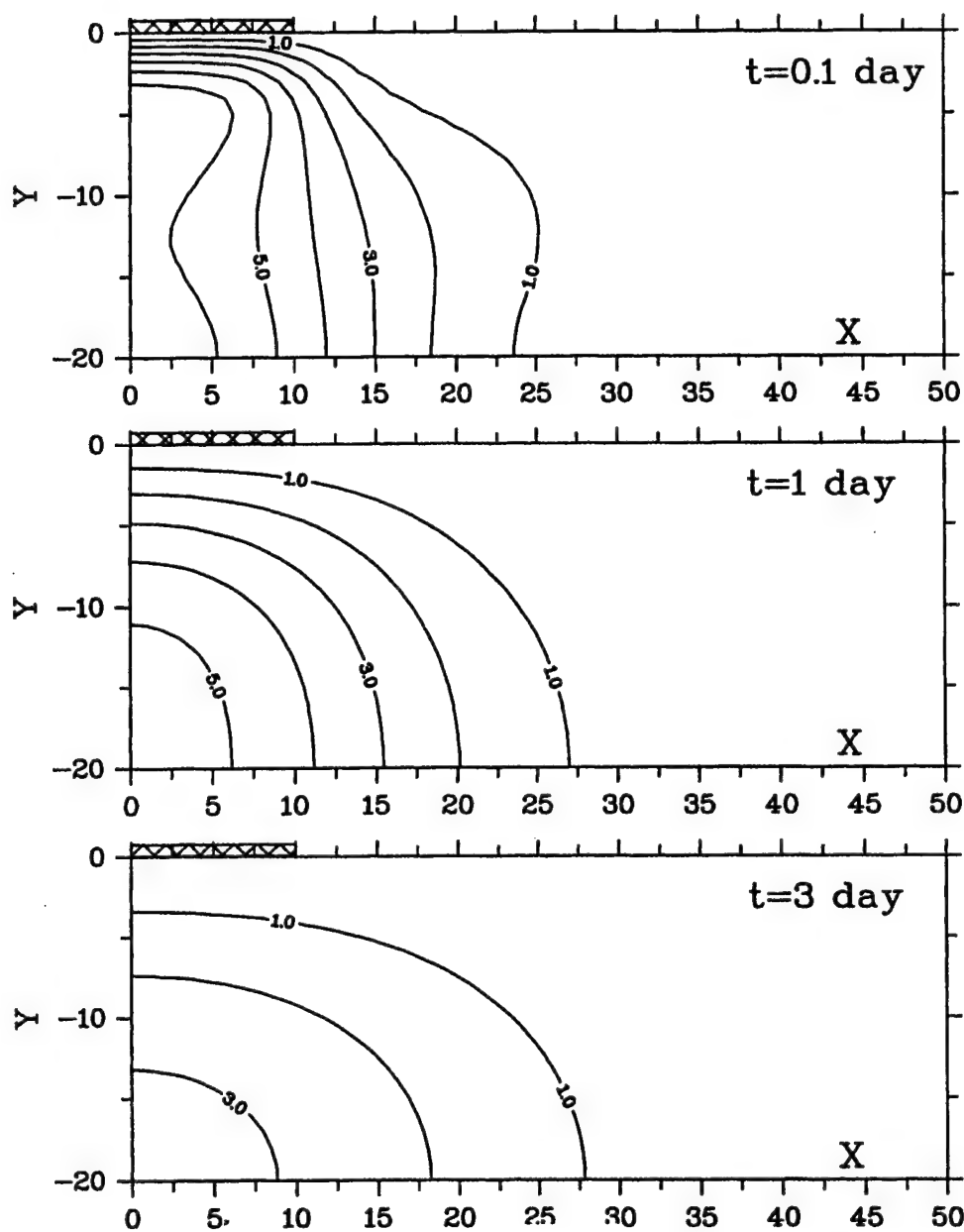


Figure 6.2

Settlement of the Upper Boundary $V=V(x|y=0)$
of Horizontal Layer under Undrained Strip Load

$K=1600 \text{ t/m}^2\text{m}$, $G=1000 \text{ t/m}^2\text{m}$, $k=0.01 \text{ m/day}$

$H=20 \text{ m}$, $L=50 \text{ m}$, $b=10 \text{ m}$, $F=10 \text{ t/m}$

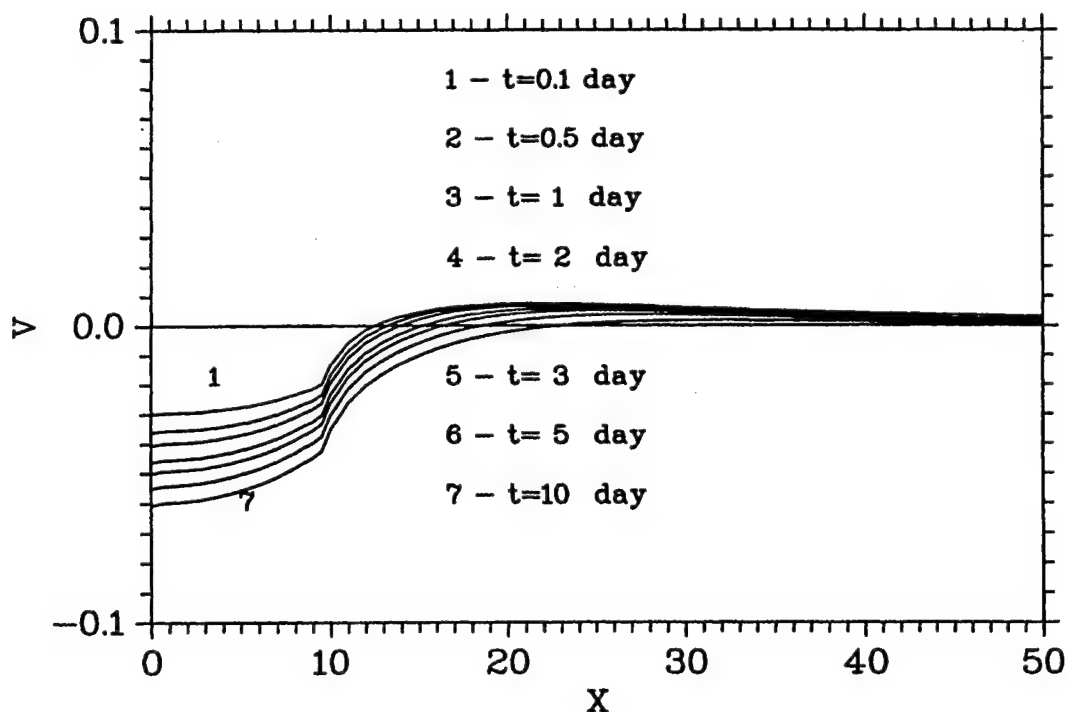


Figure 6.3

Strip Load. Drained Loading Surface.
Displacement vector field

$K=1600 \text{ t/m}^2\text{m}$, $G=1000 \text{ t/m}^2\text{m}$, $k=0.01 \text{ m/day}$

$H=20 \text{ m}$, $L=50 \text{ m}$, $b=10 \text{ m}$, $F=10 \text{ t/m}$

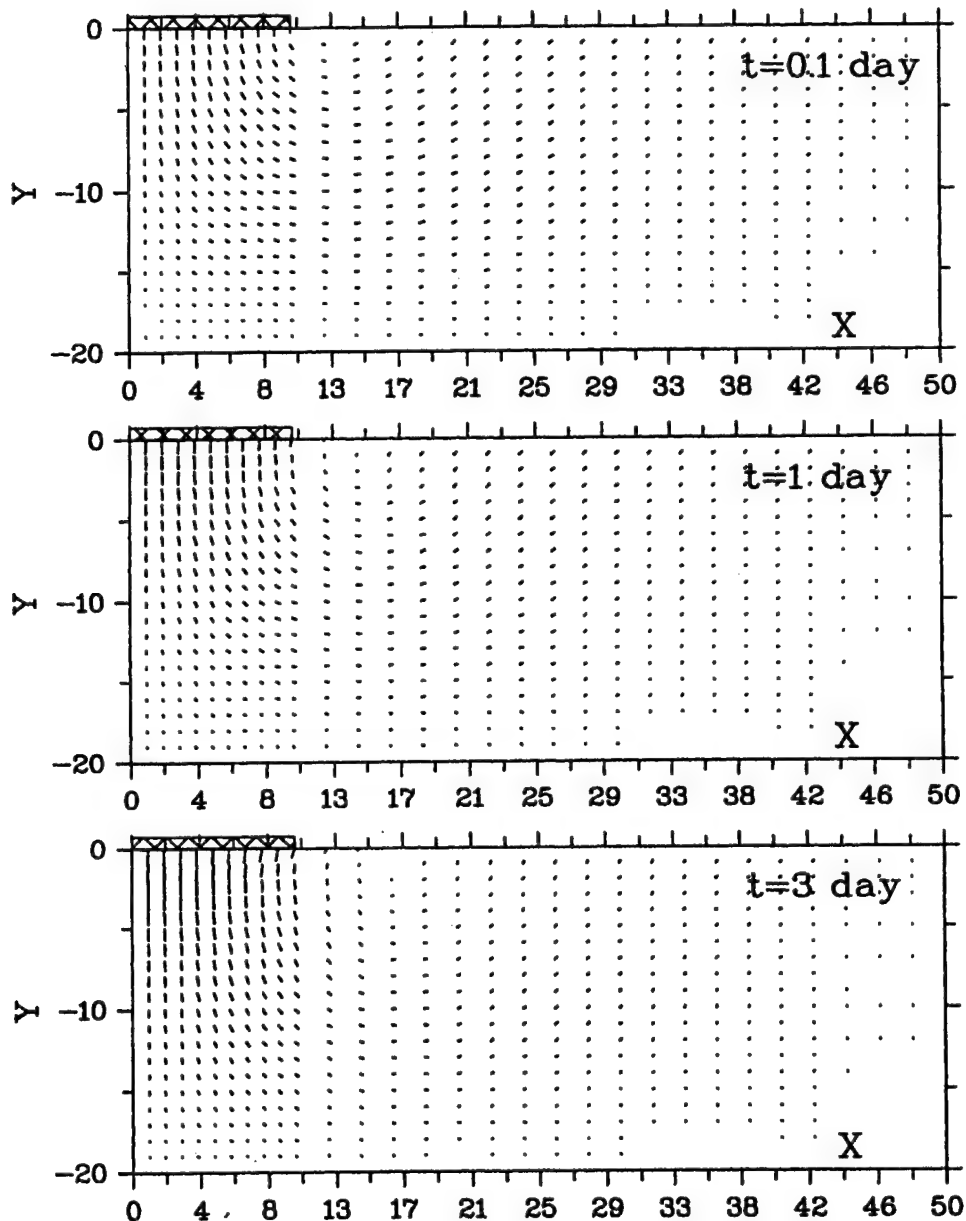


Figure 6.4

Strip Load. Undrained Loading Surface.
Pore pressure

$K=1600 \text{ t/m}^2\text{m}$, $G=1000 \text{ t/m}^2\text{m}$, $k=0.01 \text{ m/day}$

$H=20 \text{ m}$, $L=50 \text{ m}$, $b=10 \text{ m}$, $F=10 \text{ t/m}$

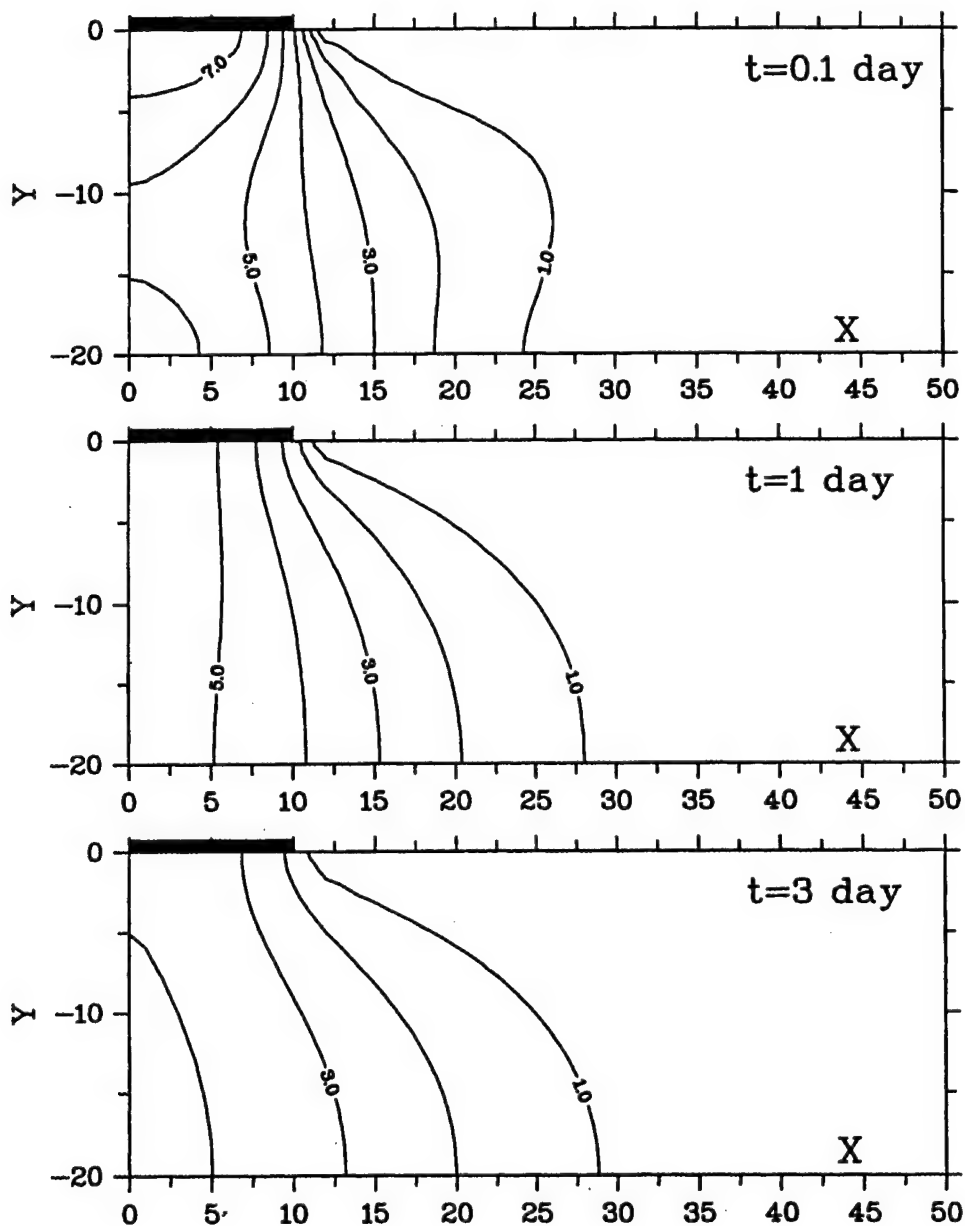


Figure 6.5

Settlement of the Upper Boundary $V=V(x|y=0)$
of Horizontal Layer under Undrained Strip Load

$K=1600 \text{ t/m}^2\text{m}$, $G=1000 \text{ t/m}^2\text{m}$, $k=0.01 \text{ m/day}$

$H=20 \text{ m}$, $L=50 \text{ m}$, $b=10 \text{ m}$, $F=10 \text{ t/m}$

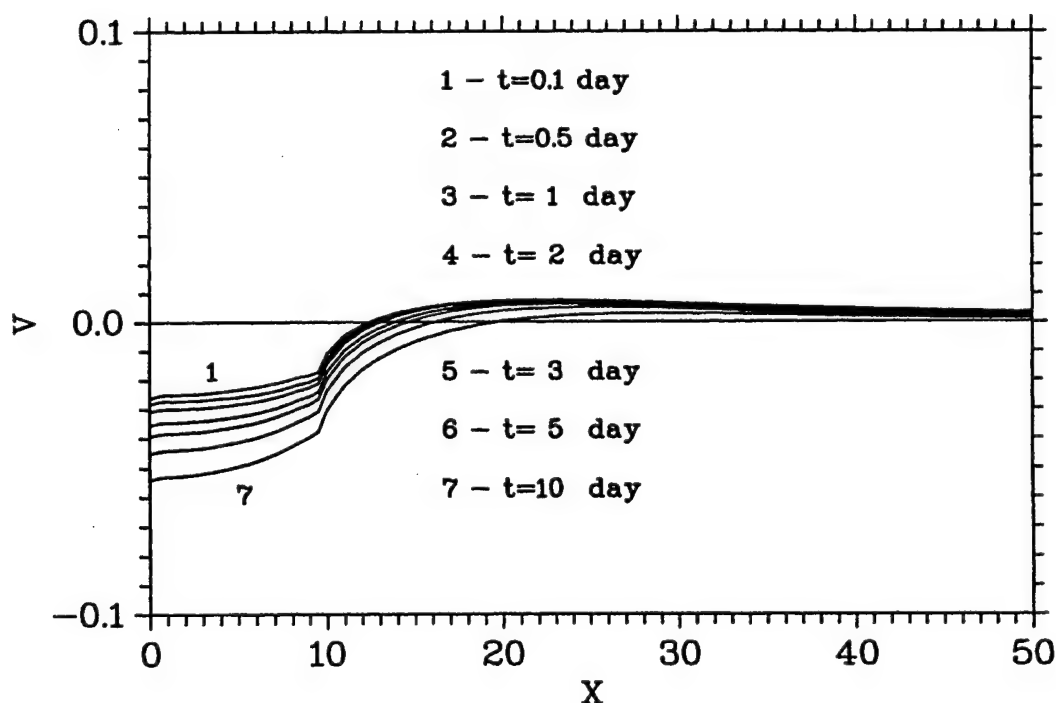


Figure 6.6

Strip Load. Undrained Loading Surface.
Displacement vector field

$K=1600 \text{ t/m}^2\text{m}$, $G=1000 \text{ t/m}^2\text{m}$, $k=0.01 \text{ m/day}$

$H=20 \text{ m}$, $L=50 \text{ m}$, $b=10 \text{ m}$, $F=10 \text{ t/m}$

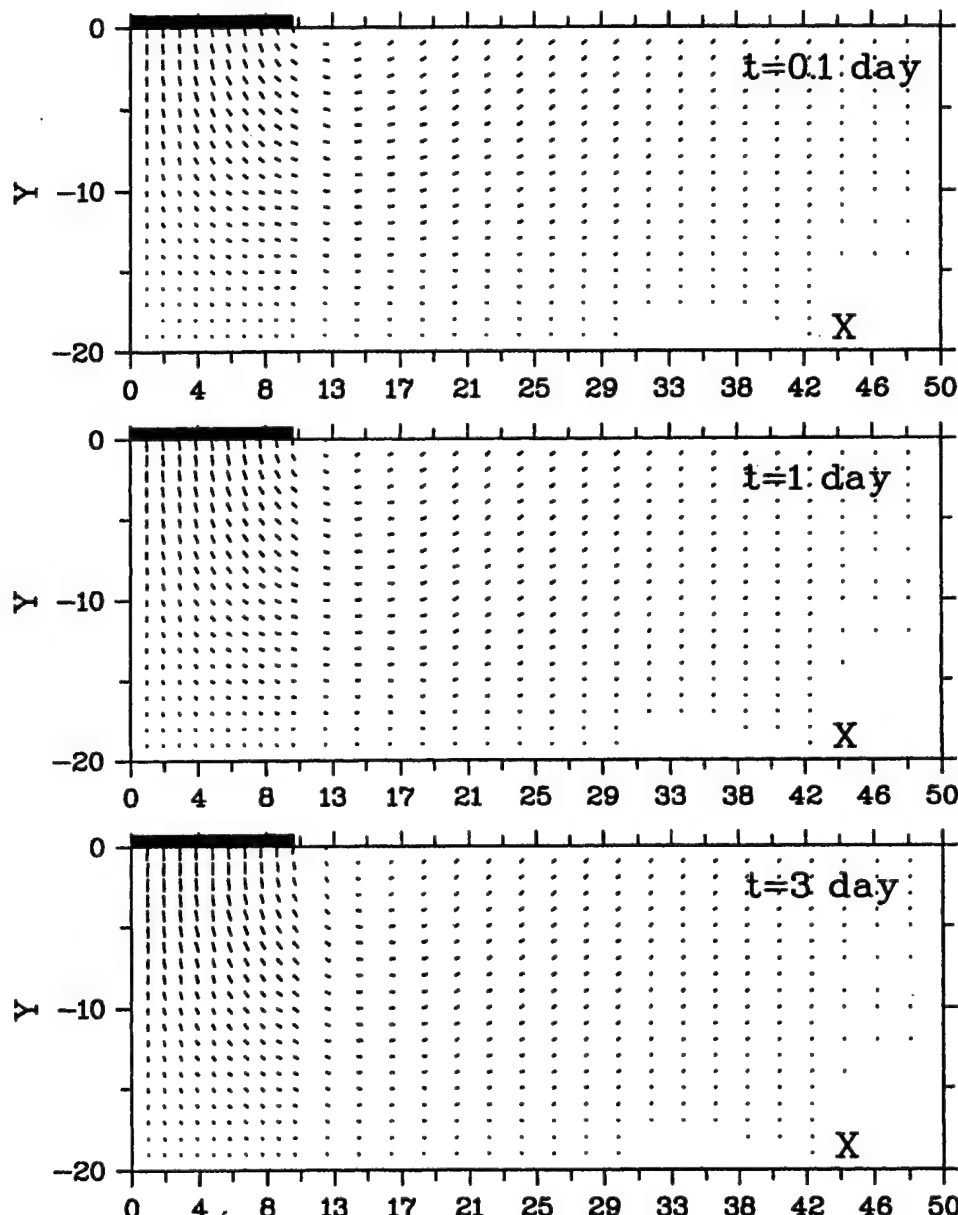


Figure 6.7

Settlement under the central point vs. time

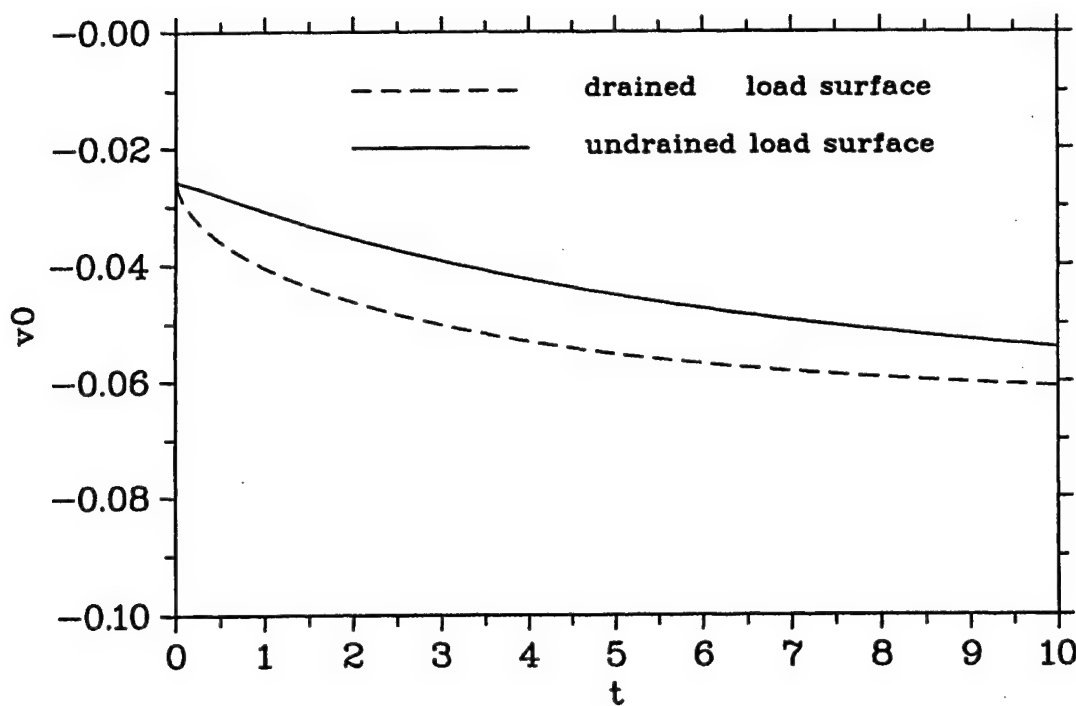
 $K=1600 \text{ t/m}^2\text{m}, G=1000 \text{ t/m}^2\text{m}, k=0.01 \text{ m/day}$ $H=20 \text{ m}, L=50 \text{ m}, b=10 \text{ m}, F=10 \text{ t/m}$ 

Figure 6.8

Integral volume deformation vs. time

$K=1600 \text{ t/m}^2\text{m}$, $G=1000 \text{ t/m}^2\text{m}$, $k=0.01 \text{ m/day}$

$H=20 \text{ m}$, $L=50 \text{ m}$, $b=10 \text{ m}$, $F=10 \text{ t/m}$

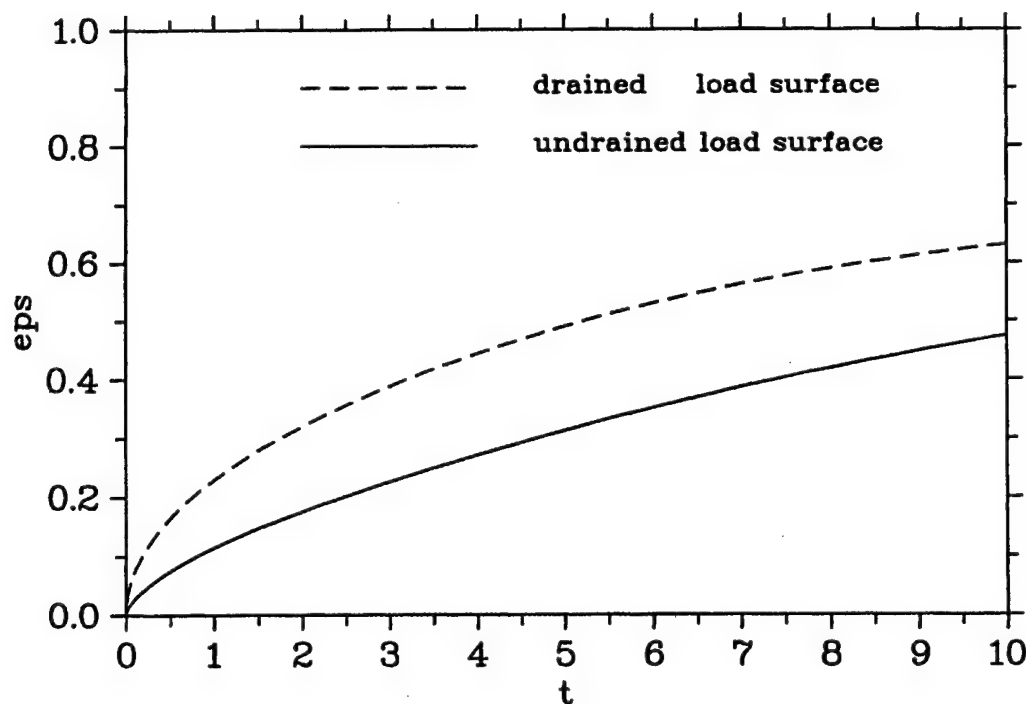


Figure 6.9

Strip Tangential Load. Drained Loading
Surface. Pore pressure

$K=1600 \text{ t/m}^2\text{m}$, $G=1000 \text{ t/m}^2\text{m}$, $k=0.01 \text{ m/day}$

$H=20 \text{ m}$, $L=100 \text{ m}$, $2b=20 \text{ m}$, $F=10 \text{ t/m}$

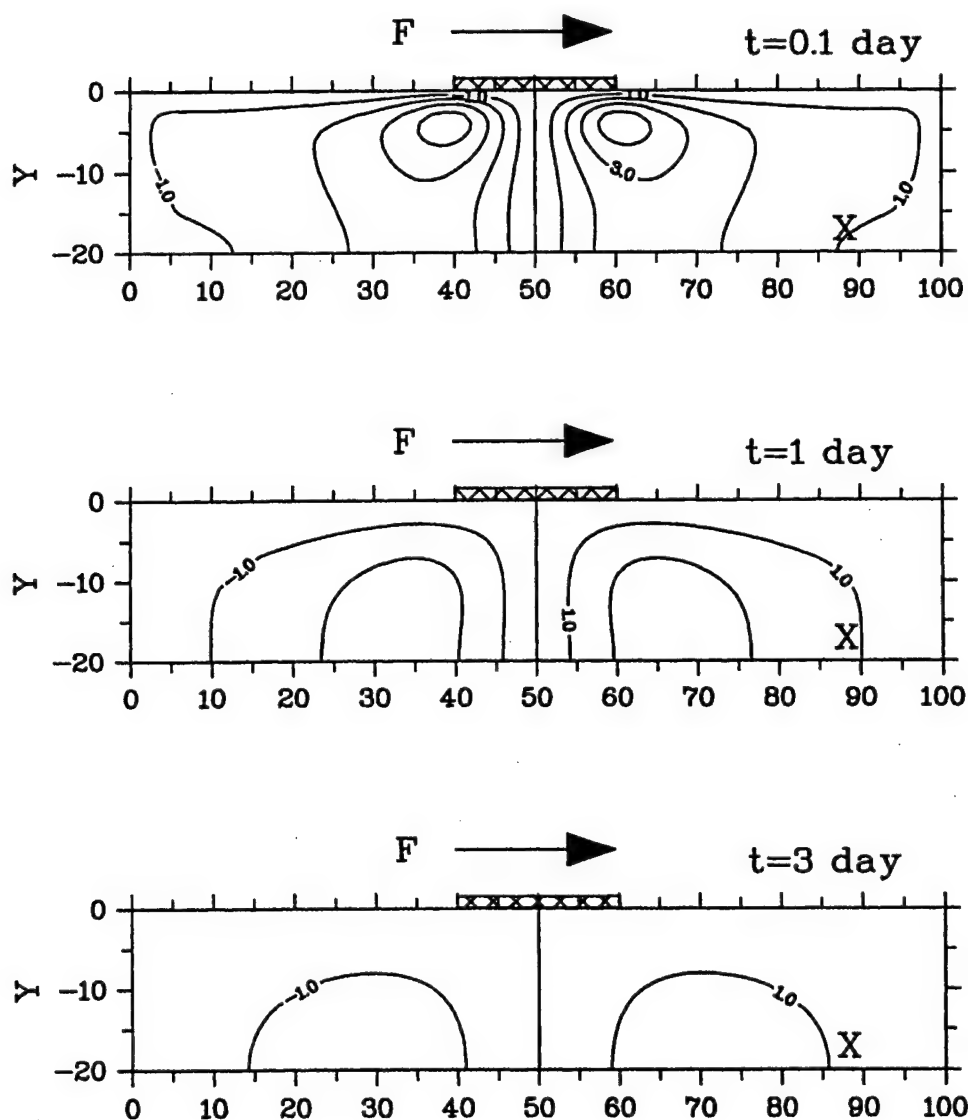


Figure 6.10

Settlement of the Upper Boundary $V=V(x|y=0)$
of Horizontal Layer under Drained Strip
Tangential Load

$K=1600 \text{ t/m}^2\text{m}$, $G=1000 \text{ t/m}^2\text{m}$, $k=0.01 \text{ m/day}$
 $H=20 \text{ m}$, $L=100 \text{ m}$, $2b=20 \text{ m}$, $F=10 \text{ t/m}$

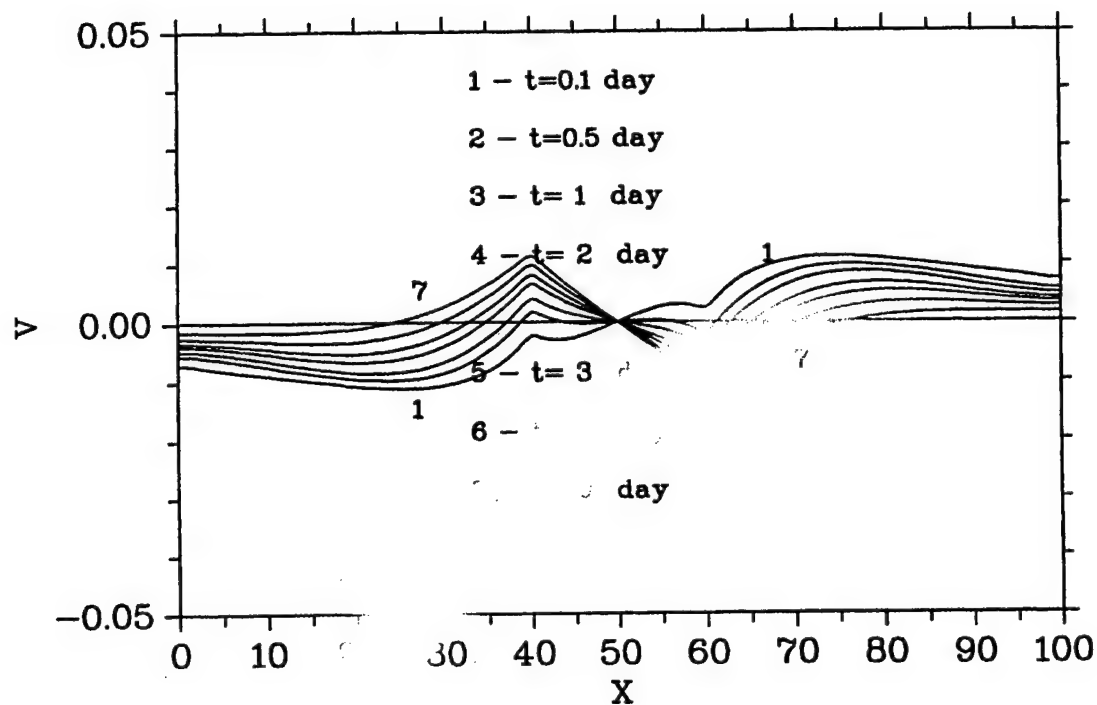


Figure 6.11

Strip Tangential Load.
 Drained Loading Surface.
 Displacement vector field

$K=1600 \text{ t/m}^2\text{m}$, $G=1000 \text{ t/m}^2\text{m}$, $k=0.01 \text{ m/day}$
 $H=20 \text{ m}$, $L=100 \text{ m}$, $2b=20 \text{ m}$, $F=10 \text{ t/m}$

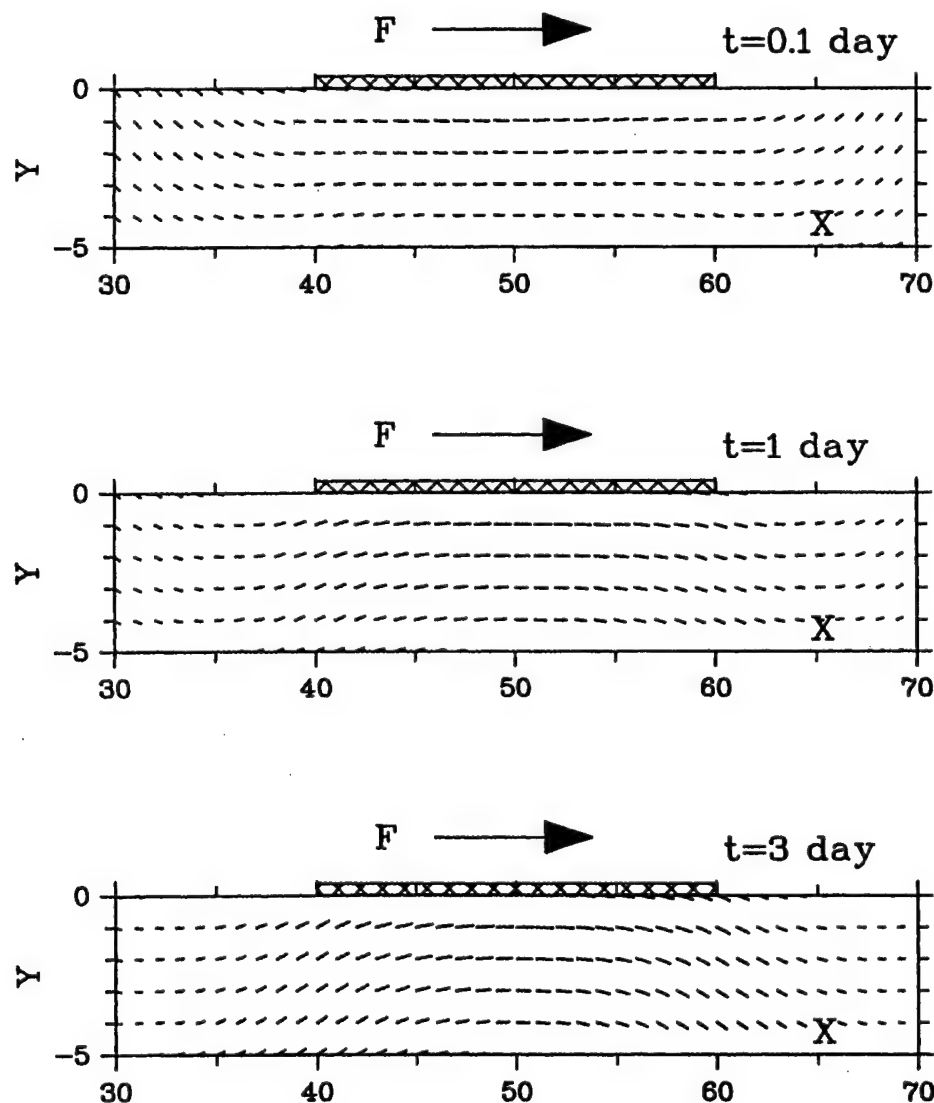


Figure 6.12

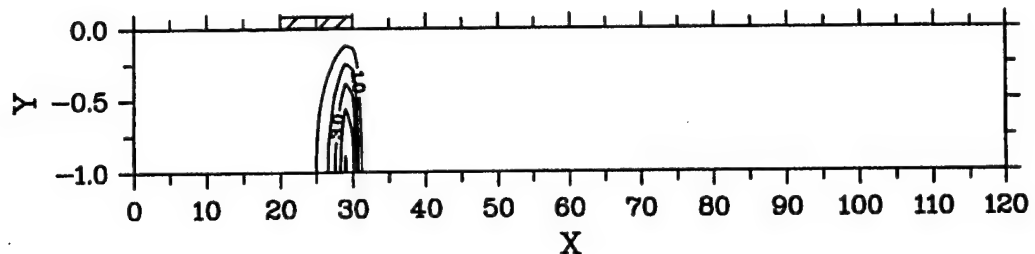
Moving Load.

Pore pressure

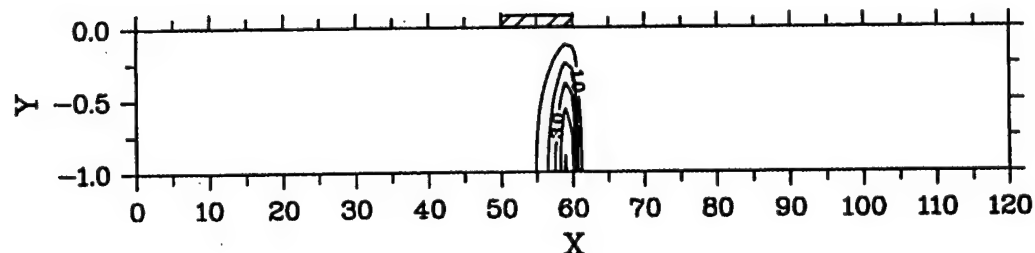
$$K = 160 \text{ t/m}^2\text{m}, G = 100 \text{ t/m}^2\text{m}, k = 1 \text{ m/day}$$

$$H = 1 \text{ m}, b = 10 \text{ m}, F = 10 \text{ t/m}, v = 60 \text{ m/hour}$$

$$t = 0.0066 \text{ day} = 9.5 \text{ min}$$



$$t = 0.0264 \text{ day} = 38 \text{ min}$$



$$t = 0.0528 \text{ day} = 76 \text{ min}$$

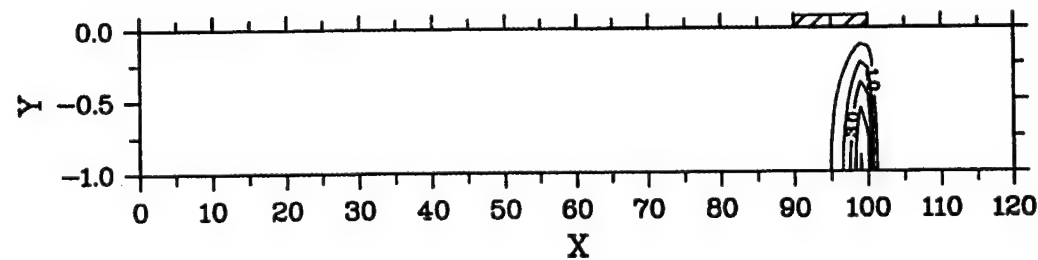


Figure 6.13

Moving Load.

Displacement of the upper boundary, $V=V(x|y=0)$

$$K = 160 \text{ t/m}^2, G = 100 \text{ t/m}^2, k = 1 \text{ m/day}$$

$$H = 1 \text{ m}, b = 10 \text{ m}, F = 10 \text{ t/m}, v = 60 \text{ m/hour}$$

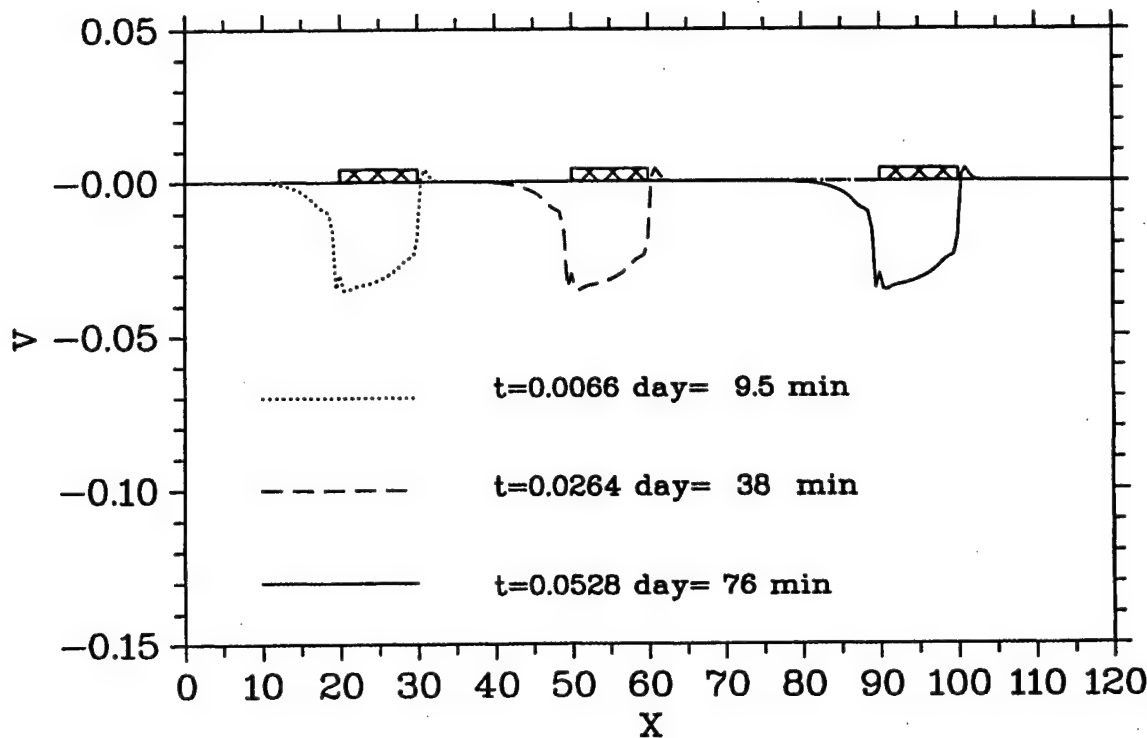


Figure 6.14

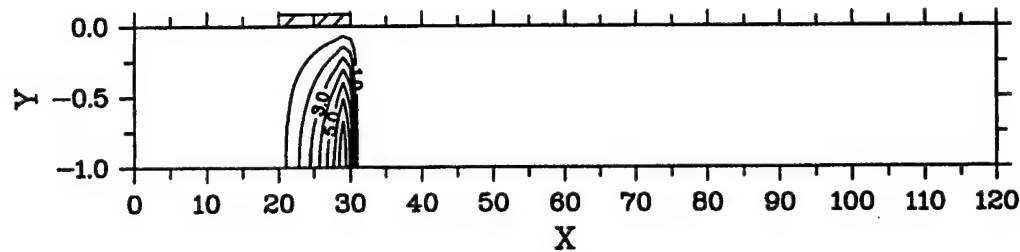
Moving Load.

Pore pressure

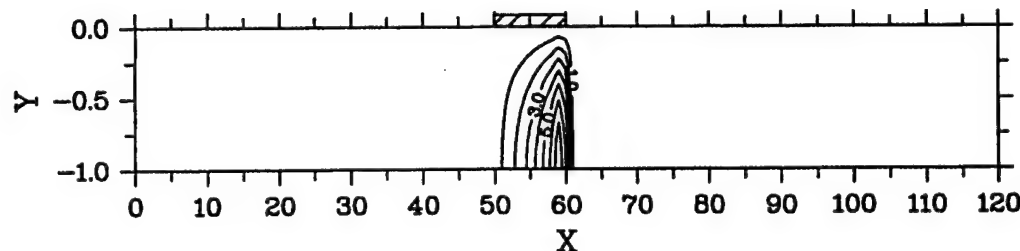
$$K = 160 \text{ t/m}^2\text{m}, G = 100 \text{ t/m}^2\text{m}, k = 1 \text{ m/day}$$

$$H = 1 \text{ m}, b = 10 \text{ m}, F = 10 \text{ t/m}, v = 120 \text{ m/hour}$$

$$t = 0.0033 \text{ day} = 4.75 \text{ min}$$



$$t = 0.0132 \text{ day} = 19 \text{ min}$$



$$t = 0.0264 \text{ day} = 38 \text{ min}$$

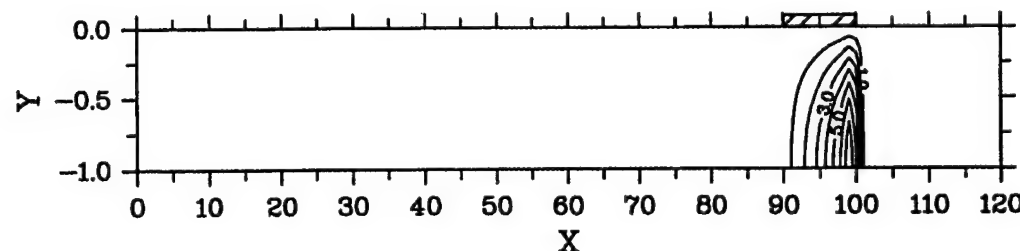


Figure 6.15

Moving Load.

Displacement of the upper boundary, $V=V(x|y=0)$

$K = 160 \text{ t/m}^2, G = 100 \text{ t/m}^2, k = 1 \text{ m/day}$

$H = 1 \text{ m}, b = 10 \text{ m}, F = 10 \text{ t/m}, v = 120 \text{ m/hour}$

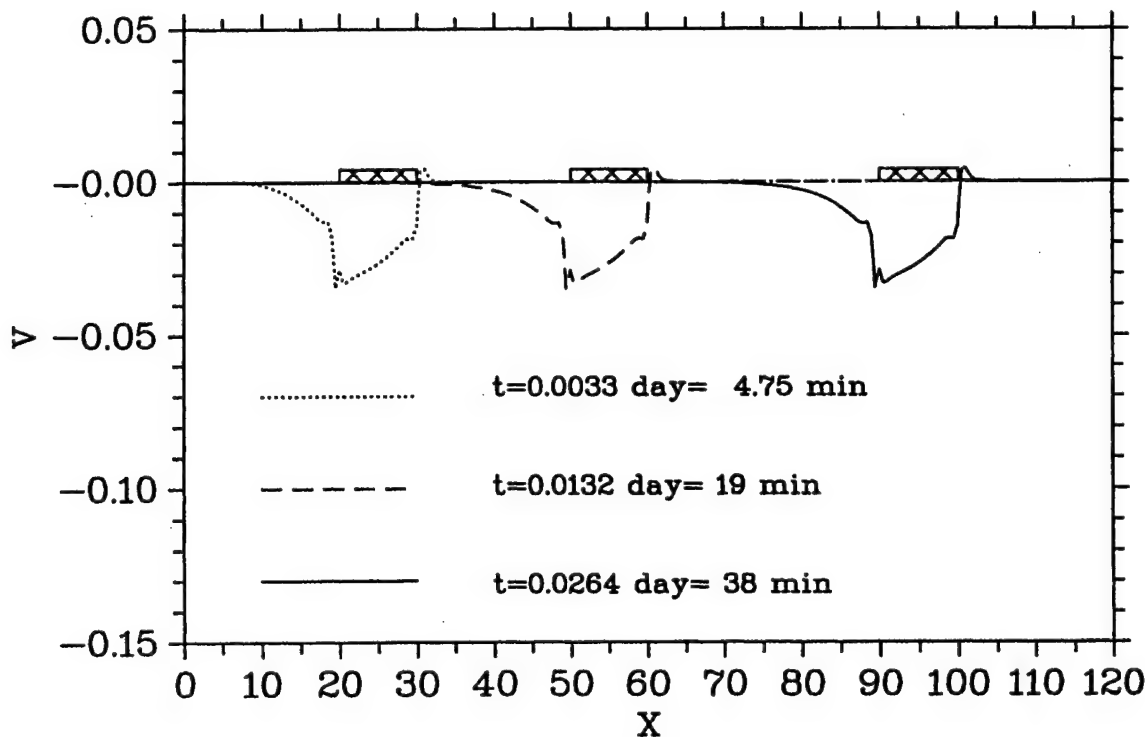


Figure 6.16

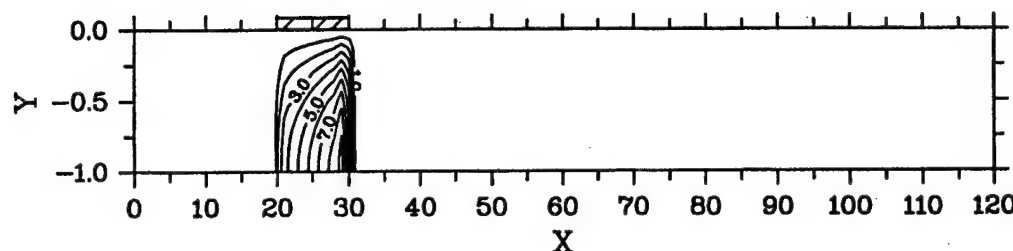
Moving Load.

Pore pressure

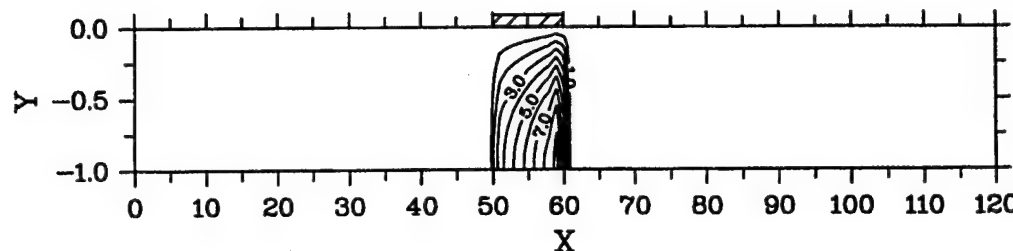
$$K = 160 \text{ t/m}^2\text{m}, G = 100 \text{ t/m}^2\text{m}, k = 1 \text{ m/day}$$

$$H = 1 \text{ m}, b = 10 \text{ m}, F = 10 \text{ t/m}, v = 240 \text{ m/hour}$$

$$t = 0.00165 \text{ day} = 2.37 \text{ min}$$



$$t = 0.0066 \text{ day} = 9.5 \text{ min}$$



$$t = 0.0132 \text{ day} = 19 \text{ min}$$

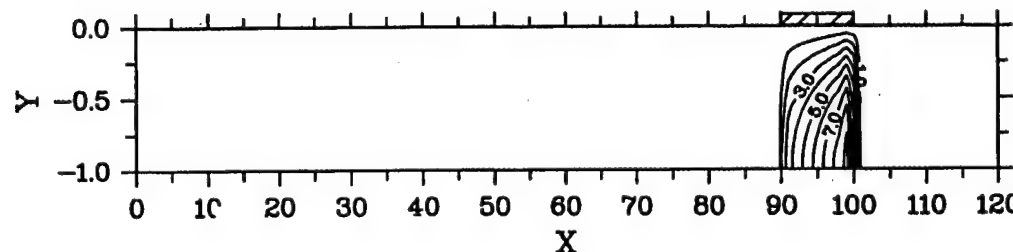


Figure 6.17

Moving Load.

Displacement of the upper boundary, $V=V(x|y=0)$

$$K = 160 \text{ t/m}^2, G = 100 \text{ t/m}^2, k = 1 \text{ m/day}$$

$$H = 1 \text{ m}, b = 10 \text{ m}, F = 10 \text{ t/m}, v = 240 \text{ m/hour}$$

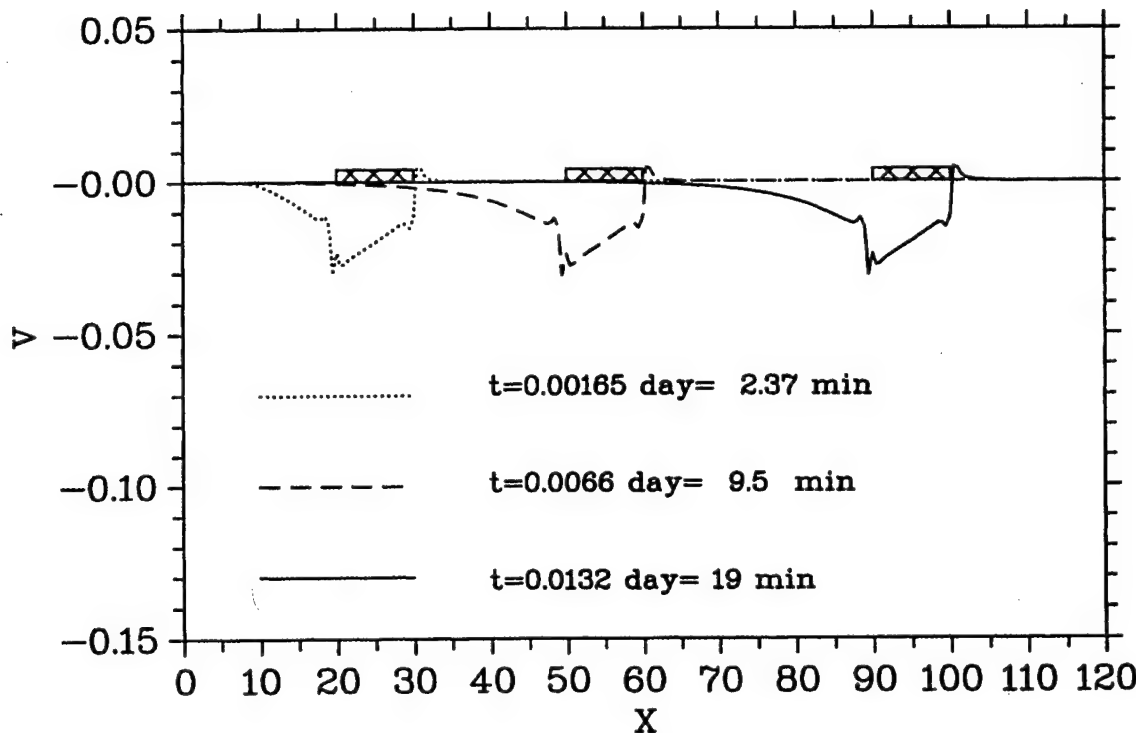


Figure 6.18

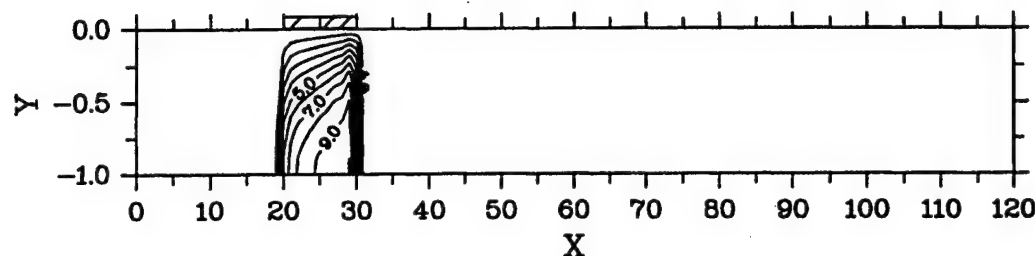
Moving Load.

Pore pressure

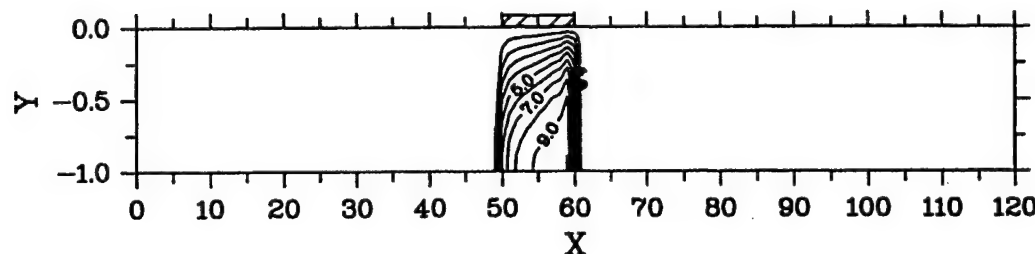
$K = 160 \text{ t/m}^2\text{m}$, $G = 100 \text{ t/m}^2\text{m}$, $k = 1 \text{ m/day}$

$H = 1 \text{ m}$, $b = 10 \text{ m}$, $F = 10 \text{ t/m}$, $v = 600 \text{ m/hour}$

$t = 0.00066 \text{ day} = 0.95 \text{ min}$



$t = 0.00264 \text{ day} = 3.8 \text{ min}$



$t = 0.00528 \text{ day} = 7.6 \text{ min}$

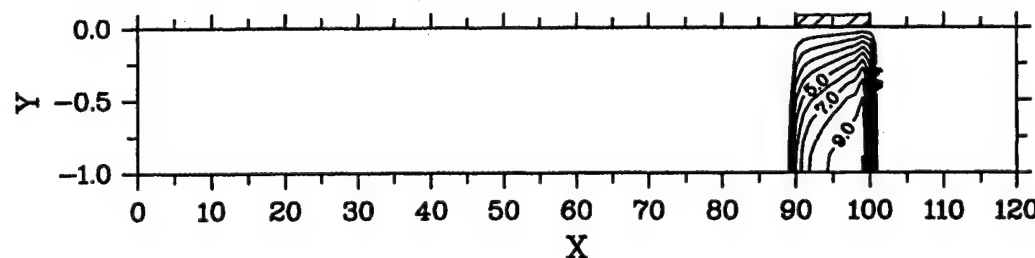


Figure 6.19

Moving Load.

Displacement of the upper boundary, $V=V(x|y=0)$

$$K = 160 \text{ t/m}^2, G = 100 \text{ t/m}^2, k = 1 \text{ m/day}$$

$$H = 1 \text{ m}, b = 10 \text{ m}, F = 10 \text{ t/m}, v = 600 \text{ m/hour}$$

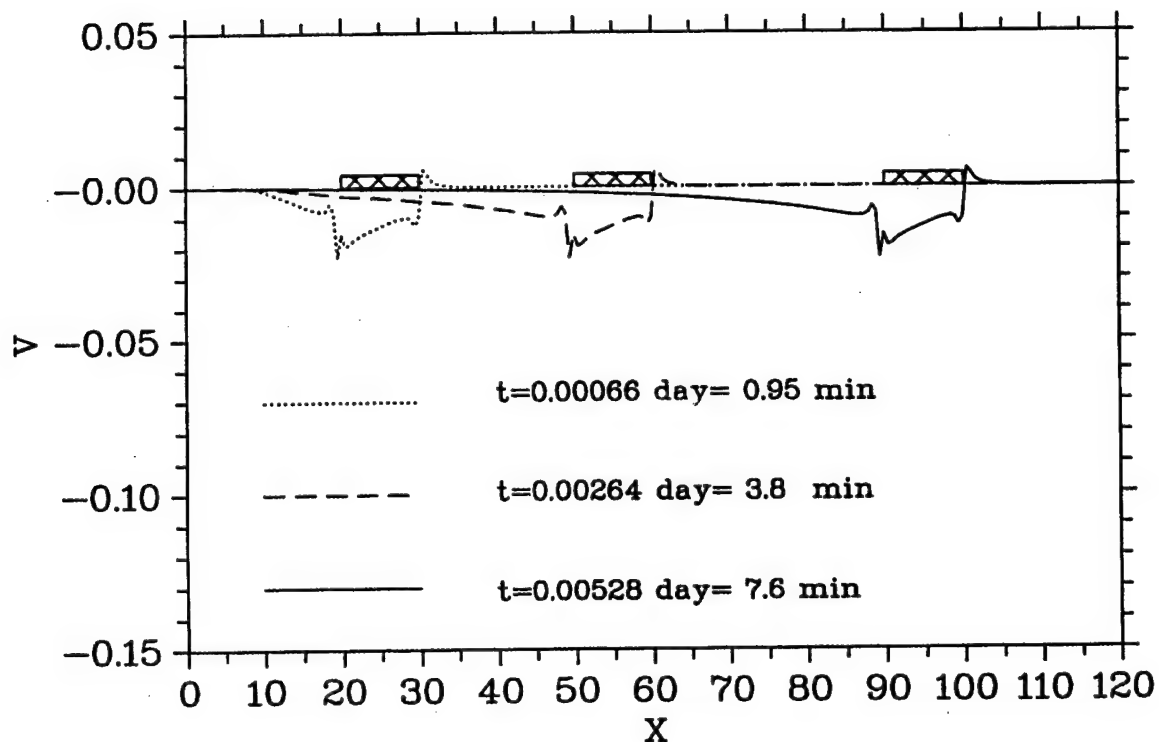


Figure 6.20

Moving Load.

Displacement of the upper boundary, $V=V(x|y=0)$

$$K = 160 \text{ t/m}^2, G = 100 \text{ t/m}^2, k = 1 \text{ m/day}$$

$$H=1 \text{ m}, b=10 \text{ m}, F=10 \text{ t/m}$$

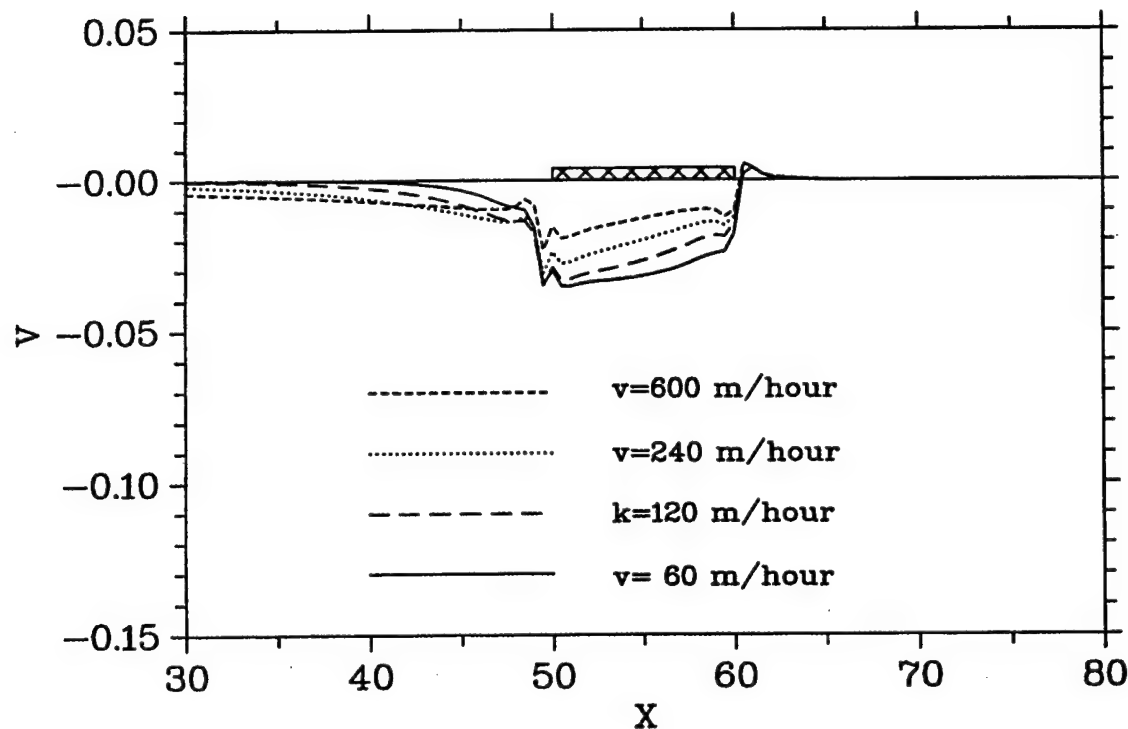


Figure 6.21

Moving Load.
 Dimensionless pore pressure
 $b/H = 10$

Calculated at
 $K = 160 \text{ t/m}^2\text{m}, G = 100 \text{ t/m}^2\text{m}, k = 1 \text{ m/day}$
 $H = 1 \text{ m}, b = 10 \text{ m}, F = 10 \text{ t/m}$

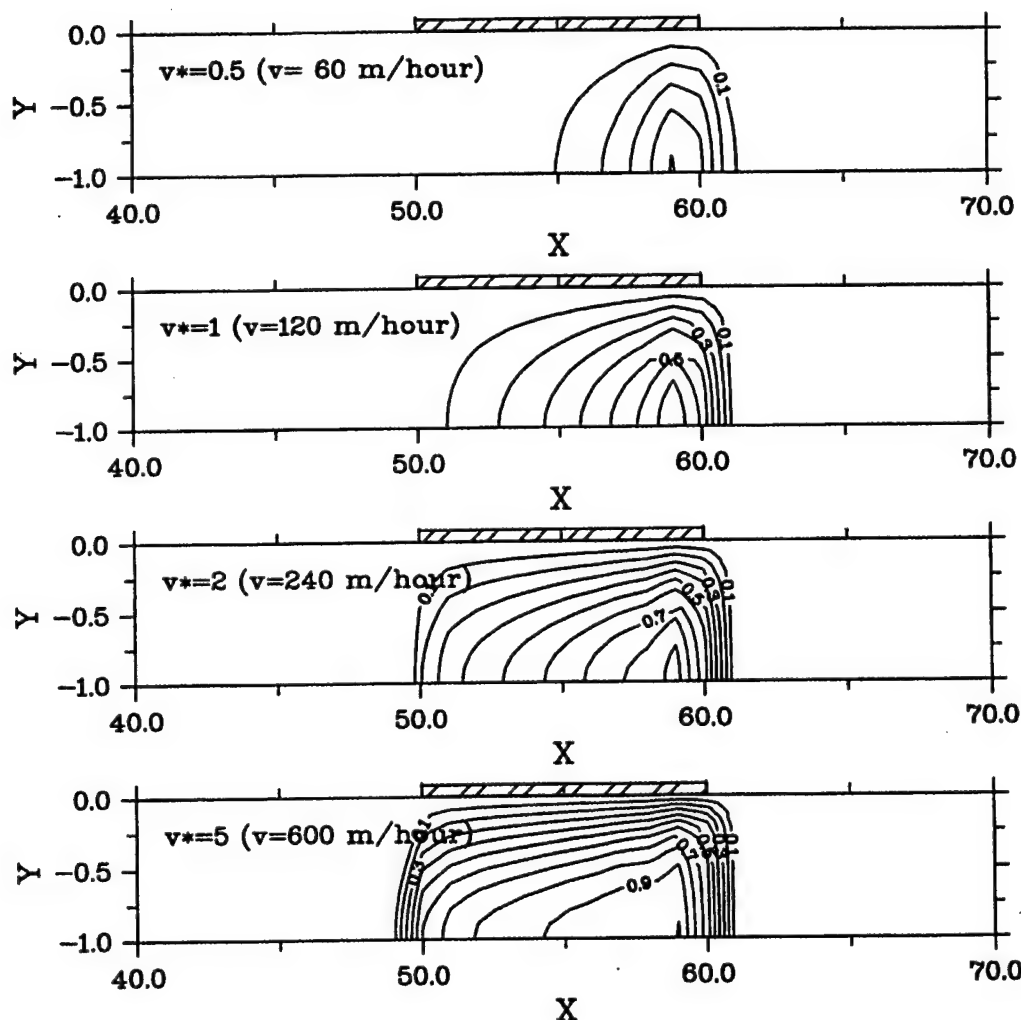


Figure 6.22

Moving Load.

Dimensionless displacement of the upper boundary

$$b/H = 10$$

Calculated at

$$K = 160 \text{ t/m}^* \text{m}, G = 100 \text{ t/m}^* \text{m}, k = 1 \text{ m/day}$$

$$H = 1 \text{ m}, b = 10 \text{ m}, F = 10 \text{ t/m}$$

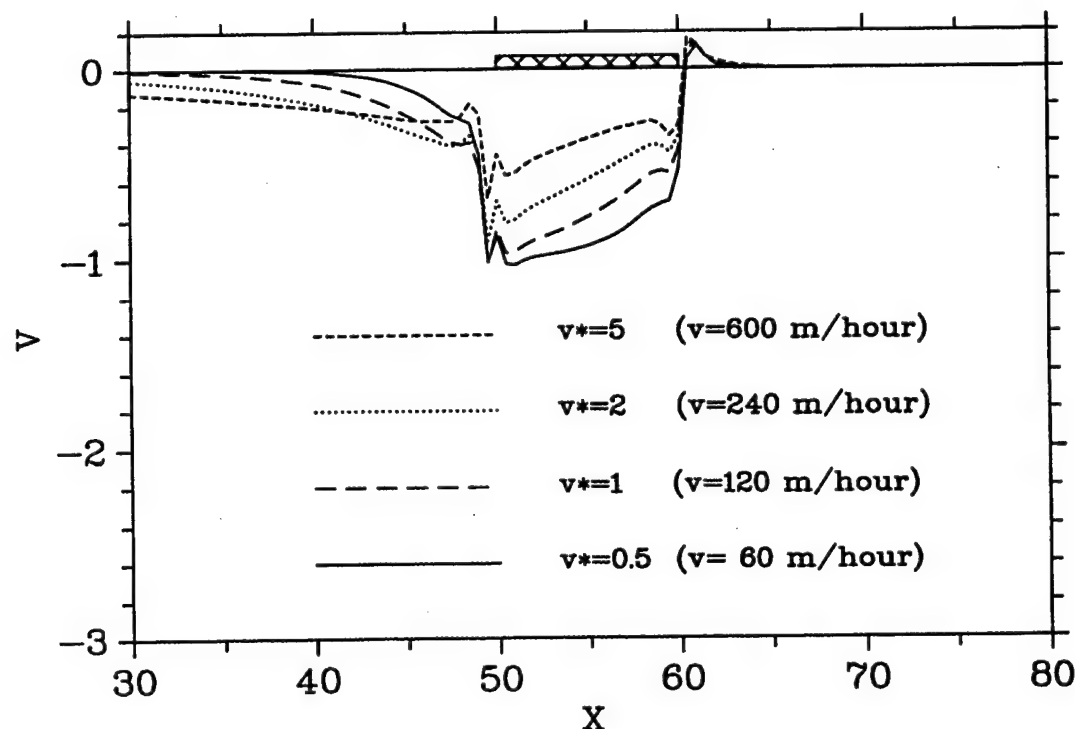


Figure 6.23

Moving Load.
 Dimensionless pore pressure
 $b/H = 5$

Calculated at

$$K = 160 \text{ t/m}^2\text{m}, G = 100 \text{ t/m}^2\text{m}, k = 1 \text{ m/day}$$

$$H = 2 \text{ m}, b = 10 \text{ m}, F = 10 \text{ t/m}$$

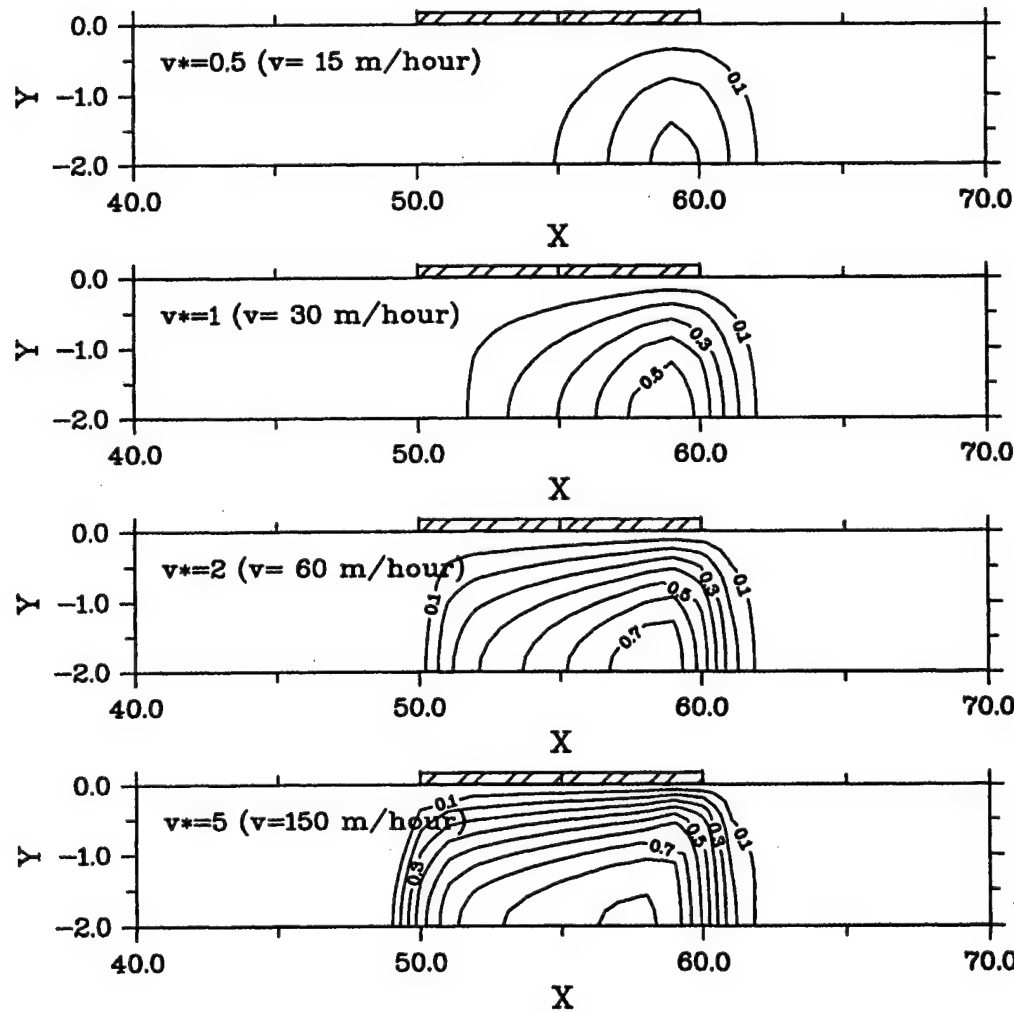


Figure 6.24

Moving Load.

Dimensionless displacement of the upper boundary

$$b/H = 5$$

Calculated at

$$K = 160 \text{ t/m}^2, G = 100 \text{ t/m}^2, k = 1 \text{ m/day}$$

$$H = 2 \text{ m}, b = 10 \text{ m}, F = 10 \text{ t/m}$$

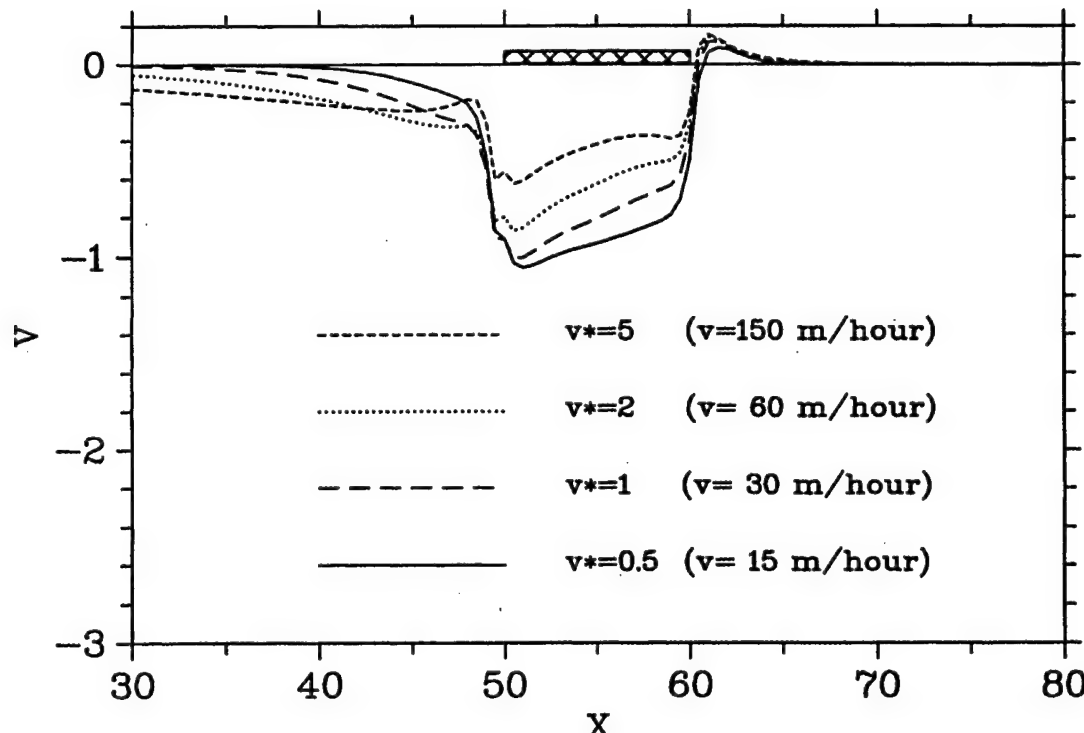


Figure 6.25

Moving Load.

Displacement of the upper boundary, $V=V(x|y=0)$

$$K = 160 \text{ t/m}^2, G = 100 \text{ t/m}^2, k = 1 \text{ m/day}$$

$$H = 1 \text{ m}, b = 10 \text{ m}, F = 10 \text{ t/m}, v = 120 \text{ m/hour}$$

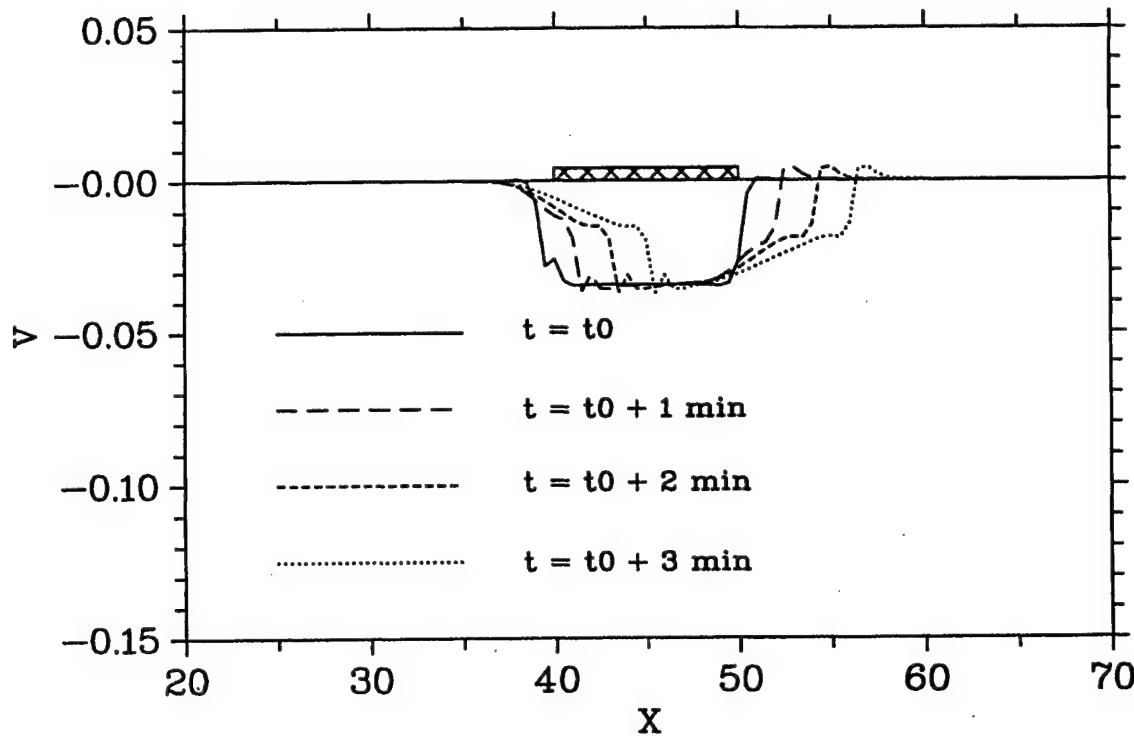


Figure 6.26

Classical Biot Consolidation.
 Strip Load. Drained Loading Surface.
 Deformed grid

(Small strain. The solution is calculated using unmoving grid)

$$\begin{aligned} K &= 160 \text{ t/m*m}, \quad G = 100 \text{ t/m*m}, \quad k = 0.01 \text{ m/day} \\ H &= 10 \text{ m}, \quad L = 50 \text{ m}, \quad b = 10 \text{ m}, \quad F = 100 \text{ t/m} \end{aligned}$$

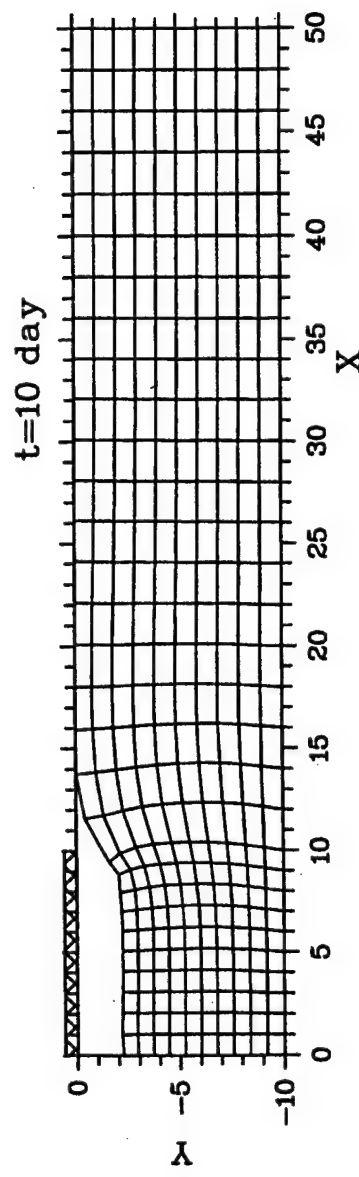


Figure 6.27

Classical Biot Consolidation.
 Strip Load. Drained Loading Surface.
 Deformed grid

(Small strain. The solution is calculated using moving grid)

$$K=160 \text{ t/m}^2\text{m}, \quad G=100 \text{ t/m}^2\text{m}, \quad k=0.01 \text{ m/day}$$

$$H=10 \text{ m}, \quad L=50 \text{ m}, \quad b=10 \text{ m}, \quad F=100 \text{ t/m}$$

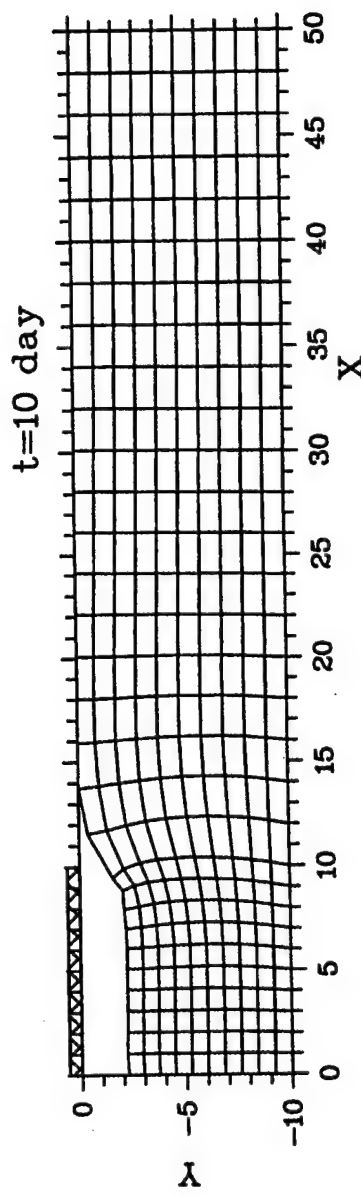


Figure 6.28

Consolidation and Viscoelasticity.
 Strip Load. Drained Loading Surface.
 Deformed grid

(Small strain. The solution is calculated using unmoving grid)

$$K=160 \text{ t/m}^2\text{m}, G=100 \text{ t/m}^2\text{m}, \eta=3000 \text{ t/m}^2\text{day}, k=0.01 \text{ m/day}$$

$$H=10 \text{ m}, L=50\text{m}, b=10\text{m}, F=100 \text{ t/m}$$

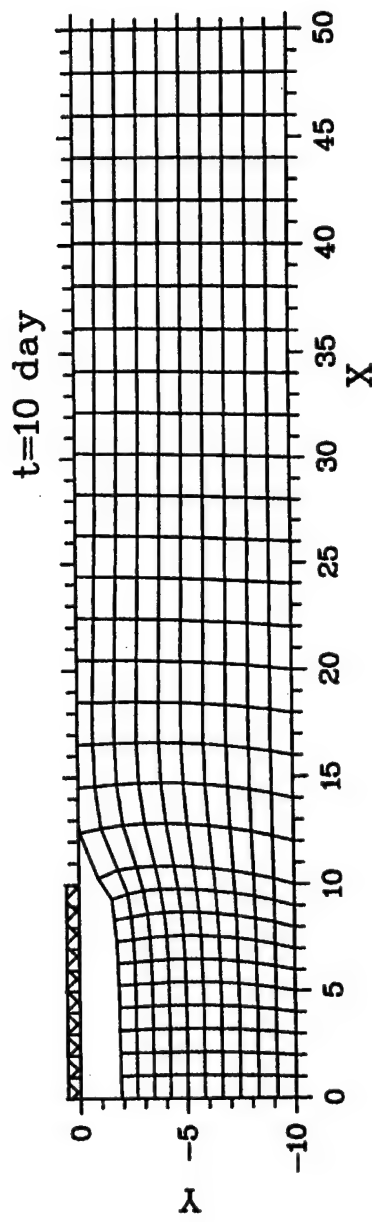


Figure 6.29

Consolidation and Viscoelasticity.
 Strip Load. Drained Loading Surface.
 Deformed grid

(Small strain. The solution is calculated using moving grid)

$K=160 \text{ t/m}^2\text{m}, G=100 \text{ t/m}^2\text{m}, \eta=3000 \text{ t/m}^2\text{day}, k=0.01 \text{ m/day}$

$H=10 \text{ m}, L=50\text{m}, b=10\text{m}, F=100 \text{ t/m}$

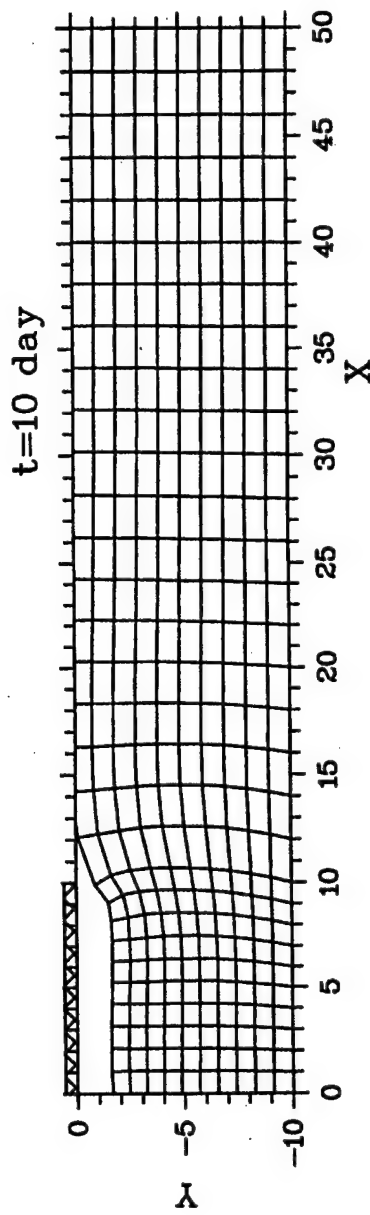


Figure 6.30

Settlement of the central point vs. time
for classical Biot and viscoelastic
consolidation models

$K=160 \text{ t/m}^2\text{m}, G=100 \text{ t/m}^2\text{m}, k=0.01 \text{ m/day}$

$H=10 \text{ m}, L=50 \text{ m}, b=10 \text{ m}, F=100 \text{ t/m}$

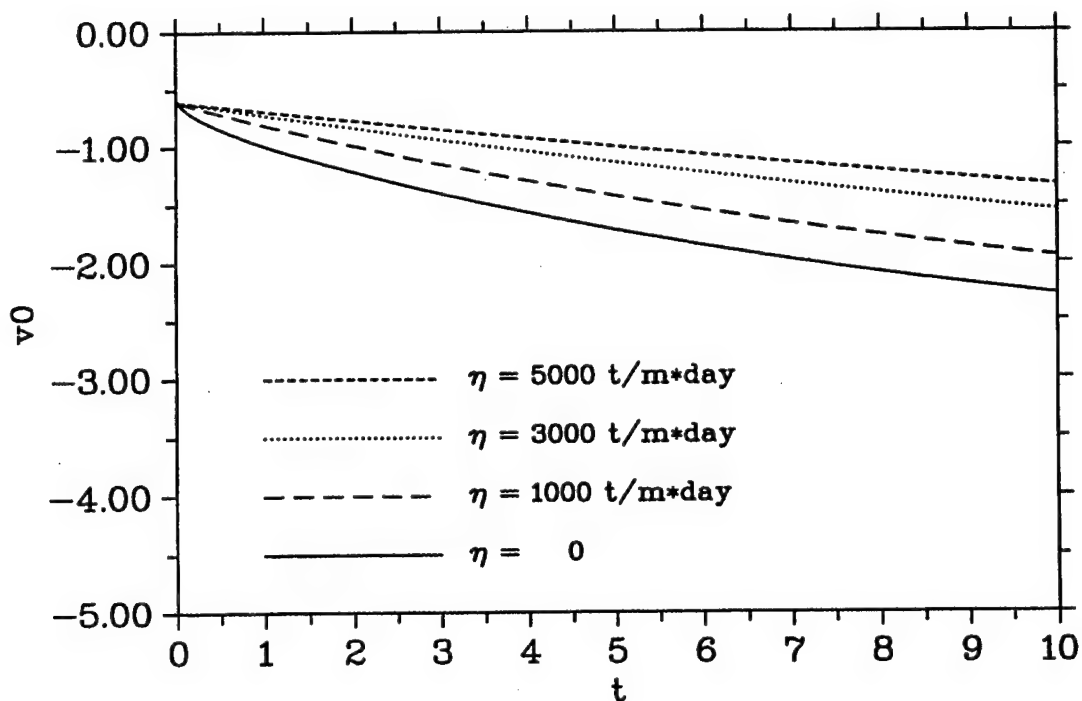


Figure 6.31

VI. Students partially supported by this work

- 1) Robert Smits
- 2) Guliermo
- 3) Bill Stroud
- 4) Joseph Kleyn

VII. Publications and Presentations

Papers that have already appeared are given in appendices 1-4. Additionally there are five papers under review which have been outline in sections I-V above. Approximately 8 seminars on the topic of this report have been presented at various national and international meetings. In addition, several lectures have been presented at various universities around the world.

Langmuir

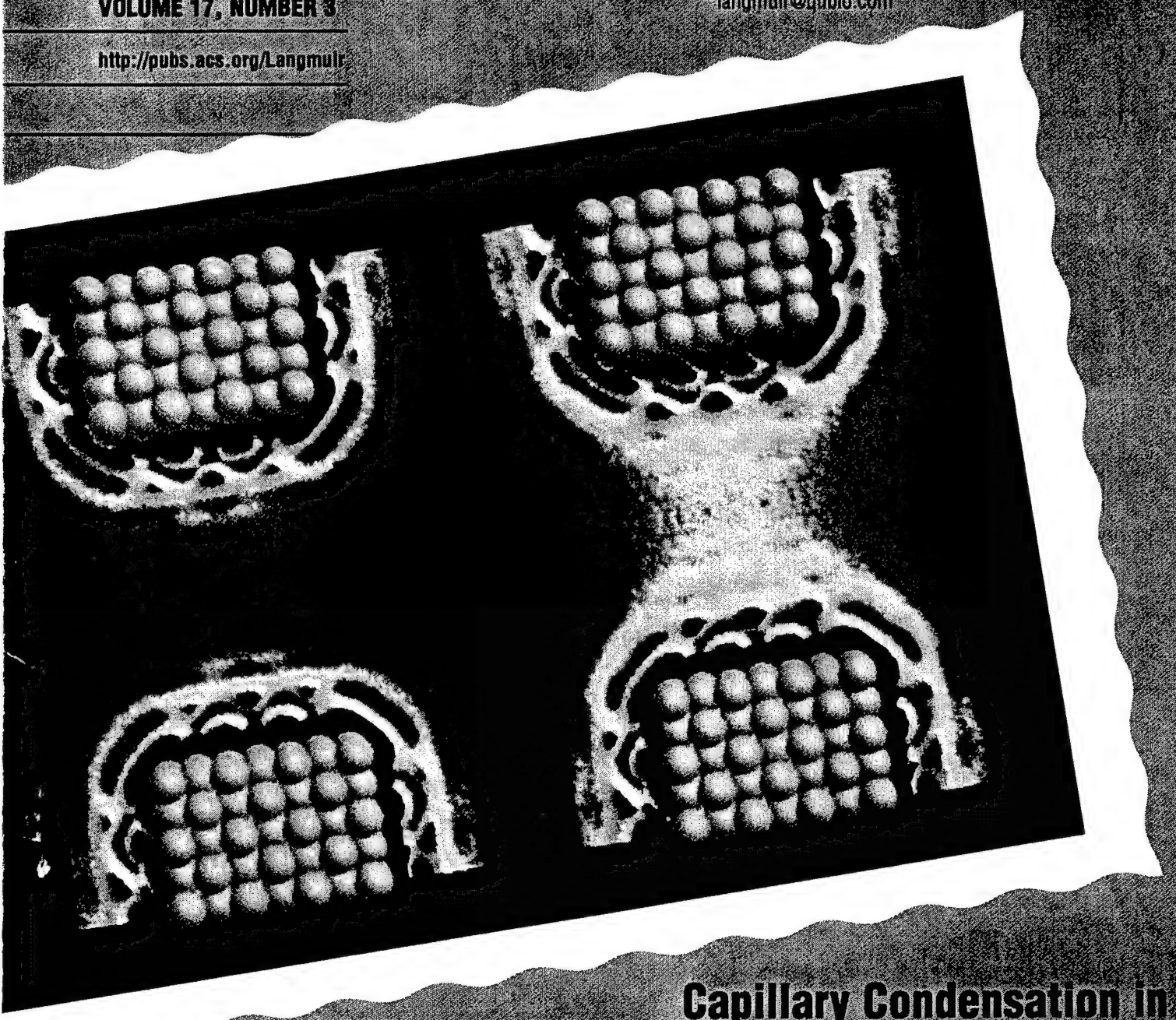
The ACS Journal of Surfaces and Colloids

FEBRUARY 6, 2001

VOLUME 17, NUMBER 3

<http://pubs.acs.org/Langmuir>

NOTICE: The new address for Dr. Whitten is
LANGMUIR, QTL Biosystems, LLC, 1322
Paseo De Peralta, Santa Fe, NM 87501
langmuir@qtlbio.com



Capillary Condensation in
Nanoscale Contacts (see p. 683)

Capillary Condensation and Snap-off in Nanoscale Contacts

William J. Stroud,[‡] Joan E. Curry,^{*,§} and John H. Cushman[‡]

*Center for Applied Mathematics, Purdue University, West Lafayette, Indiana 47907, and
Department of Soil, Water and Environmental Science, University of Arizona,
Tucson, Arizona 85721*

Received September 12, 2000. In Final Form: November 1, 2000

When a surface is placed in a vapor, several layers of molecules may adsorb depending on the intermolecular forces involved. As two such surfaces are brought together, a critical point is reached at which the gas condenses between the surfaces, forming a capillary across the gap. A cohesive force is associated with the condensed bridge. The reverse process wherein the capillary bridge degenerates as the surfaces are moved apart is called snap-off. These processes play a profound role on scales from the nano to the macro. We have studied this phenomenon via isostrain grand canonical Monte Carlo statistical mechanical simulations for Lennard-Jones fluids. Specifically, we have examined capillary condensation and snap-off between nanocontacts, infinite rectilinear nanowires, and finite rectilinear nanoplatelets, where macroscale concepts and theories are just about impossible to apply. These results are compared to condensation between infinite parallel plates. We discuss our results in terms of the Kelvin equation and van der Waals film-thickening model.

Introduction

Unless very special precautions are taken, even carefully prepared surfaces are not clean; they are covered with a thin layer of molecules such as water and other contaminants adsorbed from the atmosphere. When a critical distance separates two such surfaces, a liquid bridge spontaneously condenses across the gap. A cohesive force that tends to pull the surfaces together is associated with the condensed bridge.

Capillary condensation of water around surface contact sites (e.g., in cracks and pores) can have a profound effect on the strength of adhesion joints. The mechanical and adhesive properties of many substances are very sensitive to the presence of even trace amounts of vapors in the atmosphere.¹ For instance, in soils, concrete, and porous media in general, capillary forces can cause deformation of the solid phase, shrinkage, and cracking.² In granular materials it has been proposed that thermal activation of capillary condensed bridges between nanoscale interstices on the rough particles is related to the observed increase in static friction between different layers of the granular system with time.³

On the nanoscale, capillary forces are important in atomic force microscopy (AFM). When scanning hydrophilic samples under ambient conditions with AFM, the water meniscus between the tip and the sample formed by capillary condensation predominantly governs the force exerted by the tip of the microscope onto the sample. This makes it difficult to image soft samples in humid conditions. Working under very dry conditions will improve

the performance of the tips, but electrostatic charging of tip and sample can then be a problem.⁴ However, capillary condensation is not always a disadvantage; it was recently shown that it is possible to deposit silicate nanostructures on a silicon surface by oxidizing the silicon in the capillary condensed bridge between the AFM tip and the sample.⁵

Despite its importance in emerging nanotechnology applications, capillary condensation is still not well understood. Fundamentally, capillary condensation is a vapor–liquid transition shifted as a result of symmetry breaking. The Laplace pressure across the curved meniscus acts to pull the surfaces together. The relationship between the equilibrium meniscus curvature and the relative vapor pressure is described classically by the Kelvin equation

$$k_B T \ln\left(\frac{p}{p^*}\right) = \gamma V_m \left(\frac{1}{R_1} + \frac{1}{R_2} \right)$$

where γ is the surface energy of the liquid–vapor interface, p/p^* is the relative vapor pressure, V_m is the molar volume, k_B is the Boltzmann constant, T is the temperature, and R_1 and R_2 are the radii of curvature of the liquid–vapor interface. Practically, the Kelvin equation is routinely employed to predict pore size distributions in porous media, but it is known to be inadequate for nanoscale pores.⁶ In nanoscale devices we can envision menisci radii on the order of nanometers. Accordingly, it is important to understand the validity and applicability of the Kelvin equation for nanoscale capillary condensates. Much work has been done to determine the limits of applicability of the Kelvin equation.^{7–17} It appears that even though it is

* To whom correspondence should be addressed. E-mail: curry@ag.arizona.edu.

[†] Purdue University.

[‡] University of Arizona.

(1) Israelachvili, J. N. *Intermolecular and Surface Forces*, 2nd ed.; Academic Press: San Diego, 1992.

(2) Bentz, D. P.; Quenard, D. A.; Baroghel-Bouny, V.; Garboczi, E. J.; Jennings, H. M. *Mater. Struct.* 1995, 28, 450.

(3) Bocquet, L.; Charlaix, E.; Ciliberto, S.; Crassous, J. *Nature* 1998, 396, 735.

(4) Knapp, H. F.; Stemmer, A. *Surf. Interface Anal.* 1999, 27, 324.

(5) Garcia, R.; Calleja, M.; Rohrer, H. J. *Appl. Phys.* 1999, 86, 1898.

(6) Seaton, N. A.; Walton, J. P. R. B.; Quirke, N. *Carbon* 1989, 27, 853.

(7) Christenson, H. K.; Fang, J.; Israelachvili, J. N. *Phys. Rev. B* 1989, 39, 11750.

(8) Christenson, H. K. *J. Colloid Interface Sci.* 1985, 104, 234.

(9) Fisher, L. R.; Israelachvili, J. N. *J. Colloid Interface Sci.* 1981, 80, 528.

based on macroscale thermodynamic parameters, it is valid for very small menisci. Fischer and Israelachvili⁹ have verified the Kelvin equation for cyclohexane condensed between crossed mica cylinders for radii as small as 4 nm using a surface force apparatus (SFA). More recently, Kohonen and Christenson¹⁶ used the SFA to verify the Kelvin equation for water capillary condensates with radii as small as 5 nm. In an attempt to verify the Kelvin equation using computer simulation, Peterson and Gubbins¹⁷ concluded that the Kelvin equation overestimates the bulk vapor pressure for any reasonable choice of the meniscus radius of curvature for a cylindrical pore with radius five times the fluid diameter. However, the vapor pressure calculated from density functional theory agreed better with the Kelvin equation prediction. Miyahara¹⁵ simulated a N₂-like Lennard-Jones fluid in cylindrical pores with diameters from 2 to 4 nm and found agreement between their molecular dynamics simulations and a modified Kelvin equation that incorporates the influence of the surfaces as well as curvature effects on surface tension. It is expected that molecular scale effects will invalidate the Kelvin equation for nanoscale menisci.

In general capillary condensation has been studied for many years via experiments,^{7–9,18} theory,^{11,19–20} and computer simulations.^{21–22} In a series of studies, Gubbins and co-workers^{12,17,23} studied pore filling and emptying by incrementing the chemical potential, keeping the pore dimensions constant. Below a capillary critical point they observed hysteresis on both adsorption and desorption although hysteresis on desorption was later attributed to the neglect of pore end effects in the infinite pore models.²⁴ Gac et al.²⁵ showed that pore wall surface energy heterogeneity causes differences in adsorption compared to that on homogeneous surfaces.

In most capillary condensation simulation studies to date the pore consists of either two infinite parallel plates or an infinite cylinder with smooth (no atomic structure) walls. With these types of systems a meniscus can only be produced with canonical molecular dynamics simulations; therefore, few simulations have studied meniscus formation directly despite the effect on desorption hysteresis. Heffelfinger and co-workers used molecular dynamics to create menisci in infinite pores first with a temperature quench¹² and then by changing the pore length while keeping the number of particles fixed.²³ Variations in the attractiveness of the walls have also been used to create a meniscus. The simulation cell is divided so that the middle of the pore represents a pore with finite length in one dimension and the ends of the

cell are the reservoirs. Papadopoulou et al.²⁴ took the walls bounding the reservoirs to be purely repulsive while Miyahara et al.¹⁵ employed a potential buffering field at both ends of the pore that vanished linearly. No simulation has included the edges of the particles explicitly. Additionally, most studies have focused on adsorption and capillary condensation in pores of fixed width as a function of bulk vapor pressure; however, in SFA studies, where direct comparison may be possible, the surface separation is varied at constant chemical potential. The dimensions of the contact area must also be important, and indeed in recent AFM studies with carbon nanotube tips capillary condensation only had a minimal influence on the measurements.²⁶ To our knowledge simulations have not been used to study the formation and snap-off of a capillary condensate between nanoscale contacts where the size of the contact area is important.

With these motivations we have used Monte Carlo computer simulations in the isostrain Grand canonical ensemble to study capillary condensation between finite structured nanowires and nanoplatelets. We find that as the dimensions of the nanocontacts decrease, the surface separation that can support a liquid condensate decreases. We find that capillary condensation is preceded by accumulation of a dense vapor between the surfaces. The menisci in these nanoscale contacts are diffuse, and snap-off occurs as a gradual decrease in liquid density across the gap rather than a sudden disappearance of the condensate as the gap width gets larger.

Model. The simulation model consists of a Lennard-Jones gas in equilibrium with two surfaces constructed from the 100 plane of a face-centered cubic lattice that are parallel to one another and perpendicular to the z-axis. Fluid and wall atoms are identical, spherical, nonpolar, Lennard-Jones (LJ) atoms with mass taken to be that of argon characterized by diameter σ and interaction energy ϵ . To take into account interaction beyond the first layer of surface atoms, each surface is comprised of five layers of atoms. Figure 1 shows atomic representations of the three surface models employed. Nanoplatelets that are finite in both the x and y directions are shown in the upper panel. The nanoplatelet surfaces are square with the x and y dimensions being $3l$ and $5l$ or, as shown in the figure, $10l$ where l is the length of a unit cell, taken to be 1.5985σ . The simulation cell includes the platelets and the space both between and outside the platelets, and is outlined by solid white lines. The region outside the platelets extends $5l$ from the surface edges in the x and y directions. Periodic boundary conditions are applied in all directions in order to simulate an infinite system. The middle panel shows the infinite rectilinear nanowires that are finite in the x direction but effectively infinite in the y direction. In the x direction the simulation cell consists of surfaces $3l$, $5l$, or $10l$ in width bounded by $5l$ regions on either side. The width of the cell in the y direction is $5l$, and periodic boundary conditions are applied to simulate the infinite wire. The infinite slit pore, which has been studied extensively for the past 20 years,²⁷ is shown in the lower panel. The length of the sides of the simulation cell is $5l$. Periodic boundary conditions are employed in the x and y directions to model the infinite slit pore.

The total potential energy of the confined fluid is approximated as a pairwise sum of shifted force Lennard-

- (10) Crassous, J.; Charlaix, E.; Gayvallet, H.; Loubet, J. *Langmuir* **1993**, *9*, 1995.
- (11) Derjaguin, B. V.; Churaev, N. V. *J. Colloid Interface Sci.* **1976**, *54*, 157.
- (12) Heffelfinger, G. S.; Van Swol, F.; Gubbins, K. E. *Mol. Phys.* **1987**, *61*, 1381.
- (13) Marconi, U. M. B.; Van Swol, F. *Phys. Rev. A* **1989**, *39*, 4109.
- (14) Luedtke, W. D.; Landman, U. *Comput. Mater. Sci.* **1992**, *1*, 1.
- (15) Miyahara, M.; Kanda, H.; Yoshioka, T.; Okazaki, M. *Langmuir* **2000**, *16*, 4293.
- (16) Kohonen, M. M.; Christenson, H. K. *Langmuir*, in press.
- (17) Peterson, B. K.; Gubbins, K. E. *Mol. Phys.* **1987**, *62*, 215.
- (18) Curry, J. E.; Christenson, H. K. *Langmuir* **1996**, *12*, 5729.
- (19) Evans, R.; Tarazona, P. *Phys. Rev. Lett.* **1984**, *52*, 557.
- (20) Evans, R.; Marconi, U. M. B. *Chem. Phys. Lett.* **1985**, *114*, 415.
- (21) Lane, J. E.; Spurling, T. H. *Aust. J. Chem.* **1980**, *33*, 231.
- (22) Van Megen, W.; Snook, I. K. *Mol. Phys.* **1985**, *54*, 741.
- (23) Heffelfinger, G. S.; Van Swol, F.; Gubbins, K. E. *J. Chem. Phys.* **1988**, *89*, 5202.
- (24) Papadopoulou, A.; Van Swol, F.; Marconi, U. M. B. *J. Chem. Phys.* **1992**, *97*, 6942.
- (25) Gac, W.; Patrykiejew, A.; Sokolowski, S. *Surf. Sci.* **1994**, *306*, 434.

(26) Woolley, A. T.; Guillemette, C.; Cheung, C. L.; Housman, D. E.; Lieber, C. M. *Nature Biotechnol.* **2000**, *18*, 760.

(27) Schoen, M.; Diestler, D. J.; Cushman, J. H. *J. Chem. Phys.* **1987**, *87*, 5464.

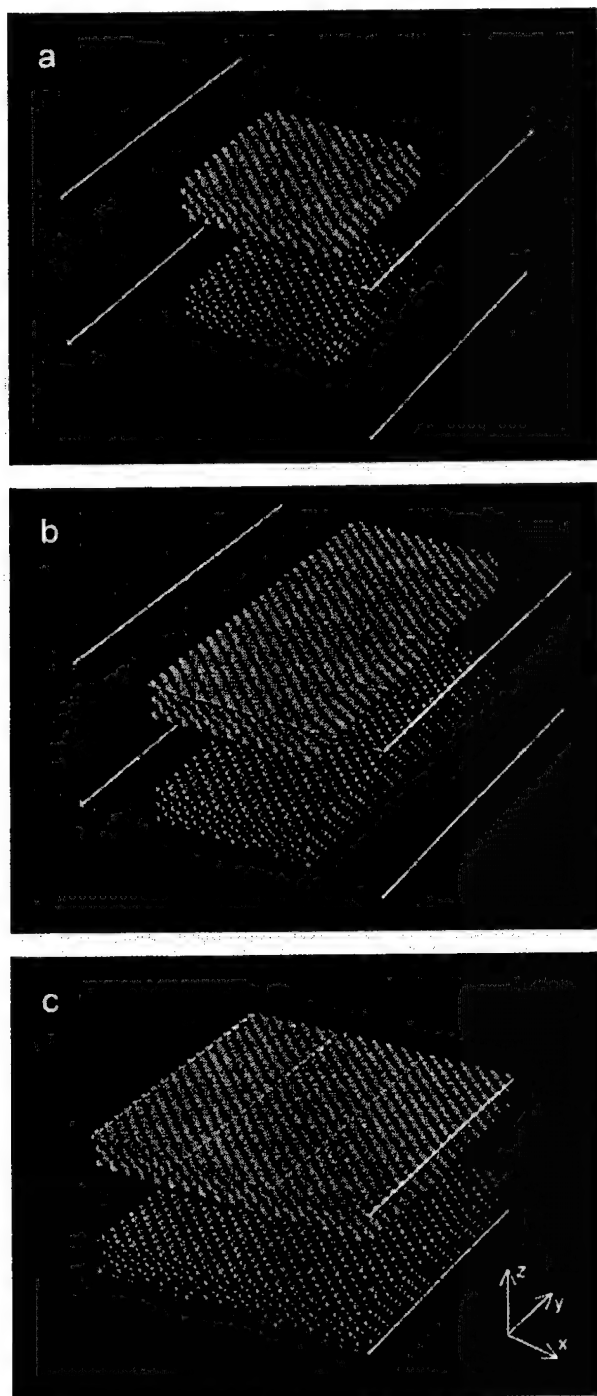


Figure 1. Schematic of the (a) nanoplatelet, (b) nanowire, and (c) infinite slit pore systems. The solid atoms are shown as spheres, and the solid white lines outline the simulation cell. The infinite slit pore is finite in the z direction only, the nanowires are finite in both the x and z directions, and the platelets are finite in all directions.

Jones (12,6) interactions with radial cutoff $r_c = 4.0\sigma$.²⁸ The interaction energy between atoms i and j is

$$U_{SF}(r_{ij}) = 4\epsilon \left[\left(\frac{\sigma}{r_{ij}} \right)^{12} - \left(\frac{\sigma}{r_{ij}} \right)^6 - U(r_c) - U'(r_c)(r_{ij} - r_c) \right] \quad (1)$$

Table 1. Reduced Units

$$\begin{aligned} h^* &= h/\sigma \\ T^* &= kT/\epsilon \\ \mu^* &= \mu/\epsilon \\ \rho^* &= \rho\sigma^3 \end{aligned}$$

for $r < r_c$ and 0 otherwise. $U(r)$ is the usual full Lennard-Jones potential. Reduced dimensionless variables, defined in terms of the Lennard-Jones well depth ϵ and "diameter" σ , where $\epsilon/k_B = 119.8$ K and $\sigma = 3.405$ Å, are used throughout (see Table 1).

The distance between the pore walls, h , is measured from the center of the surface layer of wall atoms. The relative lateral alignment of the walls, or registry, in the x and y directions must be specified to uniquely define the system. The coordinates of the wall atoms are related as follows: $x_i^{(2)} = x_i^{(1)}$; $y_i^{(2)} = y_i^{(1)}$; $z_i^{(2)} = z_i^{(1)} + h$, where the superscripts (1) and (2) refer to the lower and upper walls, respectively.

Structural features are presented in terms of a local density, $\rho(x,y,z)$, which is calculated as

$$\rho(x,y,z) = \langle N(x,y,z) \rangle / \Delta x \Delta y \Delta z \quad (2)$$

where $\langle N(x,y,z) \rangle$ is the mean number of fluid atoms in a cell of size $\Delta x \Delta y \Delta z$ centered on x, y, z . Here x and z run over the entire computational cell and y is either 0 for the midplane or 0.5 for the midplane shifted by $0.5l$. For these simulations $\Delta x = \Delta y = \Delta z = \sigma/20$.

Bulk simulations are also conducted for this Lennard-Jones fluid in order to construct an adsorption isotherm so that the chemical potential corresponding to the gas-liquid transition can be identified. The chemical potential is chosen so that the bulk fluid is in the vapor phase for all simulations.

A standard grand canonical Monte Carlo simulation scheme is used.^{27,28} The number of equilibration steps is approximately 10^6 , and the number of production steps is greater than 60 000 times the average number of atoms in the simulation. The simulations at each pore width are independent in that each simulation begins with no atoms in the cell. With this approach, metastable states are avoided.

Results

While Lennard-Jones fluids have a very elementary potential (van der Waals attraction and Born repulsion), they exhibit incredibly complex and anomalous behavior when confined in at least one dimension at the molecular scale.²⁹ Among these unusual behaviors are order-disorder transitions, second-order liquid-solid phase changes in monolayers confined to slit pores, stick-slip phenomena, layered structuring, destruction/formation of nanocapillaries as a function of shear strain, anomalous (fractal) diffusion in monolayers, and strain-induced liquefaction.

Though the potential is mathematically simple, computationally it presents considerable numerical difficulties, especially near critical points. Specifically, when using Monte Carlo simulators, the realized Markov chain is often nonergodic on any reasonable computational time frame. This is illustrated by the bulk adsorption isotherm shown as the squares in Figure 2. For comparison the adsorption isotherm for a fluid in an infinite pore at $h^* = 4.8$ is also plotted as circles. When moving to the right on the phase diagram (as a function of increasing chemical potential),

(28) Allen, M. P.; Tildesley, D. J. *Computer Simulation of Liquids*; Clarendon: Oxford, 1987.

(29) Cushman, J. H. *The Physics of Hierarchical Porous Media: Angstroms to Miles*; Kluwer: New York, 1997.

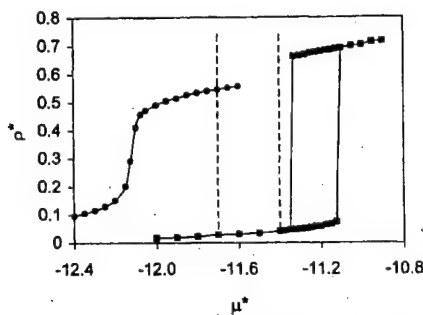


Figure 2. Adsorption isotherm at $T^* = 1.0$, $h^* = 4.8$, and registration $\alpha = 0.0$ for an infinite slit pore with surfaces five atomic layers thick (●), and the corresponding bulk phase condensation isotherm (■). The chemical potentials used in the simulations are marked as dashed lines on the plot and are clearly outside the bulk phase hysteresis loop.

the bulk gas-liquid transition occurs near $-\mu^* = 11.1$ while, when moving toward the left, it occurs at $-\mu^* = 11.35$. The appearance of the hysteresis loop always manifests near critical points, even though we know the Markov chain underlying the Monte Carlo method is ergodic (in the asymptotic limit) and even though we know from classical statistical mechanics³⁰ that such hysteresis loops cannot exist at equilibrium (except through some mathematical approximations to the true dynamics, such as with the van der Waals approximation, which results in van der Waals loops). Running much longer simulations can reduce this hysteresis loop. It is interesting that when a Lennard-Jones fluid is confined in at least one dimension on a molecular scale, these loops are reduced in size. But in any case, the results to be presented are for a fluid which is well into the gas regime ($-\mu^* = 11.7, 11.4$, marked as dashed lines in Figure 2), outside the computationally induced hysteresis loop for the bulk fluid.

We used computer simulations to investigate the condensation of a Lennard-Jones vapor between infinite parallel plates, nanowires, and nanoplatelets. The structure of a fluid confined between infinite parallel plates has been extensively studied,²⁹ and we will discuss it in comparison to the rectilinear wires and platelets. The fluid structure is most easily discussed in terms of the local density. Consider first liquid condensation between two closely spaced nanowires. Figure 3 shows the local density in the $x-z$ plane at a succession of six interwire separations, $h^* = 3.4, 4.3, 5.0, 5.6, 6.1, 6.3$. This particular wire is 5 unit cells wide and of infinite length perpendicular to the page with $\mu^* = -11.7$. As shown in the scale in the figure, red indicates the highest probability of finding an atom and blue the lowest, except black indicates zero probability. The entire simulation cell is large enough so that at the outer edges in the lateral (x) direction the fluid density is equivalent to that of the bulk vapor. The vapor phase is then in equilibrium with the condensed fluid phase perturbed by the solid. In general, as the interwire spacing is increased, the dimensions of the condensed fluid change. The condensate becomes elongated in the z direction and narrower in the x direction. The condensate eventually disappears for large enough spacing.

In more detail, we have shown panel a corresponding to $h^* = 3.4$ because it displays a characteristic phenomenon typically found when the fluid can epitaxially align with the solid and when h^*, μ^*, T^* , and the relative registry are consistent with the formation of a solid phase. In this particular panel the fluid is essentially frozen into a solid,

commensurate with the fcc structure of the wire. Between the surfaces, fluid can only diffuse in regions that are nonblack; thus, there is essentially no diffusion in the interior. However, near the edges, there is a diffuse cloud around the lattice sites indicating increased mobility, that is, hopping between lattice sites. At this chemical potential two layers of fluid cover the external surfaces of the wires. The layer closest to the solid is well ordered, and the fluid occupies localized lattice sites. The second layer is more diffuse but with the highest density at appropriate lattice sites. Beyond two layers, the system behaves essentially as the bulk. At this surface separation the layering of the fluid on the external surfaces is only slightly disrupted by the presence of the fluid-filled space between the wires. The layering on the external surfaces is essentially continuous, connecting the wires smoothly together.

In panel b, $h^* = 4.3$, a fourth layer between the surfaces is being formed and the fluid is liquidic. The surface layer atoms diffuse into and out of the central layers, and the two central layers of atoms hop very frequently back and forth. The highest probability of finding an atom in either of the two central layers lies at the lateral lattice sites for a single central layer (panel a). In other words, if you took the central layer and spread it in the z direction in panel a, and added roughly the number of atoms in a layer, then you obtain an approximation for panel b. Panel c depicts a completed four-layer system ($h^* = 5.0$) that is again liquid; however, the contact layers are much less mobile than the inner layers. You can see the beginning of the formation of a meniscus on the lateral edges between the wire surfaces, though it is poorly defined. In panel d we see the addition of a fifth layer ($h^* = 5.6$). There is the highest probability of finding atoms on the fcc lattice sights, though the fluid is liquidic. Note that in the central layer only the two most inner lattice sites have a high probability of being occupied. The two outer sites are diffusely occupied. A similar statement can be made about the second inner layer, but in this case the three most central lattice sites are occupied with higher probability than the two outer sites. Panel e ($h^* = 6.1$) shows the beginning of capillary snap-off, that is, when the interior region begins to gasify. The innermost layer has disintegrated, with only the slightest vestiges of the central lattice sites being visible. By panel f ($h^* = 6.3$) snap-off has occurred. Note that the fluid which is centrally located between the two surfaces is gaseous, but with a density slightly higher than that of the bulk phase. Additionally, order in the second layer of fluid remains enhanced by the presence of the gaseous fluid. The second fluid layer becomes as diffuse as the second layer around the outside of the nanowire with further surface separation. The transition between a liquidic state for the inner layer fluid and the gaseous state does not appear to be abrupt, but rather a somewhat gradual change with surface separation. The process is of course reversible.

Figure 4 shows a more detailed view of snap-off and condensate evaporation for interacting nanowires three unit cells wide at $\mu^* = -11.7$ for interwire separations ranging from $h^* = 5.2$ to 5.9 . The wires are connected by a four-layer liquidic condensate at $h^* = 5.2$. As the surfaces are separated, the density decreases and a diffuse fifth layer is added at $h^* = 5.4$. The meniscus curvature is not smooth but rather is a series of steps corresponding to the fluid layers. This is more pronounced for the 3-wire case compared to the 5-wire case in Figure 3 where the meniscus is more smoothly rounded. As the surfaces are further separated, the condensate remains layered, and from $h^* = 5.5$ to 5.9 the central fifth layer gradually evaporates. The vapor density between the surfaces as

(30) Hill, T. L. *An Introduction to Statistical Thermodynamics*; Addison-Wesley: Reading, MA, 1960.

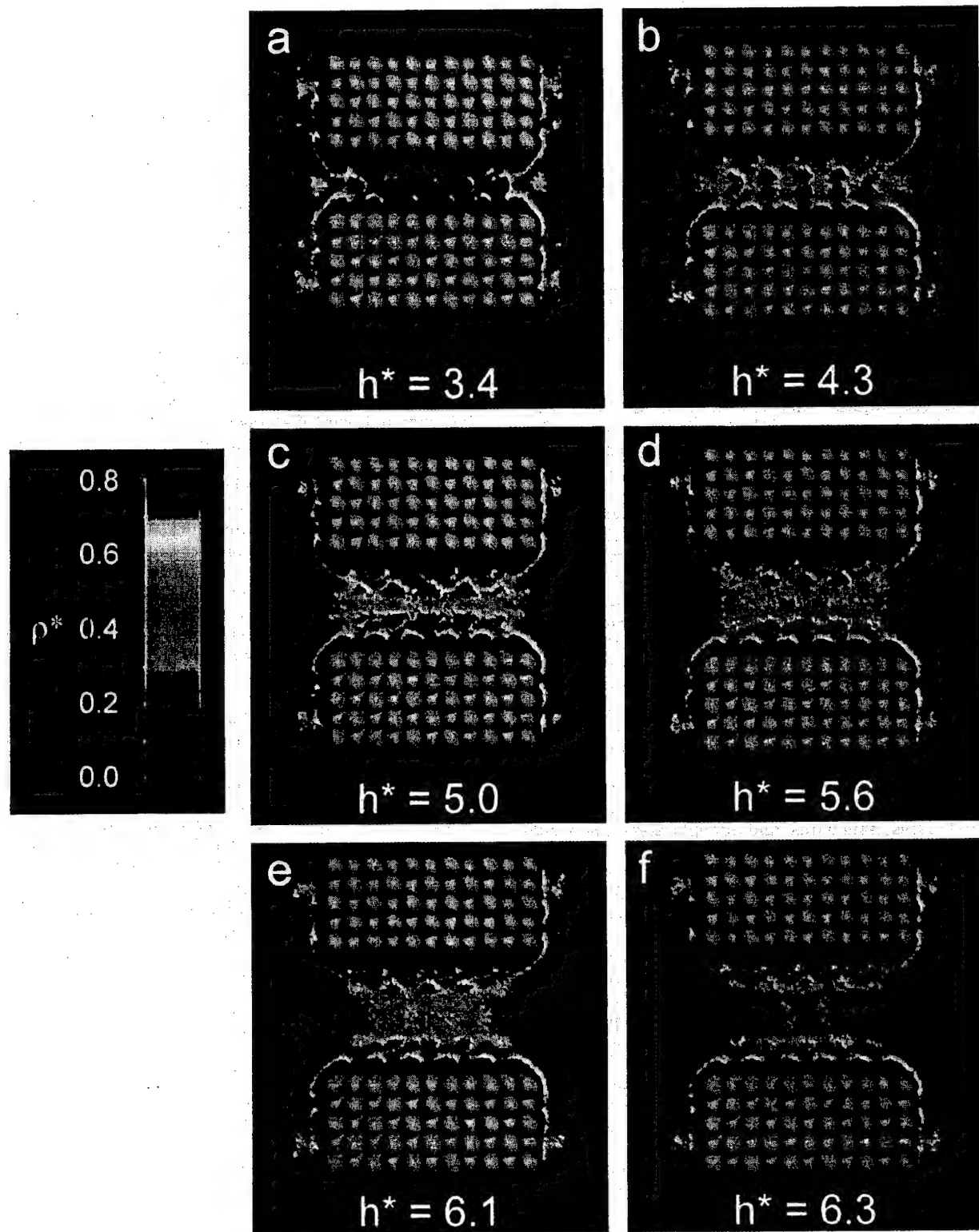


Figure 3. Maps of two-dimensional slices through the three-dimensional, ensemble-averaged particle density in the plane $y = 0$ for $\mu^* = -11.7$, $T^* = 1.0$, $\alpha = 0.0$, and $h^* = 3.4, 4.3, 5.0, 5.6, 6.1$, and 6.3 for the fluid condensed between nanowires five unit cells wide.

well as the density of the second layer of fluid wetting the surfaces remains enhanced even though the liquid condensate is no longer present. Considering the process in reverse, these illustrations also show that as surfaces approach in vapor the vapor density as well as the density of the second layer is enhanced before a fluid condenses between the surfaces.

Figure 5 is similar to Figure 4, except that in Figure 5 the chemical potential is increased to $\mu^* = -11.4$. In this latter case the sequence of panels goes from $h^* = 8.7$ to 9.4 and indicates the increasing size of the capillary condensate with increasing vapor pressure. The fluid is clearly layered within the condensate; for instance, at $h^* = 8.7$ eight fluid layers can be distinguished in the center

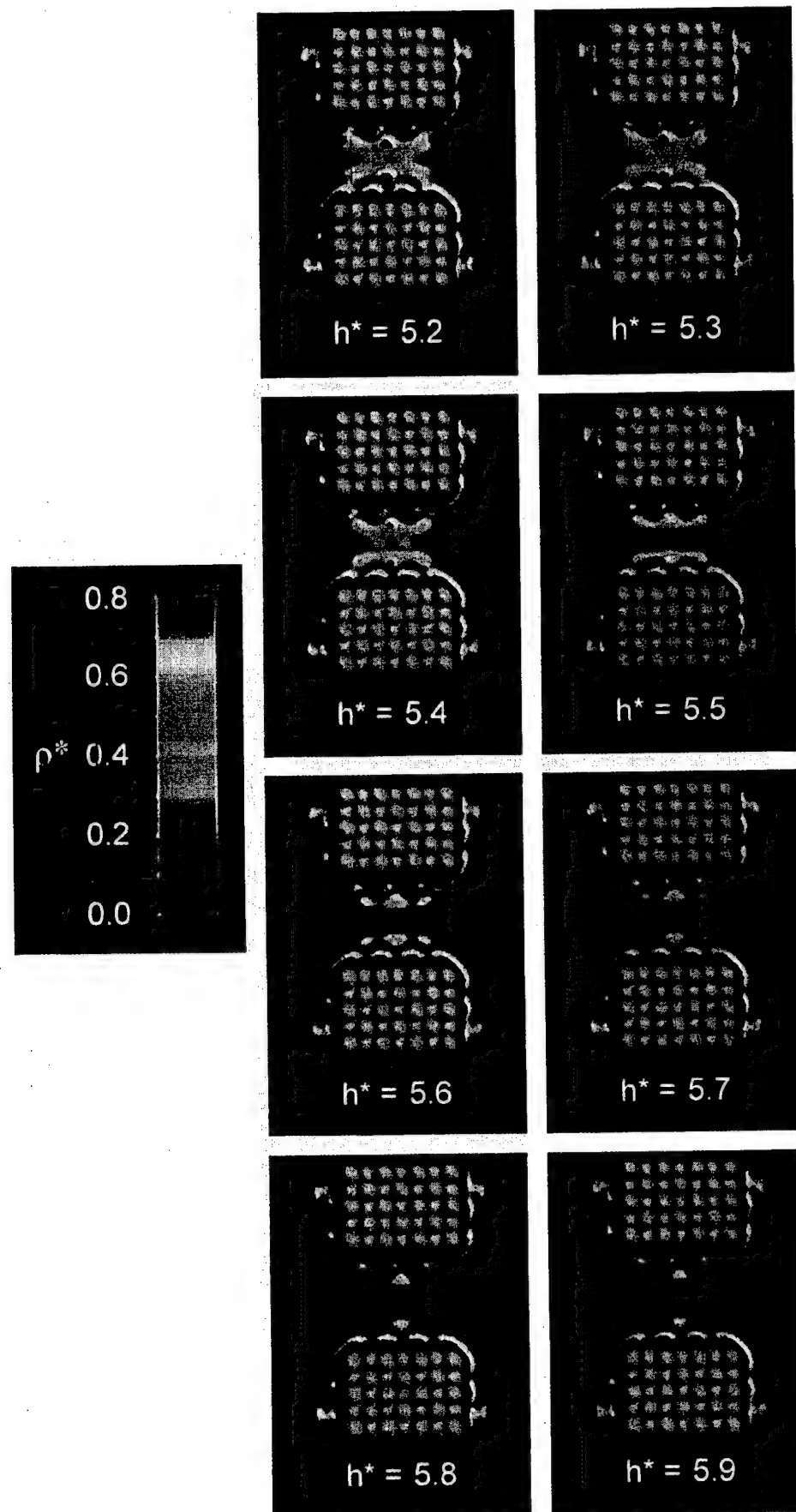


Figure 4. As for Figure 3 but for nanowires three unit cells wide at $h^* = 5.2-5.9$.

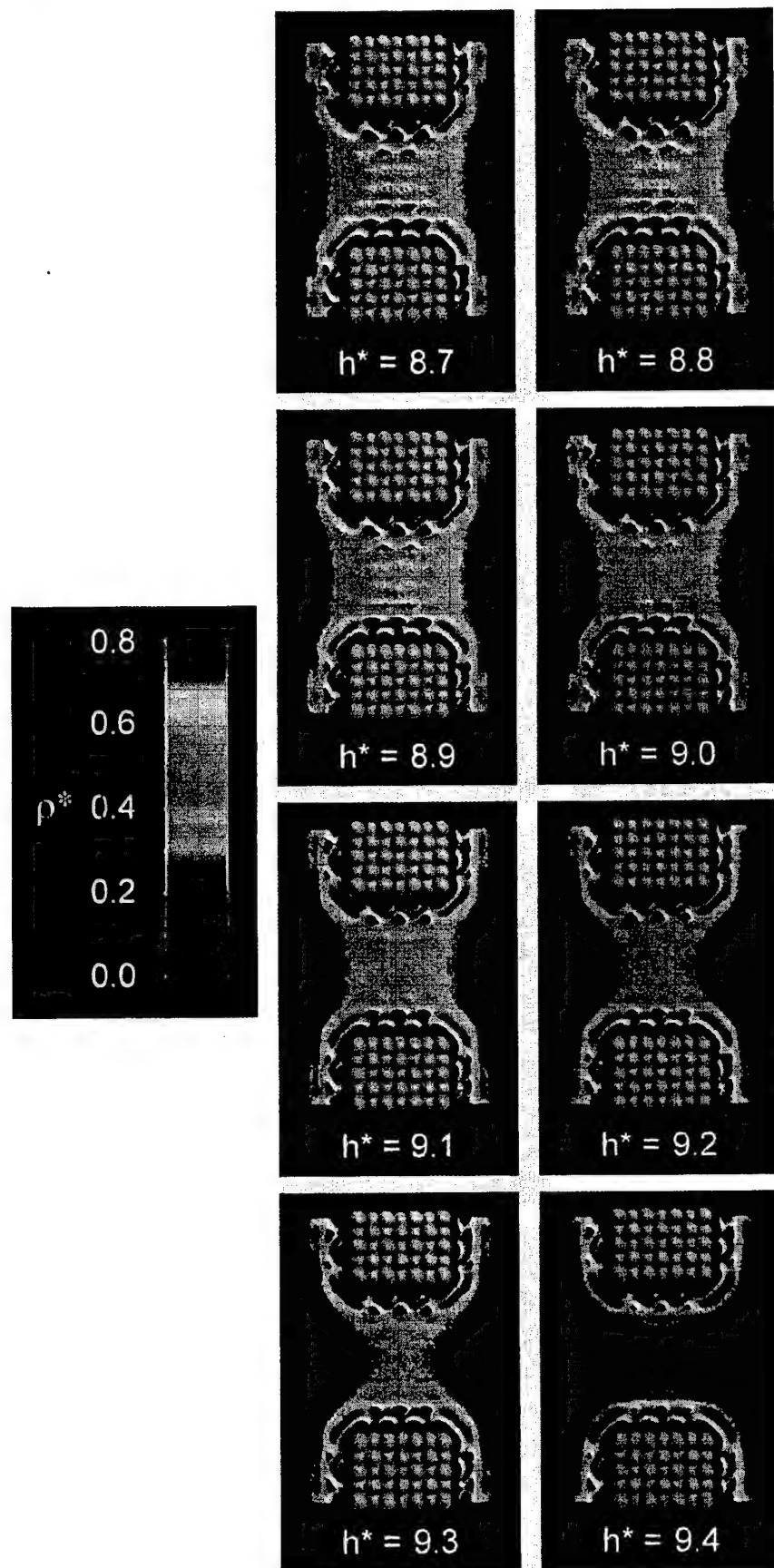


Figure 5. As for Figure 3 but for nanowires three unit cells wide at $\mu^* = -11.4$ and $h^* = 8.7-9.4$.

of the condensate. There is also inplane order within the three layers adjacent to each surface, as evidenced by the

regions of high density within the layers that correspond to discrete lattice locations. At $h^* = 9.0$ the two middle

layers are no longer distinguishable and the fluid density appears homogeneous in the center of the condensate. The condensate narrows with increasing surface separation and snaps off between $h^* = 9.3$ and 9.4 . At $h^* = 9.3$ the two layers adjacent to the surfaces are still highly ordered but inplane order in the third layer is no longer present. For $\mu^* = -11.7$ discussed above, the condensate was never larger than three molecular layers and the condensate remained layered until snap-off. There was no evidence of a bulk fluid between the surfaces. The shape of the meniscus is also affected by the chemical potential. For $\mu^* = -11.7$ the meniscus was not smoothly curved but rather contained stepwise discontinuities due to the layered fluid. For $\mu^* = -11.4$ the meniscus is diffuse but appears to be much less affected by fluid layering within the condensate.

Increasing the chemical potential also increases the film thickness on the nanowire surfaces. For $\mu^* = -11.4$ the nanowires are covered by three-layer films, as can be seen clearly for $h^* = 9.4$ in Figure 5. The two layers adjacent to the surfaces are highly ordered while the third layer appears to be a diffuse cloud. In fact, on careful examination of panel h for $h^* = 9.4$, it is possible to see that the diffuse clouds are actually connected across the gap. The vapor-phase density between the wires is enhanced due to the presence of the wires. Further separation would be necessary to see a bulk vapor phase between the wires.

Figure 6 provides a comparison of snap-off between the 5-wire, 10-wire, and infinite slit models at $\mu^* = -11.7$. Not surprisingly, the wires snap off before the planar system, and the 5-wire snaps off before the 10-wire. In panel a at $h^* = 5.5$, a 5-layer condensate is present for all three systems. At $h^* = 6.4$ the 5-wire condensate has just snapped off but a vapor more dense than the bulk remains between the surfaces. On further increasing the surface separation to $h^* = 7.00$, the 10-wire condensate has just snapped, leaving a dense vapor between the surfaces. Note, however, that bulk vapor now separates the 5-wires. For $h^* = 7.5$ the fluid phase in the infinite slit pore has evaporated, leaving a dense vapor phase. The systems with larger surface area maintain a liquid condensate for greater surface separation.

In Figure 7 we compare condensation between nanowires three unit cells wide with condensation between nanoplatelets that are three units cells in extent in both the x and y directions at $\mu^* = -11.7$. As expected, as the surface separation increases, the condensate is stable at larger surface separations for the nanowire system compared to the platelets. In other words, the system with smaller surface area snaps off at a smaller surface separation. Additionally, at all surface separations the condensate in the nanoplatelet system is never as large or well ordered as that in the 3-wire system. The 3-wire prior to snap-off has four well-defined liquidic layers and begins to add the fifth layer, while the 3×3 system never has more than four well-defined layers. The film thickness on the external surfaces is different for the 3-wire and the nanoplatelet systems. The second film layer is noticeably more dense for the 3-wire case as compared to the platelet system.

Discussion

This work shows that capillary condensation, where a liquid condenses across a gap when the surfaces are close enough, is preceded by an accumulation of dense vapor in the gap. This is clear in Figure 6, where for $h^* = 6.4$ the vapor separating the surfaces is more dense than the bulk vapor that fills the gap at $h^* = 7.5$. In fact, the fluid density

in the gap increases continuously from bulk vapor to liquid density as the surfaces approach from a sufficiently large separation. Capillary evaporation occurs in reverse. The condensate gradually thins to a dense vapor as the surfaces are separated, until finally a bulk vapor separates the surfaces. As the chemical potential increases, the surface separation at which evaporation occurs increases. The snap-off separation also increases with the number of sides that have infinite dimensions in the nanocontact, which is discussed below. Since a new simulation was started for each surface separation, no hysteresis was observed; only thermodynamically stable states were simulated.

On closer examination, it is clear that the liquid condensates are layered. This is consistent with the widely accepted idea based on both computer simulations²⁹ and SFA experiments¹ that fluids confined between surfaces sufficiently close together are layered. We show here that this also applies for fluids condensed in nanoscale contacts even though the lateral size of the contact in at least one direction is on the nanoscale. This is consistent with simulation results for fluid-filled pores where the confining surfaces are grooved, allowing the fluid to be distinctly layered in some regions and not in others.^{31,32} Transverse order is also apparent within the fluid layers closest to the surfaces due to epitaxial alignment with the surfaces. This is also a well-known phenomenon that has been studied via computer simulations for both structured²⁹ and perfectly smooth solid surfaces.^{29,33} Since the surfaces are immersed in bulk vapor, we can directly examine the meniscus as the condensate forms. The meniscus is not necessarily a smoothly varying surface that divides the liquid and vapor phases. Rather it is diffuse and actually appears to have steps that become more pronounced with smaller contacts and lower chemical potential.

The number of fluid layers that can be supported between the nanocontacts depends on the chemical potential. At $\mu^* = -11.7$ the 3-wire supports four layers whereas with an increase in chemical potential to $\mu^* = -11.4$ the 3-wire supports up to eight fluid layers. A significant result of this work is that the size of the nanocontact surfaces also affects the number of fluid layers that can be supported. At $\mu^* = -11.7$ the 5-wire supports up to five fluid layers. At the same chemical potential the fifth layer is never fully developed for the 3-wire. A similar conclusion is drawn on examination of Figure 7 for the 5-wire, 10-wire, and infinite parallel platelets. If the contact region is large enough, the number of layers supported and the condensation separation are independent of contact size. From this work it is clear that, in order for the nanocontact size to be unimportant, the lateral dimensions must be greater than 10σ .

This work also indicates the threshold where the size of the nanocontact affects application of macroscopic relationships such as the Kelvin equation. The Kelvin equation theoretically predicts the relationship between the maximum surface separation that will support a condensate and the bulk vapor pressure. Generally¹⁸ the shape and size of the contact region is not important in applying the Kelvin equation because the dimensions of the contact region are much larger than the smallest meniscus radius of curvature. The larger radius of curvature can be taken equal to infinity so that the meniscus curvature and hence the maximum surface separation only depend on the vapor pressure, temper-

(31) Curry, J. E.; Zhang, F.; Cushman, J. H.; Schoen, M.; Diestler, D. *J. Chem. Phys.* **1994**, *101*, 10824.

(32) Gao, J.; Luedtke, W. D.; Landman, U. *Science* **1995**, *270*, 605.

(33) Jiang, S.; Rhykerd, C. L.; Gubbins, K. E. *Mol. Phys.* **1993**, *79*, 373.

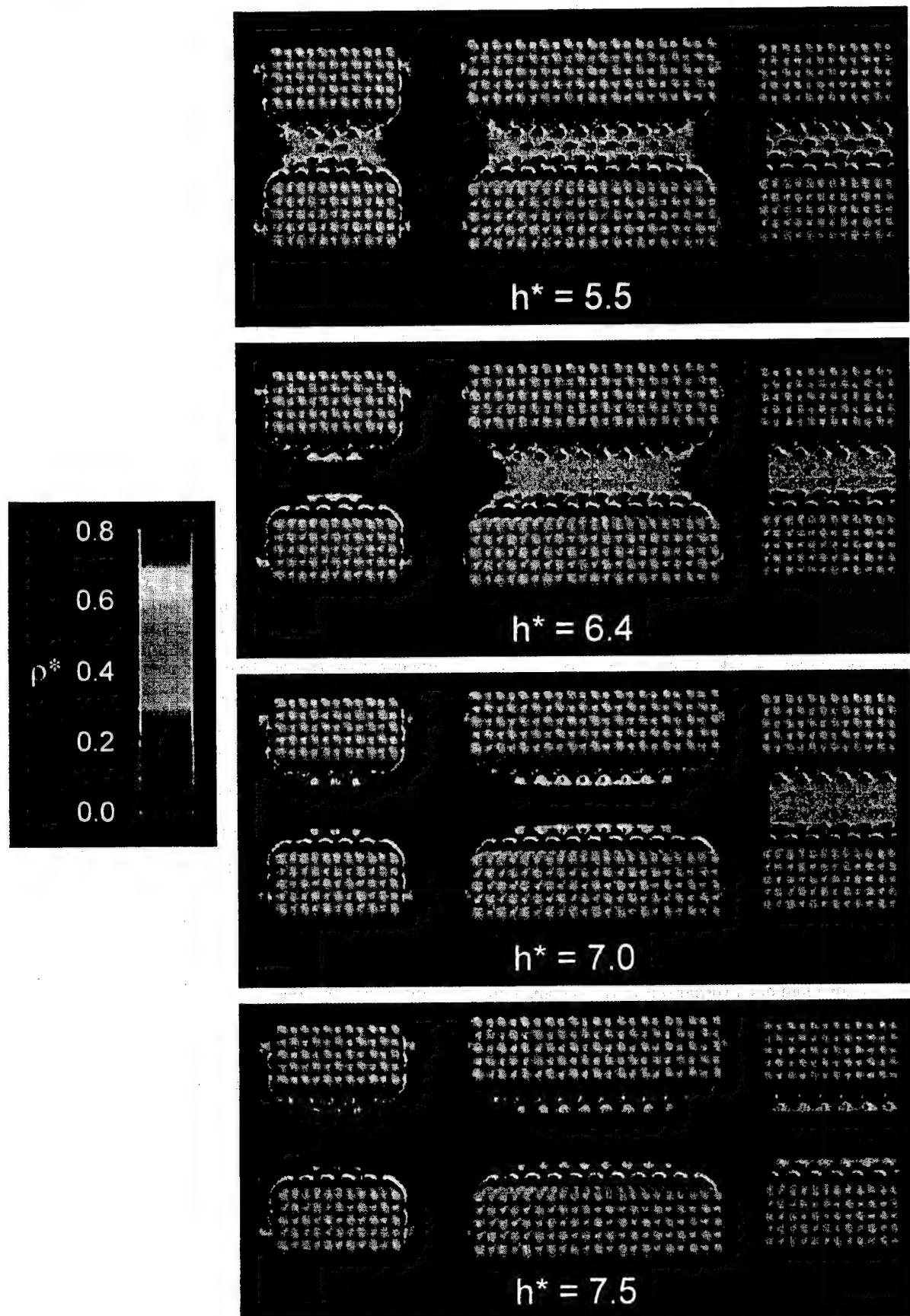


Figure 6. As for Figure 3 but for (from left to right) a 5-wire, 10-wire, and ∞ -slit pore at $h^* = 5.5, 6.4, 7.0$, and 7.5 .

ature, and surface tension. The size of the contact region is not contained in the approximate Kelvin expression for

large contacts. If, however, a dimension of the contact region approaches the size of the meniscus, the Kelvin

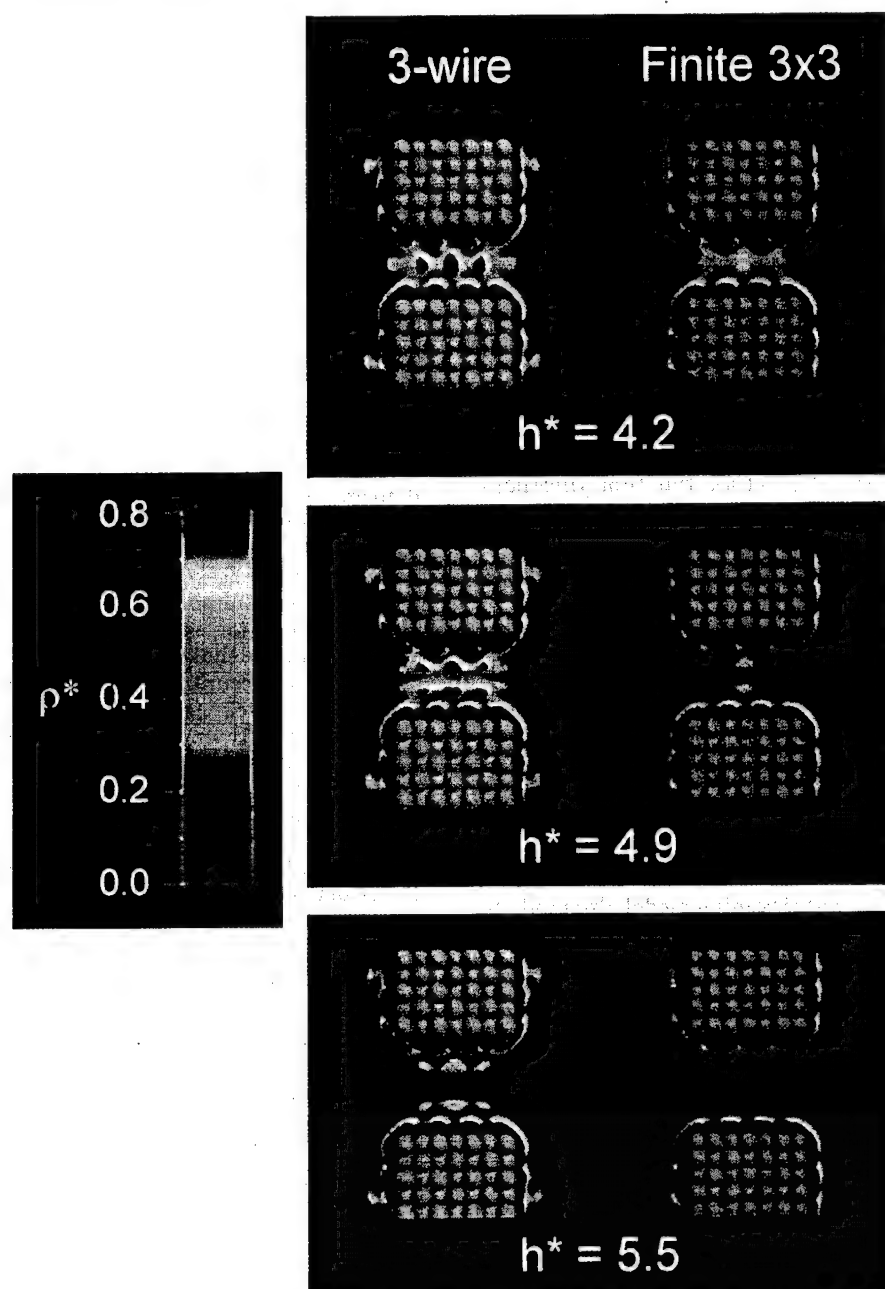


Figure 7. Maps of two-dimensional slices through the three-dimensional, ensemble-averaged particle density of the fluid condensed between nanowires three unit cells wide (left, slice taken at $y = 0.0$) and finite platelets with dimensions three unit cells in both the x and y directions (right, slice taken across the center of the contact at $y = 0.5$) for $\mu^* = -11.7$, $T^* = 1.0$, $\alpha = 0.0$, and $h^* = 4.2$, 4.9, and 5.6.

equation is only sensible if the meniscus is axisymmetric. For the nanowires, which are not axisymmetric, if the surface tension is invariant with meniscus curvature (which it almost certainly is not),³⁴ then the Kelvin equation predicts the same condensation separation irrespective of the width of the wire. These simulations show that the condensation separation decreases as the wire narrows. This is because the menisci are not independent. Even the condensation separation for the widest nanowire studied (10-wire) is less than the separation for the infinite platelets, indicating that the menisci are still interdependent. If the criterion of independent menisci is used to set a threshold for the applicability of the Kelvin equation in nanocontact

systems, then from this model the wires must be wider than 10σ .

For the nanoplatelets the limit of applicability of the Kelvin equation is not as easy to define. The nanoplatelets are axisymmetric, and geometrically the size of the contact region would not limit applying the Kelvin equation. The Kelvin equation predicts that the mean radius of curvature $(1/r_1 + 1/r_2)^{-1}$ is fixed by the vapor pressure, temperature, and surface tension, so that as one radius decreases, the other also decreases. So as the size of the contact decreases and the width of the meniscus shrinks, the evaporation distance also decreases. This is what is observed with 3×3 and 5×5 contacts. The 5×5 contact maintains a meniscus at a greater surface separation than that for the 3×3 contact. While the trend is qualitatively sensible,

the molecular nature of the fluid must limit the applicability of the Kelvin equation. Presumably in these studies we are well below this threshold; however, this can only be verified by directly calculating the surface tension, which was not attempted in this work.

In addition to capillary condensation, we can also examine film thickness on isolated surfaces as a function of chemical potential. Ellipsometry has been used extensively to measure film thickness on isolated surfaces in the laboratory.^{35,36} Films are condensed from the vapor on all exposed nanowire surfaces. When the surfaces are sufficiently far apart so that bulk vapor separates the surfaces, the film thicknesses in the contact region and on the external surfaces are the same. At $\mu^* = -11.7$ (see Figure 4, $h^* = 5.9$) two layers of fluid cover the nanowire surfaces. The first layer is dense and well ordered while the second layer is rather diffuse. As expected for a higher chemical potential ($\mu^* = -11.4$), the film thickness increases to three layers (see Figure 5, $h^* = 9.4$). The van der Waals film-thickening model predicts that the thickness of a film on an isolated surface will be increased by the presence of another surface due to van der Waals interactions across the gap separating the surfaces.¹¹ Christenson³⁷ observed van der Waals thickening for thick (~10 nm) *tert*-butyl alcohol films adsorbed on mica with a surface forces apparatus. We notice that the density of the outermost film layer is enhanced even after snap off as long as the vapor density in the gap is higher than the bulk vapor density. It is illustrated clearly in Figure 6, where for the 5-wire case the density of the second layer is higher for $h^* = 6.4$, where the surfaces are separated by a dense vapor, compared to $h^* = 7.5$, where bulk vapor separates the surfaces.

The van der Waals film-thickening model also predicts that the relationship between the surface separation and the film thickness at the capillary condensation transition is approximately $h_c = 3t_c$, where h_c and t_c are the critical surface separation and the film thickness, respectively.¹¹ To test this, we take the capillary condensation separation to be the separation where bulk vapor remains just after the condensate evaporates. Assuming the Lennard-Jones

(35) Rhykerd, C. L.; Cushman, J. H.; Low, P. F. *Langmuir* 1991, 7, 2219.

(36) Beaglehole, D.; Christenson, H. K. *J. Phys. Chem.* 1992, 96, 3395.

(37) Christenson, H. K. *Phys. Rev. Lett.* 1994, 73, 1821.

diameter defines the surface edge, we measure h_c as $h - \sigma$, since h is defined as the distance between the centers of surface atoms on opposing surfaces. The film thickness is estimated from the density profile as the distance from the surface to the edge of the green region denoting the extent of the outer film layer. We find in all cases that $h_c/t_c \sim 3$, in agreement with the van der Waals film-thickening model. Specifically, for the 3-wire, $\mu^* = -11.7$, $h^* = 5.9$ (Figure 4), $h_c/t_c = 3.1$, for the 3-wire, $\mu^* = -11.4$, $h^* = 9.4$ (Figure 5), $h_c/t_c = 3.4$, and for the 5-wire, $\mu^* = -11.7$, $h^* = 6.4$ (Figure 6), $h_c/t_c = 3.4$.

Conclusions

We have directly studied capillary condensation in nanoscale contacts via isostrain grand canonical Monte Carlo computer simulations. We have purposely examined contacts with dimensions on the molecular scale to determine the effect of contact area size on capillary condensation and the reverse process, snap-off. The condensates are layered, and in-plane order is apparent particularly in the layers nearest the surfaces. The film thickness on isolated surfaces increases with increasing chemical potential, as expected. As the surfaces approach in bulk vapor, the critical surface separation where condensation occurs is approximately three times the critical film thickness, in agreement with the van der Waals film-thickening model. The meniscus is smooth for high enough chemical potential, but for low chemical potential and small contact size the meniscus is not smoothly rounded but contains steps. A qualitative analysis in terms of the Kelvin equation shows that the Kelvin equation could be applied for condensation of simple fluids between nanoplatelets but not for nanowires.

Even in this system where the intermolecular potentials are relatively simple, the fluid behavior is complex. More complex intermolecular potentials necessary to simulate metallic surfaces and aqueous solutions almost certainly will bring to light further complexity. These will be the subjects of future work.

Acknowledgment. This work was supported by the Army Research Office and the Petroleum Research Fund. We thank Hugo Christenson for helpful comments on the manuscript.

LA0013143

Coupled Solvent and Heat Transport of a Mixture of Swelling Porous Particles and Fluids: Single Time-Scale Problem

LYNN SCHREYER BENNETHUM¹ and JOHN H. CUSHMAN²

¹*Center for Computational Mathematics, University of Colorado at Denver, PO Box 173364,
Campus Box 170, Denver, CO 80217-3364, U.S.A.*

²*Center for Applied Math, Math Sciences Building, Purdue University, West Lafayette, IN
47907-1395, U.S.A.*

(Received: 5 February 1998; in final form: 16 November 1998)

Abstract. A three-spatial scale, single time-scale model for both moisture and heat transport is developed for an unsaturated swelling porous media from first principles within a mixture theoretic framework. On the smallest (micro) scale, the system consists of macromolecules (clay particles, polymers, etc.) and a solvating liquid (vicinal fluid), each of which are viewed as individual phases or nonoverlapping continua occupying distinct regions of space and satisfying the classical field equations. These equations are homogenized forming overlaying continua on the intermediate (meso) scale via hybrid mixture theory (HMT). On the mesoscale the homogenized swelling particles consisting of the homogenized vicinal fluid and colloid are then mixed with two bulk phase fluids: the bulk solvent and its vapor. At this scale, there exists three nonoverlapping continua occupying distinct regions of space. On the largest (macro) scale the saturated homogenized particles, bulk liquid and vapor solvent, are again homogenized forming four overlaying continua: doubly homogenized vicinal fluid, doubly homogenized macromolecules, and singly homogenized bulk liquid and vapor phases. Two constitutive theories are developed, one at the mesoscale and the other at the macroscale. Both are developed via the Coleman and Noll method of exploiting the entropy inequality coupled with linearization about equilibrium. The macroscale constitutive theory does not rely upon the mesoscale theory as is common in other upscaling methods. The energy equation on either the mesoscale or macroscale generalizes de Vries classical theory of heat and moisture transport. The momentum balance allows for flow of fluid via volume fraction gradients, pressure gradients, external force fields, and temperature gradients.

Key words: swelling, heat transfer, polymer, clay, liquid/vapor transfer, drying, unsaturated, mixture.

1. Introduction

As technology becomes more sophisticated, it is becoming increasingly necessary to model porous materials over a hierarchy of scales. Consider, for example, natural smectitic clays. The macroscopic properties of clay are primarily due to clay particles, which are clusters of clay mineral platelets (a solid phase) and adsorbed water (or vicinal water). The vicinal water is adsorbed to the clay minerals via electro-chemical forces, and the proximity of the vicinal fluid to the solid may

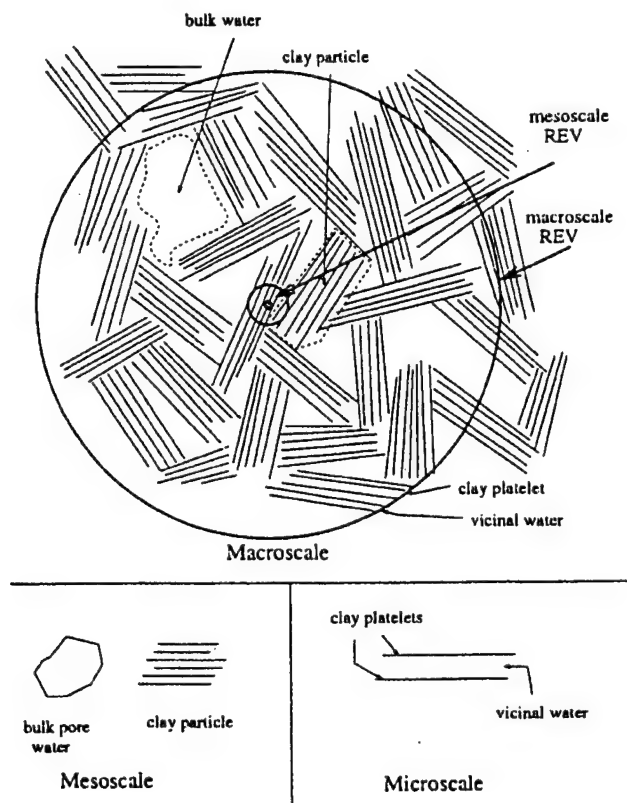


Figure 1. Three scales of an idealized smectitic clay.

strongly affect the thermodynamic properties of the adsorbed fluid [30, 42, 43]. In naturally occurring clay soils, the clay is composed of clay particles with voids which may be filled with a bulk phase liquid (water) and/or air. Thus the clay particles swell or shrink as water transfers between the bulk and vicinal phase. This particular porous medium is an example in which there are three distinct scales of observation — a microscale, in which clay minerals and adsorbed water are distinguishable; a mesoscale, in which the homogenized particles and bulk phase fluid are distinguishable; and a macroscale, in which the medium appears to be homogeneous (see Figure 1) with saturated particles, but possibly unsaturated large-scale pores.

A prototypical model governing heat and moisture transfer through porous media postulated by de Vries [23] is given by

$$C \frac{\partial T}{\partial t} - \rho^l W \frac{\partial \varepsilon^l}{\partial t} = \nabla \cdot (K \nabla T) - L \hat{e}_l^g - (c_p^g \rho^g v^g + c_p^l \rho^l v^l) \nabla T, \quad (1)$$

where T is the temperature, ρ^l and ρ^g are the densities of the liquid and gas phases respectively, v^l and v^g are the velocities of the liquid and gas phases respectively, K is the thermal conductivity of the porous media, L is the heat of vaporization, C is the volumetric heat capacity, ε^l is the volumetric liquid content, W is the differential heat of wetting, \hat{e}_l^g is the rate of evaporation, and c_p^g and c_p^l are the specific heat

of water vapor and liquid, respectively. This model is widely recognized as being practically useful for a wide range of porous media. However, it has limitations, especially under conditions in which the temperature fluctuates (for correction factor, see e.g. [32]). This model was *posited* and subsequent models have been built upon this model. The goal of this paper is to *derive* governing heat and moisture transfer equations, which are based on knowledge of the microstructure.

There are several methods which can be used to upscale information from the microscale, including homogenization [12], and averaging [53]. These methods take all information from the microscale and propagate up, either by asymptotic expansion or averaging, the microscale equations to the larger scale. The advantage of these approaches is that macroscopic coefficients are defined precisely in terms of microscopic thermodynamic properties and the geometry. The disadvantage of such approaches are that microscopic physics must be precisely known. In a material, such as swelling porous media, the interactions between the phases are not well-understood, and so we choose an alternate upscaling approach, hybrid mixture theory (HMT).

Hybrid mixture theory is a slight modification of classical mixture theory. In the two-scale approach, HMT involves volume averaging field equations (conservation of mass, momentum balance, energy balance, entropy inequality) from the microscale to the mesoscale. This yields explicit relations between the mesoscopic field variables and their microscopic counterparts. Restrictions on the constitutive equations are obtained within the framework of rational thermodynamics, i.e. the entropy inequality is exploited in the sense of Coleman and Noll [17]. These ideas were first introduced by Hassanizadeh and Gray [35–37] in 1979 for a multi-phase nonswelling porous medium. They have since been expanded to include multi-constituents [33, 34] and multi-constituent with interfaces for swelling porous media [2]. This work has generated many new insights into the macroscopic behavior of porous media, including nonequilibrium swelling and capillary pressures [1, 39], Darcy and non-Darcy type flow with and without interfacial effects, [9, 27, 28, 38, 40], the macroscale chemical potential [10, 21], and the macroscopic stress tensors for swelling porous media [11, 45, 46]. A three-scale model for swelling porous media by Bennethum and Cushman [7, 8] incorporates multiple phases, multiple species, and interfacial effects. The three scales include a microscale, mesoscale, and macroscale. In this setting HMT was employed by averaging the field equations twice: once going from the microscale to the mesoscale, and then again from the mesoscale to the macroscale. The entropy inequality is exploited to obtain constitutive restrictions only in terms of macroscopic variables.

The resulting model is a parallel flow type model, as opposed to a dual porosity or distributed microstructure model. Parallel flow type models, [49], are models which view the vicinal and bulk water velocities as super-imposed, with no distinction between the time-scales for the vicinal water and bulk water. For modeling consolidation problems, the time scales involved may become critical. However, for heat transfer problems with unsaturated drainage, we feel the distinction in

time scales is not as important, although this theory can be extended to incorporate such cases. Incorporating different time scales results in constitutive equations with nonlocal behavior, i.e. the resulting constitutive equations involve integrals in time.

This work is extremely general, and a wealth of information has yet to be exploited from it. For a summary of these works see Cushman [21]. We concentrate the discussion on moisture transport and heat transfer in combination with solid stresses which result from these processes.

2. Two-Scale Model

In this section we discuss the development of the two-scale model. Here we assume that the particle is composed of two phases, a liquid phase, l , and a solid phase, s . At the microscale, see Figure 1, one can distinguish between the solid and vicinal (adsorbed liquid) phases, while at the mesoscale the particle appears to be continuous. It is assumed that the thermodynamic properties of the liquid phase are strongly affected by its proximity to the solid phase, interfacial properties are negligible, the solid and fluid are nonpolar so that conservation of angular momentum for each phase implies the stress tensors of each phase are symmetric, and that each phase behaves as a single constituent, i.e. there are no chemical reactions within a phase. We do allow for transfer between phases. A summary of the definitions of all variables is provided in Appendix A.

2.1. MESOSCALE FIELD EQUATIONS AND ASSUMPTIONS

Within the framework of HMT, the microscale field equations are averaged with respect to some volumetric weight function [3]. If there is a distinct scale separation, then this weight function is commonly taken as a characteristic function consistent with an REV in the sense of Bear [5]. However, from a purely formal perspective, an REV need not exist, nor need there be scale separation. The averaged equations with respect to a general weight function will take the same form as those with an REV [18]. Care must be taken, however, when there is no scale separation, as constitutive theories in this case will in general be nonlocal (cf. [19, 22]) and the entropy inequality must be considered as a functional inequality in the sense of Frechet derivatives [31]. This latter point has not been well understood, as in the hydrology literature wherein localized constitutive equations have often been assumed (as in [4]), irregards to whether there is scale separation. Throughout this article we will assume scale separation between the micro, meso and macro scales. And thus, constitutive relations will be constrained using the Coleman and Noll method of exploiting the entropy inequality, which is considered as a nonfunctional equation. The averaging of the microscale field equations to the mesoscale, along with the relationships between the mesoscopic variables are presented in several papers [6, 36].

Conservation of mass for the α -phase is

$$\frac{D^\alpha(\varepsilon^\alpha \rho^\alpha)}{Dt} + \varepsilon^\alpha \rho^\alpha \nabla \cdot \mathbf{v}^\alpha = \hat{e}_\beta^\alpha, \quad \alpha, \beta = l, s, \quad \alpha \neq \beta, \quad (2)$$

where ε^α is the volume fraction of phase α , ρ^α and \mathbf{v}^α denote the averaged density and mass-averaged velocity of the α -phase, respectively, \hat{e}_β^α represents the net mass gained by the α -phase from the other phase per unit time, and D^α/Dt denotes the material time derivative following the α -phase, i.e. $D^\alpha/Dt = \partial/\partial t + \mathbf{v}^\alpha \cdot \nabla$.

Conservation of momentum for each phase is

$$\varepsilon^\alpha \rho^\alpha \frac{D^\alpha \mathbf{v}^\alpha}{Dt} - \nabla \cdot (\varepsilon^\alpha \mathbf{t}^\alpha) - \varepsilon^\alpha \rho^\alpha \mathbf{g} = \widehat{\mathbf{T}}_\beta^\alpha, \quad \alpha, \beta = l, s, \quad \alpha \neq \beta, \quad (3)$$

where \mathbf{t}^α denotes the average symmetric stress tensors for phase α , \mathbf{g} is the body force (i.e. gravity), and $\widehat{\mathbf{T}}_\beta^\alpha$ denotes the net gain of momentum of the α -phase due to mechanical interactions with the other phase.

Conservation of energy for phase α is given by

$$\varepsilon^\alpha \rho^\alpha \frac{D^\alpha E^\alpha}{Dt} - \varepsilon^\alpha \mathbf{t}^\alpha : \mathbf{d}^\alpha - \nabla \cdot (\varepsilon^\alpha \mathbf{q}^\alpha) + \varepsilon^\alpha \rho^\alpha h^\alpha = \widehat{Q}_\beta^\alpha, \\ \alpha, \beta = l, s, \quad \alpha \neq \beta, \quad (4)$$

where E^α is the average internal energy per unit mass of the α -phase, \mathbf{q}^α denotes the heat flux, \mathbf{d}^α is the symmetric part of $\nabla \mathbf{v}^\alpha$, $\mathbf{A} : \mathbf{B} = \text{tr}(\mathbf{AB}^T)$ denotes the classical inner product between tensors, h^α is the external heat source per unit mass per unit time, and \widehat{Q}_β^α denotes the gain of energy by the α -phase due to non-mechanical interactions with the other phase. If we sum over all phases, one recovers the familiar form of the energy equation

$$\rho \frac{DE}{Dt} - \mathbf{t} : \nabla \mathbf{v} - \nabla \cdot \mathbf{q} - \rho h = 0, \quad (5)$$

where the relationships between the medium and phase thermodynamic variables are

$$\rho = \sum_{\alpha=l,s} \varepsilon^\alpha \rho^\alpha, \quad (6)$$

$$\rho \mathbf{v} = \sum_{\alpha=l,s} \varepsilon^\alpha \rho^\alpha \mathbf{v}^\alpha, \quad (7)$$

$$\mathbf{u}^\alpha = \mathbf{v}^\alpha - \mathbf{v}, \quad (8)$$

$$\mathbf{t} = \sum_{\alpha=l,s} (\varepsilon^\alpha \mathbf{t}^\alpha - \varepsilon^\alpha \rho^\alpha \mathbf{u}^\alpha \mathbf{u}^\alpha), \quad (9)$$

$$\rho E = \sum_{\alpha=l,s} (\varepsilon^\alpha \rho^\alpha E^\alpha + \varepsilon^\alpha \rho^\alpha \mathbf{u}^\alpha \cdot \mathbf{u}^\alpha), \quad (10)$$

$$\mathbf{q} = \sum_{\alpha=1,s} [\varepsilon^\alpha \mathbf{q}^\alpha + \mathbf{t}^\alpha \cdot \mathbf{u}^\alpha - \rho^\alpha \mathbf{u}^\alpha (E^\alpha + \frac{1}{2} \mathbf{u}^\alpha \cdot \mathbf{u}^\alpha)], \quad (11)$$

$$\rho h = \sum_{\alpha=1,s} \varepsilon^\alpha \rho^\alpha h^\alpha. \quad (12)$$

Note that relative velocities, \mathbf{u}^α , of the liquid phase over the mass averaged bulk velocity contribute to the net heat flux.

Further, we have restrictions which arise from the fact that the thermodynamic properties of the interface are negligible. This results in the following relations:

$$\hat{e}_s^l + \hat{e}_s^s = 0, \quad (13)$$

$$\sum_{\alpha=1,s} (\widehat{\mathbf{T}}_\beta^\alpha + \hat{e}_\beta^\alpha \mathbf{v}^\alpha) = \mathbf{0}, \quad \beta = 1, s \neq \alpha, \quad (14)$$

$$\sum_{\alpha=1,s} [\widehat{Q}_\beta^\alpha + \widehat{\mathbf{T}}_\beta^\alpha \cdot \mathbf{v}^\alpha + \hat{e}_\beta^\alpha (E^\alpha + \frac{1}{2} \mathbf{v}^\alpha \cdot \mathbf{v}^\alpha)] = 0, \quad \beta = 1, s \neq \alpha. \quad (15)$$

The first equation states that the ls-interface is massless, and the second and third equations state that no momentum nor energy are lost through the interface. By design, we also have $\varepsilon^l + \varepsilon^s = 1$.

After upscaling, the system is now viewed as two co-existing continua, so that at each point in space there exist thermodynamic properties for both the liquid and solid phase. At this point we perform a change of variables using a Legendre transformation to eliminate the energy density, E^α in favor of the Helmholtz free energy, A^α ,

$$A^\alpha = E^\alpha - T \eta^\alpha. \quad (16)$$

The unknowns in our system are thus:

$$\varepsilon^l, \rho^\alpha, \mathbf{v}^\alpha, T \quad (17)$$

$$A^\alpha, \eta^\alpha, \mathbf{t}^\alpha, \widehat{\mathbf{T}}_s^l, \hat{e}_s^l, \mathbf{q}^\alpha, \widehat{Q}_s^l, \quad \alpha = 1, s. \quad (18)$$

To arrive at a system which has the same number of equations as unknowns, we consider the second row of variables (18) to be dependent, or constitutive. These variables are assumed to be functions of a set of independent variables which we henceforth denote constitutive independent variables. However, even with these constitutive variables a careful count indicates that there is still an additional unknown for which there is no corresponding equation. Making a comparison with classical mixture theory for a single phase, we see that the volume fraction is the variable unaccounted for. Thus, there is a problem of closure associated with the loss of information in the upscaling process. To close the system, we follow Bowen

[13] and postulate a constitutive relation for the material time derivative of the volume fraction.

We assume the macroscopic fluid is viscous and the fluid and solid phases are compressible. Further, we assume that the temperature of the solid and fluid phases are the same at each point in space, so that the rate at which heat transfers between phases is much faster than the time scale of the problem.

By the Principle of Equipresence (Truesdell and Toupin [52]), we assume that every constitutive variable is a function of all the following macroscopic constitutive independent variables:

$$\varepsilon^l, T, \rho^\alpha, \mathbf{E}^s, \mathbf{v}^{l,s}, \mathbf{d}^l, \nabla \varepsilon^l, \nabla T, \nabla \rho^\alpha, \nabla \mathbf{E}^s, \quad \alpha = l, s, \quad (19)$$

where \mathbf{E}^s and \mathbf{d}^l are the macroscopic strain tensor of the solid phase and rate of deformation tensor, respectively, defined by

$$\mathbf{E}^s = \frac{1}{2}[(\mathbf{F}^s)^T \mathbf{F}^s - \mathbf{I}], \quad \mathbf{d}^l = \frac{1}{2}[\nabla \mathbf{v}^l + (\nabla \mathbf{v}^l)^T], \quad (20)$$

in which $\mathbf{F}^s = \text{grad } \mathbf{x}^s$ denotes the deformation gradient (with grad denoting the differentiation with respect to a macroscopic material particle). Here we have implicitly assumed that the constitutive variables are local functions, i.e. the value of each constitutive variable is determined by the values of the constitutive independent variables at the same material point, so that there is no non-locality in space. With this assumption, the variables and their gradients (19) can be considered independent, since it is possible to have different processes which at a single point can have, for example, the same temperature but varying gradients of the temperature.

The macroscopic strain is a measure of the solid phase geometry, so that by including \mathbf{E}^s and $\nabla \mathbf{E}^s$ in the list of constitutive independent variables we are assuming the behavior of the system is partially dictated by the separation and distortion of the solid phase and their spatial variations. It should be noted however, that \mathbf{E}_s , ε_l , and ρ^s are closely coupled through the continuity equation, and specifically that they are not independent if there is no exchange of mass between phases. If there is no exchange of mass, then it is necessary to include only two of these variables, and further, if the solid phase is considered incompressible, then it is necessary to choose one of \mathbf{E}^s and ε^l as an independent constitutive variable.

To simplify the quantity of algebra which follows, we deviate slightly from the axiom of equipresence [25], and assume the Helmholtz free energy densities of the phases depend only on a subset of the set of constitutive independent variables. If it is assumed that the Helmholtz free energies are a function of all constitutive independent variables listed in (19), then exploitation of the entropy inequality requires that both energies are not a function of $\mathbf{v}^{l,s}$, ∇T , and $\nabla \mathbf{E}^s$. Here we additionally assume that the liquid free energy is not a function of ρ^s and likewise that the solid free energy is not a function of ρ^l . Incorporating these additional dependencies still produces the results presented herein if one slightly modifies the thermodynamic

definitions of the pressure and chemical potential (see [6, 8] for details). For the system under consideration, it is thus postulated that

$$A^s = A^s(\varepsilon^l, T, \rho^s, \mathbf{E}^s), \quad A^l = A^l(\varepsilon^l, T, \rho^l, \mathbf{E}^s). \quad (21)$$

By assuming the liquid phase energy is a function of the volume fraction, we are allowing the adsorbed liquid structure to be a function of the separation of the solid phase minerals. Recall that the definition of vicinal or adsorbed water is water whose properties vary with the distance from the solid phase. In an ideal case, in which the solid phase is composed of flat parallel platelets, the adsorption of additional water causes the platelets to move further apart, changing the properties (density, viscosity, etc. [43]) of the vicinal fluid. Thus incorporating the volume fraction as an independent variable of A^l allows for this property – the further apart the solid platelets, the larger the volume fraction of the liquid phase. This allows us to model particles at medium to high moisture content. At low moisture content (five or fewer layers of water between solid platelets), the liquid phase can also be affected by relative shearing of the solid phase [20, 41, 48]. This is represented in the model by assuming the liquid phase energy is a function of the solid strain tensor which, by definition, is the strain of the ‘smeared out’ solid phase. So as the platelets separate, the solid phase strain tensor is altered. Similarly, if the platelets are sheared relative to each other, this again affects the strain tensor. Using assumption (21) gives us a framework to *derive* a constitutive relation for swelling pressure previously obtained only empirically by Low [43] for the first time [2].

To complete the set of definitions, we introduce the thermodynamic pressures (p^α), the classical effective stress tensor (\mathbf{t}_e^s) in the sense of Terzaghi [51], and the hydration stress tensor (\mathbf{t}_s^l) [8, 46]. Within the current framework they are defined as follows:

$$p^\alpha = (\rho^\alpha)^2 \frac{\partial A^\alpha}{\partial \rho^\alpha}, \quad (22)$$

$$\mathbf{t}_e^s = \rho^s \mathbf{F}^s \frac{\partial A^s}{\partial \mathbf{E}^s} (\mathbf{F}^s)^T, \quad \mathbf{t}_s^l = \rho^l \mathbf{F}^s \frac{\partial A^l}{\partial \mathbf{E}^s} (\mathbf{F}^s)^T, \quad (23)$$

The definition of \mathbf{t}_e^s is analogous to the Cauchy stress tensor for an elastic medium (see Eringen [25]) although applied to a porous skeleton. In soil mechanics this stress tensor is referred to as the Terzaghi stress tensor. The hydration stress tensor, \mathbf{t}_s^l is a result of the physico-chemical forces between the fluid and solid phases (see [46] for further discussion). If one of the phases is incompressible, then there is no thermodynamic definition for pressure, but a corresponding term is still obtained by treating the continuity equation as a restriction enforced weakly using a Lagrange multiplier. In this case, the pressure becomes an unknown in the problem (see [6, 8, 21]).

The entropy inequality can be formulated in the usual manner [2, 6, 37], and in the sense of Coleman and Noll [17] the entropy inequality is exploited to obtain

restrictions on the forms of constitutive equations. We present the results in the next section.

2.2. CONSTITUTIVE RESTRICTIONS

In this section, we present relations resulting from the exploitation of the entropy inequality which are pertinent to the formulation of the flow and heat transfer within the two-scale model. We present two sets of results which represent a small portion of the results derived in [2, 6] in much greater detail. The first set consists of results which hold at equilibrium and far from equilibrium, and come from the assumption that $D^s T / Dt$ and d^s are not constitutive independent variables:

$$\varepsilon^l \rho^l \left(\frac{\partial A^l}{\partial T} + \eta^l \right) + \varepsilon^s \rho^s \left(\frac{\partial A^s}{\partial T} + \eta^s \right) = 0, \quad (24)$$

$$\varepsilon^s \mathbf{t}^s = -\varepsilon^s p^s \mathbf{I} + \varepsilon^s \mathbf{t}_e^s + \varepsilon^l \mathbf{t}_s^l. \quad (25)$$

Equation (24) is a generalization of the classical result stating that temperature and entropy are dual variables. Equation (25) is a constitutive relation for \mathbf{t}^s and indicates that the solid stress is composed of a thermodynamic pressure, the effective stress tensor, which is a measure of solid-solid interaction, and the hydration stress tensor which incorporates the effects of the fluid-solid interactions.

The second set of results hold near equilibrium and come from quadratic terms in the entropy inequality so that the entropy generated is always nonnegative. The fact that this comes from a linearization process means that terms of cubic and higher order have been neglected; thus these results hold only near equilibrium. They include

$$\mathbf{t}^l = -p^l \mathbf{I} + \rho^l \mathbf{v}^l : \mathbf{d}^l, \quad (26)$$

$$p^l - p^s = \varepsilon^l \rho^l \frac{\partial A^l}{\partial \varepsilon^l} + \varepsilon^s \rho^s \frac{\partial A^s}{\partial \varepsilon^l} + \hat{\mu}^l \frac{D^s \varepsilon^l}{Dt}, \quad (27)$$

$$\begin{aligned} \mathbf{v}^{l,s} = & \mathbf{K}^l \left[-\widehat{\mathbf{T}}_s^l + p^l \nabla \varepsilon^l - \varepsilon^l \rho^l \frac{\partial A^l}{\partial \varepsilon^l} \nabla \varepsilon^l - \varepsilon^l \rho^l \frac{\partial A^l}{\partial \mathbf{E}^s} : (\nabla \mathbf{E}^s) - \right. \\ & \left. - \varepsilon^l \rho^l \left(\frac{\partial A^l}{\partial T} + \eta^l \right) \nabla T \right], \end{aligned} \quad (28)$$

$$\begin{aligned} \mathbf{v}^{l,s} = & \mathbf{K}^l \left[-\varepsilon^l \nabla p^l + \varepsilon^l \rho^l \mathbf{g} - \varepsilon^l \rho^l \frac{\partial A^l}{\partial \varepsilon^l} \nabla \varepsilon^l - \right. \\ & \left. - \varepsilon^l \rho^l \frac{\partial A^l}{\partial \mathbf{E}^s} : (\nabla \mathbf{E}^s) - \varepsilon^l \rho^l \left(\frac{\partial A^l}{\partial T} + \eta^l \right) \nabla T \right], \end{aligned} \quad (29)$$

$$G^s - G^l = C^l \hat{e}_s^l, \quad (30)$$

$$\varepsilon^l \mathbf{q}^l + \varepsilon^s \mathbf{q}^s = \mathbf{K} \cdot \nabla T. \quad (31)$$

The coefficients v^l , $\hat{\mu}^l$, \mathbf{K}^l , C^l , and \mathbf{K} are constants which arise from the linearization procedure and may be a function of temperature, densities, volume fraction or solid strain [2, 8]. G^α of Equation (30) is the Gibbs free energy for phase α and is given by $G^\alpha = p^\alpha / \rho^\alpha + A^\alpha$. Equation (26) is the constitutive restriction on t^l and when used to eliminate t^l in the momentum equation, the Navier-Stokes equation results. At equilibrium \mathbf{d}^l is zero and we get that the stress tensor in the liquid phase is the hydrostatic pressure.

Equation (27) gives an expression for nonequilibrium interfacial pressure jump, and implies that the pressure difference between the liquid and solid phase is a function of the dynamic rate of change of the volume fraction (see [1] for a discussion on this topic and its relation to nonequilibrium interfacial pressure).

Equation (29) is a generalized Darcy-type law and arises when the constitutive equation for \hat{T}_s^l , (28), and the momentum Equation, (3), are used to eliminate \hat{T}_s^l . Recall that \hat{T}_s^l represents the exchange of momentum between phases. Thus Equation (29) is the conservation of momentum with linearized constitutive equations for \hat{T}_s^l and t^l inserted. In this expression, the inertial effects are neglected and the hydrostatic form of the stress tensor is used (see [2, 6] for details). The first two terms on the right-hand-side give what is typically known as Darcy's law, i.e., the flow of fluid is directly proportional to the gradient of pressure plus a gravitational effect. In a swelling porous medium in which the free energy of the vicinal phase may be a function of the volume fraction, the third term on the RHS indicates that flow will occur from regions of high volume fraction (high moisture content) to regions of low volume fraction. In a nonswelling medium this term would be negligible, as the energy of the fluid would not be affected by its proximity to the solid phase. Further, flow will also occur in the presence of a temperature gradient. The coefficient of this last term is zero when interfacial effects are negligible, as argued by Hassanzadeh and Gray [37]. However, in clays where the specific surface is large, in general we do not have $\partial A_l / \partial T = -\eta_l$.

Equation (30) states that the rate of transfer from the solid to liquid phase is directly proportional to the difference of the Gibbs free energies. If the liquid and solid were composed of identical materials (water and ice for example) this statement says that at equilibrium the chemical potential of two phases must be equal.

Finally, Equation (31) states that the partial heat flux of the system is proportional to the temperature gradient, causing a coupling between this generalized Fourier's law of heat conduction and the generalized Darcy's law (29). A further coupling is obtained when the definition of the net heat flux, (11), is used, since this relation also involves the stress tensors. Hence, heat flux, fluid flow, and deformation are all coupled within this system of equations.

We end this section by listing the unknowns along with the equations necessary to describe the swelling and heat transfer of a swelling porous media. The unknowns in our final system of equations are

$$\rho^l, \rho^s, \mathbf{v}^l, \mathbf{U}^s, T, \varepsilon^l, \quad (32)$$

$$\mathbf{t}^l, \mathbf{t}^s, \hat{\mathbf{e}}_s^l, \widehat{\mathbf{T}}_s^l, \mathbf{q}, A^l, A^s, \eta^l, \eta^s, \quad (33)$$

where \mathbf{U}^s is the displacement of the solid phase. The equations include (roughly corresponding to the above unknowns): The conservation of mass (2), generalized Darcy's law for the fluid phase (29), conservation of momentum for the solid phase (3), the energy equation (5), nonequilibrium capillary pressure (or constitutive equation for $D^s \varepsilon^l / Dt$) (27), constitutive equations for the stress tensors (26, 25), constitutive equations for the exchange of mass and momentum terms [28, 30], and the constitutive equation for the partial heat flux (31) combined with (11). The remaining four variables (Helmholtz energies and entropies) require constitutive equations for which no restrictions on their forms have been obtained. They may be a function of all variables listed in (19).

The energy equation (5), is not in a practical form and so we make use of the constitutive relations in order to rewrite it. We begin with Equations (4) and eliminate the internal energy in favor of the Helmholtz potential. Making use of constitutive assumptions (21) and (31), using the chain rule, and summing over the two equations, we obtain

$$\begin{aligned} \gamma_1 \dot{T} + \gamma_2 \dot{\varepsilon}^l + \gamma_3 \cdot \mathbf{v}^{l,s} + \Gamma_4 : \dot{\mathbf{E}}^s + \Gamma_5 : \mathbf{d}^l + \gamma_6 \dot{\mathbf{e}}_s^l + \\ + \nabla \cdot (\mathbf{K} \nabla T) + \varepsilon^s \rho^s h^s + \varepsilon^l \rho^l h^l = 0, \end{aligned} \quad (34)$$

where $\gamma_1, \gamma_2, \gamma_6$ are scalar functions, γ_3 is a vector valued function, and Γ_4 and Γ_5 are second order tensor valued functions. Using $\dot{\mathbf{E}}^s = (\mathbf{F}^s)^T \cdot \mathbf{d}^s \cdot \mathbf{F}^s$, it can be shown that these coefficients are related to the Helmholtz potential, A^α , by

$$\begin{aligned} \gamma_1 &= T \left[\varepsilon^s \rho^s \frac{\partial^2 A^s}{\partial T^2} + \varepsilon^l \rho^l \frac{\partial^2 A^l}{\partial T^2} \right] \\ &= T \rho \frac{\partial^2 A}{\partial T^2} = -\rho c_p, \end{aligned} \quad (35)$$

$$\begin{aligned} \gamma_2 &= p^l - p^s - \varepsilon^l \rho^l \frac{\partial A^l}{\partial \varepsilon^l} - \varepsilon^s \rho^s \frac{\partial A^s}{\partial \varepsilon^l} - \\ &- T \frac{\partial}{\partial T} \left(p^l - p^s - \varepsilon^l \rho^l \frac{\partial A^l}{\partial \varepsilon^l} - \varepsilon^s \rho^s \frac{\partial A^s}{\partial \varepsilon^l} \right) \end{aligned} \quad (36)$$

$$\begin{aligned} &= \widehat{\mu}^l \dot{\varepsilon}^l - T \frac{\partial}{\partial T} (\widehat{\mu}^l \dot{\varepsilon}^l) \\ &= \left(\widehat{\mu}^l - T \frac{\partial \widehat{\mu}^l}{\partial T} \right) \dot{\varepsilon}^l - T \widehat{\mu}^l \frac{\partial \dot{\varepsilon}^l}{\partial T}, \end{aligned} \quad (37)$$

$$\begin{aligned}
\gamma_3 &= -\varepsilon^l \rho^l \frac{\partial A^l}{\partial \varepsilon^l} \nabla \varepsilon^l + p^l \nabla \varepsilon^l - \varepsilon^l \rho^l \frac{\partial A^l}{\partial \mathbf{E}^s} : \mathbf{E}^s \nabla + \varepsilon^l \rho^l T \frac{\partial^2 A^l}{\partial T^2} \nabla T + \\
&\quad + T \frac{\partial}{\partial T} \left[\varepsilon^l \rho^l \frac{\partial A^l}{\partial \varepsilon^l} \nabla \varepsilon^l - p^l \nabla \varepsilon^l + \varepsilon^l \rho^l \frac{\partial A^l}{\partial \mathbf{E}^s} : (\mathbf{E}^s \nabla) \right] \\
&= \mathbf{K}^{-1} \cdot \mathbf{v}^{l,s} + \widehat{\mathbf{T}}_s^l + \varepsilon^l \rho^l \left(\frac{\partial A^l}{\partial T} + \eta^l - c_p^l \right) \nabla T - \\
&\quad - T \frac{\partial}{\partial T} \left[\mathbf{K}^{-1} \cdot \mathbf{v}^{l,s} + \widehat{\mathbf{T}}_s^l + \varepsilon^l \rho^l \left(\frac{\partial A^l}{\partial T} + \eta^l \right) \nabla T \right], \tag{38}
\end{aligned}$$

$$\begin{aligned}
\Gamma_4 &= -\varepsilon^s \rho^s \frac{\partial A^s}{\partial \mathbf{E}^s} - \varepsilon^s \rho^s \frac{\partial A^l}{\partial \mathbf{E}^s} + \varepsilon^s (\mathbf{F}^s)^{-1} \cdot \mathbf{t}^s \cdot (\mathbf{F}^s)^{-T} + \varepsilon^s p^s (\mathbf{F}^s)^{-1} \cdot (\mathbf{F}^s)^{-T} + \\
&\quad + T \frac{\partial}{\partial T} \left(\varepsilon^s \rho^s \frac{\partial A^s}{\partial \mathbf{E}^s} + \varepsilon^s \rho^s \frac{\partial A^l}{\partial \mathbf{E}^s} - \varepsilon^s p^s (\mathbf{F}^s)^{-1} \cdot (\mathbf{F}^s)^{-T} \right) \\
&= T \frac{\partial}{\partial T} \left(\varepsilon^s \rho^s \frac{\partial A^s}{\partial \mathbf{E}^s} + \varepsilon^s \rho^s \frac{\partial A^l}{\partial \mathbf{E}^s} - \varepsilon^s p^s (\mathbf{F}^s)^{-1} \cdot (\mathbf{F}^s)^{-T} \right) \\
&= T \frac{\partial \tilde{\mathbf{t}}^s}{\partial T}, \tag{39}
\end{aligned}$$

$$\Gamma_5 = \varepsilon^l p^l \mathbf{I} + \varepsilon^l \mathbf{t}^l - \varepsilon^l T \frac{\partial p^l}{\partial T} \mathbf{I} = \varepsilon^l \rho^l \mathbf{v}^l : \mathbf{d}^l - \varepsilon^l T \frac{\partial p^l}{\partial T} \mathbf{I}, \tag{40}$$

$$\gamma_6 = \frac{p^s}{\rho^s} - \frac{p^l}{\rho^l} - T \frac{\partial}{\partial T} \left(\frac{p^s}{\rho^s} - \frac{p^l}{\rho^l} \right), \tag{41}$$

where $\rho A = \varepsilon^l \rho^l A^l + \varepsilon^s \rho^s A^s$, $\tilde{\mathbf{t}}^s = (\mathbf{F}^s)^{-1} \mathbf{t}^s (\mathbf{F}^s)^{-T}$ is analogous to the Piola-Kirchhoff stress tensor of the second kind, and the molar heat capacities, (see [14], pp. 84, 186),

$$c_p^l = T \left(\frac{\partial \eta^l}{\partial T} \right), \quad c_p = -T \frac{\partial^2 A}{\partial T^2}, \tag{42}$$

$$\rho c_p = \varepsilon^l \rho^l c_p^l + \varepsilon^s \rho^s c_p^s \tag{43}$$

may be a function of the volume fraction ε^l . The second form of equations (36)–(40) was obtained by incorporating constitutive relations (25)–(28).

Term by term: The term associated with γ_2 is related to the differential swelling of the two phases; γ_3 is associated with convective heat transfer; Γ_4 is related to the thermally induced stress change of the solid phase; Γ_5 , up to first order, is related to the thermally induced pressure change of the liquid phase; γ_6 is related to transfer of latent heat by solidification/liquidification; and \mathbf{K} is related to heat conduction; see for example, de Vries, [23].

Let us now make some simplifying assumptions. Assume that the material time rate of change of the volume fraction is small, so that $\gamma_2 \dot{\varepsilon}^l$ is on the order of $(\dot{\varepsilon}^l)^2$ and can be neglected. Similarly, since inertial terms of the momentum equation were neglected in deriving (29), all terms of order $\mathbf{v}^{l,s} \cdot \mathbf{v}^{l,s}$ and $\mathbf{d}^l : \mathbf{d}^l$ can also be consistently neglected. Further, assume there is no exchange of mass between the liquid and solid phases. If there is no external source of body heat ($h^l = h^s = 0$), then the heat equation is of a more familiar form:

$$c_p \dot{T} + \left[\varepsilon^l \rho^l \left(\frac{\partial A^l}{\partial T} + \eta^l - c_p^l \right) \nabla T + \widehat{\mathbf{T}}_s^l - T \frac{\partial \widehat{\mathbf{T}}_s^l}{\partial T} \right] \cdot \mathbf{v}^{l,s} + \\ + T \frac{\partial \tilde{\mathbf{t}}^s}{\partial T} : \dot{\mathbf{E}}^s - \varepsilon^l T \frac{\partial p^l}{\partial T} \nabla \cdot \mathbf{v}^l + \nabla \cdot (\mathbf{K} \nabla T) = 0, \quad (44)$$

where the exchange of momentum term $\widehat{\mathbf{T}}_s^l$ can be eliminated using Equation (28).

3. Three-Scale Model

In this section we consider three-scales, denoted by micro, meso, and macro. As in the two-scale model, the field equations are upscaled via averaging to obtain field equations of Section 2.1. Figure 2 illustrates the setting where we may have some portion of a swelling colloid particle (denoted by lA and sA) and two other phases. The colloid particle may swell and shrink due to transfer from the vicinal to bulk phase, but it remains saturated.

The averaging of the field equations along with the relationships between the microscopic and macroscopic variables are presented in other papers [6, 7] so here we only present the resulting equations.

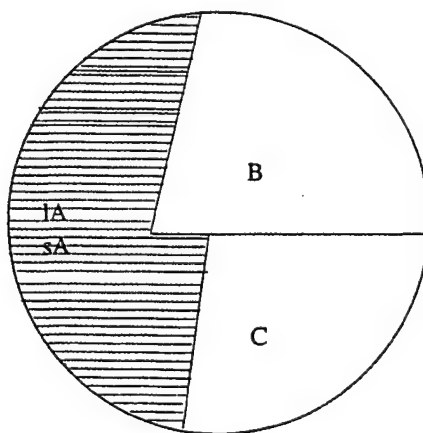


Figure 2. A colloidal phase which may swell (denoted by lA and sA) and two other phases, B and C .

3.1. MACROSCALE FIELD EQUATIONS AND ASSUMPTIONS

In this section, we discuss the development of the three-scale model. We assume the particle is composed of two phases, a liquid phase $1A$, and a solid phase sA , but now there may be interactions with two other phases. It is assumed that there are three distinct scales. At the microscale, (see Figure 1) one can distinguish between the solid and adsorbed liquid phase, at the mesoscale the particle can be distinguished from the other bulk phases, and at the macroscale, the medium appears to be continuous. It is assumed that interfacial properties are negligible, and that each phase behaves as a single constituent, i.e. there are no chemical reactions within a phase. We do allow for mass transfer between phases.

3.2. MACROSCALE FIELD EQUATIONS AND ASSUMPTIONS

In this model the field equations are upscaled twice. Averaging of the equations along with the relationships between the macroscopic and microscopic variables are presented in several papers [6, 7], so here again, we only present the resulting equations.

There are now four phases: $1A$, sA , B , and C . For each phase, the conservation of mass is

$$\frac{D^K(\varepsilon^K \rho^K)}{Dt} + \varepsilon^K \rho^K \nabla \cdot \mathbf{v}^K = \sum_{M \neq K} \hat{e}_M^K, \quad K, M = 1A, sA, B, C, \quad (45)$$

where $\varepsilon^{1A} = \varepsilon^{sA} = \varepsilon^A$ is the local volume fraction of the colloidal phase, ε^B and ε^C are the volume fractions of phases B and C , ρ^K is the mass density of the K -phase on the macroscale so that $\varepsilon^K \rho^K$ is the total mass of the K -phase per unit volume. Further, \mathbf{v}^K is the mass-averaged macroscale velocity of phase K , \hat{e}_M^K represents the net mass gained by the K -phase from the M phase, and D^K/Dt denotes the material time derivative following the K -phase.

Conservation of momentum for the K -phase ($K = 1A, sA, B, C$) is

$$\varepsilon^A \rho^K \frac{D^K \mathbf{v}^K}{Dt} - \nabla \cdot (\varepsilon^K \mathbf{t}^K) - \varepsilon^A \rho^K \mathbf{g} = \sum_{L \neq K} \widehat{\mathbf{T}}_L^K, \quad (46)$$

where \mathbf{t}^K denotes the average symmetric stress tensors for phase K , \mathbf{g} is the body force (i.e. gravity), and $\widehat{\mathbf{T}}_L^K$ denotes the net gain of momentum of the K -phase due to mechanical interactions with phase L .

Conservation of energy for phase K is given by

$$\varepsilon^K \rho^K \frac{D^K E^K}{Dt} - \varepsilon^K \mathbf{t}^K : \nabla \mathbf{v}^K - \nabla \cdot (\varepsilon^K \mathbf{q}^K) - \varepsilon^K \rho^K h^K = \sum_{L \neq K} \widehat{Q}_L^K, \quad (47)$$

where E^K is the average internal energy density per unit mass of the K -phase, \mathbf{q}^K denotes the heat flux, and \widehat{Q}_L^K denotes the gain of energy by the K -phase due to

nonmechanical interactions with phase L . If we sum over all phases, one recovers the familiar form of the energy equation

$$\rho \frac{D E}{D t} - \mathbf{t} : \nabla \mathbf{v} - \nabla \cdot \mathbf{q} - \rho h = 0, \quad (48)$$

where the relationships between the medium and phase thermodynamic variables are

$$\rho = \sum_K \varepsilon^K \rho^K, \quad (49)$$

$$\rho \mathbf{v} = \sum_K \varepsilon^K \rho^K \mathbf{v}^K, \quad (50)$$

$$\mathbf{u}^K = \mathbf{v}^K - \mathbf{v}, \quad (51)$$

$$\mathbf{t} = \sum_K (\varepsilon^K \mathbf{t}^K - \varepsilon^K \rho^K \mathbf{u}^K \mathbf{u}^K), \quad (52)$$

$$\rho E = \sum_K (\varepsilon^K \rho^K E^K + \varepsilon^K \rho^K \mathbf{u}^K \cdot \mathbf{u}^K), \quad (53)$$

$$\mathbf{q} = \sum_K [\varepsilon^K \mathbf{q}^K + \mathbf{t}^K \cdot \mathbf{u}^K - \rho^K \mathbf{u}^K (E^K + \frac{1}{2} \mathbf{u}^K \cdot \mathbf{u}^K)], \quad (54)$$

$$\rho h = \sum_K \varepsilon^K \rho^K h^K, \quad (55)$$

where all sums are over $K = 1A, sA, B, C$. Note that relative velocities of one phase over the mass averaged medium velocity contribute to a macroscopic heat flux.

Further, we have restrictions which arise from the fact that the thermodynamic properties of the interface are negligible. This results in the following relations:

$$\hat{e}_M^K + \hat{e}_K^M = 0, \quad (56)$$

$$(\hat{\mathbf{T}}_M^K + \hat{e}_M^K \mathbf{v}^K) + (\hat{\mathbf{T}}_K^M + \hat{e}_K^M \mathbf{v}^M) = \mathbf{0}, \quad (57)$$

$$[\hat{Q}_M^K + \hat{\mathbf{T}}_M^K \cdot \mathbf{v}^K + \hat{e}_M^K (E^K + \frac{1}{2} \mathbf{v}^K \cdot \mathbf{v}^K)] + \\ + [\hat{Q}_K^M + \hat{\mathbf{T}}_K^M \cdot \mathbf{v}^M + \hat{e}_K^M (E^M + \frac{1}{2} \mathbf{v}^M \cdot \mathbf{v}^M)] = 0, \quad (58)$$

where $K, M = 1A, sA, B, C$ and $K \neq M$. The first equation states that the interfaces are massless, and the second and third equations state that no momentum nor energy are lost through the interfaces. Further, we have the relation that

$$\varepsilon^A + \varepsilon^B + \varepsilon^C = 1. \quad (59)$$

After upscaling, the system is viewed as four co-existing continua, so that at each point in space there exists thermodynamic properties for all phases. At this point we perform a change of variables using a Legendre transformation to eliminate the energy density, E^K , in favor of the Helmholtz free energy, A^K ,

$$A^K = E^K - T\eta^K. \quad (60)$$

The unknowns in our system are

$$\varepsilon^A, \varepsilon^B, \rho^K, \mathbf{v}^K, T, \quad (61)$$

$$A^K, \eta^K, \mathbf{t}^K, \hat{\mathbf{e}}_M^K, \hat{\mathbf{T}}_M^K, \mathbf{q}^K, \hat{\mathbf{Q}}_M^K, \\ K = 1A, sA, B, C, \quad M = 1A, sA, B, C \neq K, \quad (62)$$

subject to restrictions (56)–(59).

To arrive at a system which has the same number of equations as unknowns, we consider the second row of variables (62) to be dependent, or constitutive. These variables are assumed to be functions of a set of constitutive independent variables. As in the two-scale case, a careful count indicates that there are two additional unknowns for which there is no corresponding equation, namely ε^A and ε^B . To close the system, we postulate a constitutive relation for the material time derivative of the volume fractions.

We assume the macroscopic vicinal fluid, $1A$, and two bulk phase fluids, B and C , are viscous and the fluid and solid phases are compressible. As before, we still assume that the temperature of all phases are the same at each point in space.

By the Principle of Equipresence (Truesdell and Toupin [52]), we assume that every constitutive variable is a function of *all* the following macroscopic constitutive independent variables:

$$\varepsilon^A, \varepsilon^B, T, \rho^K, \mathbf{E}^{sA}, \mathbf{v}^{K,sA}, \quad (63)$$

$$\nabla\varepsilon^A, \nabla\varepsilon^B, \nabla T, \nabla\rho^K, \nabla\mathbf{E}^{sA}, \mathbf{d}^K, \quad K = 1A, sA, B, C, \quad (64)$$

where \mathbf{E}^{sA} and \mathbf{d}^K are the macroscopic strain tensor of the solid phase and rate of deformation tensor of phase K , respectively, defined by

$$\mathbf{E}^{sA} = \frac{1}{2}[(\mathbf{F}^{sA})^T \mathbf{F}^{sA} - \mathbf{I}], \quad (65)$$

$$\mathbf{d}^K = \frac{1}{2}[\nabla\mathbf{v}^K + (\nabla\mathbf{v}^K)^T], \quad (66)$$

in which $\mathbf{F}^{sA} = \text{grad } \mathbf{x}^{sA}$ denotes the deformation gradient (with grad denoting the differentiation with respect to a macroscopic material particle). As in the two-scale case we assume the constitutive variables are local functions. With this assumption, the variables and their gradients (63, 64) can be considered independent.

The macroscopic strain is a measure of the solid phase geometry, so that by including \mathbf{E}^{sA} and $\nabla\mathbf{E}^{sA}$ in the list of constitutive independent variables we are still

assuming the behavior of the system is partially dictated by the separation, distortion, and entanglement of the solid platelets and their spatial variations. Contrary to the two-scale case, ε^A and \mathbf{E}^{sA} are not closely coupled in general due to the potentially large amount of fluid which could be transferred between the vicinal, 1A, and bulk phase, B.

To simplify the quantity of algebra which follows, we deviate slightly from the axiom of equipresence [52], and assume the Helmholtz free energy densities of the phases depend only on a subset of the set of constitutive independent variables. It can be shown that if it is assumed the Helmholtz free energies are a function of all constitutive independent variables listed in (63), that the exploitation of the entropy inequality requires that all energies are not a function of $\mathbf{v}^{K,sA}$, ∇T , and $\nabla \mathbf{E}^{sA}$. Here we additionally assume that the free energies are not a function of densities of other phases. Incorporating these additional dependencies still produce the results presented herein if one slightly modifies the thermodynamic definitions of the pressure and chemical potential (see [6, 8] for details). For the system under consideration it is thus postulated that

$$A^{1A} = A^{1A}(\varepsilon^A, \varepsilon^B, T, \rho^{1A}, \mathbf{E}^{sA}), \quad (67)$$

$$A^{sA} = A^{sA}(\varepsilon^A, \varepsilon^B, T, \rho^{sA}, \mathbf{E}^{sA}), \quad (68)$$

$$A^K = A^K(\varepsilon^A, \varepsilon^B, T, \rho^K). \quad (69)$$

In this simplification, we are still allowing the free energy of the vicinal water to be a function of its proximity to the solid phase by assuming its dependence on the solid phase strain tensor and the volume fraction of the particles. However, the bulk phase fluids (B and C) are, by definition, not affected by the proximity to the solid phase, so that their dependence on the solid phase strain tensor is not included. The inclusion of the volume fractions as independent variables in (69) provides a weak dependence of the free energies on the interfaces, because of the volume fractions' ability to capture some geometric effects. However, to obtain the full effects of interfaces, interfacial balance laws must be introduced, and additional constitutive independent variables such as interfacial area density must be incorporated [2, 6–8].

To complete the set of definitions, we introduce macroscale thermodynamic pressures (p^K), the macroscale effective stress tensor (\mathbf{t}_e^{sA}), and the macroscale hydration stress tensor (\mathbf{t}_{sA}^{1A}) [8, 46]. Within the current framework they are defined as follows:

$$p^K = (\rho^K)^2 \frac{\partial A^K}{\partial \rho^K}, \quad K = 1A, sA, B, C, \quad (70)$$

$$\mathbf{t}_e^{sA} = \rho^{sA} \mathbf{F}^{sA} \frac{\partial A^{sA}}{\partial \mathbf{E}^{sA}} (\mathbf{F}^{sA})^T, \quad \mathbf{t}_{sA}^{1A} = \rho^{1A} \mathbf{F}^{sA} \frac{\partial A^{1A}}{\partial \mathbf{E}^{sA}} (\mathbf{F}^{sA})^T. \quad (71)$$

The effective stress tensor \mathbf{t}_e^{sA} captures the effects of entanglement in a porous medium with a disjoint solid phase. Again, the hydration stress tensor, \mathbf{t}_{sA}^{lA} , captures the physico-chemical forces between the vicinal fluid and the solid phase. Note that the macroscale pressure is not the average of mesoscale pressures, which is the average of a partial derivative, but it is the partial derivative of averaged quantities.

The entropy inequality can be formulated in the usual manner [6, 8], and in the sense of Coleman and Noll [17] exploited to obtain restrictions on the forms of constitutive equations. We present the results in the next section.

3.3. CONSTITUTIVE RESTRICTIONS

In this section, we present relations resulting from exploiting the entropy inequality. These are pertinent to the formulation of the flow and heat transfer within the three-scale model. We present two sets of results which are a small portion of the more general results derived in [6, 8]. The first set of results hold at equilibrium and far from equilibrium, and come from the assumption that $D^{sA}T/Dt$ and \mathbf{d}^{sA} are not constitutive independent variables:

$$\sum_{K=1A, sA, B, C} \varepsilon^K \rho^K \left(\frac{\partial A^K}{\partial T} + \eta^K \right) = 0, \quad (72)$$

$$\mathbf{t}^{sA} = -p^{sA} \mathbf{I} + \mathbf{t}_e^{sA} + \mathbf{t}_{sA}^{lA}. \quad (73)$$

As in the two-scale case, Equation (72) is a generalization of the classical result stating that temperature and entropy are dual variables. Equation (73) is a constitutive relation for \mathbf{t}^{sA} and indicates that the solid stress is composed of a thermodynamic pressure, the effective stress tensor, which is a measure of solid-solid interaction, and the hydration stress tensor which incorporates the effects of the fluid-solid interactions.

The second set of results hold near equilibrium and come from forming quadratic terms in the entropy inequality so that the entropy generated is always non-negative for any process. The fact that this comes from a linearization process means that terms of cubic and higher order have been neglected; thus these results hold only near equilibrium. Linearizing about the rate of deformation tensor, \mathbf{d}^K , we obtain

$$\mathbf{t}^K = -p^K \mathbf{I} + \rho^K \mathbf{v}^K : \mathbf{d}^K, \quad K = 1A, B, C. \quad (74)$$

As in the two-scale case, at equilibrium $\mathbf{d}^K = \mathbf{0}$ and the stress tensor of any of the fluid phases is proportional to the hydrostatic pressure.

Linearizing about $D^{sA}\varepsilon^A/Dt$ and $D^{sA}\varepsilon^B/Dt$ yields nonequilibrium capillary pressure relations:

$$\begin{aligned} p^{lA} + p^{sA} - p^C &= \varepsilon^A \rho^{lA} \frac{\partial A^{lA}}{\partial \varepsilon^A} + \varepsilon^A \rho^{sA} \frac{\partial A^{sA}}{\partial \varepsilon^A} + \\ &\quad + \varepsilon^B \rho^B \frac{\partial A^B}{\partial \varepsilon^A} + \varepsilon^C \rho^C \frac{\partial A^C}{\partial \varepsilon^A} + \hat{\mu}^A \frac{D^{sA}\varepsilon^A}{Dt}, \end{aligned} \quad (75)$$

$$\begin{aligned} p^B - p^C &= \varepsilon^A \rho^{lA} \frac{\partial A^{lA}}{\partial \varepsilon^B} + \varepsilon^A \rho^{sA} \frac{\partial A^{sA}}{\partial \varepsilon^B} + \\ &\quad + \varepsilon^B \rho^B \frac{\partial A^B}{\partial \varepsilon^B} + \varepsilon^C \rho^C \frac{\partial A^C}{\partial \varepsilon^B} + \hat{\mu}^B \frac{D^{sA}\varepsilon^B}{Dt}. \end{aligned} \quad (76)$$

Note that the natural quantity which appears in regards to the pressure of the particles is the sum of the liquid and solid pressures. This can be interpreted as being the thermodynamic pressure of the particle phase, i.e. $p^A = p^{lA} + p^{sA}$.

In these expressions we are *defining* capillary pressure to be the difference of pressures between two phases. The corresponding expression for cases in which interfacial effects are incorporated are given in Appendix C. Even without directly incorporating interfacial effects, the quantity of each liquid at any given time in space is determined by what configuration minimizes the energy of the system. The further away from this minimum energy configuration, the more quickly the system will try to re-establish itself through increasing the material time rate of change of the volume fractions. In a nonswelling system, a change in variables on the volume fraction is directly related to the change in saturation (if s is saturation, then $s = \varepsilon^B/(1 - \varepsilon^A)$). See [1] for further discussion on nonequilibrium capillary pressure and its relation to nonequilibrium interfacial pressure.

The constitutive relations for the exchange of momentum terms arise by linearizing about $\mathbf{v}^{K,sA}$:

$$\begin{aligned} \mathbf{v}^{lA,sA} &= \mathbf{K}^{lA} \left[- \sum_{K=sA,B,C} \widehat{\mathbf{T}}_K^{lA} + p^{lA} \nabla \varepsilon^A - \varepsilon^A \rho^{lA} \frac{\partial A^{lA}}{\partial \varepsilon^A} \nabla \varepsilon^A - \right. \\ &\quad \left. - \varepsilon^A \rho^{lA} \frac{\partial A^{lA}}{\partial \varepsilon^B} \nabla \varepsilon^B - \varepsilon^A \rho^{lA} \frac{\partial A^{lA}}{\partial \mathbf{E}^{sA}} : (\mathbf{E}^{sA} \nabla) - \right. \\ &\quad \left. - \varepsilon^A \rho^{lA} \left(\frac{\partial A^{lA}}{\partial T} + \eta^{lA} \right) \nabla T \right], \end{aligned} \quad (77)$$

$$\begin{aligned} \mathbf{v}^{K,sA} &= \mathbf{K}^K \left[- \sum_{M=lA,sA,B,C \neq K} \widehat{\mathbf{T}}_M^K + p^K \nabla \varepsilon^K - \varepsilon^K \rho^K \frac{\partial A^K}{\partial \varepsilon^A} \nabla \varepsilon^A - \right. \\ &\quad \left. - \varepsilon^K \rho^K \frac{\partial A^K}{\partial \varepsilon^B} \nabla \varepsilon^B - \varepsilon^K \rho^K \left(\frac{\partial A^K}{\partial T} + \eta^K \right) \nabla T \right], \quad K = B, C. \end{aligned} \quad (78)$$

These relations are then used to eliminate the exchange of momentum terms, $\hat{\mathbf{T}}_M^K$, from the momentum equations to obtain generalized Darcy relationships:

$$\mathbf{v}^{lA,sA} = \mathbf{K}^{lA} \left[-\varepsilon^A \nabla p^{lA} + \varepsilon^A \rho^{lA} \mathbf{g} - \varepsilon^A \rho^{lA} \frac{\partial A^{lA}}{\partial \varepsilon^A} \nabla \varepsilon^A - \varepsilon^A \rho^{lA} \frac{\partial A^{lA}}{\partial \varepsilon^B} \nabla \varepsilon^B - \right. \\ \left. - \varepsilon^A \rho^{lA} \frac{\partial A^{lA}}{\partial \mathbf{E}^{sA}} : (\nabla \mathbf{E}^{sA}) - \varepsilon^A \rho^{lA} \left(\frac{\partial A^{lA}}{\partial T} + \eta^{lA} \right) \nabla T \right], \quad (79)$$

$$\mathbf{v}^{K,sA} = \mathbf{K}^K \left[-\varepsilon^K \nabla p^K + \varepsilon^K \rho^K \mathbf{g} - \varepsilon^K \rho^K \frac{\partial A^K}{\partial \varepsilon^A} \nabla \varepsilon^A - \varepsilon^K \rho^K \frac{\partial A^K}{\partial \varepsilon^B} \nabla \varepsilon^B - \right. \\ \left. - \varepsilon^K \rho^K \left(\frac{\partial A^K}{\partial T} + \eta^K \right) \nabla T \right], \quad K = B, C. \quad (80)$$

This is the macroscale form of the conservation of linear momentum where inertial terms are neglected and the hydrostatic forms of each liquid phase are used, i.e. $\mathbf{t}^K = -p^K \mathbf{I}$ (see [6, 8] for details). Changes in volume fractions, pressure, and temperature all cause the energy of the system to change, and these relations all reflect that fluid flows in such a way as to minimize the energy of the entire system [6, 8, 9].

If $G^K = p^K / \rho^K + A^K$ is the Gibbs free energy, then the rate at which one phase is transferred to another phase is governed by

$$G^M - G^K = C^K \hat{e}_M^K, \quad K, M = lA, sA, B, C, \quad K \neq M. \quad (81)$$

This equation is especially important for the case when $M = lA$ and $K = B$, where B is the bulk liquid phase. Then \hat{e}_M^K is the rate at which mass is transferred from the vicinal water to the bulk water. If the Gibbs free energy is higher in the bulk phase, then particles begin swelling, and if the opposite, the particles shrink.

Finally, we have the equation which governs heat transfer, which is similar to the two-scale case, i.e.,

$$\varepsilon^A \mathbf{q}^{lA} + \varepsilon^A \mathbf{q}^{sA} + \varepsilon^B \mathbf{q}^B + \varepsilon^C \mathbf{q}^C = \mathbf{K} \cdot \nabla T. \quad (82)$$

The gradient of the temperature couples the heat transfer with the flow of the liquid, which in turn governs the deformation of the porous medium. Note that because of relation (54) the left hand side is not the medium-wide heat flux unless there is no relative motion of phases.

All coefficients ν^K , $\hat{\mu}^K$, \mathbf{K}^K , C^K and K arise from the linearization procedure and may be a function of temperature, densities, volume fractions, and solid strain [8].

As in the two-scale case, the energy Equation (48), can be re-written making use of constitutive relations. We begin with Equations (47) and eliminate the internal energy in favor of the Helmholtz potential. Making use of constitutive assumptions

(67)–(69) and (82), using the chain rule, and summing over the four equations, we obtain

$$\begin{aligned} & \gamma_1 \dot{T} + \gamma_2 \dot{\varepsilon}^A + \gamma_3 \dot{\varepsilon}^B + \gamma_4 \cdot \mathbf{v}^{lA,sA} + \gamma_5 \cdot \mathbf{v}^{B,sA} + \gamma_6 \cdot \mathbf{v}^{C,sA} + \\ & + \Gamma_7 : \dot{\mathbf{E}}^{sA} + \Gamma_8 : \mathbf{d}^{lA} + \Gamma_9 : \mathbf{d}^B + \Gamma_{10} : \mathbf{d}^C + \\ & + \sum_{K=lA,sA,B,C} \sum_{M \neq K} \gamma_{KM} \hat{e}_M^K + \nabla \cdot (\mathbf{K} \nabla T) + \rho h = 0, \end{aligned} \quad (83)$$

where scalar coefficient functions are denoted as γ , vector valued functions are denoted as γ , and Γ denote second order tensor valued functions. The relationship between these coefficients and the Helmholtz potential are given in Appendix B.

Term by term: The terms associated with γ_2 and γ_3 are due to the differential swelling of the three phases; γ_4 , γ_5 , and γ_6 are due to convective heat transfer, sometimes referred to as sensible heat transfer; Γ_7 is due to thermally induced stress change of the solid phase; Γ_8 , Γ_9 , Γ_{10} , up to first order, are due to thermally induced pressure changes of the liquid phases; γ_{KM} are due to phase transformations; and \mathbf{K} is due to heat conduction; see for example, de Vries [23].

As in the two-scale case, let us now consider some simplifying assumptions. Assume that the material time rates of change of the volume fractions are small, so that the terms involving γ_2 and γ_3 can be neglected. Similarly, since inertial terms of the momentum equation were neglected in deriving (29), all terms of order $\mathbf{v}^{lA,sA} \cdot \mathbf{v}^{lA,sA}$, $\mathbf{v}^{B,sA} \cdot \mathbf{v}^{B,sA}$, $\mathbf{v}^{C,sA} \cdot \mathbf{v}^{C,sA}$, $\mathbf{d}^{lA} : \mathbf{d}^{lA}$, $\mathbf{d}^B : \mathbf{d}^B$, $\mathbf{d}^C : \mathbf{d}^C$, can also be consistently neglected. Further, assume there is no exchange of mass involving the solid phase so that $\hat{e}_{sA}^{lA} = \hat{e}_{lA}^{sA} = \hat{e}_B^{sA} = \hat{e}_{sA}^B = \hat{e}_C^{sA} = \hat{e}_{sA}^C = 0$. If there is no external source of body heat ($h = 0$), then the heat equation is of the form:

$$\begin{aligned} & \left(\rho T \frac{\partial^2 A}{\partial T^2} \right) \dot{T} + \left[\varepsilon^A \rho^{lA} \left(\frac{\partial A^{lA}}{\partial T} + \eta^{lA} - c_p^{lA} \right) \nabla T + \right. \\ & + \left. \sum_{K=sA,B,C} \left(\widehat{\mathbf{T}}_K^{lA} - T \frac{\partial \widehat{\mathbf{T}}_K^{lA}}{\partial T} \right) \right] \cdot \mathbf{v}^{lA,sA} + \\ & + \left[\varepsilon^B \rho^B \left(\frac{\partial A^B}{\partial T} + \eta^B - c_p^B \right) \nabla T - \sum_{K=lA,sA,C} T \frac{\partial \widehat{\mathbf{T}}_K^B}{\partial T} \right] \cdot \mathbf{v}^{B,sA} + \\ & + \left[\varepsilon^C \rho^C \left(\frac{\partial A^C}{\partial T} + \eta^C - c_p^C \right) \nabla T - \sum_{K=lA,sA,B} T \frac{\partial \widehat{\mathbf{T}}_K^C}{\partial T} \right] \cdot \mathbf{v}^{C,sA} + \\ & + T \frac{\partial}{\partial T} [\varepsilon^A (\mathbf{F}^{sA})^{-1} \cdot \mathbf{t}^{sA} \cdot (\mathbf{F}^{sA})^{-T}] : \dot{\mathbf{E}}^{sA} - \\ & - \varepsilon^A T \frac{\partial p^{lA}}{\partial T} \nabla \cdot \mathbf{v}^{lA} - \varepsilon^B T \frac{\partial p^B}{\partial T} \nabla \cdot \mathbf{v}^B - \varepsilon^C T \frac{\partial p^C}{\partial T} \nabla \cdot \mathbf{v}^C + \end{aligned}$$

$$\begin{aligned}
 & + \sum_{K=1,2,3} \sum_{M \neq (K,sA)} \hat{e}_M^K [G^M - G^K + T(\eta^M - \eta^K) - \\
 & - T \frac{\partial}{\partial T} \left(\frac{p^M}{\rho^M} - \frac{p^K}{\rho^K} \right)] + \nabla \cdot (\mathbf{K} \cdot \nabla T) = 0. \quad (84)
 \end{aligned}$$

Thus, rate of flow of a fluid phase is driven by (1) the gradient of the temperature, which is strongly affected by the interaction of the phases; (2) how temperature affects momentum transfer between phases; (3) the rate at which the solid phase is deforming; (4) the effect of temperature on the pressure of each phase individually – note that if there is no exchange of mass between phases and the fluid phases are considered incompressible, these terms would vanish; and (5) the rate of mass exchanged between phases.

4. Discussion

Consider the following system. Let colloidal sized molecules (polymers, clay platelets, or any sub-micron sized particle) be in a solvent bath such that all the solvent is adsorbed to the molecules. The solvent plus the colloid sized molecules considered as a single body can be thought of as a swelling particle. Now place a large number of the swelling particles in a bulk solvent bath. If the bath is suitably small, then the particles and solvent bath will form a partially saturated porous medium consisting of swelling porous particles. The solvent continues to saturate the particles, but the spaces between particles may contain vapor and/or liquid solvent. The net result is a swelling unsaturated porous medium with three distinct scales. The microscale consists of two phases, the macromolecule and the adsorbed solvent. The mesoscale consists of a homogenization of the macromolecules with the adsorbed solvent. The mesoscale particles when homogenized with the bulk liquid and vapor phase solvent form the macroscale. Such a model is consistent with many natural soils, foods, drug delivery substrates, wood and many other systems. The model proposed herein allows one to simulate flows of mass and energy in such systems.

The governing equations obtained using classical irreversible thermodynamics results in a generalization of De Vries' model (1). In particular, it suggests moisture flow in a porous medium can be driven by temperature gradients [15, 16, 50]. In addition, early experiments [24, 47] also suggest flows may be driven by thermal gradients. We believe the analysis presented here provides a rational framework for this phenomenon. Of specific note in this regard is that the coefficients multiplying ∇T in (38), (44), (B.4–B.6), (84) are nonzero and strongly affected by the phase-interactions due to the heat capacity terms and the fact that the entropy inequality does not mandate that $\partial A^l / \partial T = -\eta^l$ on the mesoscale, nor does it mandate $\partial A^K / \partial T = -\eta^K$ on the macroscale. In both unsaturated media where there is a liquid/vapor interface, and in colloids where the solvent energy is strongly perturbed by the surface, the interfaces liquid–vapor and solid–liquid play a predominant role.

This theoretical work suggests that to improve the understanding of heat and moisture transport in swelling porous media, experiments are needed to study the effects temperature has on the exchange of mechanical momentum between phases, as well as differential swelling of the various phases. In addition, the relative importance of thermal stresses induced on the solid and liquid phases should also be studied.

Appendix A. Nomenclature

Superscripts, subscripts, and other notations

$\mathbf{u} \cdot \mathbf{v}$	$\sum_{i=1}^3 u_i v_i$.
$\mathbf{A} : \mathbf{B}$	$\sum_{i=1}^3 \sum_{j=1}^3 A_{ij} B_{ij}$.
${}^\alpha$	α -phase on mesoscale.
${}^{\alpha\beta}$	$\alpha\beta$ -interface on mesoscale.
${}^{\alpha A}$	α -phase in mesoscale region A on macroscale.
K	K -phase in macroscale REV ($K = A, B, C$) (see Figure 2).
$\hat{\cdot}$	denotes exchange from other interface or phase.
k,l	difference of the two quantities, i.e., ${}^k - {}^l$.
\cdot	Material time derivative with respect to the solid phase (D^s/Dt or D^{sA}/Dt) (2).

Latin symbols

A^α, A^K, A^{KM}	Macroscopic internal (excess surface) specific Helmholtz free energy [J/kg] (16).
$\mathbf{d}^\alpha, \mathbf{d}^K, \mathbf{d}^{KM}$	Symmetric gradient of phase/interface velocity (deformation rate tensor) [1/s] (20).
$\hat{e}_\beta^\alpha, \hat{e}_M^K \hat{e}_{KM}^K$	Mass transfer from phase/interface (subscript) to phase (superscript) per unit REV volume [kg/(s m ³)] (see the conservation of mass equation).
\hat{e}_{KLM}^{KM}	Mass transfer from contact line (subscript) to interface (superscript) per unit REV volume [kg/s-m ³] (see the conservation of mass for interfaces in Appendix C).
E^α, E^K	Energy density [J/kg] (see conservation of energy equation).
E^{KM}	Surface excess energy density [J/kg] (see interfacial conservation of energy equation in Appendix C).
$\mathbf{E}^s, \mathbf{E}^{sA}$	Macroscopic strain tensor of solid phase [-] (20).
\mathbf{E}^{KM}	Macroscopic strain tensor of interface [-] (Appendix C).
\mathbf{F}^{sA}	Gradient of function relating averaged material coordinates of solid phase, \mathbf{X} , and their spatial coordinates, \mathbf{x} ,

	denoted as $\nabla_X \mathbf{X}(\mathbf{X})[m]$ (20).
\mathbf{F}^{KM}	Gradient of function relating averaged material coordinates of interface to their spatial coordinates [m] (20).
\mathbf{g}	External supply of momentum (gravity) [m/s^2].
G^α, G^K, G^{KM}	(excess surface) Gibbs free energy [J/kg] (30).
h^α, h^K, h^{KM}	External supply of energy of phase/interface [$J/(kg s)$] (see conservation of energy).
\mathbf{K}	Second-order tensor coefficient defined in (31) [$J/(m s K)$]. For a thermally isotropic medium, it represents thermal conductivity.
$\mathbf{K}^l, \mathbf{K}^K, \mathbf{K}^{KM}$	Second-order tensor coefficient defined in (28) [$m^3 s/kg$]. Related to hydraulic conductivity in Darcy's law.
p^α, p^K, p^{KM}	Macroscopic thermodynamic pressure of phase/interface [N/m^2] (22).
$\mathbf{q}^\alpha, \mathbf{q}^K, \mathbf{q}^{KM}$	Heat flux vector for the phase/interface [$J/(m^2 s)$], or interface [$J/(m s)$] (see conservation of energy).
$\widehat{Q}_\beta^\alpha, \widehat{Q}_M^K, \widehat{Q}_{KM}^K$	Energy transfer from phase/interface (subscript) to phase (superscript) per unit REV volume [$J/(m^3 s)$] (see the conservation of energy equation).
\widehat{Q}_{KLM}^{KM}	Energy transfer from contact line (subscript) to interface (superscript) per unit REV volume [$J/(m^3 s)$] (see the conservation of energy for interfaces in Appendix C).
t	Time [s].
T	Temperature [K].
$\mathbf{t}^\alpha, \mathbf{t}^K, \mathbf{t}^{KM}$	Stress tensor for the phase [N/m^2], or interface [N/m] (see the conservation of momentum equation).
$\mathbf{t}_e^s, \mathbf{t}_e^{sA}$	Stress in solid phase due to solid matrix strain [N/m^2] (23).
$\mathbf{t}_s^l, \mathbf{t}_{sA}^{sA}$	Stress in liquid phase due to solid matrix strain [N/m^2] (23).
$\widehat{\mathbf{T}}_\beta^\alpha, \widehat{\mathbf{T}}_M^K, \widehat{\mathbf{T}}_{KM}^K$	Momentum transfer through mechanical interactions from phase/interface (subscript) to phase (superscript) per unit REV volume [N/m^3] (see the conservation of momentum equation).
$\widehat{\mathbf{T}}_{KLM}^{KM}$	Momentum transfer through mechanical interactions from contact line (subscript) to interface (superscript) per unit REV volume [N/m^3] (see the conservation of momentum for interfaces in Appendix C).
$\mathbf{u}^\alpha, \mathbf{u}^K$	Velocity of phase (superscript) relative to the medium [m/s].
$\mathbf{v}^\alpha, \mathbf{v}^K$	Velocity of phase (superscript) [m/s].
\mathbf{v}^{KM}	Velocity of interface [m/s].

Greek Symbols

ε^α	Volume fraction of α -phase in mesoscale REV [-].
ε^K	Volume fraction of macroscale region A in macroscale REV [-].
ε^{KM}	Area fraction of KM -interface in macroscale REV [1/m].
$\eta^\alpha, \eta^K, \eta^{KM}$	Entropy of phase/interface [J/(kg-K)].
ν	Fourth-order tensor coefficient defined in (26) [m ² /s]. For an isotropic fluid, this coefficient represents the dynamic viscosity.
$\hat{\mu}$	Constitutive coefficient defined in near-equilibrium capillary relationship (27) [N s/m ²].
ρ^α	Mass density of α -phase averaged over mesoscale REV [kg/m ³].
ρ^K	Mass density of K -phase on macroscale [kg/m ³] so that $\varepsilon^K \rho^K$ is the total mass of K -phase in macroscopic REV divided by the volume of macroscopic REV.
ρ^{KM}	Excess mass density of KM -interface averaged over macroscale REV [kg/m ²] so that $\varepsilon^{KM} \rho^{KM}$ is the total mass of KM -interface in macroscale REV divided by the volume of the macroscale REV.

Appendix B. Thermodynamic Definitions of Coefficients for Three-Scale Heat Equation

The thermodynamic definitions of the coefficients for the three-scale heat equation, given by Equation (83), are given here. Recall that scalar coefficient functions are denoted as γ , vector valued functions are denoted as $\boldsymbol{\gamma}$, and Γ denote second order tensor valued functions. Using $\dot{\mathbf{E}}^s = (\mathbf{F}^s)^T \cdot \mathbf{d}^s \cdot \mathbf{F}^s$, it can be shown that these coefficients are related to the Helmholtz potential by

$$\gamma_1 = T\rho \frac{\partial^2 A}{\partial T^2} = -\rho c_p, \quad (\text{B.1})$$

$$\begin{aligned} \gamma_2 = & p^{1A} + p^{sA} - p^C - \varepsilon^A \rho^{sA} \frac{\partial A^{sA}}{\partial \varepsilon^A} - \varepsilon^A \rho^{1A} \frac{\partial A^{1A}}{\partial \varepsilon^A} - \\ & - \varepsilon^B \rho^B \frac{\partial A^B}{\partial \varepsilon^A} - \varepsilon^C \rho^C \frac{\partial A^C}{\partial \varepsilon^C} - T \frac{\partial}{\partial T} \left(p^{1A} + p^{sA} - p^C - \varepsilon^A \rho^{sA} \frac{\partial A^{sA}}{\partial \varepsilon^A} - \right. \\ & \left. - \varepsilon^A \rho^{1A} \frac{\partial A^{1A}}{\partial \varepsilon^A} - \varepsilon^B \rho^B \frac{\partial A^B}{\partial \varepsilon^A} - \varepsilon^C \rho^C \frac{\partial A^C}{\partial \varepsilon^A} \right) \\ = & \left(\hat{\mu}^A - T \frac{\partial \hat{\mu}^A}{\partial T} \right) \dot{\varepsilon}^A + T \hat{\mu}^A \frac{\partial \dot{\varepsilon}^A}{\partial T}, \end{aligned} \quad (\text{B.2})$$

$$\begin{aligned}
\gamma_3 = & p^B - p^C - \varepsilon^A \rho^{sA} \frac{\partial A^{sA}}{\partial \varepsilon^B} - \varepsilon^A \rho^{lA} \frac{\partial A^{lA}}{\partial \varepsilon^B} - \\
& - \varepsilon^B \rho^B \frac{\partial A^B}{\partial \varepsilon^B} - \varepsilon^C \rho^C \frac{\partial A^C}{\partial \varepsilon^B} - T \frac{\partial}{\partial T} \left(p^B - p^C - \varepsilon^A \rho^{sA} \frac{\partial A^{sA}}{\partial \varepsilon^B} - \right. \\
& \left. - \varepsilon^A \rho^{lA} \frac{\partial A^{lA}}{\partial \varepsilon^B} - \varepsilon^B \rho^B \frac{\partial A^B}{\partial \varepsilon^B} - \varepsilon^C \rho^C \frac{\partial A^C}{\partial \varepsilon^B} \right) \\
= & \left(\widehat{\mu}^B - T \frac{\partial \widehat{\mu}^B}{\partial T} \right) \dot{\varepsilon}^B + T \widehat{\mu}^A \frac{\partial \dot{\varepsilon}^B}{\partial T}, \tag{B.3}
\end{aligned}$$

$$\begin{aligned}
\gamma_4 = & -\varepsilon^A \rho^{lA} \frac{\partial A^{lA}}{\partial \varepsilon^A} \nabla \varepsilon^A - \varepsilon^A \rho^{lA} \frac{\partial A^{lA}}{\partial \varepsilon^B} \nabla \varepsilon^B + p^{lA} \nabla \varepsilon^A - \\
& - \varepsilon^A \rho^{lA} \frac{\partial A^{lA}}{\partial \mathbf{E}^{sA}} : (\mathbf{E}^{sA} \nabla) + \varepsilon^A \rho^{lA} T \frac{\partial^2 A^{lA}}{\partial T^2} \nabla T + T \frac{\partial}{\partial T} \left[\varepsilon^A \rho^{lA} \frac{\partial A^{lA}}{\partial \varepsilon^A} \nabla \varepsilon^A + \right. \\
& \left. + \varepsilon^A \rho^{lA} \frac{\partial A^{lA}}{\partial \varepsilon^B} \nabla \varepsilon^B - p^{lA} \nabla \varepsilon^A + \varepsilon^A \rho^{lA} \frac{\partial A^{lA}}{\partial \mathbf{E}^{sA}} : (\mathbf{E}^{sA} \nabla) \right] \tag{B.4}
\end{aligned}$$

$$\begin{aligned}
= & (\mathbf{K}^{lA})^{-1} \cdot \mathbf{v}^{lA,sA} + \sum_{K=sA,B,C} \widehat{\mathbf{T}}_K^{lA} + \varepsilon^A \rho^{lA} \left(\frac{\partial A^{lA}}{\partial T} + \eta^{lA} - c_p^{lA} \right) \nabla T - \\
& - T \frac{\partial}{\partial T} \left[(\mathbf{K}^{lA})^{-1} \cdot \mathbf{v}^{lA,sA} + \sum_{K=sA,B,C} \widehat{\mathbf{T}}_K^{lA} + \varepsilon^A \rho^{lA} \left(\frac{\partial A^{lA}}{\partial T} + \eta^{lA} \right) \nabla T \right],
\end{aligned}$$

$$\begin{aligned}
\gamma_5 = & -\varepsilon^B \rho^B \frac{\partial A^B}{\partial \varepsilon^A} \nabla \varepsilon^A - \varepsilon^B \rho^B \frac{\partial A^B}{\partial \varepsilon^B} \nabla \varepsilon^B + p^B \nabla \varepsilon^B + \varepsilon^B \rho^B T \frac{\partial^2 A^B}{\partial T^2} \nabla T + \\
& + T \frac{\partial}{\partial T} \left[\varepsilon^B \rho^B \frac{\partial A^B}{\partial \varepsilon^A} \nabla \varepsilon^A + \varepsilon^B \rho^B \frac{\partial A^B}{\partial \varepsilon^B} \nabla \varepsilon^B - p^B \nabla \varepsilon^B \right] \tag{B.5}
\end{aligned}$$

$$\begin{aligned}
= & (\mathbf{K}^B)^{-1} \cdot \mathbf{v}^{B,sA} + \sum_{K=lA,sA,C} \widehat{\mathbf{T}}_K^B + \varepsilon^B \rho^B \left(\frac{\partial A^B}{\partial T} + \eta^B - c_p^B \right) \nabla T - \\
& - T \frac{\partial}{\partial T} \left[(\mathbf{K}^B)^{-1} \cdot \mathbf{v}^{B,sA} + \sum_{K=lA,sA,C} \widehat{\mathbf{T}}_K^B + \varepsilon^B \rho^B \left(\frac{\partial A^B}{\partial T} + \eta^B \right) \nabla T \right],
\end{aligned}$$

$$\gamma_6 = -\varepsilon^C \rho^C \frac{\partial A^C}{\partial \varepsilon^A} \nabla \varepsilon^A - \varepsilon^C \rho^C \frac{\partial A^C}{\partial \varepsilon^B} \nabla \varepsilon^B + p^C \nabla \varepsilon^C + \varepsilon^C \rho^C T \frac{\partial^2 A^C}{\partial T^2} \nabla T +$$

$$\begin{aligned}
& + T \frac{\partial}{\partial T} \left[\varepsilon^C \rho^C \frac{\partial A^C}{\partial \varepsilon^A} \nabla \varepsilon^A + \varepsilon^C \rho^C \frac{\partial A^C}{\partial \varepsilon^B} \nabla \varepsilon^B - p^C \nabla \varepsilon^C \right] \\
= & (\mathbf{K}^C)^{-1} \cdot \mathbf{v}^{C,sA} + \sum_{K=IA,sA,B} \widehat{\mathbf{T}}_K^C + \varepsilon^C \rho^C \left(\frac{\partial A^C}{\partial T} + \eta^C - c_p^C \right) \nabla T - \\
& - T \frac{\partial}{\partial T} \left[(\mathbf{K}^C)^{-1} \cdot \mathbf{v}^{C,sA} + \sum_{K=IA,sA,B} \widehat{\mathbf{T}}_K^C + \varepsilon^C \rho^C \left(\frac{\partial A^C}{\partial T} + \eta^C \right) \nabla T \right],
\end{aligned} \tag{B.6}$$

$$\begin{aligned}
\Gamma_7 = & -\varepsilon^A \rho^{sA} \frac{\partial A^{sA}}{\partial \mathbf{E}^{sA}} - \varepsilon^A \rho^{lA} \frac{\partial A^{lA}}{\partial \mathbf{E}^{sA}} + \varepsilon^A (\mathbf{F}^{sA})^{-1} \cdot \mathbf{t}^{sA} \cdot (\mathbf{F}^{sA})^{-T} + \\
& + \varepsilon^A p^{sA} (\mathbf{F}^{sA})^{-1} \cdot (\mathbf{F}^{sA})^{-T} + T \frac{\partial}{\partial T} \left[\varepsilon^A \rho^{sA} \frac{\partial A^{sA}}{\partial \mathbf{E}^{sA}} + \right. \\
& \left. + \varepsilon^A \rho^{lA} \frac{\partial A^{lA}}{\partial \mathbf{E}^{sA}} - \varepsilon^A p^{sA} (\mathbf{F}^{sA})^{-1} \cdot (\mathbf{F}^{sA})^{-T} \right] \\
= & T \frac{\partial}{\partial T} \left[\varepsilon^A \rho^{sA} \frac{\partial A^{sA}}{\partial \mathbf{E}^{sA}} + \varepsilon^A \rho^{lA} \frac{\partial A^{lA}}{\partial \mathbf{E}^{sA}} - \varepsilon^A p^{sA} (\mathbf{F}^{sA})^{-1} \cdot (\mathbf{F}^{sA})^{-T} \right] \\
= & T \frac{\partial}{\partial T} [\varepsilon^A (\mathbf{F}^{sA})^{-1} \cdot \mathbf{t}^{sA} \cdot (\mathbf{F}^{sA})^{-T}], \tag{B.7}
\end{aligned}$$

$$\begin{aligned}
\Gamma_8 = & \varepsilon^A p^{lA} \mathbf{I} + \varepsilon^A \mathbf{t}^{lA} - \varepsilon^A T \frac{\partial p^{lA}}{\partial T} \mathbf{I} \\
= & \varepsilon^A \rho^{lA} \mathbf{v}^{lA} : \mathbf{d}^{lA} - \varepsilon^A T \frac{\partial p^{lA}}{\partial T} \mathbf{I}, \tag{B.8}
\end{aligned}$$

$$\begin{aligned}
\Gamma_9 = & \varepsilon^B p^B \mathbf{I} + \varepsilon^B \mathbf{t}^B - \varepsilon^B T \frac{\partial p^B}{\partial T} \mathbf{I} \\
= & \varepsilon^B \rho^B \mathbf{v}^B : \mathbf{d}^B - \varepsilon^B T \frac{\partial p^B}{\partial T} \mathbf{I}, \tag{B.9}
\end{aligned}$$

$$\begin{aligned}
\Gamma_{10} = & \varepsilon^C p^C \mathbf{I} + \varepsilon^C \mathbf{t}^C - \varepsilon^C T \frac{\partial p^C}{\partial T} \mathbf{I} \\
= & \varepsilon^C \rho^C \mathbf{v}^C : \mathbf{d}^C - \varepsilon^C T \frac{\partial p^C}{\partial T} \mathbf{I}, \tag{B.10}
\end{aligned}$$

$$\gamma_{KM} = \frac{p^M}{\rho^M} - \frac{p^K}{\rho^K} - T \frac{\partial}{\partial T} \left(\frac{p^M}{\rho^M} - \frac{p^K}{\rho^K} \right), \tag{B.11}$$

where $\rho A = \varepsilon^l \rho^l A^l + \varepsilon^s \rho^s A^s$, and the molar heat capacities for each fluid phase and the porous medium are (see [14], pp. 84, 186)

$$c_p^K = T \left(\frac{\partial \eta^K}{\partial T} \right), \quad K = lA, B, C, \quad (\text{B.12})$$

$$\rho c_p = \sum_{K=lA, sA, B, C} \varepsilon^K \rho^K c_p^K, \quad (\text{B.13})$$

where c_p^K may be a function of the volume fractions. The second form of equations (B.2)–(B.10) were obtained by incorporating constitutive relations (73)–(80).

Appendix C. Three-Scale Governing Equations with Interfacial Effects

In this section, we provide the governing equations for the three-scale model where interfacial effects are not neglected. The derivation of the equations are not provided, as the ideas are presented in Section 3. The details regarding the physical interpretation of interfacial thermodynamic variables at the mesoscale (two-phase model) are given in [26, 44], and for the three-scale model in [6, 7]. Referring to Figure 2, there are six interfaces. Interface lAB is the macroscopic interface between the vicinal fluid of the clay particle and the bulk phase B , where B is a fluid phase – either gas or liquid. Other interfaces include lAC , sAB , sAC , lsA and BC . It is assumed that contact lines (the intersection of three interfaces) have negligible thermodynamic properties, although this too can be incorporated into the current model [29]. The definition of the variables presented in the following equations are given in Appendix A.

The conservation of mass for the bulk phase $K = lA, sA, B, C$ is given by

$$\frac{D^K(\varepsilon^K \rho^K)}{Dt} + \varepsilon^K \rho^K \nabla \cdot \mathbf{v}^K = \sum_{M \neq K} \hat{e}_{KM}^K, \quad K, M = lA, sA, B, C, \quad (\text{C.1})$$

where \hat{e}_{KM}^K represents the net mass gained by the K -phase from the KM interface.

The conservation of mass for the KM interface is given by

$$\begin{aligned} & \frac{D^{KM}(\varepsilon^{KM} \rho^{KM})}{Dt} + \varepsilon^{KM} \rho^{KM} \nabla \cdot \mathbf{v}^{KM} \\ &= \sum_{L \neq K, M} \hat{e}_{KLM}^{KM} - \hat{e}_{KM}^K - \hat{e}_{KM}^M, \quad K, L, M = lA, sA, B, C, \end{aligned} \quad (\text{C.2})$$

where ε^{KM} is the interfacial area density of interface KM , with the exception that we define $\varepsilon^{lsA} = \varepsilon^A$ (see [7] for details). Further, \hat{e}_{KLM}^{KM} represents the amount of mass gained by interface KM through the contact line KLM . The net mass the

contact line has is zero (by assumption), and hence there is a restriction on the exchange terms:

$$\sum_{PQ=KL, KM, LM} \hat{e}_{KLM}^{PQ} = 0. \quad (\text{C.3})$$

Similarly, the conservation of momentum for the KM -phase is

$$\begin{aligned} & \varepsilon^{KM} \rho^{KM} \frac{D^{KM} \mathbf{v}^{KM}}{Dt} - \nabla \cdot (\varepsilon^{KM} \mathbf{t}^{KM}) - \varepsilon^{KM} \rho^{KM} \mathbf{g} \\ &= \sum_{L \neq K, M} \widehat{\mathbf{T}}_{KLM}^{KM} - \widehat{\mathbf{T}}_{KM}^K - \widehat{\mathbf{T}}_{KM}^M, \quad K, L, M = 1A, sA, B, C, \end{aligned} \quad (\text{C.4})$$

with the restriction

$$\sum_{PQ=KL, KM, LM} (\widehat{\mathbf{T}}_{KLM}^{PQ} + \hat{e}_{KLM}^{PQ} \mathbf{v}^{PQ}) = 0. \quad (\text{C.5})$$

The conservation of energy for interface KM is given by

$$\begin{aligned} & \varepsilon^{KM} \rho^{KM} \frac{D^{KM} E^{KM}}{Dt} - \varepsilon^{KM} \mathbf{t}^{KM} : \nabla \mathbf{v}^{KM} - \nabla \cdot (\varepsilon^{KM} \mathbf{q}^{KM}) - \varepsilon^{KM} \rho^{KM} h^{KM} \\ &= \sum_{L \neq K, M} \widehat{Q}_{KLM}^{KM} - [\widehat{Q}_{KM}^K + \widehat{\mathbf{T}}_{KM}^K \cdot \mathbf{v}^{K, KM} + \\ & \quad + \hat{e}_{KM}^K (E^{K, KM} + \frac{1}{2} \mathbf{v}^{K, KM} \cdot \mathbf{v}^{K, KM})] - \\ & \quad - [\widehat{Q}_{KM}^M + \widehat{\mathbf{T}}_{KM}^M \cdot \mathbf{v}^{M, KM} + \hat{e}_{KM}^M (E^{M, KM} + \frac{1}{2} \mathbf{v}^{M, KM} \cdot \mathbf{v}^{M, KM})], \end{aligned} \quad (\text{C.6})$$

where the restriction is now

$$\sum_{PQ=KL, KM, LM} [\widehat{Q}_{KLM}^{PQ} + \widehat{\mathbf{T}}_{KLM}^{PQ} \cdot \mathbf{v}^{PQ} + \hat{e}_{KLM}^{PQ} (E^{PQ} + \frac{1}{2} \mathbf{v}^{PQ} \cdot \mathbf{v}^{PQ})] = 0. \quad (\text{C.7})$$

The constitutive independent variables for this model are

$$\begin{aligned} & \varepsilon^A, \varepsilon^B, \varepsilon^{AB}, \varepsilon^{AC}, \varepsilon^{BC}, \nabla \varepsilon^A, \nabla \varepsilon^B, \nabla \varepsilon^{AB}, \nabla \varepsilon^{AC}, \nabla \varepsilon^{BC}, \\ & T, \nabla T, \rho^K, \mathbf{d}^K, \mathbf{v}^{K, sA}, \quad K = 1A, B, C \\ & \rho^{sA}, \mathbf{E}^{sA}, \nabla \rho^{sA}, \nabla \mathbf{E}^{sA}, \rho^{KL}, \mathbf{E}^{KL}, \mathbf{v}^{KL, sA}, \nabla \rho^{KL}, \nabla \mathbf{E}^{KL}, \\ & KL = lsA, lAB, lAC, sAB, sAC, BC. \end{aligned} \quad (\text{C.8})$$

The interfacial pressures are defined thermodynamically as

$$p^{KM} = (\rho^{KM})^2 \frac{\partial A^{KM}}{\partial \rho^{KL}}. \quad (\text{C.9})$$

The near-equilibrium capillary pressure relations are

$$\begin{aligned} p^{1A} + p^{sA} + p^{lsA} - p^B &= \varepsilon^A \rho^{1A} \frac{\partial A^{1A}}{\partial \varepsilon^A} + \varepsilon^A \rho^{lsA} \frac{\partial A^{lsA}}{\partial \varepsilon^A} - \varepsilon^B \rho^B \frac{\partial A^B}{\partial \varepsilon^B} + \\ &+ \sum_{KM=1AB,1AC,sAB,sAC} \varepsilon^{KM} \rho^{KM} \frac{\partial A^{KM}}{\partial \varepsilon^A} - \\ &- \sum_{KM=1AB,sAB,BC} \varepsilon^{KM} \rho^{KM} \frac{\partial A^{KM}}{\partial \varepsilon^B} + \hat{\mu}^A \frac{D^{sA} \varepsilon^A}{Dt}, \end{aligned} \quad (C.10)$$

$$\begin{aligned} p^B - p^C &= \varepsilon^B \rho^B \frac{\partial A^B}{\partial \varepsilon^B} - \varepsilon^C \rho^C \frac{\partial A^C}{\partial \varepsilon^C} + \sum_{KM=1AB,sAB,BC} \varepsilon^{KM} \rho^{KM} \frac{\partial A^{KM}}{\partial \varepsilon^B} - \\ &- \sum_{KM=1AC,sAC,BC} \varepsilon^{KM} \rho^{KM} \frac{\partial A^{KM}}{\partial \varepsilon^C} + \hat{\mu}^B \frac{D^{sA} \varepsilon^B}{Dt}. \end{aligned} \quad (C.11)$$

Darcy's law for a bulk phase fluid K ($K = B, C$) is now

$$\begin{aligned} \mathbf{v}^{K,sA} &= \mathbf{K}^K \left[-\varepsilon^K \nabla p^K + \varepsilon^K \rho^K \mathbf{g} - \varepsilon^K \rho^K \frac{\partial A^K}{\partial \varepsilon^K} \nabla \varepsilon^K - \right. \\ &\quad \left. - \varepsilon^K \rho^K \frac{\partial A^K}{\partial \varepsilon^{AK}} \nabla \varepsilon^{AK} - \varepsilon^K \rho^K \frac{\partial A^K}{\partial \varepsilon^{BC}} \nabla \varepsilon^{BC} + \nabla \cdot (\varepsilon^K \rho^K \mathbf{v}^K : \mathbf{d}^K) \right]. \end{aligned} \quad (C.12)$$

The heat equation has the following form

$$\begin{aligned} \gamma_1 \dot{T} + \gamma_2 \dot{\varepsilon}^A + \gamma_3 \dot{\varepsilon}^B + \sum_{KM} \gamma_4^{KM} \dot{\varepsilon}^{KM} + \sum_K \gamma_5^K \cdot \mathbf{v}^{K,sA} + \sum_{KM} \gamma_6^{KM} \cdot \mathbf{v}^{KM,sA} + \\ + \boldsymbol{\Gamma}_7 : \dot{\mathbf{E}}^{sA} + \sum_{KM} \boldsymbol{\Gamma}_8^{KM} : \dot{\mathbf{E}}^{KM} + \sum_K \boldsymbol{\Gamma}_9^K : \mathbf{d}^K + \sum_K \sum_{M \neq K} \gamma_{KM}^K \hat{e}_{KM}^K + \\ + \sum_{KM} \sum_{L \neq K,M} \gamma_{KLM}^{KM} \hat{e}_{KLM}^{KM} + \nabla \cdot (\mathbf{K} \nabla T) + \rho h = 0, \end{aligned} \quad (C.13)$$

where scalar coefficient functions are denoted as γ , vector valued functions are denoted as $\boldsymbol{\gamma}$, and $\boldsymbol{\Gamma}$ denote second order tensor valued functions. It can be shown that these coefficients are related to the Helmholtz potential by [6, 8]

$$\gamma_1 = -\rho c_p, \quad (C.14)$$

$$\gamma_2 = \hat{\mu}^A \dot{\varepsilon}^A - T \frac{\partial}{\partial T} (\hat{\mu}^A \dot{\varepsilon}^A), \quad (C.15)$$

$$\gamma_3 = \widehat{\mu}^B \dot{\varepsilon}^B - T \frac{\partial}{\partial T} (\widehat{\mu}^B \dot{\varepsilon}^B), \quad (\text{C.16})$$

$$\gamma_4^{KM} = \widehat{\mu}^{KM} \dot{\varepsilon}^{KM} - T \frac{\partial}{\partial T} (\widehat{\mu}^{KM} \dot{\varepsilon}^{KM}), \quad (\text{C.17})$$

$$\begin{aligned} \gamma_5^K &= \mathbf{K}_K^{-1} \cdot \mathbf{v}^{K,sA} + \sum_{M \neq K} \widehat{\mathbf{T}}_{KM}^K + \varepsilon^K \rho^K \left(\frac{\partial A^K}{\partial T} + \eta^K - c_p^K \right) \nabla T - \\ &- T \frac{\partial}{\partial T} \left[\mathbf{K}_K^{-1} \cdot \mathbf{v}^{K,sA} + \sum_{M \neq K} \widehat{\mathbf{T}}_{KM}^K + \varepsilon^K \rho^K \left(\frac{\partial A^K}{\partial T} + \eta^K \right) \nabla T \right], \end{aligned} \quad (\text{C.18})$$

$$\begin{aligned} \gamma_6^{KM} &= \mathbf{K}_{KM}^{-1} \cdot \mathbf{v}^{KM,sA} + \sum_{L \neq K,M} \widehat{\mathbf{T}}_{KLM}^{KM} - \widehat{\mathbf{T}}_{KM}^K - \widehat{\mathbf{T}}_{KM}^M + \\ &+ \varepsilon^{KM} \rho^{KM} \left(\frac{\partial A^{KM}}{\partial T} + \eta^{KM} - c_p^{KM} \right) \nabla T - \\ &- T \frac{\partial}{\partial T} \left[\mathbf{K}_{KM}^{-1} \cdot \mathbf{v}^{KM,sA} + \sum_{L \neq K,M} \widehat{\mathbf{T}}_{KLM}^{KM} - \widehat{\mathbf{T}}_{KM}^K - \widehat{\mathbf{T}}_{KM}^M + \right. \\ &\left. + \varepsilon^{KM} \rho^{KM} \left(\frac{\partial A^{KM}}{\partial T} + \eta^{KM} \right) \nabla T \right], \end{aligned} \quad (\text{C.19})$$

$$\Gamma_7 = T \frac{\partial}{\partial T} [\varepsilon^A (\mathbf{F}^{sA})^{-1} \cdot \mathbf{t}^{sA} \cdot (\mathbf{F}^{sA})^{-T}], \quad (\text{C.20})$$

$$\Gamma_8^{KM} = T \frac{\partial}{\partial T} [\varepsilon^{KM} (\mathbf{F}^{KM})^{-1} \cdot \mathbf{t}^{KM} \cdot (\mathbf{F}^{KM})^{-T}], \quad (\text{C.21})$$

$$\Gamma_9^K = \varepsilon^K \rho^K \mathbf{v}^K : \mathbf{d}^K - \varepsilon^K T \frac{\partial p^K}{\partial T} \mathbf{I}, \quad (\text{C.22})$$

$$\gamma_{KM}^K = \frac{p^{KM}}{\rho^{KM}} - \frac{p^K}{\rho^K} - T \frac{\partial}{\partial T} \left(\frac{p^{KM}}{\rho^{KM}} - \frac{p^K}{\rho^K} \right), \quad (\text{C.23})$$

$$\gamma_{KLM}^{KM} = - \frac{p^{KM}}{\rho^{KM}} + T \frac{\partial}{\partial T} \left(\frac{p^{KM}}{\rho^{KM}} \right). \quad (\text{C.24})$$

Acknowledgements

Partial support for this work arises from NSF Grant #9510066-BES, and ARO grant #DAAG55-98-1-0228.

References

1. Achanta, S. and Cushman, J. H.: Non-equilibrium swelling and capillary pressure relations for colloidal systems, *J. Col. Int. Sci.* **168** (1994), 266–268.
2. Achanta, S., Cushman, J. H. and Okos, M. R.: On multicomponent, multiphase thermomechanics with interfaces, *Int. J. Engng. Sci.* **32**(11) (1994), 1717–1738.
3. Anderson, T. B. and Jackson, R.: Fluidized beds: equations of motion, *Ind. Engng. Chem. Fundam.* **6**(4) (1967), 527–536
4. Baveye, P. and Sposito, G.: The operational significance of the continuum hypothesis in the theory of water movement through soils and aquifers, *Water Resour. Res.* **20**(5) (1984), 521–530.
5. Bear, J.: *Dynamics of Fluids in Porous Media*, Dover, New York, 1972.
6. Bennethum, L. S.: Multiscale, hybrid mixture theory for swelling systems with interfaces, PhD Thesis, Purdue University, West Lafayette, Indiana, 47907, 1994.
7. Bennethum, L. S. and Cushman, J. H.: Multiscale, hybrid mixture theory for swelling systems – I: Balance laws, *Int. J. Engng. Sci.* **34**(2) (1996a), 125–145.
8. Bennethum, L. S. and Cushman, J. H.: Multiscale, hybrid mixture theory for swelling systems – II: Constitutive theory, *Int. J. Engng. Sci.* **34**(2) (1996b), 147–169.
9. Bennethum, L. S. and Giorgi, T.: Generalized Forchheimer Law for two-phase flow based on hybrid mixture theory, *Transport in Porous Media*, **26**(3) (1997), 261–275.
10. Bennethum, L. S., Murad, M. A. and Cushman, J. H.: Clarifying mixture theory and the macroscale chemical potential for porous media, *Int. J. Engng. Sci.* **34**(14) (1996), 1611–1621.
11. Bennethum, L. S., Murad, M. A. and Cushman, J. H.: Modified Darcy's law, Terzaghi's effective stress principle and Fick's law for swelling clay soils, *Comput. Geotech.* **20**(3/4) (1997), 245–266.
12. Bouddour, A., Auriault, J.-L. and Mhamdi-Alaoui, M.: Heat and mass transfer in wet porous media in presence of evaporation condensation. *Int. J. Heat Mass Transfer* **41** (1993), 2263–2277.
13. Bowen, R. M.: Compressible porous media models by use of the theory of mixtures. *Int. J. Engng. Sci.* **20** (1982), 697–735.
14. Callen, H. B.: *Thermodynamics and an Introduction to Thermostatistics*, John Wiley and Sons, New York, 1985.
15. Carey, J. W.: Onsager's relation and nonisothermal diffusion of water vapor, *J. Phys. Chem.* **67** (1963), 126–129.
16. Carey, J. W.: An evaporation experiment and its irreversible thermodynamics, *Int. J. Heat Mass Transfer* **7** (1964), 531–538.
17. Coleman, B. D. and Noll, W.: The thermodynamics of elastic materials with heat conduction and viscosity, *Arch. Rat. Mech. Anal.* **13** (1963), 167–178.
18. Cushman, J. H.: Multiphase transport based on compact distributions, *Acta Applicandae Mathematicae* **3** (1985), 239–254.
19. Cushman, J. H.: An introduction to fluids in hierarchical porous media, In: J. H. Cushman (ed.), *Dynamics of Fluid in Hierarchical Porous Media*, Academic Press, New York, 1990a, pp. 1–6.
20. Cushman, J. H.: Molecular-scale Lubrication, *Nature* **347**(6290) (1990b), 227–228.
21. Cushman, J. H.: *The Physics of Fluids in Hierarchical Porous Media: Angstroms to Miles*, Kluwer Academic, Dordrecht–Boston, 1997.
22. Cushman, J. H., Hu, X. and Ginn, T. R.: Nonequilibrium statistical mechanics of preasymptotic dispersion, *J. Stat. Phys.* **75** (1994), 859–878.
23. de Vries, D. A.: Simultaneous transfer of heat and moisture in porous media, *Transac. Am. Geophys. Union* **39**(5) (1958), 909–916.
24. Deryaguin, B. V. and Melnikova, M. K.: Experimental study of the migration of water through the soil under the influence of salt concentration, temperature, and moisture gradients, In: *Int. Congr. Soil Sci.*, Trans. 6th (Paris), 1956, pp. 305–314.

25. Eringen, A. C.: *Mechanics of Continua*, John Wiley and Sons, New York, 1967.
26. Gray, W. G. and Hassanizadeh, S. M.: Averaging theorems and averaged equations for transport of interface properties in multiphase systems, *Int. J. Multiphase Flow* **15** (1989), 81–95.
27. Gray, W. G. and Hassanizadeh, S. M.: Paradoxes and realities in unsaturated flow theory, *Water Resour. Res.* **27** (1991a), 1847–1854.
28. Gray, W. G. and Hassanizadeh, S. M.: Unsaturated flow theory including interfacial phenomena, *Water Resour. Res.* **27** (1991b), 1855–1863.
29. Gray, W. G. and Hassanizadeh, S. M.: Macroscale continuum mechanics for multiphase porous–media flow including phases, interfaces, common lines, and common points, *Adv. Water Resour.* **21**(4) (1998), 261–281.
30. Grim, R. E.: *Clay Mineralogy*, McGraw-Hill, New York, 1968.
31. Groetsch, C. W.: *Elements of Applicable Functional Analysis*, Marcel Dekker, New York, 1980.
32. Hadas, A.: Evaluation of theoretically predicted thermal conductivities of soils under field and laboratory conditions, *Soil Sci. Soc. Am. J.* **41** (1980), 460–466.
33. Hassanizadeh, S. M.: Derivation of basic equations of mass transport in porous media, Part 1. Macroscopic balance laws, *Adv. Water Resour.* **9** (1986a), 196–206.
34. Hassanizadeh, S. M.: Derivation of basic equations of mass transport in porous media, Part 2. Generalized Darcy's and Fick's laws, *Adv. Water Resour.* **9** (1986b), 207–222.
35. Hassanizadeh, S. M. and Gray, W. G.: General conservation equations for multiphase systems: 1. Averaging procedure, *Adv. Water Resour.* **2** (1979a), 131–144.
36. Hassanizadeh, S. M. and Gray, W. G.: General conservation equations for multiphase systems: 2. Mass, momenta, energy, and entropy equations, *Adv. Water Resour.* **2** (1979b), 191–208.
37. Hassanizadeh, S. M. and Gray, W. G.: General conservation equations for multiphase systems: 3. Constitutive theory for porous media, *Adv. Water Resour.* **3** (1980), 25–40.
38. Hassanizadeh, S. M. and Gray, W. G.: High velocity flow in porous media, *Transport in Porous Media* **2** (1987), 521–531.
39. Hassanizadeh, S. M. and Gray, W. G.: Thermodynamic basis of capillary pressure in porous media, *Water Resour. Res.* **29**(10) (1993a), 3389–3405.
40. Hassanizadeh, S. M. and Gray, W. G.: Toward an improved description of the physics of two-phase flow, *Adv. Water Resour.* **16** (1993b), 53–67.
41. Israelachvili, J.: *Intermolecular and Surface Forces*, Academic Press, New York, 1992.
42. Low, P. F.: Nature and properties of water in montmorillonite-water systems, *J. Soil Sci. Soc. Am.* **43** (1979), 651–658.
43. Low, P. F.: The swelling of clay, II. Montmorillonites-water systems, *J. Soil Sci. Soc. Am.* **44** (1980), 667–676.
44. Moeckel, G. P.: Thermodynamics of an interface, *Arch. Rat. Mech. Anal.* **57** (1975), 255–280.
45. Murad, M. A., Bennethum, L. S. and Cushman, J. H.: A multi-scale theory of swelling porous media: I. Application to one-dimensional consolidation, *Transport in Porous Media* **19** (1995), 93–122.
46. Murad, M. A. and Cushman, J. H.: Multiscale flow and deformation in hydrophilic swelling porous media, *Int. J. Engng. Sci.* **34**(3) (1996), 313–336.
47. Rollins, R. L., Spangler, M. G. and Kirkham, D.: Movement of Soil Moisture Under a Thermal Gradient, *Highway Research Board Proc.* **33** (1954), 492–508.
48. Schoen, M., Diestler, D. J. and Cushman, J. H.: Fluids in micropores. I. Structure of a simple classical fluid in a slit-pore, *J. Chem. Phys.* **87**(9) (1987), 5464–5476.
49. Showalter, R.: Diffusion models with microstructure, *Transport in Porous Media* **6** (1991), 567–580.
50. Taylor, S. A. and Carey, J. W.: Analysis of simultaneous flow of water and heat or electricity with the thermodynamics of irreversible processes, In: *7th Int. Congr. of Soil Sci. Trans.*, Vol. 1. 1960, pp. 80–90.
51. Terzaghi, K.: *Theoretical Soil Mechanics*, John Wiley and Sons, New York, 1943.

52. Truesdell, C. and Toupin, R. A. The classical field theories, In: S. Flügge ed., *Handbuch der Physik*, Springer-Verlag, New York, 1960.
53. Whitaker, S.: Simultaneous heat, mass, and momentum transfer in porous media: A theory of drying, *Adv. Heat Transfer* (1977), pp. 119-203.



PERGAMON

International Journal of Engineering Science 38 (2000) 517–564

International
Journal of
Engineering
Science

www.elsevier.com/locate/ijengsci

Thermomechanical theories for swelling porous media with microstructure

Márcio A. Murad^{a,b,*}, John H. Cushman^c

^a Laboratorio Nacional de Computacao Cientifica, Petropolis, RJ, Caixa postal 95113, Brazil

^b Instituto Politecnico/UERJ, Nova, Friburgo, RJ 28601, Brazil

^c Center for Applied Math, Math Sciences Building, Purdue University, W. Lafayette, IN 47907, USA

Received 4 March 1998; received in revised form 3 February 1999; accepted 26 April 1999

Abstract

Thermomechanical microstructural dual porosity models for swelling porous media incorporating coupled effects of hydration, heat transfer and mechanical deformation are proposed. These models are obtained by generalizing the three-scale system of Murad and Cushman [56,57] to accommodate heat transfer effects and their influence on swelling. The microscale consists of macromolecular structures (clay platelets, polymers, shales, biological tissues, gels) in a solvent (adsorbed water), both of which are considered as distinct nonoverlaid continua. These continua are homogenized to the meso (intermediate scale) in the spirit of hybrid mixture theory (HMT), so that at the mesoscale they may be thought of as two overlaying continua. Application of HMT leads to a two-scale model which incorporates coupled thermal and physico-chemical effects between the macromolecules and adsorbed solvent. Further, a three-scale model is obtained by homogenizing the particles (clusters consisting of macromolecules and adsorbed solvent) with the bulk solvent (solvent not within but next to the swelling particles). This yields a macroscopic microstructural model of dual porosity type. In the macroscopic swelling medium the mesoscale particles act as distributed sources/sinks of mass, momentum and energy to the macroscale bulk phase system. A modified Green's function method is used to reduce the dual porosity system to a single-porosity system with memory. The resultant theory provides a rigorous derivation of creep phenomena which are due to delayed intra-particle drainage (e.g. secondary consolidation of clay soils). In addition, the model reproduces a class of lumped-parameter models for fluid flow, heat conduction and momentum transfer where the distributed source/sink transfer function is a classical exchange term assumed proportional to the difference between the potentials in the bulk phase and swelling particles. © 2000 Elsevier Science Ltd. All rights reserved.

Keywords: Swelling clay; Mixture theory; Homogenization; Dual porosity thermal effects; Secondary consolidation; Physico-chemical effects

* Corresponding author. Tel.: +55-2-4233-6149; fax: +55-2-4233-6165.
E-mail address: murad@incc.br (M.A. Murad).

1. Introduction

Due to the physico-chemical forces between phases, many porous media (macromolecular-solvent systems) can swell or shrink resulting in macroscopic behavior which may differ significantly from non-swelling media. Examples of such media include polymers, shales, clays and cartilages. It is crucial to understand the constitutive behavior of these materials for applications involving almost all aspects of life. Swelling polymers have numerous technological applications in drug delivery, contact lenses, semiconductor manufacturing and food stuffs. In oil and gas production swelling shales form 75% of drilled formations and have been responsible for 90% of wellbore instability problems. Clay soils covers 80% of the earth's crust and consequently they play a critical role in all aspects of nutrition on earth. In foundation engineering the clay soil swells and heaves upward or dries out and shrinks causing damage to the foundations of buildings, bridges, highways, and runways. All of these systems have in common a structure that can be loosely identified as a mixture of macromolecules (polymers, clay platelets) and solvent (water, organic fluid). The solvent is either adsorbed to the macromolecules or in bulk (i.e. free of any adsorptive force). The clusters of macromolecules and adsorbed solvent form fine particles which swell under imbibition and shrink under drainage. Although everything derived in this paper can be applied to a wide variety of swelling systems, for ease of exposition, we henceforth restrict our discussion to swelling clay soils.

The thermomechanical response of swelling clays has received great attention. Due to their low hydraulic conductivity, plasticity, swelling and adsorptive capacity for contaminants, clays have been used to inhibit the migration of contaminants to the environment. In isolating contaminants from the biosphere, clays act as natural barriers. In the case of nuclear, heat-generating wastes, canisters of vitrified radioactive waste are buried in compacted clay. The clay acts as a geochemical filter to prevent the migration of radionuclides in groundwater. Efficient heat transfer between the vitrified nuclear wastes and surrounding rocks is one of the desired properties required for the engineered barrier. The heating of compacted bentonitic clays may also lead to expansion and cracking and thus enhance the migration of radionuclides. Other applications of the coupling between mechanical and thermal effects appear in enhanced oil recovery technology, extraction of energy from pressurized geothermal reservoirs and frost heave.

Thermomechanical models for granular non-swelling porous media (e.g. rock or sandstone) have been widely discussed in the literature (see e.g. [7,14,68]). A major assumption underlying these models is that no other forces except those of direct contact (effective stresses and pore pressure) are present. Porous media characterized by the absence of physico-chemical interaction between the pore water and solid matrix, such as granular materials, are governed by the above theories. On the other hand, hydrophilic clays such as smectites (montmorillonites) with 2:1 lattice exhibit complex physico-chemical interaction and their constitutive behavior is significantly more complicated.

Smectitic minerals have a negative charge which is neutralized by exchangeable cations. When a montmorillonite is exposed to water, the water penetrates the superimposed layers and forces them apart causing swelling. The attraction (hydrophilicity) of montmorillonite to water is one of the causes of swelling. The force causing clay to swell upon hydration is commonly called *the hydration force*. Hydration causes the water properties to vary with the proximity to the solid surface [50–52]. The interlamellar water is termed adsorbed water (or vicinal water) to distinguish

it from its bulk or free-phase counterpart (i.e. water free of any adsorptive force). The properties of vicinal water depend in a complex way on the structure of the surfaces and the distance between surfaces [23]. In addition, the large specific surface areas of the 2:1 layer silicates and their charged character magnify the effects of hydration forces. Consequently, unlike granular non-swelling media, whose thermoelastic theories assume non-interacting bulk phase water, the thermomechanics of swelling clays is somewhat different. A macroscopic model for smectic clays requires an accurate description of the anomalous behavior of the vicinal fluid. Hence, the treatment of the adsorbed water as a separate phase from the bulk water is mandatory.

Clusters of clay platelets when hydrated form “particles” consisting of an assemblage of stacked silicate layers and adsorbed water. These particles swell under hydration and shrink under desiccation. In general, intermolecular forces between the adsorbed water and clay minerals have three contributions: (i) a molecular Van der Walls component arising from the long-ranged attraction between clay platelets and the vicinal fluid; (ii) an electrostatic part arising from ionic double layer interaction and (iii) a structural component associated with the hydration forces. Both electrostatic double layer and hydration forces cause the stacked silicate layers to repulse one another and thereby lead to particle swelling. Experimental evidence indicates that for interstices smaller than 50 Å, swelling is due primarily to hydration forces and diffuse double layer forces are believed too weak to explain the anomalous behavior of the adsorbed water (see [25,40,51,52]). At the finest scale (microscale), the adsorbed water is viewed as a thin film coating the mineral surfaces. The presence of hydration forces modifies the behavior of a confined thin film relative to the bulk phase from which the film was formed [23,25,69], Derjaguin [25] defined the microscopic concept of disjoining pressure as an excess in film pressure relative to the bulk phase. The averaged counterpart of the disjoining pressure is the swelling pressure Π defined as an overburden pressure P relative to the bulk pressure p_B ($\Pi \equiv P - p_B$) that must be applied to a saturated mixture of clay and adsorbed water in equilibrium with the bulk water to keep the layers from moving apart. The relationship between Π and the void fraction e , $e \equiv \phi_1/(1 - \phi_1)$ (ϕ_1 denotes the volume fraction) was experimentally measured by Low [50,51] in a classical reverse osmosis swelling experiment with a parallel packing of lamellar montmorillonite clay (see Fig. 1).

Considering $p_B = p_{atm}$, with p_{atm} denoting the atmospheric pressure, Low examined the equilibrium swelling pressure of different montmorillonites saturated with incompressible adsorbed water and found that the dimensionless swelling pressure (Π/p_{atm}) satisfies the empirical relation

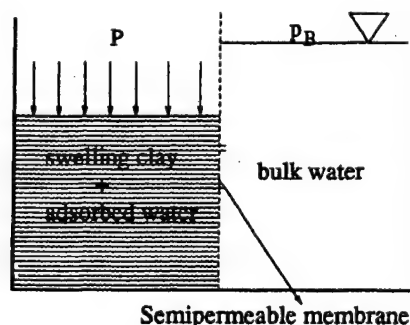


Fig. 1. Low's swelling pressure experiment.

$$\Pi + 1 = \exp \left(\alpha \left(\frac{1}{e} - \frac{1}{e^*} \right) \right) = B \exp \left(\frac{a}{e} \right), \quad (1.1)$$

where e^* is the void fraction when $\Pi = 0$ (when $P = p_B$), α is a constant related to the specific surface area and cation exchange capacity, $B = \exp(-\alpha/e^*)$ and the notation Π for the dimensionless swelling pressure has been maintained.

The effects of temperature on hydration stresses have also been discussed in the literature. (see e.g. [77]). Derjaguin et al. [26] have shown that the effective thermal expansion of the adsorbed water was higher than that of bulk water at low temperatures. Dehydration of the adsorbed water due to heating is a widely accepted phenomenon which has been verified experimentally. As temperature increases the mobility of the adsorbed water increases and it gradually becomes free water. This thermally induced adsorbed water degeneration has been modeled within the framework of the mixture theory by Ma and Hueckel [53]. In this framework the adsorbed water is treated as an immobile phase and the inter-phase adsorbed-bulk water mass transfer is modeled as a source term in the bulk fluid mass balances which are assumed to depend linearly on a temperature rate.

The derivation of macroscale governing equations for thermomechanical processes in porous media may be accomplished within the framework of the hybrid mixture theory (HMT), which is a slight modification of the classical mixture theory of Bowen [15]. In classical mixture theory a single-phase medium composed of N constituents is viewed as N overlaying continua. Bowen [15] extended this idea to model a porous medium so that at the macroscale a two-phase medium is viewed as two overlaying continua. In his work, macroscopic forms of the field equations incorporating exchange terms between the overlaying continua, are postulated. Hassanizadeh and Gray [32,33] showed that if the microscopic field equations are averaged then the terms in Bowen's macroscopic field equations can be identified precisely with microscopic counterparts. The combination of averaging and mixture theory is referred to as *hybrid mixture theory* (HMT). In both of these formulations, the constitutive restrictions are determined at the macroscale by exploiting the entropy inequality using the Coleman and Noll method [21]. HMT has been extensively used by Hassanizadeh and Gray [34] to improve our understanding of two-phase flow in non-swelling porous media.

The mixture theory approach has also been applied to derive a comprehensive macroscopic constitutive theory for swelling porous media (see [28,37,42,53]). In reference [28] Eringen was able to reproduce the extra ad-hoc overburden potential component in Darcy's law for swelling systems (see [61]). Hydration swelling effects have also been captured within alternative non-equilibrium thermodynamic approaches. Using the general principles of irreversible thermodynamics, Biot [13] formulated a theory of poroelastic systems undergoing finite deformations. His framework incorporates a fluid adsorptive component wherein hydration effects are captured upon selection of a proper set of independent constitutive variables for the free energy of the mixture. Biot [13] also obtained a generalized form of Darcy's law wherein the driving mechanism for water flow is the gradient of a gravi-chemical potential. Contrary to classical belief, this chemical potential gradient is more general than a pressure gradient as it involves an additional interaction potential gradient accounting for the adsorptive character of the clay platelets. Further, Achanta et al. [1] formulated an isothermal HMT theory for highly compacted clays wherein constitutive equations, capable of reproducing Low's swelling pressure relation (1.1) at equilib-

rium, were obtained within the Coleman–Noll method of exploitation of the entropy inequality. Achanta's approach provided a rational basis for explaining the water adsorption component in swelling clay pastes. Furthermore, Heidug and Wong [35] formulated a non-equilibrium thermodynamics approach for shale–water–electrolyte systems which also includes the electrostatic component of swelling. The approach is based on the general Onsager's reciprocity relations and leads to a theory of constitution which generalizes Biot's theory of poroelasticity to account for perturbations in the pore fluid's chemistry due to physical-chemical interaction. The theory was improved by Huyghe and Janssen [38] who, neglecting hydration stresses, adopted a Lagrangian form of the entropy inequality to derive a quadriphasic theory of swelling porous media which incorporates both Donnan osmosis and electrical potential as driving forces for fluid flow.

Despite the aforementioned works have attempted to formulate thermodynamically the complex nature of solid–fluid physico-chemical interaction in swelling systems, to the author's knowledge few works have discussed the additional difficulties that arise from the complex hierarchical structure of these systems. Swelling porous media are more accurately treated within *three-scale models*, i.e. the derivation of macroscopic governing equations requires two levels of averaging (micro to meso and meso to macro). Depicted in Fig. 2 is a three-scale porous matrix. Swelling particles are in contact with one another and bulk water. Each particle consists of clay colloids and adsorbed water. At the microscale the model has two phases, the disjoint clay platelets and adsorbed water. The mesoscale (the homogenized microscale) corresponds to the Darcy-scale for adsorbed water, wherein mesoscopic transport equations are obtained by averaging the point microscopic equations. These averaged equations are coupled with Stokesian bulk water equations. At the macroscale, bulk water is homogenized with the mesoscale particles and large scale averaged equations are derived by upscaling the mesoscopic structure. A first attempt towards the extension of HMT to three-scale isothermal swelling systems was presented in [10,11,55–57], (see also [24] for a summary of this early work). In a three-scale picture, the appearance of two levels of hydrodynamics related to adsorbed and bulk water phases occurring simultaneously at disparate space and time scales increases substantially the complexity of the macroscopic governing equations, as the macroscopic model now inherits the fading memory effects associated with the difference in the time scales between the adsorbed and bulk water flows.

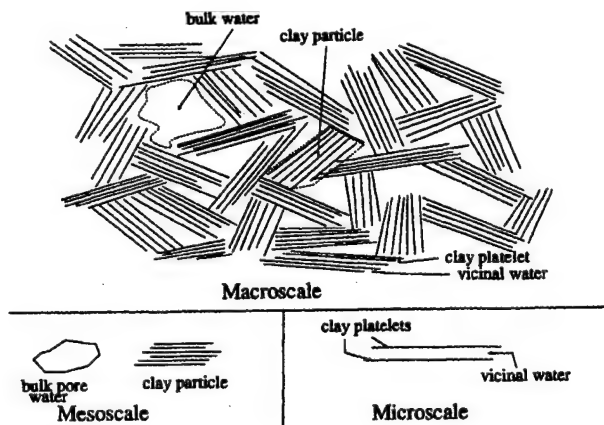


Fig. 2. Three-scale model for clay.

A three-scale model for a swelling medium resembles in form a dual porosity model for fractured media (see e.g. [9,74]). In the macroscopic picture of a dual porosity model, an interconnected network of fractures (playing the role of the bulk system) provides most of the global permeability for macroscopic fluid flow whereas most of the fluid storage takes place in the relatively low permeability matrix block system (analogous to the clay particles). These two systems are coupled via a distributed source/sink transfer function which quantifies the mass exchange between them. In dual porosity systems, one component is essentially responsible for storage and the other for transport. Thus, an accurate description of the source/sink transfer function between the two systems is of utmost importance. Early approaches proposed to describe this mass-transfer function were based on lumped-parameter hydrodynamic models (e.g. [9,74]) wherein the distributed source/sink is given as a classical exchange term, assumed proportional to the difference between the corresponding fractured and matrix (mean) potentials. First proposed for single-phase compressible flow in rigid fissured porous media, lumped-parameter models have been extended to two-phase flows [78], anisotropic systems ([63] within the framework of large scale averaging), isothermal poroelastic fissured media [75] and coupled thermo-poroelasticity ([8]). Lumped-parameter models make use of a time scale assumption where at each time, the intra-block (or intra-particle) fluid is assumed uniformly distributed throughout the block (particle) domain reaching equilibrium instantaneously when disturbed by the bulk phase. By treating the blocks in a lumped-parameter fashion, the particle geometry is suppressed and the distinction between the space and time scales of the bulk phase and clay particles are overlooked [70].

In order to overcome the aforementioned drawbacks of lumped parameter models, *microstructural dual porosity models* for flow in rigid fractured media have been proposed by Arbogast and coworkers [3,4,27]. In this framework, the macroscopic medium is covered by two distinct interacting coexisting systems: the macroscopic system, which is related to the global fracture flow, and the mesoscopic system, which is represented by the matrix blocks at the mesoscale. The macroscopic picture associated to a microstructural dual porosity model is a continuous distribution of mesoscopic matrix blocks with prescribed geometry over the macroscopic fracture domain. These two systems are coupled via a microstructural mass transfer function. Rather than treated it in a simplified lumped parameter manner, (i.e. proportional to a pressure difference), this function is explicitly calculated by solving and averaging the matrix block equations. By incorporating details of the flow inherent to particle geometry the microstructural model explicitly captures the length scales of the physical problem. Consequently the dual porosity model provides a more accurate portrait of the distributed mass exchange between the two coexisting systems.

Extensions of Arbogast and coworkers microstructural models have been proposed by Peszynska [60] for non-isothermal flow in rigid media and by Murad and Cushman [57] for isothermal flow in deformable porous media. Here, we derive microstructural dual porosity models for non-isothermal swelling porous media with the aim of coupling thermal and physico-chemical effects.

We also exploit some consequences of the proposed dual porosity model. We show that our approach is capable of reproducing other well-known models. We begin by showing that application of a modified Green's function technique, developed by Feng and Michaelides [30] for the heat equation, reduces the dual porosity model to a single integro-differential equation of Volterra type. The integro-differential equation is related to some viscoelastic models for secondary con-

solidation (continued deformation of the clay skeleton after the bulk water has been substantially drained). The secondary consolidation stage has been characterized by creep viscoelastic behavior (see e.g. [16,31,41,44,48,73,76]) which arise from the delayed drainage of the adsorbed water after the bulk water has been drained from the larger pores (see [37,72]). Macroscopic viscoelastic models with fading memory, with the macroscopic stress/strain relation represented in terms of hereditary constitutive laws (e.g. Hooke's law with memory), have been postulated to describe delayed exchange processes between micro and macropores (see e.g. [22]). In particular, such hereditary models have also been postulated by Biot [13] aiming at capturing the delayed penetration of the fluid in the micropores due to possible adsorption effects in swelling systems. Within the proposed approach, we show that application of the Green's function method leads to an explicit relation between the microstructural dual porosity model and the parameters appearing in the single-porosity model with memory (e.g. the convolution kernel). Thus, a notable consequence of the approach proposed herein is that it provides a rational basis for explaining hereditary constitutive laws governing secondary compression in terms of micromechanical analysis. Since the macroscopic parameters can explicitly be correlated with microstructure response, our approach furnishes a new direction for a proper interpretation of these coefficients in terms of the knowledge of particle geometry. This correlation provides a better way of representing memory effects in terms of the double-porosity structure of the medium.

We also show how lumped-parameter models can be viewed as special cases of the general microstructural model. Firstly, we reproduce the lumped-heat-capacity system [36] by assuming that particle thermal conductivity is sufficiently large compared to the particle surface-convection heat transfer coefficient. In this context we examine the so-called two-equation models in the sense of Quintard and Whitaker [62,64,65] (see also [43]) wherein different temperatures are assigned to the clay particles and bulk water and the distributed energy transfer function is treated in a lumped parameter fashion. Then we discuss the validity of the one-equation model for which the principle of local thermal equilibrium is valid with a single temperature locally assigned to both clay particles and bulk water. The ideas underlying the validity of two-equation models for heat transfer in rigid porous media have been extensively discussed by Quintard and Whitaker [62,64,65] and Kaviany [43] within the context of volume averaging and also in the context of homogenization by Auriault [5]. Here we clarify the assumptions underlying this approach for swelling porous media. Further, departing from the general microstructural dual porosity model and adopting a time scale assumption in the flow problem we reproduce the lumped-parameter hydrodynamical models wherein a Warren–Root type coupling (proportional to a potential difference) dictates the constitutive behavior of the mass transfer between particles and bulk phase water. Moreover, we relate this result with the well known lumped-parameter isothermal and non-isothermal consolidation theories with double porosity [8,75].

Throughout the development of the article we assume that physico-chemical forces are due to primarily hydration forces. The exchangeable cations are condensed on the clay surface, i.e., they are concentrated in the Stern layer, in such a way that the negative surface charge is effectively screened. In other words, following Low [52], surface hydration is the dominant component of swelling and the diffuse layer contributes only weakly to the swelling pressure. Extensions of the proposed model to the case wherein swelling is due to a combination of electrostatic and hydration forces can be obtained by coupling the proposed approach with the thermodynamical framework developed by Huyghe and Janssen [38].

2. Two-scale thermomechanical model for the clay particles

We begin by reviewing the two-scale results of the mesoscale constitutive theory of Murad and Cushman [56,57] obtained within the framework of the HMT for an isothermal system composed of clay platelets and adsorbed-water (the clay particle). Then we follow the approach of Eringen [28] and incorporate the coupling between thermal and physico-chemical effects by manipulating the energy equation. In this fashion we obtain a proper form of the energy balance for swelling media which incorporate new quantities such as mechanical work of hydration stresses and intrinsic dissipation.

2.1. Non-equilibrium results

Consider the clay particles as a mixture of two phases (the solid clay platelets and liquid adsorbed water) viewed as coexisting continua, which undergo independent motions $x = x_\alpha(X_\alpha, t)$, $\alpha = l, s$ with respect to each reference configuration (here x denotes the spatial position of the particle in the α -phase at time t with respect to a reference position X_α). Let the subscript $\alpha = l, s$ denote the adsorbed liquid and solid phase, respectively, and let ρ_α , t_α , ϕ_α , T_α and A_α denote the averaged density, symmetric stress tensor, volume fraction, temperature and intensive Helmholtz potential of phase α . Further, let the average mesoscopic strain tensor of the solid phase, E_s , be given as

$$E_s = \frac{1}{2}(\mathbf{C}_s - \mathbf{I})$$

where $\mathbf{C}_s = \mathbf{F}_s^T \mathbf{F}_s$ with $\mathbf{F}_s = \text{grad } x_s$ denoting the deformation gradient of the solid phase (with grad denoting differentiation with respect to a material particle on the mesoscale). We shall restrict our analysis to the range of *moderate moisture contents* (see [57]) which includes moisture content greater than that occupied by 10 adsorbed fluid monolayers. In this range, at equilibrium, hydration forces are able to withstand the normal hydrostatic swelling pressure but, on the other hand, deviatoric shear stresses are only supported by effective stresses at equilibrium. Within the framework of HMT, the goal in deriving a constitutive theory capable of capturing particle swelling in the range of moderate moisture content is to postulate dependence of A_l on ϕ_l . This allows the adsorbed liquid structure to be a function of the separation of the clay platelets. Recall that the definition of vicinal or adsorbed water is that water whose properties vary with distance from the solid phase. This change is accounted for on the mesoscale by the volume fraction which is the mesoscopic thermodynamic internal variable which accounts for physico-chemical effects. At the mesoscale, ϕ_l plays an analogous role to thin film thickness, h , at the microscale which is the internal state variable accounting for the structural component of disjoining pressure (see e.g. [25]). If one wants to consider a dryer system, say of an order of one to ten layers of water (2.5 to 25 Å), then the vicinal fluid is even more anomalous. In this case the vicinal water molecules are more ordered and are layered parallel to the surface, so that the fluid, on the microscale, is structured, inhomogeneous, anisotropic, relatively immobile and can actually support a shearing force at equilibrium. In this range A_l also depends on the alignment of the clay platelets and consequently to capture swelling one must replace ϕ_l by the strain tensor E_s .

For simplicity, assume that interfaces contain no thermodynamic properties, entropy fluxes are solely due to heat fluxes, solid and fluid are non-polar, non-reacting phases, all external sources are negligible, the microscopic solid phase is incompressible, and the adsorbed water at the mesoscale is non-viscous. In addition, assume a priori the validity of the principle of local thermal equilibrium between adsorbed water and clay minerals ($T_s = T_l = T$) so that one can locally assign a single temperature to both phases and consequently adopt a one-energy two-scale model in the sense of Quintard and Whitaker [65].

By postulating constitutive dependence of the free energies in the form $A_s = A_s(T, E_s)$ and $A_l = A_l(T, \rho_l, \phi_l)$ and using the Coleman and Noll method of exploiting the entropy inequality [21], Murad and Cushman [56,57] obtained the following constitutive equations for the entropies η_α and the stress tensors t_α

$$\eta_\alpha = -\frac{\partial A_\alpha}{\partial T} \quad \alpha = l, s, \quad (2.1)$$

$$t_l = -p_l I, \quad (2.2)$$

$$t_s = -p_s I + \frac{1}{\phi_s} (t_s^e + t_s^l), \quad (2.3)$$

where the tensors t_s^e and t_s^l are defined by

$$t_s^e \equiv \rho_s \phi_s F_s \frac{\partial A_s}{\partial E_s} F_s^T, \quad t_s^l \equiv \phi_l \phi_s p_* I, \quad p_* \equiv \rho_l \frac{\partial A_l}{\partial \phi_l} \quad (2.4)$$

with p_α denoting the thermodynamic pressure of the α -phase. The pressure p_l of the compressible vicinal fluid has the classical definition

$$p_l \equiv \rho_l^2 \frac{\partial A_l}{\partial \rho_l}. \quad (2.5)$$

For the incompressible clay platelets, p_s is identified with a Lagrange multiplier which arises from exploiting a modified entropy inequality formulation in the sense of Liu [49], obtained by adding the incompressible solid phase mass balance (treated as an internal constraint) to the original entropy inequality (see [55,56] for details).

From (2.3), the difference between granular and swelling media is the physico-chemical stress component t_s^l (or p_*) which arises because we postulated that A_l depends on ϕ_l . To obtain a physical interpretation for this physico-chemical quantity we follow [56,57] and introduce the total particle stress tensor t and the particle thermodynamic pressure p

$$t = \phi_s t_s + \phi_l t_l, \quad p = \phi_l p_l + \phi_s p_s. \quad (2.6)$$

If we multiply (2.2) and (2.3) by ϕ_l and ϕ_s , respectively, and add them we obtain after using (2.6)

$$t = -p I + t_s^e + t_s^l, \quad t_s^l = \phi_l \phi_s p_* I. \quad (2.7)$$

The physical interpretation of (2.7) has been discussed in [56,57] who form an analogy with the results of Hassanizadeh and Gray [33] for non-swelling granular media. If we consider a fixed solid strain E_s and then define the bulk phase (denoted by the subscript B) to be fluid whose properties are unaffected by the solid phase with absence of physico-chemical effects (as in the case of non-swelling granular media), then, by definition, the free energy of a bulk fluid A_B does not change with the proximity of the solid and therefore is independent of ϕ_1 . In this case from (2.4), t_s^l and p_* are zero for a granular medium and t_s^e remains unaltered, as it only depends on the fixed solid strain E_s . Hence the reduced form of (2.7) for granular non-swelling media is

$$\mathbf{t}_B = -p_B \mathbf{I} + \mathbf{t}_s^e \quad (\text{for a non-swelling medium}). \quad (2.8)$$

In classical soil mechanics the above result resembles in form Terzaghi's effective stress principle at the mesoscale for non-swelling media with p_B and \mathbf{t}_s^e normally referred to as pore pressure (or bulk phase pressure) and effective stress tensor, respectively. In classical stress analysis of non-swelling media, p_B has a classical pore pressure definition, analogous to p in (2.6), except that it is equal to both the thermodynamic fluid and solid pressures, (see e.g. [12,33]), i.e.

$$p_B = \phi_s p_s + \phi_l p_l = p_l = p_s, \quad (\text{for a non-swelling medium}). \quad (2.9)$$

The effective stress tensor, \mathbf{t}_s^e , measures stresses induced by mineral to mineral contact and primarily controls the deformation of non-swelling systems such as sands, silts, and low and medium plastic clays such as kaolinite or illite. The modified effective stress principle (2.7) for swelling media has the additional term, t_s^l , which is the stress due to the change in the free energy of the vicinal fluid with volume fraction. In contrast with coarse-grained materials where stress mechanisms are primarily controlled by the contact stresses \mathbf{t}_s^e , the deformation of smectitic clays such as montmorillonite is governed by the additional stress t_s^l . Clearly this additional term accounts for the solid–fluid physico-chemical interactions and can be viewed as a stress structural component arising from surface hydration. Whence, as in Murad and Cushman [56,57], we henceforth call t_s^l and p_* the *hydration stress tensor* and *hydration pressure*, respectively. Note that the modified Terzaghi's principle (2.7) shows an explicit decoupling between elastic and hydration stresses. Other thermodynamic approaches, such as the one proposed by Biot [13], considered the vicinal fluid as part of the solid phase. Consequently the bonding energy associated with the swelling pressure is somewhat obscure, as it is incorporated in the free energy of the “wetted solid phase”. In our approach, physico-chemical effects appear explicitly decoupled from elastic stresses as they are taken into account by postulating the additional dependence of the adsorbed fluid free energy, on an internal variable (the intra-cluster volume fraction). This led to the modified Terzaghi's principle (2.7), which is consistent with some heuristic principle postulated by Hueckel [37], Lambe [46], Morgenstern and Balasubramonian [54], Sridharan and Rao [71] to account for net attractive (A)–repulsive (R) forces between the clay particles (commonly denoted by $(R-A)$).

2.2. One energy equation model

Let v_α be the mass-average velocity of phase α and let D_α/Dt denote the material time derivative following the α -phase satisfying

$$\frac{D_\alpha}{Dt} \equiv \frac{\partial}{\partial t} + \mathbf{v}_\alpha \cdot \nabla, \quad \frac{D_l}{Dt} = \frac{D_s}{Dt} + \mathbf{v}_{l,s} \cdot \nabla, \quad \alpha = l, s, \quad (2.10)$$

where $\mathbf{v}_{l,s} = \mathbf{v}_l - \mathbf{v}_s$ denotes the velocity relative to the solid phase. Since we have assumed that the clay minerals and adsorbed water are at local thermal equilibrium there is no need to consider individual energy balances for each phase. Rather, an energy equation for the mixture as a whole is considered by summing up the energy balances for the individual phases. In terms of the Helmholtz free energy, A_α , the overall energy balance can be expressed as (see [33])

$$\sum_{\alpha=l,s} \phi_\alpha \rho_\alpha \frac{D_\alpha A_\alpha}{Dt} + \phi_\alpha \rho_\alpha \eta_\alpha \frac{D_\alpha T}{Dt} + \phi_\alpha \rho_\alpha T \frac{D_\alpha \eta_\alpha}{Dt} - \phi_\alpha \mathbf{t}_\alpha : \mathbf{d}_\alpha + \text{div}(\phi_\alpha \mathbf{h}_\alpha) - \widehat{Q}_\alpha = 0, \quad (2.11)$$

where $\mathbf{A} : \mathbf{B} = \text{tr}(\mathbf{AB}^T)$ denotes the classical inner product between tensors, \mathbf{d}_α is the symmetric part of $\nabla \mathbf{v}_\alpha$, \mathbf{h}_α is the heat flux, and \widehat{Q}_α is the net exchange of energy between phases. If we denote by $\widehat{\mathbf{T}}_\alpha$ the exchange of momentum to phase α from the other phase, it satisfies the momentum balance

$$\phi_\alpha \rho_\alpha \frac{D_\alpha \mathbf{v}_\alpha}{Dt} - \text{div}(\phi_\alpha \mathbf{t}_\alpha) = \widehat{\mathbf{T}}_\alpha, \quad \alpha = l, s. \quad (2.12)$$

Conservation of momentum and energy for the mixture as a whole requires

$$\sum_{\alpha=l,s} \widehat{\mathbf{T}}_\alpha = \mathbf{0}, \quad \sum_{\alpha=l,s} \widehat{Q}_\alpha = - \sum_{\alpha=l,s} \widehat{\mathbf{T}}_\alpha \cdot \mathbf{v}_\alpha = - \widehat{\mathbf{T}}_l \cdot \mathbf{v}_{l,s}. \quad (2.13)$$

Recalling our constitutive assumptions $A_l = A_l(T, \rho_l, \phi_l)$ and $A_s = A_s(T, E_s)$, using (2.1), (2.4) and (2.5), by the chain rule, the expansions for $D_l A_l / Dt$ and $D_s A_s / Dt$ are

$$\phi_l \rho_l \frac{D_l A_l}{Dt} + \phi_l \rho_l \eta_l \frac{D_l T}{Dt} = \frac{\phi_l p_l}{\rho_l} \frac{D_l \rho_l}{Dt} + \phi_l p_s \frac{D_l \phi_l}{Dt}, \quad (2.14)$$

$$\phi_s \rho_s \frac{D_s A_s}{Dt} + \phi_s \rho_s \eta_s \frac{D_s T}{Dt} - \mathbf{t}_s^e : \mathbf{d}_s = 0, \quad (2.15)$$

where the solid was assumed incompressible ($D_s \rho_s / Dt = 0$) and the relation $D_s E_s / Dt = \mathbf{F}_s^T \mathbf{d}_s \mathbf{F}_s$ [29] was used. Since ρ_s is constant, by adding the mass balances $(\phi_l / \rho_l) D_l \rho_l / Dt + D_l \phi_l / Dt + \phi_l \text{div} \mathbf{v}_l = 0$ and $D_s \phi_s / Dt + \phi_s \text{div} \mathbf{v}_s = 0$ yields

$$\frac{\phi_l}{\rho_l} \frac{D_l \rho_l}{Dt} = - \sum_{\alpha=l,s} \left(\phi_\alpha \text{div} \mathbf{v}_\alpha + \frac{D_\alpha \phi_\alpha}{Dt} \right) = - \sum_{\alpha=l,s} \phi_\alpha \text{div} \mathbf{v}_\alpha - \mathbf{v}_{l,s} \cdot \nabla \phi_l,$$

where the relation (2.10) and the constraint $\phi_l + \phi_s = 1$ have been used. By adding (2.14) to (2.15), using the above result, and (2.10) we obtain

$$\begin{aligned}
\sum_{\alpha=1,s} \phi_\alpha \rho_\alpha \frac{D_\alpha A_\alpha}{Dt} + \sum_{\alpha=1,s} \phi_\alpha \rho_\alpha \eta_\alpha \frac{D_\alpha T}{Dt} - \mathbf{t}_s^e : \mathbf{d}_s &= \phi_1 p_* \frac{D_1 \phi_1}{Dt} + \frac{\phi_1 p_1}{\rho_1} \frac{D_1 \rho_1}{Dt} \\
&= \phi_1 p_* \frac{D_1 \phi_1}{Dt} - p_1 \sum_{\alpha=1,s} \phi_\alpha \operatorname{div} \mathbf{v}_\alpha - p_1 \mathbf{v}_{1,s} \cdot \nabla \phi_1 \\
&= \phi_1 p_* \frac{D_s \phi_1}{Dt} - p_1 \sum_{\alpha=1,s} \phi_\alpha \operatorname{div} \mathbf{v}_\alpha + (\phi_1 p_* - p_1) \mathbf{v}_{1,s} \cdot \nabla \phi_1.
\end{aligned}$$

Together with the constitutive Eqs. (2.2) and (2.3) for the stress tensors and the mass balance for the incompressible solid $D_s \phi_1 / Dt = \phi_s \operatorname{div} \mathbf{v}_s = \phi_s \mathbf{I} : \mathbf{d}_s$ this gives

$$\begin{aligned}
\sum_{\alpha=1,s} \phi_\alpha \rho_\alpha \frac{D_\alpha A_\alpha}{Dt} + \sum_{\alpha=1,s} \phi_\alpha \rho_\alpha \eta_\alpha \frac{D_\alpha T}{Dt} - (\phi_1 p_* - p_1) \mathbf{v}_{1,s} \cdot \nabla \phi_1 \\
&= -p_1 \sum_{\alpha=1,s} \phi_\alpha \operatorname{div} \mathbf{v}_\alpha + (\phi_1 p_* + p_1 - p_s) \frac{D_s \phi_1}{Dt} + \mathbf{t}_s^e : \mathbf{d}_s + (p_s - p_1) \frac{D_s \phi_1}{Dt} \\
&= -p_1 \sum_{\alpha=1,s} \phi_\alpha \mathbf{I} : \mathbf{d}_\alpha + \phi_s (p_1 - p_s + \phi_1 p_*) \mathbf{I} : \mathbf{d}_s + \mathbf{t}_s^e : \mathbf{d}_s + (p_s - p_1) \frac{D_s \phi_1}{Dt} \\
&= -\sum_{\alpha=1,s} \phi_\alpha p_\alpha \mathbf{I} : \mathbf{d}_\alpha + \phi_s \phi_1 p_* \mathbf{I} : \mathbf{d}_s + \mathbf{t}_s^e : \mathbf{d}_s + (p_s - p_1) \frac{D_s \phi_1}{Dt} \\
&= \sum_{\alpha=1,s} \phi_\alpha \mathbf{t}_\alpha : \mathbf{d}_\alpha + (p_s - p_1) \frac{D_s \phi_1}{Dt}.
\end{aligned}$$

Using the above expression and (2.13) in the energy balance (2.11) gives

$$\sum_{\alpha=1,s} \phi_\alpha \rho_\alpha T \frac{D_\alpha \eta_\alpha}{Dt} + \operatorname{div}(\phi_\alpha \mathbf{h}_\alpha) = \Phi, \quad (2.16)$$

where Φ denotes the intrinsic dissipation function

$$\Phi \equiv (p_1 - p_s) \frac{D_s \phi_1}{Dt} - (\widehat{\mathbf{T}}_1 + (\phi_1 p_* - p_1) \nabla \phi_1) \cdot \mathbf{v}_{1,s} \quad (2.17)$$

Note from (2.9) that in the case of a non-swelling granular media, $p_1 = p_s$ and therefore the first term in the r.h.s. of (2.17) vanishes. In this case Φ has only one contribution due to the Darcy velocity $\mathbf{v}_{1,s}$.

2.3. Equilibrium

At thermodynamic equilibrium $\{\mathbf{v}_{1,s}, D_s \phi_1 / Dt, \nabla T\}$ vanish. Following [33], it is postulated that at equilibrium entropy is a maximum and entropy generation is a minimum. Application of these conditions to the entropy inequality yields at equilibrium (see [56] for details)

$$\hat{\mathbf{T}}_1 = (p_l - p_* \phi_l) \nabla \phi_l, \quad (2.18)$$

$$p_l = p_s = p, \quad (2.19)$$

$$\sum_{\alpha=l,s} \phi_\alpha \mathbf{h}_\alpha = \mathbf{0}. \quad (2.20)$$

Eq. (2.20) shows that the overall heat flux vanishes at equilibrium. Relation (2.19) states that at equilibrium, the thermodynamic pressures of the solid and adsorbed fluid phases are equal. Recall that this result reproduces (2.9) which is a result that has been extensively used for granular non-swelling media even away from equilibrium (see e.g. [33]). By combining (2.18) with (2.2) and (2.12) we obtain at equilibrium

$$\nabla p_l + p_* \nabla \phi_l = 0. \quad (2.21)$$

Note from (2.21) that the pressure gradient is counter-balanced by a gradient in the volume fraction. This implies that it is possible to have no flow even with a net pressure difference across the clay. Defining the chemical potential (molar Gibbs free energy) μ_l of the adsorbed water as

$$\mu_l \equiv A_l + \rho_l^{-1} p_l, \quad (2.22)$$

and using definitions (2.5), (2.1) and (2.4) for p_l , η_l and p_* we have by the chain rule

$$d\mu_l = d\left(\frac{p_l}{\rho_l}\right) + dA_l = d\left(\frac{p_l}{\rho_l}\right) + \frac{p_l}{\rho_l^2} d\rho_l - \eta_l dT + \frac{p_*}{\rho_l} d\phi_l = \frac{1}{\rho_l} (dp_l + p_* d\phi_l) - \eta_l dT \quad (2.23)$$

which represents the Gibbs–Duhem relation for the vicinal liquid. Using (2.21) and recalling that $dT = 0$ at equilibrium we get

$$d\mu_l = 0 \rightarrow \mu_l = \text{constant}.$$

This is the well known result that at equilibrium the chemical potential is constant everywhere [18]. We make use of this to characterize a local reference bulk phase pressure p_B . The reason for this characterization is because in Low's swelling pressure experiment of Fig. 1, the reference bulk phase pressure p_B is defined in the domain occupied by the bulk water. Therefore, the generalization of Low's equilibrium definition for Π to the case where particles undergo non-equilibrium processes requires a pointwise definition for the reference pressure $p_B(x, t)$. We define the reference pressure of a virtual bulk water, constructed at instantaneous thermal and mechanical equilibrium with the adsorbed water such that their chemical potentials, densities and temperatures are equal. Setting $d\mu_l = dT = 0$ in (2.23) yields $dp_l = -p_* d\phi_l$. Considering the volume fraction $\phi_l^* = e^*/(1 - e^*)$ defined in Low's relation (1.1) where hydration forces are absent, for $\phi_l = \phi_l^*$, $A_l(\phi_l^*) = A_B$, where A_B denotes the free energy of the reference bulk fluid. Hence, integrating from ϕ_l to ϕ_l^* and using the condition $p_l(\phi_l^*) = p_B$ gives

$$p_B = p_l - \int_{\phi_l}^{\phi_l^*} p_*(s) ds. \quad (2.24)$$

Hence, for given ϕ_1 , p_1 and ϕ_1^* , (2.24) can be used to characterize locally the reference bulk phase pressure $p_B = p_B(p_1, \phi_1, \phi_1^*)$. In this approach, the difference $p_1 - p_B$ denotes a pressure excess due to the physico-chemical interaction between water and clay. In other words, if there is no physico-chemical interaction, the excess in adsorbed fluid pressure, $p_1 - p_B$, would be zero and the properties of the water would be unaffected by the interaction with the solid phase, as in the case of a bulk fluid. Moreover, since p_1 affects the total particle thermodynamic pressure, p , through (2.6), we are led to introduce an excess in total particle pressure p relative to the bulk phase p_B . We refer to this difference as an *excess in pore pressure*, (Π_B) (see [57]),

$$\Pi_B \equiv p - p_B. \quad (2.25)$$

In analogy to the excess in fluid pressure, $p_1 - p_B$, the above definition reflects locally the excess in pore pressure due to the physico-chemical interaction between the adsorbed water and the minerals. In other words, Π_B would be zero if the properties of the water are not perturbed by the presence of the clay platelets.

With the local reference bulk phase pressure p_B characterized by (2.24) we may now pursue a pointwise definition for the swelling pressure Π away from equilibrium and also rewrite the modified Terzaghi's principle (2.7) in terms of p_B rather than p . For t and t_B given in (2.7) and (2.8), define Π as

$$\Pi(x, t)\mathbf{I} \equiv -(t - t_B). \quad (2.26)$$

From (2.7), (2.8) and definition (2.25) the above r.h.s. reduces to $p - p_B - \phi_1\phi_s p_*$ or $\Pi_B - \phi_1\phi_s p_*$. This shows that the swelling pressure is a scalar and also $\phi_1\phi_s p_*$ can be interpreted as the difference $\Pi_B - \Pi$. To show that at equilibrium the above definition is consistent with Low's swelling pressure, recall that for a well ordered particle depicted in Fig. 1, $t_s^e = 0$, $t_B = -p_B\mathbf{I}$ and $t = -P\mathbf{I}$ (P denotes the overburden pressure). Thus (2.26) reduces to the classical swelling pressure definition $\Pi = P - p_B$. Since $\Pi = \Pi_B - p_*\phi_1\phi_s$, in conjunction with (2.7) with (2.25) we also have

$$t = -(p - p_*\phi_1\phi_s)\mathbf{I} + t_s^e = -(p_B + \Pi_B - p_*\phi_1\phi_s)\mathbf{I} + t_s^e = -(p_B + \Pi)\mathbf{I} + t_s^e. \quad (2.27)$$

Eq. (2.27) is an alternative form of writing the mesoscopic modified effective stress principle (2.7) with p replaced by p_B . In this case physico-chemical forces are dictated by the swelling pressure Π . This alternative way of expressing the modified Terzaghi's principle resembles in form some heuristic modified effective stress principles for clays discussed in Lambe [46] or Shridaran and Rao [71]. Historically, physico-chemical forces have heuristically been modeled at the macroscale with an additional term in Terzaghi's principle which measures the effect of net repulsive (RI) and attractive (AI) forces between particles. This stress is commonly denoted by $(R - A)\mathbf{I}$ (see [46,71]). We have

$$t = -p_B\mathbf{I} + t_s^e + (R - A)\mathbf{I}. \quad (2.28)$$

Eq. (2.27) provides a rigorous derivation of the above heuristic modified Terzaghi's principle. When comparing (2.27) with (2.28) we have $R - A = -\Pi$, which shows that the net attractive-

repulsive intra particles forces arising from hydration stresses are governed by the swelling pressure. This clarifies some controversial aspects in stress analysis in cohesive soils.

3. Near equilibrium

We begin by presenting the near equilibrium results of Murad and Cushman [56] in the range of moderate moisture content. These results were derived by linearizing the entropy inequality about equilibrium. In particular, when linearizing about $\{v_{l,s}, D_s \phi_l / Dt, \nabla T\}$ the following results were obtained

$$(p_* \phi_l - p_l) \nabla \phi_l + \hat{T}_l = -R_l v_{l,s}, \quad (3.1)$$

$$p_l - p_s = \mu_* \frac{D_s \phi_l}{Dt}, \quad (3.2)$$

$$\sum_{\alpha=l,s} \phi_\alpha h_\alpha = -K^T \nabla T, \quad (3.3)$$

where R_l , K^T and μ_* are positive definite material coefficients. Eq. (3.3) is the classical Fourier's law of heat conduction for the overall heat flux. If the medium is isotropic, $K^T = K^T I$, where K^T is the thermal conductivity of the mixture. Eq. (3.1) leads to a modified form of Darcy's law for the vicinal fluid. Denoting $K_l = \phi_l^2 R_l^{-1}$ the mesoscopic permeability tensor of the clay particles (recall that R_l is positive definite), using (2.2) and (3.1) in (2.12) and neglecting inertial effects we obtain the mesoscopic Darcy's law for the adsorbed water

$$\phi_l v_{l,s} = -K_l (\nabla p_l + p_* \nabla \phi_l). \quad (3.4)$$

The first term on the r.h.s. of (3.4) is the driving force for the traditional Darcy's law. The last term shows that due to the hydrophilic attraction between the adsorbed water and the minerals, the vicinal fluid tends to flow from regions of high volume fraction to regions of low volume fraction. Note from (3.4) and (2.12) that with $\nabla T = 0$, the driving force for vicinal fluid flow is the gradient of the chemical potential which consists of the same form postulated by Biot [13].

Eq. (3.2) tells us that near equilibrium, the thermodynamic pressure of the adsorbed fluid and solid phases are not necessarily equal. The coefficient μ_* may be thought of as a relaxation factor which among other effects, accounts for the re-ordering of the adsorbed water, i.e. the redistribution of the fluid molecules over the interlamellar spaces. Flow towards equilibrium is characterized by the fluid thermorelaxation time which depends on the size of the pores. For bulk fluids in macropores the relaxation time is usually much smaller than the macroscopic flow time [17]. It follows that for a granular medium, $\mu_* \approx 0$, since there is very little re-ordering of the bulk liquid phase. On the other hand, the combination of physico-chemical forces and narrow pores increases the relaxation time of the vicinal fluid to the same order of the macroscopic flow consequently leading to a natural relaxation viscoelastic constitutive behavior. The evaluation of the coefficient μ_* requires experimental study, and most likely it varies depending on the composition and the interaction of the vicinal fluid and solid minerals. In Murad and Cushman [57], μ_* was identified with the excess in the volumetric viscosity of the thin film relative to the bulk phase.

Using (3.2), (2.24) and the second definition in (2.6) in (2.25), the near equilibrium relation for Π_B is

$$\Pi_B = p - p_B = \phi_s p_s + \phi_l p_l - p_B = \phi_s(p_s - p_l) + p_l - p_B = \int_{\phi_l}^{\phi_s^*} p_*(s) ds - \phi_s \mu_* \frac{D_s \phi_l}{Dt}. \quad (3.5)$$

In addition, we have for the swelling pressure

$$\Pi = \Pi_B - p_* \phi_l \phi_s = \int_{\phi_l}^{\phi_s^*} p_*(s) ds - p_* \phi_l \phi_s - \phi_s \mu_* \frac{D_s \phi_l}{Dt}. \quad (3.6)$$

Using (3.2) and (3.5) in the modified Terzaghi's principle (2.7) gives near equilibrium

$$\mathbf{t} - \mathbf{t}_s^e - p_* \phi_l \phi_s \mathbf{I} = -p \mathbf{I} = (-p_l + \phi_s(p_l - p_s)) \mathbf{I} = \left(-p_l + \mu_* \phi_s \frac{D_s \phi_l}{Dt} \right) \mathbf{I}. \quad (3.7)$$

Note that even though a priori the solid is considered to be elastic, the last term in the r.h.s. of (3.7) shows a viscoelastic behavior for the volumetric stresses.

Finally, we derive a near-equilibrium relation from the intrinsic dissipation function by using (3.1), (3.2) in definition (2.17) to obtain

$$\Phi = \mu_* \left(\frac{D_s \phi_l}{Dt} \right)^2 + R_l |\mathbf{v}_{l,s}|^2, \quad (3.8)$$

where $|\cdot|$ denotes the Euclidean norm and $\mathbf{R}_l = R_l \mathbf{I}$ for an isotropic medium.

4. Two-scale linear thermomechanical model

The two-scale infinitesimal thermomechanical model for the clay particles is obtained following the standard linearization procedure [29]. Consider that particles are initially in a homogeneous, equilibrium and isotropic state and assume small deformations and small deviations in temperature and adsorbed fluid density from their reference values. Expand A_α ($\alpha = l, s$) in a Taylor series about equilibrium and retain quadratic terms in A_α and linear terms in the set of governing equations. Assume A_s is an isotropic function of E_s , depending only on its invariants to fulfill the usual objectivity requirements [29]. At the initial equilibrium state denote $T = \bar{T}$, $\rho_l = \bar{\rho}_l$, $\mathbf{E}_s = \mathbf{0}$, $\phi_l = \bar{\phi}_l$ and $\phi_s = \bar{\phi}_s$ ($\bar{\phi}_s = 1 - \bar{\phi}_l$) and also denote $\{\bar{A}_\alpha, \bar{\eta}_\alpha, \bar{p}_l\}$ the values of $\{A_\alpha, \eta_\alpha, p_l\}$ in the reference state. For simplicity, assume initially a well ordered parallel platelet arrangement such that the reference configuration is free of effective stresses in the solid phase and consider that the only non-zero stresses in the reference configuration are due to hydration stresses. Let $\{\bar{p}_*, \bar{K}_l, \bar{K}^T, \bar{\mu}_*\}$ be the values of $\{p_*, K_l, K^T, \mu_*\}$ at the reference configuration. Further let the infinitesimal strain tensor be given as

$$\mathbf{E}_s = \nabla^s \mathbf{u}_s, \quad (4.1)$$

where $\nabla^s \mathbf{u}_s = 1/2(\nabla \mathbf{u}_s + \nabla \mathbf{u}_s^T)$, with \mathbf{u}_s denoting the displacement of the mesoscale solid phase. Let $\{\mu_s, \lambda_s\}$ denote the pair of Lame coefficients of the platelet matrix and let α_s and C_s denote the coefficients of thermal expansion and the constant volume specific heat of the α -phase defined as follows

$$C_l \equiv \bar{T} \frac{\partial \eta_l}{\partial \theta_T} \Big|_{\rho_l, \phi_l}, \quad C_s \equiv \bar{T} \frac{\partial \eta_s}{\partial \theta_T} \Big|_{E_s}, \quad \alpha_s \equiv \frac{\partial \text{tr } E_s}{\partial \theta_T} \Big|_{\text{tr } E_s}, \quad \alpha_l \equiv -\frac{1}{\bar{\rho}_l} \frac{\partial \rho_l}{\partial \theta_T} \Big|_{\rho_l, \phi_l},$$

where $\theta_T \equiv T - \bar{T}$. Additionally let K_0 denote the bulk modulus for hydration stresses, defined as the coefficient of proportionality between p_* and ϕ_l and also introduce the physico-chemical coefficient of thermal expansion α_{ls} in the sense of Campanella and Mitchell [19] to account for changes in volume resulting from a temperature induced change in physico-chemical forces. Within the current framework, these new physico-chemical coefficients are defined as

$$\alpha_{ls} \equiv \frac{\partial \phi_l}{\partial \theta_T} \Big|_{\rho_l, p_*}, \quad K_0 = \bar{\phi}_l \frac{\partial p_*}{\partial \phi_l} \Big|_{\rho_l, \theta_T}.$$

Consider the relation $\rho_l = \rho_l(\theta_T, p_l, \phi_l)$ (obtained by inverting the equation of state $p_l = p_l(\theta_T, \rho_l, \phi_l)$) and assume that induced changes in ρ_l , due to p_l and p_* are small compared to those induced by changes in θ_T (this weak dependence of ρ_l on p_* due to physico-chemical interaction was experimentally verified by Low [52] who observed that changes in ρ_l due to the proximity of the solid are negligible compared to the other properties). Under this assumption the fluid compressibility due to mechanical and physico-chemical perturbations is neglected and p_l is now identified with a Lagrange multiplier rather than thermodynamically defined from (2.5) (see [56,57]). The linearized version of $\rho_l = \rho_l(\theta_T)$ is

$$\rho_l - \bar{\rho}_l = -\bar{\rho}_l \alpha_l \theta_T. \quad (4.2)$$

Postulate now the quadratic expansions

$$\rho_s \phi_s A_s = \rho_s \bar{\phi}_s \bar{A}_s - \rho_s \bar{\phi}_s \bar{\eta}_s \theta_T + \frac{\lambda_s}{2} (\text{tr } E_s)^2 + \mu_s \text{tr } E_s^2 - (3\lambda_s + 2\mu_s) \alpha_s \text{tr } E_s \theta_T - \frac{\rho_s C_s \bar{\phi}_s}{2\bar{T}} \theta_T^2, \quad (4.3)$$

$$\rho_l A_l = \bar{\rho}_l \bar{A}_l - \bar{\rho}_l \bar{\eta}_l \theta_T + \bar{p}_* (\phi_l - \bar{\phi}_l) + \frac{K_0}{2\bar{\phi}_l} (\phi_l - \bar{\phi}_l)^2 - \frac{K_0 \alpha_{ls}}{\bar{\phi}_l} (\phi_l - \bar{\phi}_l) \theta_T - \frac{\bar{\rho}_l C_l}{2\bar{T}} \theta_T^2. \quad (4.4)$$

Together with (2.4) this gives

$$\mathbf{t}_s^e = (\lambda_s \text{tr } E_s - K_s \alpha_s \theta_T) \mathbf{I} + 2\mu_s E_s, \quad (4.5)$$

$$p_* = \bar{p}_* + \frac{K_0}{\bar{\phi}_l} (\phi_l - \bar{\phi}_l) - \frac{\alpha_{ls} K_0}{\bar{\phi}_l} \theta_T, \quad (4.6)$$

where $K_s \equiv 3\lambda_s + 2\mu_s$ is the solid matrix bulk modulus. Using (4.3) and (4.4) in (2.1), gives the linearized entropy relations

$$\eta_s = \bar{\eta}_s + \frac{C_s}{\bar{T}} \theta_T + \frac{K_s \alpha_s}{\bar{\rho}_s \bar{\phi}_s} \operatorname{tr} \mathbf{E}_s, \quad (4.7)$$

$$\eta_l = \bar{\eta}_l + \frac{C_l}{\bar{T}} \theta_T + \frac{K_0 \alpha_{ls}}{\bar{\rho}_l \bar{\phi}_l} (\phi_l - \bar{\phi}_l). \quad (4.8)$$

Eq. (4.5) is the classical linear thermoelastic constitutive equation for the effective stresses. Defining $K'_{ls} \equiv \bar{\phi}_s^2 K_0 + \bar{p}_* \bar{\phi}_s (\bar{\phi}_s - \bar{\phi}_l)$ and $\alpha'_{ls} \equiv \bar{\phi}_s \alpha_{ls} K_0 / K'_{ls}$, by linearizing $\mathbf{t}_s^l = \phi_s \phi_l p_* \mathbf{I}$ we have from (4.6)

$$\mathbf{t}_s^l = p_* \phi_l \phi_s \mathbf{I} = \left(\bar{p}_* \bar{\phi}_l \bar{\phi}_s + \frac{K'_{ls}}{\bar{\phi}_s} (\phi_l - \bar{\phi}_l) - \alpha'_{ls} K'_{ls} \theta_T \right) \mathbf{I}, \quad (4.9)$$

By neglecting all inertial and convective effects, using (4.2), the linearized mass balances of the incompressible solid and adsorbed fluid are

$$\begin{aligned} \frac{\bar{\phi}_l}{\bar{\phi}_s} \frac{\partial \phi_l}{\partial t} - \bar{\phi}_l \operatorname{div} \frac{\partial \mathbf{u}_s}{\partial t} &= 0, \\ - \bar{\phi}_l \alpha_l \frac{\partial \theta_T}{\partial t} + \frac{\partial \phi_l}{\partial t} + \bar{\phi}_l \operatorname{div} \mathbf{v}_l &= 0. \end{aligned} \quad (4.10)$$

After adding the above equations and rewriting the result in terms of the Darcy velocity $\mathbf{q}_l = \phi_l \mathbf{v}_{ls}$ we have

$$-\bar{\phi}_l \alpha_l \frac{\partial \theta_T}{\partial t} + \operatorname{div} \mathbf{q}_l + \operatorname{div} \frac{\partial \mathbf{u}_s}{\partial t} = 0.$$

Let $\mathbf{h}_T = \sum_{\alpha=l,s} \phi_\alpha \mathbf{h}_\alpha$ be the overall heat flux. Neglecting convective effects, using relations (4.7) and (4.8) and the mass balance (4.10) in the linearized energy (2.16) gives,

$$\begin{aligned} \operatorname{div} \mathbf{h}_T - \Phi &= -\bar{T} \sum_{\alpha=l,s} \bar{\phi}_\alpha \bar{\rho}_\alpha \frac{\partial \eta_\alpha}{\partial t} = -\bar{\rho} C_T \frac{\partial \theta_T}{\partial t} - \alpha_{ls} \bar{T} K_0 \frac{\partial \phi_l}{\partial t} - \bar{T} K_s \alpha_s \operatorname{div} \frac{\partial \mathbf{u}_s}{\partial t} \\ &= -\bar{\rho} C_T \frac{\partial \theta_T}{\partial t} - \bar{T} (\bar{\phi}_s \alpha_{ls} K_0 + K_s \alpha_s) \operatorname{div} \frac{\partial \mathbf{u}_s}{\partial t}, \end{aligned} \quad (4.11)$$

where $\bar{\rho} C_T \equiv \rho_s \bar{\phi}_s C_s + \bar{\rho}_l \bar{\phi}_l C_l$, $\bar{\rho} \equiv \rho_s + \bar{\rho}_l$. The last two terms of the r.h.s. of (4.11) measure, respectively, the mechanical work of hydration and effective stresses.

4.1. Linearized thermoviscoelastic governing equations

In the absence of inertial and convective effects, with Φ given as in (3.8), in terms of the unknowns $\{\mathbf{u}_s, \mathbf{q}_l, \mathbf{t}_s^l, \phi_l, p_*, p_l, t, \theta_T, \mathbf{h}_T\}$ our mesoscopic linearized governing equations are

Mass of the solid phase.

$$\frac{\partial \phi_1}{\partial t} - \bar{\phi}_s \operatorname{div} \frac{\partial \mathbf{u}_s}{\partial t} = 0.$$

Total mass.

$$-\alpha_1 \bar{\phi}_1 \frac{\partial \theta_T}{\partial t} + \operatorname{div} \mathbf{q}_1 + \operatorname{div} \frac{\partial \mathbf{u}_s}{\partial t} = 0.$$

Total momentum.

$$\operatorname{div} \mathbf{t} = 0.$$

Modified Terzaghi's effective principle.

$$\mathbf{t} = -p \mathbf{I} + \mathbf{t}_s^e + \left(\phi_1 \phi_s p_* + \bar{\phi}_s \bar{p}_* \frac{\partial \phi_1}{\partial t} \right) \mathbf{I}.$$

Linearized effective stress constitutive relation.

$$\mathbf{t}_s^e = (\lambda_s \operatorname{div} \mathbf{u}_s - \alpha_s K_s \theta_T) \mathbf{I} + 2\mu_s \nabla^s \mathbf{u}_s.$$

Linearized hydration stress constitutive relation.

$$\phi_1 \phi_s p_* = \bar{p}_* \bar{\phi}_1 \bar{\phi}_s + \frac{K'_{ls}}{\bar{\phi}_s} (\phi_1 - \bar{\phi}_1) - \alpha'_{ls} K'_{ls} \theta_T \mathbf{I}.$$

Modified Darcy's law for the adsorbed water.

$$\mathbf{q}_1 = -\bar{K}_1 (\nabla p_1 + \bar{p}_* \nabla \phi_1). \quad (4.1)$$

Energy equation for the mixture.

$$\operatorname{div} \mathbf{h}_T + \bar{\rho} C_T \frac{\partial \theta_T}{\partial t} = -\bar{T} \alpha_* \operatorname{div} \frac{\partial \mathbf{u}_s}{\partial t} + \Phi. \quad (4.1)$$

Fourier's law of heat conduction.

$$\mathbf{h}_T = -\bar{K}^T \nabla \theta_T,$$

where $\alpha_* = \alpha_s K_s + \alpha'_{ls} \bar{\phi}_s K_0 = \alpha_s K_s + \alpha'_{ls} K'_{ls}$. The above two-scale linearized system governs particle swelling when physico-chemical forces are primarily due to hydration stresses. Next we establish the coupling between this system and bulk phase governing equations to obtain the mesoscale particle–bulk phase coupled system. For simplicity we henceforth adopt a partially decoupled formulation in the sense of Bai and Abousleiman [7] wherein the dissipation function and mechanical work (due to effective and hydration stresses) in the r.h.s. of (4.13) are negligible.

5. Mesoscopic thermomechanical model for clay particles and bulk water

Let Ω_l and Ω_f denote the clay particle and bulk water domains respectively and let Γ represent the interface between them. The above two-scale linearized equations govern the swelling of the particles in Ω_l . In addition, let Ω_f be occupied by bulk phase water and denote by μ_f the bulk water viscosity and the other corresponding bulk water properties by the subscript f (to distinguish from the subscript B used for the reference bulk fluid in Ω_l). Assume initially the bulk water is at equilibrium at a constant temperature \bar{T}_f . Neglect fluid compressibility due to mechanical effects by assuming $\rho_f = \rho_f(\theta_f)$, with $\theta_f \equiv T_f - \bar{T}_f$. Further, neglect convective effects, source terms and mechanical work and dissipation in the energy equation. By linearizing the mass balance, Stokes equations, energy balance, Fourier's law of heat conduction and the relation $\rho_f = \rho_f(\theta_f)$ the bulk water governing equations are

$$\begin{aligned} \frac{\partial \rho_f}{\partial t} + \bar{\rho}_f \operatorname{div} v_f &= 0, \\ \operatorname{div} t_f &= 0, \\ t_f &= -p_f I + 2\mu_f \nabla^s v_f \quad \text{in } \Omega_f, \\ \operatorname{div} h_f &= -\bar{\rho}_f C_f \frac{\partial \theta_f}{\partial t}, \\ h_f &= -\bar{K}_f^T \nabla \theta_f, \\ \rho_f - \bar{\rho}_f &= -\bar{\rho}_f \alpha_f \theta_f. \end{aligned}$$

5.1. Boundary conditions

The above system is supplemented by boundary conditions on the particle bulk-water interface Γ . Continuity of mass, heat flux, and the normal component of the stress tensor on Γ lead to

$$\begin{aligned} q_l \cdot n &= \left(v_f - \frac{\partial u_s}{\partial t} \right) \cdot n, \\ h_T \cdot n &= h_f \cdot n \quad \text{on } \Gamma, \\ tn &= t_f n, \end{aligned}$$

where n is the unit normal exterior to Ω_l . Consider now Dirichlet boundary conditions for the hydrodynamical problem and follow Murad et al. [55,56] who postulated continuity of the variable whose gradient is the driving force for fluid flow. According to Darcy's law (3.4) and (2.23), the driving force is the chemical potential (for fixed T). Hence as in [55,56], postulate

$$\mu_l = \mu_f \quad \text{on } \Gamma \tag{5.1}$$

where as in (2.22), $\mu_f \equiv A_l + \rho_f^{-1} p_f$. The above boundary condition can be used to quantify the discontinuity in the liquid pressure ($p_l - p_f$) on Γ . By the same arguments leading to (2.24), after linearizing, we can rewrite (5.1) as:

$$p_l - p_f = \int_{\phi_l}^{\phi_l^*} p_*(s) ds = \int_{\phi_l}^{\phi_l^*} \bar{p}_*(s) ds - \bar{p}_*(\phi_l - \bar{\phi}_l) = \bar{\Pi}_B - \bar{p}_*(\phi_l - \bar{\phi}_l) \quad \text{on } \Gamma, \quad (5.2)$$

where $\bar{\Pi}_B$ is the equilibrium value of the excess in pore pressure Π_B , obtained by setting $\mu_* = 0$ in (3.5). Hence, due to the presence of the hydration pressure p_* , we observe a discontinuity between p_l and p_f on the interface. Further using (2.24), the above boundary condition can be rewritten as:

$$p_B = p_f \quad \text{on } \Gamma$$

which in contrast to (5.2) shows continuity in the reference bulk fluid pressure. Note that the classical boundary condition between a granular non-swelling medium and a free bulk fluid ($p_l = p_f$ on Γ) can be recovered by setting $p_* = 0$ in (5.2).

In what follows we also discuss the general case where the particle–bulk phase interfaces may exhibit resistance to fluid flow and heat transfer. This leads to “slip” boundary conditions for pressure and temperature (see e.g. [66]), where discontinuity in temperature and reference pressure on the boundary may arise due to an interfacial barrier resistance accounting for the local variations in both thermal and hydraulic conductivities near the particle–bulk phase interface. In the analysis that follows we consider the classical case where the interfacial resistance is proportional to the difference in the corresponding potential. This leads to the following first-order “slip” boundary conditions

$$\begin{aligned} \mathbf{h}_T \cdot \mathbf{n} &= \delta_T(\theta_T - \theta_f) \quad \text{on } \Gamma, \\ \mathbf{q}_l \cdot \mathbf{n} &= \delta'_P(\mu_l - \mu_f) = \delta_P(p_B - p_f) \quad \text{on } \Gamma, \end{aligned} \quad (5.3)$$

where δ_T , δ'_P and δ_P denote the slip coefficients for heat transfer and fluid flow.

5.2. Alternative mesoscopic formulation

Following Murad and Cushman [57] an alternative way of formulating our two-scale HMT model is to rewrite it in terms of the pair of auxiliary variables $\{p_B, \Pi\}$ replacing $\{p_l, p_*, \Pi\}$ in the set of primary unknowns. In analogy to (5.2), by linearizing (2.24) we find

$$p_B - p_l = - \int_{\phi_l}^{\phi_l^*} p_*(s) ds = - \bar{\Pi}_B + \bar{p}_*(\phi_l - \bar{\phi}_l). \quad (5.4)$$

Using this result in (4.12) we can rewrite Darcy’s law in terms of a reference pressure gradient as follows:

$$\mathbf{q}_l = -\bar{K}_l(\nabla p_l + \bar{p}_* \nabla \phi_l) = -\bar{K}_l \nabla p_B.$$

Further, if we define the initial equilibrium swelling pressure $\bar{\Pi} = \bar{\Pi}_B - \bar{\phi}_l \bar{\phi}_s \bar{p}_*$, by linearizing (3.6) together with (4.9) we get:

$$\Pi = \bar{\Pi} - \frac{K_{ls}}{\bar{\phi}_s} (\phi_l - \bar{\phi}_l) - \bar{\phi}_s \mu_* \frac{\partial \phi_l}{\partial t} + \alpha_{ls}^* K_{ls} \theta_T$$

with $K_{ls} \equiv K'_{ls} + \bar{p}_*$ and $\alpha_{ls}^* = \alpha'_{ls} K'_{ls} / K_{ls}$. The above results together with the modified Terzaghi principle (2.27) and boundary condition (5.3) lead to the following alternative mesoscopic formulation in terms of the primary unknowns $\{\mathbf{u}_s, \mathbf{q}_l, \mathbf{t}_s^e, \phi_l, \Pi, p_B, \mathbf{t}, \theta_T, \mathbf{h}_T\}$ and $\{\mathbf{t}_f, \mathbf{v}_f, p_f, \theta_f, \mathbf{h}_f\}$

$$\mathbf{t}_f = -p_f \mathbf{I} + 2\mu_f \nabla^s \mathbf{v}_f \quad \text{in } \Omega_f,$$

$$\operatorname{div} \mathbf{t}_f = 0 \quad \text{in } \Omega_f,$$

$$\mathbf{h}_f = -K_f^T \nabla \theta_f \quad \text{in } \Omega_f,$$

$$\operatorname{div} \mathbf{h}_f = -\bar{\rho}_f C_f \frac{\partial \theta_f}{\partial t} \quad \text{in } \Omega_f,$$

$$-\alpha_f \frac{\partial \theta_f}{\partial t} + \operatorname{div} \mathbf{v}_f = 0 \quad \text{in } \Omega_f,$$

$$\operatorname{div} \mathbf{t} = 0 \quad \text{in } \Omega_l,$$

$$\mathbf{t} = -p_B \mathbf{I} + \mathbf{t}_s^e - \Pi \mathbf{I} \quad \text{in } \Omega_l,$$

$$\mathbf{t}_s^e = (\lambda_s \operatorname{div} \mathbf{u}_s - \alpha_s K_s \theta_T) \mathbf{I} + 2\mu_s \nabla^s \mathbf{u}_s \quad \text{in } \Omega_l,$$

$$\Pi = \bar{\Pi} - \frac{K_{ls}}{\bar{\phi}_s} (\phi_l - \bar{\phi}_l) - \bar{\phi}_s \mu_* \frac{\partial \phi_l}{\partial t} + \alpha_{ls}^* K_{ls} \theta_T \quad \text{in } \Omega_l,$$

$$\bar{\phi}_l \alpha_l \frac{\partial \theta_T}{\partial t} = \operatorname{div} \mathbf{q}_l + \operatorname{div} \frac{\partial \mathbf{u}_s}{\partial t} \quad \text{in } \Omega_l,$$

$$\frac{\partial \phi_l}{\partial t} - \bar{\phi}_s \operatorname{div} \frac{\partial \mathbf{u}_s}{\partial t} = 0 \quad \text{in } \Omega_l,$$

$$\mathbf{q}_l = -K_l \nabla p_B \quad \text{in } \Omega_l,$$

$$\mathbf{h}_T = -K^T \nabla \theta_T \quad \text{in } \Omega_l,$$

$$\operatorname{div} \mathbf{h}_T = -\bar{\rho} C_T \frac{\partial \theta_T}{\partial t} \quad \text{in } \Omega_l,$$

$$\mathbf{q}_l \cdot \mathbf{n} = \left(\mathbf{v}_f - \frac{\partial \mathbf{u}_s}{\partial t} \right) \cdot \mathbf{n} \quad \text{on } \Gamma,$$

$$\mathbf{t} \mathbf{n} = \mathbf{t}_f \mathbf{n} \quad \text{on } \Gamma,$$

$$\mathbf{h}_T \cdot \mathbf{n} = \mathbf{h}_f \cdot \mathbf{n} \quad \text{on } \Gamma,$$

$$\mathbf{q}_l \cdot \mathbf{n} = \delta_P (p_B - p_f) \quad \text{on } \Gamma,$$

$$\mathbf{h}_T \cdot \mathbf{n} = \delta_T (\theta_T - \theta_f) \quad \text{on } \Gamma.$$

$$\theta_f = 0 \quad \text{in } \Omega_f, t = 0,$$

$$\phi_l = \bar{\phi}_l \quad \text{in } \Omega_l, t = 0,$$

$$\begin{aligned}\theta_T &= 0 \quad \text{in } \Omega_l, t = 0, \\ \operatorname{div} \boldsymbol{u}_s &= 0 \quad \text{in } \Omega_l, t = 0.\end{aligned}$$

Henceforth, to simplify the notation the overbars used to denote the initial equilibrium values of the coefficients $\{K_l, K^T, K_f^T, \mu_*\}$ have been dropped. Note that after solving for p_B and ϕ_l , within the alternative mesoscopic formulation p_l can be computed from (5.4) using a post-processing approach.

6. Macroscopic dual porosity model for heat transfer and fluid flow

We upscale to the macroscale using the homogenization procedure. In this framework our macroscopic swelling clay is idealized as a bounded domain Ω^ε with a mesoscale periodic structure. Following the general framework of Sanchez-Palencia [67], the mesoscale characteristic length is denoted by l while the characteristic length-scale associated to the macroscopic region is denoted by L . Let the ratio $\varepsilon \equiv l/L$. Consider Ω^ε as the union of disjoint parallelepiped cells, Q^ε , congruent to a standard Q which consists of the union of several clay particles, Q_l , completely surrounded by a connected bulk water domain Q_f . Let the systems of bulk phase water and clay particles in Ω^ε be denoted by Ω_f^ε and Ω_l^ε , respectively. Our starting point, $\varepsilon = 1$, corresponds to our mesoscopic model. The ε -model in Ω^ε consists of properly scaled two-scale equations on a lattice of copies εQ . The basic problem is to investigate the asymptotics of the solution as $\varepsilon \rightarrow 0$. The picture corresponding to the limiting model is depicted in Fig. 3, where a mesoscopic cell, Q , is assigned to each point x of the macroscopic domain. As we shall illustrate next, this leads to a macroscopic model of *dual porosity* type wherein the swelling clay soil is represented as two distinct structures coexisting at each macroscopic point: one representing the global macroscopic transport equations and the other representing the local cell problems at the mesoscale. In this picture the macroscopic Darcy velocity is that of the bulk water alone, and fluid storage occurs in the system of clay particles. This technique has been successfully used to model naturally fractured reservoirs in which the system of fractures play the role of the global system (where the macroscopic flow takes place) and the matrix blocks behave as the analogue of the clay particles (see [27]). The main feature of dual porosity approaches is the accurate description of the interaction

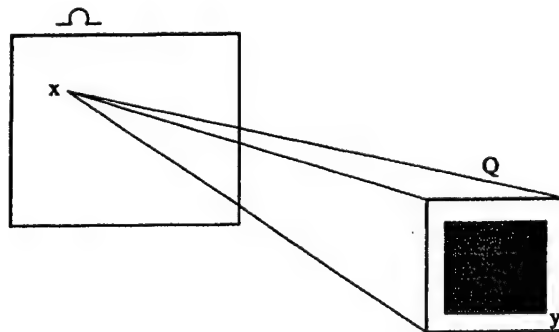


Fig. 3. Macroscopic picture of a dual porosity model with microstructure.

between the two structures. Within this framework the interaction between the two coexisting systems is manifested in a mass transfer function (also termed the secondary flux) which appears as a source term in the mass balance for the fracture flow distributed over the whole macroscopic domain. (see e.g. [3,4,27]). Here we pursue the derivation of a general microstructural dual porosity model for swelling media which incorporate distributed sources of mass, momentum and energy. In what follows we consider a totally fissured medium in the sense of Douglas and Arbogast [27] or Showalter [70] wherein particles are completely isolated from each other by the bulk phase fluid with no direct mass, energy and momentum transfer from particle to particle.

The formal homogenization process is accomplished by considering every property of the alternative mesoscopic formulation of Section 5.2 to be of the form $f(x, y)$ (where x and y denote the macroscopic and mesoscopic coordinates, respectively, with $y = \varepsilon^{-1}x$) and then postulating two-scale asymptotic expansions for the set \mathbf{u}^ε of the unknowns $\{\mathbf{u}_s, \mathbf{q}_l, \phi_l, p_B, t, \mathbf{h}_T, \theta_T, \mathbf{r}_s^\varepsilon, \Pi\}$ and $\{\mathbf{t}_f, \mathbf{v}_f, p_f, \theta_f, \mathbf{h}_f\}$ in terms of the perturbation parameter ε

$$\mathbf{u}^\varepsilon = \mathbf{u}^0 + \varepsilon \mathbf{u}^1 + \varepsilon^2 \mathbf{u}^2 + \dots \quad (6.1)$$

with the coefficients \mathbf{u}^i , Q -periodic in y . The coefficients of the two-scale coupled model must be properly scaled in order to describe the physics correctly. From the standard homogenization procedure of the Stokes problem, the bulk water viscosity coefficient μ_f is rescaled by ε^2 [67]. In addition, to control the secondary flux with a fixed volume as $\varepsilon \rightarrow 0$ it is also necessary to scale the hydraulic conductivity of the clay particles K_l^ε . Following Arbogast and co-workers [4,27] this is done by the scaling law $K_l^\varepsilon = K_l \varepsilon^2$ (see also [56]). This scaling has the effect of making the particles progressively less permeable as $\varepsilon \rightarrow 0$ and consequently prevents the degeneration of the secondary flux. In addition, recall that intuitively it is not evident that heat conduction mechanisms are the same as those governing fluid flow. Hence, the same scaling law for K_l^ε may not necessarily hold for $K^{T\varepsilon}$. Nevertheless, experimental observations show that even though particle thermal conductivity is higher than the bulk phase, particle heat capacity is significantly more pronounced. This suggests that particle thermal diffusivity $\alpha_D \equiv \rho K^T / C_T$ is smaller than that of the bulk water and therefore particles have strong potential to act as a storage sites of thermal energy (the difference is even more pronounced between particles and saturated bulk vapor). Hence, in analogy to the hydrodynamical problem we begin by adopting the same scaling law $K^{T\varepsilon} = K^T \varepsilon^2$. Under this assumption we consider that heat transfer at the macroscale takes place primarily through the global system and the thermal energy storage takes place in the local mesoscopic system of clay particles.

In order to quantify how particles respond to both thermal and hydrodynamic perturbations in the bulk phase we consider the Biot numbers for heat transfer and fluid flow $Bi_T \equiv \delta_T l / K^T$ and $Bi_P \equiv \delta_P l / K_l$. Physically these dimensionless quantities measure the ratio between particle and interfacial resistances (thermal and hydraulic) $1/K$ and $l/\delta l$. Clay particles with high conductivities are characterized by low Biot numbers. In this range the variation of the potentials for fluid flow and heat transfer over the particle is often neglected and surface resistance dominates. On the other hand, $Bi \rightarrow \infty$ corresponds to the absence of interface resistance and therefore continuity of the potentials for fluid flow and heat transfer on the particle–bulk phase interface is valid. In what follows we begin by assuming the scaling laws $Bi_T^\varepsilon = \varepsilon Bi_T$ and $Bi_P^\varepsilon = \varepsilon Bi_P$ and subsequently we analyze the influence of this scaling on the form of the macroscopic governing

equations. This analysis was carried out by Auriault [5] within the framework of homogenization of heat transfer in rigid composites. We pursue a similar analysis in order to reproduce lumped-parameter models in terms of different scalings of the Biot number.

Insert the expansions (6.1) into the set of mesoscopic governing equations with the differential operator ∂/∂_x replaced by $\partial/\partial_x + \varepsilon^{-1}\partial/\partial_y$. After a formal matching of the powers of ε , we obtain successive cell problems. For bulk water we get

$$\mathbf{t}_f^0 = -p_f^0 \mathbf{I}, \quad (6.2)$$

$$\mathbf{t}_f^1 = -p_f^1 \mathbf{I} + 2\mu_f \nabla_y^s \mathbf{v}_f^0, \quad (6.3)$$

$$\operatorname{div}_y \mathbf{t}_f^0 = -\nabla_y p_f^0 = \nabla_y \theta_f^0 = 0, \quad (6.4)$$

$$\operatorname{div}_x \mathbf{t}_f^0 + \operatorname{div}_y \mathbf{t}_f^1 = 0, \quad (6.5)$$

$$\operatorname{div}_y \mathbf{v}_f^0 = \operatorname{div}_y \mathbf{h}_f^0 = 0, \quad (6.6)$$

$$\alpha_f \frac{\partial \theta_f^0}{\partial t} = \operatorname{div}_x \mathbf{v}_f^0 + \operatorname{div}_y \mathbf{v}_f^1, \quad (6.7)$$

$$\mathbf{h}_f^0 = -K_f^T (\nabla_x \theta_f^0 + \nabla_y \theta_f^1), \quad (6.8)$$

$$\bar{\rho}_f C_f \frac{\partial \theta_f^0}{\partial t} + \operatorname{div}_x \mathbf{h}_f^0 + \operatorname{div}_y \mathbf{h}_f^1 = 0, \quad (6.9)$$

and for clay particles

$$\mu_s \Delta_{yy} \mathbf{u}_s^0 + (\lambda_s + \mu_s) \nabla_y \operatorname{div}_y \mathbf{u}_s^0 = 0, \quad (6.10)$$

$$\operatorname{div}_y \mathbf{t}^0 = 0, \quad (6.11)$$

$$\operatorname{div}_x \mathbf{t}^0 + \operatorname{div}_y \mathbf{t}^1 = 0, \quad (6.12)$$

$$\mathbf{t}^0 = -(p_B^0 + \Pi^0) \mathbf{I} + \mathbf{t}_s^{e0}, \quad (6.13)$$

$$\mathbf{t}^1 = -(p_B^1 + \Pi^1) \mathbf{I} + \mathbf{t}_s^{e1}, \quad (6.14)$$

$$\mathbf{t}_s^{e0} = (\lambda_s (\operatorname{div}_x \mathbf{u}_s^0 + \operatorname{div}_y \mathbf{u}_s^1) - \alpha_s K_s \theta_T^0) \mathbf{I} + 2\mu_s (\nabla_x^s \mathbf{u}_s^0 + \nabla_y^s \mathbf{u}_s^1), \quad (6.15)$$

$$\Pi^0 = \bar{\Pi} - \frac{K_{ls}}{\bar{\phi}_s} (\phi_l^0 - \bar{\phi}_l) - \bar{\phi}_s \mu_* \frac{\partial \phi_l^0}{\partial t} + \alpha_{ls}^* K_{ls} \theta_T^0, \quad (6.16)$$

$$\frac{1}{\bar{\phi}_s} \frac{\partial \phi_l^0}{\partial t} = \operatorname{div}_x \frac{\partial \mathbf{u}_s^0}{\partial t} + \operatorname{div}_y \frac{\partial \mathbf{u}_s^1}{\partial t}, \quad (6.17)$$

$$\bar{\phi}_l \alpha_l \frac{\partial \theta_T^0}{\partial t} = \operatorname{div}_y \mathbf{q}_l^1 + \operatorname{div}_x \frac{\partial \mathbf{u}_s^0}{\partial t} + \operatorname{div}_y \frac{\partial \mathbf{u}_s^1}{\partial t}, \quad (6.18)$$

$$\mathbf{h}_T^0 = \mathbf{q}_l^0 = 0, \quad (6.19)$$

$$\mathbf{q}_l^1 = -K_l \nabla_y p_B^0, \quad (6.20)$$

$$\mathbf{h}_T^1 = -K^T \nabla_y \theta_T^0, \quad (6.21)$$

$$\bar{\rho} C_T \frac{\partial \theta_T^0}{\partial t} + \operatorname{div}_y \mathbf{h}_T^1 = 0, \quad (6.22)$$

along with the boundary conditions

$$\left(\mathbf{v}_f^0 - \frac{\partial \mathbf{u}_s^0}{\partial t} \right) \cdot \mathbf{n} = 0 \quad \text{on } \Gamma, \quad (6.23)$$

$$\mathbf{q}_l^1 \cdot \mathbf{n} = \left(\mathbf{v}_f^1 - \frac{\partial \mathbf{u}_s^1}{\partial t} \right) \cdot \mathbf{n} \quad \text{on } \Gamma, \quad (6.24)$$

$$(2\mu_s \nabla_y \mathbf{u}_s^0 + \lambda_s \operatorname{div}_y \mathbf{u}_s^0 \mathbf{I}) \cdot \mathbf{n} = 0 \quad \text{on } \Gamma, \quad (6.25)$$

$$(\mathbf{t}^0 - \mathbf{t}_f^0) \cdot \mathbf{n} = 0 \quad \text{on } \Gamma, \quad (6.26)$$

$$(\mathbf{t}^1 - \mathbf{t}_f^1) \cdot \mathbf{n} = 0 \quad \text{on } \Gamma, \quad (6.27)$$

$$\mathbf{h}_f^0 \cdot \mathbf{n} = 0 \quad \text{on } \Gamma, \quad (6.28)$$

$$\mathbf{h}_T^1 \cdot \mathbf{n} = \mathbf{h}_f^1 \cdot \mathbf{n} \quad \text{on } \Gamma, \quad (6.29)$$

$$\mathbf{q}_l^1 \cdot \mathbf{n} = \delta_P (p_B^0 - p_f^0) \quad \text{on } \Gamma, \quad (6.30)$$

$$\mathbf{h}_T^1 \cdot \mathbf{n} = \delta_T (\theta_T^0 - \theta_f^0) \quad \text{on } \Gamma, \quad (6.31)$$

and initial conditions

$$\phi_l^0 = \bar{\phi}_l, \quad \text{in } \Omega_l, \quad t = 0, \quad (6.32)$$

$$\operatorname{div}_x \mathbf{u}_s^0 = \operatorname{div}_y \mathbf{u}_s^1 = 0, \quad \text{in } \Omega_l, \quad t = 0, \quad (6.33)$$

$$\theta_T^0 = 0 \quad \text{in } \Omega_l, \quad t = 0, \quad (6.34)$$

$$\theta_f^0 = 0 \quad \text{in } \Omega_f, \quad t = 0. \quad (6.35)$$

Next we formally collect our homogenized results. We remark that in postulating the boundary conditions, we have assumed that the displacement of the interface Γ is small compared to the mesoscopic length of the periodic cell l so that boundary conditions are applied on the initial (undeformed) position of the interface. The extension of this analysis to allow for higher order interfacial displacement (for instance of the same order of the macroscopic displacement) can be obtained by adopting the Lagrangian framework proposed by Lee and Mei [47].

Recall that since p_l was replaced by p_B within this alternative formulation, p_l^0 still needs to be evaluated by collecting $O(\epsilon^0)$ in the post processing (5.4) as follows

$$p_l^0 = p_B^0 + \bar{\Pi}_B - \bar{p}_*(\phi_l^0 - \bar{\phi}_l). \quad (6.36)$$

Non-oscillating variables. From (6.4) we have $p_f^0 = p_f^0(x, t)$ and $\theta_f^0 = \theta_f^0(x, t)$. Also note that \mathbf{u}_s^0 satisfies the Neumann problem given by (6.10) and (6.25), whose solution is $\mathbf{u}_s^0 = \mathbf{u}_s^0(x, t)$. This shows that the leading order neighboring platelets move together as a rigid body in each cell.

Darcy's law for the bulk water flow. The macroscopic Darcy's law for the bulk water flow relative to the solid phase follows from the well known upscaling of the Stokes problem (6.2)–(6.6), together with boundary condition (6.23) (see e.g. [67]). Introduce the mean value operator

$$\tilde{\gamma} = |\mathcal{Q}|^{-1} \int_{\mathcal{Q}} dQ_i, \quad i = l, f$$

and for each macroscopic point, x , define the macroscopic volume fractions of the particles and bulk phase by $n_\alpha = |Q_\alpha|/|\mathcal{Q}|$, $\alpha = l, f$, and the averaged bulk phase Darcy velocity relative to the solid phase by $\tilde{\mathbf{q}}_f^0 \equiv \tilde{\mathbf{v}}_f^0 - n_f \partial \mathbf{u}_s^0 / \partial t$. We then have

$$\tilde{\mathbf{q}}_f^0 = -K_F \nabla p_f^0,$$

which is the classical Darcy's law governing the macroscopic bulk water movement with K_F denoting the permeability coefficient. For a macroscopic isotropic medium, $K_F = K_F I$.

Fourier's law for bulk water. By combining (6.6) and (6.8) together with the boundary condition (6.28), θ_f^1 satisfies the following Neumann problem

$$\begin{aligned} \Delta_{yy} \theta_f^1 &= 0 \quad \text{in } Q_f, \\ (\nabla_x \theta_f^0 + \nabla_y \theta_f^1) \cdot \mathbf{n} &= 0 \quad \text{on } \Gamma. \end{aligned}$$

By linearity we have

$$\theta_f^1(x, y, t) = \psi(y) \cdot \nabla_x \theta_f^0(x, t) + \theta_f^*(x, t), \quad (6.37)$$

where ψ is a auxiliary Q -periodical vector valued function (determined up to an additive constant) whose components ψ_j satisfy the canonical cell problem

$$\begin{aligned} \Delta_{yy} \psi_j &= 0 \quad \text{in } Q_f \\ \nabla_y \psi_f \mathbf{n} &= -e_j \mathbf{n} = -n_j \quad \text{on } \Gamma, \quad j = 1, 2, 3, \end{aligned} \quad (6.38)$$

where $\psi = \sum_j \psi_j e_j$ with e_j denoting the unit vector in the direction of the j -axis. Using (6.37) in (6.8) we get after averaging

$$\tilde{\mathbf{h}}_f^0 = -K_F^T \nabla \theta_f^0, \quad \text{with } K_F^T = |\mathcal{Q}|^{-1} \int_{Q_f} K_f^T (I + \nabla_y \psi) dQ_f, \quad (6.39)$$

which is the macroscopic Fourier's law for the bulk water with $K_F^T = K_F^T I$ for an isotropic medium.

Overall momentum balance. To derive the overall momentum balance we apply the mean value operator to (6.12)–(6.14), use the boundary condition (6.27) together with (6.5), (6.2) to obtain (recall that \mathbf{n} was chosen outward to Q_l)

$$\begin{aligned} \operatorname{div}_x \tilde{\mathbf{t}}^0 &= \operatorname{div}_x \tilde{\mathbf{t}}_s^0 - \nabla_x \tilde{p}_B^0 - \nabla_x \tilde{\Pi}^0 = -|\mathcal{Q}|^{-1} \int_{Q_l} \operatorname{div}_y \mathbf{t}^1 \mathbf{n} dQ_l = -|\mathcal{Q}|^{-1} \int_{\Gamma} \mathbf{t}^1 \mathbf{n} d\Gamma \\ &= -|\mathcal{Q}|^{-1} \int_{\Gamma} \mathbf{t}_f^1 \mathbf{n} d\Gamma = |\mathcal{Q}|^{-1} \int_{Q_f} \operatorname{div}_y \mathbf{t}_f^1 dQ_f = |\mathcal{Q}|^{-1} \int_{Q_f} \nabla_x p_f^0 dQ_f = n_f \nabla_x p_f^0, \end{aligned}$$

where the divergence theorem and periodicity assumptions have also been used. Whence

$$\operatorname{div}_x \tilde{\mathbf{t}}_s^0 - \nabla_x \tilde{p}_B^0 - \nabla_x \tilde{\Pi}^0 - (1 - n_l) \nabla_x p_f^0 = 0. \quad (6.40)$$

We now rewrite (6.40) in a more convenient form. To this end integrate (6.17) and use the initial conditions (6.32) and (6.33) to get $\phi_1^0 - \bar{\phi}_1 = \bar{\phi}_s(\operatorname{div}_x \mathbf{u}_s^0 + \operatorname{div}_y \mathbf{u}_s^1)$. Using this relation in (6.16) yields:

$$\Pi^0 - \bar{\Pi} = -K_{ls}(\operatorname{div}_x \mathbf{u}_s^0 + \operatorname{div}_y \mathbf{u}_s^1) - \mu_{ls} \left(\operatorname{div}_x \frac{\partial \mathbf{u}_s^0}{\partial t} + \operatorname{div}_y \frac{\partial \mathbf{u}_s^1}{\partial t} \right) + \alpha_{ls}^* K_{ls} \theta_T^0 \quad (6.41)$$

with $\mu_{ls} = \bar{\phi}_s \mu_*$. Since \mathbf{u}_s^0 depends only on (x, t) , Eqs. (6.13)–(6.16) together with (6.41) suggest the following decompositions

$$\mathbf{t}_s^0 = \boldsymbol{\sigma}_0(x, t) + \boldsymbol{\sigma}_1(x, y, t), \quad (6.42)$$

$$\Pi^0 = \Pi_0(x, t) + \Pi_1(x, y, t),$$

$$\mathbf{t}^0 = \mathbf{t}_0(x, t) + \mathbf{t}_1(x, y, t),$$

$$\mathbf{t}^0 = \mathbf{t}_0^*(x, t) + \mathbf{t}_1^*(x, y, t), \quad (6.43)$$

with

$$\boldsymbol{\sigma}_0(x, t) \equiv \lambda_s \operatorname{div}_x \mathbf{u}_s^0 \mathbf{I} + 2\mu_s \nabla_x^s \mathbf{u}_s^0, \quad (6.44)$$

$$\boldsymbol{\sigma}_1(x, y, t) \equiv (\lambda_s \operatorname{div}_y \mathbf{u}_s^1 - \alpha_s K_s \theta_T^0) \mathbf{I} + 2\mu_s \nabla_y^s \mathbf{u}_s^1, \quad (6.45)$$

$$\Pi_0(x, t) \equiv \bar{\Pi} - K_{ls} \operatorname{div}_x \mathbf{u}_s^0 - \mu_{ls} \operatorname{div}_x \frac{\partial \mathbf{u}_s^0}{\partial t}, \quad (6.46)$$

$$\Pi_1(x, y, t) \equiv -K_{ls} \operatorname{div}_y \mathbf{u}_s^1 - \mu_{ls} \operatorname{div}_y \frac{\partial \mathbf{u}_s^1}{\partial t} + \alpha_{ls}^* K_{ls} \theta_T^0, \quad (6.47)$$

$$\mathbf{t}_0(x, t) \equiv \boldsymbol{\sigma}_0 - (p_f^0 + \Pi_0) \mathbf{I}, \quad (6.48)$$

$$\mathbf{t}_1(x, y, t) \equiv \boldsymbol{\sigma}_1 - (p_b^0 + \Pi_1) \mathbf{I}, \quad (6.49)$$

$$\mathbf{t}_0^*(x, t) \equiv -\Pi_0 \mathbf{I} + \boldsymbol{\sigma}_0, \quad (6.50)$$

$$\mathbf{t}_1^*(x, y, t) \equiv -(p_B^0 + \Pi_1) \mathbf{I} + \boldsymbol{\sigma}_1, \quad (6.51)$$

$$p_b^0 \equiv p_B^0 - p_f^0. \quad (6.52)$$

Using (6.42) in (6.11) gives $\operatorname{div}_y \mathbf{t}_1 = 0$. Further, using the above decompositions in (6.40) we get:

$$\begin{aligned} \operatorname{div}_x \widetilde{\boldsymbol{\sigma}_0} - \nabla_x \widetilde{\Pi}_0 - (1 - n_l) \nabla_x p_f^0 &= -\operatorname{div}_x \widetilde{\boldsymbol{\sigma}_1} + \nabla_x \widetilde{\Pi}_1 + \nabla_x \widetilde{p}_B^0 \\ &= -\operatorname{div}_x \widetilde{\boldsymbol{\sigma}_1} + \nabla_x \widetilde{\Pi}_1 + \nabla_x \widetilde{p}_b^0 + n_l \nabla_x p_f^0, \end{aligned}$$

which when combined with (6.49) gives

$$\operatorname{div}_x \widetilde{\sigma_0} - \nabla_x \widetilde{\Pi_0} - \nabla_x p_f^0 = -\operatorname{div}_x \widetilde{t}_1. \quad (6.53)$$

The above result is an alternative form of (6.40). The decompositions allow us to rewrite the macroscopic overall momentum balance with the l.h.s. of (6.53) containing only global variables (functions of (x, t)). The r.h.s. represents a distributed source/sink of momentum transfer from the mesoscopic system to the global one.

Overall mass balance. We now derive the overall macroscopic mass balance. By averaging (6.7) and (6.18) using the boundary condition (6.24) along with the divergence theorem and the periodicity assumption gives

$$\begin{aligned} -\alpha_f n_f \frac{\partial \theta_f^0}{\partial t} + \widetilde{\operatorname{div}_x v_f^0} &= -|Q|^{-1} \int_{Q_f} \operatorname{div}_y v_f^1 dQ_f = |Q|^{-1} \int_{\Gamma} v_f^1 \cdot \mathbf{n} d\Gamma = |Q|^{-1} \int_{\Gamma} \left(\mathbf{q}_f^1 + \frac{\partial u_s^1}{\partial t} \right) \cdot \mathbf{n} d\Gamma \\ &= |Q|^{-1} \int_{Q_l} \left(\operatorname{div}_y \mathbf{q}_l^1 + \operatorname{div}_y \frac{\partial u_s^1}{\partial t} \right) dQ_l = -(1 - n_f) \operatorname{div}_x \frac{\partial u_s^0}{\partial t} + \bar{\phi}_l \alpha_l \frac{\partial \widetilde{\theta}_T^0}{\partial t}. \end{aligned}$$

In terms of the bulk water Darcy velocity, \widetilde{q}_f^0 , the above result can be rewritten as:

$$-\alpha_f n_f \frac{\partial \theta_f^0}{\partial t} + \operatorname{div}_x \frac{\partial u_s^0}{\partial t} + \operatorname{div}_x \widetilde{q}_f^0 = \bar{\phi}_l \alpha_l \frac{\partial \widetilde{\theta}_T^0}{\partial t}. \quad (6.54)$$

Overall energy equation. Applying the same procedure to the energy balances (6.9) and (6.22) and using the boundary condition (6.29) gives

$$\begin{aligned} \bar{\rho}_f C_f n_f \frac{\partial \theta_f^0}{\partial t} + \operatorname{div}_x \widetilde{\mathbf{h}_f^0} &= -|Q|^{-1} \int_{Q_f} \operatorname{div}_y \mathbf{h}_f^1 dQ_f = |Q|^{-1} \int_{\Gamma} \mathbf{h}_f^1 \cdot \mathbf{n} d\Gamma = |Q|^{-1} \int_{\Gamma} \mathbf{h}_T^1 \cdot \mathbf{n} d\Gamma \\ &= |Q|^{-1} \int_{Q_l} \operatorname{div}_y \mathbf{h}_T^1 dQ_l = -\bar{\rho} C_T \frac{\partial \widetilde{\theta}_T^0}{\partial t}, \end{aligned} \quad (6.55)$$

which is our macroscopic energy balance.

Boundary and initial condition. Using (6.2) and the decomposition (6.43) and (6.51), boundary condition (6.26) can be rewritten as:

$$-p_f^0 \mathbf{n} = \mathbf{t}^0 \mathbf{n} = (\mathbf{t}_0^* + \mathbf{t}_1^*) \mathbf{n} = (\mathbf{t}_0^* - (p_B^0 + \Pi_1) \mathbf{I} + \boldsymbol{\sigma}_1) \mathbf{n} \quad \text{on } \Gamma.$$

Together with (6.49) and (6.52) this yields

$$\mathbf{t}_1 \mathbf{n} = (\boldsymbol{\sigma}_1 - (p_B^0 + \Pi_1) \mathbf{I}) \mathbf{n} = -\mathbf{t}_0^* \mathbf{n} \quad \text{on } \Gamma. \quad (6.56)$$

The above together with the boundary conditions (6.30) and (6.31), initial conditions (6.32) to (6.35) and the post processing (6.36) for p_l^0 establishes our macroscopic microstructural model of dual porosity type.

6.1. Summary of the dual porosity model

Let $\lambda_s \equiv \lambda_s n_l$, $\mu_s = n_l \mu_s$, $K_{ls} \equiv K_{ls} n_l$, $\mu_{ls} \equiv \mu_{ls} n_l$. The application of the formal homogenization procedure leads to the following dual porosity model: Find $\{u_s^0, \widetilde{\sigma}_0, \widetilde{\Pi}_0, p_f^0, \theta_f^0, \widetilde{q}_f^0, \widetilde{h}_f^0\}$ functions of (x, t) and $\{p_b^0, t_1, u_s^1, \sigma_1, \Pi_1, \theta_T^0, h_T^1\}$ functions of (x, y, t) such that

$$\begin{aligned} \operatorname{div}_x \widetilde{\sigma}_0 - \nabla_x \widetilde{\Pi}_0 - \nabla_x p_f^0 &= F_*(x, t), \\ \widetilde{\sigma}_0 &= \lambda_s \operatorname{div}_x u_s^0 I + 2\mu_s \nabla_x^s u_s^0, \\ \widetilde{\Pi}_0 &= n_l \overline{\Pi} - K_{ls} \operatorname{div}_x u_s^0 - \mu_{ls} \operatorname{div}_x \frac{\partial u_s^0}{\partial t}, \\ \alpha_f n_f \frac{\partial \theta_f^0}{\partial t} + \operatorname{div}_x \widetilde{q}_f^0 + \operatorname{div}_x \frac{\partial u_s^0}{\partial t} &= Q_*(x, t), \\ \widetilde{q}_f^0 &= -K_F \nabla_x p_f^0, \\ n_f \bar{\rho}_f C_f \frac{\partial \theta_f^0}{\partial t} + \operatorname{div}_x \widetilde{h}_f^0 &= E_*(x, t), \\ \widetilde{h}_f^0 &= -K_F^T \nabla_x \theta_f^0 \quad x \in \Omega_f, \quad t > 0, \end{aligned}$$

with

$$F_* \equiv -\frac{1}{|Q|} \operatorname{div}_x \int_{Q_l} t_1 dQ_l, \quad Q_* \equiv \frac{\bar{\phi}_l \alpha_l}{|Q|} \int_Q \frac{\partial \theta_T^0}{\partial t} dQ_l, \quad E_* \equiv -\frac{\bar{\rho} C_T}{|Q|} \int_{Q_l} \frac{\partial \theta_T^0}{\partial t} dQ_l, \quad (6.57)$$

and

$$\begin{aligned} \operatorname{div}_y t_1 &= 0, \\ t_1 &= -(p_b^0 + \Pi_1) I + \sigma_1, \\ \sigma_1 &= (\lambda_s \operatorname{div}_y u_s^1 - \alpha_s K_s \theta_T^0 I) + 2\mu_s \nabla_y^s u_s^1, \\ \Pi_1(x, t) &= -K_{ls} \operatorname{div}_y u_s^1 - \mu_{ls} \operatorname{div}_y \frac{\partial u_s^1}{\partial t} + \alpha_{ls}^* K_{ls} \theta_T^0, \\ -\bar{\phi}_l \alpha_l \frac{\partial \theta_T^0}{\partial t} + \operatorname{div}_y q_l^1 + \operatorname{div}_y \frac{\partial u_s^1}{\partial t} &= H(x, t), \\ q_l^1 &= -K_l \nabla_y p_b^0, \\ \bar{\rho} C_T \frac{\partial \theta_T^0}{\partial t} + \operatorname{div}_y h_T^1 &= 0, \\ h_T^1 &= -K^T \nabla_y \theta_T^0 \quad y \in Q_l, \quad t > 0, \end{aligned}$$

with

$$H(x, t) = -\operatorname{div}_x \frac{\partial u_s^0}{\partial t}.$$

For t_0^* given as in (6.50), the above is supplemented with the following boundary and initial conditions

$$\begin{aligned} t_1 \mathbf{n} &= -t_0^* \mathbf{n} \quad \text{on } \Gamma, \\ \mathbf{q}_1^1 \cdot \mathbf{n} &= \delta_{PP} p_b^0 \quad \text{on } \Gamma, \\ \mathbf{h}_T^1 \cdot \mathbf{n} &= \delta_T(\theta_T^0 - \theta_f^0) \quad \text{on } \Gamma, \\ \operatorname{div}_x \mathbf{u}_s^0 &= \operatorname{div}_y \mathbf{u}_s^1 = 0, \quad \text{in } \Omega_l, t = 0, \\ \theta_T^0 &= 0, \quad \text{in } \Omega_l, t = 0, \\ \theta_f^0 &= 0, \quad \text{in } \Omega_f, t = 0. \end{aligned} \tag{6.58}$$

together with the post-processing for p_l^0

$$p_l^0 = p_B^0 + \bar{\Pi}_B - \bar{p}_*(\phi_l^0 - \bar{\phi}_l). \tag{6.59}$$

We have obtained a homogenized microstructural dual porosity model wherein the macroscopic mass, momentum and energy transport equations are coupled to a family of mesoscopic cell problems through distributed source/sink transfer functions Q_* , \mathbf{F}_* and E_* . For each point x in the macroscopic domain, there is a magnified or scaled local cell Q which represents the effect of microstructure near x (Fig. 3). The way the family of local cell problems affect the macroscopic global swelling medium is analogous to the approaches of Douglas and Arbogast [27] and Peszynska [60] for isothermal and non-isothermal flow in rigid media. The novelty is the appearance of the additional distributed source of momentum \mathbf{F}_* . For rigid media ($\mathbf{u}_s = 0$) our model reduces to the one proposed by Peszynska [60]. On the other hand there are basic conceptual differences between the microstructural models for rigid and swelling media. In the former the global medium is the fracture system while the local family of cells is the collection of matrix blocks. In the latter the global medium also incorporates the non-oscillatory part of the solid variables $\{\sigma_0, \Pi_0, \mathbf{u}_s^0\}$. Also, for rigid media, the influence on the global medium on each local cell occurs only through the cell boundary Γ (see [27]). In our model the global medium also affects the clay particles system at the mesoscale throughout the clay particle domain via the distributed mass source term $H(x, t)$.

Next, let $\lambda_s^* = \lambda_s + K_{ls}$, $\lambda_s^* = \lambda_s + K_{LS}$, and $\alpha_* = \alpha_s K_s + \alpha_{l,s}^* K_{ls}$. In terms of $\{\mathbf{u}_s^0, p_f^0, \theta_f^0\}$ and $\{\mathbf{u}_s^1, p_B^0, \theta_T^0\}$ the above system can be rewritten as

$$\begin{aligned} \mu_S \Delta_{xx} \mathbf{u}_s^0 + (\lambda_s^* + \mu_S) \nabla_x \operatorname{div}_x \mathbf{u}_s^0 + \mu_{LS} \nabla_x \operatorname{div}_x \frac{\partial \mathbf{u}_s^0}{\partial t} - \nabla_x p_f^0 &= \mathbf{F}_*, \\ -\alpha_f n_f \frac{\partial \theta_f^0}{\partial t} + \operatorname{div}_x \frac{\partial \mathbf{u}_s^0}{\partial t} - K_F \Delta_{xx} p_f^0 &= Q_*, \\ \bar{p}_f n_f C_f \frac{\partial \theta_f^0}{\partial t} - K_F^T \Delta_{xx} \theta_f^0 &= E_* \quad x \in \Omega_f, \quad t > 0, \end{aligned} \tag{6.60}$$

with

$$\mathbf{F}_*(\mathbf{x}, t) = -2\mu_s \operatorname{div}_x \widetilde{\nabla_y^s \mathbf{u}_s^1} - \lambda_s^* \nabla_x \operatorname{div}_y \widetilde{\mathbf{u}_s^1} + \nabla_x \widetilde{p_b^0} - \mu_{ls} \nabla_x \frac{\partial}{\partial t} \widetilde{\operatorname{div}_y \mathbf{u}_s^1} + \alpha_* \nabla_x \widetilde{\theta_T^0}$$

and

$$\begin{aligned} \mu_s \Delta_{yy} \mathbf{u}_s^1 + (\lambda_s^* + \mu_s) \nabla_y \operatorname{div}_y \mathbf{u}_s^1 - \nabla_y p_b^0 + \mu_{ls} \nabla_y \operatorname{div}_y \frac{\partial \mathbf{u}_s^1}{\partial t} - \alpha_* \nabla_y \theta_T^0 &= 0, \\ -\alpha_l \bar{\phi}_l \frac{\partial \theta_T^0}{\partial t} + \operatorname{div}_y \frac{\partial \mathbf{u}_s^1}{\partial t} - K_l \Delta_{yy} p_b^0 &= -\operatorname{div}_x \frac{\partial \mathbf{u}_s^1}{\partial t}(\mathbf{x}, t), \\ \bar{\rho} C_T \frac{\partial \theta_T^0}{\partial t} - K^T \Delta_{yy} \theta_T^0 &= 0, \quad y \in Q_l, \quad t > 0. \end{aligned} \quad (6.61)$$

Finally, using the solid phase mass balance $\phi_l^0 - \bar{\phi}_l = \bar{\phi}_s \operatorname{div} \mathbf{u}_s^0$ in the post processing (6.36) gives

$$p_l^0 = p_B^0 + \bar{\Pi}_B - \bar{p}_* (\phi_l^0 - \bar{\phi}_l) = p_B^0 + \bar{\Pi}_B - \bar{p}_* \bar{\phi}_s (\operatorname{div}_y \mathbf{u}_s^1 + \operatorname{div}_x \mathbf{u}_s^0).$$

7. Reduced models

We now exploit several consequences of the dual porosity model with microstructure. We begin by showing that application of the Green's function method reduces the microstructural system in seven variables (x, y, t) to a reduced system in (x, t) with fading memory. Subsequently we show how lumped-parameter models such as the one developed by Wilson and Aifantis [75] and Khaled et al. [45] can be recovered from the general microstructural model.

7.1. Green's function method and memory effects

Within the context of microstructural dual porosity models for flow in rigid fissured media, Arbogast [2] and Peszynska [59] have shown that application of the Green's function method reduces the dual porosity equations to a single integro-differential equation of Volterra type. Next we exploit this idea and illustrate how application of the same technique to the proposed dual porosity model for swelling media leads to integrodifferential governing equations. In particular we exploit a notable consequence of this procedure in providing a rational basis to rigorously explain some secondary consolidation stress constitutive equations of viscoelastic type which account for creep effects due to the delayed drainage of the adsorbed water in the secondary consolidation stage (see e.g. [22]).

Green's functions (GFs) have been used in the solution of transient heat conduction equations for over a century. Carslaw and Jaeger [20] and Ozisik [58] present an introduction to the method for heat conduction problems and derive the pertinent Green's function by using a Laplace transform. Physically a $GF(y, y', t)$ represents the temperature field at position y and time t due to an instantaneous point source of unit strength at position y' . Recently Feng and Michaelides [30]

pointed out some drawbacks of the classical GFs formulation such as its dependence not only on the geometry of the solid, but also on the position of the source y' . To overcome this difficulty they proposed a modified Green's function method (MGFs) which represents the temperature induced by a unit impulse $\delta(t - \tau)$ on the boundary of the solid at time $t = \tau$. The main difference is that the MGF's depend only on the geometry of the solid considered and not on the position of the source y' . The MGFs technique has proved to be a powerful tool for deriving averaged properties of solids, such as averaged heat transfer.

To illustrate the application of the MGFs method to the proposed dual porosity system, we consider the case of large Biot numbers (δ_T and $\delta_p \rightarrow \infty$) such that we may assume that the reference pressure and temperature are continuous on the interface Γ ($p_B = p_f$ and $\theta_T = \theta_f$ on Γ). Begin by considering the local cell heat equation (6.21), (6.22) and define the modified Green's function for temperature $G_\theta(y, t)$ as the solution of (see [30])

$$\begin{aligned} \bar{\rho}C_T \frac{\partial G_\theta}{\partial t} - K^T \Delta_{yy} G_\theta &= 0 \quad \text{in } Q_1, \\ G_\theta &= \delta(t) \quad \text{on } \Gamma, \\ G_\theta &= 0 \quad \text{in } Q_1, t = 0, \end{aligned} \tag{7.1}$$

where $\delta(t)$ denotes the Dirac measure at $t = 0$. Following the usual procedure we express $\theta_T^0(y, t)$, the solution of the heat equation (6.21) and (6.22) with boundary and initial conditions in (6.58) (with $\delta_T \rightarrow \infty$), in terms of $\theta_f^0(x, t)$ and $G_\theta(y, t)$. To this end define the Laplace transform

$$Lf(t) = \int_0^\infty \exp(-St)f(t)dt = \widehat{f}(S).$$

In Laplace space, the heat equations for $\widehat{\theta}_T^0$ and \widehat{G}_θ^0 are

$$\begin{aligned} K^T \Delta_{yy} \widehat{\theta}_T^0 &= \bar{\rho}C_T S \widehat{\theta}_T^0 \quad \text{in } Q_1, \quad \widehat{\theta}_T^0 = \widehat{\theta}_f^0 \quad \text{on } \Gamma \\ K^T \Delta_{yy} \widehat{G}_\theta &= \bar{\rho}C_T S \widehat{G}_\theta \quad \text{in } Q_1, \quad \widehat{G}_\theta = 1 \quad \text{on } \Gamma. \end{aligned}$$

We then have by linearity

$$\widehat{\theta}_T^0(x, y, S) = \widehat{G}_\theta(y, S) \widehat{\theta}_f^0(x, S). \tag{7.2}$$

Hence, by inverting the Laplace transform we get the convolution relation

$$\theta_T^0(x, y, t) = G_\theta * \theta_f^0 \equiv \int_0^T G_\theta(y, t - \tau) \theta_f^0(x, \tau) d\tau. \tag{7.3}$$

Averaging this result and combining it with the mass and energy balances (6.54) and (6.55) and Darcy's and Fourier's laws for the bulk water we find

$$-\alpha_f n_f \frac{\partial \theta_f^0}{\partial t} + \operatorname{div}_x \frac{\partial \mathbf{u}_s^0}{\partial t} - K_f \Delta_{xx} p_f^0 = \bar{\phi}_f \alpha_l \left(\widetilde{G}_\theta * \frac{\partial \theta_f^0}{\partial t} \right), \quad (7.4)$$

$$\bar{\rho}_f n_f C_f \frac{\partial \theta_f^0}{\partial t} - K_f^T \Delta_{xx} \theta_f^0 = -\bar{\rho} C_T \left(\widetilde{G}_\theta * \frac{\partial \theta_f^0}{\partial t} \right), \quad (7.5)$$

where the convolution product property $\partial(f_1 * f_2)/\partial t = f_1(0)f_2(t) + (\partial f_1/\partial t * f_2)$ has been used together with the initial condition (6.35).

We now pursue the derivation of analogous convolution relations for the pair $\{\mathbf{u}_s^1, p_b^0\}$. Using (7.2), in the Laplace space, problem (6.61) for \mathbf{u}_s^1 and p_b^0 , supplemented by the initial conditions together with first and second boundary conditions in (6.58) (with $\delta_P \rightarrow \infty$) is given by:

$$\begin{aligned} \mu_s \Delta_{yy} \widehat{\mathbf{u}}_s^1 + (\lambda_s^* + \mu_s + S\mu_{ls}) \nabla_y \operatorname{div}_y \widehat{\mathbf{u}}_s^1 - \nabla_y \widehat{p}_b^0 &= \alpha_* \nabla_y \widehat{\theta}_T^0 = \alpha_* \widehat{\theta}_f^0 \nabla_y \widehat{G}_\theta \quad \text{in } Q_l, \\ S \operatorname{div}_y \widehat{\mathbf{u}}_s^1 - K_l \Delta_{yy} \widehat{p}_b^0 + S \operatorname{div}_x \widehat{\mathbf{u}}_s^0(x, S) &= \alpha_l \bar{\phi}_l S \widehat{\theta}_T^0 = \alpha_l \bar{\phi}_l S \widehat{\theta}_f^0 \widehat{G}_\theta \quad \text{in } Q_l, \\ \left[-\widehat{p}_b^0 \mathbf{I} + ((\lambda_s^* + S\mu_{ls}) \mathbf{I} : +2\mu_s) \nabla_y^s \widehat{\mathbf{u}}_s^1 \right] \mathbf{n} &= \left(-\widehat{\mathbf{t}}_0^* + \alpha_* \widehat{\theta}_f^0 \widehat{G}_\theta \mathbf{I} \right) \mathbf{n} \quad \text{on } \Gamma, \\ \widehat{p}_b^0 &= 0 \quad \text{on } \Gamma, \end{aligned} \quad (7.6)$$

with the Neumann boundary condition $\widehat{\mathbf{t}}_1 \mathbf{n} = -\widehat{\mathbf{t}}_0^* \mathbf{n}$ modified appropriately by making use of the constitutive laws (6.45), (6.47) and (6.49). Now turn to the task of defining the MGF's for displacement and pressure. To this end, for given $\{\mathbf{f}, g, \mathbf{h}\}$ depending on (y, t) , consider the isothermal version of (6.61) and define the problem

$$\begin{aligned} \mu_s \Delta_{yy} \mathbf{u}_s^1 + (\lambda_s^* + \mu_s) \nabla_y \operatorname{div}_y \mathbf{u}_s^1 - \nabla_y p_b^0 + \mu_{ls} \nabla_y \operatorname{div}_y \frac{\partial \mathbf{u}_s^1}{\partial t} &= \mathbf{f} \quad \text{in } Q_l, \\ \operatorname{div}_y \frac{\partial \mathbf{u}_s^1}{\partial t} - K_l \Delta_{yy} p_b^0 &= g \quad \text{in } Q_l, \\ \mathbf{t}_1 \mathbf{n} &= \mathbf{h} \mathbf{n} \quad \text{on } \Gamma, \\ p_b^0 &= 0 \quad \text{on } \Gamma. \end{aligned} \quad (7.7)$$

Define the pairs of modified Green's functions $\{\mathbf{G}_u^h, G_p^h\}$, $\{\mathbf{G}_u^g, G_p^g\}$, as the pair $\{\mathbf{u}_s^1, p_b^0\}$, solution to the above problem with $\{\mathbf{f} = g = 0, \mathbf{h} = -\delta(t)\mathbf{I}\}$ and $\{\mathbf{f} = \mathbf{h} = 0, g = -\delta(t)\}$, respectively. In addition, for given G_θ , satisfying (7.1), define the auxiliary functions $\{\mathbf{G}_{u\theta}^h, G_{p\theta}^h\}$ and $\{\mathbf{G}_{u\theta}^g, G_{p\theta}^g\}$ the solutions of the above problem with $\{\mathbf{f} = \alpha_* \nabla_y G_\theta, g = 0, \mathbf{h} = \alpha_* G_\theta \mathbf{I}\}$ and $\{\mathbf{f} = \mathbf{h} = 0, g = \alpha_l \bar{\phi}_l G_\theta\}$.

With the MGFs defined above, we now show that problems (7.7) and (7.6) are linearly related. To show this we generalize to the $\{\mathbf{u}_s^1, p_b^0\}$ system, the arguments leading to (7.2), based on linearity. To accomplish this consider the variational formulations of (7.6) and (7.7). Let $L^2(Q_l)$ denote the usual set of square integrable, scalar valued, Q -periodic functions defined on Q_l , with inner product

$$(f, g) \equiv \int_{Q_1} fg dQ_1 \quad \forall f, g \in L^2(Q_1)$$

and let $H^1(Q_1)$ denote the Sobolev subspace of $L^2(Q_1)$ consisting of functions with the derivative ∂f in the distributional sense satisfying $\partial f \in L^2(Q_1)$. Further, let U and V denote respectively the spaces of vectorial and scalar functions

$$U(Q_1) \equiv \left\{ f \in (L^2(Q_1))^3, \nabla f \in (L^2(Q_1))^9, \int_{Q_1} f dQ_1 = 0 \right\},$$

$$V(Q_1) \equiv H_0^1(Q_1) \equiv \{ f \in H^1(Q_1), f = 0 \text{ on } \Gamma \}.$$

The variational formulation of (7.6) consists in, for each $S \in (0, \infty)$, find $\{\widehat{\mathbf{u}}_s^1(s), \widehat{p}_b^0(s)\} \in U \times V$ such that:

$$\begin{aligned} 2\mu_s(\nabla_y^s \widehat{\mathbf{u}}_s^1, \nabla_y^s v) + (\lambda_s^* + S\mu_{ls})(\operatorname{div}_y \widehat{\mathbf{u}}_s^1, \operatorname{div}_y v) - (\widehat{p}_b^0, \operatorname{div}_y v) &= \alpha_* \widehat{\theta}_f^0(\widehat{G}_\theta, \operatorname{div}_y v) - (\widehat{\mathbf{t}}_0^*, v) \quad \forall v \in V \\ (S \operatorname{div}_y \widehat{\mathbf{u}}_s^1, q) + K_l(\nabla_y \widehat{p}_b^0, \nabla_y q) &= -(S \operatorname{div}_x \widehat{\mathbf{u}}_s^0, q) + \alpha_l \bar{\phi}_l S \widehat{\theta}_f^0(\widehat{G}_\theta, q) \quad \forall q \in V, \end{aligned}$$

where

$$(\widehat{\mathbf{t}}_0^*, v)_\Gamma \equiv \int_\Gamma \widehat{\mathbf{t}}_0^* \cdot \mathbf{n} \cdot v d\Gamma.$$

This formulation can be rewritten in terms of the weak form of a single elliptic problem in the product space $U \times V$. To show this define the bilinear form

$$\begin{aligned} A(\widehat{\mathbf{u}}_s^1, \widehat{p}_b^0; v, q) &\equiv 2\mu_s(\nabla_y^s \widehat{\mathbf{u}}_s^1, \nabla_y^s v) + (\lambda_s^* + S\mu_{ls})(\operatorname{div}_y \widehat{\mathbf{u}}_s^1, \operatorname{div}_y v) - (\widehat{p}_b^0, \operatorname{div}_y v) \\ &\quad + (S \operatorname{div}_y \widehat{\mathbf{u}}_s^1, q) + K_l(\nabla_y \widehat{p}_b^0, \nabla_y q) \end{aligned}$$

and the linear function

$$F(v, q) = \alpha_* \widehat{\theta}_f^0(\widehat{G}_\theta, \operatorname{div}_y v) + \alpha_l \bar{\phi}_l S \widehat{\theta}_f^0(\widehat{G}_\theta, q) - (\widehat{\mathbf{t}}_0^*, v)_\Gamma - S(\operatorname{div}_x \widehat{\mathbf{u}}_s^0, q). \quad (7.8)$$

Thus we can rewrite the variational formulation as, for each $S \in (0, \infty)$, find $\{\widehat{\mathbf{u}}_s^1(s), \widehat{p}_b^0(s)\} \in U \times V$ such that:

$$A(\widehat{\mathbf{u}}_s^1, \widehat{p}_b^0; v, q) = F(v, q), \quad \forall \{v, q\} \in U \times V. \quad (7.9)$$

This defines a robust elliptic problem in the Laplace space. A straightforward application of Korn's and Poincaré's inequalities shows coercivity of $A(v, v; q, q)$ in the product space $U \times V$. Hence, existence of a unique solution follows from application of the Lax–Milgram lemma.

From (7.8), the corresponding variational problems for the Green's functions are

$$\begin{aligned} A(\widehat{\mathbf{G}_u^h}, \widehat{\mathbf{G}_p^h}; \mathbf{v}, \mathbf{q}) &= -(\mathbf{I}, \mathbf{v})_{\Gamma}, \quad A(\widehat{\mathbf{G}_{u\theta}^h}, \widehat{\mathbf{G}_{p\theta}^h}; \mathbf{v}, \mathbf{q}) = \alpha_* (\widehat{\mathbf{G}_\theta}, \operatorname{div}_y \mathbf{v}), \\ A(\widehat{\mathbf{G}_u^g}, \widehat{\mathbf{G}_p^g}; \mathbf{v}, \mathbf{q}) &= -(1, \mathbf{q}), \quad A(\widehat{\mathbf{G}_{u\theta}^g}, \widehat{\mathbf{G}_{p\theta}^g}; \mathbf{v}, \mathbf{q}) = \alpha_1 \bar{\phi}_1 (\widehat{\mathbf{G}_\theta}, \mathbf{q}), \quad \forall \{\mathbf{v}, \mathbf{q}\} \in U \times V. \end{aligned} \quad (7.10)$$

With F given in (7.8), the linearity between (7.9) and (7.10) gives

$$\begin{aligned} \widehat{\mathbf{u}}_s^1 &= \widehat{\mathbf{G}_u^h} \widehat{\mathbf{t}_0^*}(\mathbf{x}, S) + \widehat{\mathbf{G}_u^g}(\mathbf{y}) S \operatorname{div}_x \mathbf{u}_s^0(\mathbf{x}, S) + \widehat{\mathbf{G}_{u\theta}^h} \widehat{\theta_f^0}(\mathbf{x}, S) + \widehat{\mathbf{G}_{u\theta}^g} S \widehat{\theta_f^0}(\mathbf{x}, S), \\ \widehat{\mathbf{p}}_b^0 &= \widehat{\mathbf{G}_p^h} \widehat{\mathbf{t}_0^*}(\mathbf{x}, S) + \widehat{\mathbf{G}_p^g}(\mathbf{y}) S \operatorname{div}_x \mathbf{u}_s^0(\mathbf{x}, S) + \widehat{\mathbf{G}_{p\theta}^h} \widehat{\theta_f^0}(\mathbf{x}, S) + \widehat{\mathbf{G}_{p\theta}^g} S \widehat{\theta_f^0}(\mathbf{x}, S), \end{aligned}$$

which after inverting the Laplace transform yields

$$\begin{aligned} \mathbf{u}_s^1(\mathbf{x}, \mathbf{y}, t) &= \mathbf{G}_u^h * \mathbf{t}_0^* + \mathbf{G}_u^g * \operatorname{div}_x \frac{\partial \mathbf{u}_s^0}{\partial t} + \mathbf{G}_{u\theta}^h * \theta_f^0 + \mathbf{G}_{u\theta}^g * \frac{\partial \theta_f^0}{\partial t}, \\ \mathbf{p}_b^0(\mathbf{x}, \mathbf{y}, t) &= \mathbf{G}_p^h * \mathbf{t}_0^* + \mathbf{G}_p^g * \operatorname{div}_x \frac{\partial \mathbf{u}_s^0}{\partial t} + \mathbf{G}_{p\theta}^h * \theta_f^0 + \mathbf{G}_{p\theta}^g * \frac{\partial \theta_f^0}{\partial t}. \end{aligned}$$

Using the above relations in (6.45), (6.47) and (6.49) we obtain after averaging

$$\begin{aligned} \widetilde{\mathbf{t}}_1 &= -(\widetilde{\mathbf{p}}_b^0 + \widetilde{\Pi}_1) \mathbf{I} + \widetilde{\sigma}_1 = -\widetilde{\mathbf{p}}_b^0 \mathbf{I} + (\lambda_s^* \mathbf{I} : + 2\mu_s) \widetilde{\nabla_y^s \mathbf{u}_s^1} + \mu_{ls} \frac{\partial}{\partial t} \widetilde{\operatorname{div}_y \mathbf{u}_s^1} \mathbf{I} - \alpha_* \widetilde{\theta_T^0} \mathbf{I}, \\ &= \widetilde{\mathbf{K}_h} * \mathbf{t}_0^* + \widetilde{\mathbf{K}_g} * \operatorname{div}_x \frac{\partial \mathbf{u}_s^0}{\partial t} \mathbf{I} + (\widetilde{\mathbf{K}_h^0} - \alpha_* \widetilde{\mathbf{G}_\theta}) * \theta_f^0 \mathbf{I} + \widetilde{\mathbf{K}_g^0} * \frac{\partial \theta_f^0}{\partial t} \mathbf{I} + \mu_{ls} \frac{\partial}{\partial t} \\ &\quad \times \left(\widetilde{\operatorname{div}_y \mathbf{G}_u^h} * \mathbf{t}_0^* + \widetilde{\operatorname{div}_y \mathbf{G}_u^g} * \operatorname{div}_x \frac{\partial \mathbf{u}_s^0}{\partial t} + \widetilde{\operatorname{div}_y \mathbf{G}_{u\theta}^h} * \theta_f^0 + \widetilde{\operatorname{div}_y \mathbf{G}_{u\theta}^g} * \frac{\partial \theta_f^0}{\partial t} \right) \end{aligned} \quad (7.11)$$

with

$$\begin{aligned} \mathbf{K}_J(\mathbf{y}, t) &= (\lambda_s^* \mathbf{I} : + 2\mu_s) \nabla_y^s \mathbf{G}_u^J - \mathbf{G}_p^J \mathbf{I}, \\ \mathbf{K}_J^0(\mathbf{y}, t) &= (\lambda_s^* \mathbf{I} : + 2\mu_s) \nabla_y^s \mathbf{G}_{u\theta}^J - \mathbf{G}_{p\theta}^J \mathbf{I}, \quad J = h, g, \end{aligned}$$

and (7.3) was also used. Hence, the fluctuating part of the macroscopic stress tensor, $\widetilde{\mathbf{t}}_1$, exhibits a viscoelastic constitutive behavior with memory which is represented by the convolution products in (7.11). Denoting $\widetilde{\mathbf{K}_h^*} = \widetilde{\mathbf{K}_h^0} - \alpha_* \widetilde{\mathbf{G}_\theta}$, and collecting the results (6.44), (6.46), (6.50), (6.53), (7.4), (7.5) and (7.11), we obtain the following system in (\mathbf{x}, t) with memory in terms of $\{\widetilde{\mathbf{t}}_0^*, \mathbf{p}_f^0, \widetilde{\mathbf{t}}_1, \theta_f^0, \mathbf{u}_s^0\}$.

$$\begin{aligned}
\operatorname{div}_x \tilde{\mathbf{t}}_0^* - \nabla_x p_f^0 &= -\operatorname{div}_x \tilde{\mathbf{t}}_1, \\
\tilde{\mathbf{t}}_0^* &= n_l \bar{\Pi} + \lambda_s^* \operatorname{div}_x \mathbf{u}_s^0 + \mu_s \nabla_x^s \mathbf{u}_s^0 + \mu_{ls} \operatorname{div}_x \frac{\partial \mathbf{u}_s^0}{\partial t}, \\
\tilde{\mathbf{t}}_1 &= \widetilde{K}_h * \mathbf{t}_0^* + \widetilde{K}_g * \operatorname{div}_x \frac{\partial \mathbf{u}_s^0}{\partial t} \mathbf{I} + \widetilde{K}_h^\theta * \theta_f^0 \mathbf{I} + \widetilde{K}_g^\theta * \frac{\partial \theta_f^0}{\partial t} \mathbf{I} + \mu_{ls} \frac{\partial}{\partial t} \\
&\quad \times \left(\widetilde{\operatorname{div}_y \mathbf{G}_u^h} * \mathbf{t}_0^* + \widetilde{\operatorname{div}_y \mathbf{G}_u^g} * \operatorname{div}_x \frac{\partial \mathbf{u}_s^0}{\partial t} + \widetilde{\operatorname{div}_y \mathbf{G}_u^h} * \theta_f^0 + \widetilde{\operatorname{div}_y \mathbf{G}_u^g} * \frac{\partial \theta_f^0}{\partial t} \right), \quad (7.12) \\
&\quad - \alpha_f n_f \frac{\partial \theta_f^0}{\partial t} + \operatorname{div}_x \frac{\partial \mathbf{u}_s^0}{\partial t} - K_f \Delta_{xx} p_f^0 = \bar{\phi}_l \alpha_l \left(\widetilde{G}_\theta * \frac{\partial \theta_f^0}{\partial t} \right), \\
\bar{\rho}_f n_f C_f \frac{\partial \theta_f^0}{\partial t} - K_f^T \Delta_{xx} \theta_f^0 &= -\bar{\rho} C_T \left(\widetilde{G}_\theta * \frac{\partial \theta_f^0}{\partial t} \right).
\end{aligned}$$

Thus, we have shown that the application of the modified Green's function technique reduces the microstructural dual porosity model to a system of integro-differential equations of Volterra type in which the dependence on the microstructure is incorporated in the convolution products appearing in the r.h.s. of (7.12). The convolution kernels ($K_J, K_J^\theta, J = h, g$) are related to the MGFs and can be calculated explicitly for a given particle geometry. In this formulation, the memory appears related to the delayed response of the vicinal water to local variations in the bulk phase. Among other effects, this delay is responsible for the creep viscous behavior of the clay structure under consolidation. This creep effect gives rise to a secondary compression stage, after the bulk water has been drained from the larger pores in the primary structure.

7.2. Isothermal models for secondary consolidation and creep

A simplified form of the above integro-differential system can be derived when thermal effects and the relaxation of the vicinal water (due to the coefficient μ_{ls}) are negligible. Under these assumptions the generalized non-isothermal system of integro-differential (7.12) reduce to an isothermal system resembling in form some rheological models for secondary consolidation and creep in clay soils. Setting $\theta_f^0 = \theta_T^0 = 0$ and neglecting the relaxation coefficient μ_{ls} in (7.11) we obtain

$$\tilde{\mathbf{t}}_1 = \widetilde{K}_h * \mathbf{t}_0^* + \widetilde{K}_g * \operatorname{div}_x \frac{\partial \mathbf{u}_s^0}{\partial t} \mathbf{I}.$$

Under these assumptions, the system (7.12) reduces to

$$\begin{aligned}
\operatorname{div}_x \tilde{\mathbf{t}}_0^* - \nabla_x p_f^0 &= -\operatorname{div}_x \tilde{\mathbf{t}}_1, \\
\tilde{\mathbf{t}}_0^* &= n_l \bar{\Pi} + \lambda_s^* \operatorname{div}_x \mathbf{u}_s^0 + \mu_s \nabla_x^s \mathbf{u}_s^0, \quad (7.13) \\
\tilde{\mathbf{t}}_1 &= \widetilde{K}_h * \mathbf{t}_0 + \widetilde{K}_g * \operatorname{div}_x \frac{\partial \mathbf{u}_s^0}{\partial t} \mathbf{I}, \\
\operatorname{div}_x \frac{\partial \mathbf{u}_s^0}{\partial t} - K_F \Delta_{xx} p_f^0 &= 0.
\end{aligned}$$

This result shows that the overall macroscopic stress tensor is decomposed into a non-oscillatory elastic component (\mathbf{t}_0^*) and a fluctuation ($\tilde{\mathbf{t}}_1$) governed by a viscoelastic constitutive behavior. The viscoelastic component exhibits fading memory as $\tilde{\mathbf{t}}_1$ depends on the history of the strain. This macroscale isothermal model resembles in form some viscoelastic models which have been proposed for creep during secondary consolidation (see e.g. [16,22,39,73]). Note that for the case where the convolution kernels are Dirac measures, (7.13) reduces to a macroscopic system exhibiting short term memory rather than fading memory. In this case, secondary consolidation is governed by the Kelvin Voigt viscoelastic constitutive equations, consisting of springs in combination with dashpots (see e.g. [31,48,76]).

7.3. Lumped-parameter first-order kinetic models

We now turn to the task of reproducing some of the classical lumped-parameter models for heat, mass and momentum transfer ([9,64,74,75]) as particular cases of the general microstructural dual porosity model of Section 6. We begin by reproducing lumped-parameter first-order kinetic models which correspond to small particles with high conductivities (relative to the surface film coefficient) so that local pressure and temperature gradients within the particles may be neglected. Under this assumption, p_b^0 and θ_T^0 are independent of the local variable y and consequently their time evolution is dictated by the interfacial resistance. In terms of the Biot numbers, this asymptotic case corresponds to the limit $Bi_j \rightarrow 0$, ($j = P, T$) where particle resistance to heat conduction and fluid flow is small compared to the convection resistance at the particle surface.

First-order kinetic model for heat conduction. We begin by discussing a first-order kinetic model for heat conduction. Assume that the particle thermal conductivity K^T tends to infinity so that local temperature gradients within the particles are negligible ($\nabla_y \theta_T = 0$ and $\theta_T = \theta_T(\mathbf{x}, t)$). This is equivalent to a time scale assumption, wherein for each instant of time t , we have local thermal equilibrium within the particle domain.

Using definition (6.57) for E_* and Q_* , by averaging the energy (6.22) together with the boundary condition (6.31) gives

$$E_* = -\frac{\bar{\rho}C_T}{|Q|} \int_{Q_l} \frac{\partial \theta_T^0}{\partial t} dQ_l = \frac{1}{|Q|} \int_{\Gamma} \mathbf{h}_T^l \mathbf{n} d\Gamma = \widetilde{\delta}_T (\theta_T^0(\mathbf{x}, t) - \theta_f^0(\mathbf{x}, t)), \quad \widetilde{\delta}_T \equiv \frac{1}{|Q|} \int_{\Gamma} \delta_T d\Gamma.$$

Whence

$$Q_* = \frac{\bar{\phi}_l \alpha_l}{|Q|} \int_{Q_l} \frac{\partial \theta_T^0}{\partial t} dQ_l = \widetilde{h}_T (\theta_f^0(\mathbf{x}, t) - \theta_T^0(\mathbf{x}, t)), \quad \widetilde{h}_T \equiv \frac{\bar{\phi}_l \alpha_l \widetilde{\delta}_T}{\bar{\rho}C_T}.$$

The dual porosity model (6.60) and (6.61) reduces to

$$\begin{aligned} \mu_S \Delta_{xx} \mathbf{u}_S^0 + (\lambda_S^* + \mu_S) \nabla_x \operatorname{div}_x \mathbf{u}_S^0 + \mu_{LS} \nabla_x \operatorname{div}_x \frac{\partial \mathbf{u}_S^0}{\partial t} - \nabla_x p_f^0 - n_l \alpha_* \nabla_x \theta_T^0 &= \mathbf{F}_*(\mathbf{x}, t), \\ - \alpha_f n_f \frac{\partial \theta_f^0}{\partial t} + \operatorname{div}_x \frac{\partial \mathbf{u}_S^0}{\partial t} - K_f \Delta_{xx} p_f^0 &= \widetilde{h}_T (\theta_f^0 - \theta_T^0), \end{aligned} \quad (7.14)$$

$$\bar{\rho}_f n_f C_f \frac{\partial \theta_f^0}{\partial t} - K_F^T \Delta_{xx} \theta_f^0 = \widetilde{\delta_T} (\theta_T^0 - \theta_f^0),$$

$$\bar{\rho} n_l C_T \frac{\partial \theta_T^0}{\partial t} = -\widetilde{\delta_T} (\theta_T^0 - \theta_f^0), \quad x \in \Omega_f, \quad t > 0$$

with

$$F_*(x, t) = -2\mu_s \operatorname{div}_x \widetilde{\nabla_y u_s^1} - \lambda_s^* \nabla_x \operatorname{div}_y \widetilde{u_s^1} + \nabla_x \widetilde{p_b^0} - \mu_{ls} \nabla_x \frac{\partial}{\partial t} \operatorname{div}_y \widetilde{u_s^1} \quad (7.15)$$

and

$$\mu_s \Delta_{yy} u_s^1 + (\lambda_s^* + \mu_s) \nabla_y \operatorname{div}_y u_s^1 - \nabla_y p_b^0 + \mu_{ls} \nabla_y \operatorname{div}_y \frac{\partial u_s^1}{\partial t} = 0, \quad (7.16)$$

$$\operatorname{div}_y \frac{\partial u_s^1}{\partial t} - K_l \Delta_{yy} p_b^0 = -\operatorname{div}_x \frac{\partial u_s^1}{\partial t} (x, t) - \widetilde{\delta_T} (\theta_T^0 - \theta_f^0), \quad y \in Q_l, \quad t > 0.$$

The exchange of mass and energy between the local and global systems is given in terms of simplified relations, assumed proportional to a temperature difference. The remaining distributed source/sink term whose evaluation still requires averaging the solution of the cell problem (7.16), is the momentum transfer function F_* .

Lumped-parameter first-order kinetic hydrodynamical model. We now make use of a similar lumped-parameter assumption for the fluid flow problem. In analogy to the previous heat transfer analysis, we consider a time scale assumption wherein the intra-particle fluid is assumed uniformly distributed throughout the local cell, at instantaneous mechanical and thermal equilibrium as it is disturbed by the global system. The intra-particle non-equilibrium effects are overlooked, the hydraulic conductivity, K_l , tends to infinity and the relaxation coefficient μ_* tends to zero. Hence, p_B^0 is independent of the fast variable y and consequently the cell behaves as a single point for both fluid flow and heat transfer. Next we show that under these assumptions the adsorbed/bulk water mass transfer function is governed by a simplified Warren–Root-type coupling. Averaging the mass balance (6.18) and using boundary condition (6.30) gives

$$\frac{\bar{\phi}_l \alpha_l}{|Q_l|} \int_{Q_l} \frac{\partial \theta_T^0}{\partial t} dQ_l = \int_{\Gamma} q_l^1 d\Gamma + \frac{1}{|Q_l|} \int_{Q_l} \operatorname{div}_y \frac{\partial u_s^1}{\partial t} dQ_l + n_l \operatorname{div}_x \frac{\partial u_s^1}{\partial t}$$

$$= \frac{\partial}{\partial t} \operatorname{div}_y \widetilde{u_s^1} + n_l \operatorname{div}_x \frac{\partial u_s^1}{\partial t} + \widetilde{\delta_P} (p_B^0 - p_f^0), \quad \widetilde{\delta_P} \equiv \frac{1}{|Q_l|} \int_{\Gamma} \delta_P d\Gamma. \quad (7.17)$$

With absence of intra-particle non-equilibrium effects, a simplified elasticity solution can be obtained for the fluctuating displacement u_s^1 . Denote δ_{ij} the Kronecker delta symbol and a^* a fourth-order tensor with components $a_{ijkl} = \lambda_s^* \delta_{ij} \delta_{kl} + \mu_s (\delta_{ik} \delta_{jl} + \delta_{il} \delta_{jk})$. Without loss of generality and ease of exposition, we restrict subsequent discussion to the case of absence of swelling stresses at the reference configuration ($\bar{\Pi} = 0$). Using the fact that $p_b = p_b(x, t)$ and $\mu_{ls} = 0$ in (7.16) together

with boundary condition (6.56) shows that \mathbf{u}_s^1 satisfies the following elasticity problem with Neumann boundary conditions

$$\begin{aligned}\operatorname{div}_y(\mathbf{a}^* \nabla_y \mathbf{u}_s^1) &= 0 \quad \text{in } Q_1, \\ \mathbf{t}_1 \mathbf{n} &= [\mathbf{a}^* \nabla_y^s \mathbf{u}_s^1 - (\alpha_* \theta_T^0 + p_b^0) \mathbf{I}] \mathbf{n} = -\mathbf{t}_0^* \mathbf{n} = -(\mathbf{a}^* \nabla_x^s \mathbf{u}_s^0) \mathbf{n} \quad \text{on } \Gamma,\end{aligned}$$

where constitutive (6.44)–(6.50) for \mathbf{t}_1 and \mathbf{t}_0^* have been used. Let $\Pi = \delta_{ij} \delta_{kl}$ denote the unity fourth-order tensor and let Ψ and \mathbf{v} be respectively a third-order tensor and a vector satisfying the following canonical cell problems

$$\begin{aligned}\operatorname{div}_y(\mathbf{a}^* \nabla_y^s \Psi) &= 0 \quad \text{in } Q_1, \\ \mathbf{a}^* \nabla_y^s \Psi \cdot \mathbf{n} &= -\mathbf{a}^* \Pi \cdot \mathbf{n} \quad \text{on } \Gamma, \quad (\mathbf{a}^* \nabla_y^s \mathbf{v}) \mathbf{n} = \mathbf{In} \quad \text{on } \Gamma.\end{aligned}$$

By linearity, \mathbf{u}_s^1 is given by:

$$\mathbf{u}_s^1 = \Psi(y) \nabla_s \mathbf{u}_s^0(\mathbf{x}, t) + \mathbf{v}(y) [p_b^0(\mathbf{x}, t) + \alpha_* \theta_T^0(\mathbf{x}, t)]. \quad (7.18)$$

Using this result in (7.15), the distributed source term is then given by

$$\mathbf{F}_* = -\operatorname{div}_x(\mathbf{a}^* \widetilde{\nabla_y^s \mathbf{u}_s^1}) + n_l \nabla_x p_b^0 = -\operatorname{div}_x(\mathbf{a}^* \widetilde{\nabla_y^s \Psi} \nabla_x^s \mathbf{u}_s^0) + (n_l \mathbf{I} - \mathbf{a}^* \widetilde{\nabla_y^s \mathbf{v}}) \nabla_x p_b^0 - \alpha_* \mathbf{a}^* \widetilde{\nabla_y^s \mathbf{v}} \nabla_x \theta_T^0$$

which when combined with the first equation in (7.14), with $\mu_{LS} = 0$, gives

$$\operatorname{div}_x(c \nabla_x^s \mathbf{u}_s^0) - \nabla_x p_f^0 - (n_l \mathbf{I} - \mathbf{a}^* \widetilde{\nabla_y^s \mathbf{v}}) \nabla_x p_b^0 - \alpha_*(n_l \mathbf{I} - \mathbf{a}^* \widetilde{\nabla_y^s \mathbf{v}}) \nabla_x \theta_T^0 = 0,$$

where c denotes the fourth-order tensor $c \equiv n_l \mathbf{a}^* + \mathbf{a}^* \widetilde{\nabla_y^s \Psi}$. Further, with isotropy, $\operatorname{div}_y \widetilde{\Psi} = \operatorname{div}_y \widetilde{\Psi} \mathbf{I}$ and c and $\widetilde{\nabla_y^s \mathbf{v}}$ admit the representations

$$c_{ijkl} = \lambda_s^0 \delta_{ij} \delta_{kl} + \mu_s^0 (\delta_{ik} \delta_{jl} + \delta_{il} \delta_{jk}), \quad \mathbf{a}^* \widetilde{\nabla_y^s \mathbf{v}} = (3\lambda_s^* + 2\mu_s) \widetilde{\operatorname{div}_y \mathbf{v} \mathbf{I}} = -\widetilde{\operatorname{div}_y \Psi \mathbf{I}}.$$

Hence, denoting $\gamma' \equiv \widetilde{\operatorname{div}_y \mathbf{v}}$, $\gamma_1 \equiv n_l - \gamma(3\lambda_s^* + 2\mu_s) = n_l + \widetilde{\operatorname{div}_y \Psi}$ and $\gamma_2 \equiv 1 - \gamma_1$, since $p_b^0 = p_B^0 - p_f^0$, the overall momentum equation can be rewritten as:

$$\mu_s^0 \Delta_{xx} \mathbf{u}_s^0 + (\lambda_s^0 + \mu_s^0) \nabla_x \operatorname{div}_x \mathbf{u}_s^0 - \gamma_1 \nabla_x p_B^0 - \gamma_2 \nabla_x p_f^0 - \alpha_* \gamma_1 \nabla_x \theta_T^0 = 0.$$

Substituting relation (7.18) for \mathbf{u}_s^1 in the mass balance (7.17), we obtain

$$-\bar{\phi}_l \alpha_l n_l \frac{\partial \theta_T^0}{\partial t} + n_l \operatorname{div}_x \frac{\partial \mathbf{u}_s^0}{\partial t} + \tilde{\delta}_P (p_B^0 - p_f^0) = -\widetilde{\operatorname{div}_y \Psi} \operatorname{div}_x \frac{\partial \mathbf{u}_s^0}{\partial t} - \gamma' \left(\frac{\partial p_b^0}{\partial t} + \alpha_* \frac{\partial \theta_T^0}{\partial t} \right).$$

Whence

$$-\gamma_* \frac{\partial \theta_T^0}{\partial T} + \gamma_1 \operatorname{div}_x \frac{\partial \mathbf{u}_s^0}{\partial t} = -\tilde{\delta}_P (p_B^0 - p_f^0) - \gamma' \frac{\partial (p_B^0 - p_f^0)}{\partial t}, \quad \gamma_* \equiv \bar{\phi}_l \alpha_l n_l - \alpha_* \gamma'.$$

Using the same lumped parameter assumptions in the bulk water mass balance (6.7) and using the boundary conditions (6.24) and (6.30) gives

$$\begin{aligned} -n_f \alpha_f \frac{\partial \theta_f^0}{\partial t} + \widetilde{\operatorname{div}_x v_f^0} &= |Q|^{-1} \int_{\Gamma} v_f^1 \cdot \mathbf{n} d\Gamma = |Q|^{-1} \int_{\Gamma} \left(q_1^1 + \frac{\partial u_s^1}{\partial t} \right) \cdot \mathbf{n} d\Gamma \\ &= \frac{\partial}{\partial t} \widetilde{\operatorname{div}_y u_s^1} + \widetilde{\delta_P}(p_B^0 - p_f^0). \end{aligned}$$

Since $\widetilde{v}_f^0 = \widetilde{q}_f^0 + n_f(\partial u_s^0 / \partial t)$, the above result combined with (7.18) gives

$$-\gamma' \alpha_* \frac{\partial \theta_T^0}{\partial t} - \alpha_f n_f \frac{\partial \theta_f^0}{\partial t} + \gamma_2 \operatorname{div}_x \frac{\partial u_s^0}{\partial t} + \operatorname{div}_x \widetilde{q}_f^0 = \widetilde{\delta_P}(p_B^0 - p_f^0) + \gamma' \frac{\partial(p_B^0 - p_f^0)}{\partial t}.$$

Hence the dual porosity model reduces to the following system in (x, t)

$$\begin{aligned} \mu_s^0 \Delta_{xx} u_s^0 + (\lambda_s^0 + \mu_s^0) \nabla_x \operatorname{div}_x u_s^0 - \gamma_2 \nabla_x p_f^0 - \gamma_1 \nabla_x p_B^0 - \alpha_* \gamma_1 \nabla_x \theta_T^0 &= 0, \\ -\gamma' \alpha_* \frac{\partial \theta_T^0}{\partial t} - \alpha_f n_f \frac{\partial \theta_f^0}{\partial t} + \gamma_2 \operatorname{div}_x \frac{\partial u_s^0}{\partial t} - K_F \Delta_{xx} p_f^0 &= \widetilde{\delta_P}(p_B^0 - p_f^0) + \gamma' \frac{\partial(p_B^0 - p_f^0)}{\partial t}, \\ -\gamma_* \frac{\partial \theta_T^0}{\partial t} + \gamma_1 \operatorname{div}_x \frac{\partial u_s^0}{\partial t} &= -\widetilde{\delta_P}(p_B^0 - p_f^0) - \gamma' \frac{\partial(p_B^0 - p_f^0)}{\partial t}, \\ \bar{\rho}_f n_f C_f \frac{\partial \theta_f^0}{\partial t} - K_F \Delta_{xx} \theta_f^0 &= \widetilde{\delta_T}(\theta_T^0 - \theta_f^0), \\ \bar{\rho} n_l C_T \frac{\partial \theta_T^0}{\partial t} &= -\widetilde{\delta_T}(\theta_T^0 - \theta_f^0) \quad x \in \Omega_f, \quad t > 0. \end{aligned}$$

In the above model, the only contributions to the macroscopic heat conduction and fluid flow are due to the bulk phase system. As in the microstructural dual porosity theory, particles act as storage sites for mass and thermal energy. Their contributions to the global problem are manifest in terms of the simplified first-order mass and heat transfer functions. Also note that, since we have neglected the non-equilibrium coefficient μ_{ls} in the above model, physico-chemical effects are manifest in the post-processing approach for p_l^0 and in the equilibrium isothermal and non-isothermal components of the swelling pressure (terms involving K_{ls} and α_{ls}^* in (6.41)). In the resultant macroscopic governing equations, these components are incorporated in the coefficients λ_s^0 and α_* .

In addition to the classical lumped-parameter mass transfer function ($\widetilde{\delta_P}(p_B^0 - p_f^0)$) we may note the appearance of an additional exchange term ($\gamma'(\partial(p_B^0 - p_f^0)/\partial t)$) in the macroscopic mass balances. Within the framework of homogenization this latter component appears strongly related to mass transfer induced by particle consolidation, as it arises from the dependence of the fluctuating displacement, u_s^1 , on the pressure excess p_b^0 through (7.18). Clearly, for rigid media this extra mass transfer component vanishes.

In what follows we pursue the derivation of two-equation models wherein particle flow and heat transfer also appear in the global macroscopic equations. Subsequently, in order to provide

physical interpretation for the coefficients γ_1 and γ_2 , arising from the homogenization procedure, we proceed by identifying the resultant lumped-parameter two-equation model with the one developed by Wilson and Aifantis ([75]).

7.4. Lumped-parameter two-equation models

In the previous models, particles conductivities were scaled by ε^2 . This led to macroscopic models where heat conduction and fluid flow at the macroscale take place only in the global medium. Particles act as storage sites for mass and thermal energy. In what follows, two-equation models can be derived by considering the pair of conductivities $\{K^{T\varepsilon}, K_l^\varepsilon\}$ of the same order of $\{K_f^{T\varepsilon}, K_f^\varepsilon\}$ so that $\{K^{T\varepsilon}, K_l^\varepsilon\}$ are now scaled by ε^0 . In this new setting Eqs. (6.18)–(6.22) are now replaced by

$$-\bar{\phi}_l \alpha_l \frac{\partial \theta_T^0}{\partial t} + \operatorname{div}_x \mathbf{q}_l^0 + \operatorname{div}_y \mathbf{q}_l^1 + \operatorname{div}_x \frac{\partial \mathbf{u}_s^0}{\partial t} + \operatorname{div}_y \frac{\partial \mathbf{u}_s^1}{\partial t} = 0, \quad (7.19)$$

$$\operatorname{div}_y \mathbf{q}_l^0 = \operatorname{div}_y \mathbf{h}_T^0 = 0, \quad (7.20)$$

$$\mathbf{h}_T^0 = -K^T(\nabla_x \theta_T^0 + \nabla_y \theta_T^1), \quad (7.21)$$

$$\bar{\rho} C_T \frac{\partial \theta_T^0}{\partial t} + \operatorname{div}_x \mathbf{h}_T^0 + \operatorname{div}_y \mathbf{h}_T^1 = 0, \quad (7.22)$$

$$\mathbf{q}_l^0 = -K_l(\nabla_x p_B^0 + \nabla_y p_B^1). \quad (7.23)$$

Under the same scaling law in the Biot numbers, this system is now supplemented by the boundary conditions $\mathbf{h}_T^0 \cdot \mathbf{n} = \mathbf{q}_l^0 \cdot \mathbf{n} = 0$ on Γ . Using (7.21) and (7.23) in (7.20), together with the above boundary conditions, θ_T^1 and p_B^1 satisfy the following Neumann problems

$$\Delta_{yy} \theta_T^1 = 0 \quad \text{in } Q_l, \quad -K^T(\nabla_x \theta_T^0 + \nabla_y \theta_T^1) = 0 \quad \text{on } \Gamma,$$

$$\Delta_{yy} p_B^1 = 0 \quad \text{in } Q_l, \quad -K_l(\nabla_x p_B^0 + \nabla_y p_B^1) = 0 \quad \text{on } \Gamma,$$

which by the same arguments leading to (6.37) and (6.39) gives

$$\theta_T^1(\mathbf{x}, y, t) = \boldsymbol{\omega}(y) \cdot \nabla_x \theta_T^0(\mathbf{x}, t) + \theta_T^*(\mathbf{x}, t), \quad p_B^1(\mathbf{x}, y, t) = \boldsymbol{\omega}(y) \cdot \nabla_x p_B^0(\mathbf{x}, t) + p_B^*(\mathbf{x}, t)$$

$$\tilde{\mathbf{h}}_T^0 = -\mathbf{K}_L^T \nabla \theta_T^0, \quad \text{with } \mathbf{K}_L^T = |Q_l|^{-1} \int_{Q_l} K^T(I + \nabla_y \boldsymbol{\omega}) dQ_l,$$

$$\tilde{\mathbf{q}}_l^0 = -\mathbf{K}_L \nabla p_B^0 \quad \text{with } \mathbf{K}_L = |Q_l|^{-1} \int_{Q_l} K_l(I + \nabla_y \boldsymbol{\omega}) dQ_l,$$

with $\boldsymbol{\omega}$ satisfying the Neumann problem (6.38) in Q_l . With isotropy and adopting the same procedure one obtains the following two-equation model

$$\begin{aligned}
& \mu_s^0 \Delta_{xx} \mathbf{u}_s^0 + (\lambda_s^0 + \mu_s^0) \nabla_x \operatorname{div}_x \mathbf{u}_s^0 - \gamma_2 \nabla_x p_f^0 - \gamma_1 \nabla_x p_B^0 - \alpha_* \gamma_1 \nabla_x \theta_T^0 = 0, \\
& -\gamma' \alpha_* \frac{\partial \theta_T^0}{\partial t} - \alpha_f n_f \frac{\partial \theta_f^0}{\partial t} + \gamma_2 \operatorname{div}_x \frac{\partial \mathbf{u}_s^0}{\partial t} - K_F \Delta_{xx} p_f^0 = \widetilde{\delta}_P (p_B^0 - p_f^0) + \gamma' \frac{\partial (p_B^0 - p_f^0)}{\partial t}, \\
& -\gamma_* \frac{\partial \theta_f^0}{\partial t} + \gamma_1 \operatorname{div}_x \frac{\partial \mathbf{u}_s^0}{\partial t} - K_L \Delta_{xx} p_B^0 = -\widetilde{\delta}_P (p_B^0 - p_f^0) - \gamma' \frac{\partial (p_B^0 - p_f^0)}{\partial t}, \\
& \bar{\rho}_f n_f C_f \frac{\partial \theta_f^0}{\partial t} - K_F^T \Delta_{xx} \theta_f^0 = \widetilde{\delta}_T (\theta_T^0 - \theta_f^0), \\
& \bar{\rho} n_f C_T \frac{\partial \theta_T^0}{\partial t} - K_L^T \Delta_{xx} \theta_T^0 = -\delta_T (\theta_T^0 - \theta_f^0), \quad x \in \Omega_f, \quad t > 0.
\end{aligned}$$

When comparing this result with the previous first order Kinetic models, the difference is the appearance of the extra diffusion terms in the macroscopic energy and mass balance ($\operatorname{div}_x \widetilde{\mathbf{h}}_T^0 = -K_L^T \Delta_{xx} \theta_T^0$ and $\operatorname{div}_x \widetilde{\mathbf{q}}_1^0 = -K_L \Delta_{xx} p_B^0$) governing particle heat conduction and adsorbed fluid flow at the macroscale.

If we neglect the term involving the coefficient γ' in the mass transfer and the terms involving physico-chemical effects, then the resultant model resembles in form the reduced version of the lumped-parameter thermomechanical model developed by Bai and Roegier [8] for incompressible solid phase. Physical interpretation of the coefficients γ_1 and γ_2 can be obtained by considering the isothermal version of Bai and Roegier's model developed by Wilson and Aifantis [75]. If we denote K_1 the overall bulk modulus of the compacted clay (without the bulk phase) and K_2 the overall bulk modulus of the macroscopic system, following [75], for incompressible solid phase, we have $\gamma_1 = 1 - K_2/K_1$ and $\gamma_2 = K_2/K_1$.

7.5. One-equation models: local equilibrium

Local thermal equilibrium. When θ_f^0 and θ_T^0 are sufficiently close to each other, the principle of local thermal equilibrium is valid and a single macroscopic temperature can be assigned to both clay particles and bulk water [63]. Within the framework of homogenization this is imposed by assuming large values of the Biot number. For example one may scale Bi_T^0 by $O(\epsilon^{-1})$. This scaling replaces boundary condition (6.31) by $\theta_T^0 = \theta_f^0$ on Γ . Moreover, since these variables only depend on (x, t) this yield $\theta_T^0 = \theta_f^0 = \theta^0(x, t)$. Hence, as in the two-scale model, there is no need to consider individual energy balances for the particles and bulk phase. By adding them up we obtain the following one-equation heat transfer model

$$\begin{aligned}
& \mu_s^0 \Delta_{xx} \mathbf{u}_s^0 + (\lambda_s^0 + \mu_s^0) \nabla_x \operatorname{div}_x \mathbf{u}_s^0 - \gamma_2 \nabla_x p_f^0 - \gamma_1 \nabla_x p_B^0 - \alpha_* \gamma_1 \nabla_x \theta^0 = 0, \\
& -\gamma_* \frac{\partial \theta^0}{\partial t} + \gamma_2 \operatorname{div}_x \frac{\partial \mathbf{u}_s^0}{\partial t} - K_F \Delta_{xx} p_f^0 = \widetilde{\delta}_P (p_B^0 - p_f^0) + \gamma' \frac{\partial (p_B^0 - p_f^0)}{\partial t}, \\
& -\gamma_* \frac{\partial \theta^0}{\partial t} + \gamma_1 \operatorname{div}_x \frac{\partial \mathbf{u}_s^0}{\partial t} - K_L \Delta_{xx} p_B^0 = -\widetilde{\delta}_P (p_B^0 - p_f^0) - \gamma' \frac{\partial (p_B^0 - p_f^0)}{\partial t}, \\
& \bar{\rho}_* C \frac{\partial \theta^0}{\partial t} - K_*^T \Delta_{xx} \theta^0 = 0, \quad x \in \Omega_f, \quad t > 0,
\end{aligned}$$

where $\gamma^* \equiv \gamma'\alpha_* + \alpha_f n_f$, $K_*^T \equiv K^T + K_F^T$ and $\bar{\rho}_* C \equiv \bar{\rho} n_l C_l + \bar{\rho}_f n_f C_f$ (with $\bar{\rho}_* \equiv \bar{\rho}_f + \bar{\rho}$) denote respectively the macroscopic effective thermal conductivity and specific heat capacity.

Local hydrodynamic equilibrium. In analogy to the previous model the scaling $Bi_p^\epsilon = Bi_p \epsilon^{-1}$ together with boundary condition (5.3) leads to $p_B^0 = p_f^0 = P^0(x, t)$. This condition has been referred to as large-scale mechanical equilibrium [63]. Since $\gamma_1 + \gamma_2 = 1$, after adding the mass balances of adsorbed and bulk water, we are led with the following one-equation hydrodynamical model.

$$\begin{aligned} \mu_s^0 \Delta_{xx} \mathbf{u}_s^0 + (\lambda_s^0 + \mu_s^0) \nabla_x \operatorname{div}_x \mathbf{u}_s^0 - \nabla_x P^0 - \alpha^* \gamma_1 \nabla_x \theta^0 &= 0, \\ -\gamma \frac{\partial \theta^0}{\partial t} + \operatorname{div}_x \frac{\partial \mathbf{u}_s^0}{\partial t} - K_L^* \Delta_{xx} P^0 &= 0, \\ \bar{\rho}_* C \frac{\partial \theta^0}{\partial t} - K_*^T \Delta_{xx} \theta^0 &= 0, \quad x \in \Omega_f, \quad t > 0, \end{aligned}$$

with $K_L^* \equiv K_L + K_F$ and $\gamma = \gamma_* + \gamma^*$ denoting respectively the macroscopic effective hydraulic conductivity and overall liquid coefficient of thermal expansion.

7.6. Isothermal poroelastic model

In the isothermal case the above system reduces to

$$\begin{aligned} \mu_s^0 \Delta_{xx} \mathbf{u}_s^0 + (\lambda_s^0 + \mu_s^0) \nabla_x \operatorname{div}_x \mathbf{u}_s^0 - \nabla_x P^0 &= 0, \\ \operatorname{div}_x \frac{\partial \mathbf{u}_s^0}{\partial t} - K_L^* \Delta_{xx} P^0 &= 0, \quad x \in \Omega_f, \quad t > 0, \end{aligned}$$

which resembles in form Biot's consolidation model of linear elastic media for incompressible solid phase. If we neglect the physico-chemical component incorporated in the coefficient λ_s^0 , by setting $K_{ls} = 0$ so that $\lambda_s^* = \lambda_s$, then the above model reduces exactly to the Biot model.

Thus, we have exploited the ability of the microstructural dual porosity system in reproducing a class of well known models as particular cases of the general framework.

8. Conclusions

A three-scale thermomechanical model for swelling porous media (2:1 lattice silicates and lyophilic polymers) is proposed. The upscaling is based on combination of hybrid mixture theory (HMT) and homogenization. Application of these two levels of averaging led to a generalized microstructural dual porosity model wherein the macroscopic swelling soil is covered by two distinct interacting coexisting systems: a macroscopic medium which incorporates the global properties and a local family of cells representing storage sites for mass, momentum and energy. The two sheets are coupled via exchange transfer functions of mass, momentum and energy. A notable consequence of the three-scale model proposed herein is that it provides an accurate portrait of the complicated distributed exchange processes between the global and local systems.

Application of the HMT approach led to a two-scale thermomechanical model which governs particle swelling when physico-chemical forces between the adsorbed water and the minerals are dominated by surface hydration stresses. Within the HMT framework, hydration effects are incorporated upon selection of a proper set of internal variables coupled with the Coleman–Noll method of exploitation of the entropy inequality for derivation of a proper constitutive theory. In the isothermal case, hydration effects are manifested: (i) in a modified effective stress principle through an additional hydration component (t_s^1); (ii) in a modified form of Darcy's law for the vicinal water in terms of an additional potential (volume fraction gradient) accounting for flow induced by physico-chemical effects; (iii) in the appearance of a retardation viscosity coefficient (μ_r) related to the viscoelastic behavior of the volumetric stresses. In the non-isothermal case the coupling between hydration and thermal effects is manifest through a physico-chemical coefficient of thermal expansion (α_{ls}) which appears in the overall momentum balance, and also governs the mechanical work of hydration stresses in the overall two-scale energy balance.

The proposed theory was also capable of reproducing other classical theories, such as creep models for secondary consolidation and lumped-parameter models. The classical approaches for secondary consolidation and creep, based on viscoelastic constitutive equations with fading memory, were recovered by reducing the dual porosity model to a single porosity system using a modified Green's function method. This yields global balances of mass, momentum and energy with fading memory. Lumped-parameter models were reproduced by assuming high conductivities (thermal and hydraulic) for the swelling particles such that local variations of the potentials (pressure for vicinal water flow and temperature for heat transfer) within the particle are neglected. This yields Warren–Root type systems wherein simplified constitutive equations for the exchange terms (e.g. proportional to a potential difference) are postulated. We remark that lumped-parameter models require the introduction of a time scale constraint where at each instant of time, the adsorbed water is assumed at equilibrium and uniformly distributed throughout the particle domain. If the constraint is not satisfied, then the resultant model must incorporate memory effects accounting for retardation mechanisms as suggested by Auriualt and Royer [6].

Acknowledgements

MM was supported by CNPq/Brazil through proc. 300810/91-1. JHC thanks aro contract daag55-98-1-0228 for support.

References

- [1] S. Achanta, J.H. Cushman, M.R. Okos, On multicomponent multiphase thermomechanics with interfaces, *Int. J. Engrg. Sci.* 32 (11) (1994) 1717–1738.
- [2] T. Arbogast, A simplified dual-porosity model for two-phase flow, in: T.F. Russel, R.E. Ewing, C.A. Brebbia, W.G. Gray, G.F. Pinder (Eds.), *Computational Methods in Water Resources, Computational Mechanics Publication*, Southampton, UK, 1992, pp. 419–426.
- [3] T. Arbogast, Gravitational forces in dual-porosity systems, *Transport in Porous Media* 13 (1993) 179–220.
- [4] T. Arbogast, J. Douglas, U. Hornung, Modeling of naturally fractured reservoirs by formal homogenization techniques, in: R. Dautray (Ed.), *Frontiers in Pure and Applied Mathematics*, Elsevier, Amsterdam, 1991, pp. 1–19.

- [5] J.L. Auriault, H. Ene, Macroscopic modeling of heat transfer in composites with interfacial thermal barrier, *Int. J. Heat Mass Transfer* 37 (18) (1994) 2885–2892.
- [6] J.L. Auriault, P. Royer, Double conductivity media: a comparison between phenomenological and homogenization approaches, *Int. J. Heat Mass Transfer* 36 (10) (1993) 2613–2621.
- [7] M. Bai, Y. Abousleiman, Thermoporoelastic coupling with application to consolidation, *Internat. J. Numer. Anal. Methods. Geomech.* 21 (1997) 121–132.
- [8] M. Bai, J.C. Roegiers, Fluid flow and heat flow in deformable fractured porous media, *Int. J. Engrg. Sci.* 32 (10) (1994) 1615–1633.
- [9] G.I. Barenblatt, I.P. Zhelton, I.N. Kochina, Basic concepts in the theory of seepage of homogeneous liquids in fissured rocks, *J. Appl. Math. Mech.* 24 (1960) 1286–1303.
- [10] L.S. Bennethum, J.H. Cushman, Multiscale hybrid mixture theory for swelling systems: Part I: Balance laws, *Int. J. Engrg. Sci.* 34 (2) (1996) 125–145.
- [11] L.S. Bennethum, J.H. Cushman, Multiscale hybrid mixture theory for swelling systems: Part II: Constitutive theory, *Int. J. Engrg. Sci.* 34 (2) (1996) 147–169.
- [12] M. Biot, General theory of three-dimensional consolidation, *J. Appl. Phys.* 12 (1941) 155–164.
- [13] M. Biot, Theory of finite deformations of porous solids, *Indiana University Mathematics J.* 21 (1972) 597–620.
- [14] J.R. Booker, C. Savvidou, Consolidation around a heat source, *Int. J. Numer. Anal. Methods Geomech.* 9 (1985) 173–184.
- [15] R.M. Bowen, Theory of mixtures, in: A.C. Eringen (Ed.), *Continuum Physics*, vol. 3, Academic Press, New York, 1976.
- [16] B. Budkowska, Q. Fu, Some aspects of numerical analysis of creep in layered granular medium, *Computers and Geotechnics* 5 (1988) 285–306.
- [17] Y.A. Buyevich, Towards a theory of nonequilibrium multiphase filtration flow, *Transport in Porous Media* 21 (1995) 145–162.
- [18] H. Callen, *Thermodynamics*, Wiley, New York, 1980.
- [19] R.G. Campanella, J.K. Mitchell, Influence of temperature variations on soil behavior, *J. Soil Mechs. and Found. Div. (ASCE) SM* 94 (3) (1968) 709–734.
- [20] H.S. Carslaw, J.C. Jaeger, *Conduction of Heat in Solids*, University Press, London, 1959.
- [21] B.D. Coleman, W. Noll, The thermodynamics of elastic materials with heat conduction and viscosity, *Arch. Rat. Mech. Anal.* 13 (1963) 167–178.
- [22] O. Coussy, *Mechanics of Porous Continua*, Wiley, New York, 1995.
- [23] J. Cushman, Molecular-scale lubrication, *Nature* 347 (1990) 227–228.
- [24] J.H. Cushman, *The Physics of fluids in hierarchical porous media: Angstroms to miles*, Kluwer Academic Publishers, New York, 1997.
- [25] B.V. Derjaguin, N.V. Churaev, V.M. Muller, *Surface Forces*, Plenum press, New York, 1987.
- [26] B.V. Derjaguin, V. Karasev, E. Khromova, Thermal expansion of water in fine pores, *J. Colloid Interface Sci.* 109 (2) (1986) 586–587.
- [27] J. Douglas, Jr., T. Arbogast, Dual porosity models for flow in naturally fractured reservoirs, in: J.H. Cushman (Ed.), *Dynamics of fluid in hierarchical porous media*, Academic Press, New York, 1990, pp. 177–222.
- [28] A. Eringen, A continuum theory of swelling porous elastic soils, *Int. J. Engrg. Sci.* 32 (8) (1994) 1337–1349.
- [29] A.C. Eringen, *Mechanics of Continua*, Wiley, New York, 1967.
- [30] Z. Feng, E. Michaelides, The use of modified Green's functions in unsteady heat transfer, *Int. J. Heat Mass Transfer* 40 (12) (1997) 2997–3002.
- [31] R.E. Gibson, K.Y. Lo, A theory of consolidation for soils exhibiting secondary compression, *Norweg. Geotech. Inst. Publ.* 41 (1961) 1–16.
- [32] S.M. Hassanzadeh, W.G. Gray, General conservation equations for multiphase systems: 2. Mass, momenta, energy, and entropy equations, *Adv. Water Resour.* 2 (1979) 191–208.
- [33] S.M. Hassanzadeh, W.G. Gray, General conservation equations for multiphase systems: 3. Constitutive theory for porous media, *Adv. Water Resour.* 3 (1980) 25–40.
- [34] S.M. Hassanzadeh, W.G. Gray, Toward an improved description of the physics of two-phase flow, *Adv. Water Resour.* 16 (1993) 53–67.

- [35] W.K. Heidug, S.W. Wong, Hydration swelling of water-adsorbing rocks: A constitutive model, *Int. J. Numer. Anal. Methods Geomech.* 20 (1996) 403–430.
- [36] J.P. Holman, *Heat Transfer*, McGraw-Hill, New York, 1997.
- [37] T. Hueckel, Water mineral interaction in hygromechanics of clays exposed to environmental loads: a mixture theory approach, *Can. Geotech. J.* 29 (1992) 1071–1086.
- [38] J.M. Huyghe, J.D. Janssen, Quadriphasic mechanics of swelling incompressible porous media, *Int. J. Engrg. Sci.* 25 (8) (1997) 793–802.
- [39] Y. Ichikawa, J. Wang, G.C. Jeong, Micro macro properties of geomaterials: a homogenization method for viscoelastic problem, *Structural Engrg. Mech.* 4 (6) (1996) 631–644.
- [40] J. Israelachvili, *Intermolecular and Surface Forces*, Academic Press, New York, 1991.
- [41] J. Feda, Creep of soils and related phenomena, *Developments in Geotechnical Engineering*, vol. 68, Elsevier, New York, 1992.
- [42] T.K. Karalis, Water flow in non-saturated swelling soil, *Int. J. Engrg. Sci.* 31 (1993) 751–774.
- [43] M.J. Kaviany, *Principles of heat transfer in porous media*, Springer, New York, 1991.
- [44] M.J. Keedwell, *Rheology and Soil Mechanics*, Elsevier, New York, 1984.
- [45] M. Khaled, D. Beskos, E. Aifantis, On the theory of consolidation with double porosity: III. A finite element formulation, *Int. J. Numer. Anal. Methods Geomech.* 8 (1984) 101–123.
- [46] T.W. Lambe, A mechanistic picture of shear strength in clay, in: *Proceedings of The ASCE Research Conference on Shear Strength of Cohesive Soils*, Boulder, Colorado, 1960, pp. 503–532.
- [47] C. Lee, C. Mei, Re-examination of the equations of poroelasticity, *Int. J. Engrg. Sci.* 35 (4) (1997) 329–352.
- [48] R. Lewis, D. Tran, Numerical simulation of secondary consolidation of soil: Finite element formulation, *Int. J. Numer. Anal. Methods Geomech.* 13 (1989) 1–18.
- [49] I.S. Liu, Method of Lagrange multipliers for exploitation of the entropy principle, *Arch. Rat. Mech. Anal.* 46 (1972) 131–148.
- [50] P.F. Low, The swelling of clay: II. Montmorillonite-water systems, *Soil Sci. Soc. Am. J.* 44 (4) (1980) 667–676.
- [51] P.F. Low, Structural component of the swelling pressure of clays, *Langmuir* 3 (1987) 18–25.
- [52] P.F. Low, The clay/water interface and its role in the environment, *Prog. Colloid Polym. Sci.* 95 (1994) 98–107.
- [53] C. Ma, T. Hueckel, Effects of inter-phase mass transfer in heated clays: A mixture theory, *Int. J. Engrg. Sci.* 30 (11) (1992) 1567–1582.
- [54] N.M. Morgenstern, B.I. Balasubramonian, Effects of pore fluid on the swelling of clay-shale, in: *Proceedings of the Fourth International Conference on Expansive Soils*, Denver, CO, 1980, pp. 190–205.
- [55] M.A. Murad, L.S. Bennethum, J.H. Cushman, A multiscale theory of swelling porous media: I application to one-dimensional consolidation, *Transport in Porous Media* 19 (1995) 93–122.
- [56] M.A. Murad, J.H. Cushman, Multiscale flow and deformation in hydrophilic swelling porous media, *Int. J. Engrg. Sci.* 34 (3) (1996) 313–336.
- [57] M.A. Murad, J.H. Cushman, A Multiscale theory of swelling porous media: II. Dual porosity models for consolidation of clays incorporating physico-chemical effects, *Transport in Porous Media* 28 (1) (1997) 69–108.
- [58] M.N. Ozisik, *Heat Conduction*, Wiley, New York, 1980.
- [59] M. Peszynska, Mathematical analysis and numerical approach to flowthrough fissured media, P.hD. Thesis, University Augsburg (1992).
- [60] M. Peszynska, On a model of nonisothermal flow through fissured media, *Diff. Integral Eqs.* 8 (6) (1995) 1497–1516.
- [61] J.R. Philip, Hydrostatics and hydrodynamics in swelling soils, *Water Resour. Res.* 5 (1969) 1070–1077.
- [62] M. Quintard, M. Kaviany, S. Whitaker, Two-medium treatment of heat transfer in porous media: numerical results for effective properties, *Adv. Water Resour.* 38 (15) (1995) 2779–2796.
- [63] M. Quintard, M. Kaviany, S. Whitaker, Transport in chemically and mechanically heterogeneous porous media, *Adv. Water Resour.* 19 (1) (1996) 29–60.
- [64] M. Quintard, S. Whitaker, One- and two-equation models for transient diffusion processes in two-phase systems, in: *Advances in Heat Transfer*, vol. 369, Academic Press, New York, 1993, pp. 369–465.
- [65] M. Quintard, S. Whitaker, Local thermal equilibrium for transient heat conduction: theory and comparison with numerical experiments, *Int. J. Heat Mass Trasnfer* 20 (1997) 77–94.

- [66] M. Sahraout, M. Kaviany, Slip and no-slip temperature boundary conditions at interface of porous, plain media: conduction, *Int. J. Heat Mass Transfer* 36 (4) (1993) 1019–1033.
- [67] E. Sanchez-Palencia, Non-homogeneous media and vibration theory, in: J. Ehlers (Ed.), *Lecture Notes in Physics*, Springer, New York, 127, 1980.
- [68] R.L. Schifman, A thermoelastic theory of consolidation, in: C.J. Cremers, F. Kreith, J.A. Clark (Eds.), *Environmental and Geophysical Heat Transfer*, vol. 4, ASME, 1971, pp. 78–84.
- [69] M. Schoen, D.J. Diestler, J.H. Cushman, Fluids in micropores: I. structure of a simple classical fluid in a slitpore, *J. Chem. Phys.* 87 (9) (1987) 5464–5476.
- [70] R.E. Showalter, Distributed microstructure models of porous media, in: U. Hornung (Ed.), *Homogenization and Porous Media, Interdisciplinary Applied Mathematics*, vol. 6, Springer, New York, 1996, pp. 1–27.
- [71] A. Sridharan, G.V. Rao, Mechanisms controlling volume change of saturated claysand the role of the effective stress concept, *Geotechnique* 23 (3) (1973) 359–382.
- [72] A. Sridharan, G.V. Rao, Mechanisms controlling the secondary compression ofclays, *Geotechnique* 32 (3) (1982) 249–260.
- [73] Y. Wang, V. Murti, S. Valliappan, A transient finite element analysis of linear viscoelastic material model, *Int. J. Numer. Anal. Methods Geomech.* 16 (1992) 265–294.
- [74] J. Warren, P. Root, The behavior of naturally fractured reservoirs, *Soc. Pet. Engrg.* 3 (1963) 245–255.
- [75] R. Wilson, E. Aifantis, On the theory of consolidation with double porosity, *Int. J. Engrg. Sci.* 20 (9) (1982) 1009–1035.
- [76] L. Zeevart, Consolidation in the intergranular viscosity of highly compressible soils, in: N. Yong, F.C. Townsend (Eds.), *Consolidation of Soils: Testing and Evaluation*, American Society for Testing and Materials ASTM 892, Philadelphia, 1986, pp. 257–281.
- [77] F. Zhang, Z. Zhang, P. Low, C. Roth, The effect of temperature on the swelling of montmorillonite, *Clay Minerals* 28 (1993) 25–31.
- [78] R. Zimmerman, T. Hadgu, G. Bodvarsson, A new lumped-parameter model for flow in unsaturated dual-porosity media, *Adv. Water Resour.* 19 (5) (1996) 317–327.

Macroscale Thermodynamics and the Chemical Potential for Swelling Porous Media

LYNN SCHREYER BENNETHUM, MÁRCIO A. MURAD and
JOHN H. CUSHMAN

Department of Mathematics, C.U. Denver, Campus Box 170, PO Box 17 3364, Denver,
CO 80217-3364, U.S.A. e-mail: bennethum@math.cudenver.edu

(Received: 13 August 1998; in final form: 11 March 1999)

Abstract. The thermodynamical relations for a two-phase, N -constituent, swelling porous medium are derived using a hybridization of averaging and the mixture-theoretic approach of Bowen. Examples of such media include 2-1 lattice clays and lyophilic polymers. A novel, scalar definition for the macroscale chemical potential for porous media is introduced, and it is shown how the properties of this chemical potential can be derived by slightly expanding the usual Coleman and Noll approach for exploiting the entropy inequality to obtain near-equilibrium results. The relationship between this novel scalar chemical potential and the tensorial chemical potential of Bowen is discussed. The tensorial chemical potential may be discontinuous between the solid and fluid phases at equilibrium; a result in clear contrast to Gibbsian theories. It is shown that the macroscopic scalar chemical potential is completely analogous with the Gibbsian chemical potential. The relation between the two potentials is illustrated in three examples.

Key words: macroscale, chemical potential, mixture theory, porous media, swelling porous media.

Nomenclature

In general, a subscript Greek letter indicates a macroscale quantity from that phase. Superscript minuscules indicate the constituent, so that, e.g., v_α^j is the macroscopic velocity of constituent j in the α -phase. A caret over the symbol, $\hat{\cdot}$, is used to emphasize that the quantity represents a transfer from either another phase or from other constituents.

A_α^j	Helmholtz free energy density of j th constituent in α -phase $A_\alpha^j = E_\alpha^j - T\eta_\alpha^j$.
b_α^j	external entropy source for j th constituent in α -phase.
C_α^j	mass concentration.
d_α^j	symmetric part of ∇v_α^j .
\hat{e}_α^j	rate of mass exchange from other phase to α -phase of j th constituent.
E_α^j	energy density.
E_s	macroscale strain tensor of solid phase.
\hat{E}_α^j	energy gained by constituent j in phase α due to non-chemical, non-mechanical interactions with other constituents within phase α .
F_s	deformation gradient, $\text{grad}x_s$, of the solid phase.

\mathbf{g}	gravity.
G_α	Gibbs free energy.
h_α^j	external supply of energy.
$\hat{\mathbf{i}}_\alpha^j$	gain of momentum of constituent i of phase α due to mechanical interactions with other species within the same phase.
\mathbf{n}_α	unit outward normal to phase α .
p_α	thermodynamic pressure.
\mathbf{q}_α^j	heat flux of constituent j in α -phase.
\hat{Q}_α^j	gain of energy of constituent j in phase α due to nonmass transfer interactions with the other phase.
\hat{r}_α^j	rate of j th constituent mass gained within phase α .
\mathbf{t}_α^j	stress tensor of j th constituent in α -phase.
T	temperature.
$\hat{\mathbf{T}}_\alpha^j$	gain of momentum of phase α due to mechanical interactions with the other phase.
\mathbf{u}_α^j	diffusive velocity, $\mathbf{v}_\alpha^j - \mathbf{v}_\alpha$.
\mathbf{v}_α^j	mass averaged velocity of j th constituent in phase α .
\mathbf{v}_α	velocity of phase α = $\sum_{j=1}^N C_\alpha^j \mathbf{v}_\alpha^j$.
δV	representative elementary volume (REV).
δV_α	portion of REV within α -phase.
$\mathbf{w}_{\alpha\beta}^j$	velocity of j th constituent in the interface.
ε^α	volume fraction of α -phase in REV = $ \delta V_\alpha / \delta V $.
γ_α	indicator function for phase α .
λ_α	Lagrange multiplier for continuity equation of phase α .
λ_α^j	Lagrange multiplier for continuity equation of j th constituent in phase α .
Γ_α^N	Lagrange multiplier for restrictions on sum of gradients of diffusive velocities.
Λ_α^j	entropy production density.
μ_α^j	scalar chemical potential of j th constituent in phase α .
ν_α^j	tensorial chemical potential of j th constituent in phase α .
η_α^j	entropy density.
$\hat{\eta}_\alpha^j$	entropy gain of j th constituent in α -phase due to nonmass transfer interactions with other constituents within phase α .
ϕ_α^j	entropy flux.
$\hat{\Phi}_\alpha^j$	entropy gained by j th constituent in α -phase due to nonmass transfer interactions with the other phase.
ρ_α^j	averaged mass density of j th constituent in α -phase = $C_\alpha^j \rho_\alpha$.
ρ_α	averaged mass density of α -phase = $\sum_{j=1}^N \rho_\alpha^j$.

1. Introduction

The purpose of this paper is three-fold: to introduce a novel definition of the macroscale chemical potential for a porous medium, to show how one can derive the properties of this chemical potential by slightly expanding the usual Coleman and Noll approach for exploiting the entropy inequality to obtain near-equilibrium

results, and to discuss the application of mixture theory to swelling porous media. By our modified approach and by using an appropriate definition of the chemical potential, we have been able to derive properties of the chemical potential which corresponds exactly with the properties of the classical Gibbsian chemical potential. We illustrate these techniques and the motivation for a new definition of the chemical potential within the context of swelling porous media.

Due to the chemical and physical forces between phases, many porous media can swell or shrink resulting in macroscopic behavior which may differ significantly from granular media. Examples of such media include lyophilic polymers and clay soils. The understanding of the constitutive behavior of these materials is crucial in applications involving almost all aspects of life. Swelling polymers have numerous technological applications in drug delivery, contact lenses, semiconductor manufacturing and food stuffs, and clay soils are widely distributed in the earth's crust. Hence they play a critical role in the transport of nutrients and pesticides in agriculture, in various high level nuclear waste isolation scenarios, in barriers for commercial land fills, and in consolidation and failure of foundations, highways and runways. Although everything derived in this paper can be applied to a wide variety of swelling systems, for ease of exposition we restrict our discussion to swelling clay soils.

The complex mechanisms underlying the constitutive behavior of a hydrophilic clay soil are a consequence of its complicated microstructure. Clay minerals consist of hydrous aluminum and magnesium silicates with an expanding layer lattice. Their tremendous specific surface area and their charged character cause hydrated clay platelets to form 'particles'. These particles swell under hydration and shrink under desication. The platelet–water bonding forces are usually referred to as 'hydration forces' and cause the macroscopic behavior of clays to differ significantly from the behavior of granular nonswelling media. In the case of hydrophilic colloidal particles (e.g. smectites), the hydration forces are believed to arise from the hydrophilic character of the mineral surfaces. These interactions modify the thermodynamical properties of the water in the interlamellar spaces and consequently its properties vary with the proximity to the solid surface [38, 54–56]. Hence, the interlamellar water is termed *vicinal* water to distinguish it from its bulk or free-phase counterpart (i.e. water free of any adsorptive force). It has been advocated in [30–32, 35, 47, 48, 57, 58] that surface hydration forces are the dominant mechanism causing the swelling of clays, and it is these forces which we account for when developing this theory.

In this paper we illustrate the use of rational thermodynamics in developing a mathematical model for a multicomponent swelling porous media with particular emphasis on the definition of the chemical potential. This is accomplished by adopting a proper theory of constitution which includes appropriate internal variables needed to capture the swelling character of the system. In particular, the approach developed herein provides a thermodynamical basis for the role hydration forces play in the adsorption and diffusion of contaminants in a swelling medium.

In classical mixture theory a single-phase medium composed of N constituents is viewed as N co-existing continua. Biot [15–17] and later more rigorously by Bowen [19–21] extended the theory of mixtures to model a porous medium so that at the macroscale a two-phase medium is viewed as two co-existing continua. In his work, macroscopic forms of the field equations (conservation of mass, momentum balance, and conservation of energy), which incorporate exchange terms between the co-existing continua, are postulated. It has been shown [40, 41] that if the microscopic field equations are averaged then the terms in Bowen's macroscopic field equations can be identified precisely with microscopic counterparts. The combination of averaging and mixture theory is referred to hybrid mixture theory (HMT). In both of these formulations, the constitutive restrictions are determined at the macroscale by exploiting the entropy inequality using the method of Coleman and Noll [25].

Although HMT has been used in several fields (e.g. alloy solidification [10]), a porous body is the canonical model of a system to which HMT is applied [1–3, 37, 64, 65]. In fact, the first application of HMT was to model single-phase flow through a deformable, elastic porous medium in which Darcy's law, which governs the flow of the liquid phase, was recovered [42]. Later the theory was extended to describe multicomponent fluid flow in porous media, in which the derivation of Fick's law and a generalized Darcy's law were the primary objectives [39]. Soon after, the theory was again extended to include multiphase flow in porous media with interfacial effects [37, 45]. Among other results, this approach [43–45] extended the thermodynamical groundwork for the physics of two-phase flow, e.g., [21, 34, 59]. In particular, a near-equilibrium capillary pressure relation and a generalized macroscopic form of Darcy's law were derived in which the generalized Darcy's law includes an additional interaction potential involving a saturation gradient. This generalized form of Darcy's law circumvents the usual heuristic extension of the single-fluid Darcy's law to that for multiple-fluid phases with relative permeability.

We discuss in detail the consequence of postulating the existence of a constitutive relation for the time rate of change of the volume fraction as a means of closing the system of equations [21]. As in all upscaling approaches, there exists an additional variable, the volume fraction in this case, for which there is no additional equation. The appearance of the additional variable is a consequence of losing information about the microscopic geometry and is known as the closure issue [18]. The means of closing the system is crucial in our formulation since, as a result, the macroscopic system has some viscoelastic constitutive behavior. As we shall see, the results are in agreement with some empirically based constitutive theories.

The macroscale chemical potential has been defined in a variety of ways, and here we concentrate on the definitions relating the change of the intensive

Helmholtz potential with respect to the concentration, i.e. if $\tilde{\mu}_\alpha^j$ is the chemical potential of the j th constituent relative to the N th constituent, then

$$\tilde{\mu}_\alpha^j \equiv \frac{\partial A_\alpha}{\partial C_\alpha^j}, \quad j = 1, \dots, N - 1,$$

in which A_α is the intensive Helmholtz potential of phase α . We employ a modification of the traditional linearization procedure for the dissipative entropy inequality to obtain near-equilibrium relations. The traditional procedure involves linearizing coefficients which are zero at equilibrium. For a system composed of N miscible components, this traditional approach yields a generalized form of Fick's law which has not been as sharp as needed for practical applications. In [2, 39] the following form of Fick's law is derived:

$$\mathbf{R}_\alpha^j \mathbf{u}_\alpha^j = \nabla \tilde{\mu}_\alpha^j = \nabla(\mu_\alpha^j - \mu_\alpha^N), \quad j = 1, \dots, N - 1, \quad \alpha = l, s, \quad (1)$$

where $\alpha = l, s$ denotes the liquid and solid phase, respectively, and \mathbf{R}_α^j is a material tensor arising from a linearization procedure. After appropriate simplifications [28, 39] Equation (1) reduces to the classical Fick's law which states that the diffusive velocity is proportional to the concentration gradient [7]. However, we are interested in reproducing the more general form of Fick's law, which according to statistical thermodynamics, states that flow is driven by an absolute chemical potential gradient (i.e. $\nabla \mu_\alpha^j$) [80]. This is in contrast to Equation (1) which states that flow is driven by a chemical potential gradient *relative* to the N th component, implying that the diffusive velocity is a function of how the constituents are labeled.

This lack of clarity is similarly manifested in equilibrium relations obtained from the entropy principle. For example, classical Gibbsian thermodynamics tells us that at equilibrium, the chemical potential of a single constituent coexisting in two phases is constant, i.e., $\mu_s^j = \mu_l^j$, $j = 1, \dots, N$ [23]. Yet historically the only derivable comparable result obtained by exploiting the entropy inequality in mixture theory is [2]

$$\tilde{\mu}_s^j = \tilde{\mu}_l^j, \quad j = 1, \dots, N - 1. \quad (2)$$

As we shall see, there is no prescribed method for extending the above relative result to the absolute form at the macroscale. The primary reason for obtaining results in terms of the relative chemical potential is the interdependence of the concentrations ($\sum_{j=1}^N C_\alpha^j = 1$) and the interdependence of \mathbf{u}_α^j , $j = 1, \dots, N$, through the constraint

$$\sum_{j=1}^N C_\alpha^j \mathbf{u}_\alpha^j = 0. \quad (3)$$

In classical Gibbsian thermodynamics, this interdependence is avoided because extensive variables representing the number of molecules of each constituent are

used as independent variables, instead of intensive variables (concentrations). Using extensive variables, such as the number of molecules of each constituent, is not possible in HMT as the upscaling process cannot be performed on extensive variables, at least not in a physically meaningful manner. Thus, all results standardly derived [2, 39] are in terms of the relative chemical potential.

Some of the results involving the relative chemical potential can be sharpened by choosing μ_α^N appropriately and subsequently deriving results for the absolute (non-relative) chemical potentials. For example, in [19, 22], the following tensorial definition for the chemical potential was proposed and has since been used in most mixture theory derivations [2, 39]:

$$\mathbf{v}_\alpha^j \equiv A_\alpha^j \mathbf{I} - \frac{1}{\rho_\alpha^j} \mathbf{t}_\alpha^j. \quad (4)$$

This definition has the nice property that

$$\sum_{j=1}^N C_\alpha^j \mathbf{v}_\alpha^j = A_\alpha \mathbf{I} - \frac{1}{\rho_\alpha} \mathbf{t}_\alpha, \quad (5)$$

where \mathbf{t}_α are the stress tensors of phase α . For the case of a perfect fluid, $\mathbf{t}_\alpha = -p_\alpha \mathbf{I}$, and the right hand side of (5) reduces to the classical thermostatics concept of Gibbs energy [23]. This definition for the chemical potential seems to be motivated by convenience and is not easily reconciled with the classical definition, which is a scalar. The classical Gibbsian chemical potential, μ_α^j , which is defined as the derivative of the extensive Helmholtz energy with respect to the number of molecules of constituent j [23], has the following characteristics: (1) it is a scalar and measures the energy required to insert a particle into the system [61]; (2) its gradient is the driving force for diffusive flow (Fick's law) [80]; and (3) it is constant for a single constituent coexisting in two phases at equilibrium, i.e. for the solid, s, and liquid phase, l, $\mu_s^j = \mu_l^j$, $j = 1, \dots, N$ where N is the number of miscible components in each phase [23]. The fact that the tensorial definition is not a scalar has lead to some difficulty in evaluating all its components, especially the off-diagonal terms [8, 69]. Furthermore, Bowen's tensorial chemical potential (4) also does not satisfy characteristics 2 or 3.

The above issues on the chemical potential were partially addressed in [14] within the context of HMT applied to diffusion and adsorption of contaminants in a granular, or non-swelling, porous media. In this work, two definitions for the N th chemical potential were introduced, and their effects on the relative form of Fick's law (1) and equilibrium result (2) were discussed. Here the sharper results of [14] are extended to accurately describe diffusion and adsorption of a multicomponent fluid in a swelling porous media, and a new application of the Lagrange multiplier technique of Liu [52] is used to enforce the constraint on the gradient of diffusive velocities (3) weakly. Liu proved that exploiting the entropy inequality subject to constraints is equivalent to exploiting a modified entropy inequality formed by

adding linear combinations of the constraints premultiplied by Lagrange factors. The technique we use to derive our results is a modification of the Lagrange multiplier technique developed by Liu. In contrast to Liu and Muller [52, 53, 63], who view the field equations as constraints, we show how the Lagrange multiplier technique can be extended to enforce other relationships between various variables, such as the relationship given by Equation (3).

In the next section we state the governing balance laws and entropy inequality as derived by averaging, along with notation and major assumptions. In the following section, constitutive assumptions in the form of the choice of constitutive independent variables are made, and the entropy inequality is formulated in terms of Lagrange multipliers. In Section 4, we derive general nonequilibrium results (i.e. results which always hold) obtained by exploiting the entropy inequality in the sense of Coleman and Noll and present two definitions for the macroscale chemical potential. In Sections 5 and 6, results which hold at equilibrium and which are obtained by linearizing about equilibrium are derived, respectively. In Section 7, we compare several definitions of the chemical potential by studying three hypothetical experiments. In the final section, we provide a few salient concluding remarks.

2. Macroscale Balance Laws and Entropy Inequality

In this section, we briefly review the derivation of the macroscale balance laws and entropy inequality. In the process, it is shown how macroscale variables in the field equations can be precisely defined in terms of their microscopic counterparts.

Consider a multi-constituent single-phase flow (denoted by l for liquid) through a deformable porous medium (denoted by s for solid). For simplicity we consider the range of moderate moisture content which allows us to assume that interfaces contain no thermodynamic properties. Consequently, it is assumed no amount of mass, momentum, energy, or entropy are lost when being transferred between phases. Interfacial effects can easily be included by pursuing any of the approaches of [29, 37, 45]; however, since this issue is not our primary purpose, we shall omit these terms to keep the level of algebra at a minimum.

In addition, it is assumed that there exists the same N constituents in each phase. This assumption is necessary to derive the correct equilibrium results for the chemical potential [2]. For the more practical case, where there are less than N constituents per phase, the corresponding results can be obtained after exploiting the entropy inequality by setting the concentrations of the appropriate constituents to zero. Because of this restriction, it is necessary to consider the governing equations for each constituent in each bulk phase. We first present the governing microscopic equations, then the averaging procedure, and finally we present the averaged equations for the bulk phase with no assumptions made on the size of perturbation of the thermodynamic variables.

At the microscale we assume the governing equations used in mixture theory hold for each phase. Consequently, thermodynamic properties exist for each constituent at each point *within* each phase, and each constituent must satisfy the governing field equations: conservation of mass, balance of linear and angular momentum, conservation of energy, and entropy production. Assuming no surface discontinuities, the constituent, microscopic field equations can be expressed for a given phase, α , as (following the notation of [33])

$$\frac{\partial}{\partial t}(\rho^j \psi^j) + \nabla \cdot (\rho^j \mathbf{v}^j \psi^j) - \nabla \cdot \mathbf{i}^j - \rho^j f^j = \rho^j G^j + \rho^j \hat{\psi}^j, \quad (6)$$

where ψ^j is the mass-average (over the phase) thermodynamic property of constituent j , \mathbf{v}^j is the mass-average velocity vector, ρ^j is the mass density, \mathbf{i}^j is the flux vector, f^j is the external supply, G^j is the net production, and $\hat{\psi}^j$ represents the influx of ψ from all other constituents (e.g. due to chemical reactions). If there is only one constituent, $\hat{\psi}^j$ is zero.

The averaging procedure is based on ideas laid down in [72, 78, 79]. Several methods are available, but we choose the computationally simplest. Equations are averaged over a representative elementary volume (REV) by weighted integration using the indicator function of the α -phase. To avoid the mathematical difficulties of, for example, defining a derivative of the averaged quantities resulting from using such a weighting function, one must treat the averaged quantity as a distribution [68, 71].

It should be noted that using this simple weight function may mean that the averaged value may not represent the actual values being measured. To account for the measuring technique, one needs to choose a weight function which represents the instrument used to measure the physical properties [27]. Extensions of the presented theory to such cases are straight forward.

After averaging Equation (6), the system is considered to be a mixture so that each component in each phase and each bulk phase now have thermodynamic properties existing at each point within the macroscopic body. The macroscopic definition of each field variable in terms of its microscopic counterpart, making *no small perturbations assumptions*, is given in Appendix A.

Here we make the additional assumptions that all external sources except for body forces (gravity), are negligible and that the solid and fluid are at local thermal equilibrium so that a common temperature T can be assigned for both phases, i.e. $T_l = T_s = T$. Furthermore, we assume the solid and fluid are nonpolar so that conservation of angular momentum for each phase implies the stress tensors of each phase are symmetric. For ease of exposition we assume no exchange of mass exists between constituents within a phase (i.e. no chemical reactions: $\hat{r}_\alpha^j = 0$), although extending the theory to such cases is straight forward [2, 39]. We do allow exchange of mass between phases. If the macroscopic variables are defined as in Appendix A, then the form of the macroscopic field equations have the following form:

Conservation of mass

For the j th component in the α -phase, conservation of mass can be expressed as

$$\frac{D_\alpha^j(\varepsilon_\alpha \rho_\alpha^j)}{Dt} + \varepsilon_\alpha \rho_\alpha^j \nabla \cdot \mathbf{v}_\alpha^j = \widehat{e}_\alpha^j, \quad \alpha = 1, s, \quad j = 1, \dots, N, \quad (7)$$

where D_α^j/Dt denotes the material time derivative following the j th component in the α -phase, i.e.,

$$\frac{D_\alpha^j}{Dt} = \frac{\partial}{\partial t} + \mathbf{v}_\alpha^j \cdot \nabla, \quad j = 1, \dots, N, \quad \alpha = 1, s.$$

Summing over all constituents, and defining the bulk phase variables appropriately, we obtain conservation of mass for the α -phase,

$$\frac{D_\alpha(\varepsilon_\alpha \rho_\alpha)}{Dt} + \varepsilon_\alpha \rho_\alpha \nabla \cdot \mathbf{v}_\alpha = \widehat{e}_\alpha, \quad \alpha = 1, s, \quad (8)$$

where \widehat{e}_α represents the net mass gained by the α -phase from the other phase, and D_α/Dt denotes the material time derivative following the α -phase. Subtracting C_α^j times Equation (8) from (7) yields a more useful form of the continuity equation for constituents:

$$\varepsilon_\alpha \rho_\alpha \frac{D_\alpha C_\alpha^j}{Dt} + \nabla \cdot (\varepsilon_\alpha \rho_\alpha^j \mathbf{u}_\alpha^j) = (\widehat{e}_\alpha^j - C_\alpha^j \widehat{e}_\alpha), \quad \alpha = 1, s, \quad j = 1, \dots, N. \quad (9)$$

Conservation of momentum

Momentum balance for the j th component of the α -phase can be expressed as

$$\varepsilon_\alpha \rho_\alpha^j \frac{D_\alpha \mathbf{v}_\alpha^j}{Dt} - \nabla \cdot (\varepsilon_\alpha \mathbf{t}_\alpha^j) - \varepsilon_\alpha \rho_\alpha^j \mathbf{g} = \widehat{\mathbf{T}}_\alpha^j + \widehat{\mathbf{i}}_\alpha^j, \quad \alpha = 1, s, \quad j = 1, \dots, N \quad (10)$$

and for the α -phase we have

$$\varepsilon_\alpha \rho_\alpha \frac{D_\alpha \mathbf{v}_\alpha}{Dt} - \nabla \cdot (\varepsilon_\alpha \mathbf{t}_\alpha) - \varepsilon_\alpha \rho_\alpha \mathbf{g} = \widehat{\mathbf{T}}_\alpha, \quad \alpha = 1, s, \quad (11)$$

where \mathbf{t}_α denotes the average symmetric stress tensors for the α -phase, and $\widehat{\mathbf{T}}_\alpha$ denotes the net gain of momentum for the α -phase due to interactions with the other phase. This form of the momentum equation differs from [21] or [6] in that their definition for the partial stress tensor and density incorporate the volume fraction.

Conservation of energy

For the j th component of the α -phase, conservation of energy is given by

$$\varepsilon_\alpha \rho_\alpha^j \frac{D_\alpha E_\alpha^j}{Dt} - \varepsilon_\alpha \mathbf{t}_\alpha^j : \mathbf{d}_\alpha^j - \nabla \cdot (\varepsilon_\alpha \mathbf{q}_\alpha^j) = \widehat{Q}_\alpha^j + \widehat{E}_\alpha^j, \quad \alpha = 1, s, \quad j = 1, \dots, N$$

and for the α -phase by

$$\varepsilon_\alpha \rho_\alpha \frac{D_\alpha E_\alpha}{Dt} - \varepsilon_\alpha \mathbf{t}_\alpha : \mathbf{d}_\alpha - \nabla \cdot (\varepsilon_\alpha \mathbf{q}_\alpha) = \widehat{Q}_\alpha, \quad \alpha = 1, s, \quad (12)$$

where E_α is the average internal energy density, per unit mass, of the α -phase, \mathbf{q}_α denotes the heat flux, \mathbf{d}_α is the symmetric part of $\nabla \mathbf{v}_\alpha$, $\mathbf{A} : \mathbf{B} = \text{tr}(\mathbf{AB}^T)$ denotes the classical inner product between tensors, and \widehat{Q}_α denotes the gain of energy by the α -phase due to the interactions with the other phase.

Entropy inequality

The entropy inequality for the entire mixture is

$$\Lambda = \sum_{\alpha=l,s} \sum_{j=1}^N \left[\varepsilon_\alpha \rho_\alpha^j \frac{D_\alpha^j \eta_\alpha^j}{Dt} - \nabla \cdot \left(\frac{\varepsilon_\alpha \mathbf{q}_\alpha^j}{T} \right) - \widehat{\phi}_\alpha^j - \widehat{\eta}_\alpha^j \right] \geq 0,$$

where Λ is the net rate of entropy production. Here we have assumed that each constituent in each phase undergoes only simple thermodynamical processes, e.g., the entropy flux is proportional to the heat flux. As a result, using (12), the entropy inequality can be rewritten as

$$\begin{aligned} \Lambda = & \sum_{\alpha=l,s} \sum_{j=1}^N \left[-\frac{\varepsilon_\alpha \rho_\alpha^j}{T} \left(\frac{D_\alpha^j A_\alpha^j}{Dt} + \eta_\alpha^j \frac{D_\alpha^j T}{Dt} \right) + \right. \\ & \left. + \frac{\varepsilon_\alpha}{T} \mathbf{t}_\alpha^j : \mathbf{d}_\alpha^j + \frac{\varepsilon_\alpha}{T^2} \mathbf{q}_\alpha^j \cdot \nabla T + \frac{1}{T} (\widehat{E}_\alpha^j + \widehat{Q}_\alpha^j) - \widehat{\phi}_\alpha^j - \widehat{\eta}_\alpha^j \right] \geq 0, \end{aligned}$$

where we have performed a Legendre transformation to eliminate E_α^j in favor of the Helmholtz potential, A_α^j .

Recall that the bulk phase variables are defined so as to obtain bulk phase field equations which resemble the traditional form of the field equations. The various relations between the phase and species properties are [2, 39]

$$\rho_\alpha = \sum_{j=1}^N \rho_\alpha^j, \quad \widehat{e}_\alpha = \sum_{j=1}^N \widehat{e}_\alpha^j, \quad \rho_\alpha \mathbf{v}_\alpha = \sum_{j=1}^N \rho_\alpha^j \mathbf{v}_\alpha^j = \rho_\alpha \sum_{j=1}^N C_\alpha^j \mathbf{v}_\alpha^j, \quad (13)$$

$$\mathbf{t}_\alpha = \sum_{j=1}^N (\mathbf{t}_\alpha^j - \rho_\alpha^j \mathbf{u}_\alpha^j \otimes \mathbf{u}_\alpha^j), \quad \widehat{\mathbf{T}}_\alpha = \sum_{j=1}^N (\widehat{\mathbf{T}}_\alpha^j + \widehat{e}_\alpha^j \mathbf{u}_\alpha^j), \quad (14)$$

$$\eta_\alpha = \sum_{j=1}^n C_\alpha^j \eta_\alpha^j, \quad A_\alpha = \sum_{j=1}^n C_\alpha^j A_\alpha^j, \quad (15)$$

$$E_\alpha = \sum_{j=1}^N C_\alpha^j \left(E_\alpha^j + \frac{1}{2} \mathbf{u}_\alpha^j \cdot \mathbf{u}_\alpha^j \right), \quad (16)$$

$$\mathbf{q}_\alpha = \sum_{j=1}^N \left[\mathbf{q}_\alpha^j + \mathbf{t}_\alpha^j \mathbf{u}_\alpha^j - \rho_\alpha^j \left(E_\alpha^j + \frac{1}{2} \mathbf{u}_\alpha^j \cdot \mathbf{u}_\alpha^j \right) \mathbf{u}_\alpha^j \right], \quad (17)$$

$$\widehat{Q}_\alpha = \sum_{j=1}^N \left[\widehat{Q}_\alpha^j + \widehat{\mathbf{T}}_\alpha^j \cdot \mathbf{u}_\alpha^j + \widehat{e}_\alpha^j \left(E_\alpha^j - E_\alpha + \frac{1}{2} \mathbf{u}_\alpha^j \cdot \mathbf{u}_\alpha^j \right) \right], \quad (18)$$

where η_α and A_α denote the entropy and free energy of phase α , respectively, and \otimes denotes the tensorial product between vectors.

In addition, we have the following constraints [2, 39]:

$$\sum_{\alpha=l,s} \varepsilon_\alpha = 1, \quad \sum_{j=1}^N C_\alpha^j = 1, \quad \sum_{j=1}^N \rho_\alpha^j \mathbf{u}_\alpha^j = \mathbf{0}, \quad (19)$$

$$\sum_{j=1}^N \widehat{\mathbf{i}}_\alpha^j = \mathbf{0}, \quad \sum_{j=1}^N \widehat{\eta}_\alpha^j = 0, \quad \sum_{j=1}^N (\widehat{E}_\alpha^j + \widehat{\mathbf{i}}_\alpha^j \cdot \mathbf{u}_\alpha^j) = 0, \quad (20)$$

$$\sum_{\alpha=l,s} \widehat{e}_\alpha = 0, \quad \sum_{\alpha=l,s} \widehat{e}_\alpha^j = 0, \quad j = 1, \dots, N, \quad (21)$$

$$\sum_{\alpha=l,s} \left[\widehat{Q}_\alpha^j + \widehat{\mathbf{T}}_\alpha^j \cdot \mathbf{v}_\alpha^j + \widehat{e}_\alpha^j \left(E_\alpha^j + \frac{1}{2} \mathbf{v}_\alpha^j \cdot \mathbf{v}_\alpha^j \right) \right] = 0, \quad j = 1, \dots, N, \quad (22)$$

$$\sum_{\alpha=l,s} (\widehat{\mathbf{T}}_\alpha^j + \widehat{e}_\alpha^j \mathbf{v}_\alpha^j) = \mathbf{0}, \quad \sum_{\alpha=l,s} (\widehat{\phi}_\alpha^j + \widehat{e}_\alpha^j \eta_\alpha^j) = 0, \quad j = 1, \dots, N. \quad (23)$$

Relations (19) are a consequence of the definition of the variables. Restrictions (20) are a result of summing the balance laws over each constituent and requiring the bulk phase to satisfy the balance laws. Restrictions (21)–(23) are a consequence of assuming that the interfaces have no thermodynamical properties, e.g. the momentum transfer from the liquid phase to the solid phase is the same magnitude as that from the solid to the liquid phase.

Expressing the entropy inequality in terms of phase properties and using (13)–(23) we have

$$\begin{aligned} T \Lambda = & \sum_{\alpha=l,s} -\varepsilon_\alpha \rho_\alpha \left(\frac{D_\alpha A_\alpha}{Dt} + \eta_\alpha \frac{D_\alpha T}{Dt} \right) + \\ & + \sum_{\alpha=l,s} \varepsilon_\alpha \mathbf{d}_\alpha : \left(\mathbf{t}_\alpha + \sum_{j=1}^N \rho_\alpha^j \mathbf{u}_\alpha^j \otimes \mathbf{u}_\alpha^j \right) + \sum_{\alpha=l,s} \sum_{j=1}^N \varepsilon_\alpha \nabla \mathbf{u}_\alpha^j : (\mathbf{t}_\alpha^j - \rho_\alpha^j A_\alpha^j \mathbf{I}) - \\ & - \sum_{\alpha=l,s} \sum_{j=1}^N \mathbf{u}_\alpha^j \cdot [\nabla (\varepsilon_\alpha \rho_\alpha^j A_\alpha^j) + \widehat{\mathbf{i}}_\alpha^j + \widehat{\mathbf{T}}_\alpha^j] - \mathbf{v}_{l,s} \cdot \widehat{\mathbf{T}}_l + \\ & + \sum_{\alpha=l,s} \frac{\varepsilon_\alpha}{T} \nabla T \cdot \left\{ \mathbf{q}_\alpha + \sum_{j=1}^N \left[\rho_\alpha^j \mathbf{u}_\alpha^j \left(A_\alpha^j + \frac{1}{2} \mathbf{u}_\alpha^j \cdot \mathbf{u}_\alpha^j \right) - \mathbf{t}_\alpha^j \mathbf{u}_\alpha^j \right] \right\} - \end{aligned}$$

$$-\sum_{\alpha=l,s} \sum_{j=1}^N \widehat{e}_l^j \left(\frac{1}{2} \mathbf{u}_l^j \cdot \mathbf{u}_l^j - \frac{1}{2} \mathbf{u}_s^j \cdot \mathbf{u}_s^j \right) - \widehat{e}_l \left(A^l - A^s + \frac{1}{2} \mathbf{v}_{l,s} \cdot \mathbf{v}_{l,s} \right) \geq 0, \quad (24)$$

where $\mathbf{v}_{l,s} = \mathbf{v}_l - \mathbf{v}_s$ denotes the relative velocity, \mathbf{I} denotes the identity matrix, and the following relation has been employed

$$\begin{aligned} & \sum_{\alpha=l,s} \sum_{j=1}^N \varepsilon_\alpha \rho_\alpha^j \frac{D_\alpha^j A_\alpha^j}{Dt} \\ &= \sum_{\alpha=l,s} \varepsilon_\alpha \rho_\alpha \frac{D_\alpha A_\alpha}{Dt} + \sum_{\alpha=l,s} \sum_{j=1}^N [\widehat{e}_\alpha^j (A_\alpha - A_\alpha^j) + \nabla \cdot (\varepsilon_\alpha \rho_\alpha^j A_\alpha^j \mathbf{u}_\alpha^j)]. \end{aligned}$$

3. Constitution

In this section, we assume the material is a swelling colloid. We focus our discussion on clay, but the results can be applied to other swelling systems, such as lyophilic polymers. The clay systems we have in mind are smectic clays such as montmorillonite. We assume the clay systems can be described as an assemblage of mineral platelets, forming the solid phase, and vicinal water, forming the fluid phase. This system may swell under hydration and shrink under desiccation.

The unknowns in our system are:

$$\varepsilon_l, \rho_\alpha, C_\alpha^j, \mathbf{v}_\alpha, \mathbf{v}_\alpha^j, T, \quad (25)$$

$$\begin{aligned} & A_\alpha, A_\alpha^j, \eta_\alpha, \eta_\alpha^j, \mathbf{t}_\alpha, \mathbf{t}_\alpha^j, \widehat{\mathbf{T}}_l, \widehat{\mathbf{T}}_l^j, \widehat{e}_l, \widehat{e}_l^j, \mathbf{q}_\alpha, \mathbf{q}_\alpha^j, \\ & \widehat{\mathbf{i}}_\alpha^j, \widehat{\mathbf{Q}}_l, \widehat{\mathbf{Q}}_l^j, \widehat{\mathbf{E}}_\alpha^j, \quad j = 1, \dots, N-1, \quad \alpha = l, s. \end{aligned} \quad (26)$$

Note that since we only consider $N - 1$ constituents, the above variables are indeed independent. To arrive at a system which has the same number of equations as unknowns, we consider the last two rows of variables (26) to be dependent, or constitutive. These variables are assumed to be functions of a set of independent variables which we henceforth denote as the constitutive independent variables. However, even with these constitutive variables a careful count indicates that there is still an additional unknown for which there is no corresponding equation. Making a comparison with classical mixture theory for a single phase, we see that the volume fraction is the variable unaccounted for. Thus, there is a problem of closure associated with the loss of information in the upscaling process. One way of closing the system is to assume the solid phase is incompressible (e.g. $D_s \rho_s / Dt = 0$) [42]. However, we are interested in more general results so that these ideas can be extended to more complicated systems, such as systems with more than two

bulk phases, or a system for which interfacial effects cannot be neglected. One popular method, introduced first for granular media in [36] and generalized in [67] is to postulate another balance law, called the ‘balance of equilibrated forces’. Eventually constitutive relations must be postulated for these additional terms. In a fashion similar to this approach, Aifantis and co-workers have suggested that there should be additional balance equations for all internal variables [5, 77]. Again the system must be closed by introducing additional constitutive variables.

Although some nice results have been obtained using this approach, we have not chosen to close our system of equations in this manner for several reasons. First, the additional balance equation has no microstructural origin. Within HMT all balance equations are upscaled from the microscale. Not relating each additional variable to a microscale counterpart has resulted in confusion as to the physical interpretation of these variables [4]. Further, many of the physical interpretations attributed to the variables in the additional balance equation correspond to terms within the original macroscale balance laws, especially if one includes the interfacial balance equations as well. Lastly, we feel the system should be closed by a constitutive relation. The change in the volume fraction is a consequence of the constitution of each phase of the porous media, as well as the state of each phase.

Although we feel this issue needs to be examined more closely, the closure method we feel most comfortable with is that of postulating a constitutive relation for the material time derivative of the volume fraction, which was first introduced in [21]. Note that this method of closure can be viewed as a simplified version of adding an additional balance equation; within the additional balance law for the volume fraction, if it is assumed there is no external supply of the volume fraction, all variables except for the time rate of change of the volume fraction are considered constitutive. Thus, there is a relation between the aforementioned closure method and this one. Additionally this closure approach allows the derivation of results which had only been previously heuristically derived [2].

We assume the macroscopic medium is nonheat conducting, the macroscopic fluid is nonviscous, and the fluid and solid phases are compressible. By the Principle of Equipresence [76], we assume that every constitutive variable is a function of all the following macroscopic constitutive independent variables:

$$\begin{aligned} T, \rho_\alpha, \mathbf{E}_s, \mathbf{v}_{l,s}, \mathbf{u}_\alpha^j, C_\alpha^j, \nabla C_\alpha^j, \nabla \rho_\alpha, \nabla \mathbf{E}_s, \\ j = 1, \dots, N - 1, \quad \alpha = l, s, \end{aligned} \quad (27)$$

where \mathbf{E}_s is the macroscopic strain tensor of the solid phase defined by

$$\mathbf{E}_s = \frac{1}{2}(\mathbf{F}_s^T \mathbf{F}_s - \mathbf{I}), \quad (28)$$

in which $\mathbf{F}_s = \text{grad} \mathbf{x}_s$ denotes the deformation gradient (with grad denoting the differentiation with respect to a macroscopic material particle). Here we have implicitly assumed the constitutive variables are local functions, that is, the value of each constitutive variable is determined by the values of the constitutive independent variables at that same material point, so that there is no nonlocality in space.

With this assumption, the variables and their gradients (27) can be considered independent, since it is possible to have different processes which at a single point can have e.g. the same strain but varying gradients of the strain. As we shall see in the next section, including the gradient of the strain tensor in the list of constitutive independent variables is crucial for deriving a proper form of Darcy's law for the vicinal fluid.

The macroscopic strain is a measure of the solid phase geometry, so by including \mathbf{E}_s and $\nabla \mathbf{E}_s$ in the list of constitutive independent variables, we assume that the behavior of the system is partially dictated by the separation and distortion of the solid platelets and their spatial variations. Moreover, although both ε_l and \mathbf{E}_s could be considered as independent variables [11, 13], \mathbf{E}_s is closely related to ε_l through the continuity equation, especially if the mass transfer of constituents between phases is negligible (see Section 8), so that we choose to include only \mathbf{E}_s as an independent constitutive variable. In addition, \mathbf{u}_α^N and C_α^N are not considered independent variables since they are coupled with other independent variables through (19).

To simplify manipulations of the entropy inequality, we use Liu's Lagrange multiplier technique [52]. We first choose to view conservation of mass equations as constraints which are weakly enforced in the entropy inequality using scalar Lagrange multipliers, λ_α and λ_α^j . We further use Lagrange multipliers to enforce the relationship between $\nabla \mathbf{u}_\alpha^j$, $j = 1, \dots, N$ obtained by differentiating (3). This approach differs from the more commonly used method which involves eliminating $\nabla \mathbf{u}_\alpha^N$ directly via (3) [2, 14, 39]. The two techniques give identical results, but this procedure provides a more systematic method, simplifying the manipulations required to exploit the entropy inequality. Let Γ_α^N denote the second order tensorial Lagrange multiplier corresponding to the constraint on $\nabla \mathbf{u}_\alpha^j$. The superscript N is carried to remind us that we view the constraints as restrictions on \mathbf{u}_α^N , that is they depend on the labeling of the constituents.

Let $\Lambda_{\text{old}} \equiv \Lambda$ of (24). Modifying the entropy inequality we get

$$\begin{aligned} T\Lambda_{\text{new}} &= T\Lambda_{\text{old}} + \sum_{\alpha=l,s} \lambda_\alpha \left[\frac{D_\alpha(\varepsilon_\alpha \rho_\alpha)}{Dt} + \varepsilon_\alpha \rho_\alpha \nabla \cdot \mathbf{v}_\alpha - \widehat{\mathbf{e}}_\alpha \right] + \\ &\quad + \sum_{\alpha=l,s} \sum_{j=1}^{N-1} \lambda_\alpha^j \left[\varepsilon_\alpha \rho_\alpha \frac{D_\alpha C_\alpha^j}{Dt} + \nabla \cdot (\varepsilon_\alpha \rho_\alpha^j \mathbf{u}_\alpha^j) - (\widehat{\mathbf{e}}_\alpha^j - C_\alpha^j \widehat{\mathbf{e}}_\alpha) \right] + \\ &\quad + \sum_{\alpha=l,s} \varepsilon_\alpha \Gamma_\alpha^N : \left[\sum_{j=1}^N \nabla(\rho_\alpha^j \mathbf{u}_\alpha^j) \right] \geq 0. \end{aligned}$$

Next we invoke the theorem of Liu [52], which states equivalence between the entropy inequality with restrictions and the modified entropy inequality above.

To simplify the quantity of algebra which follows, we deviate slightly from the axiom of equipresence [33], and assume the Helmholtz free energy densities of the phases depend only on a subset of the set of constitutive independent variables. It

can be shown that if it is assumed the Helmholtz free energies are a function of all constitutive independent variables listed in (27), that the exploitation of the entropy inequality requires that both energies are not a function of $\mathbf{v}_{l,s}$, \mathbf{u}_α^j , $\nabla \rho_\alpha^j$, ∇C_α^j , and $\nabla \mathbf{E}_s$. Here we additionally assume that the liquid free energy is not a function of ρ_s and C_s^j , and likewise that the solid free energy is not a function of ρ_l and C_l^j . Incorporating these additional dependencies still produces the results presented herein if one slightly modifies the thermodynamic definitions of the pressure and chemical potential [13, 11]. For the system under consideration it is thus postulated that

$$\begin{aligned} A_s &= A_s(T, \rho_s, C_s^j, \mathbf{E}_s) \\ A_l &= A_l(T, \rho_l, C_l^j, \mathbf{E}_s), \quad j = 1, \dots, N - 1. \end{aligned} \quad (29)$$

By assuming the liquid phase energy as a function of the solid phase strain tensor, we are adopting the framework of [13, 65] in order to allow the adsorbed liquid structure to be a function of the separation and shear strain of the macroscopic solid phase. Recall that the definition of vicinal or adsorbed water is water whose properties vary with the distance from the solid phase. In an ideal case, in which the solid phase is composed of flat parallel platelets, the adsorption of additional water causes the platelets to move further apart, changing the properties (density, viscosity, etc. [56] of the vicinal fluid. This change is represented by the strain tensor which, by definition, is the strain of the ‘smeared out’ solid phase. So as the platelets separate, the solid phase strain tensor is altered. Similarly, if the platelets are sheared relative to each other, this again affects the strain tensor. This is a generalization of the work [2] where it was assumed that the liquid phase energy is a function of ε_l instead of \mathbf{E}_s . In Achanta’s work, an empirical result for the swelling pressure obtained in [56] was derived for the first time using this constitutive assumption and the exploitation of the entropy inequality. The derivation of this result in our formulation is presented in Section 7. In the more general theory considered here, we are assuming that the Helmholtz free energy of the adsorbed liquid is not only a function of the separation of clay platelets, but also of the shear strain of the macroscopic solid phase. By including shear strains, we are attempting to capture the behavior of clay soils at low moisture content (interlayer spacings less than 10 molecular diameters of water or 25) where the behavior of the microscopic vicinal water may be neither liquid-like nor solid-like, but glassy [26, 47, 70]. In this state the fluid molecules are more ordered and are layered parallel to the surface so that the fluid, on the microscale, is structured, inhomogeneous, and anisotropic. The interlamellar fluid is relatively immobile due to the higher viscosity, allowing the fluid to support a shear stress.

To complete the set of definitions, we introduce the thermodynamic pressures (p_α), the Gibbs energy density of the α -phase, G_α , the chemical potentials of the j th component relative to the N th component in the α -phase ($\widetilde{\mu}_\alpha^j$) [19], the

classical effective stress tensor (\mathbf{t}_s^e) in the sense of [74], and the hydration stress tensor (\mathbf{t}_s^l) [13, 65]. Within the current framework they are defined as follows:

$$p_\alpha = \rho_\alpha^2 \frac{\partial A_\alpha}{\partial \rho_\alpha}, \quad G_\alpha = A_\alpha + \rho_\alpha^{-1} p_\alpha, \quad (30)$$

$$\mathbf{t}_s^e = \rho_s \mathbf{F}_s \frac{\partial A_s}{\partial \mathbf{E}_s} \mathbf{F}_s^T, \quad \mathbf{t}_s^l = \rho_l \mathbf{F}_s \frac{\partial A_l}{\partial \mathbf{E}_s} \mathbf{F}_s^T, \quad (31)$$

$$\tilde{\mu}_\alpha^j = \frac{\partial A_\alpha}{\partial C_\alpha^j}, \quad \alpha = l, s, \quad j = 1, \dots, N-1. \quad (32)$$

The definition of \mathbf{t}_s^e is analogous to the Cauchy stress tensor for an elastic medium [33] although applied to a porous skeleton. In soil mechanics this stress tensor is referred to as the Terzaghi stress tensor. The hydration stress tensor, \mathbf{t}_s^l , is novel, and is a result of the physico-chemical forces between the vicinal fluid and the clay minerals.

The Coleman and Noll method [25] is now used to exploit the restrictions placed by the entropy inequality on the constitutive theory. Within this framework the total derivatives of the free energies are rewritten in terms of partial derivatives using the chain rule and the functional forms postulated in (29). Using the relations $D_l/Dt = D_s/Dt + \mathbf{v}_{l,s} \cdot \nabla$ and $D_s \mathbf{E}_s/Dt = \mathbf{F}_s^T \mathbf{d}_s \mathbf{F}_s$ [33] and the above definitions we then have

$$\frac{D_l A_l}{Dt} = \frac{\partial A_l}{\partial T} \frac{D_l T}{Dt} + \frac{p_l}{\rho_l^2} \frac{D_l \rho_l}{Dt} + \sum_{j=1}^{N-1} \tilde{\mu}_l^j \frac{D_l C_l^j}{Dt} + \frac{1}{\rho_l} \mathbf{t}_s^l : \mathbf{d}_s + \mathbf{v}_{l,s} \cdot \left(\frac{\partial A_l}{\partial \mathbf{E}_s} : \nabla \mathbf{E}_s \right)$$

and

$$\frac{D_s A_s}{Dt} = \frac{\partial A_s}{\partial T} \frac{D_s T}{Dt} + \frac{p_s}{\rho_s^2} \frac{D_s \rho_s}{Dt} + \sum_{j=1}^{N-1} \tilde{\mu}_s^j \frac{D_s C_s^j}{Dt} + \frac{1}{\rho_s} \mathbf{t}_s^e : \mathbf{d}_s,$$

where the term in the parenthesis in indicial notation is $(\partial A / \partial E_{ij}) E_{ij,k}$ in which repeated indices imply summation and a comma denotes a partial derivative.

To minimize the required algebra, we restrict our analysis to the case where temperature gradients and heat fluxes are absent. Using the above expansions entropy inequality (24) can be rewritten as

$$\begin{aligned} T \Lambda = & \sum_{\alpha=l,s} \frac{D_s \rho_\alpha}{Dt} \left(\varepsilon_\alpha \lambda_\alpha - \varepsilon_\alpha \frac{p_\alpha}{\rho_\alpha} \right) + \sum_{\alpha=l,s} \sum_{j=1}^{N-1} \frac{D_s C_\alpha^j}{Dt} (\varepsilon_\alpha \rho_\alpha \lambda_\alpha^j - \varepsilon_\alpha \rho_\alpha \tilde{\mu}_\alpha^j) - \\ & - \sum_{\alpha=l,s} \varepsilon_\alpha \rho_\alpha \frac{D_s T}{Dt} \left(\frac{\partial A_\alpha}{\partial T} + \eta_\alpha \right) + \varepsilon_l \mathbf{d}_l : \left(\mathbf{t}_l + \rho_l \lambda_l \mathbf{I} + \sum_{j=1}^N \rho_l^j \mathbf{u}_l^j \otimes \mathbf{u}_l^j \right) + \\ & + \varepsilon_s \mathbf{d}_s : \left(\mathbf{t}_s + \rho_s \lambda_s \mathbf{I} - \mathbf{t}_s^e - \frac{\varepsilon_l}{\varepsilon_s} \mathbf{t}_s^l + \sum_{j=1}^N \rho_s^j \mathbf{u}_s^j \otimes \mathbf{u}_s^j \right) + \end{aligned}$$

$$\begin{aligned}
& + \mathbf{v}_{l,s} \cdot \left(-\varepsilon_l \frac{p_l}{\rho_l} \nabla \rho_l - \sum_{j=1}^{N-1} \varepsilon_l \rho_l \tilde{\mu}_l^j \nabla C_l^j - \varepsilon_l \rho_l \frac{\partial A_l}{\partial \mathbf{E}_s} : \nabla \mathbf{E}_s + \varepsilon_l \lambda_l \nabla \rho_l + \right. \\
& + \sum_{j=1}^{N-1} \varepsilon_l \rho_l \lambda_l^j \nabla C_l^j + \rho_l \lambda_l \nabla \varepsilon_l - \widehat{\mathbf{T}}_l \Big) + \\
& + \frac{D_s \varepsilon_l}{Dt} (\rho_l \lambda_l - \rho_s \lambda_s) + \sum_{\alpha=l,s} \sum_{j=1}^N \varepsilon_\alpha \nabla \mathbf{u}_\alpha^j : (\mathbf{t}_\alpha^j + \rho_\alpha^j (\lambda_\alpha^j - A_\alpha^j) \mathbf{I} + \rho_\alpha^j \Gamma_\alpha^N) + \\
& + \sum_{\alpha=l,s} \sum_{j=1}^N \mathbf{u}_\alpha^j \cdot [\lambda_\alpha^j \nabla (\varepsilon_\alpha \rho_\alpha^j) - \nabla (\varepsilon_\alpha \rho_\alpha^j A_\alpha^j) - (\widehat{\mathbf{i}}_\alpha^j + \widehat{\mathbf{T}}_\alpha^j) + \varepsilon_\alpha \Gamma_\alpha^N \nabla \rho_\alpha^j] - \\
& - \sum_{j=1}^N \widehat{e}_l^j (\lambda_l^j - \lambda_s^j + \Delta^2) - \widehat{e}_l \left(\lambda_l - \lambda_s + \sum_{j=1}^{N-1} (C_s^j \lambda_s^j - C_l^j \lambda_l^j) + A_l - A_s \right) \geq 0, \tag{33}
\end{aligned}$$

where $\tilde{\mu}_\alpha^N$ and λ_α^N are defined to be zero for notational convenience, and where $\Delta^2 = (1/2)(\mathbf{u}_l^j \cdot \mathbf{u}_l^j + \mathbf{v}_{l,s} \cdot \mathbf{v}_{l,s} - \mathbf{u}_s^j \cdot \mathbf{u}_s^j)$. Note that because the restriction associated with the Lagrange multiplier Γ_α^N , $\nabla \mathbf{u}_\alpha^j$, $j = 1, \dots, N$, can be considered independent when exploiting the entropy inequality. However, \mathbf{u}_α^j , $j = 1, \dots, N$, may not be considered independent.

4. General Nonequilibrium Results and Two Definitions for the N th Chemical Potential

As usual, Λ is a linear function of the following set of variables which are neither independent – set (27), nor constitutive – set (26), and thus are arbitrary:

$$\frac{D_s \rho_\alpha}{Dt}, \quad \frac{D_s C_\alpha^j}{Dt}, \quad \frac{D_s T}{Dt}, \quad \mathbf{d}_\alpha, \quad \nabla \mathbf{u}_\alpha^j, \quad \alpha = l, s,$$

where $j = 1, \dots, N-1$ for $D_s C_\alpha^j / Dt$ and $j = 1, \dots, N$ for $\nabla \mathbf{u}_\alpha^j$. Note that the index on $\nabla \mathbf{u}_\alpha^j$ ranges from 1 to N because we have used a Lagrange multiplier to enforce the relation between these variables so that we can consider them to be independent. In order to satisfy the entropy inequality for all possible processes, the coefficients of these variables must be identically zero. This yields

$$\lambda_\alpha = \frac{p_\alpha}{\rho_\alpha}, \tag{34}$$

$$\lambda_\alpha^j = \tilde{\mu}_\alpha^j, \quad j = 1, \dots, N-1, \tag{35}$$

$$\sum_{\alpha=l,s} \varepsilon_\alpha \rho_\alpha \left(\frac{\partial A_\alpha}{\partial T} + \eta_\alpha \right) = 0, \tag{36}$$

$$\mathbf{t}_l = -p_l \mathbf{I} - \sum_{j=1}^N \rho_l^j \mathbf{u}_l^j \otimes \mathbf{u}_l^j, \quad (37)$$

$$\mathbf{t}_s = -p_s \mathbf{I} + \mathbf{t}_s^e + \frac{\varepsilon_l}{\varepsilon_s} \mathbf{t}_s^l - \sum_{j=1}^N \rho_s^j \mathbf{u}_s^j \otimes \mathbf{u}_s^j, \quad (38)$$

$$\mathbf{t}_\alpha^j = \rho_\alpha^j A_\alpha^j \mathbf{I} - \rho_\alpha^j \tilde{\mu}_\alpha^j \mathbf{I} - \rho_\alpha^j \Gamma_\alpha^N, \quad j = 1, \dots, N. \quad (39)$$

Equations (34) and (35) determine the Lagrange multipliers. If any phase or constituent is incompressible, then there is no equation for the corresponding Lagrange multiplier, and it becomes an unknown of the problem. *For the remainder of this paper, we will replace the Lagrange multipliers by their corresponding definitions given in (34) and (35).* Equation (36) is a classical result stating that entropy and temperature are dual variables [23]. The macroscopic stress tensor for the vicinal liquid (37) is, in a first order theory, a scalar multiple of the identity. Note that if ∇E_s had not been included in the list of independent variables, then it would have been included in the above list of variables which are neither independent nor constitutive. This would have resulted in the conclusion that A_l is not a function of E_s , and the above results could only be used to model nonswelling porous media.

Equation (38) gives important insight into the behavior of the stress tensor for the swelling particles. If we introduce the total stress tensor $\mathbf{t} = \varepsilon_s \mathbf{t}_s + \varepsilon_l \mathbf{t}_l$ and total thermodynamic pressure $p = \varepsilon_l p_l + \varepsilon_s p_s$, then by using (37) and (38) we obtain

$$\mathbf{t} + p \mathbf{I} = \varepsilon_l \mathbf{t}_s^l + \varepsilon_s \mathbf{t}_s^e - \sum_{\alpha=l,s} \sum_{j=1}^N \varepsilon_\alpha \rho_\alpha^j \mathbf{u}_\alpha^j \otimes \mathbf{u}_\alpha^j. \quad (40)$$

Equation (40) is a modified Terzaghi's effective stress principle for swelling clays which incorporates the effect of hydration stresses. It states that the equilibrium part of the stress tensor for a swelling medium is composed of both the classical effective stress tensor in the sense of Terzaghi [74], \mathbf{t}_s^e , and an additional stress, \mathbf{t}_s^l , which accounts for the stress in the adsorbed water due to hydration forces. The effective stress tensor, \mathbf{t}_s^e , measures stresses induced by solid-solid interaction and hence is the dominant factor when considering nonswelling systems such as sands, silts, and low and medium plastic clays such as kaolinite or illite. On the other hand, \mathbf{t}_s^l dominates when there is a significant amount of solid-fluid interaction, such as swelling particles. Clearly this additional stress component is due to the presence of physico-chemical forces arising from surface hydration. Whence, as in [13, 65], we term the coupling tensor \mathbf{t}_s^l the 'hydration stress tensor'. Other attempts to obtain the hydration stress tensor have been primarily heuristic [46, 51, 62, 73].

Equation (39) relates the chemical potential to the stress tensor of the components within each phase, \mathbf{t}_α^j . One consequence of (39) is that by letting $j = N$ we obtain the definition of the Lagrange multiplier, Γ_α^N

$$\Gamma_\alpha^N = A_\alpha^N \mathbf{I} - \frac{1}{\rho_\alpha^N} \mathbf{t}_\alpha^N. \quad (41)$$

But more importantly, Equation (39) illustrates that applying the Coleman and Noll method only yields results relative to the N th constituent. This is due to the interdependence of the concentrations (19). In order to derive more specific results, a definition for the absolute chemical potential must be postulated, and this strongly affects the form of the final results. This procedure is mostly avoided in classical and statistical thermodynamics because extensive variables, namely the number of molecules of each constituent, are used as independent variables instead of intensive variables (concentrations).

We believe the appropriate definition of the absolute chemical potential within mixture theory needs to be carefully examined. Indeed, one can find a variety of definitions in the literature. Here we mention a few. In terms of our notation, Kremer *et al.* [50] define the chemical potential at equilibrium to be $\partial(\rho_\alpha A_\alpha)/\partial\rho_\alpha^j$ for fixed vibrational energy. In [4] the chemical potential is defined to be $\partial(C_\alpha^j A_\alpha^j)/\partial C_\alpha^j$. Probably the most popularly used definition is the tensorial definition of [19, 22]

$$\nu_\alpha^j \equiv A_\alpha^j \mathbf{I} - \frac{1}{\rho_\alpha^j} \mathbf{t}_\alpha^j, \quad j = 1, \dots, N, \quad (42)$$

see, e.g., [2, 39]. To determine the most appropriate definition, a criteria must be established, and we believe that the criteria should be that *the macroscale chemical potential should have the same properties as that of the classical Gibbsian chemical potential*. Further, these properties should be consistent with the entropy inequality.

In classical Gibbsian thermodynamics, the chemical potential is defined to be the change of the total extensive Helmholtz potential, A , with respect to the number of molecules of constituent j , n^j , keeping temperature, volume, and the number of molecules of all other constituents fixed, i.e. $\partial A / \partial n^j|_{T, V, n_i}$ [24]. In this setting, the chemical potential has the following properties [24]:

- (1) It is a scalar quantity representing the amount of chemical energy required to insert/remove a molecule of constituent j (by definition).
- (2) At equilibrium, the chemical potential of a single constituent in different phases is the same.
- (3) The chemical potential is the driving force for diffusive flow. In particular, at equilibrium the gradient of the chemical potential is zero.

Note that the above properties do not imply that at equilibrium the chemical potentials of two different constituents are the same, an error commonly found in the literature. It is especially important that property 3 holds, as it is the property used to indirectly measure the chemical potential [24].

Of the definitions given above, only Bowen's arises naturally within our framework. In fact, using Bowen's definition (42) we get from (41) and (39)

$$\nu_\alpha^N \equiv \Gamma_\alpha^N, \quad (43)$$

$$\tilde{\mu}_\alpha^j \mathbf{I} = \nu_\alpha^j - \nu_\alpha^N, \quad (44)$$

respectively. By multiplying (42) through by C_α^j and summing on j from 1 to N , we find that

$$\sum_{j=1}^N C_\alpha^j \mathbf{v}_\alpha^j = A_\alpha \mathbf{I} - \frac{1}{\rho_\alpha} \mathbf{t}_\alpha, \quad (45)$$

where we have used the relationship between the phase stress tensor and partial stress tensors in (14) and neglected second order terms involving diffusive velocities. This definition for the chemical potential seems to be motivated by convenience and is not easily reconciled with the classical definition, which is a scalar. Although for a single constituent liquid, the classical scalar and Bowen's tensorial definitions agree, i.e., $\mathbf{v}_l = \mu_l \mathbf{I} = (p_l/\rho_l + A_l) \mathbf{I}$, the question remains as to how to interpret this tensorial quantity in the solid phase, which, according to classical statistical theory, is physically interpreted as a measure of the amount of chemical energy required to place a particle in the system (property 1, see also [61]). Indeed, we will show that Bowen's tensorial chemical potential definition is not reconciled with classical properties 1–3 when considering a stressed solid phase. This has caused some problems with measuring the tensorial stress tensor [8, 69].

Alternatively, by defining the chemical potential slightly differently, we can reproduce in form classical Gibbsian results. To this end, note that beginning with the relationship between the stress tensors of the components and phases, (14), and eliminating $\sum_{j=1}^N \mathbf{t}_\alpha^j$, \mathbf{t}_α , and Γ_α^N using (39), (37, 38), and (41), respectively, gives

$$\begin{aligned} -\frac{1}{\rho_l^N} \mathbf{t}_l^N &= \left(\frac{1}{\rho_l} p_l + A_l - \sum_{j=1}^N C_l^j \tilde{\mu}_l^j - A_l^N \right) \mathbf{I}, \\ -\frac{1}{\rho_s^N} \mathbf{t}_s^N + \frac{1}{\rho_s} \left(\mathbf{t}_s^e + \frac{\varepsilon_l}{\varepsilon_s} \mathbf{t}_s^l \right) &= \left(\frac{1}{\rho_s} p_s + A_s - \sum_{j=1}^N C_s^j \tilde{\mu}_s^j - A_s^N \right) \mathbf{I}. \end{aligned}$$

This tells us that the left-hand sides of the above equations are scalar multiples of the identity. By using (39) we can show that the above quantities on the left-hand-side are scalars for all j , $j = 1, \dots, N$. With this as a motivation, define the scalar chemical potentials

$$\mu_l^j \mathbf{I} \equiv A_l^j \mathbf{I} - \frac{1}{\rho_l^j} \mathbf{t}_l^j, \quad (46)$$

$$\mu_s^j \mathbf{I} \equiv A_s^j \mathbf{I} - \frac{1}{\rho_s^j} \mathbf{t}_s^j + \frac{1}{\rho_s} \left(\mathbf{t}_s^e + \frac{\varepsilon_l}{\varepsilon_s} \mathbf{t}_s^l \right), \quad j = 1, \dots, N, \quad (47)$$

where we have used the nonbold symbol, μ_α^j , to distinguish it from Bowen's tensorial chemical potential which we continue to write in bold face. Multiplying (46, 47) by C_α^j and then summing on j gives us the relationship analogous to (45)

$$\sum_{j=1}^N C_\alpha^j \mu_\alpha^j = A_\alpha + \frac{1}{\rho_\alpha} p_\alpha = G_\alpha, \quad \alpha = l, s, \quad (48)$$

where definition (30) for G_α has been used. Moreover, if we define the pressure of the j th component, p_α^j , as

$$-p_l^j \mathbf{I} \equiv \mathbf{t}_l^j, \quad -p_s^j \mathbf{I} \equiv \mathbf{t}_s^j - C_s^j \left(\mathbf{t}_s^e + \frac{\varepsilon_l}{\varepsilon_s} \mathbf{t}_s^l \right), \quad j = 1, \dots, N,$$

then (46) and (47) can be expressed as

$$A_\alpha^j + \frac{1}{\rho_\alpha^j} p_\alpha^j = \mu_\alpha^j, \quad \alpha = l, s, \quad (49)$$

which shows consistency with (48). Summing (49) over all components and comparing with (48) implies $p_\alpha = \sum_{j=1}^N p_\alpha^j$ so that in particular, this gives us an alternative way of interpreting p_s .

Comparing the two definitions of the tensorial and scalar chemical potentials (42), (46, 47), we arrive at the following relationships:

$$\mu_l^j \mathbf{I} = \nu_l^j, \quad (50)$$

$$\mu_s^j \mathbf{I} - \nu_s^j = \frac{1}{\rho_s} \left(\mathbf{t}_s^e + \frac{\varepsilon_l}{\varepsilon_s} \mathbf{t}_s^l \right), \quad j = 1, \dots, N. \quad (51)$$

For future reference, if definition (32) is combined with the above result and (44), we obtain the relation

$$\tilde{\mu}_\alpha^j \mathbf{I} \equiv \frac{\partial A_\alpha}{\partial C_\alpha^j} \mathbf{I} \equiv \nu_\alpha^j - \nu_\alpha^N = (\mu_\alpha^j - \mu_\alpha^N) \mathbf{I}, \quad (52)$$

which is also obtained by using the interdependence of C_α^j , $j = 1, \dots, N$ and the chain rule [28]. If one assumes *a priori* that the absolute chemical potential satisfies (52), then it is only necessary to define the N th chemical potential, which is a much weaker postulate than the assumptions presented in this section. Furthermore, note that the difference between the tensorial and scalar chemical potentials (51) is due to the effective and hydration stresses. If, for example, the solid phase is replaced by another immiscible fluid, we would get equality between the two definitions. As we shall illustrate in next section, the right-hand side of (51) plays a crucial role in the deviation of the tensorial chemical potential from classical Gibbsian results. Also note that constitutive theory for a granular media falls out naturally by setting $\mathbf{t}_s^l = \mathbf{0}$. In this case the difference between the tensorial and scalar definitions are only due to the effective stresses, \mathbf{t}_s^e .

5. Equilibrium Restrictions

For the system under consideration, equilibrium is defined when $D_s \varepsilon_l / D_t$, $\nu_{l,s}$, \mathbf{u}_α^j , \hat{e}_l^j , \hat{e}_l vanish for $j = 1, \dots, N - 1$. It is postulated that at equilibrium entropy is maximum and entropy generation is minimum. Therefore, we must have

$(\partial \Lambda / \partial z_a)_e = 0$ and $(\partial^2 \Lambda / \partial z_a \partial z_b)_e$ positive definite where z_a and z_b denote any of the above set of variables. Before applying these conditions, it is necessary to rewrite the term in entropy inequality (33) associated with \mathbf{u}_α^j , $j = 1, \dots, N$ in terms of independent variables \mathbf{u}_α^j , $j = 1, \dots, N - 1$. To do so, we use the following result obtained by using restriction (3):

$$\sum_{j=1}^N \mathbf{u}_\alpha^j \cdot \mathbf{w}_\alpha^j = \sum_{j=1}^{N-1} \mathbf{u}_\alpha^j \cdot \left(\mathbf{w}_\alpha^j - \frac{C_\alpha^j}{C_\alpha^N} \mathbf{w}_\alpha^N \right),$$

where \mathbf{w}_α^j is the vector representing the coefficient of \mathbf{u}_α^j in (33). Using (41) and (35) we can now express this term as

$$\begin{aligned} \sum_{j=1}^{N-1} \mathbf{u}_\alpha^j \cdot & \left\{ \tilde{\mu}_\alpha^j \nabla (\varepsilon_\alpha \rho_\alpha^j) - \nabla [\varepsilon_\alpha \rho_\alpha^j (A_\alpha^j - A_\alpha^N)] - (\hat{\mathbf{i}}_\alpha^j + \hat{\mathbf{T}}_\alpha^j) + \right. \\ & \left. + \frac{C_\alpha^j}{C_\alpha^N} (\hat{\mathbf{i}}_\alpha^N + \hat{\mathbf{T}}_\alpha^N) - \varepsilon_\alpha \mathbf{t}_\alpha^N \nabla \left(\frac{C_\alpha^j}{C_\alpha^N} \right) \right\}. \end{aligned}$$

We thus obtain the following results which hold at equilibrium:

$$p_l = p_s, \quad (53)$$

$$\hat{\mathbf{T}}_l = p_l \nabla \varepsilon_l - \varepsilon_l \rho_l \frac{\partial A_l}{\partial \mathbf{E}_s} : \nabla \mathbf{E}_s, \quad (54)$$

$$\nabla \cdot \varepsilon_\alpha \rho_\alpha^j \left[\tilde{\mu}_\alpha^j \mathbf{I} - (A_\alpha^j - A_\alpha^N) \mathbf{I} + \left(\frac{1}{\rho_\alpha^j} \mathbf{t}_\alpha^j - \frac{1}{\rho_\alpha^N} \mathbf{t}_\alpha^N \right) \right] = \varepsilon_\alpha \rho_\alpha^j \nabla \tilde{\mu}_\alpha^j, \quad (55)$$

$$\tilde{\mu}_l^j = \tilde{\mu}_s^j, \quad (56)$$

$$\left(\frac{p_l}{\rho_l} + A_l \right) \mathbf{I} - \sum_{j=1}^N C_l^j \mathbf{v}_l^j + \mathbf{v}_l^N = \left(\frac{p_s}{\rho_s} + A_s \right) \mathbf{I} - \sum_{j=1}^N C_s^j \mathbf{v}_s^j + \mathbf{v}_s^N, \quad (57)$$

where we have used the definition of the Lagrange multipliers given in (34) and (35). Further, we used the momentum equation for species, (10), at equilibrium in the derivation of (55), and Equation (44) was used in the derivation of (57). Relation (53) states that at equilibrium, the thermodynamic pressures of the two phases are equal. Relation (56) resembles in form the classical Gibbsian result stating that at equilibrium, the chemical potentials of a single constituent in two phases are equal, although it is not yet in the sharpest form since it is expressed only in terms of the relative chemical potential. Expression (57) gives a relationship between the Gibbs energy and the weighted sum of the chemical potentials. To obtain a more physically intuitive interpretation for (54), begin by eliminating $\hat{\mathbf{T}}_l$

by using the momentum equation for the liquid phase (11), and then eliminate \mathbf{t}_l using (37) to get

$$\nabla p_l - \rho_l \mathbf{g} = -\rho_l \frac{\partial A_l}{\partial \mathbf{E}_s} : \nabla \mathbf{E}_s. \quad (58)$$

This shows that in contrast with a bulk liquid, the vicinal fluid does not satisfy the classical hydrostatic relation $\nabla p_l = \rho_l \mathbf{g}$. This result will be exploited in the next section to obtain a modified form of Darcy's law for the vicinal fluid.

Using (39) to eliminate \mathbf{t}_α^j in (55) yields

$$\nabla \tilde{\mu}_\alpha^j = \nabla(\mu_\alpha^j - \mu_\alpha^N) = \nabla \cdot (\mathbf{v}_\alpha^j - \mathbf{v}_\alpha^N) = 0, \quad (59)$$

where (52) is used for $\tilde{\mu}_\alpha^j$. This resembles the classical Gibbsian result stating that at equilibrium, the chemical potential is constant, but, similar to (56), it is expressed only in terms of the relative chemical potential.

We now use the two definitions of the chemical potential to obtain nonrelative results corresponding to (56) and (59). The non-relative results corresponding to (57) are given by Equations (45) and (48) for the tensorial and scalar definitions, respectively.

Eliminating the stress tensors in (45) using Equations (37) and (38) at equilibrium, and then eliminating $\sum_{j=1}^N C_\alpha^j \mathbf{v}_\alpha^j$ and $\mathbf{v}_l^N - \mathbf{v}_s^N$ using (57) and (56), respectively, gives, in terms of the tensorial chemical potential,

$$\mathbf{v}_l^j - \mathbf{v}_s^j = \frac{1}{\rho_s} \left(\mathbf{t}_e^s + \frac{\varepsilon_l}{\varepsilon_s} \mathbf{t}_s^l \right), \quad j = 1, \dots, N. \quad (60)$$

To get the equivalent expression in terms of the scalar chemical potential subtract (51) from (50) and combine this result with (60). This yields

$$\mu_l^j = \mu_s^j, \quad j = 1, \dots, N, \quad (61)$$

which tells us that the scalar chemical potential satisfies the classical Gibbsian result stating that the chemical potentials of a single species in two phases are equal at equilibrium. In contrast, when the solid phase is stressed, (60) indicates the macroscale tensorial chemical potential does not recover the classical result. This is due to the definition of the *macroscale* tensorial chemical potential, (42), and in no way should this be applied at the microscale. We may interpret the right hand side of (60), the effective and hydration stress tensors, as being an external source. It is nonzero, for example, when an external load is applied to the medium. Also note that if the solid phase is replaced by, e.g., another immiscible fluid we would get, by following the same procedure, equality between the two tensorial chemical potentials.

We now turn to the derivation of the absolute form of (59). This requires the derivation of an extended form of the Gibbs–Duhem relation for the vicinal fluid.

To this end, begin by taking the gradient of the constitutive assumption for A_1 (29). Using the chain rule and the constraint $\sum_{j=1}^N C_1^j = 1$ we get

$$\begin{aligned}\nabla A_1 &= \frac{p_1}{(\rho_1)^2} \nabla \rho_1 + \sum_{j=1}^{N-1} \tilde{\mu}_1^j \nabla C_1^j + \frac{\partial A_1}{\partial \mathbf{E}_s} : \nabla \mathbf{E}_s \\ &= \frac{p_1}{(\rho_1)^2} \nabla \rho_1 + \sum_{j=1}^N \mu_1^j \nabla C_1^j + \frac{\partial A_1}{\partial \mathbf{E}_s} : \nabla \mathbf{E}_s.\end{aligned}\quad (62)$$

By taking the gradient of (48) and setting $\alpha = 1$ we also have

$$\nabla A_1 = \frac{p_1}{(\rho_1)^2} \nabla \rho_1 - \frac{1}{\rho_1} \nabla p_1 + \sum_{j=1}^N (C_1^j \nabla \mu_1^j + \mu_1^j \nabla C_1^j). \quad (63)$$

Eliminating ∇A_1 via (62) and (63) and using equilibrium result (58) yields

$$\sum_{j=1}^N C_1^j \nabla \mu_1^j = \frac{1}{\rho_1} \nabla p_1 + \frac{\partial A_1}{\partial \mathbf{E}_s} : \nabla \mathbf{E}_s = \mathbf{g}, \quad (64)$$

which is the Gibbs–Duhem relation for the vicinal liquid. This relation can be used to obtain a sharper form of the relative result (59). By multiplying the scalar version of (59) by C_1^j and summing over all constituents, we find, by using the above result, that $\nabla \mu_1^N = \mathbf{g}$. Combining this with (61) and (59) gives

$$\nabla \mu_1^j = \nabla \mu_s^j = \mathbf{g}, \quad j = 1, \dots, N. \quad (65)$$

The above result provides a sharper description of equilibrium condition (59) and shows consistency with the classical result of Gibbsian thermodynamics which states that in the absence of gravity, the scalar chemical potential is constant at equilibrium. The corresponding result for the tensorial chemical potential can be easily obtained by combining the above expression, (65), with (50) and (51):

$$\nabla \cdot \nu_1^j = \mathbf{g}, \quad \nabla \cdot \nu_s^j = \mathbf{g} - \nabla \cdot \left[\frac{1}{\rho_s} \left(\mathbf{t}_s^e + \frac{\varepsilon_1}{\varepsilon_s} \mathbf{t}_s^l \right) \right], \quad (66)$$

which confirms that in the absence of gravity, Bowen's tensorial chemical potential for the solid phase is not constant at equilibrium.

By incorporating the effective and hydration stress tensors into the definition of the scalar chemical potential in the solid phase (47), we have in some sense incorporated an 'external' source. Physically, both μ_α^j and $(1/3)\text{tr}(\nu_\alpha^j)$ may be interpreted as the amount of chemical energy required to place a particle into the system. But we must keep in mind the slight difference between them, that is that the scalar definition incorporates the amount of energy associated with $\text{tr}(\mathbf{t}_s^e) + (\varepsilon_1/\varepsilon_s)\text{tr}(\mathbf{t}_s^l)$. When viewing the hydration and effective stresses as a source

term, we see that the scalar chemical potential is analogous to the well-known ‘gravi-chemical potential’ of classical thermodynamics whose definition incorporates the energy due to gravity. In Section 8, we shall illustrate this analogy with some examples.

6. Near-Equilibrium Theory

To derive near-equilibrium results, the coefficients of $D_s \varepsilon_l / Dt$, \mathbf{u}_α^j , $\mathbf{v}_{l,s}$, \hat{e}_α^j , \hat{e}_α in entropy inequality (33) are linearized about the above variables since they vanish at equilibrium. Strictly speaking the coefficients should be linearized about all variables of the above set [2, 39]. However, here we pursue the approach of [14] and choose to linearize only about the one variable which gives a positive quadratic form in the entropy inequality. So for example, if z is a variable which vanishes at equilibrium and f is the coefficient of z within the entropy inequality, the linearization procedure gives an approximation for the near-equilibrium value of f as,

$$f_{\text{neq}} \approx f_{\text{eq}} + Cz, \quad (67)$$

where C is the linearization constant. Using this procedure for the coefficients of $D_s \varepsilon_l / Dt$, $\mathbf{v}_{l,s}$, and \hat{e}_α^j , we have

$$p_l - p_s = \mu_* \frac{D_s \varepsilon_l}{Dt}, \quad (68)$$

$$p_l \nabla \varepsilon_l - \varepsilon_l \rho_l \frac{\partial A_l}{\partial \mathbf{E}_s} : \nabla \mathbf{E}_s - \hat{\mathbf{T}}_l = R_l \mathbf{v}_{l,s}, \quad (69)$$

$$\tilde{\mu}_l^j - \tilde{\mu}_s^j = K^j \hat{e}_\alpha^j \quad j = 1, \dots, N-1, \quad (70)$$

where μ_* , R_l , R_α^j and K^j are material coefficients which may be a function of the independent variables which are not necessarily zero at equilibrium.

The above relations are nice in some sense because the term f_{eq} is zero. This is not true of the coefficient for \mathbf{u}_α^j , so for this case it is necessary to do some further manipulations. Consider the term involving \mathbf{u}_α^j in entropy inequality (33). Eliminating the Lagrange multipliers using (35) and (43), and adding $\sum_{j=1}^N \mathbf{u}_\alpha^j [\rho_\alpha^j \mathbf{v}_\alpha^N \nabla \varepsilon_\alpha]$, which is zero by constraint (3), we have

$$\begin{aligned} & \sum_{\alpha=l,s} \sum_{j=1}^N \mathbf{u}_\alpha^j \cdot [\mathbf{v}_\alpha^j \nabla (\varepsilon_\alpha \rho_\alpha^j) - \mathbf{v}_\alpha^N \nabla (\varepsilon_\alpha \rho_\alpha^j) - \nabla (\varepsilon_\alpha \rho_\alpha^j A_\alpha^j) - (\hat{\mathbf{i}}_\alpha^j + \hat{\mathbf{T}}_\alpha^j) + \\ & \quad + \varepsilon_\alpha \mathbf{v}_\alpha^N \nabla \rho_\alpha^j + \rho_\alpha^j \mathbf{v}_\alpha^N \cdot \nabla \varepsilon_\alpha] \\ &= \sum_{\alpha=l,s} \sum_{j=1}^N \mathbf{u}_\alpha^j \cdot [\mathbf{v}_\alpha^j \nabla (\varepsilon_\alpha \rho_\alpha^j) - \nabla (\varepsilon_\alpha \rho_\alpha^j A_\alpha^j) - (\hat{\mathbf{i}}_\alpha^j + \hat{\mathbf{T}}_\alpha^j)]. \end{aligned}$$

Linearizing this term about equilibrium using (67) and eliminating $\widehat{\mathbf{i}}_\alpha^j + \widehat{\mathbf{T}}_\alpha^j$ using momentum Equation (10) we have

$$\begin{aligned} & [\mathbf{v}_\alpha^j \nabla (\varepsilon_\alpha \rho_\alpha^j) - \nabla (\varepsilon_\alpha \rho_\alpha^j A_\alpha^j) + \nabla \cdot (\varepsilon_\alpha \mathbf{t}_\alpha^j) + \varepsilon_\alpha \rho_\alpha^j \mathbf{g}]_{\text{neq}} \\ & = [\mathbf{v}_\alpha^j \nabla (\varepsilon_\alpha \rho_\alpha^j) - \nabla (\varepsilon_\alpha \rho_\alpha^j A_\alpha^j) + \nabla \cdot (\varepsilon_\alpha \mathbf{t}_\alpha^j) + \varepsilon_\alpha \rho_\alpha^j \mathbf{g}]_{\text{eq}} + \mathbf{R}_\alpha^j \mathbf{u}_\alpha^j, \end{aligned}$$

where \mathbf{R}_α^j is the linearization constant which in general is a second order tensor and where we have assumed the inertial term in the momentum equation is negligible near equilibrium. Using (42) to rewrite this expression in terms of the tensorial chemical potential yields

$$(-\varepsilon_\alpha \rho_\alpha^j \nabla \cdot \mathbf{v}_\alpha^j + \varepsilon_\alpha \rho_\alpha^j \mathbf{g})_{\text{neq}} = (-\varepsilon_\alpha \rho_\alpha^j \nabla \cdot \mathbf{v}_\alpha^j + \varepsilon_\alpha \rho_\alpha^j \mathbf{g})_{\text{eq}} + \mathbf{R}_\alpha^j \mathbf{u}_\alpha^j.$$

At equilibrium we can use (66) so that we obtain generalized Fick's laws,

$$\begin{aligned} R_1^j \mathbf{u}_1^j &= -\varepsilon_l \rho_l^j (\nabla \cdot \mathbf{v}_1^j - \mathbf{g}), \\ R_s^j \mathbf{u}_s^j &= -\varepsilon_s \rho_s^j (\nabla \cdot \mathbf{v}_s^j - \mathbf{g}) - \varepsilon_s C_s^j \nabla \cdot \left(\mathbf{t}_s^e + \frac{\varepsilon_l}{\varepsilon_s} \mathbf{t}_s^l \right), \quad j = 1, \dots, N. \\ R_\alpha^j \mathbf{u}_\alpha^j &= -\varepsilon_\alpha \rho_\alpha^j (\nabla \mu_\alpha^j - \mathbf{g}), \quad j = 1, \dots, N, \quad \alpha = l, s, \end{aligned}$$

that is a form of Fick's law which is identical in form to the statistical thermodynamical result [80]. Note that this is a much sharper result than what has been previously obtained, (1). The coefficients R_α^j must be such that the constraint on the diffusive velocities, (19), is satisfied. This extends to swelling media the results of [14] where a macroscopic form of Fick's law involving the absolute chemical potential gradient was derived for granular media. The above results are consistent with equilibrium relations (65) and (66) and in particular, indicate that stressing the solid phase affects the diffusive velocity of solid constituents.

Equation (68) tells us that near equilibrium, the thermodynamic pressure of the vicinal fluid and solid phases are not necessarily equal, especially for colloidal systems. The coefficient μ_* may be thought of as a retardation factor which among other effects, accounts for the re-ordering of the water molecules as they are disturbed, that is an entropic effect. If this is the only source of retardation, then it follows that for a granular media, $\mu_* \approx 0$, since there is very little ordering of the liquid phase in such a medium. We remark that an equation identical to (68) with $p_s = 0$ was heuristically derived and used in polymer physics [75] and in the mechanics of thin films [49]. In this latter reference the authors discuss the appearance of a viscous disjoining pressure component due to the excess in viscosity of the thin liquid film relative to the bulk phase [66]. Furthermore, using (68) in expressions (38) and (40) for \mathbf{t}_s and \mathbf{t} , respectively, we obtain the near-equilibrium

relations,

$$\begin{aligned}\mathbf{t}_s &= \left(-p_l + \mu_* \frac{D_s \varepsilon_l}{Dt} \right) \mathbf{I} + \mathbf{t}_s^e + \frac{\varepsilon_l}{\varepsilon_s} \mathbf{t}_s^l - \sum_{j=1}^N \rho_s^j \mathbf{u}_s^j \otimes \mathbf{u}_s^j, \\ \mathbf{t} &= \left(-p_l + \varepsilon_s \mu_* \frac{D_s \varepsilon_l}{Dt} \right) \mathbf{I} + \varepsilon_s \mathbf{t}_s^e + \varepsilon_l \mathbf{t}_s^l - \sum_{\alpha=l,s} \sum_{j=1}^N \varepsilon_\alpha \rho_\alpha^j \mathbf{u}_\alpha^j \otimes \mathbf{u}_\alpha^j.\end{aligned}$$

The above result can be viewed as a near-equilibrium modified Terzaghi principle, which in our notation can be stated as $\mathbf{t} = -p_l \mathbf{I} + \varepsilon_s \mathbf{t}_s^e$. Note that though the solid is considered elastic, the appearance of the retardation factor in (68) leads to a viscoelastic behavior for the volumetric stresses.

By neglecting inertial effects and using analogous arguments to those which gave rise to the vicinal fluid hydrostatic relation (58), Equation (69) leads to the modified Darcy's law

$$\frac{1}{\varepsilon_l} R_l \mathbf{v}_{l,s} = -\nabla p_l - \rho_l \frac{\partial A_l}{\partial \mathbf{E}_s} : \nabla \mathbf{E}_s + \rho_l \mathbf{g}.$$

In addition to a pressure gradient, the above form of Darcy's law contains a gradient of a generalized interaction potential which accounts for flow of vicinal water induced by the deformation of the clay particle. The appearance of this additional term indicates that strain gradients provide a potential for vicinal water flow in a swelling medium. If vicinal water flow due to particle shearing is neglected, then this interaction potential reduces to $(\rho_l \partial A_l / \partial \varepsilon_l) \nabla \varepsilon_l$, as was shown in [2, 64] by positing $A_l = A_l(T, \rho_l, \varepsilon_l, C_l^j)$ rather than the constitutive dependency of (29). We also remark that an extended form of Darcy's law for multiphase flows which incorporates an interaction potential was first derived within the current framework for nonswelling, granular systems in [43, 45].

Equation (70) governs the near-equilibrium adsorption/desorption of the j th component by the solid phase. The coefficient K^j may be identified with the kinetic constant of linear chemical adsorption [60]. Since it is expressed in terms of the relative chemical potentials, we turn to the task of sharpening it. To this end, we begin by rewriting the \widehat{e}_l^j term of entropy inequality (33). Neglecting higher order terms near equilibrium (i. e. Δ^2) we have

$$\sum_{j=1}^N \widehat{e}_l^j (-\tilde{\mu}_l^j + \tilde{\mu}_s^j) = \sum_{j=1}^N \widehat{e}_l^j (-\mu_l^j + \mu_s^j) - \sum_{j=1}^N \widehat{e}_l^j (-\mu_l^N + \mu_s^N).$$

Note that by using (61), we can show that each coefficient (given in parenthesis) is zero at equilibrium. The last coefficient is independent of j , so it will contribute to the coefficient of \widehat{e}_l in the entropy inequality (recall that $\sum_{j=1}^N \widehat{e}_l^j = \widehat{e}_l$). Linearizing the remaining coefficient using Equation (67) yields

$$K^j \widehat{e}_l^j = \mu_s^j - \mu_l^j, \quad j = 1, \dots, N,$$

which is the absolute form of the near-equilibrium adsorption/desorption relation in terms of the scalar chemical potential. Again using (50) and (51) to express the adsorption law in terms of the tensorial chemical potential we obtain

$$K_l^j \hat{e}_l^j \mathbf{I} = \mathbf{v}_s^j - \mathbf{v}_l^j + \frac{1}{\rho_s} \left(\mathbf{t}_s^e + \frac{\varepsilon_l}{\varepsilon_s} \mathbf{t}_s^l \right), \quad j = 1, \dots, N,$$

which again emphasizes the recurring theme that replacing the scalar chemical potential by the tensorial chemical potential yields an additional source term due to \mathbf{t}_s^e and \mathbf{t}_s^l . This result indicates a stressed solid matrix affects the adsorption rate of the constituents.

7. Comparing the Chemical Potentials for Selected Examples

Our goal in this section is to compare the scalar and tensorial chemical potentials in selected one-dimensional examples. In doing so we provide a better physical feel for the two potentials. In this section we assume there is no net exchange of mass between the liquid and solid phases, and that the solid phase is incompressible so that $D_s \rho_s / D t = 0$.

We begin with Equation (51) which relates the solid phase scalar and tensorial chemical potentials:

$$\mu_s^j \mathbf{I} = \mathbf{v}_s^j + \frac{1}{\rho_s} (\mathbf{t}_s^e + \frac{\varepsilon_l}{\varepsilon_s} \mathbf{t}_s^l). \quad (71)$$

To compare the two quantities at equilibrium, we define their scalar difference

$$\Delta \mu_s^j \equiv \frac{1}{3} \text{tr} \mathbf{v}_s^j - \mu_s^j. \quad (72)$$

Using (71) in (72) gives

$$\Delta \mu_s^j = -\frac{1}{3} \frac{1}{\rho_s} \left(\text{tr} \mathbf{t}_s^e + \frac{\varepsilon_l}{\varepsilon_s} \text{tr} \mathbf{t}_s^l \right),$$

which, when using the definitions of \mathbf{t}_s^e (31), \mathbf{t}_s^l (31), and \mathbf{E}_s (28) yields

$$\begin{aligned} \Delta \mu_s^j &= -\frac{1}{3} \frac{\partial A_s}{\partial \mathbf{E}_s} : \mathbf{C}_s - \frac{1}{3} \frac{\varepsilon_l \rho_l}{\varepsilon_s \rho_s} \frac{\partial A_l}{\partial \mathbf{E}_s} : \mathbf{C}_s \\ &= -\frac{2}{3} \frac{\partial A_s}{\partial \mathbf{C}_s} : \mathbf{C}_s - \frac{2}{3} \frac{\varepsilon_l \rho_l}{\varepsilon_s \rho_s} \frac{\partial A_l}{\partial \mathbf{C}_s} : \mathbf{C}_s, \end{aligned} \quad (73)$$

where $\mathbf{C}_s = \mathbf{F}_s^T \mathbf{F}_s$.

Next we rewrite the above expression for the case in which we assume the free energies are independent of the shearing components (or deviatoric part) of \mathbf{E}_s , i.e., for the one-dimensional problem in which the free energy, A_α , depends on the volume change of the solid phase. Let $J_s = \det \mathbf{F}_s$ be the Jacobian of the solid

phase motion, which represents the volumetric change in the solid phase [33]. For an incompressible solid, the macroscopic volumetric deformation of the matrix is governed by changes in the volume fraction. Therefore, if we denote the volume fraction of the reference configuration by $\bar{\varepsilon}_s = \bar{\varepsilon}_s(\mathbf{X}_s)$, we have

$$J_s \varepsilon_s = \bar{\varepsilon}_s. \quad (74)$$

Using the identity $(\partial J_s^2 / \partial \mathbf{C}_s) : \mathbf{C}_s = 3J_s^2$ [33], and using (74) leads to

$$\begin{aligned} \frac{2}{3} \frac{\partial A_\alpha}{\partial \mathbf{C}_s} : \mathbf{C}_s &= \frac{2}{3} \frac{\partial A_\alpha}{\partial J_s^2} \frac{\partial J_s^2}{\partial \mathbf{C}_s} : \mathbf{C}_s = 2J_s^2 \frac{\partial A_\alpha}{\partial J_s^2} = 2J_s^2 \frac{\partial A_\alpha}{\partial \varepsilon_s} \frac{\partial \varepsilon_s}{\partial J_s^2} \\ &= -\frac{\bar{\varepsilon}_s}{J_s} \frac{\partial A_\alpha}{\partial \varepsilon_s} = \varepsilon_s \frac{\partial A_\alpha}{\partial \varepsilon_l}. \end{aligned}$$

Combining the above result with (73) gives

$$\Delta \mu_s^j = -\varepsilon_s \frac{\partial A_s}{\partial \varepsilon_l} - \frac{\varepsilon_l \rho_l}{\rho_s} \frac{\partial A_l}{\partial \varepsilon_l}, \quad (75)$$

which is a simplified one-dimensional relationship between the tensorial and scalar chemical potentials. The terms on the right-hand side of (75) represent the one-dimensional version of the effective stress tensor and the hydration stress tensor, respectively.

To illustrate the effects of the effective and hydration stress components on $\Delta \mu_s^j$, we consider the consolidation of nonswelling and swelling media in two one-dimensional examples. But before proceeding to these examples, we consider a classical static fluids example with the purpose of setting up an analogy between our scalar tensorial chemical potentials and the gravitational classical chemical potentials.

Example 1: Classical Static Fluid Column Problem.

Consider a static column filled with an incompressible fluid (see Figure 1(a)). In this example, we assume the fluid is composed of a single constituent so that its classical (scalar) chemical potential is equal to the Gibbs free energy of the fluid, G_l . We denote the potential function due to both chemical energy and gravity as the gravi-chemical potential G_l^g and define it in terms of G_l to be

$$G_l^g \equiv G_l - \psi, \quad (76)$$

where ψ is the gravitational potential, i.e. $\nabla \psi = \mathbf{g}$. The gravitational potential in (76) plays the same role as the effective and hydration stresses in (75). Orienting the coordinate system as depicted in Figure 1(a), we set $\mathbf{g} = g \mathbf{i}_z$, where \mathbf{i}_z is the unit vector along the z -axis. Hence $\psi = gz$, where we have set $\psi = 0$ at $z = 0$ (i.e. the gravi-chemical and chemical potentials are identical at the top of the column). Thus,

$$G_l - G_l^g = gz. \quad (77)$$

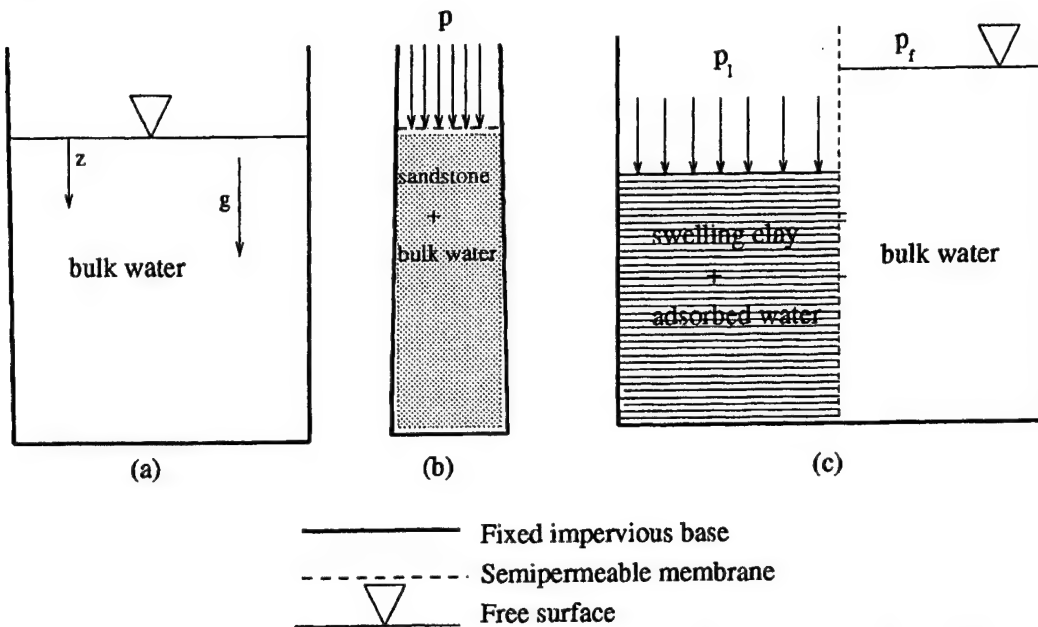


Figure 1. One-dimensional examples: (a) classical static fluid column, (b) Terzaghi's consolidation column example with components, (c) Low's swelling pressure experiment with components.

Also, since the single constituent fluid is incompressible, (62) reduces to $\nabla A_1 = 0$. Thus, taking the gradient in (48) and using equilibrium expression (64) yields

$$\nabla G_1 = \frac{1}{\rho_1} \nabla p_1 = g,$$

so that when combined with (77) we obtain

$$\nabla G_1^g = \mathbf{0}. \quad (78)$$

Results (77) and (78) show that G_1^g is constant throughout the length of the column while G_1 must increase linearly as z increases. Consequently, the chemical energy required to place a particle in the bottom of the column is greater than the chemical energy required at the top due to the gravitational potential.

We have thus illustrated an analogy between gravity, which acts as an external source when using the classical Gibbs free energy, G_1 , and the effective and hydration stresses which act as an external source when using the tensorial chemical potentials. Keeping these results in mind, we consider the role of effective and hydration stress tensors on $\Delta\mu_s^j$.

Example 2: Terzaghi's Consolidation Problem

To illustrate the influence of the effective stress tensor on $\Delta\mu_s^j$, we consider Terzaghi's one-dimensional consolidation problem for a nonswelling elastic medium as described in [74]. In our formulation, these results can be easily reproduced by setting $t_s^l = 0$. As depicted in Figure 1(b), a porous elastic column is bounded

on the sides and bottom by a rigid, adiabatic, impermeable wall. At the top, a load is applied and the bulk water is free to drain. We consider the equilibrium configuration and assume each phase contains N miscible components. By neglecting the dependency of A_1 on ε_1 in (75) we have

$$\Delta\mu_s^j = -\varepsilon_s \frac{\partial A_s}{\partial \varepsilon_1}. \quad (79)$$

We assume the porous medium is linearly elastic and neglect gravitational effects. If the system under consideration is initially free of stress with a constant volume fraction $\bar{\varepsilon}_1$, then we can assume the following quadratic form for A_s [33]:

$$A_s = \frac{1}{2}C(\varepsilon_1 - \bar{\varepsilon}_1)^2,$$

where C is a constant representing the compressibility of the solid matrix. Using (79) we then have

$$\Delta\mu_s^j \equiv \frac{1}{3}\text{tr } \mathbf{v}_s^j - \mu_s^j = -C\varepsilon_s(\varepsilon_1 - \bar{\varepsilon}_1) \approx -\bar{C}(\varepsilon_1 - \bar{\varepsilon}_1), \quad (80)$$

where we have linearized the above expression about equilibrium ($\varepsilon_1 = \bar{\varepsilon}_1$) so that $\bar{C} = \bar{\varepsilon}_s C$. In addition, we can derive the linear relationship between the effective pressure (p_s^e) and volume fraction

$$p_s^e \equiv -\frac{1}{3}\text{tr } \mathbf{t}_s^e = -\varepsilon_s \rho_s \frac{\partial A_s}{\partial \varepsilon_1} = -\bar{C} \rho_s (\varepsilon_1 - \bar{\varepsilon}_1)$$

which is similar in form to the one heuristically proposed by Terzaghi. Equation (80) can be interpreted physically in a manner similar to the previous example. As the overburden pressure is increased, ε_1 decreases, and since μ_s^j is constant at equilibrium (see Equation (65)), then $\text{tr } \mathbf{v}_s^j$ increases. Hence, the chemical energy required to insert a solid particle into the compressed system is greater than at the unstressed (initial) state.

Example 3: Swelling Pressure Experiment.

To illustrate the influence of the hydration stress tensor, \mathbf{t}_s^l , on $\Delta\mu_s^j$ we consider the classical reverse osmosis swelling pressure experiment of Low [56] or Achanta *et al.* [2]. As depicted in Figure 1 (c), a saturated mixture of montmorillonite clay and adsorbed (incompressible) fluid is separated from a bulk (nonadsorbed) fluid by a semi-permeable membrane which only allows fluid to pass. An overburden pressure is applied to the clay mixture and the shrinkage due to the loss of fluid is recorded. As in the previous example, gravity is assumed negligible and each phase is assumed to be composed of the same N miscible components where the concentrations of some of these components within a phase may be zero. It is assumed the clay mineral consists of flat plates and the clay medium is such

that the flat plates are parallel so that the effective stress tensor, \mathbf{t}_s^e , is negligible. Consequently, Equation (75) reduces to

$$\Delta\mu_s^j = -\frac{\varepsilon_l\rho_l}{\rho_s} \frac{\partial A_l}{\partial \varepsilon_l}. \quad (81)$$

Next, following Achanta *et al.* [2], we will show that, in contrast with the previous example, $\Delta\mu_s^j$ appears inversely proportional to the volume fraction, ε_l . Begin by assuming the macroscopic solid phase stress tensor in the clay mixture is negligible ($\mathbf{t}_s = 0$) so that all the overburden pressure is supported by the adsorbed liquid (recall that the total stress is given by $\varepsilon_s \mathbf{t}_s + \varepsilon_l \mathbf{t}_l$). Since we have already assumed \mathbf{t}_s^e is negligible, the equation for the solid phase stress tensor (38) reduces to

$$p_l \mathbf{I} = \frac{\varepsilon_l}{\varepsilon_s} \mathbf{t}_s^l, \quad (82)$$

where we have used the equilibrium condition $p_s = p_l$ (Equation (53)). This tells us that the pressure in the adsorbed fluid is balanced by the hydration forces (otherwise all the fluid would pass through the membrane with minimal applied pressure). Taking the trace of (82), using definition (31) and using the same reasoning as in Equations (73)–(75), we have for the one-dimensional case,

$$p_l = \frac{1}{3} \frac{\varepsilon_l}{\varepsilon_s} \text{tr}(\mathbf{t}_s^l) = \varepsilon_l \rho_l \frac{\partial A_l}{\partial \varepsilon_l}. \quad (83)$$

Moreover, by design we have that the concentrations of all constituents are constant. Since the scalar chemical potentials of the liquid phase are constant at equilibrium (Equation (65)) we have that the Gibb's free energy is also constant by (48), i.e.,

$$G_l = A_l + \frac{1}{\rho_l} p_l = \text{const.}$$

Hence, since adsorbed water was assumed incompressible

$$\frac{\partial A_l}{\partial \varepsilon_l} = -\frac{1}{\rho_l} \frac{\partial p_l}{\partial \varepsilon_l}$$

or when combining with (83)

$$p_l = -\varepsilon_l \frac{\partial p_l}{\partial \varepsilon_l}. \quad (84)$$

Upon integrating and using the condition that when $\varepsilon_l = 1$, the pressure in the adsorbed fluid, p_l , is equal to the bulk fluid pressure, p_f , we get

$$p_l = \frac{p_f}{\varepsilon_l}. \quad (85)$$

Combining (83) and (81) and eliminating p_l using (85) gives

$$\frac{1}{3} \operatorname{tr} \nu_s^j - \mu_s^j = \Delta\mu_s^j = -\frac{p_l}{\rho_s} = -\frac{p_f}{\varepsilon_l \rho_s}. \quad (86)$$

We note that $\Delta\mu_s^j$ is never zero due to the assumption that there is always some hydration force between the adsorbed liquid and solid phase. We conclude, contrary to the Terzaghi problem, that increasing the overburden pressure, which causes ε_l to decrease, results in a decrease in the magnitude of the $\operatorname{tr} \nu_s^j$. Hence it is easier to insert a solid particle into a compressed swelling media. This can be physically attributed to the stronger adsorption forces in the compressed system due to the closer proximity of the liquid and solid phases.

As was done in [2], we can rewrite the above result in terms of the separation of platelets, λ . Denote the thickness of a clay platelet by λ_s , so that the volume fraction can be expressed as

$$\varepsilon_l = \frac{\lambda}{\lambda + \lambda_s}. \quad (87)$$

Using (87), we can express (84) in terms of the separation between platelets as

$$\left(\frac{\lambda^2}{\lambda_s} + \lambda \right) \frac{\partial p_l}{\partial \lambda} = -p_l.$$

At high moisture contents, $\lambda \ll \lambda^2/\lambda_s$ and hence after integrating we obtain

$$p_l = p_f \exp(\lambda_s/\lambda),$$

where the thickness of the solid platelets, λ_s , is assumed constant. This result is identical to the swelling pressure result obtained empirically by Low [56]. Thus, by rewriting the dependency of $\Delta\mu_s^j$ in (86) in terms of λ gives the alternative expression

$$\Delta\mu_s^j = -\frac{p_f}{\rho_s} \exp(\lambda_s/\lambda).$$

8. Conclusions

Within the framework of hybrid mixture theory for multicomponent single-phase flow in a colloidal porous medium, we have introduced a novel definition of the macroscale chemical potential. Unlike Bowen's tensorial chemical potential, this new chemical potential is a scalar which satisfies three properties consistent with the classical Gibbsian chemical potential for a single phase medium: (1) it is a scalar; (2) at equilibrium, the chemical potential of a single constituent in different phases is the same; and (3) the chemical potential is the driving force for diffusive flow (generalized Fick's law). After defining this chemical potential, the aforementioned properties were derived by exploiting the entropy inequality and using a

generalized Gibbs–Duhem relation. Of particular note is that we used a Lagrange multiplier to enforce the gradient of the relationship between the diffusive velocities (3). Further, near-equilibrium results were obtained by linearizing coefficients which were not necessarily zero at equilibrium. This is an extension to what has been traditionally done [1, 45] where coefficients of constitutive variables such as $D_s \varepsilon_1 / Dt$ and \bar{e}^l are linearized about equilibrium. Here we have linearized about variables which are not constitutive, but are explicitly related to other independent variables, e.g., \mathbf{u}_α^N . In fact, one can linearize the coefficient of any variable (independent, constitutive, or directly dependent), using Equation (67); however, it may not be trivial to determine the coefficient at equilibrium. It should be noted that this philosophy cannot be applied when deriving nonequilibrium or equilibrium results, as the argument requires the entropy inequality to be expressed as linear combinations of variables which are independent.

From the entropy inequality, we rederived in a unified manner macroscopic constitutive results which captured the physics of swelling particles. Principle results include:

- (1) A modified effective stress principle for swelling porous media which incorporates an additional stress component (t_s^l) accounting for hydration stresses of physico-chemical nature.
- (2) A modified form of Darcy's law governing the flow of vicinal water which involves an additional interaction potential gradient accounting for the adsorptive character of the clay platelets.
- (3) The appearance of a retardation viscosity coefficient (μ_*) as a natural consequence of the topological law [18] used to close the system. Among other effects this coefficient led to a viscoelastic behavior for the volumetric stresses even though the solid is considered a priori to be elastic. The coefficient may provide an important rational basis for the rheology of polymers and thin films as it may account for the re-ordering of the vicinal water molecules as they are disturbed. In contrast, for a granular media there is very little ordering of the bulk liquid phase and consequently, we may expect very little viscous behavior in such a medium due to this mechanism.
- (4) Improved forms of Fick's law and the adsorption/desorption relationship between phases, which are not dependent upon the labeling of the constituents.

9. Appendix A. Definition of Macroscopic Bulk Variables

The following formulas are the relationships between the microscale and macro-scale (continuum scale) variables. In previous papers [9, 11, 12, 40], the relationships are derived assuming small perturbations so that $\overline{\psi^\alpha} = \bar{\psi}^\alpha$ and $\overline{\psi - \bar{\psi}^\alpha} = 0$. Here we have made no such assumptions.

$$\overline{\rho^j}^\alpha(\mathbf{x}, t) \equiv \frac{1}{|\delta V_\alpha|} \int_{\delta V} \rho^j(\mathbf{r}, t) \gamma_\alpha(\mathbf{r}, t) d\nu(\xi) \quad (\text{average mass over } \delta V_\alpha)$$

$$\langle \psi^j \rangle^\alpha(\mathbf{x}, t) \equiv \frac{1}{|\delta V_\alpha|} \int_{\delta V} \psi^j(\mathbf{r}, t) \gamma_\alpha(\mathbf{r}, t) d\nu(\xi) \quad (\text{volume average of property } \psi^j)$$

$$\overline{\psi^j}^\alpha(\mathbf{x}, t) \equiv \frac{1}{\overline{\rho^j}^\alpha |\delta V_\alpha|} \int_{\delta V} \rho^j(\mathbf{r}, t) \psi^j(\mathbf{r}, t) \gamma_\alpha(\mathbf{r}, t) d\nu(\xi) \quad (\text{mass average of property } \psi^j).$$

A few notes regarding the notation follow. In surface integrals, the unit normal outward vector \mathbf{n}_α indicates the surface integral should be evaluated in the limit as the $\alpha\beta$ -interface is approached from the α -side. A $\widehat{}$ above the variable is used to emphasize that the quantity represents a transfer from the other phase or from other constituents.

$$\rho_\alpha^j \equiv \overline{\rho^j}^\alpha, \quad (88)$$

$$C_\alpha^j \equiv \frac{\rho_\alpha^j}{\rho_\alpha}, \quad (89)$$

$$\varepsilon_\alpha \equiv \frac{|\delta V_\alpha|}{|\delta V|}, \quad (90)$$

$$\mathbf{v}_\alpha^j \equiv \overline{\mathbf{v}^j}^\alpha, \quad (91)$$

$$\widehat{e}_\alpha^j \equiv \frac{1}{|\delta V|} \int_{\delta A_{\alpha\beta}} \rho^j (\mathbf{w}_{\alpha\beta}^j - \mathbf{v}^j) \cdot \mathbf{n}_\alpha da, \quad (92)$$

$$\widehat{r}_\alpha^j \equiv \varepsilon_\alpha \rho_\alpha^j \overline{\widehat{r}^j}^\alpha, \quad (93)$$

$$\mathbf{t}_\alpha^j \equiv \langle \mathbf{t}^j \rangle^\alpha + \rho_\alpha^j \mathbf{v}_\alpha^j \mathbf{v}_\alpha^j - \rho_\alpha^j \overline{\mathbf{v}^j \mathbf{v}^j}^\alpha, \quad (94)$$

$$\mathbf{g} \equiv \overline{\mathbf{g}}^\alpha, \quad (95)$$

$$\begin{aligned} \widehat{\mathbf{T}}_\alpha^j &\equiv \frac{1}{|\delta V|} \int_{\delta A_{\alpha\beta}} (\mathbf{t}^j + \rho^j \mathbf{v}^j (\mathbf{w}_{\alpha\beta}^j - \mathbf{v}^j)) \cdot \mathbf{n}_\alpha da - \\ &\quad - \frac{\mathbf{v}_\alpha^j}{|\delta V|} \int_{\delta A_{\alpha\beta}} \rho^j (\mathbf{w}_{\alpha\beta}^j - \mathbf{v}^j) \cdot \mathbf{n}_\alpha da, \end{aligned} \quad (96)$$

$$\widehat{\mathbf{i}}_\alpha^j \equiv \varepsilon_\alpha \rho_\alpha^j (\overline{\widehat{\mathbf{i}}^j}^\alpha + \overline{\widehat{r}^j \mathbf{v}^j}^\alpha - \widehat{r}_\alpha^j \mathbf{v}_\alpha^j), \quad (97)$$

$$E_\alpha^j \equiv \overline{E^j}^\alpha + \frac{1}{2} \overline{\mathbf{v}^j \cdot \mathbf{v}^j}^\alpha - \frac{1}{2} \mathbf{v}_\alpha^j \cdot \mathbf{v}_\alpha^j, \quad (98)$$

$$\begin{aligned} \mathbf{q}_\alpha^j &\equiv \langle \mathbf{q}^j \rangle^\alpha + \langle \mathbf{t}^j \mathbf{v}^j \rangle^\alpha - \mathbf{t}_\alpha^j \mathbf{v}_\alpha^j + \\ &\quad + \rho_\alpha^j \mathbf{v}_\alpha^j \overline{(E^j + \frac{1}{2} \mathbf{v}^j \cdot \mathbf{v}^j)}^\alpha - \rho_\alpha^j \overline{\mathbf{v}^j (E^j + \frac{1}{2} \mathbf{v}^j \cdot \mathbf{v}^j)}^\alpha, \end{aligned} \quad (99)$$

$$h_\alpha^j \equiv \overline{h^j}^\alpha + \overline{\mathbf{g}^j \cdot \mathbf{v}^j}^\alpha - \mathbf{g}_\alpha^j \cdot \mathbf{v}_\alpha^j, \quad (100)$$

$$\begin{aligned} \widehat{Q}_\alpha^j &\equiv \frac{1}{|\delta V|} \int_{\delta A_{\alpha\beta}} \left(\mathbf{q}^j + \mathbf{t}^j \mathbf{v}^j + (E^j + \frac{1}{2} \mathbf{v}^j \cdot \mathbf{v}^j) \rho_\alpha^j (\mathbf{w}_{\alpha\beta}^j - \mathbf{v}^j) \right) \cdot \mathbf{n}_\alpha \, da - \\ &\quad - \frac{\mathbf{v}_\alpha^j}{|\delta V|} \cdot \int_{\delta A_{\alpha\beta}} \left(\mathbf{t}^j + \rho^j \mathbf{v}^j (\mathbf{w}_{\alpha\beta}^j - \mathbf{v}^j) \right) \cdot \mathbf{n}_\alpha \, da - \\ &\quad - \left(\frac{\overline{E^j + \frac{1}{2} \mathbf{v}^j \cdot \mathbf{v}^j}^\alpha - \mathbf{v}_\alpha^j \cdot \mathbf{v}_\alpha^j}{|\delta V|} \right) \int_{\delta A_{\alpha\beta}} \rho^j (\mathbf{w}_{\alpha\beta}^j - \mathbf{v}^j) \cdot \mathbf{n}_\alpha \, da - \\ &\quad - \frac{\mathbf{v}_\alpha^j}{|\delta V|} \int_{\delta A_{\alpha\beta}} \rho^j \mathbf{v}^j (\mathbf{w}_{\alpha\beta}^j - \mathbf{v}^j) \cdot \mathbf{n}_\alpha \, da, \end{aligned} \quad (101)$$

$$\begin{aligned} \widehat{E}_\alpha^j &\equiv \varepsilon_\alpha \rho_\alpha^j \left(\overline{\widehat{E}^j}^\alpha + \overline{\widehat{\mathbf{i}}^j \cdot \mathbf{v}^j}^\alpha - \widehat{\mathbf{i}}_\alpha^j \cdot \mathbf{v}_\alpha^j + \right. \\ &\quad \left. + \overline{(E^j + \frac{1}{2} \mathbf{v}^j \cdot \mathbf{v}^j) \widehat{r}^j}^\alpha - \overline{(E^j + \frac{1}{2} \mathbf{v}^j \cdot \mathbf{v}^j)}^\alpha \widehat{r}_\alpha^j \right), \end{aligned} \quad (102)$$

$$\eta_\alpha^j \equiv \overline{\eta^j}^\alpha, \quad (103)$$

$$\phi_\alpha^j \equiv \langle \phi^j \rangle^\alpha + \rho_\alpha^j \mathbf{v}_\alpha^j \eta_\alpha^j - \rho_\alpha^j \overline{\mathbf{v}^j \eta^j}^\alpha, \quad (104)$$

$$b_\alpha^j \equiv \overline{b^j}^\alpha, \quad (105)$$

$$\begin{aligned} \widehat{\Phi}_\alpha^j &\equiv \frac{1}{|\delta V|} \int_{\delta A_{\alpha\beta}} (\boldsymbol{\phi}^j + \rho^j \eta^j (\mathbf{w}_{\alpha\beta}^j - \mathbf{v}^j)) \cdot \mathbf{n}_\alpha \, da - \\ &\quad - \frac{\eta_\alpha^j}{|\delta V|} \int_{\delta A_{\alpha\beta}} \rho^j (\mathbf{w}_{\alpha\beta}^j - \mathbf{v}^j) \cdot \mathbf{n}_\alpha \, da, \end{aligned} \quad (106)$$

$$\widehat{\eta}_\alpha^j \equiv \varepsilon_\alpha \rho_\alpha^j \left(\overline{\widehat{\eta}^j}^\alpha + \overline{\widehat{r}^j \eta^j}^\alpha - \widehat{r}_\alpha^j \eta_\alpha^j \right), \quad (107)$$

$$\widehat{\Lambda}_\alpha^j \equiv \overline{\Lambda^j}^\alpha. \quad (108)$$

Acknowledgements

This work was supported by the USARO/Terrestrial Sciences under contract DAAL 03-90-G-0074 and the Army Engineering Waterways Experiment Station under contract DACA39-95-K-0056.

References

1. Achanta, S. and Cushman J. H.: Non-equilibrium swelling and capillary pressure relations for colloidal system, *J. Colloid Interface Sci.* **168** (1994), 266–268.
2. Achanta, S., Cushman, J. H. and Okos, M. R.: On multicomponent, multiphase thermomechanics with interfaces, *Int. J. Engng Sci.* **32**(11) (1994), 1717–1738.
3. Achanta, S., Okos, M. R., Cushman, J. H. and Kessler, D. P.: Moisture transport in shrinking gels during saturated drying, *AICHE* **43**(8) (1997), 2112.
4. Adams, E. E. and Brown, R. L.: A mixture theory for evaluating heat and mass transport processes in nonhomogeneous snow, *Contin. Mech. Thermodyn.* **2** (1990), 31–63.
5. Aifantis, E. C.: On the problem of diffusion in solids, *Acta Mech.* **37** (1980), 265–296.
6. Atkin, R. J. and Craine, R. E.: Continuum theories of mixtures: basic theory and historical development, *Quart. J. Mech. Appl. Math.* **29** (1976), 209–231.
7. Balzhiser, R. E., Samuels, M. R. and Eliassen, J. D.: *Chemical Engineering Thermodynamics*, Prentice Hall, New Jersey, 1972.
8. Bartholomeusz, B. J.: The chemical potential at the surface of a non-hydrostatically stressed, defect-free solid, *Philosophical Magazine A* **71** (1995), 489–495.
9. Bear, J.: *Dynamics of Fluid in Porous Media*, Elsevier, Amsterdam, 1972.
10. Beckermann, C. and Viskanta R.: Mathematical modeling of transport phenomena during alloy solidification, *Appl. Mech. Rev.* **46**(1) (1993), 1–27.
11. Bennethum, L. S.: Multiscale, hybrid mixture theory for swelling systems with interfaces, PhD Thesis, Purdue University, West Lafayette, Indiana, 1994.
12. Bennethum, L. S. and Cushman, J. H.: Multiscale hybrid mixture theory for swelling systems – I: Balance laws. *Int. J. Engng Sci.* **34**(2) (1996a), 125–145.
13. Bennethum L. S. and Cushman, J. H.: Multiscale hybrid mixture theory for swelling systems – II. Constitutive Theory, *Int. J. Engng Sci.* **34**(2) (1996b), 147–169
14. Benethum, L. S., Murad, M. A. and Cushman, J. H.: Clarifying mixture theory and the macroscale chemical potential for porous media, *Int. J. Engng Sci.* **34**(14) (1996), 1611–1621.
15. Biot, M.: General Theory of three-dimensional consolidation, *J. Appl. Phys.* **12** (1944), 155–164.
16. Biot, M.: Theory of propagation of elastic waves in a fluid-saturated porous solid, *J. Acoust. Soc. Amer.* **28**(2) (1956), 168–178.
17. Biot M.: Mechanics of deformation and acoustic propagation in porous media, *J. Appl. Phys.* **33**(4) (1962), 1482–1498.
18. Bouré, J. A.: Two-phase. flow models: the closure issue, In: G. F. Hewitt, J. M. Delhaye and N. Zuber (eds), *Multiphase Science and Technology*, Vol. 3, Marcel Dekker, New York, 1987, pp. 3–30.
19. Bowen, R. M.: Theory of Mixtures, In: A. C. Eringen (ed.), *Continuum Physics*, Vol. 3, Academic Press, New York, 1976, pp. 2–127.
20. Bowen, R. M.: Incompressible porous media models by use of the theory of mixtures, *Int. J. Engng Sci.* **18** (1980), 1129–1148.
21. Bowen, R. M.: Compressible porous media models by use of the theory of mixtures, *Int. J. Engng Sci.* **20** (1982), 697–735.
22. Bowen, R. M. and Wiese, J. C.: Diffusion in mixtures of elastic bodies, *Int. J. Engng Sci.* **7**, (1969), 689–735.
23. Callen, H.: *Thermodynamics and an Introduction to Thermostatics*, Wiley, New York, 1985.
24. Castellan, G.: *Physical Chemistry*, Addison-Wesley, Menlo Park, California, 1983.
25. Coleman, B. D. and Noll, W.: The thermodynamics of elastic materials with heat conduction and viscosity, *Archive Rational Mech. Anal.* **13** (1963), 167–178.
26. Cushman, J.: Molecular-scale lubrication, *Nature* **347** (1990), 227–228.

27. Cushman, J. H.: On unifying the concepts of scale, instrumentation and stochastics in the development of multiple phase transport theory, *Water Resour. Res.* **20** (1984), 1668–1676.
28. de Groot, S. R. and Mazure, P.: *Nonequilibrium Thermodynamics*. McGraw-Hill, New York, 1962.
29. Deemer, A. R. and Slattery, J. C.: Balance equations and structural models for phase interfaces, *Int. J. Multiphase Flow* **4** (1978), 171–192.
30. Derjaguin, B. V. and Churaev, N.: On the question of determining the concept of disjoining pressure and its role in the equilibrium and flow of thin films, *J. Colloid Interface Sci.* **66**(3) (1978), 389–398.
31. Derjaguin, B. V. and Churaev, N.: The current state of the theory of long-range surface forces, *Colloids and Surfaces* **41** (1989), 223–237.
32. Derjaguin, B. V., Churaev, N. and Muller, V. M.: *Surface Forces*. Consultants Bureau, New York, 1987.
33. Eringen, A. C.: *Mechanics of Continua*. John Wiley and Sons, New York, 1967.
34. Fremond, M. and Nicolas, P.: Macroscopic thermodynamics of porous media, *Continuum Mechanics and Thermodynamics* **2** (1990), 119–139.
35. Gee, M. L., McGuiggan, P. M., Israelachvili, J. and Homola, A. M.: Liquid to solidlike transitions of molecularly thin films under shear, *J. Chem. Phys.* **93**(3) (1990), 1895–1906.
36. Goodman, M. A. and Cowin, S. C.: A Continuum Theory for Granular Materials, *Archive Rational Mech. Anal.* **44** (1972), 249–266.
37. Gray, W. G. and Hassanizadeh, S. M.: Unsaturated flow theory including interfacial phenomena. *Water Resour. Res.* **27** (1991), 1855–1863.
38. Grim, R. E.: (1968), *Clay Mineralogy*, McGraw-Hill, New York.
39. Hassanizadeh, S. M.: 1986, Derivation of basic equations of mass transport in porous media, Part 2. Generalized Darcy's and Fick's Laws, *Adv. Water Resour.* **9**, 207–223.
40. Hassanizadeh, S. M. and Gray, W. G.: General conservation equations for multiphase systems: 1. Averaging procedure, *Adv. Water Resour.* **2** (1979a), 131–144.
41. Hassanizadeh, S. M. and Gray, W. G.: General conservation equations for multiphase systems: 2. Mass, momenta, energy, and entropy equations, *Adv. Water Resour.* **2** (1979a), 191–208.
42. Hassanizadeh, S. M. and Gray, W. G.: General conservation equations for multiphase systems: 3: constitutive theory for porous media, *Adv. Water Resour.* **3** (1980), 25–40.
43. Hassanizadeh, S. M. and Gray, W. G.: Mechanics and thermodynamics of multiphase flow in porous media including interphase boundaries, *Adv. Water Resour.* **13** (1990), 169–186.
44. Hassanizadeh, S. M. and Gray, W. G.: Thermodynamics basics of capillary pressure in porous media, *Water Resour. Res.* **29** (10) (1993a), 3389–3405.
45. Hassanizadeh, S. M. and Gray, W. G.: Toward an improved description of the physics of two phase flow, *Adv. Water Resour.* **16** (1993b), 53–67.
46. Hueckel, T.: On effective stress concepts and deformation in clays subjected to environmental loads, *Canad. Geotech. J.* **29** (1992), 1120–1125.
47. Israelachvili, J.: *Intermolecular and Surface Force*, Academic Press, New York, 1991.
48. Israelachvili, J., McGuiggan, P. M. and Homola, A. M.: Dynamic properties of molecularly thin liquid films, *Science* **240** (1988), 189–191.
49. Kralchevsky, P. A. and Ivanov, I. B.: Micromechanical description of curved interfaces, thin films, and membranes – II: Film surface tensions, disjoining pressure and interfacial stress balances, *J. Colloid Interface Sci.* **137**(1) (1990), 234–252.
50. Kremer, G. M., Dai, L. and Marques J. W.: Thermodynamics of binary mixtures of molecular and noble gases, *Contin. Mech. Thermodyn.* **4** (1992), 37–57.
51. Lambe, T. W.: A mechanistic picture of shear strength in clay, In: *Research Conference on Shear Strength of Cohesive Soils*, New York, 1960, pp. 503–532.
52. Liu, I. S.: Method of Lagrange multipliers for exploitation of the entropy principle, *Archive Rational Mech. Anal.* **46** (1972), 131–148.

53. Liu, I. S. and Muller, I.: Extended thermodynamics of classical and degenerate gases, *Archive Rational Mech. Anal.* **83** (1983), 285–332.
54. Low, P. E. Viscosity of interlayer water in montmorillonites, *Soil Sci. Soc. Amer. J.* **40** (1976), 500–505.
55. Low, P. F.: Nature and properties of water in montmorillonite-water system, *Soil Sci. Soc. America J.* **43** (1979), 651–658.
56. Low, P. F.: The swelling of clay: II. Montmorillonite-water system, *Soil Sci. Soc. America J.* **44**(4) (1980), 667–676.
57. Low, P. F.: Structural component of the swelling pressure of clays, *Langmuir* **3** (1987), 18–25.
58. Low, P. F.: The clay/water interface and its role in the environment, In: *Progress in Colloid & Polymer Science*, Vol. 95, Steinkopff Verlag, 1994, pp. 98–107.
59. Marle, C. M.: On macroscopic equations governing multiphase flow with diffusion and chemical reactions in porous media, *Int. J. Engng Sci.* **20** (1982), 643–662.
60. Marsily, G.: 1986, *Quantitative Hydrogeology: Groundwater Hydrology for Engineers*, Academic Press, London.
61. McQuarrie, D. A.: 1977, *Statistical Mechanics*, Harper and Row, New York.
62. Morgenstern, N. M. and Balasubramonian B.: Effects of pore fluid on the swelling of clay-shale, In: D. Snethen (ed.), *Proc. Fourth Int. Conf. on Expansive Soils*, New York, NY, 1980, pp. 190–205.
63. Müller, I. and Ruggeri, T.: 1993, *Extended Thermodynamics*, Springer-Verlag, New York.
64. Murad, M. A., Bennethum, L. S. and Cushman, J. H.: A multiscale theory of swelling porous media: Application to one-dimensional consolidation, *Transport in Porous Media* **19** (1995), 93–122.
65. Murad, M. A. and Cushman, J. H.: Multiscale flow and deformation in hydrophilic swelling porous media, *Int. J. of Engng Sci.* **34**(3) (1996), 313–336.
66. Murad, M. A. and Cushman, J. H.: (1997), A multiscale theory of swelling porous media: II dual porosity models for consolidation of clays incorporating physico-chemical effects, *Transport in Porous Media* **28**(1) (1997), 69–108.
67. Passman, S. L., Nunziato, J. W. and Walsh, E. K.: 1984, A theory of multiphase mixtures, In: Truesdell (ed.), *Rational Thermodynamics*, Springer-Verlag, New York.
68. Richards, J. I. and Youn, H. K.: 1990, *Theory of Distributions: A Non-Technical Introduction*, Cambridge Univ. Press, Cambridge.
69. Rusanov, A. I.: 3. Thermodynamics of solid bulk phase: Anisotropy of chemical potential, *Surface Science Reports* **23** (6–8) (1996), 178–181.
70. Schoen, M., Diestler, D. J. and Cushman, J. H.: Fluids in micropores. I. structure of a simple classical fluid in a slit-pore, *J. of Chem. Phys.* **87**(9) (1987), 5464–5476.
71. Schwartz, L.: 1950, *Théorie des Distributions*. Paris: Hermann et Cie.
72. Slattery, J. C.: Flow of viscoelastic fluids through porous media, *AICHE* **13** (1967), 1066–1071.
73. Sridharan, A. and Rao, G. V.: Mechanisms controlling volume change of saturated clays and the role of the effective stress concept, *Geotechnique* **23**(3) (1973), 359–382.
74. Terzaghi, K.: 1942, *Theoretical Soil Mechanics*, John Wiley and Sons, New York.
75. Thomas, N. L. and Windle A. H.: A theory of case II diffusion, *Polymer* **23** (1982), 529–542.
76. Truesdell, C. and Noll, W.: 1965, *The Non-Linear Field Theories of Mechanics. Handbuch der Physik III/3*, Springer-Verlag.
77. Vardoulakis, I. and Aifantis, E. C.: On the role of microstructure in the behavior of soils: Effects of higher order gradients and internal inertia, *Mechanics of Materials* **18** (1994), 151–158.
78. Whitaker, S.: Diffusion and dispersion in porous media, *AICHE* **13** (1967), 420–438.
79. Whitaker, S.: Advances in theory of fluid motion in porous media, *Ind. Engng Chem.* **61**(12) (1969), 14–28.
80. Zubarev, D. N.: 1974, *Nonequilibrium Statistical Thermodynamics*, Consultants Bureau, New York, pp. 321–322.